Université de Montréal

Département de chimie Faculté des arts et des sciences

This Thesis entitled

Lactam-peptide modulators of biased interlukin-1 receptor signaling for mitigating inflammation without compromising immuno-vigilance

Presented by

Azade Geranurimi

Thesis was evaluated by a jury composed of the following members

Prof. Samy Cecioni, President of jury

Prof. William D. Lubell, Research director

Prof. Helen Lebel, Member of jury

Prof. Monika Raj, External examiner

Résumé

Les accouchements prématurés restent un défi pour la médecine moderne. Malgré les efforts de préventions déployés, les taux de naissances prématurés sont en constante augmentation dans les pays industrialisés. Le récepteur interleukine-1 (IL-1R) a été étudié dans le but de développer des agents thérapeutiques pouvant prolonger la gestation et mener à des prognostiques néonataux. Dans cette optique, il y a été démontré que le peptide 101.10 possède a démontré une capacité à moduler le récepteur IL-1R, retarder les accouchements prématurés et réduire l'incidence de la rétinopathie prématurée par un mécanisme allostérique impliquant une signalisation biaisée. Dans le but d'étudier la conformation active du peptide 101.10 et d'en améliorer l'activité, nous avons développé une méthode pour introduire des α-amino γ-lactames β-substituées dans des séquences peptidiques. Appliquer cette stratégie au peptide 101.10 a permis d'améliorer la compréhension de la relation structure-activité pour la modulation allostérique du récepteur IL-1R.

Les composés peptidomimétiques ont le potentiel de mimer la conformation et l'activité des peptides bioactifs. Ils offrent le potentiel d'améliorer la reconnaissance moléculaire, d'optimiser le transport à travers des différentes membranes biologiques et d'augmenter la résistance métabolique. Parmi les différentes classes de composés peptidomimétiques, les α-amino γ-lactames (Agl) permet de rigidifier par des liens covalents la chaine peptidique principale favorisant les structures secondaires de type tour β. Les analogues Agl β-substituées mimer et rigidifier la chaine latérale des acides aminés.

Cette thèse introduit des méthodes efficaces pour la synthèse stéréocontrolée des résidus α-amino γ-lactames β-substituées possédant diverses fonctionnalités. L'introduction de ces résidus dans différents peptides bioactifs a été effectuée pour étudier leur relation structure-activité. En utilisant le peptide modulateur du récepteur IL-1R 101.10 comme peptide représentatif, la présente recherche a permis d'identifier de nouveaux agents tocolytiques qui peuvent prolonger la gestation et améliorer le pronostique néonatal.

Dans le chapitre 2, des stéréo-isomères de (Agl) et β-hydroxy-α-amino-γ-lactam (Hgl) ont été utilisés pour étudier l'influence de la configuration du groupement hydroxyle sur la conformation et l'activité du peptide 101.10. L'orientation de ce groupement dans les peptides Agl et Hgl s'est avéré avoir une influence conformationnelle et sur l'activité. La spectroscopie par

dichroïsme circulaire (CD) a illustré la propension de certains analogues, comme le [(3*R*,4*S*)-Hgl³]-101.10, à adopter des tours *β*. Les analogues Agl et Hgl ont été examinés dans une série d'essais *in vitro* et *in vivo* modélisant les accouchements prématurés. Dépendant de leur structure et configuration, les analogues lactames ont démontré une sélectivité fonctionnelle différente dans diverse processus biologiques, démontrant les particularités de divers phénotypes. Par exemple, l'inhibition des JNK et ROCK kinases s'est avérée importante respectivement dans leurs effets tocolytiques et dans la diminution de la vaso-oblitération. Notamment, parmi les douze analogues testés, [(3*R*,4*S*)-Hgl³]-101.10 s'est avéré démontrer la même activité *in vitro* et *in vitro* que le peptide parent.

Dans le chapitre 3, des méthodes de déplacement du groupement hydroxyle des résidus Hgl ont permis l'introduction stéréosélective de substituent en position β des résidus Agl. Une combinaison de réaction de Mitsunobu sur les résidus *trans* Hgl et une ouverture nucléophile les sulfamidates cycliques dérivés des lactames *cis*, ont mené à l'obtention de mime rigidifiés de résidus Ser, Thr, Cys, Dap, Dab, His et Met.

Dans le chapitre 4, différentes lactames β-substitués ont été introduits dans la séquence du peptide 101.10 par une combinaison de chimie en solution et sur support solide pour étudier d'avantage les éléments structurels nécessaire pour réguler l'activité et la signalisation de cette cytokine clef dans la médiation de l'inflammation. Considérant l'activité de l'analogue [(3*R*,4*S*)-Hgl³]-101.10, plusieurs analogues β-substitués possédant une orientation similaire pour la chaine principale et latérale ont été synthétisés. Certains analogues ont démontré une activité biologique prometteuse dans des modèles de rétinopathie et seront étudiés dans le futur.

En conclusion, des méthodes de synthèse d'α-amino-γ-lactames et de leur contrepartie β-substitués et leur introduction dans des peptides d'intérêt pour étudier leur relation structure-activité ont été développés. En utilisant ces méthodologies sur le modulateur allostérique du récepteur IL-1R 101.10, le conformère actif *in vivo* responsable de l'activité tocolytique et protectrice contre la rétinopathie associée aux accouchements prématures ont été identifiés. Considérant l'utilité de la synthèse de lactames pour le développement d'agents susceptibles de prolonger la gestation et d'améliorer le prognostique associé aux accouchements prématurés, cette thèse a permis la conception de prototypes de médicaments pour traiter les accouchements prématurés ainsi que l'évaluation des contraintes structurelles pertinentes pour la biologie des peptides.

Mots-clefs: Peptidomimétique, lactame de Freidinger-Veber, α-amino-γ-lactam (Agl), β-hydroxy-α-amino-γ-lactam (Hgl), tours *β*, dichroïsme circulaire, réaction de Mitsunobu, CuAAC, sulfamidate cyclique, récepteur interleukine 1, accouchements prématurés, rétinopathie associée aux prématurés, tocolytiques.

Abstract

Preterm birth (PTB) is an unmet biomedical need. Despite efforts to counter the onset of preterm labor, the rate of premature birth has increased steadily in developed countries. The interleukin-1 receptor (IL-1R) has been pursued as a target for designing agents which can prolong labor and improve neonatal outcomes. Towards these goals, a lead peptide 101.10 had been shown to modulate the IL-1R, to delay PTB and to mitigate associated retinopathy of prematurity (ROP) by an allosteric mechanism featuring biased signaling. With the goals of understanding the active conformers and improving the activity of 101.10, methods were conceived for the synthesis and introduction of β-substituted α-amino γ-lactams into peptides. Applying such methods on 101.10 has provided insight into the structure-activity relationships required for allosteric modulation of the IL-1R.

Peptidomimetics are promising structures that replicate peptide function and conformation. They offer the potential to improve molecular-recognition, to enhance transport across biological membranes, and to resist metabolism. Among peptidomimetic classes, α-amino γ-lactam (Agl) residues introduce covalent constraint to rigidify the peptide backbone and have been employed to favor turn secondary structures. β-Substituted Agl analogs offer additional potential to mimic and restrict peptide side-chain geometry.

This thesis introduces effective methods for the stereo-controlled synthesis of β-substituted α-amino γ-lactams residues having various side chain functionality. Introduction of the parent Agl residue and β-substituted counterparts into biologically active peptides has been explored to study structure-activity relationships. Employing the IL-1R modulator 101.10 as a representative peptide, the described research has furnished novel labor delaying agents that can improve neonatal outcomes.

In chapter 2, α-amino-γ-lactam (Agl) and β-hydroxy-α-amino-γ-lactam (Hgl) stereoisomers were employed to study the influence of configuration and hydroxyl group side chain on conformation and activity of the interleukin-1 receptor modulator peptide 101.10. The configuration and hydroxyl group side chain influenced the conformation and biological activity of Agl and Hgl-101.10 analogs. Circular dichroism (CD) spectroscopy illustrated *β*-turn conformers for specific analogs, such as [(3*R*,4*S*)-Hgl³]-101.10. The Agl and Hgl analogs were examined in a series of *in vitro* assays and *in vivo* models of PTB. Contingent on their structure

and configuration, the lactam analogs exhibited different functional selectivity in the various biological pathways, and indicated the requirement for specific phenotypes. For example, inhibition of the JNK and ROCK kinase pathways were respectively shown to be important for delaying labor and diminishing vaso-obliteration in the PTB and ROP models. Notably, among the twelve analogs, $[(3R,4S)\text{-}Hgl^3]$-101.10 was found to exhibit identical *in vitro* and *in vivo* activity as the parent peptide.

In chapter 3, methods were developed for displacement of the β-hydroxy-α-amino-γ-lactam (Hgl) residue alcohol to introduce stereo-selectively different β-substituents on Agl residues. A combination of Mitsunobu chemistry on the *trans* Hgl residue, and nucleophilic ring opening of the cyclic sulfamidate derived from the *cis* lactam counterpart provided constrained mimics of Ser, Thr, Cys, Dap, Dab, His and Met residues.

In chapter 4, various β-substituted lactams were introduced into the sequence of 101.10 by combination of solution and solid phases chemistry to further study the structural requirements for regulating the activity and signaling of this key cytokine mediator of inflammasome activation. Considering the activity of $[(3R,4S)\text{-}Hgl^3]$-101.10, the β-substituted Agl analogs were synthesized possessing similar backbone and side chain configurations. Certain analogs exhibited promising biological activity in the ROP model meriting further study.

In sum, methods were conceived for the synthesis and application of α-amino-γ-lactams and their β-substituted analogs to study peptide structure-activity relationships. Employing this chemistry on the IL-1R allosteric modulator 101.10 has identified the active conformer and *in vitro* activity responsible for ability to delay labor and mitigate retinopathy of prematurity. Considering the utility of the lactam synthesis methods for the development of improved agents for delaying labor and improving neonatal outcomes, this thesis has conceived useful prototypes for drugs to treat PTB, as well as useful methods for dissecting the structural requirements for peptide chemical biology.

Keywords: Peptidomimetic, Freidinger-Veber lactam, α-amino-γ-lactam (Agl), β-hydroxy-α-amino-γ-lactam (Hgl), *β*-turn, circular dichroism, Mitsunobu reaction, CuAAC, cyclic sulfamidate, interleukin 1 receptor, preterm birth, retinopathy of prematurity, tocolytic.

Note

This thesis describes my research on the synthesis of β-substituted-α-amino-γ-lactams as constrained amino acid residue mimics with constrained backbone and side chain conformations, and their insertion into the IL-1 allosteric modulating peptide 101.10 to study the influence of side chain functional group, configuration and conformation on biological activity. This thesis has been written employing published manuscripts. I specify herein my contributions to each of the chapters.

The introduction (Chapter 1), and unless specified otherwise below, the following chapters, all were written by me and edited by Professor William D. Lubell.

The manuscript in chapter 2 entitled "Probing anti-inflammatory properties independent of NF-κB through conformational constraint of peptide-based interleukin-1 receptor biased ligands" describes the synthesis of a library of twelve 101.10 derivatives containing various stereochemical isomers of α-amino-γ-lactam (Agl) and α-amino-β-hydroxy-γ-lactam (Hgl) residues to constrain the D-Thr-D-Val dipeptide residue. Their CD spectra were measured to study the influence of Agl and Hgl residues on conformation. This manuscript has been published in the *Frontiers in Chemistry* as an original research manuscript. I performed the synthesis, isolation and chemical and spectroscopic characterization of all derivatives. Dr. Daniel J. St-Cyr, Ms. Kim Beauregard, and Dr. Vadim Bernard-Gauthier performed preliminary chemical and biological investigations. All final peptide analogs that I synthesized and purified were tested in a panel of *in vitro* cellular assays, as well as for *in vivo* activity in murine models of PTB and ROP by our collaborators Professor Sylvain Chemtob, Dr. Christiane Quiniou, Dr. Xin Hou, Dr. Tang Zhu, Dr. José Carlos Rivera, and Mr. Colin W. H. Cheng from the Département de pédiatrie, Université de Montréal. Colin and I wrote the original draft of the manuscript which was edited by Professor Lubell, Professor Chemtob, Dr. Quiniou and Dr. Daniel J. St-Cyr.

The manuscript in chapter 3 entitled "Diversity-oriented syntheses of β-substituted α-amino γ-lactam peptide mimics with constrained backbone and side chain residues" and the Proceeding of the 35th European Peptide Symposium entitled "Stereoselective synthesis of a β-methylthio α-amino γ-lactam dipeptide, a *S*-methyl-Cys-Val mimic" describe my original syntheses, isolation and characterization of a series of β-substituted α-*N*(Fmoc)amino-γ-lactams employing, respectively, Mitsunobu chemistry and cyclic sulfamidate nucleophilic ring opening from *trans*- and *cis*-β-hydroxy-α-amino-γ-lactam precursors. The manuscript has been published

in *Organic Letters*. I performed all experiments, and the isolation and characterization of all compounds. I wrote the first draft of the manuscript and contributed to its revision which was edited by Professor Lubell.

The manuscript in Chapter 4 entitled "Solid-phase synthesis and diversification of β-substituted α-amino-γ-lactam peptide allosteric modulators of the inteleukin-1 receptor" describes synthesis of fifteen β-substituted-Agl^3-101.10 peptides by a combination of solution- and solid-phase methods employing *N*-Fmoc-β-substituted-Agl^3-Val-OH dipeptide building blocks. The manuscript is in preparation for submission to *Frontiers in Chemistry*. I performed all the experiments to synthesize the peptide analogs and their isolation and characterization. The analogs are currently being tested in a panel of *in vitro* cellular assays as well as *in vivo* activity in murine models of PTB and ROP by our collaborators Professor Chemtob, Dr. Quiniou, Dr. Hou and Mr. Cheng from the Département de pédiatrie, Université de Montréal. Colin and I wrote the original draft of the manuscript which has been edited by Professors Lubell and Chemtob, and Dr. Quiniou.

In Chapter 5, I have written the conclusion and perspectives of this thesis, which were edited by Professor Lubell. The perspective describes the synthesis of constrained dipeptides bearing lactam and cyclopropyl amino acid components. I performed the synthesis and characterization of the dipeptide analogs using cyclopropyl amino acid components, which were synthesized and characterized by Ms. Emmanuelle Allouche.

Table of contents

Contents

Geranurimi, A.; Cheng, C. W. H.; Quiniou, C.; Hou, X.; Zhu, T.; Rivera, J. C.; St-Cyr, D.; Beauregard, K.; Bernard-Gauthier, V.; Chemtob, S.; Lubell, W. D. *Frontiers Chem.,* **2019**, *7*, Article 23.

Geranurimi, A.; Lubell, W. D. *Org. Lett.,* **2018**, *20* (19), 6126-6129.

Geranurimi, A.; Lubell, W. D. **2018**. In P. B. Timmons, Ch. M. Hewage, M. Lebl (Eds.), Proceedings of the 35th European Peptide Symposium, Dublin City University, Ireland, pp. 18-20.

List of Figures

List of Schemes

List of Tables

List of abbreviations

$[\alpha]^D$	specific rotations
°C	degree Celsius
Acc	1-aminocyclopropane-1-carboxylic acid
Agl	α-amino-γ-lactam
AP	alkaline phosphatase
ARVO	Association for Research in Vision and Ophthalmology
Bgl	β-amino-γ-lactam
Bn	Benzyl
Boc$_2$O	di-*tert*-butyl dicarbonate
br	broad (in NMR)
BSA	bovine serum albumin
c	Concentration
Cbz	Benzyloxycarbonyl
CCBs	calcium channel blockers
CD	circular dichroism
cDNA	complementary DNA
CIHR	Canadian Institute of Health Research
^{13}C NMR	carbon nuclear magnetic resonance
COSY	correlation spectroscopy
COX-2	cyclooxygenase-2
CuAAC	copper-catalyzed azide alkyne cycloadditions
d	doublet (in NMR)
Dab	Diaminobutyrate
DAMPs	damage-associated molecular patterns
Dap	diaminoproprionic acid
DCC	*N,N'*-dicyclohexylcarbodiimide
DCM	Dichloromethane
dd	doublet of doublet (in NMR)
DEAD	diethyl azodicarboxylate

DIAD	diisopropyl azodicarboxylate
DIEA	*N,N*-diisopropylethylamine
DMEM	Dulbecco's modified Eagle medium
DMF	Dimethylformamide
DPPA	diphenylphosphoryl azide
DVB	Divinylbenzene
Erk1/2	extracellular signal-regulated kinase
ESI	electrospray ionization
Et_2O	Ether
EtOAc	ethyl acetate
eq	Equivalent
FA	formic acid
FESP	Faculté des études supérieures et postdoctorales
Fmoc	fluorenylmethyloxycarbonyl
Fmoc-OSu	9-fluorenylmethyl *N*-succinimidyl carbonate
FP	prostaglandin F2α
FT-IR	fourier-transform infrared
HBTU	2-(1H-benzotriazol-1-yl)-1,1,3,3- tetramethyluronium hexafluorophosphate
HFIP	hexafluoro isopropanol
hGH	human growth hormone
Hgl	β-hydroxy-α-amino-γ-lactam
HMBC	heteronuclear multiple bond correlation
^{1}H NMR	Hydrogen nuclear magnetic resonance
HOBt	hydroxy benzotriazole
HPLC	high performance liquid chromatography
HRMS	high resolution mass spectrometry
Hz	Hertz
ICAM	intercellular adhesion molecule
IL-1β	interleukin-1β
IL-1R	IL-1 receptor
IL-1Ra	IL-1R antagonist

IL-1RacP	IL-1R accessory protein
i-Pr	*iso*-propyl
IR	Infrared
J	coupling constant (in NMR)
JNK	c-Jun *N*-terminal kinases
LCMS	liquid chromatography mass spectrometry
LC-MSD	liquid chromatography/mass selective detector
LH-RH	luteinizing hormone-releasing hormone
IκB	inhibitor of kappa B kinase
LPS	lipopolysaccharide
LTA	lipoteichoic acid
m	multiplet (in NMR)
MAPK	mitogen-activated protein kinase
m-CPBA	*meta*-chloroperoxybenzoic acid
MHz	megahertz (in NMR)
mp	melting point
NF-κB	nuclear factor kappa-light-chain-enhancer of activated B cells
NOESY	nuclear overhauser effect spectroscopy
NSAID	non-steroid anti-inflammatory drug
NSERC	Natural Sciences and Engineering Research Council of Canada
OD	optical density
OIR	oxygen-induced retinopathy
OTR	oxytocin receptor
p38	p38 mitogen-activated protein kinases
PAMPs	pathogen-associated molecular patterns
PCR	polymerase chain reaction
PDVF	polyvinylidene difluoride
PGE2	prostaglandin E2
PhF	9-phenylfluoren-9-yl
Pmc	2,2,5,7,8-pentamethylchroman-6-sulphonyl
PMSF	phenylmethylsulfonyl fluoride

PPh$_3$	Triphenylphosphine
ppm	parts per million (in NMR)
Prep LC	high performance liquid chromatography
PTB	preterm birth
PTGHS2	Prostaglandin H synthetase 2
qPCR	Quantitative polymerase chain reaction
R$_f$	retention factor (in chromatography)
Rho/ROCK	Rho/Rho-associated coiled-coil containing protein kinase
ROCK2	Rho-associated coiled-coil-containing protein kinase 2
ROP	retinopathy of prematurity
RP	reverse phase
RPE	retinal pigment epithelium
RPM	revolutions per minute
rt	room temperature
RT	retention time
s	singlet (in NMR)
SAR	structure-activity relationship
Sema	semaphorin-3A
SPPS	solid-phase peptide synthesis
t	triplet (in NMR)
t-Bu	*tert*-butyl
TCEP	tris(2-carboxyethyl)phosphine hydrochloride
TEA	Triethylamine
TFE	Trifluoroethanol
TES	Triethylsilane
TFA	trifluoroacetic acid
THF	tetrahydrofuran
TLC	thin layer chromatography
TLRs	toll-like receptors
TNF-α	tumor necrosis factor-α
UAPs	uterine activation proteins

UV	Ultraviolet
μW	Microwave
VEGF	vascular endothelial growth factor

To my family

With love and eternal appreciation

Acknowledgement

First and foremost, I would like to thank my research director, Professor William D. Lubell, for accepting me into his research group, as well as for his support and ideas throughout the years. I am honored to be his Ph.D. student, and thankful for his teachings and advice in chemistry, communicational skills, real life values and coping with cultural and social differences. His knowledge, patient guidance and encouragement enabled this great desire of my life to become a reality. This thesis would never have been possible without his tireless efforts. No words can express my respect and gratitude for him.

I would like to thank my thesis committee, Professor Samy Cecioni, Professor Alexis Vallée-Bélisle and Professor Helene Lebel for their encouragement and valuable guidance. I would like to thank you all for being a part of my thesis committee and for the evaluation of this thesis.

I would like to acknowledge my external examiner, Professor Monika Raj for reading and evaluating of this thesis.

I am grateful to all the past and present members of the Lubell group for their support and for creating a dynamic friendly and supportive work environment, especially Dr. Daniel J. St-Cyr, Dr. Yésica Garcia-Ramos, Dr. Mariam Traoré, Dr. Stephen Turcotte, Dr. Martin Strack, Dr. Ramesh Chingle, Dr. Fatemeh Mir, Dr. Nagavenkata Durga Prasad Atmuri, Dr. Antoine Douchez, Dr. Mohamed Atfani, Dr. Chiara Gamberi, Dr. Ahsanullah Ahsanullah, Dr. Ragnhild Ohm, Ms. Kelvine Chignen Possi, Dr. Pradeep Chauhan, Mr. Julien Poupart, Ms. Cynthia Crifar and Ms. Anh Minh Thao Nguyen. I have always enjoyed working with you and more than once you helped me find a solution to the difficulties encountered in my project. I am particularly grateful to Dr. Pradeep Chauhan and Dr. Fatemeh Mir who helped read and correct my thesis chapters. I also would like to thank Mr. Julien Poupart and Ms. Cynthia Crifar for helping me write the French abstract.

Thanks to all the staff of the Université de Montréal for allowing me to evolve in such a warm and welcoming environment, especially Ms. Nancy Noel, Ms. Karine Plamandon, Ms. Marya Nahil, Ms. Aida Mikhno, Ms. Audrey Morin, Ms. Catherine Fouron, Mr. Kevin Filiatrault and of course Ms. Mildred Bien-Aimé.

I acknowledge the assistance of members of the Université de Montréal facilities: Dr. Alexandra Fürtös-Matei, Ms. Karine Gilbert, Ms. Marie-Christine Tang, Ms. Louiza Mahrouche and Mr. Simon Comtois-Marotte for HPLC, HRMS and LCMS analyses; Dr. Pedro Aguiar, Dr.

Chapter 1: Introduction

1.1   Preterm birth (PTB)

Preterm birth (PTB), birth at less than 37 weeks of gestation, affects about one of every ten newborns.[1-2] Premature babies are at higher risk of cerebral palsy developmental delays, and auditory and visual problems.[3] The earlier the birth, the more serious are the risks. PTB is the second leading cause of infant death worldwide. About 70% of neonatal deaths, 36% of infant deaths, and up to 50% of cases of long-term neurological impairments in children, all are due to prematurity.[4] Moreover, in spite of improvements in neonatal care, PTB remains an important clinical challenge. The rate of PTB increased from 10.62% in 1990 to 11.72% in 2011 in the United States.[5] PTB is also costly. In 2005, the annual cost of PTB was estimated to $26.2 billion in USA.[6-8]

Multiple factors may cause PTB, including stress, systemic or maternal genital tract infections, placental ischemia, vascular lesions and uterine over distension. For this reason, PTB is considered a syndrome and not a single disease. Pathways to PTB differ in initiating factors and mediators, but ultimately, share common features leading to preterm uterine contractions and birth.[9] Significant evidence suggests that inflammation plays an important role in preterm and term labor.[10-11] The inflammatory cascade leading to PTB may be triggered by stimuli characterized as damage- and pathogen-associated molecular patterns (DAMPs and PAMPs). The initial insult may arise from the environment (infection) or can be maternally-produced by stressed cells (alarmins), the former being a source of PAMPs and the latter a source of DAMPs. Such molecular patterns activate Toll-like receptors (TLRs), which trigger immune cells (e.g., neutrophils, macrophages, T-cells) to produce pro-inflammatory cytokines and chemokines. Cytokines (primarily IL-1 and IL-6) feed forward a placental chain reaction and exert inflammatory effects upon the fetus. Activation of gestational tissue by cytokines and chemokines prepare the uterus for labor by driving so-called uterine activation proteins (UAPs), such as prostaglandin endoperoxide synthase-2, the prostaglandin F2α receptor (FP), inducible nitric oxide synthase, and the oxytocin receptor (OTR).[12] The induction of UAPs by inflammation increases myometrial contractility, drives cervical ripening and leads to the rupture of membranes promoting the onset of labor.[13]
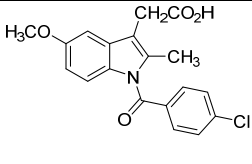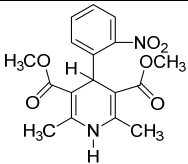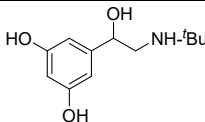
1.2   Retinopathy of prematurity (ROP)

Chapter 1

Among the consequences of PTB, retinopathy of prematurity (ROP) is a leading cause of childhood blindness throughout the world.[14] The use of oxygen therapy to treat respiratory distress syndrome of prematurity and bronchopulmonary dysplasia has been associated with ROP,[15] which is characterized by disorganized retinal blood vessel growth, scarring of the retina, and retinal detachment. Mild ROP may resolve spontaneously, but more severe cases may lead to blindness. Fetal retinal vascularization begins typically at the fourth month of pregnancy and is completed a few weeks before the normal time of delivery but is usually incomplete in preterm infants. Blood vessels grow from the central part of the retina outwards. Oxygen supply influences blood vessel formation. Oxygen toxicity and related hyperoxia can contribute to abnormal blood vessel growth and bleeding inside the eye. Reuptake of blood and reabsorbed abnormal vessels may give rise to multiple band-like membranes which can disturb retinal growth and facilitate detachment of the retina leading to blindness in neonates younger than six months.[16-17]

1.3 Tocolytic agents to prevent PTB

Traditional ways to suppress preterm contractions include bed rest, alcohol, hydration and restraining intercourse, but effectiveness is inconclusive. Tocolytic (from Greek *tókos,* "childbirth", and *lúsis,* "loosening") agents delay labor and may prevent PTB by inhibiting contractions. Different tocolytic agents have distinct mechanisms of action and risk-benefit profiles. Most are only effective for short-term (up to 48 hours) prolongation of pregnancy to allow for the administration of corticosteroids to the woman to improve newborn outcomes.[18-19] For example, the non-steroid anti-inflammatory drug (NSAID) indomethacin functions by inhibiting cyclooxygenase enzyme activity.[20] Calcium channel blockers (CCBs), such as nifedipine, are commonly used for tocolysis to inhibit calcium flow through cell membranes and prevent calcium-dependent myosin light-chain kinase-mediated phosphorylation, which results in myometrial relaxation.[21] Beta-adrenergic receptor agonists (beta-mimetics, e.g., terbutaline) bind the beta2 adrenergic receptor and decrease myometrial contractility through a cAMP-protein kinase-myosin light-chain kinase pathway.[22] Historically utilized to decreased myometrial contractions, magnesium sulfate inhibits myosin light-chain kinase activity by competing with intracellular calcium.[22]

Table 1.1. Contemporary tocolytic agents in use to delay preterm labor

Classification	Non-steroidal anti-inflammatory drugs (NSAIDs)	Calcium channel blockers (CCBs)	Beta-adrenergic receptor agonists (β-mimetics)	Magnesium sulfate
Examples	Indomethacin	Nifedipine	Terbutaline	
Structure				$MgSO_4$
Mechanism of action	inhibits cyclooxygenase enzyme activity	inhibits myosin light-chain kinase-mediated phosphorylation	Binds and activates beta2 adrenergic receptor	inhibits myosin light-chain kinase activity
potential side effects	renal failure	cardiovascular side effects	cardiovascular side effects	

Among the four classes of tocolytic mentioned above, the probability of delaying delivery by 48 hours to improve neonatal and maternal outcomes and to decrease maternal adverse effects was highest with NSAIDs, followed by magnesium sulfate, CCBs, and betamimetics. On the other hand, CCBs were better for use at and after 32 weeks of gestation to avoid premature closure of the fetal ductus arteriosus and complications due to deficiency of amniotic fluid.[19, 23]

Most common tocolytic drugs have a short-term effect (two days or less) that relaxes the uterine smooth muscle.[19, 24-25] Current tocolytic therapy does not decrease the risk of recurring preterm labor, nor improve perinatal outcomes.[26] Administration of a tocolytic serves usually only to delay preterm labor.[27] Contemporary tocolytics may maintain pregnancy for a sufficient period to enable *in utero* maturation; however, they are commonly associated with side effects to mother and fetus (Table 1).[28] The safety profile of indomethacin is limited to short-term use. Calcium channel blockers may have significant cardiovascular side effects. In spite a lack of evidence for efficacy and reported associated serious side effects, magnesium sulphate is the most commonly used tocolytic in the United States.[29] Mothers treated with beta-adrenergic receptor agonists, such as terbutaline, have exhibited negative cardiac side effects, including pulmonary edema, myocardial ischemia, cardiac arrhythmias, and hypotension.[30] In spite their ability to delay labor,

contemporary tocolytic agents do not reverse the fundamental parturitional process; instead, they reduce uterine response to stimulants driving parturition. Current tocolytic drugs prolong pregnancy by mostly blocking myometrial contractions at the late stage of pregnancy. They are not effective on PTB associated disorders caused by activation of the inflammatory cascade. Tocolytic drugs are thus needed to delay labor at earlier stages and to improve neonatal outcomes by mitigating prenatal inflammation.

1.4   Roles of Toll-like receptors (TLRs) and interleukin-1β (IL-1β) in PTB and ROP

Contingent on parturition time, bacterial infection is associated with 40% to 70% of all preterm births.[31-32] After PAMPs from invading bacteria are recognized by the TLRs,[33-34] immune cells release the pro-inflammatory cytokine interleukin-1β (IL-1β) commencing the mechanism to PTB.[35] Moreover, at term, spontaneous delivery in humans without infection is triggered by a rise in IL-1β expression. Furthermore, elevated IL-1β blood concentrations in human neonates have been associated with PTB.[36] IL-1β performs a key pro-inflammatory role in the induction of term and preterm labor.

The TLRs are present in various cells within the fetal–maternal interface: e.g., the cervix, endometrium, fallopian tubes, and placenta.[37,38,39] Up-regulated upon detection of bacterial infection before and during preterm labor, so-called chorioamnionitis, as well as during normal parturition,[40] TLRs recognize and respond to PAMPs. For example, TLR-2 is responsive to products of Gram-positive bacteria, mycoplasmas, and yeast, and TLR-4 mediates the response to lipopolysaccharides (LPS) found in the outer membrane of Gram-negative bacteria.[41-42] Engagement of TLRs leads also to the activation of nuclear factor kappa-light-chain-enhancer of activated B cells (NF-κB), a transcription factor that is involved in the expression of cytokines such as IL-1β, chemokines and defensin antimicrobial peptides.[43] The activation of NF-κB is essential for maintaining immune vigilance against invading pathogens.

Expression of TLRs in the retina is regulated during retinal ischemic diseases, such as ROP.[44] TLRs can be expressed in multiple cells in the retina, such as glial cells, retinal pigment epithelium (RPE), as well as photoreceptor cells and endothelium cells. Activation of TLRs in the retina can initiate a complex signal transduction cascade leading to production of pro-inflammatory cytokines, such as IL-1β, which play prominent roles in the pathogenesis of retinal ischemic

diseases.[44-47] IL-1β is produced by retinal microglia cells following exposure to hyperoxia, and triggers the inflammatory cascade, including of IL-6 and IL-8.[48] IL-1β contributes to deleterious effects in the retina. IL-1β-dependent retinal and sub-retinal injury to the immature subject involves direct endothelial cytotoxicity.[49-50] In oxygen-induced retinopathy (OIR), IL-1β has been indirectly associated with retinal microvascular degeneration,[51] and linked to oxidative stress.

1.5   IL-1 therapy

The major cytokine responsible for inducing local and systemic inflammation, IL-1β is a key pro-inflammatory agent associated with acute and chronic inflammation.[52] Therapy blocking the activity of IL-1β in auto-inflammatory syndromes has thus been pursued to reduce disease severity.[53] Currently, there are three approved drugs that inhibit IL-1β activity. Anakinra (Kineret; Amgen) is a recombinant form of the naturally occurring IL-1 receptor antagonist (IL-1Ra), blocks the activity of both IL-1α and IL-1β, and has been beneficial in clinical cases of rheumatoid arthritis, acute gouty arthritis, and diabetes mellitus.[54-55] Canakinumab (Novartis) is a therapeutic monoclonal antibody targeting IL-1β that was approved for the treatment of cryopyrin-associated periodic syndromes.[56] Rilonacept (Regeneron) is an "IL-1 trap", and consists of a dimeric fusion protein composed of the ligand-binding domains of the IL-1R1 and IL-1R accessory protein (IL-1RAcP) linked by an antibody Fc region.[57] All three are relatively large proteins (17.5–251 kDa) that compete with IL-1β for binding to its native ligand "orthosteric" binding site on the IL-1RI and may exhibit secondary effects such as immunosuppression, which increases the risk for opportunistic infections and pain at the site of injection. Such drawbacks may account for the failures of such therapy in clinical trials and may be related to non-selective interference of all signals triggered by IL-1β.[58-59] Although these protein drugs have exhibited effectiveness in treating certain inflammatory diseases, such as rheumatoid arthritis and inflammatory bowel disease, they do not delay labor, probably in part due to inability to cross the placenta.

Among the signaling pathways triggered by IL-1β, the activation of NF-κB is beneficial to retain anti-apoptotic activity[60] and to promote differentiation and proliferation of B and T cells, which are critical for the immune response against pathogenic insults.[61] Presently, approved therapies to block IL-1β inhibit all signaling pathways triggered by its binding to the orthosteric

ligand-binding site. Targeting IL-1β without inhibition of NF-κB signaling represents thus a novel promising strategy for developing therapy, which may be used to simultaneously delay labor, inhibit inflammation, and maintain immune vigilance to fight bacterial infection.

Allosteric ligands, which, bind at different sites other than the native orthosteric ligand binding site, may exhibit alternative modes of action with improved qualities. For example, allosteric ligands may possess higher functional selectivity, fewer adverse effects, and lower toxicity. Upon receptor binding at remote sites from the orthosteric binding site, allosteric ligands may likely change the conformation of the receptor and modulate the effects of the natural agonist. Allosteric ligand discovery has traditionally been serendipitous and often achieved through high-throughput screening. Technologic advances using computational approaches and structural data have been developed to detect allosteric binding sites and develop modulators.[62] Towards IL-1-targeting therapy for the prevention of PTL the functional selectivity provided by an allosteric ligand may be beneficial compared to strategies featuring competitive inhibition of the native ligand.[63] Current therapy which targets IL-1β prevents its binding to the orthosteric ligand-binding site of the IL-1R and inhibits activation of all downstream signaling. For example, Kineret® is a recombinant form of the native IL-1R antagonist. Canakinumab and Rilonacept are proteins that compete with IL-1R for IL-1β binding. In contrast, allosteric ligands may modulate the conformational dynamics of the IL-1R upon binding with IL-1β to modify downstream signalling.

1.6   101.10

Peptides are a particularly attractive class of therapeutic agents with potential advantages of having low toxicity and high activity. The peptide drug market has expanded significantly over recent years.[64] To employ peptides as therapeutic agents, however, certain limitations must be overcome. For example, peptides metabolize rapidly, have poor bioavailability, may interact with several subtypes of receptors, and may require intravenous administration. To address such issues while retaining the advantages of native peptides for drug discovery, strategies have been developed to prepare so-called peptidomimetics.[65] Peptidomimetics may replicate the form and function of peptides retaining desired activities such as high potency and low toxicity yet eliminating undesirable characteristics, such as rapid metabolism, lack of receptor selectivity, and poor

bioavailability. Mimicry of natural peptide conformations has been used to improve stability, binding affinity, and receptor specificity.

Based on a previously proven method for making allosteric modulators of G protein-coupled receptors,[66-67] a library of interface peptides from the flexible portions of the IL-1RAcP was created from sequences which were putative sites of interaction with IL-1RI.[68] The extracellular loops and inter-domain regions of the IL-1RAcP were identified based on the crystal structure and modeling data of the extracellular portions of the IL-1RI/IL-1β/IL-1RAcP complex and used to design an initial library of fifteen all D-configured, sense and anti-sense peptides (sense peptide is a peptide whose sequence is coded by the nucleotide sequence (read 5' → 3') of the sense (positive) strand of DNA, in contrast, an antisense peptide is coded by the corresponding nucleotide sequence (read 5' → 3') of the antisense (negative) strand of DNA) (Figure 1.1). Subsequent pharmacological testing, truncation and examination of the enantiomeric sequence led to the discovery of a selective D-peptide antagonist of IL-1RI, termed 101.10 (D-Arg^1-D-Tyr^2-D-Thr^3-D-Val^4-D-Glu^5-D-Leu^6-D-Ala^7-NH$_2$, rytvela-NH$_2$, small letters represent amino acids of D-stereochemistry), which displayed key features of an allosteric modulator and efficacy in models of acute inflammation.[68]
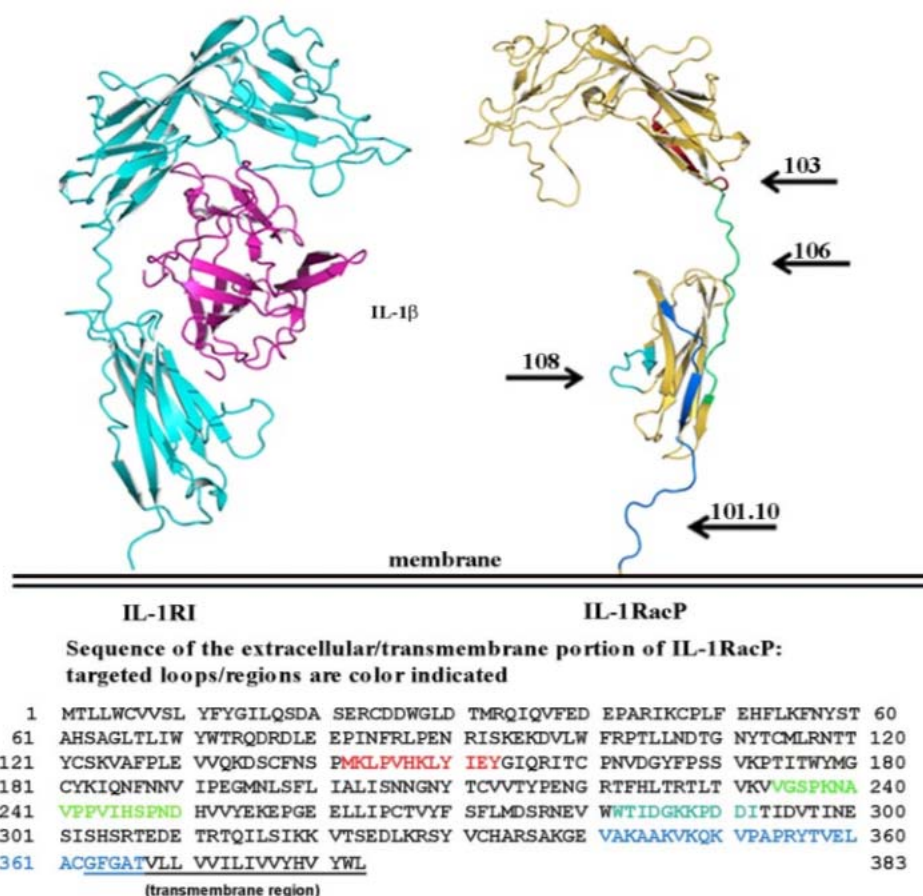
Figure 1.1. Ribbon-like model of IL-1RI/IL-1β/IL-1RAcP complex and primary sequence of the extracellular portion of IL-1RAcP. (Colored sequences refer to regions that were used to derive interface peptides) (Figure copied with publisher permission from ref. 68)

The peptides were tested for ability to modulate IL-1β-stimulated prostaglandin E2 (PGE2) production. Among the candidates exhibiting promising activity, a peptide (101, aprytvela-NH$_2$) was initially identified based on the juxta-membrane flexible loop of the accessory protein. Successive D-alanine scans, in which each D-amino acid is systematically replaced by D-alanine, and *N*-terminal truncation to shorten the sequence were conducted, and the resulting analogs were examined for activity against IL-1β-triggered proliferation of endothelial cells and phosphorylation of downstream effectors: e.g., p38 mitogen-activated protein kinases (p-38) and mitogen-activated protein kinase (MAPK) and inhibitor of kappa B kinase (IκB).[69-70] The D-heptapeptide 101.10 was shown by this method to exhibit efficacy and potency in a broad variety of *in vitro* IL1β-dependent assays, including thymocyte cell proliferation (IC$_{50}$ = 0.2 nM).[68]

In a displacement assay using radio labelled peptide, 101.10 proved to be a noncompetitive inhibitor of IL-1β binding and activity.[68] The modulatory effects of 101.10 were also shown to be selective for IL-1β without influencing activity of homologous cytokines of the IL-1 family; 101.10 exhibited no effect on IL-18-induced tumor necrosis factor (TNF-α)- and lipopolysaccharide (LPS)-dependent c-Jun *N*-terminal kinase (JNK) and p38 phosphorylation, nor IL-6-induced extracellular signal-regulated kinase (Erk1/2) phosphorylation. Moreover, 101.10 failed to bind to IL-1RI-deficient cells and was ineffective *in vivo* in IL1RI-knockout mice in a variety of assays, including IL-1-induced IL-6 and E-selectin expression and IL-1-induced fever, indicating that 101.10 binds selectively to IL-1RI.[68] The *in vivo* efficacy of 101.10 was subsequently demonstrated in animal models of hyperthermia, hypotension, inflammatory bowel disease and contact dermatitis.[68]

The efficacy of 101.10 as a modulator of IL-1R was applied to delay labor in a murine model of induced PTB using IL-1β, lipoteichoic acid (LTA, a TLR2 ligand), and LPS (a TLR4 ligand). The peptide 101.10 exhibited functional selectivity and inhibited IL-1–triggered stress-activated pathway kinase/c-jun (SAPK/c-jun) and Rho/Rho-associated coiled-coil containing protein kinase (Rho/ROCK) pathways, without affecting NF-κB activity. The resulting biased signaling pattern differs from that of the corresponding endogenous ligand and offers a novel means for delaying labor without compromising immune vigilence.[71] Moreover, 101.10 preserved vascular beds and decreased the detrimental angiogenesis associated with ischemic retinopathies such a ROP.[46]

1.7 Relationships between 101.10 activity and peptide conformation

The lead peptide 101.10 is a biopolymer possessing a primary structure consisting of a series of amino acids linked by amide bonds. The amino acid side chains of 101.10 influence the properties and folding of the peptide. Unlike longer sequences, which may exhibit particular low energy folded secondary structures (e.g., helical, sheet and turn), the circular dichroism (CD) spectrum of 101.10 exhibits a curve shape indicative of a random coil.[72-73] Although 101.10 is an attractive lead for developing treatments of inflammatory diseases with the advantages of having low toxicity and excellent activity, the peptide is rapidly cleared after administration, and has limited bioavailability. The pharmacokinetic properties of 101.10 may be linked to conformational flexibility which enables interaction with parasitic receptors involved in metabolism and clearance.

Understanding of the conformers by which 101.10 exhibits desirable biological activities would prove useful for the development of improved modulators of IL-1 activity. Identification and stabilization of the active conformation may enhance activity and avoid side effects that come from alternative conformations of 101.10. To study the active conformers of 101.10 different strategies may be used to limit the flexibility of the peptide sequence.[73-75] In the context of this thesis, successful examination of the active conformation of 101.10 has been achieved using lactam analogs as a form of covalent constraint.

1.8   Application of covalent constraint to study peptide conformation

The random coil CD spectrum of 101.10 is likely indicative of a peptide in dynamic equilibrium between multiple conformers of similar energy. Considering that certain conformers of 101.10 may be responsible for desired biological activity and others may exhibit off-target effects, efforts have been made to use covalent constraint to limit the flexibility of 101.10 to identify active conformations. In principle, covalent constraint may enhance receptor binding affinity by pre-organizing 101.10 into an active conformer and removing the entropic costs for folding. Moreover, such constraint may improve target specificity, enhance cell permeability and increase metabolic stability.

Among strategies that have been employed to generate peptides with reduced flexibility, the use of lactam heterocycles has had significant success since the early 1980s, when researchers at Merck Inc. led by R. Hirschmann, R. Freidinger and D. Veber made an analog of luteinizing hormone releasing hormone (LHRH, **1.1** Glu-His-Trp-Ser-Tyr-Gly-Leu-Arg-Pro-Gly-NH$_2$) in which glycine was replaced by an α-amino γ-lactam (Agl) residue (Figure 1.2). Relative to the parent peptide, the constrained LHRH analog, **1.2**, exhibited an 8.9 fold enhancement in potency, which was suggested to be due to the Agl constraint favoring a *β*-turn conformation.[76-77]
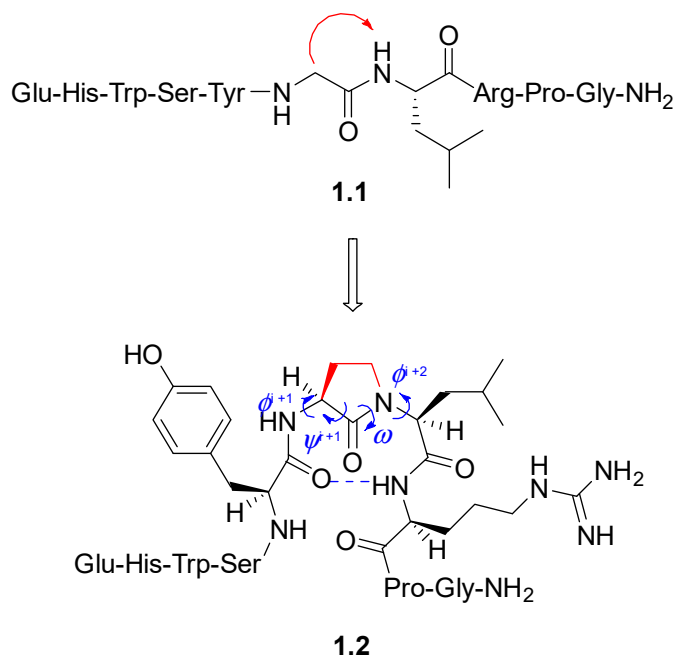
1.1

1.2

Figure 1.2. Constraining LHRH with insertion of Agl residue

The insertion of an Agl residue into a linear peptide sequence restricts rotation of the ψ dihedral angle about the N-C$^\alpha$-C-N bond within the lactam ring to a value around 120°.[78-79] The mobility about the ω dihedral angle (C$^\alpha$-C$^{c=o}$-N-C$^\alpha$) of the amide bond shared between the Agl and *C*-terminal residues is also locked within the lactam ring to the *Z-trans* geometry (180°). Moreover, steric interactions between the lactam ring and the *N*-terminal amide and *C*-terminal residue side chain and carboxylate limit the degrees of conformational freedom about their respective ϕ (C$^{c=o}$-N-C$^\alpha$-C$^{c=o}$) dihedral angles. The combination of the covalent and steric constraints can stabilize respectively type II' and II β-turn structures for L,L- and D,D-Agl-Xaa dipeptides (Xaa represents an α-amino acid residue).[76]

In the study of LHRH, the Agl-Leu dipeptide was designed by replacing the pro-*S*-hydrogen atom of Gly and *N*$^\alpha$-hydrogen of Leu with an ethylene bridge. The synthesis of the Agl-Leu dipeptide was performed in solution starting with *N*-Boc-methionyl-leucine methyl ester **1.4**. Alkylation of thioether **1.4** with methyl iodide gave sulfonium salt **1.5**, which upon treatment with sodium hydride in a mixture of DCM and DMF underwent a regioselective lactam formation to provide *N*-Boc-Agl-Leu-OMe **1.3** with expulsion of dimethyl sulfide (Scheme 1.1).[80] After ester

saponification, Boc-Agl-Leu-OH was inserted into the LHRH peptide sequence using solid-phase chemistry.[76]
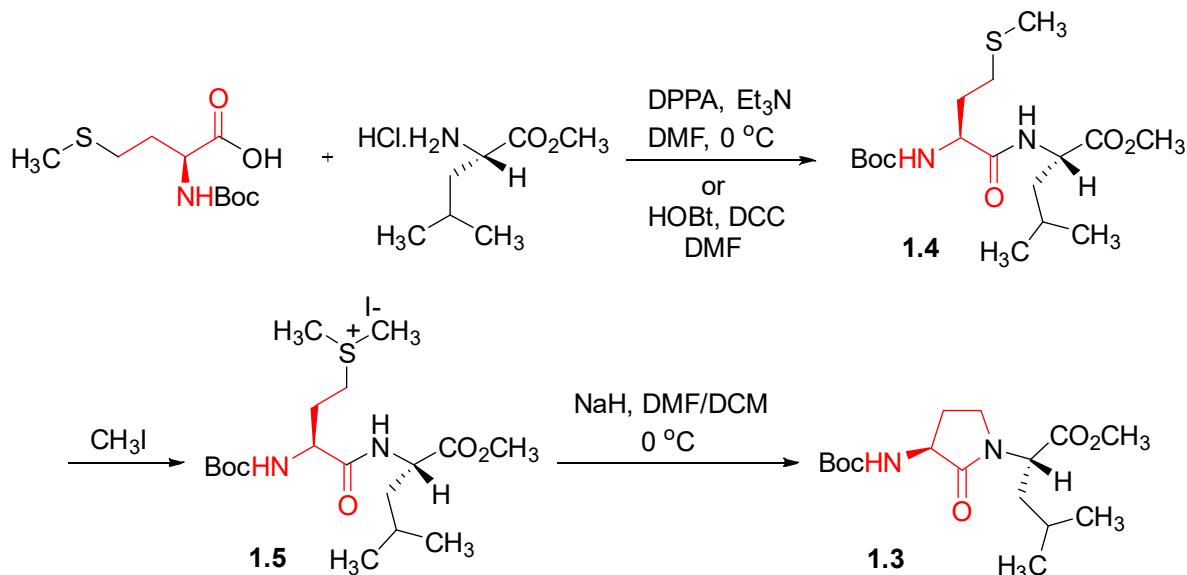
Scheme 1.1. Synthesis of Boc-Agl-Leu-OMe **1.3**

1.9 Application of lactam constraints to study 101.10

A method for the systematic replacement of each residue in a peptide by an Agl residue was developed employing solid-phase chemistry and used to study 101.10.[81] In this method, six-membered cyclic sulfamidate, (4*R*)-benzyl 2,2-dioxo-3-*N*-Fmoc-1,2,3-oxathiazinane-4-carboxylate **1.6** undergoes regioselective ring opening with an amine nucleophile and the resulting γ-amino ester is subsequently converted to the lactam by microwave irradiation. For example, employing H-Trp-OMe in solution Fmoc-Agl-Trp-OMe **1.7** was synthesized in 54% overall yield (Scheme 1.2).

Cyclic sulfamidate **1.6** was synthesized starting from L-methionine. L-Homoserine **1.8** was prepared form L-methionine by *S*-alkylation followed by pH controlled intramolecular displacement to form homoserine lactone and subsequent hydrolytic ring opening. Nitrogen and carboxylate protection gave *N*-Fmoc-homoserine benzyl ester **1.9**, which was first converted to a 4:1 mixture of cyclic sulfamidite diastereomers **1.10** using thionyl chloride and imidazole in THF. Subsequent oxidation using catalytic ruthenium (III) trichloride hydrate and sodium metaperiodate gave cyclic sulfamidate **1.6**.
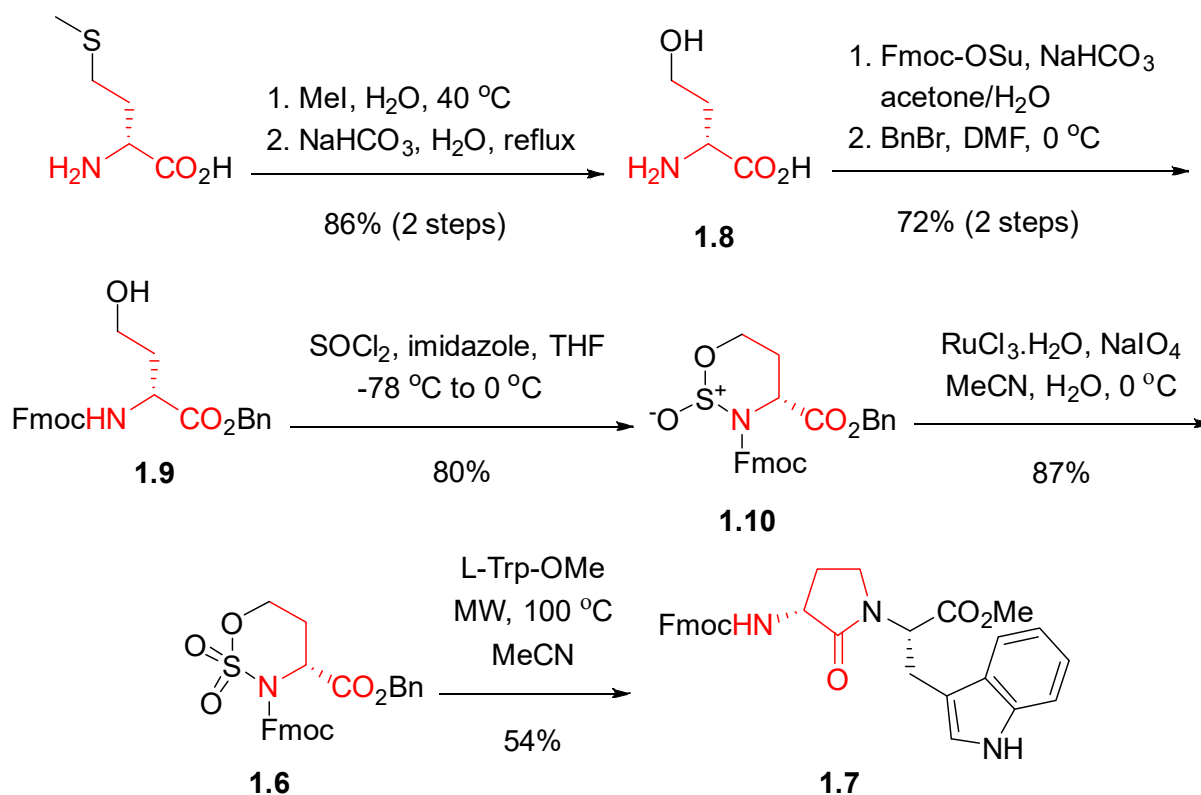
Scheme 1.2. Solution phase synthesis of lactam dipeptide **1.7**

Systematic incorporation of an Agl residue for each amino acid in the peptides was achieved by introducing a lactam formation sequence into the standard solid-phase Fmoc-based peptide synthesis protocol on Rink amide resin (Scheme 1.3). After peptide elongation, the *N*-terminal amine was initially reacted with sulfamidate **1.6**; however, due to bis-alkylation low amounts of the desired product were observed. To address this issue, a temporary silyl protection strategy was developed in which the amine was treated with *N,O*-bis(trimethylsilyl)acetamide (BSA). After silylation, secondary amine **1.11** was alkylated selectively with sulfamidate **1.6**, and silyl group removal by washing the resin with methanol to afford γ-amino ester **1.12**. As illustrated by the synthesis of [(*R*)-Agl⁴]-101.10, lactam **1.13** was next formed by heating secondary amine resin **1.12** by microwave irradiation at 100 °C in DMF (Scheme 1.3). Subsequent, removal of the Fmoc group, peptide elongation and resin cleavage gave [(*R*)-Agl⁴]-101.10 **1.14** after purification by HPLC.
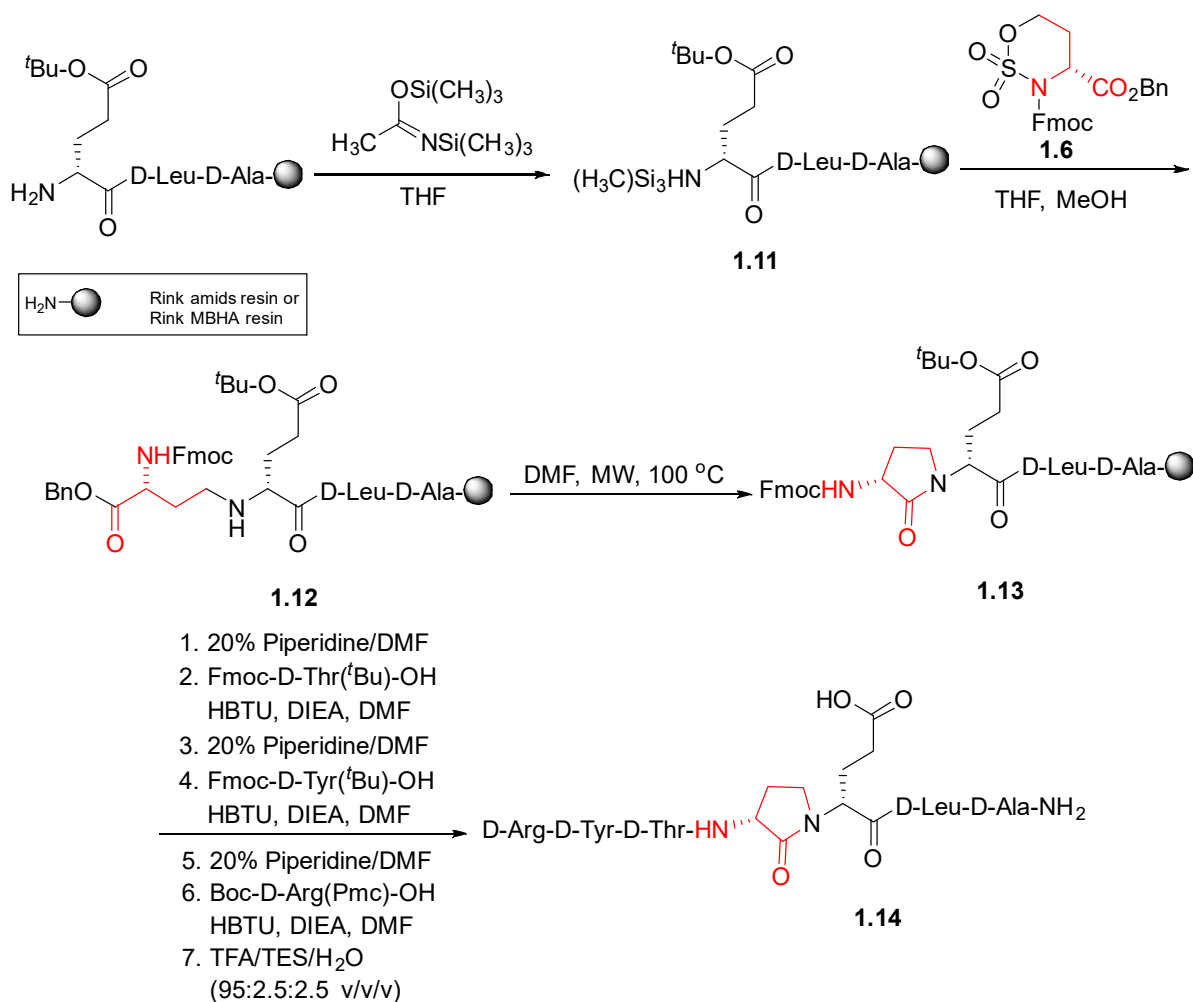
Scheme 1.3. Solid-phase synthesis of [(R)-Agl[4]]-101.10 **1.14** using cyclic sulfamidate **1.6**

Six *R*-Agl analogs were respectively prepared by using the above method to study 101.10. The Agl analogs were assessed for ability to inhibit IL-1β-induced human TF-1 thymocyte cell proliferation (Figure 1.3). The natural rate of thymocyte cell reproduction (control, 100%) increases in the presence of the pro-inflammatory agent IL-β (IL-1, 140%). In the presence of 101.10, the increased rate of IL-β-induced thymocyte cell proliferation can be restored to normal (101.10, 100%). Four of the analogs with *R*-Agl respectively at the 2, 4, 5 and 6-positions of 101.10 [tyr (y), val (v), glu (e), leu (l)], all maintained a similar inhibitory effect as the parent peptide on thymocyte cell proliferation. Moreover, [(R)-Agl[1]]-101.10 [arg (r)] exhibited improved inhibitory potency. On the other hand, [(R)-Agl[3]]-101.10 [thr (t)] was significantly less effective than the parent peptide at blocking IL-1β-induced thymocyte cell proliferation. The latter result indicated

that the side chain function and the conformations of the backbone and side chain around the thr residue, all were important for peptide activity.[81]

101.10   D-Arg-D-Tyr-D-Thr-D-Val-D-Glu-D-Leu-D-Ala

r   **(R)-Agl**-D-Tyr-D-Thr-D-Val-D-Glu-D-Leu-D-Ala

y   D-Arg-**(R)-Agl**-D-Thr-D-Val-D-Glu-D-Leu-D-Ala

t   D-Arg-D-Tyr-**(R)-Agl**-D-Val-D-Glu-D-Leu-D-Ala

v   D-Arg-D-Tyr-D-Thr-**(R)-Agl**-D-Glu-D-Leu-D-Ala

e   D-Arg-D-Tyr-D-Thr-D-Val-**(R)-Agl**-D-Leu-D-Ala

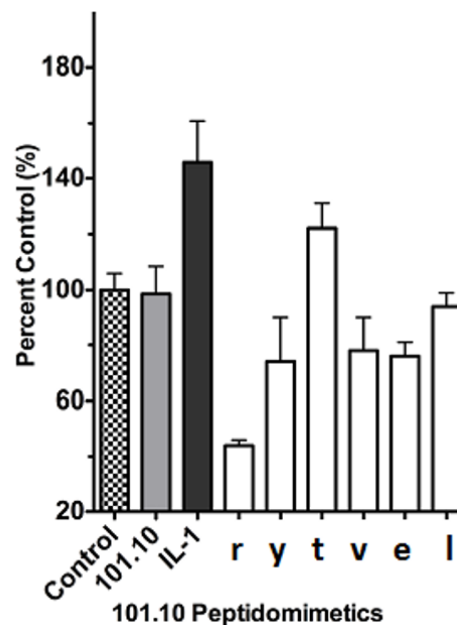**l**   D-Arg-D-Tyr-D-Thr-D-Val-D-Glu-**(R)-Agl**-D-Ala

Figure 1.3. (R)-Agl-101.10 analog inhibition of IL-1-induced human TF-1 thymocyte cell proliferation.

β-Amino γ-lactam (Bgl) residues have also been suggested to stabilize β-turn-like conformations in peptides.[73, 81] Although less frequently used to study peptide conformation, replacement of aspartate by S-Bgl in a fragment of human growth hormone (hGH) conserved insulin potentiating and hypoglycemic activities and extended the duration of action.[82-83] Effective methods for installing Bgl residues into peptides were developed using related cyclic sulfamidate chemistry and employed to study the conformation and biological activity of 101.10. Twelve Bgl analogs of 101.10 were synthesized using a similar alkylation–lactam formation sequence on solid-phase employing (R)- and (S)-cyclic sulfamidates (R)- and (S)-**1.15**, which were derived from L- and D-aspartic acid (Scheme 1.4). Examination of the inhibitory effect of the Bgl analogs on IL-1β-induced thymocyte cell proliferation using a fluorescence assay exhibited that only (S)-Bgl[4]-101.10 had better inhibitory effect than parent peptide indicating that a turn conformation at the center of the peptide may be a determinant for activity.
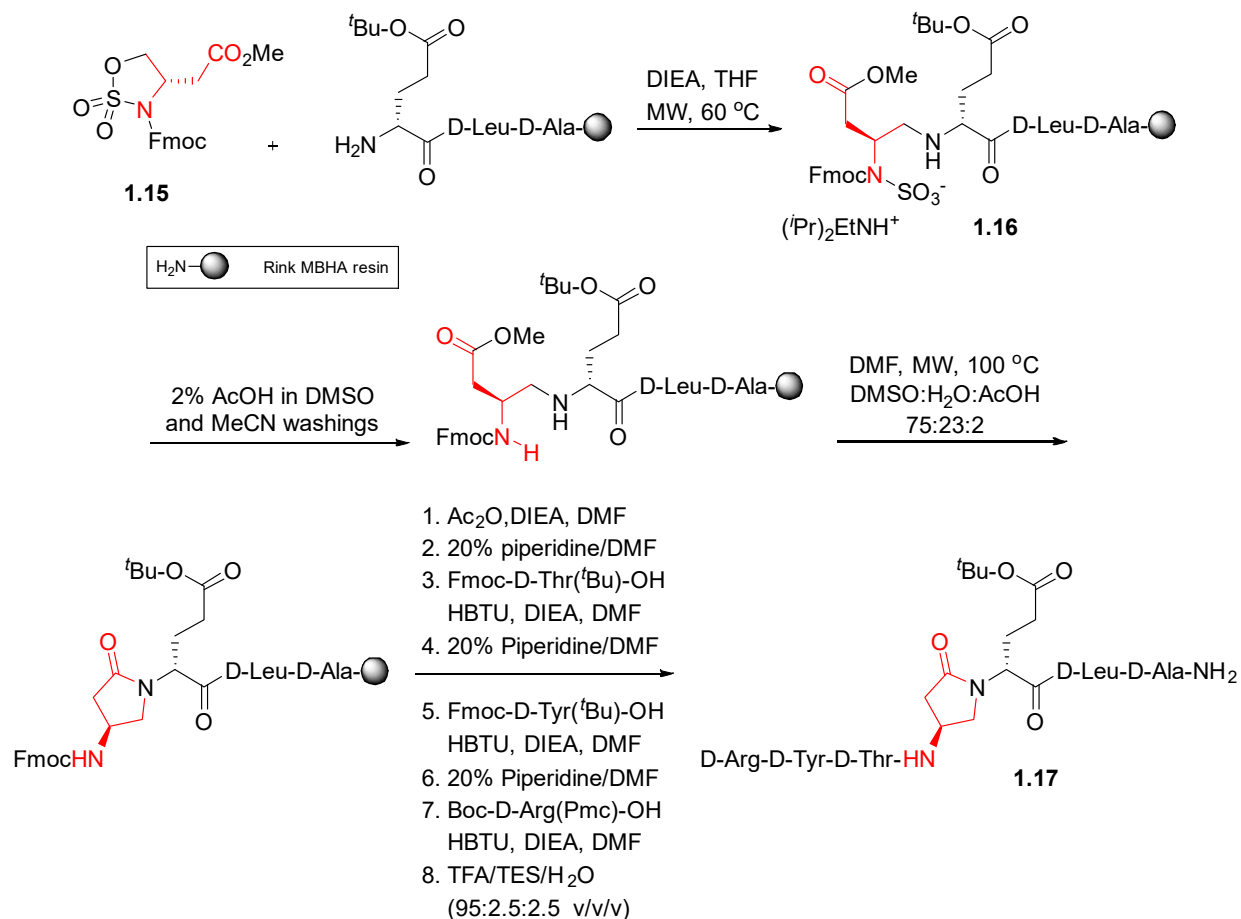
Scheme 1.4. Solid-phase synthesis of $[(S)\text{-Bgl}^4]$-101.10 **1.17** using cyclic sulfamidate **1.15**

1.10   β-Substituted α-Amino Lactams

Although Agl and Bgl residues can constrain the peptide backbone to induce specific secondary structures such as β-turn conformations, replacement of certain amino acids by such lactam constraints removes the side chain functionality, which may be important for biological activity. In such cases, the ability to add substituents to the β-position of the Agl residue could provide tools to study both the relevance and orientation of the side chain function. In the pursuit of β-substituted Agl residues, several approaches have been pursued and will be discussed further in Chapter 3.

Introduction of (R)-Agl residues into 101.10 gave typically analogs exhibiting similar and improved inhibitory potency in the IL-1β-induced thymocyte cell proliferation assay. On the other hand, replacement of D-threonine by (R)-Agl gave an analog with lower potency than 101.10

suggesting that the hydroxyl side chain may play an important role in activity of this peptide (Figure 1.3). β-Hydroxy-α-amino-γ-lactam (Hgl) residues were conceived to function as constrained threonine analogs for rigidifying both backbone and side chain dihedral angles.[81] Serine and threonine play important roles in peptide activity and secondary structure. For example, the phosphorylation and glycosylation of the β-hydroxyl group of these amino acid residues in proteins is vital for cellular signaling and function.[84-85] Notably, such post-translational modifications occur often on Ser and Thr residues at turn conformations.[86] Moreover, hydrogen bonding to the side-chain hydroxyl group may stabilize peptide secondary structure and interactions with receptors. Constrained Ser and Thr analogs are attractive targets for exploring the impact of their conformation on peptide biology. For example, 3-hydroxyproline may mimic a Ser or Thr residue with a constrained ϕ- and χ-dihedral angles.[87]

The synthesis and insertion of Hgl residues for D-threonine in 101.10 was thus pursued to explore the relevance of the alcohol function and orientation for activity. The solution-phase synthesis and purification of Fmoc-Hgl-Val-OMe dipeptide **1.17** from (2S,2$'S$)-N-(Fmoc)-oxiranylglycine methyl ester **1.18** and L-valine methyl ester was facilitated using a combination of trifluoroethanol (TFE) for epoxide ring opening and catalytic benzoic acid for γ-lactam formation. (Scheme 1.5)
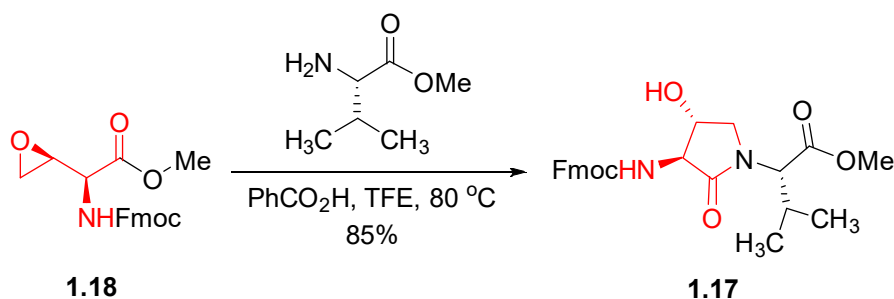
Scheme 1.5. Synthesis of Fmoc-(S)-Hgl-(S)-Val **1.17**

After saponification, lactam dipeptide **1.17** could be introduced into 101.10 peptide through a modular approach. Alternatively, the Hgl residue was incorporated into the sequence of 101.10 by a solid-phase approach featuring alkylation of the vela peptide amide linked to Synphase™ lantern **1.19** using (2S,2$'S$) oxiranyl glycine **1.18**, and lactam formation.[75] Subsequent peptide elongation, lantern cleavage, and purification by HPLC provided [(3S,4R)-Hgl³]-101.10 (**1.20**, Scheme 1.6).[75]
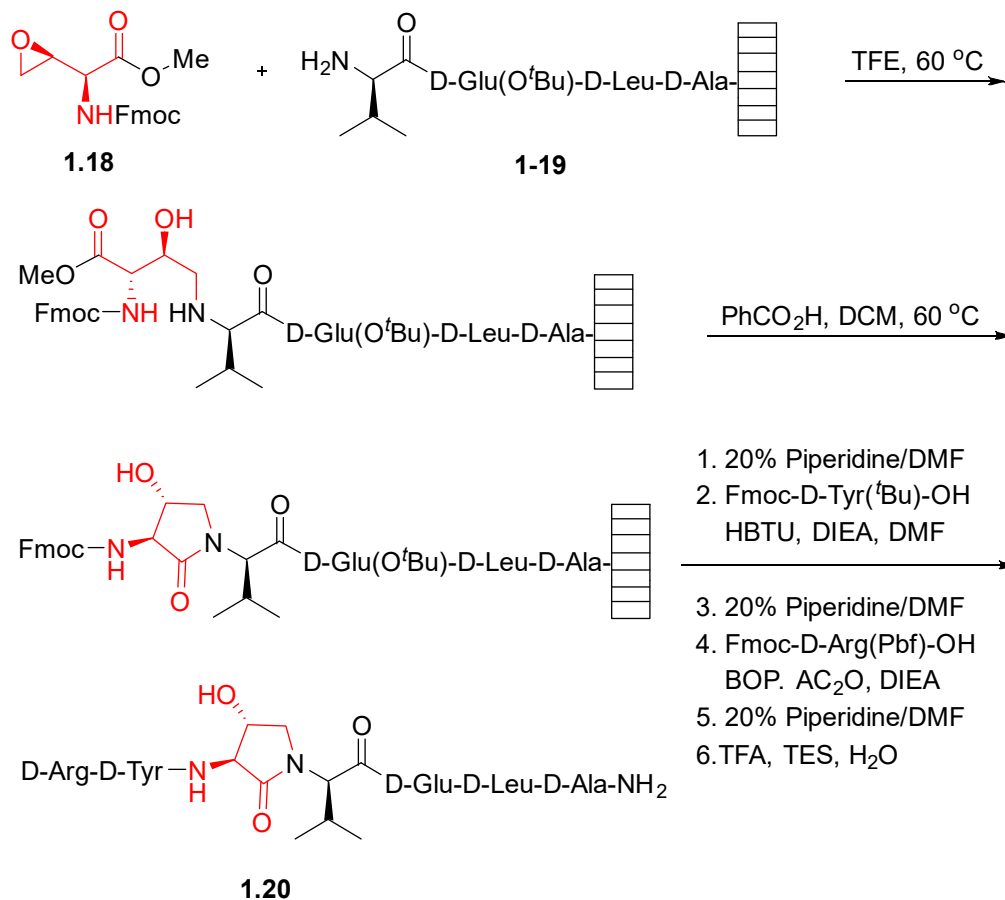
Scheme 1.6. Synthesis of Hgl peptide [(3S,4R)-Hgl^3]-101.10 **1.20**

1.11 Thesis aims

Towards development of novel tocolytic agents that can prevent PTB and improve neonatal outcomes, the all D-peptide 101.10 offers notable promise for prolonging labor and mitigating ROP in murine models. Knowledge of the active conformation and improvement of pharmacokinetic properties of 101.10 may lead the way to first in-kind therapy. Earlier research using lactams as covalent constraint to study the conformation of 101.10 has provided analogs exhibiting similar and improved properties compared with the parent peptide probably because of induced secondary structures that facilitate receptor recognition and enhance peptide biological activity.[81] On the other hand, the relevance of the conformation and hydroxyl group of the D-threonine residue for the activity of 101.10 were brought to light through such study using [(R)-Agl^3]-101.10. Propelled by the conception of the β-hydroxy-α-amino-γ-lactam (Hgl) residues and

potential for their insertion at the 3-position of 101.10, this thesis has performed a detailed study to understand the relevance of this central residue to the allosteric mechanism of the parent peptide.

The aims of this thesis have been two-fold. In the first place, a systematic study has explored the importance of the conformation and hydroxyl group of the D-threonine residue in 101.10 for biological activity. Considering the utility of Hgl residues in the latter study, strategies were next pursued to access a variety of β-substituted α-amino-γ-lactams from a common precursor. Finally, a library of β-substituted Agl^3-101.10 analogs was prepared to study in more detail the importance of the side chain function for activity in delaying labor and diminishing vaso-obliteration in models of PTB and ROP. Note, the biological analyses were performed in collaboration with the laboratory of Professor Chemtob.

In chapter 2, all stereoisomers of Agl^3-Val^4- and Hgl^3-Val^4-101.10 were synthesized to study the importance of the β-hydroxyl group of D-Thr^3, and the backbone and side chain orientations of 101.10 for biological activity. Employing a modified approach related to that developed by Freidinger, D- and L-methionine and valine were combined to prepare four diastereomers of Fmoc-Agl-Val-OH.[76] Employing oxiranyl glycine and D- and L-valine,[75] eight diastereomers of Fmoc-Hgl-Val-OH were synthesized.[72] Considering that the epoxidation of vinyl glycine provided a major oxiranyl glycine isomer suitable for preparing *trans*-Hgl isomers, a novel route was developed to prepared the *cis*-Hgl diastereomers featuring Mitsonubo chemistry to invert the configuration of the hydroxyl group of the *trans*-Hgl residue. The twelve stereoisomers of H-Agl- and H-Hgl-Val-OH were introduced into 101.10 using a solid-phase approach and the biological activity of the isomers were examined using various *in vitro* and *in vivo* assays.

In RAW- and HEK-blue cells, the activity of the lactam analogs was examined after stimulation with IL-1β by measuring influences on kinases phosphorylation using Western blot assays for JNK, p-38 and ROCK2 kinase. The influences of the lactam analogs on the expression of IL-6, cyclooxygenase-2 (COX2) and IL-1β were examined using quantitative polymerase chain reaction assays (qPCR). Finally, lactam influence on NF-☐B was ascertained using a QUANTI-blue reported assay. Finally, the analogs were assessed *in vivo* in LPS-induced mouse models of PTB and ROP. Note, the biological analyses were performed in collaboration with the laboratory of Professor Chemtob.

In chapter 3, methods to prepare β-substituted lactams were conceived. In the first method, the utility of the Mitsunobu reaction on the *trans*-Hgl diastereomer was further put to use to make

a series of β-substituted *cis*-Agl-Val dipeptides. On the other hand, the Mitsunobu chemistry on the *cis*-Hgl diastereomer failed to give β-substituted *trans*-Agl-Val dipeptides due to β-elimination. Considering that the *anti*-orientation between the pseudo axial β-hydroxyl group and α-proton favored β-elimination, the amine and alcohol groups in the *cis*-Hgl isomer were tied into a cyclic sulfamidate to both activate the alcohol for nucleophilic displacement and to avoid the undesired geometry. Nucleophilic ring opening of the cyclic sulfamidate derived from *cis*-Hgl dipeptide gave access to β-substituted *trans*-Agl-Val dipeptides. The combination of the two methods have furnished a set of constrained dipeptide mimics possessing Ser, Thr, Cys, Dap, Dab, and His residues.[88]

In chapter 4, a combination of knowledge of the bioactive conformation of 101.10 from the study of $[(3R,4S)\text{-Hgl}^3]$-101.10 in chapter 2 and methods for the synthesis of β-substituted-Agl analogs presented in chapter 3 has been used to create a set of β-substituted-Agl^3-101.10 analogs. A variety of β-substituted-Agl^3 analogs of 101.10 have been synthesized by a combination of solution- and solid-phase methods employing *N*-Fmoc-β-substituted-Agl^3-Val-OH dipeptide building blocks. Introduction of a β-azido-Agl^3 residue into the resin bound peptide and subsequent reduction and CuAAC chemistry gave access to a series of amine and triazole derivatives. The β-substituted-Agl^3 analogs of 101.10 have been tested using similar *in vitro* and *in vivo* assays as described in chapter 2 to evaluate both their mechanism and potential for delaying preterm labor and mitigating retinopathy of prematurity.

1.12   Conclusion

The conception of novel methods for the synthesis and application of β-substituted α-amino γ-lactam residues has provided effective means to apply covalent constraint to study the relevance of side chain function and the conformation of the backbone and side chain of biologically active peptides. Employing such methods, libraries of β-substituted α-amino γ-lactam analogs of the peptide 101.10 were synthesized and used to study the structural requirements for its inhibitory activity on IL-1β-induced pro-inflammatory signaling. Without inhibiting NF-κB, the lactam analogs exhibited a range of biased inhibitory effects on other IL-1-activated pathways. Immune vigilance was thus preserved by the lactam analogs which do not block activation of the NF-κB pathway. Their varying influences on different kinases has provided a toolkit to study the relevance

of such signaling in inflammatory responses of various indications involving chronic inflammation.

Among the constrained Agl and Hgl analogs, [(3*R*,4*S*)-Hgl^3]-101.10 exhibited the same activity as the parent peptide in the *in vitro* and *in vivo* assays indicating the significance of the threonine alcohol and *β*-turn conformer for the biological activity of the parent peptide. Among the β-substituted-Agl analogs, the β-(phenyl)triazole and β-thiocyanate-Agl analogs appear to exhibit activity superior to the parent peptide *in vitro* and *in vivo* assays providing novel lead structures for the further development of pro-inflammatory modulators. Overall, information gleaned from the study of the structure-activity relationships of the lactam analogs of 101.10 has provided significant understanding of the requirements for modulator activity, as well as promising leads for the development of therapeutic agents to delay labor and improve neonatal outcomes. The synthetic methods developed in this thesis may thus have significant impact in the study of biologically active peptides for various applications.

1.13   References

1.   Liu, L.; Johnson, H. L.; Cousens, S.; Perin, J.; Scott, S.; Lawn, J. E.; Rudan, I.; Campbell, H.; Cibulskis, R.; Li, M., Global, regional, and national causes of child mortality: an updated systematic analysis for 2010 with time trends since 2000. *The Lancet* **2012,** *379*, 2151-2161.

2.   Hamilton, B. E.; Hoyert, D. L.; Martin, J. A.; Strobino, D. M.; Guyer, B., Annual summary of vital statistics: 2010–2011. *Pediatrics* **2013,** *131*, 548-558.

3.   Zupancic, J. A., Burdens beyond biology for sick newborn infants and their families. *Clinics in perinatology* **2018,** *45*, 557-563.

4.   Mathews, T.; MacDorman, M. F., Infant mortality statistics from the 2006 period linked birth/infant death data set. *National Vital Statistics Reports: From the Centers for Disease Control and Prevention, National Center for Health Statistics, National Vital Statistics System* **2010,** *58* , 1-31.

5.   Hamilton, B. E.; Hoyert, D. L.; Martin, J. A.; Strobino, D. M.; Guyer, B., Annual summary of vital statistics: 2010–2011. *Pediatrics* **2013,** *131*, 548-558.

6.   Blencowe, H.; Cousens, S.; Chou, D.; Oestergaard, M.; Say, L.; Moller, A.-B.; Kinney, M.; Lawn, J., Born too soon: the global epidemiology of 15 million preterm births. *Reproductive health* **2013,** *10*, S2.

7.   Mathews, T.; MacDorman, M. F.; Thoma, M. E., Infant mortality statistics from the 2013 period linked birth/infant death data set. **2015**.

8.   Russell, R. B.; Green, N. S.; Steiner, C. A.; Meikle, S.; Howse, J. L.; Poschman, K.; Dias, T.; Potetz, L.; Davidoff, M. J.; Damus, K., Cost of hospitalization for preterm and low birth weight infants in the United States. *Pediatrics* **2007**, *120*, e1-e9.

9.   Behrman, R. E.; Butler, A. S., Biological pathways leading to preterm birth. In *Preterm Birth: Causes, Consequences, and Prevention*, National Academies Press (US): **2007**.

10.   Lee, J. Y.; Shin, N. E.; Na, Q.; Dong, J.; Chudnovets, A.; Li, S.; Novak, C. M.; McLane, M. W.; Lei, J.; Burd, I., Exposure to systemic and intrauterine inflammation leads to decreased pup survival via different placental mechanisms. *J. Reprod. Immunol.* **2019**.

11.   Rinaldi, S. F.; Hutchinson, J. L.; Rossi, A. G.; Norman, J. E., Anti-inflammatory mediators as physiological and pharmacological regulators of parturition. *Expert Rev. Clin. Immunol.* **2011,** *7*, 675-696.

12.   Xu, C.; Long, A.; Fang, X.; Wood, S. L.; Slater, D. M.; Ni, X.; Olson, D. M., Effects of PGF2α on the expression of uterine activation proteins in pregnant human myometrial cells from upper and lower segment. *J. Clin. Endocrinol. Metab.* **2013,** *98*, 2975-2983.

13.   Koga, K.; Mor, G., Toll-like receptors at the maternal–fetal interface in normal pregnancy and pregnancy disorders. *Am. J. Reprod. Immunol.* **2010,** *63*, 587-600.

14.   Chow, P. P.; Yip, W. W.; Ho, M.; Lok, J. Y.; Lau, H. H.; Young, A. L., Trends in the incidence of retinopathy of prematurity over a 10-year period. *International ophthalmology* **2019,** *39*, 903-909.

15.   Hartnett, M. E.; Lane, R. H., Effects of oxygen on the development and severity of retinopathy of prematurity. *Journal of American Association for Pediatric Ophthalmology and Strabismus* **2013,** *17*, 229-234.

16.   Lambert, S. R.; Lyons, C. J., *Taylor and Hoyt's Pediatric Ophthalmology and Strabismus E-Book*. Elsevier Health Sciences: **2016**.

17.   Stenson, B. J.; Tarnow-Mordi, W. O.; Darlow, B. A.; Simes, J.; Juszczak, E.; Askie, L.; Battin, M.; Bowler, U.; Broadbent, R.; Cairns, P., Oxygen saturation and outcomes in preterm infants. *N. Engl. J. Med.* **2013,** *368*, 2094-2104.

18.   Obstetricians, A. C. o.; Gynecologists, Practice Bulletin No. 171: Management of preterm labor. *Obstet. Gynecol.* **2016,** *128*, e155.

19.	Hanley, M.; Sayres, L.; Reiff, E. S.; Wood, A.; Grotegut, C. A.; Kuller, J. A., Tocolysis: A review of the literature. *Obstet. Gynecol. Surv.* **2019,** *74*, 50-55.

20.	Reinebrant, H. E.; Pileggi-Castro, C.; Romero, C. L.; dos Santos, R. A.; Kumar, S.; Souza, J. P.; Flenady, V., Cyclo-oxygenase (COX) inhibitors for treating preterm labour. *Cochrane database of systematic reviews* **2015,** 1-83.

21.	Conde-Agudelo, A.; Romero, R.; Kusanovic, J. P., Nifedipine in the management of preterm labor: a systematic review and metaanalysis. *Am. J. Obstet. Gynecol.* **2011,** *204*, 134. e1-134. e20.

22.	Arrowsmith, S.; Kendrick, A.; Wray, S., Drugs acting on the pregnant uterus. *Obstetrics, Gynaecology & Reproductive Medicine* **2010,** *20*, 241-247.

23.	Antonucci, R.; Zaffanello, M.; Puxeddu, E.; Porcella, A.; Cuzzolin, L.; Dolores Pilloni, M.; Fanos, V., Use of non-steroidal anti-inflammatory drugs in pregnancy: impact on the fetus and newborn. *Current drug metabolism* **2012,** *13*, 474-490.

24.	Goldenberg, R. L., The management of preterm labor. *Obstetrics & Gynecology* **2002,** *100* , 1020-1037.

25.	Stoiber, B.; Haslinger, C.; Schäffer, M. K.; Zimmermann, R.; Schäffer, L., Effect of dual tocolysis with fenoterol and atosiban in human myometrium. *Journal of perinatal medicine* **2019,** *47*, 190-194.

26.	Sanchez-Ramos, L.; Kaunitz, A. M.; Gaudier, F. L.; Delke, I., Efficacy of maintenance therapy after acute tocolysis: a meta-analysis. *Am. J. Obstet. Gynecol.* **1999,** *181*, 484-490.

27.	Pitzer, M.; Schmidt, M. H.; Esser, G.; Laucht, M., Child development after maternal tocolysis with beta-sympathomimetic drugs. *Child Psychiatry Hum. Dev.* **2001,** *31* , 165-182.

28.	Perna, R.; Loughan, A.; Perkey, H.; Tyson, K., Terbutaline and associated risks for neurodevelopmental disorders. *Child Development Research* **2014,** *2014*.

29.	Caritis, S., Adverse effects of tocolytic therapy. *BJOG: An International Journal of Obstetrics & Gynaecology* **2005,** *112*, 74-78.

30.	Nightingale, S. L., Warning on use of terbutaline sulfate for preterm labor. *JAMA* **1998,** *279*, 9-9.

31.	Kemp, M. W., Preterm birth, intrauterine infection, and fetal inflammation. *Frontiers in immunology* **2014,** *5*, 574.

32.   Agrawal, V.; Hirsch, E. In *Intrauterine infection and preterm labor*, Seminars in Fetal and Neonatal Medicine, Elsevier: 2012; pp 12-19.

33.   Elovitz, M. A.; Wang, Z.; Chien, E. K.; Rychlik, D. F.; Phillippe, M., A new model for inflammation-induced preterm birth: the role of platelet-activating factor and Toll-like receptor-4. *Am. J. Pathol.* **2003,** *163*, 2103-2111.

34.   Ilievski, V.; Lu, S.-J.; Hirsch, E., Activation of toll-like receptors 2 or 3 and preterm delivery in the mouse. *Reprod. Sci.* **2007,** *14*, 315-320.

35.   Romero, R.; Brody, D. T.; Oyarzun, E.; Mazor, M.; Wu, Y. K.; Hobbins, J. C.; Durum, S. K., Infection and labor: III. Interleukin-1: A signal for the onset of parturition. *Am. J. Obstet. Gynecol.* **1989,** *160*, 1117-1123.

36.   Skogstrand, K.; Hougaard, D. M.; Schendel, D. E.; Bent, N.-P.; Sværke, C.; Thorsen, P., Association of preterm birth with sustained postnatal inflammatory response. *Obstetrics & Gynecology* **2008,** *111*, 1118-1128.

37.   Amirchaghmaghi, E.; Taghavi, S. A.; Shapouri, F.; Saeidi, S.; Rezaei, A.; Aflatoonian, R., The role of toll like receptors in pregnancy. *International journal of fertility & sterility* **2013,** *7*, 147.

38.   Fazeli, A.; Bruce, C.; Anumba, D., Characterization of Toll-like receptors in the female reproductive tract in humans. *Human Reproduction* **2005,** *20*, 1372-1378.

39.   Holmlund, U.; Cebers, G.; Dahlfors, A. R.; Sandstedt, B.; Bremme, K.; Ekström, E. S.; Scheynius, A., Expression and regulation of the pattern recognition receptors Toll-like receptor-2 and Toll-like receptor-4 in the human placenta. *Immunology* **2002,** *107*, 145-151.

40.   Kim, Y. M.; Romero, R.; Chaiworapongsa, T.; Kim, G. J.; Kim, M. R.; Kuivaniemi, H.; Tromp, G.; Espinoza, J.; Bujold, E.; Abrahams, V. M., Toll-like receptor-2 and-4 in the chorioamniotic membranes in spontaneous labor at term and in preterm parturition that are associated with chorioamnionitis. *Am. J. Obstet. Gynecol.* **2004,** *191*, 1346-1355.

41.   Akira, S.; Takeda, K.; Kaisho, T., Toll-like receptors: critical proteins linking innate and acquired immunity. *Nature immunology* **2001,** *2*, 675-680.

42.   Choi, H.-G.; Choi, S.; Back, Y. W.; Park, H.-S.; Bae, H. S.; Choi, C. H.; Kim, H.-J., Mycobacterium tuberculosis Rv2882c protein induces activation of macrophages through TLR4 and exhibits vaccine potential. *PloS one* **2016,** *11*, e0164458.

43.   Choi, K.-S.; Scorpio, D. G.; Dumler, J. S., Anaplasma phagocytophilum ligation to toll-like receptor (TLR) 2, but not to TLR4, activates macrophages for nuclear factor-κB nuclear translocation. *J. Infect. Dis.* **2004,** *189*, 1921-1925.

44.   Xu, W.-Q.; Wang, Y.-S., The role of Toll-like receptors in retinal ischemic diseases. *International journal of ophthalmology* **2016,** *9*, 1343-1351.

45.   Beaudry-Richard, A.; Nadeau-Vallée, M.; Prairie, É.; Maurice, N.; Heckel, É.; Nezhady, M.; Pundir, S.; Madaan, A.; Boudreault, A.; Hou, X., Antenatal IL-1-dependent inflammation persists postnatally and causes retinal and sub-retinal vasculopathy in progeny. *Scientific reports* **2018,** *8*, Article 11875.

46.   Rivera, J.; Sapieha, P.; Honore, J.; Hamel, D.; Quiniou, C.; Chemtob, S., A novel modulator of the IL-1 receptor prevents development of oxygen-induced retinopathy. *Investig. Ophthalmol. Vis. Sci.* **2010,** *51*, 3336-3336.

47.   Rivera, J. C.; Holm, M.; Austeng, D.; Morken, T. S.; Zhou, T. E.; Beaudry-Richard, A.; Sierra, E. M.; Dammann, O.; Chemtob, S., Retinopathy of prematurity: inflammation, choroidal degeneration, and novel promising therapeutic strategies. *J. Neuroinflammation* **2017,** *14* , 165.

48.   Tosato, G.; Jones, K., Interleukin-1 induces interleukin-6 production in peripheral blood monocytes. *Blood* **1990,** *75*, 1305-1310.

49.   Tremblay, S.; Miloudi, K.; Chaychi, S.; Favret, S.; Binet, F.; Polosa, A.; Lachapelle, P.; Chemtob, S.; Sapieha, P., Systemic inflammation perturbs developmental retinal angiogenesis and neuroretinal function. *Investig. Ophthalmol. Vis. Sci.* **2013,** *54*, 8125-8139.

50.   Zhou, T. E.; Rivera, J. C.; Bhosle, V. K.; Lahaie, I.; Shao, Z.; Tahiri, H.; Zhu, T.; Polosa, A.; Dorfman, A.; Beaudry-Richard, A., Choroidal involution is associated with a progressive degeneration of the outer retinal function in a model of retinopathy of prematurity: early role for IL-1β. *Am. J. Pathol.* **2016,** *186*, 3100-3116.

51.   Rivera, J. C.; Sitaras, N.; Noueihed, B.; Hamel, D.; Madaan, A.; Zhou, T.; Honoré, J.-C.; Quiniou, C.; Joyal, J.-S.; Hardy, P., Microglia and interleukin-1β in ischemic retinopathy elicit microvascular degeneration through neuronal semaphorin-3A. *Arter. Thromb. Vasc. Biol.* **2013,** *33*, 1881-1891.

52.   Dinarello, C. A., Interleukin-1 in the pathogenesis and treatment of inflammatory diseases. *Blood* **2011,** *117*, 3720-3732.

53.   Dinarello, C. A.; Simon, A.; Van Der Meer, J. W., Treating inflammation by blocking interleukin-1 in a broad spectrum of diseases. *Nat. Rev. Drug Discov.* **2012,** *11*, 633-652.

54.   Ramírez, J.; Cañete, J. D., Anakinra for the treatment of rheumatoid arthritis: a safety evaluation. *Expert Opin. Drug Saf.* **2018,** *17*, 727-732.

55.   Libby, P., Interleukin-1 beta as a target for atherosclerosis therapy: biological basis of CANTOS and beyond. *J. Am. Coll. Cardiol.* **2017,** *70*, 2278-2289.

56.   Ridker, P. M.; Everett, B. M.; Thuren, T.; MacFadyen, J. G.; Chang, W. H.; Ballantyne, C.; Fonseca, F.; Nicolau, J.; Koenig, W.; Anker, S. D., Antiinflammatory therapy with canakinumab for atherosclerotic disease. *New England journal of medicine* **2017,** *377*, 1119-1131.

57.   Terkeltaub, R. A.; Schumacher, H. R.; Carter, J. D.; Baraf, H. S.; Evans, R. R.; Wang, J.; King-Davis, S.; Weinstein, S. P., Rilonacept in the treatment of acute gouty arthritis: a randomized, controlled clinical trial using indomethacin as the active comparator. *Arthritis Res. Ther.* **2013,** *15*, R25.

58.   Opal, S. M.; Fisher, C. J.; Dhainaut, J.-F. A.; Vincent, J.-L.; Brase, R.; Lowry, S. F.; Sadoff, J. C.; Slotman, G. J.; Levy, H.; Balk, R. A., Confirmatory interleukin-1 receptor antagonist trial in severe sepsis: a phase III, randomized, doubleblind, placebo-controlled, multicenter trial. *Critical care medicine* **1997,** *25*, 1115-1124.

59.   Roerink, M. E.; Van der Schaaf, M. E.; Dinarello, C. A.; Knoop, H.; Van der Meer, J. W., Interleukin-1 as a mediator of fatigue in disease: a narrative review. *J. Neuroinflammation* **2017,** *14*, 16.

60.   Castro-Alcaraz, S.; Miskolci, V.; Kalasapudi, B.; Davidson, D.; Vancurova, I., NF-κB regulation in human neutrophils by nuclear IκBα: correlation to apoptosis. *J. Immunol.* **2002,** *169*, 3947-3953.

61.   Gerondakis, S.; Siebenlist, U., Roles of the NF-κB pathway in lymphocyte development and function. *Cold Spring Harbor perspectives in biology* **2010,** *2*, a000182.

62.   Lu, S.; He, X.; Ni, D.; Zhang, J., Allosteric modulator discovery: from serendipity to structure-based design. *J. Med. Chem.* **2019,** *62*, 6405-6421.

63.   Nadeau-Vallee, M.; Obari, D.; Quiniou, C.; Lubell, W. D.; Olson, D. M.; Girard, S.; Chemtob, S., A critical role of interleukin-1 in preterm labor. *Cytokine & growth factor reviews* **2016,** *28*, 37-51.

Chapter 1

64. Lau, J. L.; Dunn, M. K., Therapeutic peptides: Historical perspectives, current development trends, and future directions. *Bioorg. Med. Chem.* **2018,** *26*, 2700-2707.

65. Marshall, G. R., A hierarchical approach to peptidomimetic design. *Tetrahedron* **1993,** *49*, 3547-3558.

66. Rihakova, L.; Quiniou, C.; Hamdan, F.; Kaul, R.; Brault, S.; Hou, X.; Lahaie, I.; Sapieha, P.; Hamel, D.; Shao, Z., VRQ397 (CRAVKY): A novel noncompetitive V2 receptor antagonist. *American Journal of Physiology-Regulatory, Integrative and Comparative Physiology* **2009,** *297*, R1009-R1018.

67. Peri, K. G.; Quiniou, C.; Hou, X.; Abran, D.; Varma, D. R.; Lubell, W. D.; Chemtob, S. In *THG113: a novel selective FP antagonist that delays preterm labor*, Seminars in perinatology, Elsevier: 2002; pp 389-397.

68. Quiniou, C.; Sapieha, P.; Lahaie, I.; Hou, X.; Brault, S.; Beauchamp, M.; Leduc, M.; Rihakova, L.; Joyal, J.-S.; Nadeau, S., Development of a novel noncompetitive antagonist of IL-1 receptor. *J. Immunol.* **2008,** *180*, 6977-6987.

69. Chemtob, S.; Quiniou, C.; Lubell, W. D.; Beauchamp, M.; Hansford, K. A., Interleukin-1 receptor antagonists, compositions, and methods of treatment. US20050122989, **2005**.

70. Chemtob, S.; Quiniou, C.; Lubell, W. D.; Beauchamp, M.; Hansford, K. A., Interleukin-1 receptor antagonists, compositions, and methods of treatment. US20050122989, **2005**.

71. Nadeau-Vallée, M.; Quiniou, C.; Palacios, J.; Hou, X.; Erfani, A.; Madaan, A.; Sanchez, M.; Leimert, K.; Boudreault, A.; Duhamel, F., Novel noncompetitive IL-1 receptor–biased ligand prevents infection-and inflammation-induced preterm birth. *J. Immunol.* **2015,** *195*, 3402-3415.

72. Geranurimi, A.; Cheng, C. W.; Quiniou, C.; Zhu, T.; Hou, X.; Rivera, J. C.; St-Cyr, D. J.; Beauregard, K.; Bernard-Gauthier, V.; Chemtob, S., Probing Anti-inflammatory Properties Independent of NF-κB Through Conformational Constraint of Peptide-Based Interleukin-1 Receptor Biased Ligands. *Frontiers in chemistry* **2019,** *7*, Article 23.

73. Boutard, N.; Turcotte, S.; Beauregard, K.; Quiniou, C.; Chemtob, S.; Lubell, W. D., Examination of the active secondary structure of the peptide 101.10, an allosteric modulator of the interleukin-1 receptor, by positional scanning using β-amino γ-lactams. *J. Pept. Sci.* **2011,** *17*, 288-296.

74.   Boutard, N.; Jamieson, A. G.; Ong, H.; Lubell, W. D., Structure–activity analysis of the growth hormone secretagogue GHRP-6 by α-and β-amino γ-lactam positional scanning. *Chemical biology & drug design* **2010,** *75*, 40-50.

75.   St-Cyr, D. J.; Jamieson, A. G.; Lubell, W. D., α-Amino-β-hydroxy-γ-lactam for constraining peptide Ser and Thr residue conformation. *Org. Lett.* **2010,** *12*, 1652-1655.

76.   Freidinger, R. M.; Veber, D. F.; Perlow, D. S.; Saperstein, R., Bioactive conformation of luteinizing hormone-releasing hormone: evidence from a conformationally constrained analog. *Science* **1980,** *210*, 656-658.

77.   Freidinger, R. M.; Perlow, D. S.; Veber, D. F., Protected lactam-bridged dipeptides for use as conformational constraints in peptides. *J. Org. Chem.* **1982,** *47*, 104-109.

78.   Paul, P. K.; Burney, P.; Campbell, M. M.; Osguthorpe, D. J., The conformational preferences of γ-lactam and its role in constraining peptide structure. *Journal of computer-aided molecular design* **1990,** *4*, 239-253.

79.   Valle, G.; Crisma, M.; Toniolo, C.; Yu, K.-L.; Johnson, R. L., Crystal-state structures of Boc-Pro-Leu-Gly-NH2, hemihydrate and two lactam-restricted analogues. *J. Chem. Soc., Perkin Transactions 2* **1989,** 83-87.

80.   Freidinger, R. M., Design and synthesis of novel bioactive peptides and peptidomimetics. *J. Med. Chem.* **2003,** *46*, 5553-5566.

81.   Jamieson, A. G.; Boutard, N.; Beauregard, K.; Bodas, M. S.; Ong, H.; Quiniou, C.; Chemtob, S.; Lubell, W. D., Positional scanning for peptide secondary structure by systematic solid-phase synthesis of amino lactam peptides. *J. Am. Chem. Soc.* **2009,** *131*, 7917-7927.

82.   Reinelt, S.; Marti, M.; Dédier, S.; Reitinger, T.; Folkers, G.; de Castro, J. A. L.; Rognan, D., β-amino acid scan of a class I major histocompatibility complex-restricted alloreactive T-cell epitope. *J. Biol. Chem.* **2001,** *276*, 24525-24530.

83.   Gentilucci, L., SNew trends in the development of opioid peptide analogues as advanced remedies for pain relief. *Curr. Top. Med. Chem.* **2004,** *4*, 19-38.

84.   Steen, P. V. d.; Rudd, P. M.; Dwek, R. A.; Opdenakker, G., Concepts and principles of O-linked glycosylation. *Crit. Rev. Biochem. Mol. Biol.* **1998,** *33*, 151-208.

85.   Pinna, L. A.; Ruzzene, M., How do protein kinases recognize their substrates? *Biochimica et Biophysica Acta (BBA)-Molecular Cell Research* **1996,** *1314*, 191-225.

86.   Julenius, K.; Mølgaard, A.; Gupta, R.; Brunak, S., Prediction, conservation analysis, and structural characterization of mammalian mucin-type O-glycosylation sites. *Glycobiology* **2005,** *15*, 153-164.

87.   Hruby, V. J.; Li, G.; Haskell-Luevano, C.; Shenderovich, M., Design of peptides, proteins, and peptidomimetics in chi space. *Peptide Science* **1997,** *43*, 219-266.

88.   Geranurimi, A.; Lubell, W. D., Diversity-oriented syntheses of β-substituted α-amino γ-lactam peptide mimics with constrained backbone and side chain residues. *Org. Lett.* **2018,** *20*, 6126-6129.

Chapter 1

Chapter 2: Probing anti-inflammatory properties independent of NF-κB through conformational constraint of peptide-based interleukin-1 receptor biased ligands

2.1 Context

In chapter 2, the relevance of the D-threonine hydroxyl group and the D-Thr-D-Val dipeptide configuration and conformation for the biological activity of 101.10 were addressed by the synthesis of Agl and Hgl analogs. The influence of the modifications of the structure on the peptide conformation was studied using circular CD spectroscopy. The biological activity of the peptides was ascertained in vitro by studying effects on phosphorylation performed by three different kinases (JNK, p-38, and ROCK2), transcription of pro-inflammatory genes (IL-6, COX2, and IL-1β), and NF-κB signaling. Their biological activity was studied *in vivo* in murine models of PTB and ROP.

The chemistry for this publication has been described in brief in the thesis introduction. In this preamble to chapter 2, brief descriptions are presented for the various *in vitro* assays: Western blot assay, qPCR experiments, and NF-κB QUANTI-Blue assay. The LPS-induced preterm model in mice and oxygen-induced retinopathy in Sprague-Dawley rats are described sufficiently in the publication.

Western blot assay

The Western blot assay is an analytical technique for quantifying the relative abundance of specific proteins in a sample using antibodies. The assay also provides information about protein size. Antibodies bind to antigens, which in the case of proteins can be specific peptide sequences known as epitopes. In a Western blot analysis, antibodies distinguish specific epitopes from a lysate that may contains thousands of different proteins. First, proteins are separated from each other using sodium dodecyl sulfate - polyacrylamide gel electrophoresis based on size and charge. The proteins are transferred from the gel to a membrane by application of an electrical current. The membrane is processed with primary antibodies specific for target proteins of interest. Next, secondary antibodies bound to enzymes are applied and finally a substrate that reacts with the secondary antibody-bound enzyme is added for detection and quantification of the antibody-protein complex.[1-2]

qPCR Experiments

Cells in all organisms control gene expression by regulation of gene transcripts. Expression of specific genes can be measured by the number of copies of their RNA transcripts in a sample. The detection and quantification of gene expression from small amounts of RNA necessitates amplification of the gene transcript, which is commonly achieved using the polymerase chain

reaction (PCR). In the quantitative polymerase chain reaction (qPCR), the RNA sample is first reverse-transcribed to complementary DNA (cDNA) with the enzyme reverse transcriptase. Amplification of targeted DNA during PCR is then carefully monitored.[3-5]

NF-κB QUANTI-Blue Assay

Nuclear factor kappa-light-chain-enhancer of activated B cells (NF-κB) is a protein complex that controls transcription of DNA, cytokine production and cell survival to control the immune responses. Ubiquitous in animal cell types, NF-κB is involved in cellular responses to stimuli such as stress, cytokines, free radicals, and bacterial and viral antigens. NF-κB plays a key role in regulating the immune response to infection. Incorrect regulation of NF-κB has been linked to cancer, inflammatory and autoimmune diseases.[6] The QUANTI-Blue assay uses a colorimetric enzyme detection method to determine levels of a secreted alkaline phosphatase (AP) reporter product from the transcription of the NF-κB gene in a biological sample, such as cell culture supernatant.

Finally, in Chapter 2, a correlation of the structure-activity relationships, conformational analysis by CD, and *in vitro* and *in vivo* activity has been performed to provide insight into the relevance of structure, configuration and conformation for the biased signaling mechanisms of 101.10 and the resulting phenotypes.

2.2. References

1.   Mahmood, T.; Yang, P.-C., Western blot: technique, theory, and trouble shooting. *North American journal of medical sciences* **2012,** *4*, 429-434.

2.   Liu, Z.-Q.; Mahmood, T.; Yang, P.-C., Western blot: technique, theory and trouble shooting. *North American journal of medical sciences* **2014,** *6*, 160.

3.   Taylor, S. C.; Nadeau, K.; Abbasi, M.; Lachance, C.; Nguyen, M.; Fenrich, J., The ultimate qPCR experiment: producing publication quality, reproducible data the first time. *Trends in biotechnology* **2019,** *37*, 761-774.

4.   Taylor, S.; Wakem, M.; Dijkman, G.; Alsarraj, M.; Nguyen, M., A practical approach to RT-qPCR—publishing data that conform to the MIQE guidelines. *Methods* **2010,** *50*, S1-S5.

5.   Taylor, S. C.; Mrkusich, E. M., The state of RT-quantitative PCR: firsthand observations of implementation of minimum information for the publication of quantitative real-time PCR experiments (MIQE). *Journal of molecular microbiology and biotechnology* **2014,** *24*, 46-52.

6.   Li, Q.; Verma, I. M., NF-κB regulation in the immune system. *Nature reviews immunology* **2002,** *2*, 725-734.

Chapter 2

Article 1

Probing anti-inflammatory properties independent of NF-κB through conformational constraint of peptide-based interleukin-1 receptor biased ligands

(Published in *Frontiers Chem.,* **2019**, *7*, Article 23)

I performed the synthesis, isolation and chemical and spectroscopic characterization of all derivatives.

All final peptide analogs that I synthesized and purified were tested in a panel of *in vitro* cellular assays, as well as for *in vivo* activity in murine models of PTB and ROP by our collaborators Professor Sylvain Chemtob, Dr. Christiane Quiniou, Dr. Xin Hou, Dr. Tang Zhu, Dr. José Carlos Rivera, and Mr. Colin W. H. Cheng from the Département de pédiatrie, Université de Montréal. Colin.

I wrote the original draft of the manuscript which was edited by Professor Lubell, Professor Chemtob, Dr. Quiniou and Dr. Daniel J. St-Cyr.

Azade Geranurimi[1#], Colin W.H. Cheng[2,3,4#], Christiane Quiniou[2], Tang Zhu[2], Xin Hou[2], José Carlos Rivera[3,4], Daniel J. St-Cyr[1], Kim Beauregard[1], Vadim Bernard-Gauthier[1], Sylvain Chemtob[2,3,4,5], William D. Lubell[1]

[1]Département de Chimie, Université de Montréal, Montréal, QC, Canada

[2]Department of Pharmacology & Therapeutics, McGill University, Montréal, QC, Canada

[3]Hôpital Sainte-Justine Research Centre, Montréal, QC, Canada

[4]Hôpital Maisonneuve-Rosemont Research Centre, Montréal, QC, Canada

[5]Departments of Pediatrics, Pharmacology and Physiology, and Ophthalmology, Université de Montréal, Montréal, QC, Canada

# These authors contributed equally.

*Correspondence:

William D. Lubell

william.lubell@umontreal.ca

Abstract

Interleukin-1β (IL-1β) binds to the IL-1 receptor (IL-1R) and is a key cytokine mediator of inflammasome activation. IL-1β signaling leads to parturition in preterm birth (PTB) and contributes to retinal vaso-obliteration characteristic of oxygen-induced retinopathy (OIR) of the premature infant. Therapeutics targeting IL-1β and IL-1R are approved to treat rheumatoid arthritis; however, all are large proteins with clinical limitations including immunosuppression, due in part to inhibition of NF-κB signaling, which is required for immuno-vigilance and cytoprotection.

The all-D-amino acid peptide **2.1** (101.10, H-D-Arg-D-Tyr-D-Thr-D-Val-D-Glu-D-Leu-D-Ala-NH$_2$) is an allosteric IL-1R modulator which exhibits functional selectivity and conserves NF-κB signaling, while inhibiting other IL-1-activated pathways. Peptide **2.1** has proven effective in experimental models of PTB and OIR. Seeking understanding of the structural requirements for the activity and biased signaling of **2.1**, a panel of twelve derivatives was synthesized employing the various stereochemical isomers of α-amino-γ-lactam (Agl) and α-amino-β-hydroxy-γ-lactam (Hgl) residues to constrain the D-Thr-D-Val dipeptide residue. Using circular dichroism spectroscopy, the peptide conformation in solution was observed to be contingent on Agl, Hgl and Val stereochemistry. Moreover, the lactam mimic structure and configuration influenced biased IL-1 signaling in an *in vitro* panel of cellular assays as well as *in vivo* activity in murine models of PTB and OIR.

Remarkably, all Agl and Hgl analogs of peptide **2.1** did not inhibit NF-κB signaling but blocked other pathways, such as JNK and ROCK2 phosphorylation contingent on structure and configuration. Efficacy in preventing preterm labor correlated with capacity to block IL-1β-induced IL-1β synthesis. Furthermore, the importance of inhibition of JNK and ROCK2 phosphorylation for enhanced activity was highlighted for prevention of vaso-obliteration in the OIR model.

Taken together, lactam mimic structure and stereochemistry strongly influenced conformation and biased signaling. Selective modulation of IL-1 signaling was proven to be

particularly beneficial for curbing inflammation in models of preterm labor and retinopathy of prematurity. A class of biased ligands has been created with potential to serve as selective probes for studying IL-1 signaling in disease. Moreover, the small peptide mimic prototypes are promising leads for developing immunomodulatory therapies with easier administration and maintenance of beneficial effects of NF-κB signaling.

Keywords: β-hydroxy-α-amino-γ-lactam (Hgl), interleukin-1 receptor antagonist, 101.10 (rytvela), *β*-turn, Freidinger lactams, circular dichroism (CD), solid-phase peptide synthesis, retinopathy, prematurity

Introduction

Among examples of synthetic methods to create folded peptides, the applications of α-amino-γ-lactam (Agl) residues to control folding is a mainstay for biomedical research to improve biological activity.[1-3] Previously[4], an Agl residue scan of the all D-amino acid linear peptide 101.10 (**2.1**, H-D-Arg-D-Tyr-D-Thr-D-Val-D-Glu-D-Leu-D-Ala-NH₂, Figure 2.1) was used to study conformation-activity relationships of this allosteric modulator of the interleukin (IL)-1 receptor (IL-1R), which is of great interest in the treatment of many inflammatory diseases given the shortcomings of currently-approved anti-IL-1 therapeutics. The resulting lactam analogs exhibited properties that were either similar or improved relative to the parent peptide **2.1**.[4-5] Inspired by the activity of the Agl analogs but wary that the absence of side chain function may diminish potency despite a favorable geometry, the corresponding β-hydroxy-α-amino-γ-lactam (Hgl) residue was conceived to examine constraint of both backbone and side chain conformation of the D-Thr residue.[3] A detailed study of **2.1** is now reported in which all configurations of Agl, Hgl and Val residues (e.g., **2.5** and **2.6**, Figure 2.1) are used to study the central D-Thr-D-Val dipeptide moiety. IL-1 is a pro-inflammatory cytokine extensively involved in many diseases[6] and has been described to play a major role in inflammatory episodes leading to preterm birth (PTB)[7-10] and its associated sequela of retinopathy of prematurity (ROP).[11] IL-1 exerts its biological effects through complexation to the ubiquitously expressed IL-1R[12] and dimerization with the IL-1R accessory protein (IL-1RacP). IL-1 activates various downstream signaling mediators, notably PGE₂ and NF-κB, which trigger hyperthermic and pro-inflammatory effects.[13] Agents that block the effects of IL-1 offer potential to treat diseases included in chronic inflammatory disorders such as

rheumatoid arthritis and Crohn's disease.[14] Currently approved IL-1R antagonists, such as the endogenous IL-1R antagonist (IL-1Ra) compete with the agonist (i.e., IL-1β) by binding at the orthosteric, native-ligand binding site.[15] Moreover, all are large proteins (17.5-251 kDa): Kineret® (recombinant IL-1ra; Biovitrium), Canakinumab (Novartis) and Gevokizumab (IL-1 monoclonal antibodies; XOMA corporation), Rilonacept (Regeneron; soluble IL-1R [Fc-bound]). The use of relatively large immunomodulators in clinical settings presents secondary effects such as immunosuppression, which increases the risk for opportunistic infections, and pain at the site of injection. Such drawbacks may account for failures in clinical trials,[16-18] and may be related to non-selective interference of all signals triggered by IL-1β because of the orthosteric competitive nature of these biologics. Preservation of the nuclear factor κ-light-chain-enhancer of activated B cells (NF-κB) has been suggested to be beneficial, due to retained anti-apoptotic activity[19] and promotion of the differentiation and proliferation of B and T cells, which are critical for the immune response against pathogenic insults.[20]

Heptapeptide **2.1** (850Da) binds at spatially distinct sites from endogenous IL-1β, and selectively and allosterically regulates downstream signaling of inflammatory pathways.[7, 21] Derived from a loop region of the IL-1RacP using a strategy for conceiving peptide modulators based on sequences from protein receptors,[22-25] peptide **2.1** significantly attenuated hyperoxia (oxidant stress)-induced increases in IL-1β, tumor necrosis factor-α (TNF-α), intercellular adhesion molecule (ICAM)-1, and semaphorin (Sema)-3A.[11] These molecular changes caused by peptide **2.1** were associated with prevention of retinal vaso-obliteration, acceleration of normal revascularization, and normalization of vascular density. In addition, fluorescein-conjugated **2.1** was shown to localize principally in microglial and endothelial cells in the inflamed retina subjected to oxygen-induced retinopathy (OIR) conditions. In contrast to currently approved IL-1 inhibitors, peptide **2.1** exhibited pharmacological selectivity, by inhibiting some IL-1-triggered pathways such as p38 mitogen-activated protein kinases (p38 MAPK) and Rho-associated coiled-coil-containing protein kinase 2 (ROCK2), while preserving NF-κB.[7] In models of hyperthermia, inflammatory bowel disease and contact dermatitis, peptide **2.1** also proved superior to corticosteroids and FDA-approved IL-1Ra.[21] In models of PTB, peptide **2.1** has been shown to be an effective early intervention for suppressing the downstream inflammatory cascade induced by bacterial lipopolysaccharide (LPS, to mimic chorioamnionitis), and for preventing premature initiation of uterine activation proteins and subsequent onset of labor in mice.[7]

Conformational restriction of natural peptides has been used to identify active geometry and to enhance therapeutic potential by mitigating issues such as low oral availability and poor metabolic stability.[26-28] Since pioneering studies by Freidinger and Veber, the application of Agl residues has proven effective for constraining the backbone sequence to favor *β*-turn geometry in various peptides.[1, 29-34] In the interest of understanding the biologically active conformation responsible for the mechanism of action, Agl residues as well as their β-amino-γ-lactam (Bgl) counterparts have been used in structure-activity relationship studies of peptide **2.1**.[4-5, 35] Although systematic replacement of each residue of peptide **2.1** with D-Ala indicated that removal of certain side chains may lead to activity loss, analogs possessing one (*R*)-Agl residue, respectively at either the D-Tyr, D-Val, D-Glu, or D-Leu positions demonstrated similar efficacy, and [(*S*)-Bgl⁴]-**2.1** increased activity compared to peptide **2.1** in inhibiting IL-1β-induced DNA primase-1-dependent thymocyte TF-1 proliferation.[4-5] An active turn conformation situated about the D-Tyr-D-Thr-D-Val triad appeared key for potent inhibition of IL-1β-induced thymocyte TF-1 proliferation; however, [(*R*)-Agl³]-**2.1** exhibited significantly diminished activity, likely due to loss of side chain.[4]

Employing all configurations of Agl, Hgl and Val residues to study the D-Thr-D-Val dipeptide of **2.1**, the influences of backbone and side chain conformation on modulation of IL-1R signaling has now been examined *in vitro* by assessing phosphorylation of downstream IL-1 modulators and transcription of inflammatory genes. Moreover, the effects of their lactam structures and configurations has been assessed *in vivo* on murine models of preterm birth (PTB) and oxygen-induced retinopathy (OIR). These investigations have illustrated the influences of the orientation of the hydroxyl group and backbone for activity and biased signaling, particularly with respect to inhibition of NF-κB.
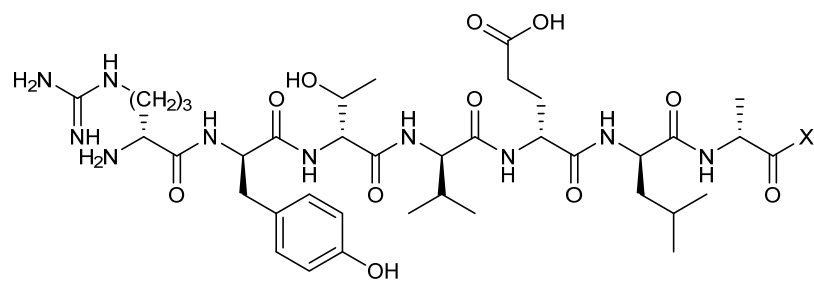
Chapter 3
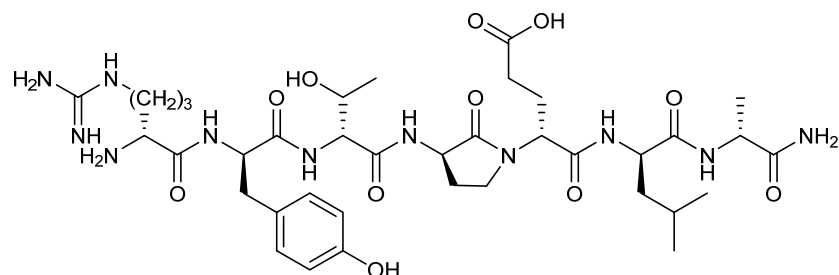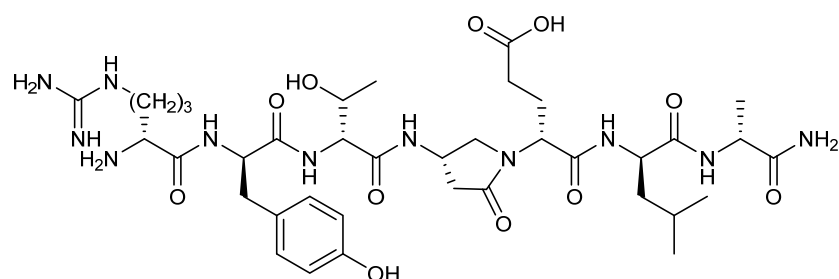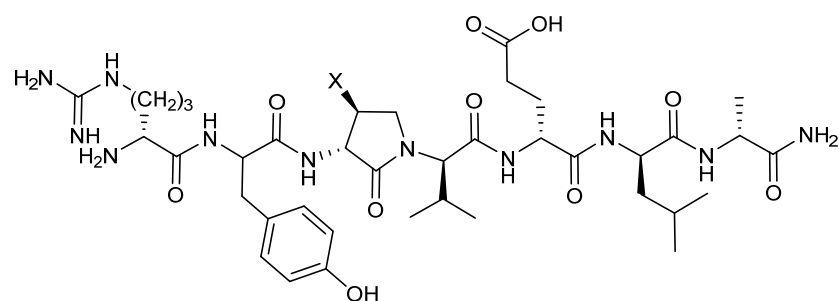
Figure. 2.1. Peptide 1 and representative Agl, Bgl and Hgl analogs

Materials and Methods

General Chemistry Methods

Unless otherwise specified, all non-aqueous reactions were performed under an inert argon atmosphere. All glassware was dried with a flame under flushing argon gas or stored in the oven, and let cool under an inert atmosphere prior to use. Anhydrous solvents (THF, DCM, MeCN, MeOH, toluene and DMF) were obtained by passage through solvent filtration systems (Glass Contour, Irvine, CA) and solvents were transferred by syringe. Reaction mixture solutions (after aqueous workup) were dried over anhydrous $MgSO_4$ or Na_2SO_4, filtered, and rotary-evaporated under reduced pressure. The syntheses under microwave conditions were performed on a 0-400 W Biotage® Robot Eight & Robot Sixty microwave synthesizer. Column chromatography was performed on 230-400 mesh silica gel, and thin-layer chromatography was performed on alumina plates coated with silica gel (Merck 60 F_{254} plates). Visualization of the developed chromatogram was performed by UV absorbance or staining with iodine or potassium permanganate solutions. Melting points were obtained on a Buchi melting point B-540 apparatus and are uncorrected. Specific rotations, $[\alpha]^D$ values, were calculated from optical rotations measured at 20 °C and 25 °C in $CHCl_3$ or MeOH at the specified concentrations (c in g/100 mL) using a 0.5 dm cell length (l) on a Anton Paar Polarimeter, MCP 200 at 589 nm, using the general formula: $[\alpha]^D_{25} = (100 \times \alpha)/(\ l \times c)$. Accurate mass measurements were performed on an LC-MSD instrument in electrospray ionization (ESI-TOF) mode at the Université de Montréal Mass Spectrometry facility. Sodium adducts $[M + Na]^+$ were used for empirical formula confirmation. Nuclear magnetic resonance spectra (^1H NMR, ^{13}C NMR) were recorded on Bruker 300, 400, 500 and 700 MHz spectrometers. ^1H NMR spectra were referenced to $CDCl_3$ (7.26 ppm), CD_3OD (3.31 ppm), C_6D_6 (7.16 ppm) or DMSO-d_6 (2.50 ppm) and ^{13}C NMR spectra were measured in $CDCl_3$ (77.16 ppm), CD_3OD (49.0 ppm), C_6D_6 (128.39 ppm) or DMSO-d_6 (39.52 ppm) as specified below. Coupling constant J values were measured in Hertz (Hz) and chemical shift values in parts per million (ppm). Infrared spectra were recorded in the neat on a Perkin Elmer Spectrometer FT-IR instrument, and are reported in reciprocal centimeters (cm^{-1}). Analytical LCMS and HPLC analyses were performed on a 5 μM, 50 mm x 4.6 mm C18 Phenomenex Gemini column™ with a flow rate of 0.5 mL/min using appropriate gradients from pure water containing 0.1% formic acid (FA), to mixtures with either CH_3CN containing 0.1% FA, or MeOH containing 0.1% FA. Peptides were purified on a preparative column (C18 Gemini column™) using appropriate gradients from pure

water containing 0.1% FA to mixtures with MeOH containing 0.1% FA at a flow rate of 10 mL/min.

Chemical Reagents

Unless specified otherwise, commercially available reagents were purchased from Aldrich, A & C American Chemicals Ltd., Fluka and Advanced Chemtech™ and used without further purification, including PPh$_3$, DIAD, *p*-nitrobenzoic acid, NaN$_3$, piperidine, DIEA, TFA, TES, TEA, CH$_3$I, NaH, Fmoc-OSu, Boc$_2$O, NaIO$_4$, *m*-CPBA, TFE and HFIP. Polystyrene Rink amide resin (0.5 mmol/g) was purchased from Advanced Chemtech™, and the manufacturer's reported resin loading was used in the calculation of yields of final product. All commercially available amino acids [e.g., Fmoc-D-Ala-OH, Fmoc-D-Leu-OH, Fmoc-D-Glu(*t*-Bu)-OH, Fmoc-D-Tyr(*t*-Bu)-OH, Fmoc-D-Arg(Pmc)-OH, Boc-D-Arg(Pmc)-OH, H-L-Met-OH, H-D-Met-OH, L-Val-O-*t*-Bu.HCl, D-Val-O-*t*-Bu•HCl, Boc-L-Met-OH and Boc-D-Met-OH] and coupling reagents (e.g., HOBt, HBTU and DCC) were purchased from GL Biochem™ and used as received. Solvents were obtained from VWR international.

H-D-Arg-D-Tyr-(*R*)-Agl-D-Val-D-Glu-D-Leu-D-Ala-NH$_2$ [(3*R*)-Agl³]-2.1, [(3*R*)-2.5]

A 10-mL plastic filtration tube equipped with a polyethylene filter was charged with polystyrene Rink amide resin, 75-100 mesh, 1%, DVB with a 0.5 mmol/g loading, (200 mg) and DCM (about 7 mL). The tube was sealed, shaken for 30 min to induce swelling and the liquid phase was removed. The Fmoc group was cleaved from the resin-bound peptide by treatment with a freshly-prepared 20% piperidine in DMF solution (about 7 mL), shaking for 30 min, and removal of the liquid phase. The resin was repeatedly (3x per solvent) washed (10 mL per wash) over a total of 6 min with DMF, DCM, and the liquid phase was removed. Generation of the free amine resin was confirmed by a positive Kaiser test. Peptide elongation was conducted by treating the DMF-swollen free amine resin with a freshly prepared acylation solution Fmoc-D-Ala-OH (3 eq), HBTU (3 eq), and DIEA (6 eq) in DMF (4-7 mL). After agitating for 3-5 h at room temperature, Fmoc cleavage and peptide elongation were reiterated using Fmoc-D-Leu-OH, Fmoc-D-Glu(*t*-Bu)-OH, *N*-Fmoc-(3*R*)-Agl³-*R*-Val-OH dipeptide, Fmoc-D-Tyr(*t*-Bu)-OH, and Fmoc-D-Arg(Pmc)-OH. For the coupling of *N*-Fmoc-(3*R*)-Agl³-*R*-Val-OH, only a stoichiometric quantity was used; for Fmoc-D-Tyr(*t*-Bu)-OH, coupling was repeated twice using a higher reaction concentration. Synthetic progress was monitored using a combination of the Kaiser test and LC-MS analyses on TFA cleaved resin aliquots, which were concentrated and dissolved in mixtures of water and

MeCN. The completed peptide sequence was cleaved from the resin by treatment with TFA/H$_2$O/TES (3 mL, 95/2.5/2.5, v/v/v) with shaking for 3 h, and the liquid phase was collected. The resin was repeatedly (2x) washed with TFA and the combined liquid phases were concentrated in vacuo. The residue was dissolved in a minimal volume of acetonitrile, precipitated with ice-cold diethyl ether, and centrifuged. The supernatant was removed by decantation and the precipitate was collected. The precipitation and collection process were repeated on the supernatant. The combined white solid precipitate was dissolved in water (5 mL), freeze-dried to give a white powder (44% crude purity), and purified using preparative HPLC on a Waters™ Prep LC instrument equipped with a reverse-phase Gemini™ C18 column (250 × 21.2 mm, 5 μm), using a gradient of MeOH (0.1% FA) in H$_2$O (0.1% FA) at a flow rate of 10.0 mL/min and UV detection at 280 nm. Fractions containing pure peptide were combined and lyophilized to afford peptide (3*R*)-**2.5** (10 mg, 12% yield of >95% purity): LCMS [10-90% MeOH (0.1% FA) in water (0.1% FA) over 14 min; RT 8 min] and [10-90% MeCN (0.1% FA) water (0.1% FA) over 14 min; RT 5.6 min]; HRMS (ESI$^+$) calcd m/z for C$_{38}$H$_{62}$N$_{11}$O$_{10}$ [M+H]$^+$, 832.4676 found 832.4682.

(3*R*, 2'*R*)-2-[3-*N*-(Fmoc)amino-2-oxopyrrolidin-1-yl]-3-methylbutanoic acid [(3*R*, 2'*R*)-2.7]
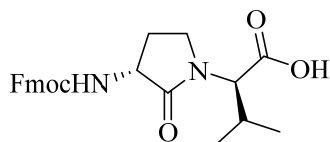
(3*R*, 2'*R*)-Acid (3*R*, 2'*R*)-**2.14** (1 eq., 67 mg, 0.27 mmol) was dissolved in 1:1 acetone (1 mL) and H$_2$O (1 mL), treated with Na$_2$CO$_3$ (2 eq., 58 mg, 0.55 mmol) followed by Fmoc-OSu (1.1 eq., 100 mg, 0.3 mmol), stirred at rt for 18 h, and concentrated to a residue that was dissolved in H$_2$O and acidified to pH 3-4 with citric acid (0.5 N solution). The aqueous solution was extracted multiple times with EtOAc until the aqueous layer no longer exhibited the carbamate by TLC. The organic layer was extracted with saturated NaHCO$_3$ (2 X 3 mL). The aqueous extractions were combined, acidified to pH 3-4 with 0.5 N citric acid solution, and extracted with EtOAc. The organic layer was washed with brine, dried over MgSO$_4$, filtered, and concentrated to afford (3*R*, 2'*R*)-carbamate (3*R*, 2'*R*)-**2.7** (87 mg, 0.21 mmol, 75 % yield): R$_f$ = 0.26 (10% MeOH:DCM); [α]$_D^{25}$ 13.2° (*c* 0.41, MeOH); ^{1}H NMR (300 MHz, MeOD) δ 7.80 (d, *J* = 7.6, 2H), 7.68 (d, *J* = 7.4, 2H), 7.40 (t, *J* = 7.1, 2H), 7.31 (t, *J* = 6.9, 2H), 5.60 (d, *J* = 5, 1H), 4.53-4.18 (m, 5H), 3.74 (t, *J* = 9.2, 1H), 3.49-3.35 (m, 1H), 2.56-2.37 (m, 1H), 2.32-2.16 (m, 1H), 2.10-1.85 (m, 1H), 1.44-1.21 (m, 1H), 1.03 (d, *J* = 6.7, 3H), 0.93 (d, *J* = 6.7, 3H); ^{13}C NMR (75 MHz, MeOD) δ 173.9, 171.6, 157.2, 143.9,

141.2, 127.4, 126.8, 124.8, 119.5, 66.7, 60.8, 52.2, 41.2, 28.1, 26.2, 18.4, 18.1; HRMS (ESI$^+$) calcd *m/z* for C$_{24}$H$_{27}$N$_2$O$_5$ [M+H]$^+$, 423.1914 found 423.1917.

(*R*)-*N*-(Boc)-Methioninyl-(*R*)-valine *tert*-butyl ester [(*R, R*)-2.10]
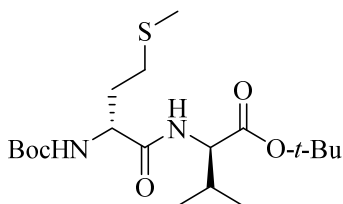
N-Boc-(*R*)-Methionine [(*R*)-**2.8**, 1 eq., 1 g, 4 mmol] and (*R*)-valine *tert*-butyl ester hydrochloride [(*R*)-**9** HCl, 1 eq., 840 mg, 4 mmol] were dissolved in dry DMF (6 mL). On treatment of the mixture with triethyl amine (1 eq., 400 mg, 0.56 mL, 4 mmol) a precipitate was formed, and HOBt (1 eq., 540 mg, 4 mmol) and DCC (1 eq., 830 mg, 4 mmol) were added to the mixture. The mixture was stirred at rt for 24 h, filtered and the filter cake was washed with DCM. The filtrate and washings were combined concentrated under vacuum. The residue was dissolved in EtOAc (6 mL), washed with 0.5 M citric acid (3 x 4 mL), 2 N aqueous NaHCO$_3$ (3 x 4 mL) and brine (4 mL), dried over Na$_2$SO$_4$, filtered and concentrated under vacuum to give (*R,R*)-dipeptide (*R,R*)-**2.10** as a white foam (1.27 g, 3.13 mmol, 78% yield): R$_f$ = 0.28 (20% EtOAc in hexane); [α]$_D^{25}$ – 4.1° (*c* 1.95, CHCl$_3$); ^{1}H NMR (300 MHz, CDCl$_3$) δ 6.61 (d, *J* = 8.4, 1H), 5.20 (d, *J* = 8.0, 1H), 4.40 (dd, *J* = 8.8, 4.6, 1H), 4.35-4.22 (br, 1H), 2.59 (t, *J* = 7.2, 2H), 2.23-1.86 (m, 5H), 1.46 (s, 9H), 1.44 (s, 9H), 0.91 (dd, *J* = 7.6, 7.1, 6H); ^{13}C NMR (75 MHz, CDCl$_3$) δ 171.4, 170.7, 155.6, 82.1, 80.2, 57.7, 53.4, 31.6, 31.4, 30.3, 28.4, 28.2, 19.1, 17.6, 15.3; HRMS (ESI$^+$) calcd *m/z* for C$_{19}$H$_{36}$N$_2$O$_5$S [M+H]$^+$, 405.2418 found 405.2433.

N-Boc-(*R*)-Methioninyl-(*R*)-valine *tert*-butyl ester methylsulfonium iodide [(*R, R*)-2.11]
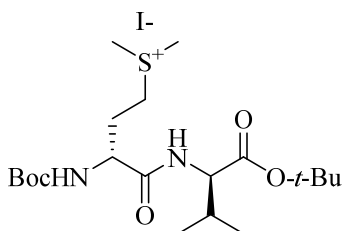
(*R,R*)-Dipeptide (*R,R*)-**2.10** (1 eq., 500 mg, 1.24 mmol) was dissolved in CH$_3$I (39 eq., 3 mL, 48.2 mmol) and stirred at rt for 24 h, concentrated under vacuum, and the volatile contaminants were removed by repeated (3x) co-evaporation with DCM to give (*R,R*)-methylsulfonium iodide (*R, R*)-**2.11** as yellow gummy foam (655 mg, 1.2 mmol, 97 % yield): R$_f$ = 0.2 (5% MeOH in DCM); [α]

$_D^{25}$ 22° (*c* 1, MeOH); ^{1}H NMR (300 MHz, CDCl$_3$) δ 7.53 (d, *J* = 7.1, 1H), 5.98 (d, *J* = 7.2, 1H), 4.60 (dd, *J* = 12.5, 7.3, 1H), 4.24 (dd, *J* = 7.8, 5.2, 1H), 3.96-3.81 (m, 1H), 3.73- 3.58 (m, 1H), 3.32 (s, 3H), 3.21 (s, 3H), 2.64-2.47 (m, 1H), 2.42-2.14 (m, 2H), 1.45 (s, 9H), 1.42 (s, 9H), 0.99 (t, *J* = 7.3, 6H); HRMS (ESI$^+$) calcd *m/z* for C$_{20}$H$_{39}$N$_2$O$_5$S [M]$^+$, 419.2574 found 419.2567.

***tert*-Butyl (3*R*, 4*S*, 2'*R*)-2-[3-(Fmoc)amino-4-hydroxy-2-oxopyrrolidin-1-yl]-3-methylbutanoate [(3*R*, 4*S*, 2'*R*)-2.12]** was prepared as previously described.[36]

(3*R*, 2'*R*)-*tert*-Butyl 2-[3-(Boc)amino-2-oxopyrrolidin-1-yl]-3-methylbutanoate [(3*R*, 2'*R*)-2.13]
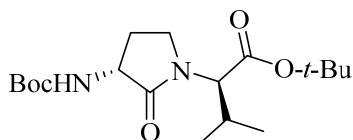
(*R,R*)-Methylsulfonium iodide (*R,R*)-**2.11** (1 eq., 158 mg, 0.289 mmol) was dissolved in a 1:1 mixture of DMF (3.5 mL) and DCM (3.5 mL) under argon, cooled to 0 °C, treated with NaH (60% dispersion in mineral oil, 1.2 eq., 14 mg, 0.347 mmol), and stirred at 0 °C for 2.5 h. The reaction was diluted with methyl acetate (2.5 mL) and H$_2$O (0.5 mL), and allowed to warm to rt with stirring overnight. The reaction mixture was concentrated under vacuum, quenched with 1 M NaH$_2$PO$_4$, and extracted three times with EtOAc. The combined EtOAc layers were dried over MgSO$_4$, filtered and concentrated to a residue that was purified by column chromatography on silica gel using 20% of EtOAc in hexane as eluent. Evaporation of the collected fractions provided (3*R*,2'*R*)-lactam (3*R*,2'*R*)-**2.13** (60 mg, 0.17 mmol, 58 % yield): R$_f$ = 0.31 (30% EtOAc in hexane); [α] $_D^{25}$ 35.8° (*c* 1.6, CHCl$_3$); ^{1}H NMR (300 MHz, CDCl$_3$) δ 5.09 (s, 1H), 4.39 (d, *J* = 9.3, 1H), 4.31-4.16 (br s, 1H), 3.72 (t, *J* = 9.1, 1H), 3.27 (m, 1H), 2.72-2.58 (m, 1H), 2.26-2.11 (m, 1H), 1.90-1.71 (m, 1H), 1.45 (s, 9H), 1.44 (s, 9H), 0.98 (d, *J* = 6.7, 3H), 0.89 (d, *J* = 6.8, 3H); ^{13}C NMR (75 MHz, CDCl$_3$) δ 173.0, 169.7, 156.1, 82.1, 80.0, 61.0, 52.4, 41.7, 29.4, 28.8, 28.5, 28.2, 19.4, 19.3; HRMS (ESI$^+$) calcd *m/z* for C$_{18}$H$_{33}$N$_2$O$_5$ [M+H]$^+$, 357.2384 found 357.2399.

(3*R*, 2'*R*)-2-[3-Amino-2-oxopyrrolidin-1-yl]-3-methylbutanoate trifluoroacetate [(3*R*, 2'*R*)-2.14]
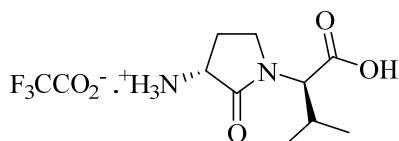
A solution of (3*R*,2'*R*)-lactam (3*S*,2'*S*)-**2.13** (1 eq., 100 mg, 0.281 mmol) in TFA (1 mL) and DCM (1 mL) was stirred at rt. After TLC analysis revealed complete consumption of the carbamate, the volatiles were evaporated on a rotary evaporator, and the residue was precipitated from ice-cooled diethyl ether and collected using a centrifuge to yield (3*R*,2'*R*)-trifluoroacetate (3*R*,2'*R*)-**2.14** (77.6 mg, 0.247 mmol, 88 % yield) as white precipitate: R_f = 0.1 (1:9:90 Et$_3$N:MeOH:DCM); $[\alpha]_D^{25}$ 45.6° (*c* 0.5, MeOH); ^{1}H NMR (400 MHz, MeOD) δ 4.40 (d, *J* = 9.3, 1H), 4.17 (dd, *J* = 11.0, 8.5, 1H), 3.92-3.81 (m, 1H), 3.60-3.45 (m, 1H), 2.66-2.54 (m, 1H), 2.35-2.19 (m, 1H), 2.14-1.97 (m, 1H), 1.05 (d, *J* = 6.7, 3H), 0.98 (d, *J* = 6.8, 3H); ^{13}C NMR (75 MHz, MeOD) δ 171.3, 170.0, 60.8, 50.3, 41.6, 28.2, 24.5, 18.3, 18.2; HRMS (ESI$^+$) calcd *m/z* for C$_9$H$_{17}$N$_2$O$_3$ [M+H]$^+$, 201.1234 found 201.1226.

N-Fmoc-(*R*)-Methionine methyl ester [(*R*)-2.15] and N-Fmoc-(*R*)-Methionine sulfoxide methyl ester [(*R*)-2.16] were prepared by a modified version (vide infra) of the previously described method.[37]

N-Fmoc-(2*R*)-Vinylglycine methyl ester [(*R*)-2.17] and (2*R*, 2'*R*)- and (2*R*, 2'*S*)-Methyl 2-(oxiranyl)-N-(Fmoc)glycinate [(2*R*, 2'*R*)-2.18 and (2*R*, 2'*S*)-2.18] were prepared as previously described.[3]

N-Fmoc-(3*R*, 4*S*, 2'*R*)-Hgl-Val-*t*Bu [(3*R*, 4*S*, 2'*R*)-2.19] and (3*R*, 4*R*, 2'*R*)-*tert*-Butyl 2-[3-(Fmoc)Amino-4-*p*-nitrobenzoyloxy-2-oxopyrrolidin-1-yl]-3-methylbutanoate [(3*R*, 4*R*, 2'*R*)-2.20] were prepared as previously described.[36]

N-Fmoc-[(3*R*)-Agl^3]-D-Val-D-Glu(*t*-Bu)-D-Leu-D-Ala-Rink amide resin (2.22)
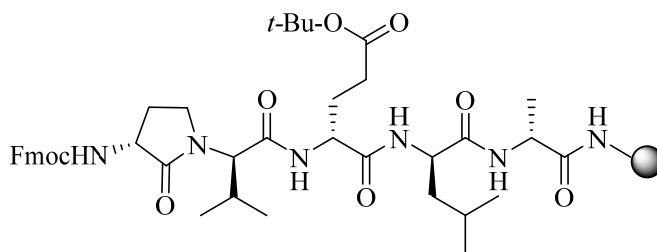
A solution of acid (3*R*,2'*R*)-**2.7** (1 eq., 87 mg, 0.2 mmol) and 2-(1H-benzotriazol-1-yl)-1,1,3,3-tetramethyluronium hexafluorophosphate (HBTU, 1 eq., 78 mg, 0.2 mmol) in dimethylformamide (DMF, 2 mL) was stirred for 1 min, treated with *N,N*-diisopropylethylamine (DIEA, 2 eq., 53.2 mg, 68 μL, 0.4 mmol), stirred for 5 min and added to H-D-Val-D-Glu(*t*-Bu)-D-Leu-D-Ala-Rink amide resin **2.21** (400 mg, 0.5 mmol/g, 0.2 mmol), which was placed earlier into a 3-mL plastic filtration tube equipped with a polyethylene filter and swollen in DMF (2 mL). The resin mixture

was shaken at rt for 5 h, and the liquid phase was removed by filtration. The resin was repeatedly (3x per solvent) washed (15 sec per wash) with DMF and DCM, and dried under vacuum to afford resin **2.22**. To assess resin-bound peptide purity, a resin aliquot (5 mg) was placed into a 1-mL plastic filtration tube equipped with a polyethylene filter and treated with 20% piperidine in DMF. After 0.5 h, the liquid phase was removed by filtration and the resin was treated with 0.5 mL of a 95:2.5:2.5 cocktail of TFA:H_2O:triethylsilane (TES) at rt for 1 h, and filtered. The filtrate was collected in a 1.5 mL tube, and concentrated by purging with an air stream. The residue was treated with Et_2O (1 mL), and centrifuged for 2 min. After decantation, the precipitate was dissolved in H_2O (1 mL) and analyzed by LCMS [10-90% MeOH (0.1% FA)/ water (0.1% FA), 14 min, RT 9.2 min] and [10-90% MeCN (0.1% FA)/ water (0.1% FA), 14 min, RT 7.6 min].

Circular Dichroism Spectroscopy

CD spectra were recorded on a Chirascan CD Spectrometer (Applied Photophysics, Leatherhead, United Kingdom) using a 1.0-cm path-length quartz cell containing 20 µM of peptide dissolved in Milli-Q water. The experimental settings were as follows: 1 nm, bandwidth; 0.5 nm, step size; 3 s, sampling time.

Animals

Timed-pregnant CD-1 mice were obtained from Charles River (Saint-Constant, QC, Canada) at gestational day 12 and were acclimatized for 4 days prior to experiments. Animals were used according to a protocol approved by the Animal Care Committee of Hôpital Sainte-Justine in accordance with the principles of the Guide for the Care and Use of Experimental Animals of the Canadian Council on Animal Care. The animals were maintained on standard laboratory chow under a 12h:12h light/dark cycle and allowed free access to chow and water.

Two-day-old (P2) Sprague Dawley rat pups and their mothers were ordered from Charles River (Saint-Constant, QC, Canada) and acclimatized for 3 days. The rats were housed in standard cages with access ad libitum to food and water and kept in a 12h:12h light/dark cycle. To control for the effects of litter size on retinal development, the sizes of litters were reduced to 12 by sacrificing excess pups by decapitation while under 2% isoflurane anesthesia. All procedures and protocols involving the use of these rats were approved by the Animal Care Committee of the research center of Hôpital Maisonneuve-Rosemont and are in accordance with the Statement for the Use of Animals in Ophthalmic and Vision Research approved by the Association for Research

in Vision and Ophthalmology (ARVO), and guidelines established by the Canadian Council on Animal Care.

Reagents

Chemicals were purchased from the following manufacturers: human rIL-1β (200-01B; PeproTech), LPS (L2630; Sigma-Aldrich), rytvela (peptide **2.1**) (Elim Biopharmaceuticals, Hayward, CA) and Kineret (Anakinra, Sobi, Biovitrum Stockholm, Sweden).

qPCR experiments

HEK-Blue IL-33/IL-1β cells were purchased from InvivoGen (San Diego, CA) and used at passages under 15. HEK-Blue cells were cultured in DMEM growth medium supplemented with 10% serum, 50 U/mL penicillin, 50 mg/mL streptomycin, 200 mg/mL zeocin, and 100 mg/mL hygromycin. Cells were grown in regular conditions (37 °C, 5% CO_2). Cells were serum starved overnight and treated with 100 ng/mL IL-1β for 4h. Cells were pre-incubated for 30 min with peptides **2.1**, **2.5** or **2.6** (10^{-6}M) or Kineret (1.0 mg/mL) prior to the experiments to reach equilibrium (n=4 each treatment). Cells were harvested and incubated for 5 min in RIBOzol (AMRESCO). RNA was extracted according to manufacturer's protocol and RNA concentration and integrity were measured with a NanoDrop 1000 spectrophotometer. A total of 500 ng RNA was used to synthetize cDNA using iScript Reverse Transcription SuperMix (Bio-Rad, Hercules, CA). Primers were designed using National Center for Biotechnology Information Primer Blast and are shown in Table 2.1. Quantitative gene expression analysis was performed on Stratagene MXPro3000 (Stratagene) with SYBR Green Master Mix (Bio-Rad). Gene expression levels were normalized to 18S universal primer (Ambion Life Technology, Burlington ON, Canada). Genes analyzed include *IL1β, IL6* and *PTGHS2* (Prostaglandin H synthetase 2 or cyclooxygenase-2 (COX-2)). Data are representative of 3 experiments (n=4).

Table 2.1. List of primers for the human genes assessed by qPCR

Gene	Forward Primer (5'→3')	Reverse Primer (5'→3')
IL1β	AGCTGGAGAGTGTAGATCCCAA	ACGGGCATGTTTTCTGCTTG
IL6	TTCAATGAGGAGACTTGCCTGG	CTGGCATTTGTGGTTGGGTC
PTGHS2	ATATTGGTGACCCGTGGAGC	GTTCTCCGTACCTTCACCCC

NF-κB QUANTI-Blue assay

HEK-Blue IL-33/IL-1β cells (InvivoGen) were pretreated with peptides **2.1**, **2.5** or **2.6** (10^{-6}M) or Kineret (1.0 mg/mL) for 30 min, followed by treatment with constant concentration of IL-1β (100 ng/mL), and then incubated at 37 °C for 4 h. Levels of secreted alkaline phosphatase in cell culture supernatant were determined using the QUANTI-Blue assay, according to the manufacturer's instructions (InvivoGen). Alkaline phosphatase activity was assessed by measuring the optical density (OD) at 620–655 nm with a micro plate reader (EnVision Multilabel reader; PerkinElmer, Waltham, MA). Data are representative of five experiments (each with n = 6).

P38 MAPK, ROCK2 and JNK Phosphorylation Assay

RAW Blue cells (Invivogen) were grown under standard conditions (37 °C, 5% CO_2) and maintained under passage number 15. Cells were equilibrated with **2.1**, **2.5** or **2.6** (10^{-6}M) or Kineret (1.0 mg/mL) for 30 min, after which time, they were exposed to IL-1β (100 ng/mL) for 15 min. Cells were harvested and lysed on ice for 30 min using a radioimmunoprecipitation assay buffer (Cell Signaling) supplemented with 1 mM phenylmethylsulfonyl fluoride (PMSF) and complete EDTA-free protease inhibitor cocktail (Roche, Mannheim, Germany, prepared according to the manufacturer's instructions). Protein concentrations were determined using a Bradford protein assay (Bio-Rad) on 96-well plates with a microplate reader (EnVision Multilabel reader) measuring OD at 595 mm. Bovine serum albumin serial dilutions were used to generate a standard curve. Lysates were then mixed with 4X reducing sample buffer (Bio-Rad).

Lysates were loaded (30 µg protein per well) in a 5% acrylamide stacking gel, and samples were electrophoresed in a 12% acrylamide resolving gel for 1.5 h at 120 V, followed by a 1 h transfer onto polyvinylidene difluoride (PDVF) membranes at 100 V. Membranes were blocked and incubated with 1:1000 dilution of primary antibody and 1:20,000 dilution of secondary antibodies according to the manufacturer's instructions. Antibodies used were for phospho-p38 MAPK (Cell Signaling, #9211), p38 MAPK (Cell Signaling, #9212), SAPK/JNK (Cell Signaling, #9252), phospho-SAPK/JNK (Cell Signaling, #9251), ROCK2 (Thermo Fisher Scientific PA5-21131), phospho-ROCK2 (Thermo Fisher Scientific PA5-34895), and goat anti-rabbit conjugated to horseradish peroxidase (Abcam, ab6721). Membranes were imaged using an Amersham Imager 600 (GE Healthcare) using Clarity Western ECL Substrate (Bio-Rad). The intensity of protein

bands was quantified using ImageJ and standardized using total (phosphorylated + non-phosphorylated) protein content. Data are representative of three independent experiments.

Radioligand Displacement Assay

Displacement of radiolabelled peptide **2.1** was performed as described previously.[21] Briefly, RAW-Blue macrophage cells (InVivogen; San Diego, CA) were preincubated for 20 min with 100 µM of non-radiolabelled ("cold") peptide **2.1**, **2.5** or **2.6** followed by incubation for 2 h at 37 °C with [^{125}I]-peptide **2.1** and 600 nM concentration to ensure maximal specific binding.[21] Cells were washed four times with PBS buffer and lysed with 0.1 N NaOH/0.1% Triton X-100. Bound radioactivity was measured on cell lysates with a Hidex AMG gamma counter (Hidex; Turku Finland).

LPS-induced preterm model in mice

Timed-pregnant CD-1 mice at 16.5 days of gestation (G16.5) were anesthetized with 2% isoflurane and received an intraperitoneal injection of LPS (n = 4 per group, a single dose of 10 µg).[7, 38] A dosage of 2 mg/kg/day of peptide **2.1**, **2.5** or **2.6** or vehicle was injected subcutaneously in the neck, every 12 h until delivery. On G16.5, a dose of 1 mg/kg was injected 30 min before stimulation with LPS (to allow distribution of drugs to target tissues) and 1 mg/kg was injected 12 h after stimulation (n = 4 each treatment). Mice delivery was assessed every hour until term (G19–G19.5). A mouse is considered as delivering prematurely if the first pup is delivered earlier than G18.5.

Oxygen-induced retinopathy in Sprague Dawley rats

On P5, litters were transferred to a controlled hyperoxic environment (Biospherix OxyCycler A84XOV), maintained at 80±1% O_2, which is used to induce vaso-obliteration of the retinal vasculature. At this timepoint, the vasculature is immature and particularly susceptible to hypoxic insults resulting in vaso-obliteration, a defining characteristic of early stage of retinopathies in premature infants.[39] Control litters were not exposed to hyperoxia and were kept in standard conditions with room air (21% O_2). To control for the effects of hyperoxia on the lactation of the dams, dams of hyperoxic litters were switched with dams of control litters on P8.

In litters exposed to hyperoxia, pups were randomized to receive phosphate-buffered saline (PBS) vehicle, 2 mg/kg/day of peptides **2.1**, **2.5** or **2.6** or 3 mg/kg/day of Kineret from P5 to P10. These doses were determined from our previous study[11] and administered in twice-daily intra-

peritoneal injections titrated to 20 µL per injection with 28-gauge insulin syringes. A total of 6 to 8 pups were used for each treatment group.

On P10, pups were euthanized by decapitation under 2% isoflurane anesthesia. Eyes were enucleated and fixed in 4% paraformaldehyde for 1 h at room temperature before washing twice with PBS and storage at 4 °C in PBS until further processing.

Retinal Flatmount and Immunohistochemistry

Under a dissecting microscope, the cornea and lens were removed from the eyes gently and remnants of the hyaloid vasculature were removed from the retinas using surgical scissors and tweezers. The retinas were gently removed from the underlying sclera and choroid.

Retinas were treated at room temperature for 1 h with a blocking solution consisting of 1% bovine serum albumin (BSA), 1% normal goat serum, 0.1% Triton X-100 and 0.05% Tween-20 in PBS. The retinas were then double-labelled overnight at 4 °C with gentle shaking in an antibody solution consisting of 1 mM $CaCl_2$, 1% Triton X-100, 1% TRITC-conjugated lectin cell endothelial marker from *Bandeiraea simplicifolia* (Sigma-Aldrich, St Louis, MO) and a 1:500 dilution of rabbit anti-Iba-1 antibody (Wako Chemicals USA) in PBS. The retinas were then washed thrice with PBS and incubated with a secondary antibody solution consisting of 1% BSA, 0.1% Triton X-100, 0.05% Tween-20 and 1:500 Alexa-594-conjugated donkey anti-rabbit IgG (ThermoFisher Scientific, Rockford, IL) in PBS for 2 h at room temperature. Retinas were washed thrice with PBS and then flat-mounted onto glass slides with coverslips and Fluoro-Gel mounting medium (Electron Microscopy Sciences, Hatfield, PA).

Microscopy

For assessment of vaso-obliteration, retinas were imaged using an epifluorescence microscope at 10X magnification (Zeiss AxioImager Z2) and version 4.8 of the AxioVision software. Images were captured and stitched together using the software's MosaiX feature. Ionized calcium-binding adapter molecule (Iba)-1 staining was assessed with the same microscope at 20X magnification, and a total of 4 fields per retina were imaged halfway between the optic nerve and the edge of the retina.

Representative images of Iba-1 staining were taken using a laser scanning confocal microscope (Olympus IX81 with Fluoview FV1000 Scanhead) with the Fluoview Software at 30X magnification.

Quantification and Data Analysis

The FIJI software was used to the quantify the area of vaso-obliteration in each retina, expressed as a percentage of the area of the whole retina. The number of Iba-1-positive cells was counted using the cell counter plug-in in FIJI, and the average of cell counts in 4 fields per retina was calculated.

Data was analyzed using GraphPad Prism 7 with one-way ANOVA and the Dunnett's test for multiple comparisons. Outliers were detected using Grubb's test. Results were treated as significant when p was less than 0.05 and expressed as mean ± SEM.

Results

Chemical Synthesis

The application of lactam-bridged dipeptides by Freidinger, Veber, Hirschmann and coworkers at Merck Sharp and Dohme Research Laboratories in the early 1980s marked an important milestone in the use of heterocycle synthesis to design constrained peptide mimics.[1, 29, 40] Such so-called Freidinger-Veber lactams (e.g., Agl and Hgl) restrict backbone conformation by limiting rotation about the ϕ-, ψ- and ω-dihedral angles such that Agl and Hgl residues prefer to situate at the i+1 residue in β-turn sequences contingent on sequence stereochemistry.[2, 40] Moreover, in the case of Hgl, the hydroxyl group side chain orientation is locked due to restriction of the χ-dihedral angle.[41] Although Freidinger-Veber lactams have been used to study a wide range of biologically active peptides,[40] to the best of our knowledge, the application of all stereoisomers of the heterocyclic dipeptide in a sequence has yet to be explored.

The syntheses of all four Agl-Val and eight Hgl-Val diastereomers of peptide **2.1** (e.g., **2.5** and **2.6**) were performed by approaches featuring preparation of the *N*-Fmoc-dipeptides in solution, followed by their incorporation into the final peptides using solid-phase peptide synthesis. Although effective means for introducing Agl and Hgl residues directly on solid phase have been developed,[3-5, 35, 37, 42] the construction of dipeptide building blocks in solution prior to coupling on resin was selected to ensure significant amounts of each isomer for biological studies, as well as to minimize concerns of epimerization during peptide assembly. The *N*-Fmoc-Agl-Val-OH dipeptide building blocks **2.7** were synthesized by extension of the original method for Agl residue assembly featuring alkylation of the thioether of *N*-Boc-methionyl dipeptide ester, followed by intramolecular displacement of the resulting sulfonium ion under basic conditions.[1, 29] As illustrated for the synthesis of *N*-Fmoc-(*R*)-Agl-(*R*)-Val-OH [(*RR*)-**2.7**, Figure 2.2], *N*-Boc-

D-methionine **2.8** was coupled to *tert*-butyl (*R*)-valinate **2.9** using DCC, HOBT and triethylamine to provide protected dipeptide **2.10** in 78% yield. The lactam was installed by *S*-alkylation using methyl iodide followed by intramolecular *N*-alkylation using sodium hydride to furnish *N*-Fmoc-(*R*)-Agl-(*R*)-Val-O*t*-Bu **2.11** in 58% yield.[1, 29] Subsequently, the acid labile carbamate and ester groups were removed using a 50% solution of TFA in DCM, and amine acylation was performed using Fmoc-OSu and sodium carbonate to provide dipeptide **7** for solid-phase synthesis. The other three diastereomers of **2.7** were respectively synthesized using different enantiomers of **2.8** and **2.9**, such that all four dipeptide building blocks were obtained in 26-32% overall yields from L- and D-methionine (Figure 2.2).
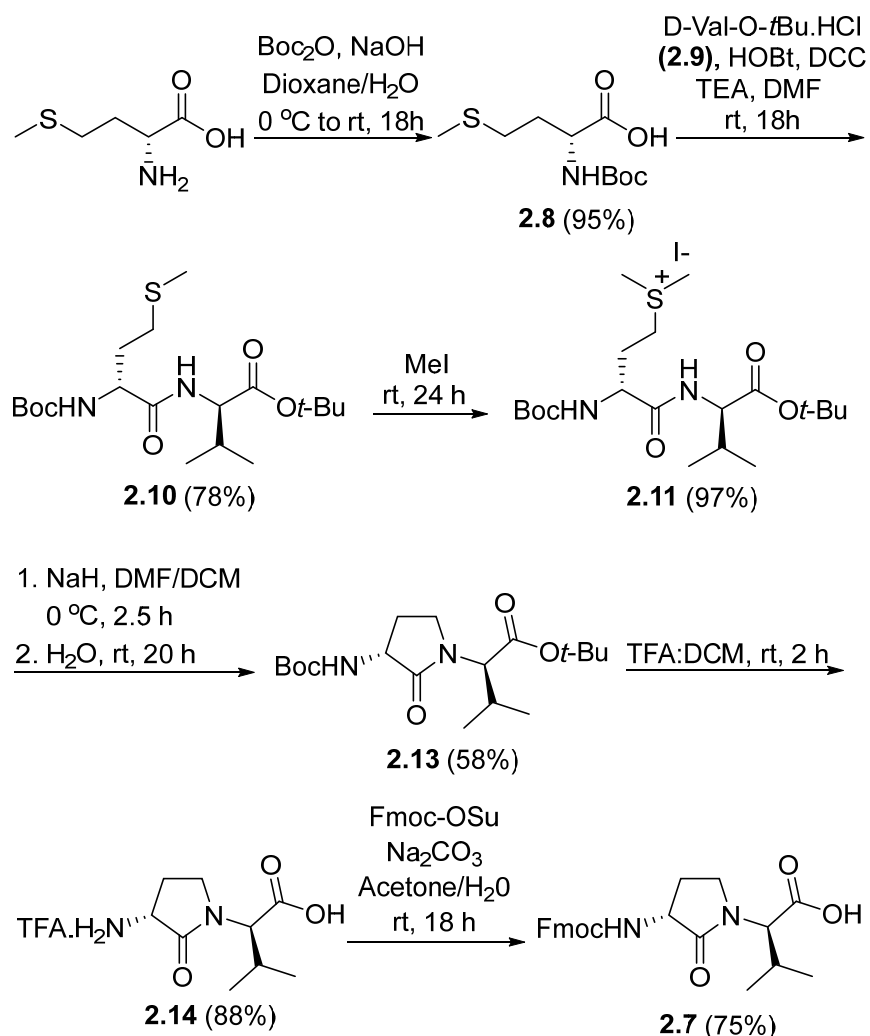
Figure 2.2. Synthesis of α-amino-γ-lactam (Agl) using protected (*R*)-methionine-(*R*)-valine dipeptide

Chapter 3

The synthesis of Hgl peptides in solution and on solid phase has been accomplished using oxiranyl glycine.[3, 37] For preparation of *N*-Fmoc-Hgl-Val-OH diastereomers **2.12** possessing the *trans*-lactam residue, oxiranyl glycines (2*R*,3*R*)- and (2*S*,3*S*)-**2.18** were prepared from *N*-Fmoc-D- and L-methionine methyl esters (*R*- and *S*-**2.15**) using a modification of the reported three-step protocol in which *N*-Fmoc-vinylglycine methyl ester **2.17** was synthesized by a flow process featuring elimination of *N*-Fmoc-methionine sulfoxide methyl ester **2.16** using 2,4-dichlorotoluene at 200 °C, and epoxidation of olefin **2.17** was performed by microwave irradiation using *m*-CPBA in toluene at 80 °C (Figure 2.3). Epoxide (2*R*,3*R*)-**2.18** was reacted with *tert*-butyl (*R*)-valinate **2.9** using catalytic amount of benzoic acid and trifluoroethanol under microwave irradiation at 80 °C for 90 min to provide *N*-Fmoc-(2*R*,3*S*,2'*R*)-Hgl-D-Val-O*t*-Bu [(2*R*,3*S*,2'*R*)-**2.19**] in 89% yield. A Mitsunobu approach was employed for the synthesis of the *cis*-Hgl isomers by inversion of the alcohol stereochemistry of their *trans*-counterparts.[36] *tert*-Butyl esters **2.19** were converted to the corresponding acids **2.12** using 1:1 TFA/DCM. Employing the respective (2*R*,3*R*)- and (2*S*,3*S*)-diasteromers of epoxide **2.18** and enantiomers of valine **2.9**, the *trans*- and *cis*-Hgl dipeptide diasteromers **2.12** were respectively synthesized in 84% and 83% yields.

Chapter 3
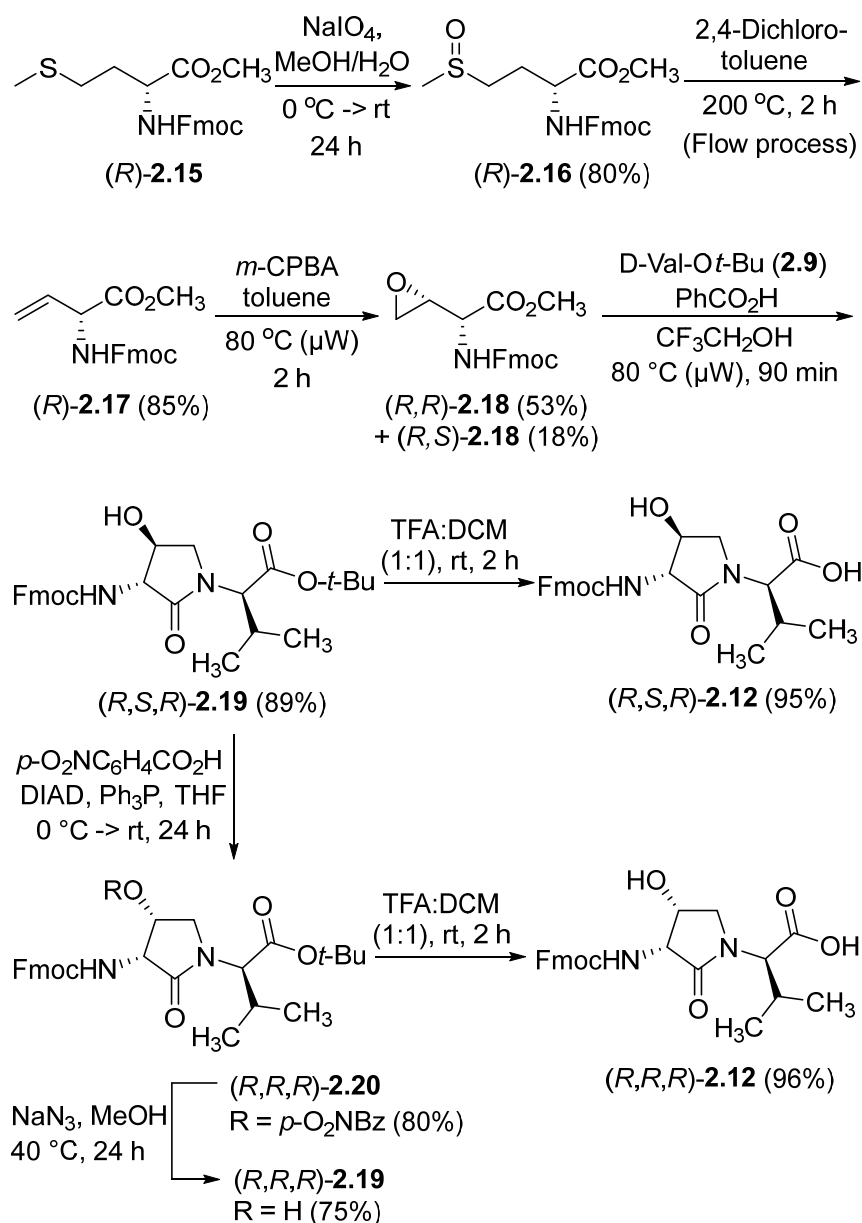
Figure 2.3. Synthesis of β-hydroxy-α-amino-γ-lactams (Hgl) dipeptides using *N*-(Fmoc)oxiranylglycine

With Agl and Hgl dipeptide diastereomers **2.7** and **2.12** in hand, the syntheses of the respective [Agl³]- and [Hgl³]-**2.1** peptides (**2.5** and **2.6**) were performed using standard Fmoc-based solid-phase synthesis on Rink amide resin (Figure 2.4).[43]
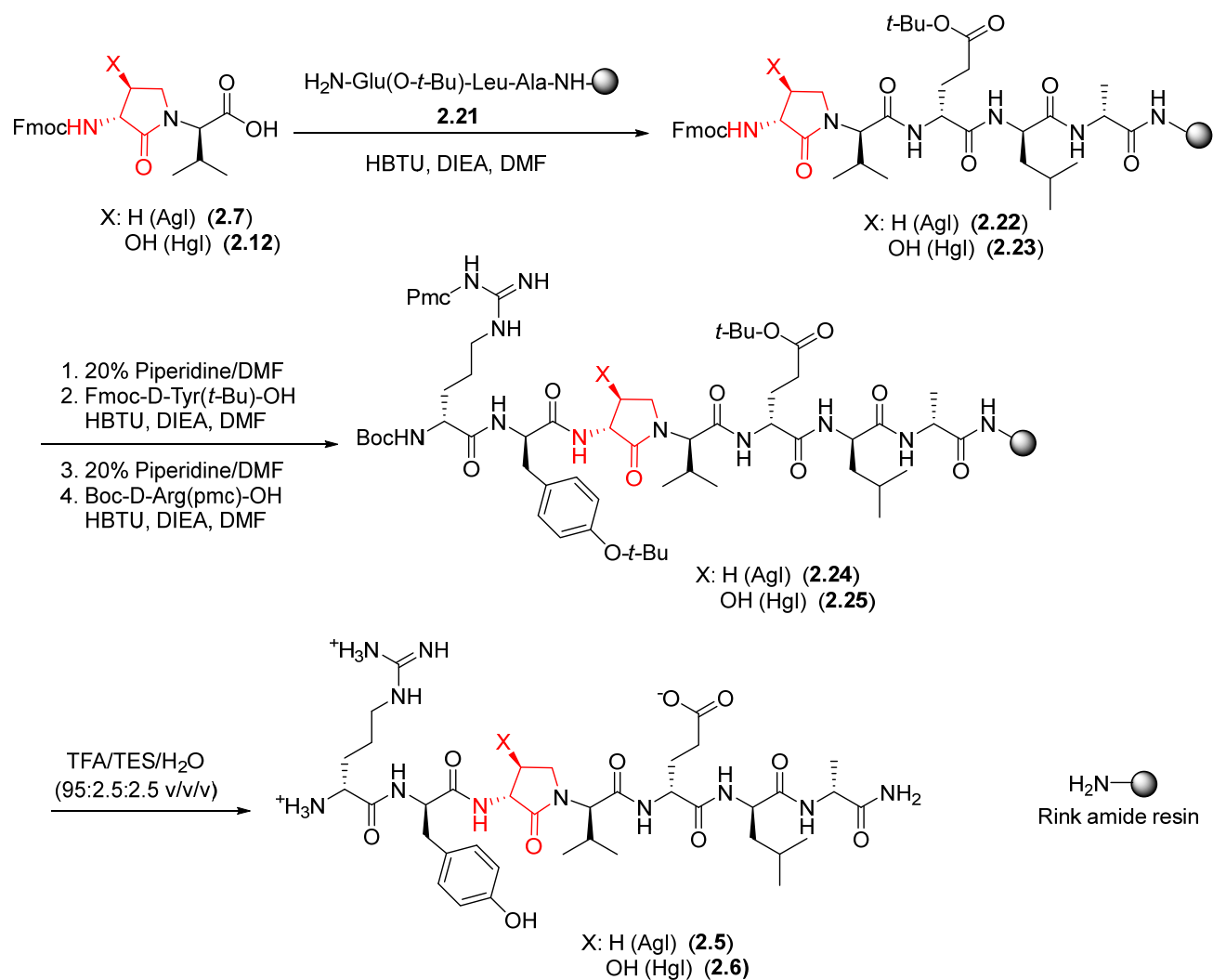
Figure 2.4. Representative protocols for solid-phase synthesis of Agl and Hgl peptides **2.5** and **2.6**

To *O-tert*-butyl D-glutamyl-D-leucinyl-D-alanine Rink amide resin **2.19**, the respective Agl and Hgl dipeptides **2.7** and **2.12** were coupled using HBTU, DIEA and DMF to give the corresponding resin-bound pentapeptides **2.20** and **2.21**. Subsequent removals of the Fmoc protection were performed using 20% piperidine in DMF, and peptide elongation was completed by sequential couplings of *N*-Fmoc-*O-tert*-butyl-tyrosine and *N*-Boc-*N*-Pmc-arginine using HBTU and DIEA in DMF to give respectively the protected heptapeptide resins **2.22** and **2.23**. Resin cleavage was performed using a cocktail of 95:2.5:2.5 TFA/H₂O/TES to furnish peptides **2.5** and **2.6** in 35-69% purities. Purification by HPLC provided peptides **2.5** and **2.6** in 8-16% overall yields (Table 2.2).

Table 2.2. Retention times, crude purity, final purity, yields and mass spectrometric data for Agl and Hgl peptids **2.5** and **2.6**

compd	RT (min)		crude purity %	final purity at 280 nm %	yield % (>95 %)	HRMS [M+1] in MeOH	
	CH₃OH	CH₃CN				m/z (calcd)	m/z (obsd)
[(3*R*)-Agl³]-**2.1**, [(3*R*)-**2.5**]	8	5.6	44	>99	12	832.4676	832.4682
[(3*R*, 4*R*)-Hgl³]-**2.1**, [(3*R*, 4*R*)-**2.6**]	7.8	5.4	42	>99	8	848.4625	848.4525
[(3*R*, 4*S*)-Hgl³]-**2.1**, [(3*R*, 4*S*)-**2.6**]	7.5	5.2	69	>99	14	848.4625	848.4573
[(3*R*)-Agl³-(*S*)-Val]-**2.1**, [(3*R*, 2'*S*)-**2.5**]	7.6	5.3	63	>97	16	832.4676	832.4687
[(3*R*, 4*R*)-Hgl³-(*S*)-Val]-**2.1**, [(3*R*, 4*R*, 2'*S*)-**2.6**]	6.8	4.9	55	>99	13	848.4625	848.4629
[(3*R*, 4*S*)-Hgl³-(*S*)-Val]-**2.1**, [(3*R*, 4*S*, 2'*S*)-**2.6**]	6.9	4.9	52	>99	13	848.4625	848.4529
[(3*S*)-Agl³]-**2.1**, [(3*S*)-**2.5**]	8	5.4	42	>99	15	832.4676	832.4680
[(3*S*, 4*R*)-Hgl³]-**2.1**, [(3*S*, 4*R*)-**2.6**]	7.8	5.4	42	>99	11	848.4625	848.4625
[(3*S*, 4*S*)-Hgl³]-**2.1**, [(3*S*, 4*S*)-**2.6**]	7.3	5.2	35	>99	9	848.4625	848.4627
[(3*S*)-Agl³-(*S*)-Val]-**2.1**, [(3*S*, 2'*S*)-**2.5**]	7.9	5.5	56	>99	13	832.4676	832.4676
[(3*S*, 4*R*)-Hgl³-(*S*)-Val]-**2.1**, [(3*S*, 4*R*, 2'*S*)-**2.6**]	7	4.9	39	>99	12	848.4625	848.4618
[(3*S*, 4*S*)-Hgl³-(*S*)-Val]-**2.1**, [(3*S*, 4*S*, 2'*S*)-**2.6**]	6.6	5.2	45	>99	12	848.4625	848.4635

Isolated purity ascertained by LC-MS using gradients of 10−90% A [H₂O (0.1% FA)/MeOH (0.1% FA)] or B [H₂O (0.1% FA)/MeCN (0.1% FA)] over 14 min.

Circular Dichroism Spectra

Understanding the relationships between the preferred conformations of peptides **2.1**, **2.5** and **2.6** and their modulator activity is critical towards the design of improved prototypes with therapeutic potential. In the absence of crystallographic data of their complex with IL-1R, circular dichroism (CD) spectroscopy of peptides **2.1**, **2.5** and **2.6** in water were first measured to begin examining the influences Agl-Val and Hgl-Val dipeptide configuration on conformation. The conformers in water represent likely the geometry that binds initially the receptor. Restraint that pre-organizes a favorable binding conformer may facilitate molecular recognition by diminishing the entropy costs for folding.

The CD spectrum of the parent peptide **2.1** exhibited a curve shape characteristic of a disordered random coil structure (Figure 2.5). Contingent on stereochemistry certain Agl and Hgl analogs exhibited CD spectroscopic curve shapes characteristic of ideal *β*-turn peptides. For example, analogs with *R,R*-backbone conformation including [(3*R*)-Agl³]-, [(3*R*,4*R*)-Hgl³]- and [(3*R*,4*S*)-Hgl³]-**2.1**, all exhibited negative and positive maximum, that were respectively observed at 198-207 and 221-227 nm indicative of a *β*-turn conformation (Figure 2.5).[44-45] Inversion of the stereochemistry of both backbone centers in [(3*S*)-Agl³-(*S*)-Val⁴]-, [(3*S*,4*S*)-Hgl³-(*S*)-Val⁴]- and

[3*S*,4*R*]-Hgl[3]-(*S*)-Val[4]]-**2.1** gave similar but inverted curve shapes typical of *β*-turn conformers with notably greater ellipticity.[45] On the other hand, among the Agl and Hgl analogs with mixed backbone stereochemistry, only [(3*R*,4*S*)-Hgl[3]-(*S*)-Val[4]]-**2.1** exhibited a curve shape indicative of a *β*-turn conformer.[45] A similar *β*-turn conformer curve shape was observed in CD spectra of [(3*R*,4*S*)-Hgl[3]]-**2.1** examined in trifluoroethanol (TFE), MeOH and hexafluoroisopropanol (HFIP), and the greatest ellipticity was seen in 5% TFE in water.
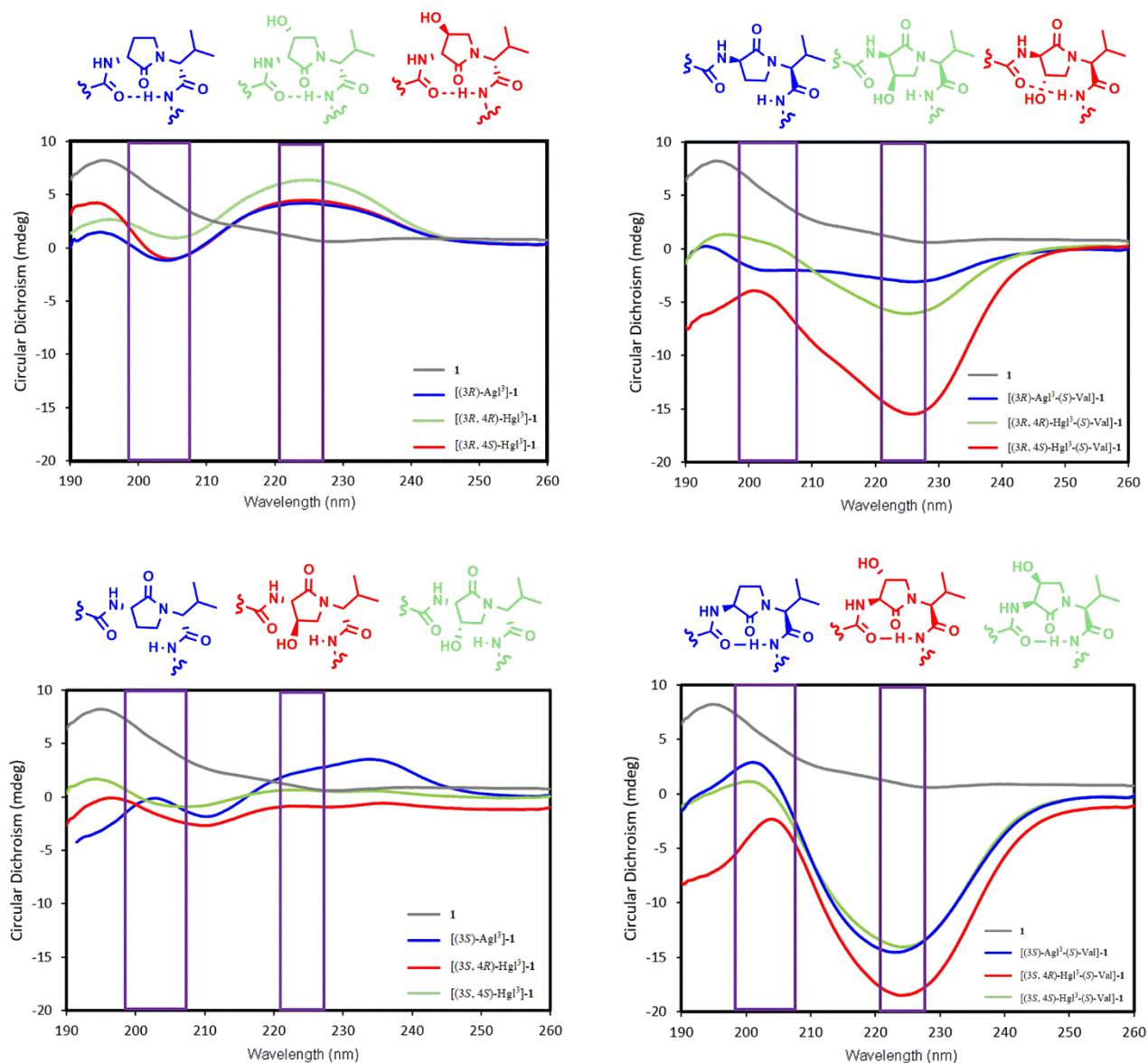
Figure 2.5. The molar ellipticity circular dichroism spectra of peptides **2.1**, **2.5** and **2.6**.

Chapter 3

In vitro inhibition of signaling pathways

The biological effects of peptide **2.1** and derivatives were ascertained *in vitro* in RAW-blue and HEK-blue cells which were stimulated with IL-1β. The QUANTI-blue assay was employed to measure concentrations of secreted alkaline phosphatase, a reporter product from the transcription of the NF-κB gene. All peptides that were tested did not exhibit any noticeable inhibition of NF-κB signaling (Figure 2.6). On the other hand, Kineret, which is an FDA-approved recombinant IL-1 receptor antagonist, inhibited NF-κB as previously reported.[7]
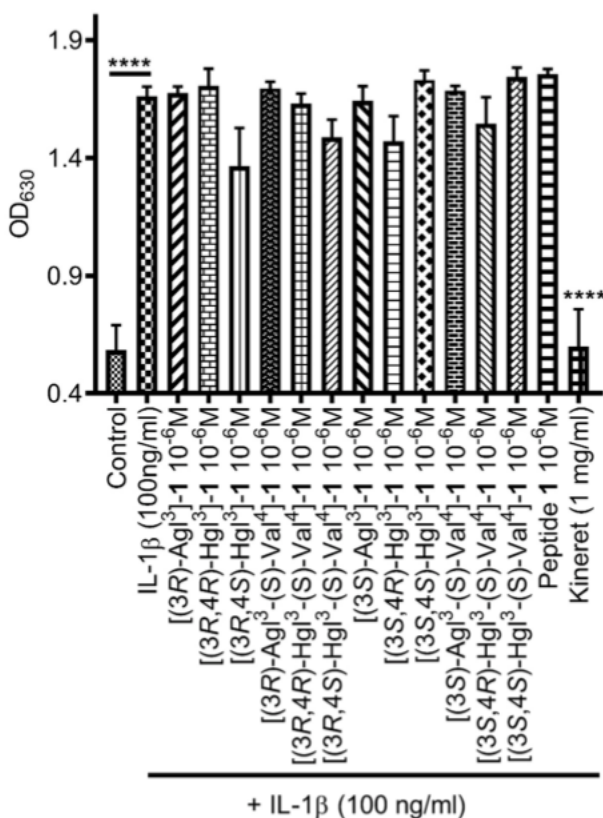
Figure 2.6. The effects of peptides 2.1, 2.5 and 2.6 on IL-1-induced NF-κB signaling. NF-κB activation was quantified on HEK-blue cells using the QUANTI-blue assay, which spectroscopically detects secreted alkaline phosphatase, a reporter product from the transcription of the NF-κB gene. HEK-blue cells were pre-incubated with peptides **2.1**, **2.5** and **2.6** or vehicle, then stimulated with IL-1β for 4 h. Data shown represents the average of 3 experiments, n = 6 each. **** $p < 0.0001$ compared to group treated only with IL-1β. Treatment groups that are not labelled with asterisks are statistically non-significant compared to group treated only with IL-1β.

Western Blots were performed to measure phosphorylation of downstream c-Jun *N*-terminal kinases (JNK), p38 mitogen-activated protein kinases (p-38) and Rho-associated, coiled-coil-containing protein kinase 2 (ROCK2) in RAW-blue cells, after pre-incubation with peptides **2.1**, **2.5** or **2.6** and stimulation with IL-1β (Figure 2.7). In contrast to peptide **2.1** which inhibited the effects of all three kinases, the Agl and Hgl analogs exhibited biased signaling contingent on stereochemistry and structure. For example, JNK phosphorylation was inhibited more profoundly by (*R*)- than (*S*)-Val^4 derivatives **2.5** and **2.6**. In the (*R*)-Val series, the Agl and *trans*-Hgl isomers were more effective than the *cis*-Hgl counterparts. Phosphorylation of p-38 was inhibited most effectively by [(3*R*,4*S*)-Hgl^3]- and [(3*R*)-Agl^3-(*S*)-Val^4]-**2.1**; [(3*S*)-Agl^3]-, [(3*R*)-Agl^3]-, [(3*R*,4*R*)-Hgl^3]- and [(3*S*,4*S*)-Hgl^3-(*S*)-Val^4]-**2.1** were inactive. Finally, ROCK2 phosphorylation was inhibited significantly (*p*<0.05) by most derivatives, except for [(3*S*)-Agl^3-(*R*)-Val^4]- and [(3*R*)-Agl^3-(*R*)-Val^4]-**2.1**. In contrast to peptide **2.1** which inhibited effectively all three kinases, the inhibitory activity of the Agl and Hgl derivatives was contingent on configuration and the presence of the hydroxyl group. Conversely, these factors did not play a role in NF-κB signaling, which was universally unaffected by all derivatives **2.5** and **2.6**.

Chapter 3
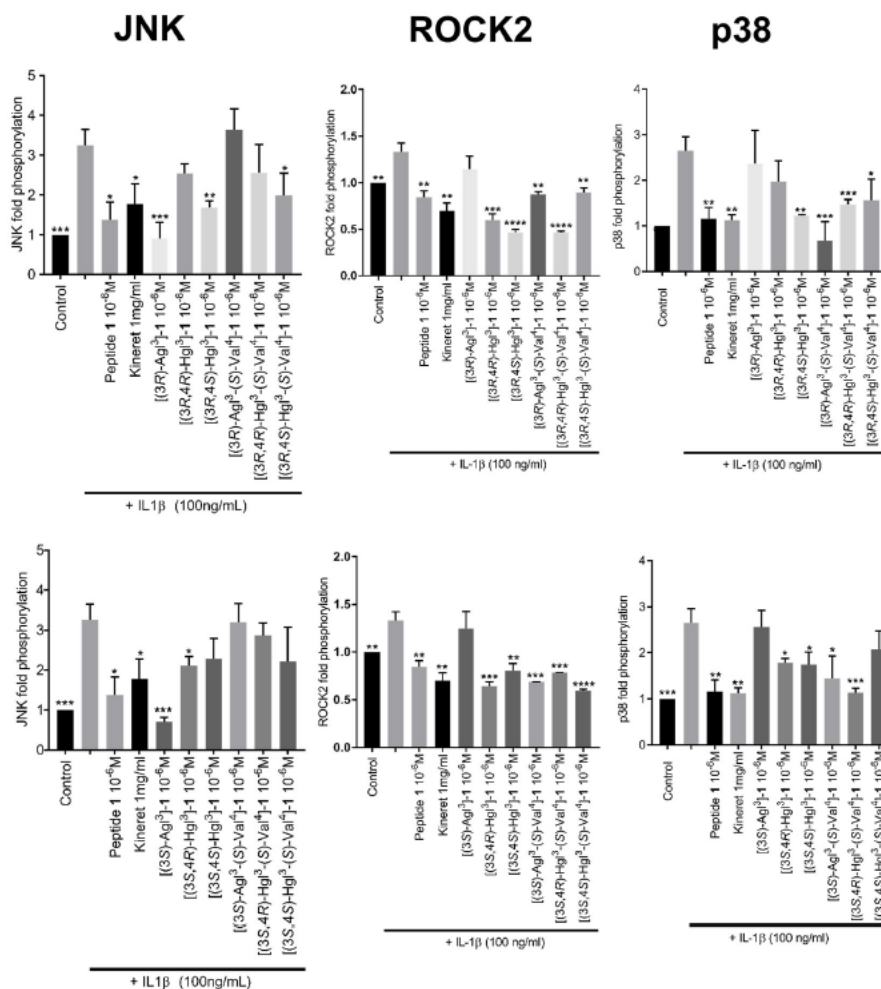
Figure 2.7. **The effects of peptides 2.1, 2.5, and 2.6 on IL-1β-induced phosphorylation of JNK, ROCK2 and p38.** Graphical representations of band density analysis of Western Blots, sorted into columns based on protein of interest (JNK, ROCK2, or p38) and rows by peptide configuration ((3*R*- or (3*S*)). RAW-blue cells were pretreated with peptides **2.1**, **2.5**, **2.6**, Kineret, or vehicle for 30 min and then stimulated with IL-1β for 15 min. Images of representative Western Blots can be found in the Supplementary Figures. Results shown are the average of 3 independent experiments: *$p<0.05$, **$p<0.01$, ***$p<0.001$, **** $p<0.0001$ compared to group treated only with IL-1β. Treatment groups that are not labelled with asterisks are statistically non-significant compared to group treated only with IL-1β.

The effects of peptides **2.1**, **2.5** and **2.6** on the transcription of downstream pro-inflammatory genes that are mediated by IL-1β were measured with focus on IL-6, cyclooxygenase-2 (COX2) and IL-1β, which positively increases expression of itself.[46] Quantitative polymerase chain reaction (qPCR) experiments were performed on HEK blue cells

to ascertain the expression levels of the mRNA transcripts after pre-treatment with peptides **2.1**, **2.5** and **2.6** and stimulation with IL-1β. Parent peptide **2.1** exhibited strong suppression of transcription of all three genes. Moreover, Agl and Hgl analogs of **2.1** maintained similar inhibitory potency as the parent peptide (Figure 2.8). On the other hand, ability to suppress the transcription of all three genes was lost in [(3*R*)-Agl^3-(*S*)-Val^4]- and [(3*S*)-Agl^3-(*S*)-Val^4]-**2.1** and recovered in part in certain Hgl^3-(*S*)-Val^4 analogs with [(3*S*, 4*S*)-Hgl^3-(*S*)-Val^4]-**2.1** exhibiting ability to inhibit the expression of all three genes.
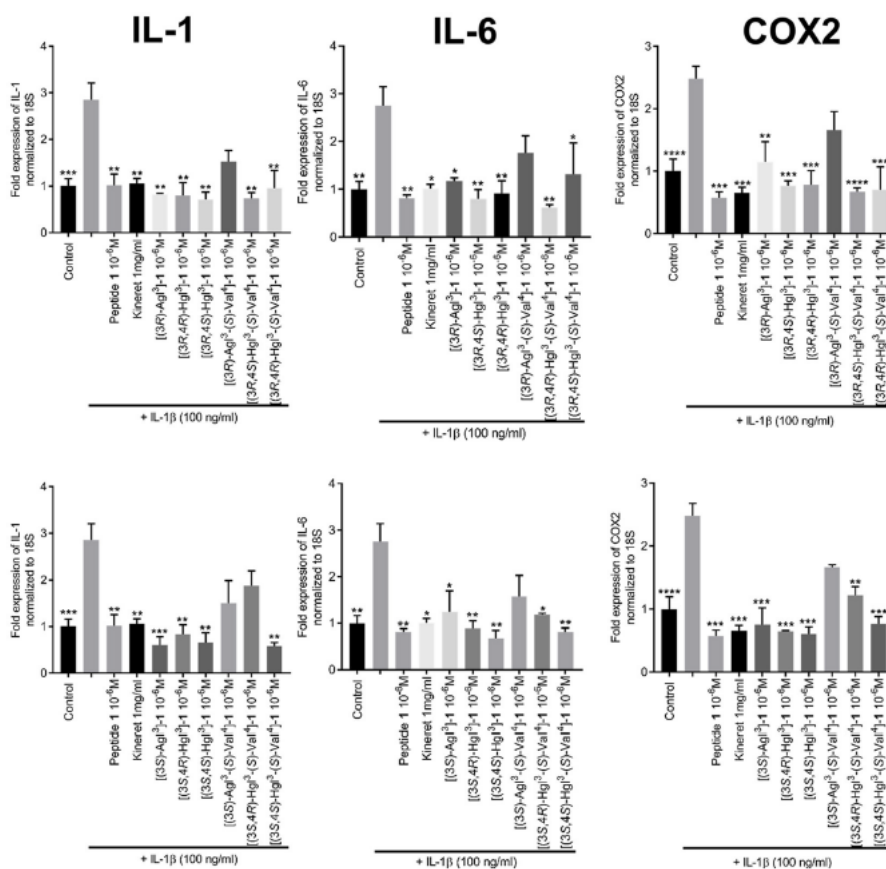
Figure 2.8. The effects of peptides 2.1, 2.5 and 2.6 on the expression of pro-inflammatory genes. HEK-Blue cells were pre-treated with peptides **2.1**, **2.5** and **2.6** as above and stimulated with IL-1β overnight. qPCR was performed on cell lysates using 18S rRNA as internal control. Graphs are sorted in columns by gene of interest (COX-2, IL-1β or IL-6) and rows by peptide configuration ((3*R*) or (3*S*)). Results are representative of an average of 3 independent experiments and are expressed as a fold-change of the non-stimulated control: *$p<0.05$, **$p<0.01$, ***$p<0.001$,

****$p<0.0001$ compared to group treated only with IL-1β. Treatment groups that are not labelled with asterisks are statistically non-significant compared to group treated only with IL-1β.

Displacement of radiolabeled peptide 2.1

Peptide **2.1** is known to bind to IL-1R.[21] To determine if the Agl and Hgl derivatives occupied the same binding site as peptide **2.1**, a radio-ligand displacement assay was used to determine the extent to which peptides **2.5** and **2.6** displaced radiolabelled **2.1**. Compared to cold unlabelled peptide **2.1**, which was used to set the baseline for specific binding, similar capacity to displace [^{125}I]-**2.1** was demonstrated by peptides **2.5** and **2.6**, except for [(3*R*,4*S*)-Hgl^3]-**2.1**, which exhibited significantly lower ($p = 0.0011$) ability to compete with radiolabelled peptide **2.1** (Table 2.3).

Table 2.3. The ability of peptides 2.1, 2.5 and 2.6 to displace radio-labelled [^{125}I]-2.1 in RAW-blue cells.

Compound	Percentage of displacement of [^{125}I]-**2.1**, relative to unlabeled peptide **2.1**, ± SEM	*p*-value
[(3*R*)-Agl^3]-**2.1**	83.55±9.02	0.9908
[(3*R*,4*S*)-Hgl^3]-**2.1***	32.13±16.94	*0.0011*
[(3*R*,4*R*)-Hgl^3]-**2.1**	104.6±6.826	0.9997
[(3*R*)-Agl^3-(*S*)-Val^4]-**2.1**	120.7±15.69	0.954
[(3*R*,4*S*)-Hgl^3-(*S*)-Val^4]-**2.1**	58.63±13.45	0.0724
[(3*R*,4*R*)-Hgl^3-(*S*)-Val^4]-**2.1**	82.12±14.12	0.9308
[(3*S*)-Agl^3]-**2.1**	106.6±12.39	0.9996
[(3*S*,4*R*)-Hgl^3]-**2.1**	78.64±21.22	0.9428
[(3*S*,4*S*)-Hgl^3]-**2.1**	69.73±8.897	0.2864

[(3S)-Agl^3-(S)-Val^4]-**2.1**	102.7±8.637	0.9999
[(3S,4R)-Hgl^3-(S)-Val^4]-**2.1**	48.32±21.13	0.0649
[(3S,4S)-Hgl^3-(S)-Val^4]-**2.1**	86.06±6.46	0.9806

* $p < 0.05$ relative to cold peptide **2.1**-treated group

In vivo inhibition of preterm labor

The spectrum of *in vitro* profiles exhibited by peptides **2.5** and **2.6** offers a unique means for probing the specific signaling pathways that contribute to the therapeutic potential of IL-1R modulators. Peptides **2.1**, **2.5** and **2.6** were first examined in an established CD-1 mouse model of preterm birth (PTB, Figure 2.9A), featuring induction on administration of lipopolysaccharide (LPS) by intraperitoneal injection into pregnant dams on day 16.5 of gestation. The Agl and *trans*-Hgl analogs of peptide **2.1** exhibited equal potency as the parent peptide in delaying labor (Figure 2.9B). On the other hand, *cis*-Hgl derivatives of peptide **2.1** and (S)-Val peptides **2.5** and **2.6** exhibited little efficacy.
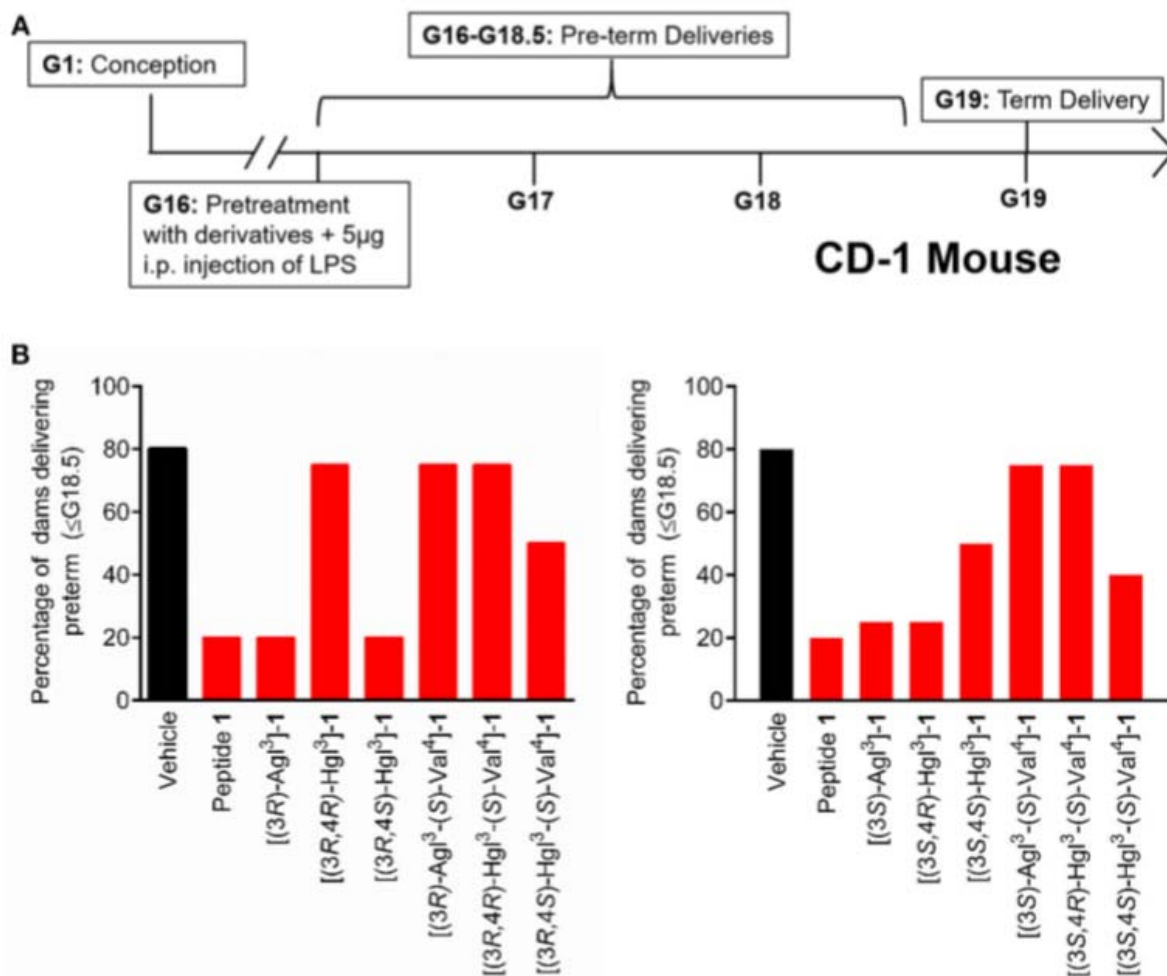
Figure 2.9. The effects of peptides 2.1, 2.5 and 2.6 on prevention of PTB. (A) Schematic of the CD-1 mouse PTB model. In brief, pregnant dams on day 16.5 of gestation (G16.5) were subcutaneously pretreated with peptides **2.1**, **2.5** and **2.6** or vehicle, followed by LPS, and observed for delivery of pups. A dam was considered as delivering preterm if at least one pup was delivered before G18.5. **(B)** The rates of PTB in dams treated with peptides **2.1**, **2.5** and **2.6** are grouped into (3*R*)- (left) and (3*S*)- (right) derivatives; n = 4-5 dams per treatment group.

In vivo inhibition of vaso-obliteration in oxygen-induced retinopathy

A model of oxygen-induced retinopathy was next used to examine peptide **2.1** and a subset of analogs **2.5** and **2.6** that were previously tested in the PTB model: e.g., [(3*S*)-Agl^3]-, [(3*R*)-Agl^3]-, [(3*S*,4*R*)-Hgl^3]- and [(3*R*,4*S*)-Hgl^3]-**2.1** which exhibited the best activity, [3*S*,4*S*-Hgl^3]-**2.1** which had partial efficacy and [3*S*,4*R*-Hgl^3-(*S*)-Val^4]-**2.1**, which was inactive in delaying labor.

Exposure of rat pups to 80% oxygen from days 5 to 10 of life resulted usually in vaso-obliteration of ~35% of the retinal capillaries, extending radially from the optic nerve (Figure

2.10A and 2.10B). Peptide **2.1** and Kineret, both diminished the extent of vaso-obliteration to 15-20% (Figure 10B) (Rivera 2013). Among the four peptides that were strongly effective in the PTB model, only two, [3R,4S-Hgl[3]]- and [3S,4R-Hgl[3]]-**2.1** exhibited efficacy in the OIR model and reduced vaso-obliteration to 15-25%. Furthermore, [3S,4S-Hgl[3]]-**2.1**, which was moderately effective (~50% efficacy) in the PTB model, demonstrated efficacy in reducing vaso-obliteration to somewhat less extent than peptide **2.1**. On the other hand, [(3S,4R)-Hgl[3]-(S)-Val[4]]-**2.1**, which had no effect in the PTB model, was also ineffective in curbing vaso-obliteration.
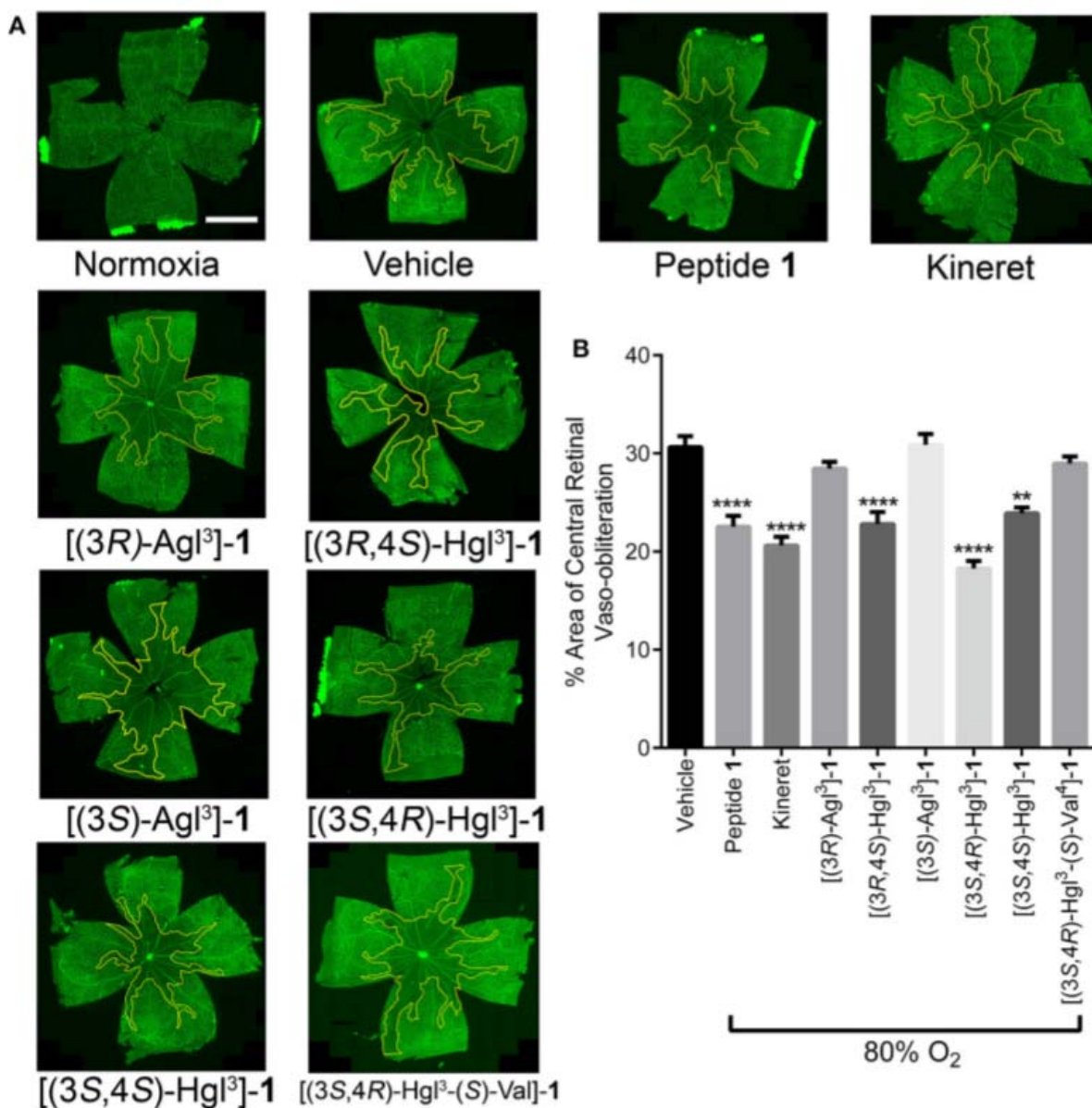
Figure 2.10. The preventive effects of peptides 2.1, 2.5 and 2.6 against vaso-obliteration in an OIR model. Five-day old Sprague Dawley pups and their mothers were kept in 80% oxygen until

the tenth day of life, receiving twice-daily intraperitoneal injections of peptides **2.1**, **2.5** and **2.6** (2mg/kg/day), Kineret (15mg/kg/day) or PBS vehicle (each injection was titrated to a volume of 20 µL). **(A)** Representative retinal flatmounts stained with FITC-conjugated *Bandeiraea simplicifolia* lectin, taken at 10X magnification and stitched with MosaiX in Axiovision 4.8. Yellow lines indicate the central area of vaso-obliteration extending from the optic nerve (centre of each retina), scale bar 2 mm. **(B)** Quantification of area of vaso-obliteration performed using ImageJ, expressed as a percentage of the total retinal area: n = 5-7 of peptides **2.5** and **2.6** and Kineret, n = 10-12 for vehicle and peptide **2.1**; **$*p<0.01$, ****$*p<0.0001$ relative to the vehicle group. Treatment groups that are not labelled with asterisks are statistically non-significant compared to the vehicle group.

Immuno-histochemical staining for Iba-1 was used to assess microglial activation and density, because microglia have been shown to be mediators of vaso-obliteration in the context of OIR.[11] Microglia morphology has been observed to change at different states of activation: microglia that are inactive and ramified possess numerous branches, which were observed in retina under normoxia and after treatment with peptide **2.1** (Figure 2.11A); on the other extreme, activated microglia retract their limbs and become amoeboid,[47] as observed in vehicle-treated retina under hypoxia. Peptides [(3S,4R)-Hgl^3]-, [(3R,4S)-Hgl^3]- and [(3S,4S)-Hgl^3]-**2.1** prevented partially the activation of microglia; [(3S)-Agl^3]-, [(3R)-Agl^3]- and [(3S,4R)-Hgl^3-(S)-Val^4]-**2.1** had no appreciable effect on microglial morphology (Figure 2.11A). Quantification of microglial density revealed similar trends (Figure 2.11B), except for [(3S)-Agl^3]-**2.1**, which modestly (<20%) reduced microglial density despite not influencing microglial morphology. Peptides **2.1**, **2.5** and **2.6**, which prevented microglia activation, caused a statistically significant reduction in vaso-obliteration area. In summary, certain [Hgl^3]-**2.1** analogs behaved like the parent peptide and exhibited protection against vaso-obliteration in the hyperoxic phase of OIR, due in part to mitigation of microglial activation.
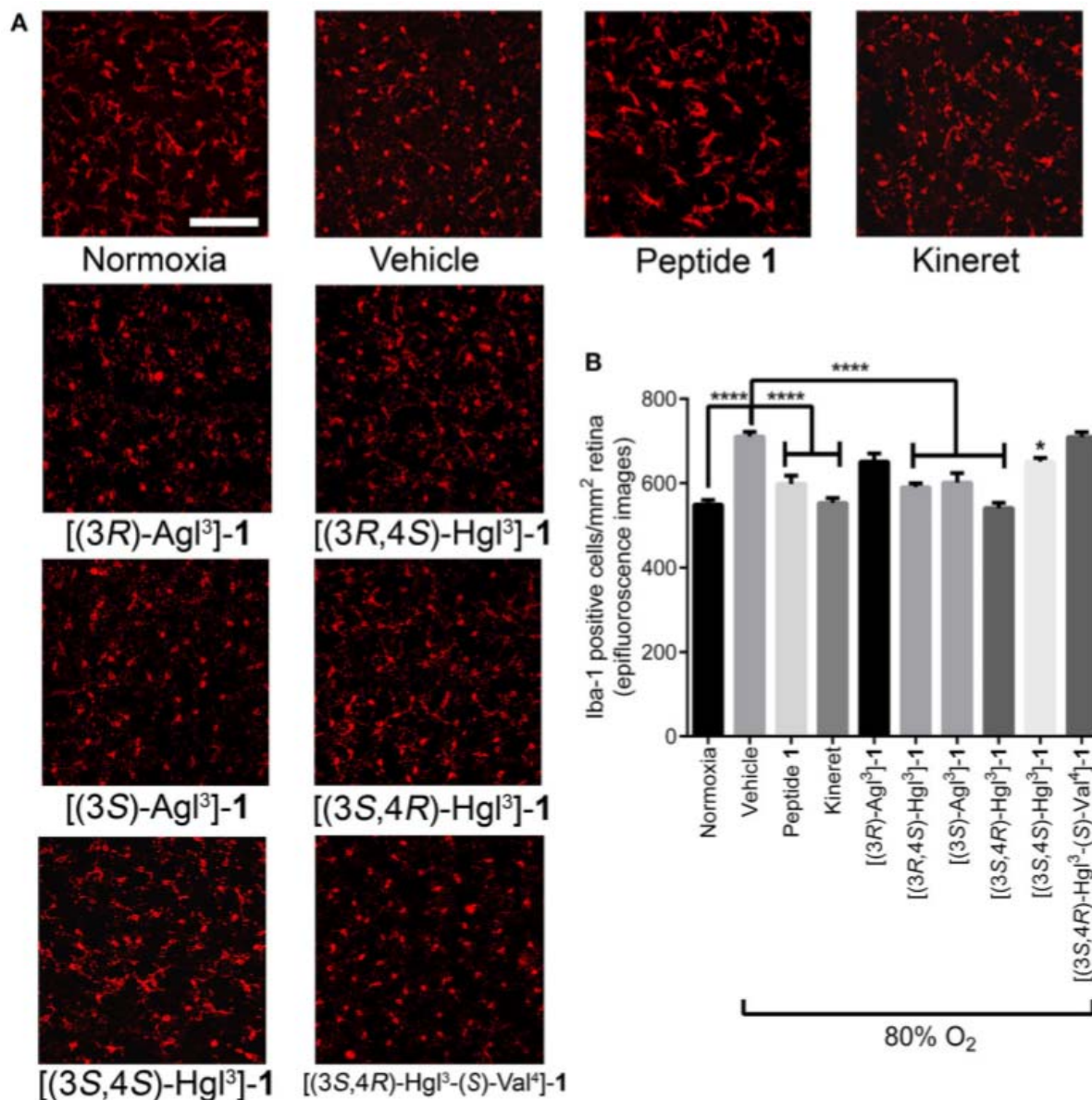
Figure 2.11. The effects of peptides 2.1, 2.5 and 2.6 on retinal microglial activation and density. Retinas were obtained for immunohistochemistry from rat pups treated with the OIR protocol, and incubated with rabbit anti-iba-1 antibody, followed by donkey anti-rabbit antibody conjugated to Alexa 594. **(A)** Representative confocal images of retinal microglia at 30X magnification: scale bar 100 μm. **(B)** Epifluorescence microscopy images at 20X magnification of retinal microglial density quantified using ImageJ: 4 images per retina were taken at a distance halfway between the optic nerve and the peripheral edge of the retina; n = 5-7 for peptide **2.1**, **2.5** and **2.6**, and Kineret; n = 8-10 for normoxia and vehicle; *$p<0.05$, ****$p<0.0001$ relative to the

vehicle group. Treatment groups that are not labelled with asterisks are statistically non-significant compared to the vehicle group.

Discussion

PTB and ROP are medical conditions strongly associated with dysregulated inflammation. Current treatments for PTB, such as oxytocin antagonists and indomethacin, are targeted at reducing the contractility of the myometrium (tocolysis) but fail to address the underlying inflammatory processes responsible for labor.[48] Current ROP treatments employ anti-vascular endothelial growth factor (VEGF) antibodies and laser photocoagulation[49] which treat the proliferative phase of the disease but fail to address earlier stage vaso-obliteration and associated inflammation. Modulation of IL-1R signaling offers potential to mitigate both PTB and ROP as indicated by the *in vivo* results herein and previously reported.[7, 11, 50]

Peptide **2.1** was shown to adopt a random coil CD spectrum. In the *in vitro* assays, peptide **2.1** exhibit inhibitory activity on the phosphorylation of the three kinases (JNK, p-38 and ROCK2) and on the transcription of downstream pro-inflammatory genes that are mediated by IL-1β (IL-6, COX2 and IL-1β), but did not affect NF-κB signaling. Moreover, peptide **2.1** delayed significantly preterm birth in mice induced with LPS and reduced vaso-obliteration in the OIR murine model. Conformational constraint of peptide **2.1** was performed by replacing $(2R,3S)$-Thr^3-(R)-Val^4 with all four possible Agl^3-Val^4 (e.g., **2.5**) and eight possible Hgl^3-Val^4 (e.g., **2.6**) diastereomers. Among the twelve analogs of peptide **2.1**, those possessing common backbone stereochemistry (e.g., R,R- and S,S-) exhibited circular dichroism spectra indicative of β-turn conformers in water: [$(3R)$-Agl^3]-, [$(3R,4R)$-Hgl^3]- and [$(3R,4S)$-Hgl^3]-, [$(3S)$-Agl^3-(S)-Val^4]-, [$(3S,4S)$-Hgl^3-(S)-Val]-, [$3S,4R)$-Hgl^3-(S)-Val]-**2.1**. Moreover, [$(3R,4S)$-Hgl^3-(S)-Val]-**2.1** also exhibited a CD curve indicative of a turn conformer.

Among the constrained analogs, [$(3R,4S)$-Hgl^3]-**2.1** exhibited the most similar activity as the parent peptide in the *in vitro* and *in vivo* assays with slightly reduced potency in inhibiting JNK. Moreover, [$(3S,4R)$-Hgl^3]-**2.1** was also typically as potent as **2.1** but had slightly reduced abilities in inhibiting p38 and ROCK2. Although their CD spectra and conformers differed in water, both isomers possess *trans*-Hgl residues and (R)-Val stereochemistry indicating the importance of the β-hydroxyl group and gauche-(−) χ-dihedral angle side chain geometry for maximum activity.

Chapter 3

The contrast of high potency and inactivity exhibited respectively in the PTB and OIR models by both [(3R)-Agl³]- and [(3S)-Agl³]-**2.1** correlates with their ability to block JNK without inhibitory potency on p-38 and ROCK2. The importance of the hydroxyl group for activity on the latter kinases and for ability to reduce vaso-obliteration in the OIR model is illustrated by the potency of the corresponding Hgl analogs. Notably, [(3S,4S)-Hgl³]-**2.1** which positions the hydroxyl group in a gauche-(+) χ-dihedral angle side chain orientation maintains some potency on all three kinases with best activity on ROCK2 and exhibits respectively moderate and strong activities in the PTB and OIR models.

Some inhibitory activity on JNK appears necessary for potency in delaying labor in the PTB model. For example, [(3R,4R)-Hgl³]-**2.1**, which inhibited strongly ROCK2, but had no effects on JNK and p-38, was inactive in the PTB model. The weaker potency in the PTB assay of the (S)-Val analogs correlated with their lack of inhibitory activity on JNK. Although (R)- instead of (S)-Val may be a prerequisite for binding IL-1R, the latter may also be more susceptible to enzymatic cleavage by proteases.[51-52]

Correlations between peptide structure, *in vitro* activity and *in vivo* potency highlight the relative importance of blocking specific IL-1 signaling pathways to treat certain pathologies (Table 2.4). For example, inhibition of JNK phosphorylation was most strongly correlated with effectiveness in PTB inhibition. In agreement with an earlier study in which the use of a specific JNK inhibitor had delayed PTB which was induced by a type of LPS that activated both NF-κB and JNK pathways,[53] blocking JNK phosphorylation alone was sufficient for PTB prevention. On the other hand, efficacy in the OIR model necessitated inhibition of both JNK and ROCK2 phosphorylation. The latter was in concordance with a study demonstrating the utility of specific ROCK inhibitors an *in vivo* model of OIR.[54] Inactivity of specific compounds may be due to their pharmacokinetics and would require further study to address such issues. For example, delivery may play a role in efficacy because entrance into the retina is more challenging than the myometrium, due to the presence of a blood-retina-barrier that limits entrance from systemic circulation[55] and may account for the enhanced activity of the Hgl relative to the Agl analogs in the OIR model.

Peptide **2.1** was previously shown to bind to IL-1R.[21] Most of peptides **2.5** and **2.6** displaced radio-labelled **2.1** to the same extent as cold peptide **2.1**, suggesting they all compete for the same binding site on IL-1R, though not necessarily with the same binding affinity. The sole

exception was [(3*R*,4*S*)-Hgl³]-**2.1**, which displaced radio-labelled **2.1** to a lesser extent despite being the most efficacious molecule *in vitro* and *in vivo* (Table 2.4). This contradiction may be due to a different IL-1R binding pattern that retains desirable biased signaling and may require crystallographic analyses to confirm this hypothesis.

Compared to the larger proteins and non-selective competitive inhibitors currently used in anti-IL-1 therapies, peptides **2.1**, **2.5** and **2.6** may offer benefits such as ease of administration, as well as potential to reduce immunosuppression, immunogenicity and related side effects. The small peptides may be further optimized for oral administration, in contrast to antibodies, which must be administered by injection predisposing patients to potentially unpleasant injection-site reactions leading to reduced patient compliance. Notably, anti-VEGF antibodies, a mainstay of ROP treatment, must be injected directly into the vitreous of the eye (i.e., intravitreally), a technique that is invasive and technically demanding.[55]

To date, there are no clinically-approved allosteric inhibitors of IL-1 or its receptor. The anti-IL-1β antibody Gevokizumab, which is currently under investigation, has been reported to bind to an allosteric site on IL-1β;[56-57] however, like other antibodies may be associated with similar drawbacks including large molecule size and high production costs.

Conclusion

The utility of conformational-constraint to create folded synthetic peptides has for the first time been studied in the context of cytokine signaling and inflammation. Towards the development of immunomodulatory therapy, lactam constraint has been used to study the central D-Thr-D-Val dipeptide sequence of the allosteric IL-1R modulator peptide **2.1**, which has previously exhibited efficacy in curbing inflammation in various models of disease, due in part to ability to maintain the beneficial effects of NF-κB signaling.[7, 19-20] Although the lactam analogs behaved like parent peptide **2.1** and did not inhibit NF-κB, they exhibited different degrees of inhibitory potency on the kinases and cytokines activated by IL-1β *in vitro*. Lactam analogs **2.5** and **2.6** are thus valuable probes for identifying specific inflammation induced signaling pathways for intervention to treat specific medical conditions. Specifically, inhibition of JNK alone and in combination with ROCK2 were respectively identified for delaying preterm labor and mitigating retinopathy of prematurity. Peptides **2.1**, **2.5** and **2.6** compose a valuable set of selective probes for studying IL-1 signaling pathways in various inflammatory diseases. As promising leads for immune modulator therapy, they offer benefits over traditional protein-based counterparts due to biased signaling, which may

avoid immunosuppression. The demonstrated methods for utilizing a combination of Agl and Hgl residues to make folded peptides may thus have broad utility for biomedical research.

Table 2.4. Heatmap summary of the *in vivo* and *in vitro* effects of peptides 2.1, 2.5 and 2.6.

		Western Blot			qPCR			Nf-κB	*In vivo*	
	Structure	JNK	p38	ROCK2	COX2	IL-1β	IL-6		PTB	OIR
(R)-Val	[(3R)-Agl³]-**2.1**	4	0	0	3	4	3	0	4	0
	[(3R,4R)-Hgl³]-**2.1**	0	0	4	4	4	4	0	0	
	[(3R,4S)-Hgl³]-**2.1**	4	4	4	4	4	4	0	4	4
	[(3R)-Agl³-(S)-Val⁴]-**2.1**	0	4	2	1	1	1	0	0	
	[(3R,4R)-Hgl³-(S)-Val⁴]-**2.1**	1	3	4	4	3	4	0	0	
	[(3R,4S)-Hgl³-(S)-Val⁴]-**2.1**	2	2	2	4	4	2	0	2	
(S)-Val	[(3S)-Agl³]-**2.1**	4	0	0	4	4	2	0	4	1
	[(3S,4R)-Hgl³]-**2.1**	3	3	3	4	4	4	0	4	4
	[(3S,4S)-Hgl³]-**2.1**	1	1	3	4	4	4	0	2	3
	[(3S)-Agl³-(S)-Val⁴]-**2.1**	0	2	3	1	1	1	0	0	
	[(3S,4R)-Hgl³-(S)-Val⁴]-**2.1**	0	3	3	3	1	3	0	0	0
	[(3S,4S)-Hgl³-(S)-Val⁴]-**2.1**	2	0	4	4	4	4	0	2	
Peptide **2.1** (H-rytvela-NH₂)		4	4	4	4	4	4	0	4	4
Kineret		4	4	4	4	4	4	4	0	3

Black = not tested

No effect | 0 | 1 | 2 | 3 | 4 | Maximum inhibition/efficacy

Chapter 3

Author Contributions

AG wrote the manuscript, synthesized and purified compounds, and conducted circular dichroism analyses. CWHC wrote the manuscript and conducted *in vivo* and *in vitro* experiments. CQ and TZ edited the manuscript and conducted *in vitro* experiments. XH and JCR edited the manuscript and conducted *in vivo* experiments. CQ, DJS-C, KB and VB-G conceptualized rytvela (peptide **2.1**) and assisted in synthesis of derivatives. SC and WDL supervised the progress of the project, edited and proofread the manuscript. All authors have read the final manuscript and agree to be accountable for the content of this work.

Conflicts of Interest

The authors declare that the research was conducted in the absence of any commercial or financial relationships that could be construed as a potential conflict of interest.

References

1.   Freidinger, R. M.; Veber, D. F.; Perlow, D. S.; Saperstein, R., Bioactive conformation of luteinizing hormone-releasing hormone: evidence from a conformationally constrained analog. *Science* **1980,** *210*, 656-658.

2.   St-Cyr, D. J.; García-Ramos, Y.; Doan, N.-D.; Lubell, W. D., Aminolactam, N-aminoimidazolone, and N-aminoimdazolidinone peptide mimics. In *Peptidomimetics I*, Springer: 2017; pp 125-175.

3.   St-Cyr, D. J.; Jamieson, A. G.; Lubell, W. D., α-Amino-β-hydroxy-γ-lactam for constraining peptide Ser and Thr residue conformation. *Org. Lett.* **2010,** *12*, 1652-1655.

4.   Jamieson, A. G.; Boutard, N.; Beauregard, K.; Bodas, M. S.; Ong, H.; Quiniou, C.; Chemtob, S.; Lubell, W. D., Positional scanning for peptide secondary structure by systematic solid-phase synthesis of amino lactam peptides. *J. Am. Chem. Soc.* **2009,** *131*, 7917-7927.

5.   Boutard, N.; Turcotte, S.; Beauregard, K.; Quiniou, C.; Chemtob, S.; Lubell, W. D., Examination of the active secondary structure of the peptide 101.10, an allosteric modulator of the interleukin-1 receptor, by positional scanning using β-amino γ-lactams. *J. Pept. Sci.* **2011,** *17*, 288-296.

6.   Dinarello, C. A.; Simon, A.; Van Der Meer, J. W., Treating inflammation by blocking interleukin-1 in a broad spectrum of diseases. *Nat. Rev. Drug Discov.* **2012,** *11*, 633-652.

7.   Nadeau-Vallée, M.; Quiniou, C.; Palacios, J.; Hou, X.; Erfani, A.; Madaan, A.; Sanchez, M.; Leimert, K.; Boudreault, A.; Duhamel, F., Novel noncompetitive IL-1 receptor–biased ligand prevents infection-and inflammation-induced preterm birth. *J. Immunol.* **2015,** *195* , 3402-3415.

8.   Romero, R.; Brody, D. T.; Oyarzun, E.; Mazor, M.; Wu, Y. K.; Hobbins, J. C.; Durum, S. K., Infection and labor: III. Interleukin-1: A signal for the onset of parturition. *Am. J. Obstet. Gynecol.* **1989,** *160*, 1117-1123.

9.   Yoshimura, K.; Hirsch, E., Effect of stimulation and antagonism of interleukin-1 signaling on preterm delivery in mice. *J. Soc. Gynecol. Investig.* **2005,** *12*, 533-538.

10.   Puchner, K.; Iavazzo, C.; Gourgiotis, D.; Boutsikou, M.; Baka, S.; Hassiakos, D.; Kouskouni, E.; Economou, E.; Malamitsi-Puchner, A.; Creatsas, G., Mid-trimester amniotic fluid interleukins (IL-1β, IL-10 and IL-18) as possible predictors of preterm delivery. *In vivo* **2011,** *25*, 141-148.

11.   Rivera, J. C.; Sitaras, N.; Noueihed, B.; Hamel, D.; Madaan, A.; Zhou, T.; Honoré, J.-C.; Quiniou, C.; Joyal, J.-S.; Hardy, P., Microglia and interleukin-1β in ischemic retinopathy elicit microvascular degeneration through neuronal semaphorin-3A. *Arter. Thromb. Vasc. Biol.* **2013,** *33*, 1881-1891.

12.   Dinarello, C., The IL-1 family and inflammatory diseases. *Clinical and experimental rheumatology* **2002,** *20*, S1-S13.

13.   Dinarello, C. A.; Gatti, S.; Bartfai, T., Fever: links with an ancient receptor. *Current biology* **1999,** *9*, R143-R146.

14.   Hallegua, D.; Weisman, M., Potential therapeutic uses of interleukin 1 receptor antagonists in human diseases. *Annals of the rheumatic diseases* **2002,** *61*, 960-967.

15.   Braddock, M.; Quinn, A., Targeting IL-1 in inflammatory disease: new opportunities for therapeutic intervention. *Nat. Rev. Drug Discov.* **2004,** *3*, 330-339.

16.   Opal, S. M.; Fisher, C. J.; Dhainaut, J.-F. A.; Vincent, J.-L.; Brase, R.; Lowry, S. F.; Sadoff, J. C.; Slotman, G. J.; Levy, H.; Balk, R. A., Confirmatory interleukin-1 receptor antagonist trial in severe sepsis: a phase III, randomized, doubleblind, placebo-controlled, multicenter trial. *Critical care medicine* **1997,** *25*, 1115-1124.

17.   Roerink, M. E.; Bredie, S. J. H.; Heijnen, M.; Dinarello, C. A.; Knoop, H.; Van der Meer, J. W. M., Cytokine inhibition in patients with chronic fatigue syndrome: a randomized trial. *Ann. Intern. Med.* **2017,** *166*, 557-564

18.   Mantero, J.; Kishore, N.; Ziemek, J.; Stifano, G.; Zammitti, C.; Khanna, D.; Gordon, J.; Spiera, R.; Zhang, Y.; Simms, R., Randomised, double-blind, placebo-controlled trial of IL1-trap, rilonacept, in systemic sclerosis. A phase I/II biomarker trial. *Clinical and experimental rheumatology* **2018,** *36*, 146-149.

19.   Castro-Alcaraz, S.; Miskolci, V.; Kalasapudi, B.; Davidson, D.; Vancurova, I., NF-κB regulation in human neutrophils by nuclear IκBα: correlation to apoptosis. *J. Immunol.* **2002,** *169*, 3947-3953.

20.   Gerondakis, S.; Siebenlist, U., Roles of the NF-κB pathway in lymphocyte development and function. *Cold Spring Harbor perspectives in biology* **2010,** *2* a000182.

21.   Quiniou, C.; Sapieha, P.; Lahaie, I.; Hou, X.; Brault, S.; Beauchamp, M.; Leduc, M.; Rihakova, L.; Joyal, J.-S.; Nadeau, S.; Heveker, N.; Lubell, W.; Sennlaub, F.; Gobeil, F.; Miller, G.; Pshezhetsky, A. V.; Chemtob, S., Development of a novel noncompetitive antagonist of IL-1 receptor. *J. Immunol.* **2008,** *180*, 6977-6987.

22.   Bourguet, C. B.; Claing, A.; Laporte, S. A.; Hébert, T. E.; Chemtob, S.; Lubell, W. D., Synthesis of azabicycloalkanone amino acid and azapeptide mimics and their application as modulators of the prostaglandin F2α receptor for delaying preterm birth. *Can. J. Chem.* **2014,** *92*, 1031-1040.

23.   Rihakova, L.; Quiniou, C.; Hamdan, F.; Kaul, R.; Brault, S.; Hou, X.; Lahaie, I.; Sapieha, P.; Hamel, D.; Shao, Z., VRQ397 (CRAVKY): a novel noncompetitive V2 receptor antagonist.

American Journal of Physiology-Regulatory, Integrative and Comparative Physiology **2009,** *297*, R1009-R1018.

24.   Hebert, T. E.; Moffett, S.; Morello, J.-P.; Loisel, T. P.; Bichet, D. G.; Barret, C.; Bouvier, M., A peptide derived from a β2-adrenergic receptor transmembrane domain inhibits both receptor dimerization and activation. *J. Biol. Chem.* **1996,** *271*, 16384-16392.

25.   Tan, D. C.; Kini, R. M.; Jois, S. D.; Lim, D. K.; Xin, L.; Ge, R., A small peptide derived from Flt-1 (VEGFR-1) functions as an angiogenic inhibitor. *FEBS letters* **2001,** *494*, 150-156.

26.   Lubell, W. D., *Peptidomimetics I*. Springer: 2017; Vol. 48.

27.   Rubin, S.; Qvit, N., Cyclic Peptides for Protein− Protein Interaction Targets: Applications to Human Disease. *Critical Reviews™ in Eukaryotic Gene Expression* **2016,** *26*, 199-221.

28.   Carney, D. W.; Schmitz, K. R.; Truong, J. V.; Sauer, R. T.; Sello, J. K., Restriction of the conformational dynamics of the cyclic acyldepsipeptide antibiotics improves their antibacterial activity. *J. Am. Chem. Soc.***2014,** *136*, 1922-1929.

29.   Freidinger, R. M.; Perlow, D. S.; Veber, D. F., Protected lactam-bridged dipeptides for use as conformational constraints in peptides. *J. Org. Chem.* **1982,** *47*, 104-109.

30.   Perdih, A.; Kikelj, D., The application of Freidinger lactams and their analogs in the design of conformationally constrained peptidomimetics. *Curr. Med. Chem.* **2006,** *13* (13), 1525-1556.

31.   Aube, J., Synthetic routes to lactam peptidomimetics. *ChemInform* **1999,** *30*.

32.   Yu, K. L.; Rajakumar, G.; Srivastava, L. K.; Mishra, R. K.; Johnson, R. L., Dopamine receptor modulation by conformationally constrained analogs of Pro-Leu-Gly-NH2. *J. Med. Chem.* **1988,** *31*, 1430-1436.

33.   Zhang, Y. L.; Dawe, A. L.; Jiang, Y.; Becker, J. M.; Naider, F., A superactive peptidomimetic analog of a farnesylated dodecapeptide yeast pheromone. *Biochemical and biophysical research communications* **1996,** *224*, 327-331.

34.   Valle, G.; Crisma, M.; Toniolo, C.; Yu, K. L.; Johnson, R., Crystal-state structural analysis of two γ-lactam-restricted analogs of Pro-Leu-Gly-NH2. *International journal of peptide and protein research* **1989,** *33*, 181-190.

35.   Ronga, L.; Jamieson, A. G.; Beauregard, K.; Quiniou, C.; Chemtob, S.; Lubell, W. D., Insertion of multiple α-amino γ-lactam (Agl) residues into a peptide sequence by solid-phase synthesis on synphase lanterns. *Peptide Science: Original Research on Biomolecules* **2010,** *94*, 183-191.

36.   Geranurimi, A.; Lubell, W. D., Diversity-oriented syntheses of β-substituted α-amino γ-lactam peptide mimics with constrained backbone and side chain residues. *Org. Lett.* **2018,** *20*, 6126-6129.

37.   Sicherl, F.; Cupido, T.; Albericio, F., A novel dipeptidomimetic containing a cyclic threonine. *Chemical Communications* **2010,** *46*, 1266-1268.

38.   Kakinuma, C.; Kuwayama, C.; Kaga, N.; Futamura, Y.; Katsuki, Y.; Shibutani, Y., Trophoblastic apoptosis in mice with preterm delivery and its suppression by urinary trypsin inhibitor. *Obstetrics & Gynecology* **1997,** *90*, 117-124.

39.   Garner, A.; Ashton, N., Retinopathy of Prematurity: Vaso-Obliteration and Retrolental Fibroplasia. SAGE Publications: 1971.

40.   Freidinger, R. M., Design and synthesis of novel bioactive peptides and peptidomimetics. *J. Med. Chem.* **2003,** *46*, 5553-5566.

41.   St-Cyr, D. J.; Maris, T.; Lubell, W. D., Crystal-state structure analysis of β-hydroxy-γ-lactam constrained Ser/Thr peptidomimetics. *Heterocycles* **2010,** *82*, 729-737.

42.   Jamieson, A. G.; Boutard, N.; Sabatino, D.; Lubell, W. D., Peptide Scanning for Studying Structure-Activity Relationships in Drug Discovery. *Chemical biology & drug design* **2013,** *81* , 148-165.

43.   Lubell, W.; Blankenship, J.; Fridkin, G.; Kaul, R., "Peptides," in Science of Synthesis, ed S. M. Weinreb (Stuttgart: Thieme), **2005,** 713-809.

44.   Bush, C. A.; Sarkar, S. K.; Kopple, K. D., Circular dichroism of *β* turns in peptides and proteins. *Biochemistry* **1978,** *17*, 4951-4954.

45.   Kelly, S. M.; Jess, T. J.; Price, N. C., How to study proteins by circular dichroism. *Biochimica et Biophysica Acta (BBA)-Proteins and Proteomics* **2005,** *1751*, 119-139.

46.   Weber, A.; Wasiliew, P.; Kracht, M., Interleukin-1 (IL-1) pathway. *Sci. Signal.* **2010,** *3* .

47.   Donat, C. K.; Scott, G.; Gentleman, S. M.; Sastre, M., Microglial activation in traumatic brain injury. *Frontiers in aging neuroscience* **2017,** *9*, 208.

48.   Olson, D. M.; Christiaens, I.; Gracie, S.; Yamamoto, Y.; Mitchell, B. F., Emerging tocolytics: challenges in designing and testing drugs to delay preterm delivery and prolong pregnancy. *Expert opinion on emerging drugs* **2008,** *13*, 695-707.

49.   Hellström, A.; Smith, L. E.; Dammann, O., Retinopathy of prematurity. *The lancet* **2013,** *382*, 1445-1457.

50.   Beaudry-Richard, A.; Nadeau-Vallée, M.; Prairie, É.; Maurice, N.; Heckel, É.; Nezhady, M.; Pundir, S.; Madaan, A.; Boudreault, A.; Hou, X., Antenatal IL-1-dependent inflammation persists postnatally and causes retinal and sub-retinal vasculopathy in progeny. *Scientific reports* **2018,** *8*, 11875.

51.   Carmona, G.; Rodriguez, A.; Juarez, D.; Corzo, G.; Villegas, E., Improved protease stability of the antimicrobial peptide Pin2 substituted with D-amino acids. *The protein journal* **2013,** *32*, 456-466.

52.   Najjar, K.; Erazo-Oliveras, A.; Brock, D. J.; Wang, T.-Y.; Pellois, J.-P., An l-to d-amino acid conversion in an endosomolytic analog of the cell-penetrating peptide TAT influences proteolytic stability, endocytic uptake, and endosomal escape. *J. Biol. Chem.* **2017,** *292*, 847-861.

53.   Pirianov, G.; MacIntyre, D. A.; Lee, Y.; Waddington, S. N.; Terzidou, V.; Mehmet, H.; Bennett, P. R., Specific inhibition of c-Jun N-terminal kinase delays preterm labour and reduces mortality. *Reproduction (Cambridge, England)* **2015,** *150*, 269-277.

54.   Yamaguchi, M.; Nakao, S.; Arita, R.; Kaizu, Y.; Arima, M.; Zhou, Y.; Kita, T.; Yoshida, S.; Kimura, K.; Isobe, T., Vascular normalization by ROCK inhibitor: therapeutic potential of Ripasudil (K-115) eye drop in retinal angiogenesis and hypoxia. *Investig. Ophthalmol. Vis. Sci.* **2016,** *57*, 2264-2276.

55.   del Amo, E. M.; Rimpelä, A.-K.; Heikkinen, E.; Kari, O. K.; Ramsay, E.; Lajunen, T.; Schmitt, M.; Pelkonen, L.; Bhattacharya, M.; Richardson, D., Pharmacokinetic aspects of retinal drug delivery. *Progress in retinal and eye research* **2017,** *57*, 134-185.

56.   Blech, M.; Peter, D.; Fischer, P.; Bauer, M. M.; Hafner, M.; Zeeb, M.; Nar, H., One target—two different binding modes: structural insights into gevokizumab and canakinumab interactions to interleukin-1β. *J. Mol. Biol.* **2013,** *425*, 94-111.

57.   Issafras, H.; Corbin, J. A.; Goldfine, I. D.; Roell, M. K., Detailed Mechanistic Analysis of Gevokizumab, an Allosteric Anti–IL-1β Antibody with Differential Receptor-Modulating Properties. *Journal of Pharmacology and Experimental Therapeutics* **2014,** *348*, 202-215.

Chapter 3

Chapter 3: Diversity-Oriented Syntheses of β-Substituted α-Amino γ-Lactam Peptide Mimics with Constrained Backbone and Side Chain Residues

3.1. Context

β-Substituted lactams offer potential as novel tools for constraining peptide backbone and side chain geometry. The synthesis of a series of constrained β-substituted Agl derivatives was inspired based on earlier success using the parent residue to induce *β*-turn geometry,[1] and the importance of side chain residues for molecular recognition at turn regions.[2] The addition of β-substituents to Agl residues was thus pursued as a means to enhance potency by simultaneously constraining the ω-, ψ-, φ- and χ-dihedral angles to pre-organize the backbone and side chain for molecular recognition with the receptor target.

Few examples have been reported of syntheses of β-substituted Agl residues. Most have focused on adding ordinary alkyl β-substituents onto the lactam ring.[3-6] In certain cases, carboxylates and hydroxy methyl β-substituents have been introduced.[7] These methods add the side chain typically at an early stage in the synthesis limiting potential for late stage diversification.

For example, β-alkyl-substituted α-amino γ-lactams were synthesized from aspartic acid as chiral precursor to prepare constrained Val-Ala, Ile-Ala, and Leu-Ala bridged dipeptides **3.1a-c** (Scheme 3.1).[3] By employing the bulky 9-phenylfluoren-9-yl (PhF) amine protecting group to shield the α-carbon proton, selective enolization the β-carboxylate of aspartate **3.2** was achieved and the enolate was reacted with a set of alkyl halides without loss of configurational integrity. Selective reduction of the β-methyl ester of β-alkyl branched aspartates to aldehydes **3.4a-c**. Reductive animation with lactam cyclization using alanine methyl ester afforded bridged dipeptides **3.1a-c**.[3]
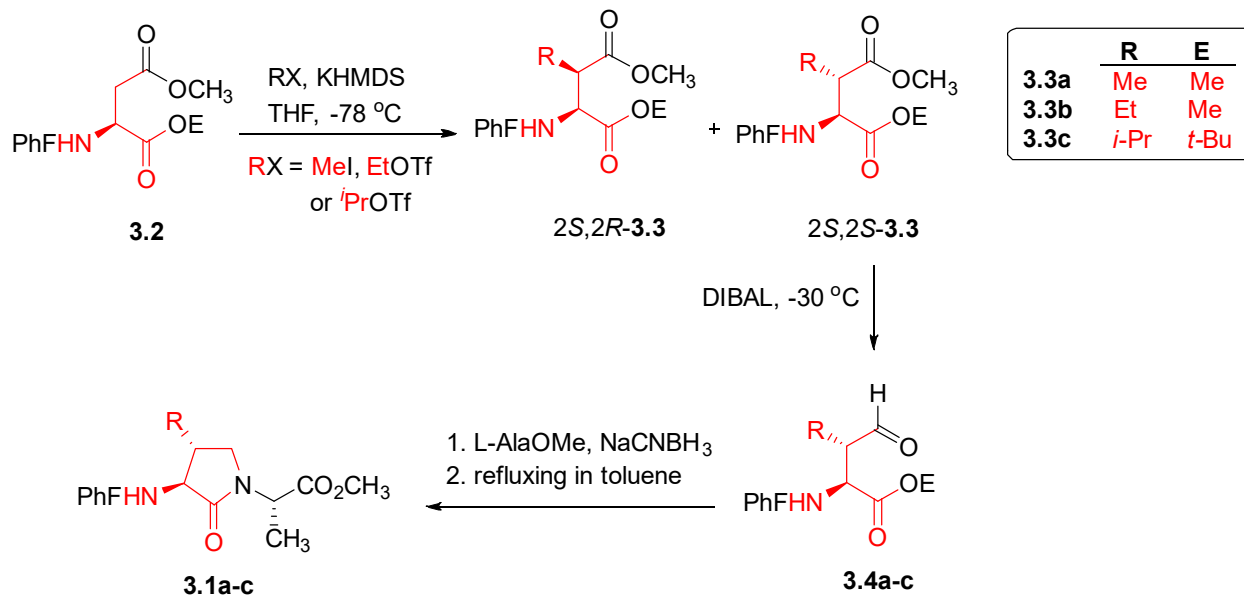
Scheme 3.1. Synthesis of constrained Val-Ala, Ile-Ala, and Leu-Ala **3.1a-c** from aspartate

Selective formylation of aspartate **3.5** using 20 equivaltents of (*tert*-butyloxy)-bis(dimethylamino)methane in cyclohexane at 40°C for 18h followed by acid mediated enamine hydrolysis gave β-formyl aspartate **3.6** in 96% yield. Subsequent reductive amination with H-Phe-NH₂ and lactam formation gave constrained Asp-Phe dipeptide amide **3.7** (Scheme 3.2). On the other hand, alkylation of β-formyl ester **3.6** with allyl iodide, followed by hydrogenation which cleaved concomitantly the benzyl ester, induced decarboxylation and reduced the olefin gave aldehyde **3.8**.[8] Subsequent reductive amination with aspartate **3.9** afforded constrained Asp-Phe dipeptide **3.10**.[8]
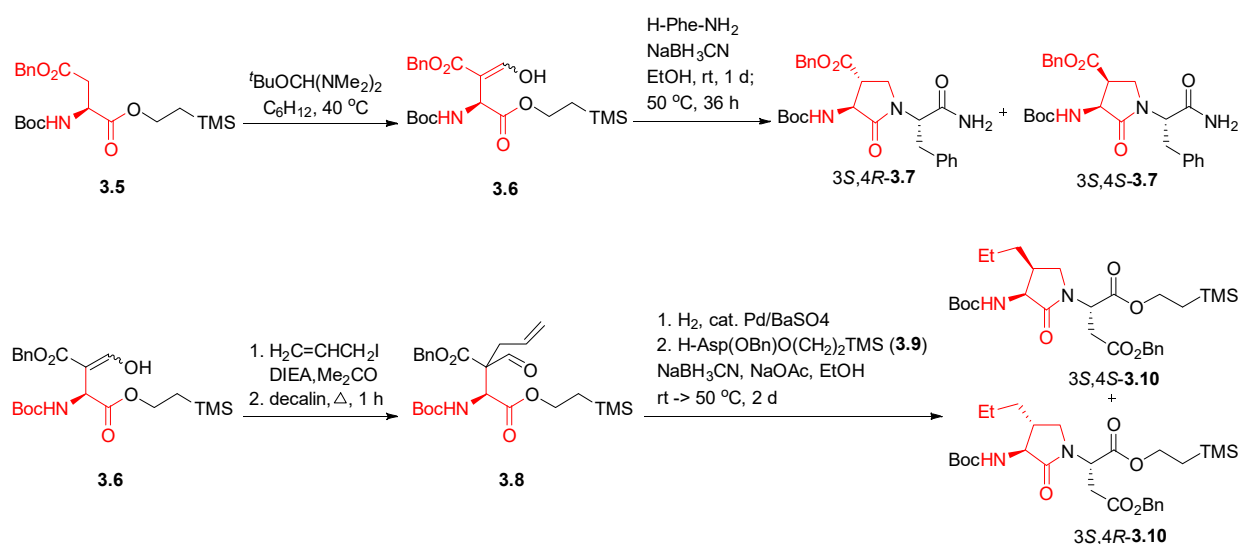
Scheme 3.2. Synthesis of constrained Asp-Phe dipeptide amide **3.7** and Asp-Phe dipeptide **3.10**

By a mechanism involving generation of a singlet bi-radical, β-hydroxy-β-phenyl-α-amino-γ-lactams **3.11** was synthesized through stereoselective photo-cyclization of glycinyl-*N*-benzoylmethyl-L-valinate **3.12**. The bi-radical intermediate preferred pro-R hydrogen abstraction, such that cyclization by radical recombination gave **3.11** as a 10:1 diastereomeric mixture (Scheme 3.3).[9]
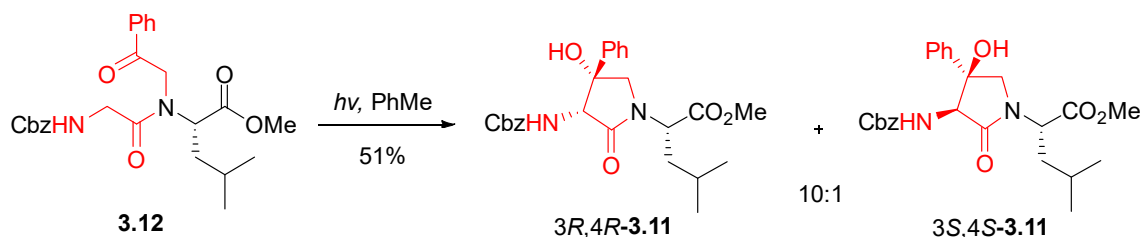
Scheme 3.3. Synthesis of diastereomers of β-hydroxy-β-phenyl-α-amino-γ-lactams **3.11**

α-Amino β-hydroxy γ-lactam (Hgl) residues are constrained forms of Ser and Thr, which may induce turn conformation.[10-13] Employing oxiranyl glycine **3.13** as a bis-electrophile in trifluoroethanol a variety of amino acid derivatives were alkylated.[11] Subsequent lactam formation using catalytic benzoic acid provided a library of Hgl dipeptides (e.g., **3.14**) in 31–85% yields (Scheme 3.4).[11]
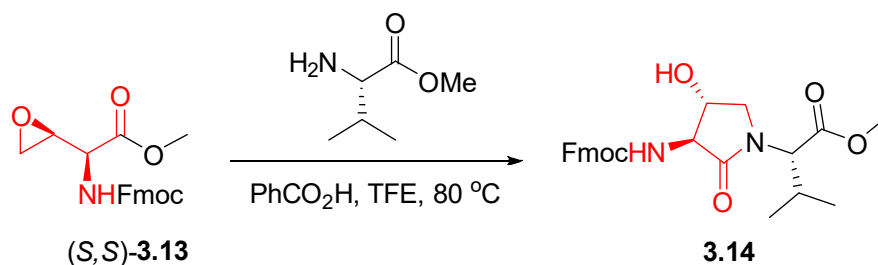
Scheme 3.4. Synthesis of *trans* Hgl-Val dipeptide

By elaboration of the hydroxy group of Hgl residue, β-bromide **3.15** and β-phosphate **3.16** were synthesized respectively using PPh$_3$Br$_2$, and POCl$_3$ in 2,6-lutidine followed by a methanol quench (Scheme 3.5).[11]
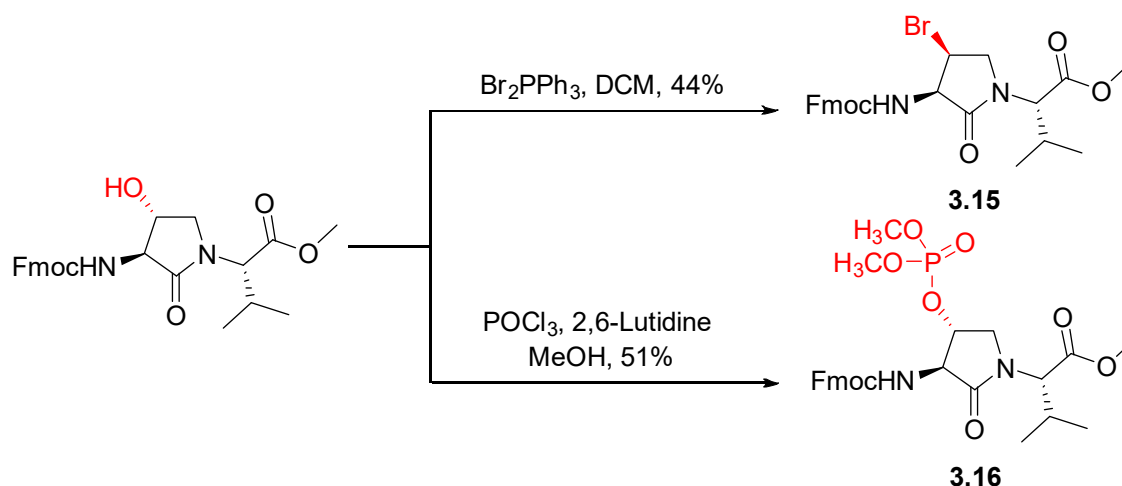
Scheme 3.5. Bromination and phosphorylation of Hgl residue

All the examples of β-substituted lactams described above have been synthesized through different methods and in most cases never introduced into the peptide. Displacement of the hydroxyl group of the Hgl residue with different nucleophiles was perceived as a potential means to add a variety of different side chains to the lactam β-position. In this chapter, the Mitsunobu reaction and cyclic sulfamidate nucleophilic ring opening were respectively employed from *trans*- and *cis*-β-hydroxy-α-amino-γ-lactam precursors to prepare series of various β-substituted α-amino-γ-lactam dipeptides.

The Mitsunobu reaction on *trans*-β-hydroxy-α-amino-γ-lactam **3.17** with 4-nitrobenzoic acid, PPh₃ and diisopropyl azodicarboxylate (DIAD) in THF, followed by benzoate removal without Fmoc cleavage using NaN₃ in MeOH afforded *cis*-β-substituted-α-amino-γ-lactam **3.18** in 60% yield (Scheme 3.6).[12]
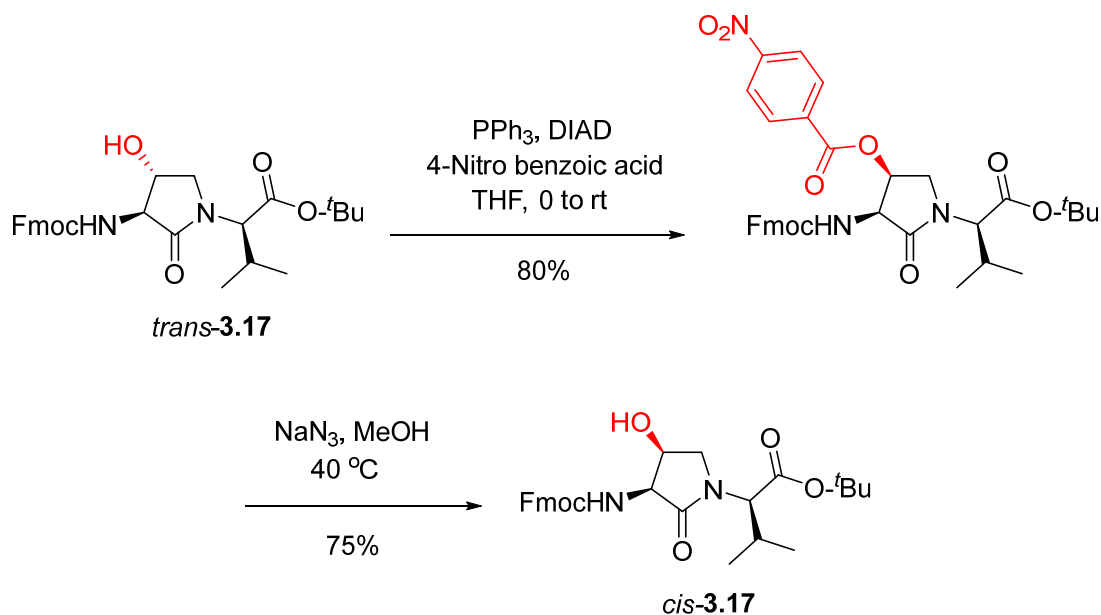
Scheme 3.6. Synthesis of *cis* Fmoc-Hgl-Val dipeptide (*cis*-**3.17**) by Mitsunobu reaction

The order of addition of the reagents in the Mitsunobu reaction can influence yield significantly. Typically, the alcohol, acid, and PPh₃ are premixed in a solvent (e.g. THF), cooled to 0 °C, treated slowly with DIAD, and stirred while warming to room temperature for several hours.[13] Alternatively, the betaine intermediate may be generated first by mixing DIAD and PPh₃ in THF at 0 °C. Subsequent addition of the alcohol and pro-nucleophile, such as 4-nitrobenzoic acid, may provide better yield of product.[14-15] Alcohol oxygen activation occurs on reaction with the phosphonium of the betaine intermediate to form an oxyphosphonium ion, which is displaced by the carboxylate anion with inversion of configuration at carbon (Figure 3.1).[15]
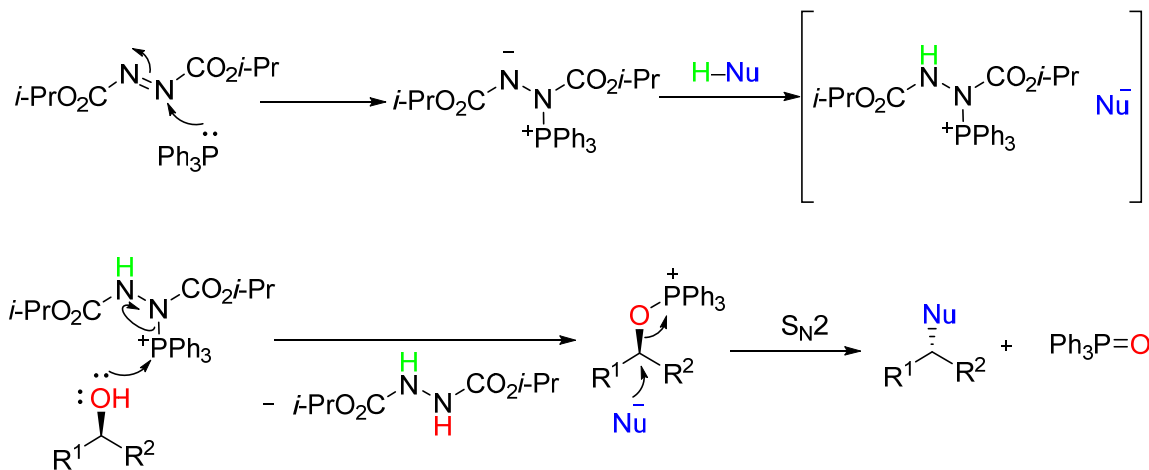
Figure 3.1. The proposed mechanism for the Mitsunobu reaction

The Mitsunobu reaction has been used to displace β-hydroxy esters to introduce a wide range of functionality. For example, the primary alcohol of L-serine ester has been reacted to make sets of β-substituted alanines;[16] however, β-elimination may occur to give dehydroalanine **3.18** (Scheme 3.7).[15, 17-18] Alternatively, oxazoline **3.19** was formed under Mitsunobu conditions using β-amido alcohol **3.20** (Scheme 3.8).[19]
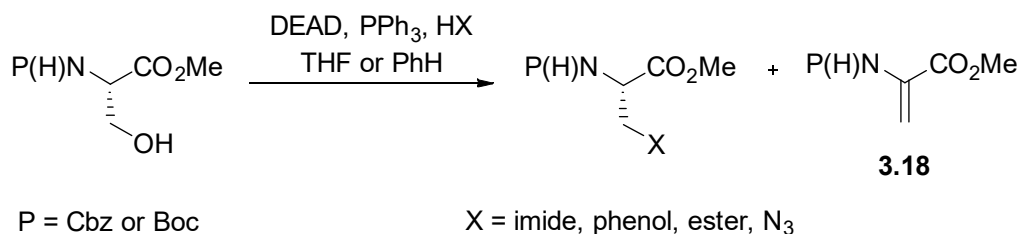
Scheme 3.7. Dehydroalanine **3.18** formation as a byproduct of Mitsunobu reaction
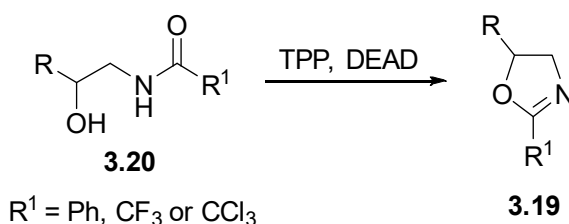
Scheme 3.8. Synthesizing oxazoline **3.19** from β-amido alcohol **3.20** as a byproduct of Mitsunobu reaction

Although the Mitsunobu reaction has been performed using pro-nucleophiles with pK_a values under 11, in the case of *trans*-Hgl **3.17** reaction was only successful with pro-nucleophiles with pK_a values between 3 and 7.

Employing Mitsunobu conditions on *cis*-Hgl **3.17** gave only dehydrolactam **3.21**, likely due to a preferred *anti* orientation between the pseudoaxial β-hydroxyl group and α-proton. To surmount this issue, the amine and alcohol were tied into a cyclic sulfamidate to provide a reactive intermediate in a geometry less prone to elimination. Cyclic sulfamidates have been used for the synthesis of various products possessing heteroatomic functional groups.[20-21] Cyclic sulfamidate **3.22** was prepared from *cis*-Hgl **3.17** by way of oxidation of cyclic sulfamidite **3.23**. Nucleophiles have reacted with five-membered cyclic sulfamidates under different conditions.[22] In the case of cyclic sulfamidate **3.22**, a mixed solvent system of DCM and DMF was used to solubilize the starting materials and favor the ring opening displacement (Scheme 3.10).
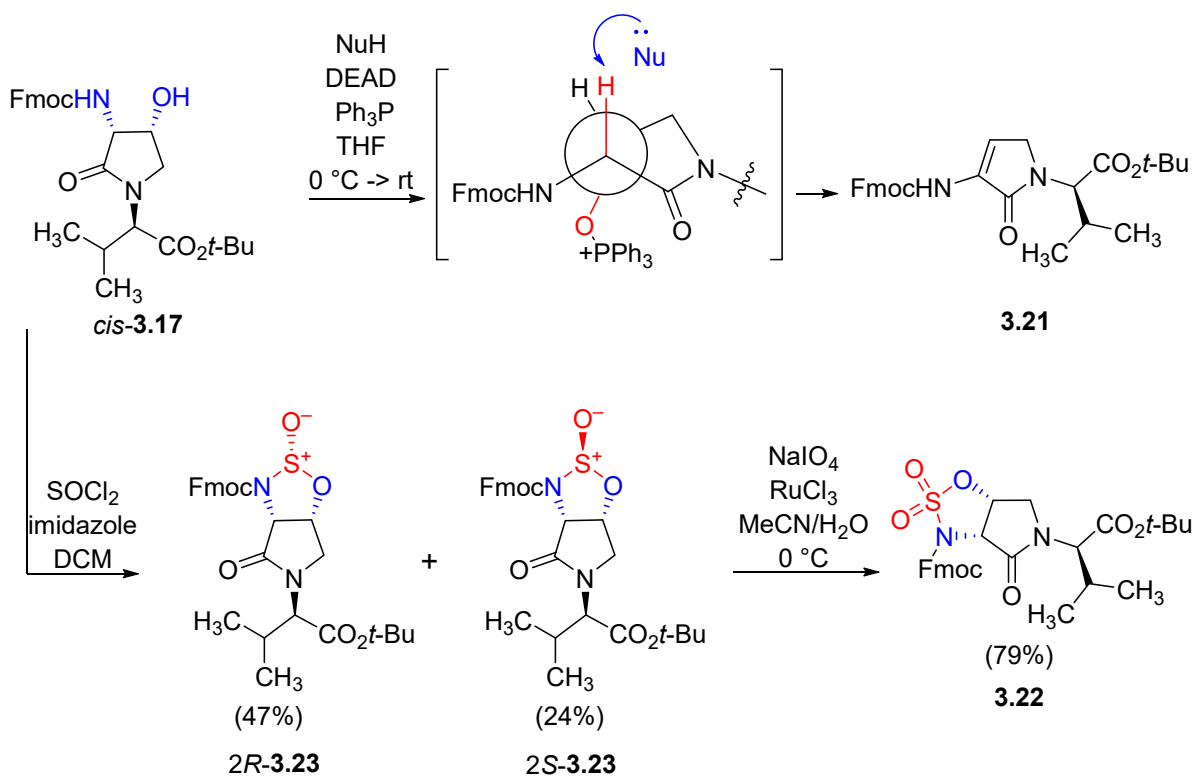
Scheme 3.9. Synthesis of sulfamidate **3.22**

Moreover, displacement of cyclic sulfamidate **3.22** using thiocyanate gave β-thiocyano-Agl residue **3.24k** (Scheme 3.10). Reduction and alkylation of β-thiocyanide **3.24k** with iodomethane gave *S*-methyl Cys or methionine analog **3.24l**. In principle, a variety of alkyl halides may be used to convert β-thiocyanide **3.24k** into a set of thio ethers **3.24l**.
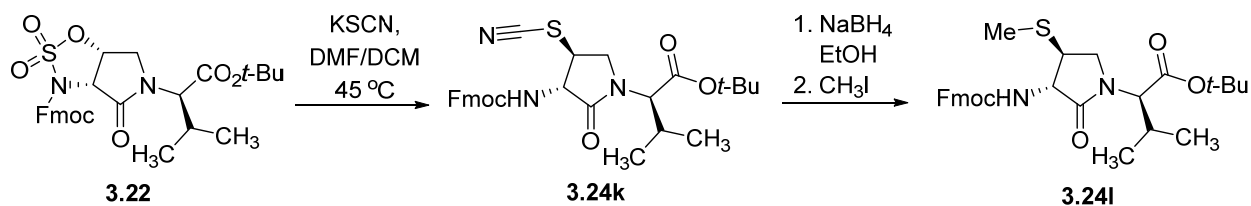
Scheme 3.10. Synthesis of constrained *S*-methyl Cys or methionine derivative **3.24l**

Various β-substituted Agl residues were synthesized stereoselectively by employing the combination of these three methods. Constrained mimics were prepared with features of Ser, Thr,

Cys, Dap, Dab, Met and His. The results of this Chapter were published in part in *Organic Letters* in 2018 and Proceedings of the 35th European Peptide Symposium in 2018.[23]

3.2. References

1.   Geranurimi, A.; Cheng, C. W.; Quiniou, C.; Zhu, T.; Hou, X.; Rivera, J. C.; St-Cyr, D. J.; Beauregard, K.; Bernard-Gauthier, V.; Chemtob, S., Probing anti-inflammatory properties independent of NF-κB through conformational constraint of peptide-based interleukin-1 receptor biased ligands. *Frontiers in chemistry* **2019,** *7*.

2.   St-Cyr, D. J.; García-Ramos, Y.; Doan, N.-D.; Lubell, W. D., Aminolactam, N-aminoimidazolone, and N-aminoimdazolidinone peptide mimics. In *Peptidomimetics I*, Springer: 2017; pp 125-175.

3.   Wolf, J. P.; Rapoport, H., Conformationally constrained peptides. Chirospecific synthesis of 4-alkyl-substituted. gamma.-lactam-bridged dipeptides from L-aspartic acid. *J. Org. Chem.* **1989,** *54*, 3164-3173.

4.   Garvey, D. S.; May, P. D.; Nadzan, A. M., 3, 4-Disubstituted. gamma.-lactam rings as conformationally constrained mimics of peptide derivatives containing aspartic acid or norleucine. *J. Org. Chem.* **1990,** *55*, 936-940.

5.   Leeson, P. D.; Williams, B. J.; Baker, R.; Ladduwahetty, T.; Moore, K. W.; Rowley, M., Effects of five-membered ring conformation on bioreceptor recognition: identification of 3R-amino-1-hydroxy-4R-methylpyrrolidin-2-one (L-687,414) as a potent glycine/N-methyl-D-aspartate receptor antagonist. *J. Chem. Soc., Chemical Communications* **1990,** , 1578-1580.

6.   Rowley, M.; Leeson, P. D.; Williams, B. J.; Moore, K. W.; Baker, R., Routes to 4-substituted analogues of the glycine/NMDA antagonist HA-996. Enantioselective synthesis of (3R, 4R) 3-amino-1-hydroxy-4-methyl-2-pyrrolidinone (L-687, 414). *Tetrahedron* **1992,** *48*, 3557-3570.

7.   Crucianelli, E.; Galeazzi, R.; Martelli, G.; Orena, M.; Rinaldi, S.; Sabatino, P., A novel conformationally restricted analogue of 3-methylaspartic acid via stereoselective methylation of chiral pyrrolidin-2-ones. *Tetrahedron* **2010,** *66*, 400-405.

8.   Garvey, D. S.; May, P. D.; Nadzan, A. M., 3, 4-disubstituted γ-lactam rings as conformationally constrained mimics of peptides derivatives containing aspartic acid of norleucine. *J. Org. Chem.* **1990,** *55*, 936-940.

9.   Wyss, C.; Batra, R.; Lehmann, C.; Sauer, S.; Giese, B., Selective photocyclization of glycine in dipeptides. *Angew. Chem.* **1996,** *35*, 2529-2531.

10.   Tashiro, T.; Fushiya, J.; Nozoe, SH., Synthesis of 2'-epi-distichonic acid A, an iron-chelating amino acid derivative. *Chem. Pharm. Bull.* **1988,** *36*, 893-901.

11.   St-Cyr, D. J.; Jamieson, A. G.; Lubell, W. D., α-Amino-β-hydroxy-γ-lactam for constraining peptide Ser and Thr residue conformation. *Org. Lett.* **2010,** *12*, 1652-1655.

12.   Pandey, A. K.; Naduthambi, D.; Thomas, K. M.; Zondlo, N. J., Proline editing: a general and practical approach to the synthesis of functionally and structurally diverse peptides. Analysis of steric versus stereoelectronic effects of 4-substituted prolines on conformation within peptides. *J. Am. Chem. Soc.* **2013,** *135*, 4333-4363.

13.   Volante, R., A new, highly efficient method for the conversion of alcohols to thiolesters and thiols. *Tetrahedron Lett.* **1981,** *22* (33), 3119-3122.

14.   Fletcher, S., The Mitsunobu reaction in the 21 st century. *Organic Chemistry Frontiers* **2015,** *2* (6), 739-752.

15.   Hughes, D. L., Progress in the Mitsunobu reaction. A review. *Organic Preparations and procedures international* **1996,** *28* (2), 127-164.

16.   Cherney, R. J.; Wang, L., Efficient Mitsunobu reactions with N-phenylfluorenyl or N-trityl serine esters. *J. Org. Chem.* **1996,** *61*, 2544-2546.

17.   Mitsunobu, O., The use of diethyl azodicarboxylate and triphenylphosphine in synthesis and transformation of natural products. *Synthesis* **1981,** *1981* (01), 1-28.

18.   Wojciechowska, H.; Pawłowicz, R.; Andruszkiewicz, R.; Grzybowska, J., Conversion of protected serine and threonine to corresponding dehydroamino acids under mild conditions. *Tetrahedron Lett.* **1978,** *19*, 4063-4064.

19.   Wiśniewski, K.; Kołdziejczyk, A. S.; Falkiewicz, B., Applications of the Mitsunobu reaction in peptide chemistry. *J. Pept. Sci.: an official publication of the European Peptide Society* **1998,** *4*, 1-14.

20.   Han, Z.; Krishnamurthy, D.; Grover, P.; Fang, Q. K.; Senanayake, C. H., Properly designed modular asymmetric synthesis for enantiopure sulfinamide auxiliaries from N-sulfonyl-1, 2, 3-oxathiazolidine-2-oxide agents. *J. Am. Chem. Soc.* **2002,** *124*, 7880-7881.

21.   Wei, L.; Lubell, W. D., Scope and limitations in the use of N-(PhF) serine-derived cyclic sulfamidates for amino acid synthesis. *Can. J. Chem.* **2001,** *79* , 94-104.

22.	Meléndez, R. E.; Lubell, W. D., Synthesis and reactivity of cyclic sulfamidites and sulfamidates. *Tetrahedron* **2003,** *15*, 2581-2616.

23.	Geranurimi, A.; Lubell, W. D., Diversity-oriented syntheses of β-substituted α-amino γ-lactam peptide mimics with constrained backbone and side chain residues. *Org. Lett.* **2018,** *20*, 6126-6129.

Chapter 3

Article 2

Diversity-Oriented Syntheses of β-Substituted α-Amino γ-Lactam Peptide Mimics with Constrained Backbone and Side Chain Residues

I performed all experiments, and the isolation and characterization of all compounds. I wrote the first draft of the manuscript and contributed to its revision which was edited by Professor Lubell.

Azade Geranurimi and William D. Lubell*

* Département de Chimie, Université de Montréal, C.P. 6128, Succursale Centre-Ville, Montréal, Québec H3C 3J7, Canada
* S Supporting Information

Abstract

α-N-(Fmoc)Amino-γ-lactam dipeptides with a variety of β-substituents were synthesized stereoselectively with minimal β-elimination by routes employing, respectively, Mitsunobu chemistry and cyclic sulfamidate nucleophilic ring opening from *trans*- and *cis*-β-hydroxy-α-amino-γ-lactam precursors. This diversity-oriented method provides stereochemically pure dipeptide mimics bearing Cys, Ser, Thr, Dap, Dab, His, and other amino acid residues with constrained backbone and side chain conformations.
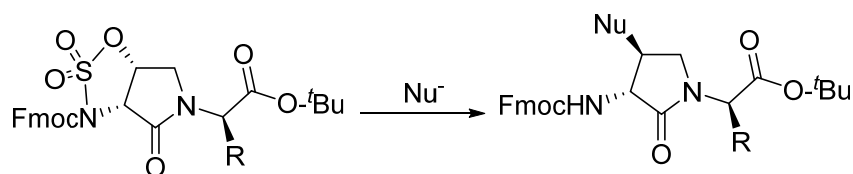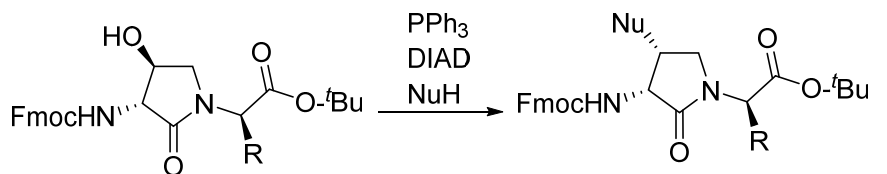
Backbone and side chain orientations are critical for natural peptide and protein biological activity. Mimicry of such natural architectures using constrained heterocycles has been a central paradigm for achieving biological activity in peptide based drug discovery since the pioneering use of α-amino-γlactams (so-called Freidinger-Veber lactams, Agl residues, Figure 3.2) to restrict the backbone ω-, ψ-, and φ-dihedral angles.[1-5] The success of Agl residues in inducing β-turn geometry combined with the importance of side chain residues for molecular recognition at turn regions has motivated synthesis of β-substituted Agl analogs.[1-2, 6-8] Their stereo controlled synthesis has, however, been challenging such that few examples with primarily simple alkyl and carboxylate β-substituents have been reported.[9-11] In addition, 4-hydroxy-4-phenyl-Agl was prepared as a 10:1 diastereomeric mixture by a photochemical C−H activation approach.[12] In spite of difficulties in their preparation, which may account in part for the rarity of applications of such analogs in the exploration of biologically active peptides,[2, 5, 11] their potential to orient both side chain and backbone geometry make Agl residues with modifiable β-substituents particularly valuable targets for the synthesis of bioconjugates to study post-translational modifications.
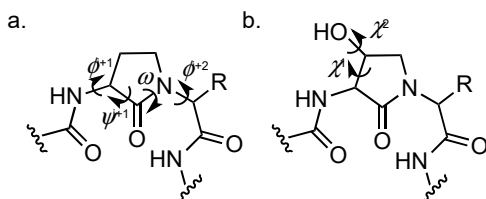
Figure 3.2. (a) Agl and (b) Hgl residues constrain backbone and side chain dihedral angles at the central residue of a β-turn.

Recently, β-hydroxy-α-amino-γ-lactam (Hgl) analogs were synthesized as constrained Ser/Thr residues,[5, 13-14] and introduced into a peptide allosteric modulator of the interleukin 1 receptor.[5] Employing oxiranyl glycine as a bis-electrophile, which was readily prepared from vinylglycine,[15] the Hgl residue was synthesized by a reaction with amino esters in solution[5, 13-14] and with N-terminal residues of peptides linked to resin.[5] Interested in employing the Hgl residue for diversity oriented synthesis of β-substituted analogs, displacement of the hydroxyl group has now been explored to introduce side chains with stereocontrol onto the Agl residue. Activation of the alcohol risks, however, β-elimination to form dehydrolactam **3.21**. To devise effective substitution chemistry without elimination, the *trans-* and *cis-*diastereomers of Fmoc-Hgl-Val-O*t*-Bu (**3.17**) have been employed as relatively bulky challenging substrates. The Fmoc protection

Chapter 3

was selected for subsequent compatibility with solid-phase peptide synthesis. Mitsunobu chemistry and cyclic sulfamidate ring opening, respectively, proved useful for displacing the β-hydroxyl group of the *trans-* and *cis* diastereomers of Hgl **3.17**. Among the set of diverse dipeptide mimics, thiol and amino side chain substituents have been introduced to provide constrained Cys and diaminoproprionic acid (Dap) analogs. The preparation of a set of β-substituted Agl residues began by synthesis of (3*R*,4*R*,2′*R*)- and (3*R*,4*S*,2′*R*)-Fmoc-Hgl-Val-O*t*-Bu [(4*R*)- and (4*S*)-**3.17**]. D-Valine *tert*-butyl ester was reacted, respectively, with (2*R*,3*R*)- and (2*R*,3*S*)-methyl *N*-(Fmoc)oxiranyl glycinates [(3*R*)- and (3*S*)-**3.13**] to provide (4*S*)- and (4*R*)-**3.17** in 89% and 85% yields (Scheme 3.11). Considering that (3*S*)-oxirane (3*S*)-**3.13** is typically the minor isomer from the diastereoselective epoxidation of methyl *N*-(Fmoc)-vinylglycinate,[5] an alternative approach to prepare (4*R*)-Hgl (4*R*)-**3.17** was conceived, employing inversion of the hydroxyl group by Mitsunobu displacement. Treatment of (4*S*)-Hgl (4*S*)-**3.17** with *p*-nitrobenzoate, diisopropyl azodicarboxylate (DIAD) and triphenylphosphine in THF at 0 °C gave the (4*R*)-ester (4*R*)-**3.24a** in 80% yield. Benzoate hydrolysis using sodium azide in MeOH at 40 °C delivered (4*R*)-Hgl (4*R*)-**3.17** without Fmoc group removal in 75% yield.
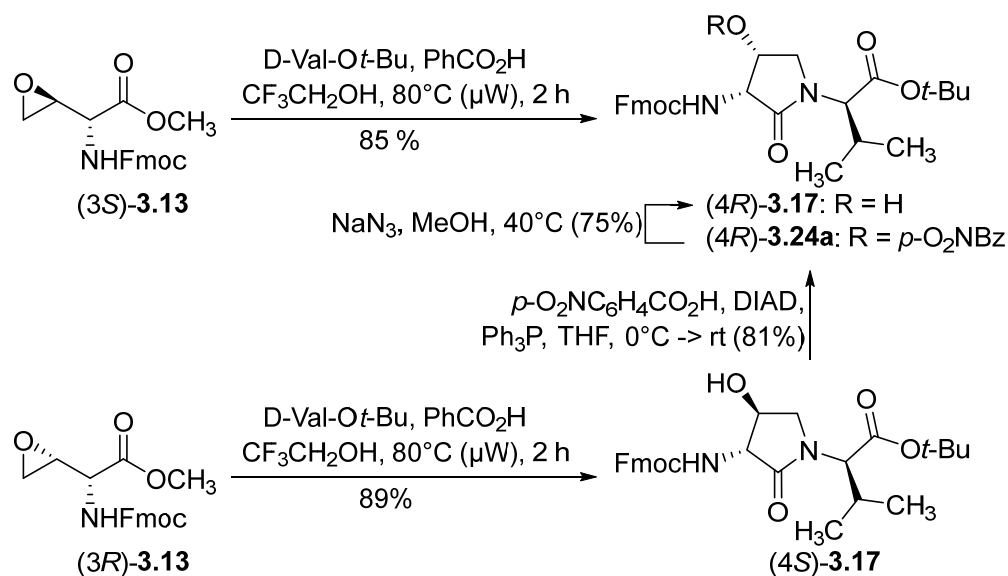
Scheme 3.11. Hgl synthesis from oxyranylglycine and hydroxyl group inversion

Assignment of configuration of (4*R*)- and (4*S*)-**3.17** was performed based on comparisons of their NMR spectra with those of the previously reported Hgl *trans*-diastereomers.[5] Notably, (3*R*,4*S*,2′*R*)-Fmoc-Hgl-Leu-OMe has been characterized by X-ray crystallography.[14] The *cis*- and

trans- diastereomer γ-proton chemical displacements of (4*R*)- and (4*S*)-**3.17** are, respectively, similar (3.44 and 3.52 ppm) and different (3.23 and 4.02 ppm) due likely to a downfield shift in the latter caused by the aromatic Fmoc group on the α-amine, which sits in a pseudoaxial orientation. Successful inversion of the *trans-* to the *cis*-diastereomer using *p*-nitrobenzoate in the Mitsunobu reaction evoked examination of the same conditions using a series of alternative pronucleophiles to prepare a set of β-substituted Agl analogs (Table 3.1). β-Amido alcohols have been previously shown to produce oxazolines under Mitsunobu conditions.[16] Although the Fmoc group prevented cyclization to the corresponding oxazoline, elimination occurred to a certain degree, particularly with less acidic pronucleophiles. β-Elimination of the oxyphosphonium salt competed with displacement to provide dehydrolactam **3.21** in 15−35% yields contingent on the nucleophile. Alcohol elimination has previously been observed as a side reaction in the Mitsunobu reaction and has been employed for olefin synthesis.[17-20] For example, Mitsunobu reactions on Ser and Thr residues have provided dehydroamino acids.[19-20] Although displacement under the Mitsunobu conditions has been typically performed on ordinary alcohols using acids having pK_a values of 11 or less,[21] reactions on (4*S*)Hgl (4*S*)-**3.17** were only successful using pronucleophiles having pK_a values of 3 to 7. Acidic pronucleophiles with pK_a values around 6 gave sluggish incomplete reactions with dehydrolactam **3.21** as a significant side product. In these cases, some improvement occurred when the betaine intermediate was generated prior to the addition of alcohol (4*S*)-**3.17**. Pronucleophiles with pK_a values higher than 7 were unsuccessful: e.g., *N*-hydroxysuccinimide, benzotriazole, phthalimide, acetylacetone, benzylamine, succinimide, phenol, and acetone cyanohydrin. In the latter cases, only elimination product **3.21** and starting material (4*S*)-**3.17** were recovered. For example, phenol gave 87% yield of dehydrolactam **3.21** after 18 h. A study of the influence of solvent was performed employing *N*-hydroxyphthalimide, which was the least successful of the reactive pronucleophiles in THF, giving *O*-alkylhydroxyphthalimide (4*R*)-**3.24g** in 42% yield along with high amounts of elimination product **3.21** (35%). The yield of displacement product (4*R*)-**3.24g** increased to 51% in DCM, which also reduced formation of dehydrolactam **3.21** to 25% yield. However, displacement to form **3.24g** in toluene and acetonitrile occurred, respectively, with similar (45%) and lower (23%) yields.[17] Attempts to improve the yield of **3.24g** using excess Ph$_3$P were unsuccessful and increased the yield of elimination product **3.21**.[18] In addition, constrained cysteine and diaminobutyrate (Dab) analogs, thiol (4*R*)-**3.24h** (−Nu = −SH) and *O*-alkylhydroxamine (4*R*)-**3.24i** (−Nu = −ONH$_2$),

were, respectively, liberated from (4*R*)-**3.24b** and (4*R*)-**3.24g** in 55% and 78% yields using sodium azide in MeOH and hydrazine monohydrate in a mixture of MeOH/DCM to demonstrate that the orthogonal protection may be suitable for Fmoc/*t*-Bu solid-phase synthesis commonly used in the preparation of peptide disulfides and oxime ligation conjugates.[22-23]

Table 3.1. 4-Substituted Agl residue synthesis by Mitsunobu displacement using pronucleophiles with various pK_a values[24]

NuH (pKa)		% **3.24**	% recovered (4*S*)-**3.17**	% **3.21**
a	O$_2$N—⬡—CO$_2$H (3.41)	80	–	16
b	⬡—C(=O)SH (3.61)	71	–	20
c	⬡—CO$_2$H (4.20)	68	6	19
d	benzotriazole-N-OH (4.30)	70	7	15
e	EtO$_2$C–C(CN)=N–OH (4.60)	57	17	23
f	⬡—SH (6.62)	49	21	28
g	N-hydroxyphthalimide (6.63)	THF: 42	23	35
		DCM: 51	0	25
		MePh: 45	0	38
		MeCN: 23	35	37

Application of diphenylphosphoryl azide (DPPA) as a hydrazoic acid equivalent under the Mitsunobu conditions with (4*S*)-Hgl (4*S*)-**3.17** and diethyl azodicarboxylate (DEAD) gave the corresponding azide (4*R*)-**3.24j** in 60% yield without detectable elimination and 25% recovered starting material (Scheme 2).[25] Azide (4*R*)-**3.24j** is suitably protected for use as a constrained Dap

analog. Moreover, azide (4*R*)-**3.24j** could be employed in copper-catalyzed azide alkyne cycloadditions (CuAAC) to prepare constrained histidine mimics.[26-27] For example, treatment of azide (4*R*)-**3.24j** with phenyl acetylene and CuI in the presence of DIEA and acetic acid gave 4-phenyltriazole **3.25** in 80% yield.[27]
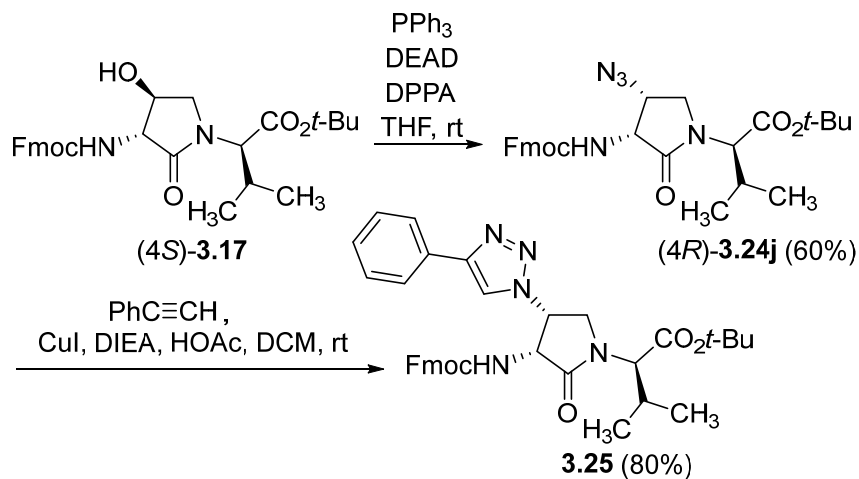
Scheme 3.12. Synthesis of β-azido-Agl (4*R*)-**3.24j** and triazole **3.25**

With a set of diverse 4-substituted Agl *cis*-diastereomers in hand, the synthesis of *trans* stereoisomers was next pursued. Attempts to employ the successful Mitsunobu conditions developed with (4*S*)-Hgl (4*S*)-**3.17** on the (3*R*)-alcohol, however, gave only dehydrolactam **3.21**. Considering that a preferred *anti*-orientation between the pseudoaxial β-hydroxyl group and α proton may favor dehydration, the amine and alcohol were tied into cyclic sulfamidate **3.22** to provide a reactive intermediate in a geometry less prone to elimination.[28] Treatment of (4*R*)-Hgl (4*R*)-**3.17** with thionyl chloride and imidazole in dichloromethane gave a separable 1:2 mixture of diastereoisomeric sulfamidites **3.23**. The minor (2*S*)-isomer (2*S*)-**3.23** was assigned based on the downfield shifted signal (5.8 vs 5.4 ppm) of the Agl β-proton due to the magnetic anisotropy of the proximal S−O bond.[28] Sulfamidate **3.22** was synthesized in 79% yield by oxidation of sulfamidites **3.23** using sodium periodate and catalytic ruthenium trichloride in 4:3 acetonitrile/water at 0 °C.[29] In preliminary studies, ring opening of sulfamidate **3.22** has been found to be contingent on solvent (Scheme 3.13). For example, β-azido Agl (4*S*)-**3.24j** was prepared from **3.22** in 35% and 80% yields using NaN₃, respectively, in DMF and 1:4 DMF/ DCM. Potassium benzothiolate reacted with sulfamidate **3.22**, respectively, in DMF and DCM, to give 30% and 90% yields of the constrained cysteine dipeptide (4*S*)-**3.24b**.
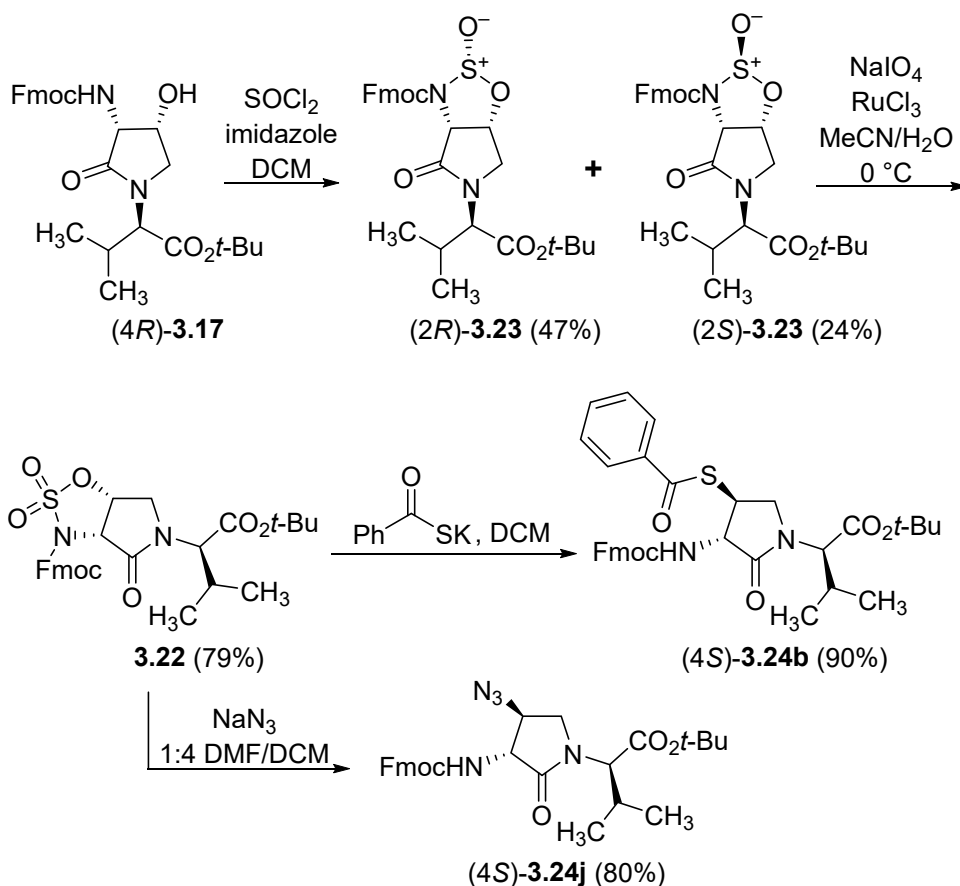
Scheme 3.13. Synthesis and ring opening of sulfamidate **3.22**

Further studies of ring opening of cyclic sulfamidate **3.22** with other nucleophiles are now in progress and will be presented in due time. Stereoselective access to a series of β-substituted α-*N*(Fmoc)amino-γ-lactam dipeptides **3.24** has been achieved through displacements of the corresponding β-hydroxy-α-amino-γ-lactams **3.17**. The Mitsunobu reaction on the *trans* diastereomer (4*S*)-**3.17** has given a variety of *cis*-β-substituted Agl analogs (3*R*)-**3.24** that may serve as constrained mimics of Ser, Thr, Cys, Dap, Dab, and His. Moreover, nucleophilic ring opening of cyclic sulfamidate **3.22** has provided entry to *trans*-β-substituted Agl derivatives (3*S*)-**3.24** for use as constrained Cys and Dap derivatives. Considering the reactivity of the β-substituents, potential exists for their elaboration into other side chain functionality, as well as for the synthesis of constrained peptide conjugates. Application of β-substituted Agl analogs **3.24** in peptide synthesis is ongoing and promises a useful means to explore a variety of biologically relevant targets.

Associated content

Supporting Information

The Supporting Information is available free of charge on the ACS Publications website at DOI: 10.1021/acs.orglett.8b02575.

Experimental procedures; characterization data (^{1}H, ^{13}C, and 2D NMR, HRMS, IR, and specific rotation) (PDF)

Author information

Corresponding Author

*E-mail: william.lubell@umontreal.ca.

ORCID

Azade Geranurimi: 0000-0002-6866-1089

Notes

The authors declare no competing financial interest.

Acknowledgments

References

1.	Freidinger, R. M.; Veber, D. F.; Perlow, D. S.; Saperstein, R., Bioactive conformation of luteinizing hormone-releasing hormone: evidence from a conformationally constrained analog. *Science* **1980,** *210*, 656-658.

2.	St-Cyr, D. J.; García-Ramos, Y.; Doan, N.-D.; Lubell, W. D., Aminolactam, N-aminoimidazolone, and N-aminoimdazolidinone peptide mimics. In *Peptidomimetics I*, Springer: 2017; pp 125-175.

3.	Khashper, A.; Lubell, W. D., Design, synthesis, conformational analysis and application of indolizidin-2-one dipeptide mimics. *Org. Biomol. Chem.* **2014,** *12*, 5052-5070.

4.	Ball, J. B.; Alewood, P. F., Conformational constraints: Nonpeptide β-turn mimics. *J. Mol. Recognit.* **1990,** *3*, 55-64.

5.   St-Cyr, D. J.; Jamieson, A. G.; Lubell, W. D., α-Amino-β-hydroxy-γ-lactam for constraining peptide Ser and Thr residue conformation. *Org. Lett.* **2010,** *12*, 1652-1655.

6.   Bhagwanth, S.; Mishra, R. K.; Johnson, R. L., Development of peptidomimetic ligands of Pro-Leu-Gly-NH2 as allosteric modulators of the dopamine D2 receptor. *Beilstein J. Org. Chem. Beilstein journal of organic chemistry* **2013,** *9* (1), 204-214.

7.   Boutard, N.; Jamieson, A. G.; Ong, H.; Lubell, W. D., Structure–Activity Analysis of the Growth Hormone Secretagogue GHRP-6 by α-and β-Amino γ-Lactam Positional Scanning. *Chemical biology & drug design* **2010,** *75* (1), 40-50.

8.   Perdih, A.; Kikelj, D., The application of Freidinger lactams and their analogs in the design of conformationally constrained peptidomimetics. *Curr. Med. Chem.* **2006,** *13*, 1525-1556.

9.   Wolf, J. P.; Rapoport, H., Conformationally constrained peptides. Chirospecific synthesis of 4-alkyl-substituted. gamma.-lactam-bridged dipeptides from L-aspartic acid. *J. Org. Chem.* **1989,** *54*, 3164-3173.

10.   Garvey, D. S.; May, P. D.; Nadzan, A. M., 3, 4-Disubstituted. gamma.-lactam rings as conformationally constrained mimics of peptide derivatives containing aspartic acid or norleucine. *J. Org. Chem.* **1990,** *55*, 936-940.

11.   Crucianelli, E.; Galeazzi, R.; Martelli, G.; Orena, M.; Rinaldi, S.; Sabatino, P., A novel conformationally restricted analogue of 3-methylaspartic acid via stereoselective methylation of chiral pyrrolidin-2-ones. *Tetrahedron* **2010,** *66* (1), 400-405.

12.   Wyss, C.; Batra, R.; Lehmann, C.; Sauer, S.; Giese, B., Selective photocyclization of glycine in dipeptides. *Angewandte Chemie International Edition in English* **1996,** *35* (21), 2529-2531.

13.   Sicherl, F.; Cupido, T.; Albericio, F., A novel dipeptidomimetic containing a cyclic threonine. *Chemical Communications* **2010,** *46* (8), 1266-1268.

14.   St-Cyr, D. J.; Maris, T.; Lubell, W. D., Crystal-state structure analysis of β-hydroxy-γ-lactam constrained Ser/Thr peptidomimetics. *Heterocycles* **2010,** *82* (1), 729-737.

15.   Afzali-Ardakani, A.; Rapoport, H., l-Vinylglycine. *J. Org. Chem.* **1980,** *45*, 4817-4820.

16.   Petersson, M. J.; Jenkins, I. D.; Loughlin, W. A., The use of phosphonium anhydrides for the synthesis of 2-oxazolines, 2-thiazolines and 2-dihydrooxazine under mild conditions. *Org. Biomol. Chem.* **2009,** *7*, 739-746.

Chapter 3

17.	Elson, K. E.; Jenkins, I. D.; Loughlin, W. A., The Hendrickson reagent and the Mitsunobu reaction: a mechanistic study. *Org. Biomol. Chem.* **2003,** *1* , 2958-2965.

18.	Huang, G.; Schramm, S.; Heilmann, J.; Biedermann, D.; Křen, V.; Decker, M., Unconventional application of the Mitsunobu reaction: Selective flavonolignan dehydration yielding hydnocarpins. *Beilstein J. Org. Chem.* **2016,** *12*, 662-669.

19.	Cherney, R. J.; Wang, L., Efficient Mitsunobu reactions with N-phenylfluorenyl or N-trityl serine esters. *J. Org. Chem.* **1996,** *61*, 2544-2546.

20.	Wiśniewski, K.; Kołdziejczyk, A. S.; Falkiewicz, B., Applications of the Mitsunobu reaction in peptide chemistry. *J. Pept. Sci.: an official publication of the European Peptide Society* **1998,** *4*, 1-14.

21.	Fletcher, S., The Mitsunobu reaction in the 21 st century. *Organic Chemistry Frontiers* **2015,** *2*, 739-752.

22.	Villadsen, K.; Martos-Maldonado, M. C.; Jensen, K. J.; Thygesen, M. B., Chemoselective reactions for the synthesis of glycoconjugates from unprotected carbohydrates. *ChemBioChem* **2017,** *18*, 574-612.

23.	Guthrie, Q. A.; Proulx, C., Oxime Ligation via in situ Oxidation of N-Phenylglycinyl Peptides. *Org. Lett.* **2018,** *20*, 2564-2567.

24.	Cox, B. G., *Acids and bases: solvent effects on acid-base strength*. OUP Oxford: 2013.

25.	Lal, B.; Pramanik, B. N.; Manhas, M.; Bose, A. K., Diphenylphosphoryl azide a novel reagent for the stereospecific synthesis of azides from alcohols. *Tetrahedron Lett.* **1977,** *18*, 1977-1980.

26.	Buysse, K.; Farard, J.; Nikolaou, A.; Vanderheyden, P.; Vauquelin, G.; Sejer Pedersen, D.; Tourwé, D.; Ballet, S., Amino triazolo diazepines (Ata) as constrained histidine mimics. *Org. Lett.* **2011,** *13*, 6468-6471.

27.	Shao, C.; Wang, X.; Zhang, Q.; Luo, S.; Zhao, J.; Hu, Y., Acid–base jointly promoted copper (I)-catalyzed azide–alkyne cycloaddition. *J. Org. Chem.* **2011,** *76*, 6832-6836.

28.	Meléndez, R. E.; Lubell, W. D., Synthesis and reactivity of cyclic sulfamidites and sulfamidates. *Tetrahedron* **2003,** *15*, 2581-2616.

29.	Wei, L.; Lubell, W. D., Racemization in the use of N-(9-(9-Phenylfluorenyl)) serine-derived cyclic sulfamidates in the synthesis of δ-keto α-amino carboxylates and prolines. *Org. Lett.* **2000,** *2*, 2595-2598.

Proceeding 1

Stereoselective synthesis of a β-methylthio α-amino γ-lactam dipeptide, a *S*-methyl-Cys-Val mimic

I performed all experiments, and the isolation and characterization of all compounds. I wrote the first draft of the Proceedings and contributed to its revision which was edited by Professor Lubell.

Azade Geranurimi and William D. Lubell

Department of chemistry, Université de Montréal, Montreal, Canada

Abstract

Pursuing β-substituted α-*N*-(Fmoc)amino-γ-lactam (Agl) dipeptides by displacements of the alcohol corresponding β-hydroxy-α-amino-γ-lactam (Hgl) residue, nucleophilic ring opening of cyclic sulfamidate **3.22** with thiocyanate has provided entry to *trans*-β-methylthio-Agl derivative **3.24l** for use as a constrained *S*-methyl Cys derivative.

Introduction

Peptides are typically flexible and may adopt multiple conformers in solution. Among methods to restrict peptide movement and improve receptor binding affinity, cyclization has proven successful since the team at Merck led by Drs. Freidinger and Veber introduced α-amino-γ-lactam (Agl) residues into LH-RH.[1] Since their pioneering research, many have used Agl residues to favor peptide turn conformations by constraining ω, φ and ψ backbone dihedral angles.[2] Adding β-substituents to Agl residues has since been perceived as a means to enhance mimicry potential by simultaneously constraining backbone and side (χ) dihedral angles.[3-5]

Recently, a set of β-substituted α-amino-γ-lactam residues were synthesized using β-hydroxy-α-amino-γ-lactam (Hgl) residue **3.17** as a convenient precursor (Figure 3.3).[5,6] Mitsunobu reactions on the *trans* isomer of Hgl *trans*-**3.17** with pro-nucleophiles having pK_a values between

3 and 7 provided a variety of *cis*-β-substituted Agl analogs **3.24a-g** in 49-80% yields.[6] Moreover, treatment of *trans*-Hgl **3.17** with diphenylphosphoryl azide (DPPA) as a hydrazoic acid equivalent under Mitsunobu conditions gave in 60% yield the corresponding β-azido-Agl residue, which was further converted to its phenyltriazole counterpart in 80% yield by copper-catalyzed azide alkyne cycloadditions.[6]

Attempts to employ Mitsunobu reaction on *cis*-Hgl *cis*-**3.17** gave however only dehydro-lactam.[6] Cyclic sulfamidate **3.22** was thus synthesized from *cis*-Hgl *cis*-**3.17** to disfavor β-elimination to dehydro-lactam.[6] Ring opening of sulfamidate **3.22** has already provided β-azido-Agl (4*S*)-**3.24j** and constrained protected cysteine (4*S*)-**3.24b** (Figure 3.3). Exploring the chemistry of sulfamidate **3.22** further, we now report a method to provide constrained *S*-alkyl Cys residues (e.g., **3.24l**).
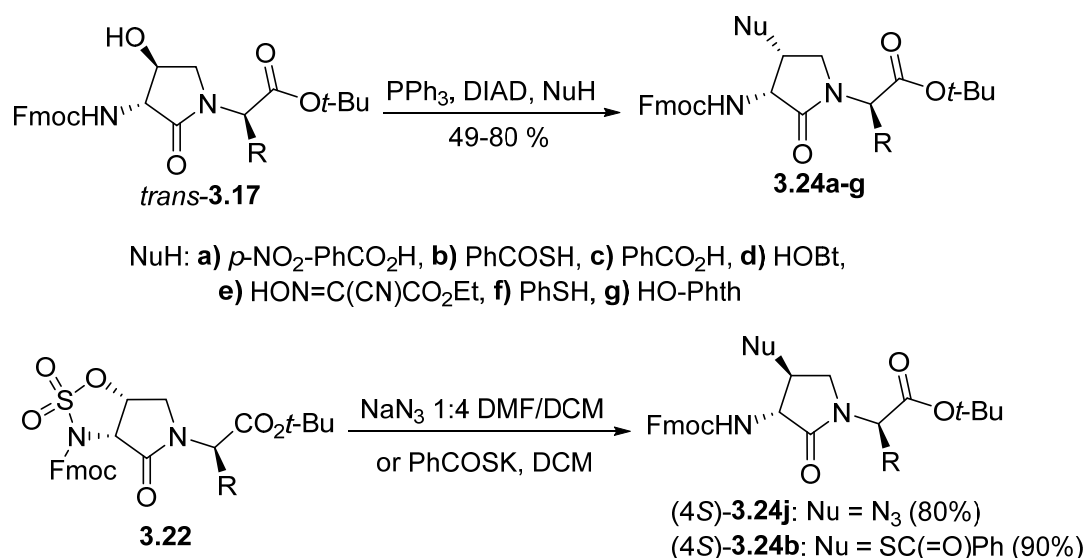
Figure 3.3. Synthesis of 4-substituted Agl residues by way of the Mitsunobu reaction and cyclic sulfamidate ring opening.

Results and discussion

β-Thiocyano-Agl **3.24k** was synthesized by reacting sulfamidate **3.22** with potassium thiocyanate in 1:1 DMF/DCM in 92% yield. Reduction of thiocyanide **3.24k** with NaBH4 and alkylation with iodomethane by way of a constrained Cys thiolate intermediate provided thioether **3.24l** in 65% yield from **3.24k** (Scheme 3.14).[7]
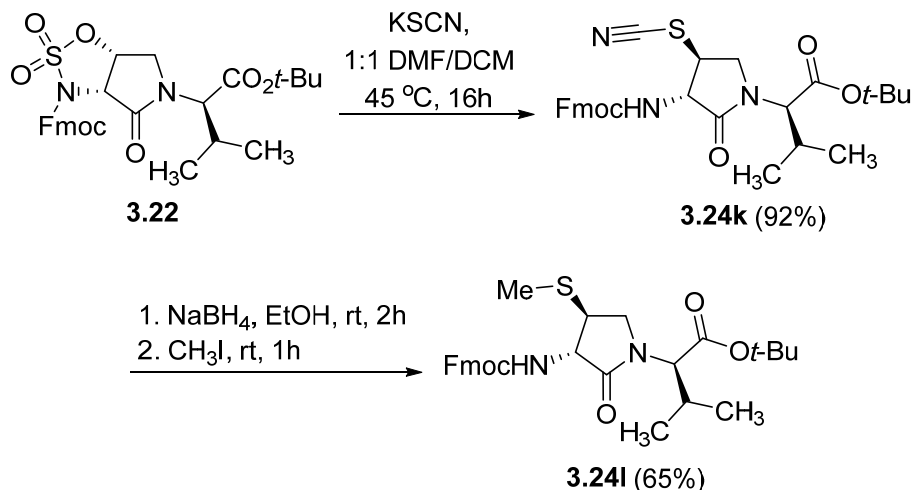
Scheme 3.14. Synthesis of constrained *S*-methyl Cys derivative **3.24l**

Conclusions

Methylthio-Agl **3.24l** may be considered a constrained isoleucine analog. Moreover, *S*-alkylation with other electrophiles may further expand the diversity of *trans*-β-substituted Agl residues. The synthesis of such amino acid residues with constrained backbone and side chain geometry, and their subsequent insertion into peptides is now under investigation and will be reported in due time.

Experimental

***tert*-Butyl (3*S*, 4*S*, 2'*R*)-2-[3-(Fmoc)amino-4-thiocyanato-2-oxopyrrolidin-1-yl]-3-methylbutanoate**

A solution of sulfamidate **3.22** (1 eq., 80 mg, 144 umol, prepared according to ref 6) in a mixture of DCM (2 mL) and DMF (2 mL) was treated with potassium thiocyanate (3 eq., 42 mg, 435 umol), stirred at 45 °C for 16 h, poured into 1 M NaH_2PO_4, and extracted with DCM. The combined organic phase was washed with brine, dried, filtered, evaporated to a residue, that was purified by column chromatography using a step gradient of 10-30% EtOAc in hexane. Evaporation of the collected fractions gave thiocyanide **3.24k** as a white solid (71. mg, 92 %): R_f= 0.3 (30% EtOAc in hexane); mp 56-60 °C; $[\alpha]_D^{25}$ 24° (c 1, $CHCl_3$); FT-IR (neat) vmax 3321, 2973, 2155, 1707, 1523, 1449, 1391, 1370, 1239, 1150, 1106, 1043, 781, 759, 738 cm^{-1}; ^{1}H NMR (500 MHz, $CDCl_3$) δ 7.76 (d, *J* = 7.6 Hz, 2H), 7.59 (ddd, *J* = 7.4, 3.8, 0.6 Hz, 2H), 7.41 (t, *J* = 7.4 Hz, 2H), 7.32 (td, *J* = 7.5, 1.0 Hz, 2H), 5.48 (s, 1H), 4.46 (m, 3H), 4.31 (s, 2H), 4.23 (t, *J* = 6.8 Hz, 1H), 3.83 (dd, *J*

= 18.1, 9.1 Hz, 1H), 3.49 (t, J = 9.4 Hz, 1H), 2.23 (m, 1H), 1.48 (s, 9H), 1.02 (d, J = 6.7 Hz, 3H), 0.97 (d, J = 6.8 Hz, 3H); ^{13}C NMR (126 MHz, CDCl$_3$) δ 169.0, 156.5, 143.5, 141.3, 127.8, 127.1, 125.1, 120.1, 109.7, 82.7, 67.6, 60.9, 57.1, 48.1, 47.0, 45.9, 29.0, 28.0, 22.0, 19.5, 19.3; HRMS (ESI-TOF) m/z [M+Na]$^+$ calcd for C$_{29}$H$_{33}$N$_3$O$_5$S 558.2033 found, 558.2017.

tert-Butyl (3*S*, 4*S*, 2'*R*)-2-[3-(Fmoc)amino-4-methylthio-2-oxopyrrolidin-1-yl]-3-methylbutanoate

A solution of thiocyanide **3.24k** (1 eq., 30 mg, 56.0 umol) in EtOH (95%, 1 mL) was added drop-wise to a stirred solution of NaBH$_4$ (5 eq., 10.6 mg, 280 umol) in EtOH (95%, 1 mL) at rt. The mixture was stirred for 2 h, treated with iodomethane (2 eq., 7 uL, 112 umol), stirried for 1h, and treated with a solution of 1N HCl (2 mL). The mixture was extracted with EtOAc (3×5 mL). The combined organic phase was washed with brine, dried, filtered, evaporated to a residue, that was purified by column chromatography using a step gradient of 10-30% EtOAc in hexane. Evaporation of the collected fractions gave thioether **3.24l** as a light yellow oil (19 mg, 65 %): R$_f$ = 0.5 (30% EtOAc in hexane); [α]$_D^{25}$ 45° (*c* 0.2, CHCl$_3$); ^{1}H NMR (500 MHz, CDCl$_3$) δ 7.76 (d, J = 7.5 Hz, 2H), 7.60 (d, J = 7.4 Hz, 2H), 7.39 (t, J = 7.5 Hz, 2H), 7.31 (td, J = 7.5, 1.0 Hz, 2H), 5.26 (s, 1H), 4.45 (d, J = 9.1 Hz, 1H), 4.43 (d, J = 7.0 Hz, 2H), 4.34 (t, J = 8.9 Hz, 1H), 4.24 (t, J = 7.0 Hz, 1H), 4.06 (dd, J = 9.4, 7.5 Hz, 1H), 3.32 – 3.24 (m, 1H), 3.21 (t, J = 9.2 Hz, 1H), 2.24 – 2.14 (m, 4H), 1.47 (s, 9H), 1.00 (d, J = 6.7 Hz, 3H), 0.94 (d, J = 6.8 Hz, 3H); ^{13}C NMR (126 MHz, CDCl$_3$) δ 171.1, 169.5, 156.4, 143.8, 141.3, 127.7, 127.1, 125.2, 120.0, 82.3, 67.3, 60.7, 57.6, 47.8, 47.1, 45.7, 28.8, 28.1, 22.0, 19.4, 13.6; HRMS (ESI-TOF) m/z [M+Na]$^+$ calcd for C$_{29}$H$_{36}$N$_2$O$_5$S 547.2237 found, 547.2228.

Acknowledgments

References

1. Freidinger, R. M.; Veber, D. F.; Perlow, D. S.; Saperstein, R., *Science* **1980,** *210*, 656-658.

2. Freidinger, R. M., *J. Med. Chem.* **2003,** *46*, 5553-5566.

3. St-Cyr, D. J.; García-Ramos, Y.; Doan, N.-D.; Lubell, W. D., Aminolactam, N-Aminoimidazolone, and N-Aminoimdazolidinone Peptide Mimics. In *Peptidomimetics I*, Springer2017; pp 125-175.

4. Wolf, J. P.; Rapoport, H., *J. Org. Chem.* **1989,** *54*, 3164-3173.

5. St.-Cyr, D.; Jamieson, A. G.; Lubell, W.D. *Org. Lett.* **2010**, 12, 1652-1655.

6. Geranurimi, A.; Lubell, W. D., *Org. Lett.* **2018,** *20*, 6126-6129.

7. Gulea, M.; Hammerschmidt, F.; Marchand, P.; Masson, S.; Pisljagic, V.; Wuggenig, F., *Tetrahedron: Asymmetry* **2003,** 14, 1829-1836.

Chapter 3

Chapter 4: Solid-Phase Synthesis and Diversification of β-Substituted α-Amino-γ-Lactam Peptide Allosteric Modulators of the Inteleukin-1 Receptor

4.1. Context

Dipeptide building blocks were synthesized in Chapter 3. Employing certain examples of the latter in solid-phase approaches, the diversity of β-substituted Agl peptides has been greatly expanded. For example, by modification of azide **4.2c**, amine, amide, urea and guanidine functionality were installed at the β-position.

The copper-catalyzed azide alkyne cycloaddition (CuAAC) chemistry has been used to synthesize a variety of triazole analogs from the azide **4.2c**. Libraries of 4-substituted 1,2,3-triazoles were synthesized with regiocontrol by employing CuI, DIEA and acetic acid.[1,2] The tertiary amine has been suggested to be essential for dissociating the polymeric structure of CuI to favor the cycloaddition reaction.[3] Moreover, acetic acid has been recognized to accelerate the protonation of the C-Cu intermediates and to buffer the basicity of the tertiary amine.[4-5]

In total fifteen novel β-substituted-Agl[3] analogs of 101.10 were synthesized. β-Substituents were installed to examine the potential for hydrogen bonds, salt bridges and aromatic interactions. Analogs with ($3R$,$4S$)-sterochemistry were synthesized because of the successful activity of the corresponding ($3R$,$4S$)-Hgl[3] isomer.

The β-substituted-Agl[3]-101.10 analogs are currently being tested *in vitro.* Based on preliminary data not reported, selected analogs are being examined a PTB murine model. The activity of the selected β-substituted-Agl analogs have been examined *in vivo* in a rodent model of OIR. In the model of ROP, five analogs exhibited identical activity as the parent peptide **4.1**. The activity of the five analogs merits their further investigation and employment as leads for treating retinopathy of prematurity, which is the leading cause of infant blindness.

4.2. References

1.	Shao, C.; Wang, X.; Zhang, Q.; Luo, S.; Zhao, J.; Hu, Y., Acid–base jointly promoted copper (I)-catalyzed azide–alkyne cycloaddition. *J. Org. Chem.* **2011,** *76*, 6832-6836.

2.	Hein, J. E.; Fokin, V. V., Copper-catalyzed azide–alkyne cycloaddition (CuAAC) and beyond: new reactivity of copper (I) acetylides. *Chemical Society Reviews* **2010,** *39*, 1302-1315.

3.	Meldal, M.; Tornøe, C. W., Cu-catalyzed azide-alkyne cycloaddition. *Chemical reviews* **2008,** *108*, 2952-3015.

4.	Shao, C.; Cheng, G.; Su, D.; Xu, J.; Wang, X.; Hu, Y., Copper (I) Acetate: A structurally simple but highly efficient dinuclear catalyst for Copper-Catalyzed Azide-Alkyne Cycloaddition. *Advanced Synthesis & Catalysis* **2010,** *352*, 1587-1592.

5.   Shao, C.; Wang, X.; Xu, J.; Zhao, J.; Zhang, Q.; Hu, Y., Carboxylic Acid-Promoted Copper (I)-Catalyzed Azide-Alkyne Cycloaddition. *J. Org. Chem.* **2010,** *75*, 7002-7005.

Chapter 4

Article 3

Solid-Phase Synthesis and Diversification of β-Substituted α-Amino-γ-Lactam Peptide Allosteric Modulators of the Inteleukin-1 Receptor

(*In preparation for Frontiers Chem.,* **2019**)

I performed all the experiments to synthesize the peptide analogs and their isolation and characterization. The analogs are currently being tested in a panel of *in vitro* cellular assays as well as *in vivo* activity in murine models of PTB and ROP by our collaborators Professor Chemtob, Dr. Quiniou, Dr. Hou and Mr. Cheng from the Département de pédiatrie, Université de Montréal. Colin and I wrote the original draft of the manuscript which has been edited by Professors Lubell and Chemtob, and Dr. Quiniou.

Azade Geranurimi[1#], Colin W.H. Cheng[2,3,4#], Christiane Quiniou[2], Xin Hou[2], Sylvain Chemtob[2,3,4,5], William D. Lubell[1]

[1]Département de Chimie, Université de Montréal, Montréal, QC, Canada

[2]Department of Pharmacology & Therapeutics, McGill University, Montréal, QC, Canada

[3]Hôpital Sainte-Justine Research Centre, Montréal, QC, Canada

[4]Hôpital Maisonneuve-Rosemont Research Centre, Montréal, QC, Canada

[5]Departments of Pediatrics, Pharmacology and Physiology, and Ophthalmology, Université de Montréal, Montréal, QC, Canada

# These authors contributed equally.

* Correspondence: Prof. William D. Lubell, *william.lubell@umontreal.ca*

Abstract

A key cytokine mediator of inflammation, interleukin-1β (IL-1β) binds to the IL-1 receptor (IL-1R) and activates various downstream signaling mediators, including NF-κB, which is required for immuno-vigilance and cytoprotection. Towards the development of IL-1-targeting therapeutics which exhibit functional selectivity, the all-D-amino acid

peptide **4.1** (101.10, H-D-Arg-D-Tyr-D-Thr-D-Val-D-Glu-D-Leu-D-Ala-NH2) was conceived as an allosteric IL-1R modulator that conserves NF-κB signaling while inhibiting other IL-1-activated pathways. Employing β-hydroxy-α-amino-γ-lactam (Hgl) stereoisomers to study the conformation about the Thr³ residue in **4.1**, among possible diastereomers, [(3R,4S)-Hgl³]-**4.1** (**4.2b**) was found to exhibit identical *in vitro* and *in vivo* activity as the parent peptide and superior activity to the α-amino-γ-lactam (Agl) counterpart. Noting the relevance of the β-hydroxyl substituent and configuration for the activity of (3R,4S)-**4.2b**, fifteen different β-substituted-Agl³ analogs of **4.1** (e.g., **4.2c-q**) have now been synthesized by a combination of solution- and solid-phase methods employing *N*-Fmoc-β-substituted-Agl³-Val-OH dipeptide building blocks. Introduction of a β-azido-Agl³ residue into the resin bound peptide and subsequent reduction and CuAAC chemistry gave access to a series of amine and triazole derivatives (e.g., **4.2h-q**). β-Substituted-Agl³-101.10 analogs **4.2c-q** exhibited generally similar circular dichroism (CD) spectra as that of Hgl analog **4.2b** in water, presenting curve shapes indicative of *β*-turn structure. In contrast, the relevance of the β-substituent was indicated in a rodent model of retinopathy of prematurity (ROP), in which only certain analogs inhibited vaso-obliteration with similar activity as 101.10 and **4.2b**. The active analogs and methods for their synthesis represent respectively useful leads for developing treatments of ROP, the leading cause of infant blindness, and effective means for exploring structure-activity relationships of biologically active peptides.

Introduction

Inflammatory factor expression is engaged primarily through signaling pathways triggered by interleukin-1β (IL-1β).[1] This major pro-inflammatory cytokine may stimulate various physiological effects contingent on the activated cascade, leading ultimately to hyperthermia, hypotension, tissue destruction, and inflammation.[2] The activity of IL-1β is critical for inflammatory responses to treat damaged tissue and to fight invasion. Imbalanced IL-1β activity is however a pathogenic characteristic of many chronic conditions.

The IL-1 receptor I (IL-1RI) complex is composed of the IL-1 receptor and accessory protein (IL-1RAcP) subunits, which on binding to IL-1β activate multiple signaling pathways.[3] For example, the nuclear factor kappa-light-chain-enhancer of

activated B cells (NF-κB) protein complex is typically activated by IL-1β signaling which prompts cellular responses responsible for immuno-vigilance to counter bacterial and viral invasion. Other IL-1β triggered signaling pathways include those mediated by kinases such as c-Jun *N*-terminal kinases (JNK)[4] and Rho-associated kinase-2 (ROCK2),[5] which regulate various aspects of the inflammation cascade including the synthesis of pro-inflammatory cytokines, and the maturation, migration and activity of T cells.

Two natural inhibitors of IL-1β signaling are the antagonist protein (IL-1Ra) and decoy receptor, IL-1 receptor type II (IL-1RII).[3] IL-1Ra competes with IL-1 for the IL-1R binding site and prevents recruitment of IL-1RAcP. IL-1RII sequesters IL-1 but cannot form a signaling complex.[1] Current therapeutic strategies to counter pathological IL-1 signaling have been based on the mechanisms of these natural proteins. The three FDA-approved proteins comprise: 1) the recombinant IL-1 receptor antagonist, Kineret, 2) the IL-1 trap composed of a dimeric fusion of the ligand-binding domains of the extracellular portions of IL-1R1 and IL-1RAcP proteins, Rilonacept, and 3), a human monoclonal antibody targeting IL-1β, Canakinumab. These relatively large protein immunomodulators have presented secondary effects in the clinical setting including immunosuppression, which increases the risk for opportunistic infections, and pain at the site of injection.[6-7] Their failures in clinical trials may be due in part to drawbacks related to non-selective interference of all signals triggered by acting directly on the native orthosteric ligand IL-1β.[6-7] Interest in selective agents to differentiate IL-1β signaling pathways leading to immuno-vigilance and inflammation has focused attention on modulation of IL-1RI using allosteric ligands, which bind remotely from the orthosteric ligand binding site and induce biased signaling. Ideally, such allosteric modulators can be smaller molecules exhibiting improved bioavailability, potential for oral administration, protease resistance and lower risks of toxicity.

The all D-amino acid heptapeptide 101.10 (**4.1**, D-Arg-D-Tyr-D-Thr-D-Val-D-Glu-D-Leu-D-Ala-NH$_2$) was identified from a library of peptide sequences derived from IL-1RAcP loop regions,[8-9] and shown to exhibit potent, selective, and reversible non-competitive inhibition of IL-1β activity. For example, peptide **4.1** blocked IL-1β–induced human thymocyte cell proliferation *in vitro*,[10] and demonstrate robust *in vivo* effects in models of hyperthermia and inflammatory bowel disease.[9] Efforts to understand the

Chapter 4

biologically active conformation of **4.1** through covalent constraint have employed α-amino-γ-lactam (Agl) residues,[10-11] so-called Freidinger-Veber lactams,[12-13] as well as their β-hydroxy-α-amino-γ-lactam (Hgl) counterpart as a rigid threonine mimic.[14-15] Among the restricted analogs, [(3*R*,4*S*)-Hgl[3]]-**4.1** exhibited identical signaling behavior as the parent peptide *in vitro*.[16] Like **4.1**, [(3*R*,4*S*)-Hgl[3]]-**4.1** did not inhibit NF-κB signaling but exhibited strong inhibitory potency on kinases (e.g., JNK and ROCK2) and cytokines [e.g., IL-6 and cyclooxygenase-2 (COX-2)] activated by IL-1β. Moreover, [(3*R*,4*S*)-Hgl[3]]-**4.1** behaved like **4.1** in *in vivo* models of preterm birth (PTB) and retinopathy of prematurity (ROP) respectively delaying IL-1β-induced labor and curbing oxygen-induced vaso-obliteration. In contrast to **4.1**, which exhibits a random coil circular dichroism (CD) spectrum in water, [(3*R*,4*S*)-Hgl[3]]-**4.1** displayed a CD curve shape indicative of a *β*-turn geometry. Although the corresponding [(3*R*)-Agl[3]]- **4.1** (**4.2a**) exhibited a similar CD curve shape as [(3*R*,4*S*)-Hgl[3]]-**4.1** (**4.2b**), the Agl analog failed to exhibit inhibitory potency on p38 mitogen-activated protein kinases (p38 MAPK) nor ROCK2, and was inactive in the ROP model indicating the significance of the β-hydroxyl group for blocking signaling and activity in the pathways leading to oxygen-induced vaso-obliteration.

To further study the influence of the β-substituent of [(3*R*,4*S*)-Hgl[3]]-**4.1** (**4.2b**) on activity, a series of β-substituted-Agl analogs were synthesized stereoselectively through routes featuring nucleophilic ring opening of cyclic sulfamidate **4.4** derived from Fmoc-(3*R*, 4*R*)-Hgl-Val-O*t*-Bu (Scheme 4.1). Subsequent ester removal has provided Fmoc-(3*R*,4*S*)-β-substituted-Agl-Val-OH analogs possessing β-azido **4.3c**, thiocyano **4.3d** and methylthio **4.3e** substituents.[15, 17] Moreover, application of hydroxyphthalimide in sulfamidate ring opening gave protected aminoxy analog **4.3f**. By employing β-substituted-Agl dipeptides **4.3c-f** as building blocks in standard Fmoc-based solid phase synthesis protocols,[18] four novel lactam analogs of **4.1** (e.g., **4.2c-f**) were synthesized. Furthermore, modification of the azide and hydroxyphthalimide moieties of the corresponding protected peptides **4.8c** and **4.8f** on resin gave β-amino and β-aminoxy-Agl[3] analogs **4.2h** and **4.2g**, accordingly. Modification of β-amino-Agl[3] resin **4.8h** by acylation, carbamylation and guanidinylation gave access to lactam analogs **4.2i-k**. Finally, copper-catalyzed azide alkyne cycloadditions (CuAAC) on β-azido-Agl[3] resin **4.8c** furnished 1,2,3-triazoles which on resin cleavage and removal of protection gave lactams **4.2l-q**. This combination of

Chapter 4

solution- and solid-phase synthesis protocols delivered fifteen new (3*R*,4*S*)-β-substituted-Agl[3] analogs of **4.1** (e.g., **4.2c-q**) in which the hydroxyl group of **4.2b** was replaced by a variety of functional groups with potential to serve in hydrogen bonds as donors and acceptors, in salt bridges as protonated ammonium ions, and in potential π-cation interactions as aromatic donors.

a. H
b. OH
c. N_3
d. SCN
e. SMe
f. O-NPhth
g. ONH_2
h. NH_2
i. -NH(C=O)Me
j. -NH(C=O)NH_2
k. -NH(C=NH)NH_2

l. R: Ph
m. R: p-MeC$_6$H$_4$
n. R: m-H$_2$N-C$_6$H$_4$
o. R: -C(CH$_3$)$_2$NH$_2$
p. R: CH$_2$NH$_2$
q. R: CH$_2$OH
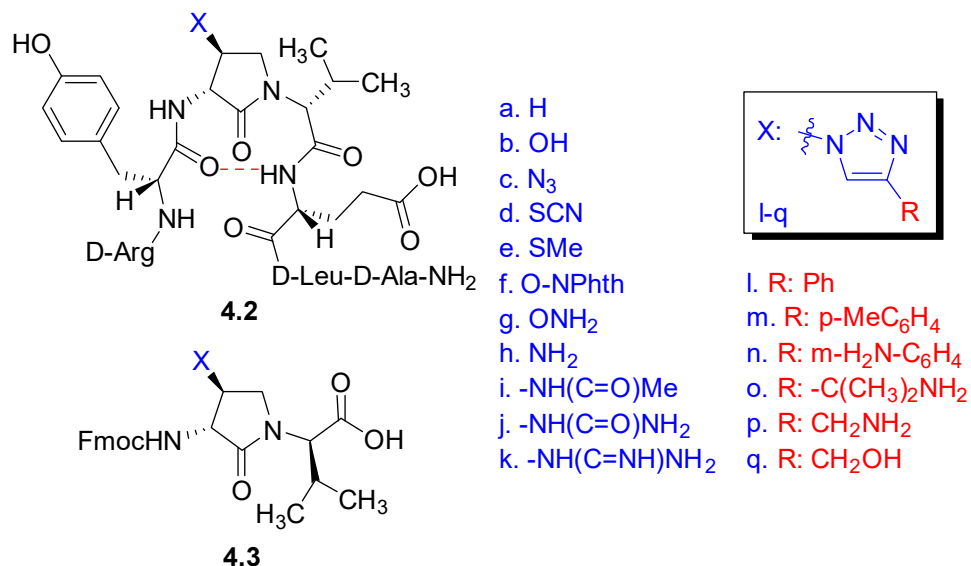
Figure 4.1. β-Substituted-Agl analogs **4.2** and **4.3**

The influence of the β-substituent on conformation was analyzed using circular dichroism (CD) spectroscopy to compare the curve of (3*R*,4*S*)-Hgl analog **4.2a** with those of other (3*R*,4*S*)-β-substituted-Agl[3] analogs. The β-substituent effects of lactams **4.2c-q** are also being examined *in vitro* by assessing their influence on the transcription of inflammatory genes corresponding to IL-1β and COX-2, and by examining activity in a reporter assay for NF-κB production. Based on preliminary *in vitro* analyses, certain analogs were selected for examination in an *in vivo* rodent model of oxygen-induced retinopathy (OIR). These investigations have identified a set of (3*R*,4*S*)-β-substituted-Agl[3] analogs that exhibited similar CD curves and *in vivo* effects as the (3*R*,4*S*)-Hgl counterpart **4.2a** and a deeper understanding of the relevance of the β-substituent on conformation and activity.

Materials and methods

General Chemistry Methods

Unless otherwise specified, all non-aqueous reactions were performed under an inert argon atmosphere. All glassware was dried with a flame under flushing argon gas or stored in the oven and let cool under an inert atmosphere prior to use. Anhydrous solvents (THF, DCM, MeCN, MeOH and DMF) were obtained by passage through solvent filtration systems (Glass Contour, Irvine, CA) and solvents were transferred by syringe. Reaction mixture solutions (after aqueous workup) were dried over anhydrous $MgSO_4$ or Na_2SO_4, filtered, and rotary-evaporated under reduced pressure. Column chromatography was performed on 230-400 mesh silica gel, and thin-layer chromatography was performed on alumina plates coated with silica gel (Merck 60 F_{254} plates). Visualization of the developed chromatogram was performed by UV absorbance or staining with iodine or potassium permanganate solutions. Specific rotations, $[\alpha]^D$ values, were calculated from optical rotations measured at 25 °C in $CHCl_3$ at the specified concentrations (c in g/100 mL) using a 0.5 dm cell length (l) on a Anton Paar Polarimeter, MCP 200 at 589 nm, using the general formula: $[\alpha]^D{}_{25} = (100 \times \alpha)/(1 \times c)$. Nuclear magnetic resonance spectra (^{1}H NMR, ^{13}C NMR) were recorded on a Bruker 300MHz spectrometer. ^{1}H NMR spectra were referenced to $CDCl_3$ (7.26 ppm), and ^{13}C NMR spectra were measured in $CDCl_3$ (77.16 ppm) as specified below. Coupling constant J values were measured in Hertz (Hz) and chemical shift values in parts per million (ppm). High resolution mass spectrometry (HRMS) data in electrospray ionization (ESI-TOF) mode were obtained by the Centre Ŕgional de Spectroḿtrie de Masse de l'Universitéde Montréal. Protonated molecular ions $[M + H]^+$, and sodium adducts $[M + Na]^+$ were used for empirical formula confirmation. Analytical LCMS and HPLC analyses were performed on either a CSH-C18, 4.6 X100 mm, 5 μm column with a flow rate of 0.8 mL/min or CE-C18 3 X 50 mm, 2.7 μm column with a flow rate of 0.4 mL/min using appropriate gradients from X-Y% of MeOH (0.1% FA) or MeCN (0.1% FA) in H_2O (0.1% FA) over Z min. a) 10-90%/10 min [10-90% MeOH (or MeCN) containing 0.1% FA in H_2O (0.1% FA) for 10.0 min] b) 50-90%/10 min [50-90% MeOH (or MeCN) containing 0.1% FA in H_2O (0.1% FA) for 10.0 min], c) 30-60/10 min [30-60% MeOH (or MeCN) containing 0.1% FA in H_2O (0.1% FA) for 10.0 min], d) 5-60%/10 min [5-60% MeOH (or MeCN) containing 0.1% FA in H_2O (0.1% FA) for 10.0 min], e) 30-90%/10 min [30-90% MeOH (or MeCN) containing 0.1% FA in H_2O (0.1% FA) for

10.0 min], f) 20-40%/10 min [20-40% MeOH (or MeCN) containing 0.1% FA in H$_2$O (0.1% FA) for 10.0 min].

All final peptides were purified using the respective conditions below on a Waters™ preparative HPLC instrument equipped with either a reverse-phase Gemini™ C18 column (21.2 x 250mm, 5 μm) using a flow rate of 10 mL/min over 40 min; a C18 Atlantis column (19 x 100 mm, 5 um) using a flow rate of 24 mL/min over 15 min; a RP-Polar column (19 x 100 mm, 4 um) using a flow rate of 24 mL/min over 15 min, and UV detection at 214, 254 and 280 nm. The appropriate gradients from X-Y% of MeOH (or MeCN) containing 0.1% FA in H$_2$O (0.1% FA) over time were used on the following collumns: A) 10-90%/30 min MeOH (0.1% FA) in H$_2$O (0.1% FA), Gemini™ C18 column; B) 10-90%/10.0 min MeOH (0.1% FA) in H$_2$O (0.1% FA), Atlantis C18 column; C) 30-90%/10 min MeOH (0.1% FA) in H$_2$O (0.1% FA), Atlantis C18 column; D) 40-90%/10 min MeCN (0.1% FA) in H$_2$O (0.1% FA), RP-Polar column; E) 30-90%/10 min MeCN (0.1% FA) in H$_2$O (0.1% FA), C18 Atlantis column; F) 0-50%/ 9 min MeOH (0.1% FA) in H$_2$O (0.1% FA), C18 Atlantis column.

Chemical Reagents

Unless specified otherwise, commercially available reagents were purchased from Aldrich, A & C American Chemicals Ltd., Fluka and Advanced Chemtech™ and used without further purification: copper(I)iodide, phenylacetylene, 4-ethynyltoluene, 3-ethynylaniline, 1,1-dimethylpropargylamine (90% remainder H$_2$O), propargylamine, propargylalcohol, acetic acid, tris(2-carboxyethyl)phosphine hydrochloride, acetic anhydride, potassium cyanate, 1,3-bis(*tert*-butoxycarbonyl)-2-methyl-2-thiopseudourea, triethylamine, mercuric chloride, piperidine, DIEA, TFA, TES, TEA, HBTU, polystyrene Rink amide resin (75-100 mesh, 1%, DVB with a 0.5 mmol/g loading). All commercially available amino acids [e.g., Fmoc-D-Ala-OH, Fmoc-D-Leu-OH, Fmoc-D-Glu(*t*-Bu)-OH, Fmoc-D-Tyr(*t*-Bu)-OH, Boc-D-Arg(Pmc)-OH] were purchased from GL Biochem™ and used as received. Solvents were obtained from VWR international.

tert-Butyl (3_R_, 4_S_, 2'_R_)-2-[3-(Fmoc)amino-4-(1,3-dioxoisoindolin-2-yl)oxy)-2-oxopyrrolidin1-yl]-3-methylbutanoate (4.5f)
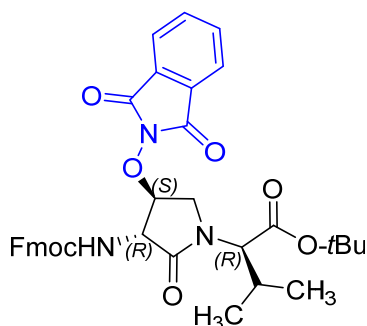
A solution of sulfamidate **4.4** (1 eq., 80 mg, 144 µmol , prepared according to reference 15) in a mixture of DCM (2 mL) and DMF (1 mL) was treated with sodium *N*-hydroxyphthalimide (1 eq., 80 mg, 431 µmol), stirred at rt for 8 h, poured into 1 M NaH$_2$PO$_4$, and extracted with DCM. The combined organic phase was washed with brine, dried, filtered, and evaporated to a residue, that was purified by column chromatography using a step gradient of 20-30% EtOAc in hexane. Evaporation of the collected fractions provided (4*S*)-phthalimide **4.5f** (81 g, 78 %) as white foam: R$_f$ = 0.37 (40% EtOAc in hexane); [α]$_D^{25}$ 16.4° (*c* 1, CHCl$_3$); ^{1}H NMR (300 MHz, CDCl$_3$) δ 7.88-7.65 (m, 8H), 7.41 (t, *J* = 7.1, 2H), 7.33 (t, *J* = 6.9, 2H), 6.53 (d, *J* = 8.6, 1H), 5.00 (t, *J* = 4.5, 1H), 4.77 (dd, *J* = 8.6, 5.1, 1H), 4.51-4.43 (m, 1H), 4.43-4.30 (m, 2H), 4.27-4.15 (m, 2H), 3.73 (dd, *J* = 12.5, 4.3, 1H), 2.29-2.11 (m, 1H), 1.41 (s, 9H), 1.02 (d, *J* = 6.6, 3H), 0.92 (d, *J* = 6.8, 3H); ^{13}C NMR (75 MHz, CDCl$_3$) δ 169.4, 168.9, 163.8, 156.7, 144.0, 143.8, 141.2, 134.7, 128.8, 127.7, 127.6, 127.1, 127.0, 125.6, 125.5, 123.8, 119.8, 82.1, 67.7, 61.0, 55.0, 47.4, 47.0, 28.7, 28.0, 21.9, 19.3; HRMS (ESI-TOF) m/z [M + H]$^+$ calcd for C$_{36}$H$_{38}$N$_3$O$_8$$^+$ 640.2653, found 640.2634.

[(3*R*, 4*S*)-4-(N$_3$)AgI^3]-4.1 (4.2c)
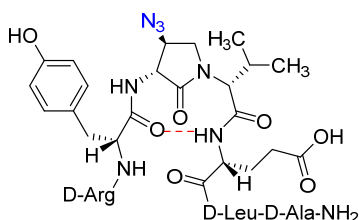
A 10-mL plastic filtration tube equipped with a polyethylene filter was charged with polystyrene Rink amide resin (75-100 mesh, 1%, DVB with a 0.5 mmol/g loading, 100 mg, 50.0 µmol), followed by DCM (7 mL). The tube was sealed, shaken for 30 min to induce

swelling and the liquid phase was removed by filtration. The Fmoc group was cleaved from the resin by treatment with a freshly-prepared 20% piperidine in DMF solution (5 mL), shaking for 30 min, and removal of the liquid phase by filtration. The resin was repeatedly (3x per solvent) washed (10 mL per wash for 6 min) with DMF and DCM, and the liquid phase was removed by filtration. The presence of the free amine resin was confirmed by a positive Kaiser test. Peptide elongation was conducted by treating the DMF-swollen free amine resin with a freshly prepared acylation solution composed of Fmoc-D-Ala-OH (3 eq), HBTU (3 eq), and DIEA (6 eq) in DMF (4-7 mL). After agitating for 3-5 h, at rt, the resin was filtered, the Fmoc group was cleaved as described above and peptide coupling was performed using the following sequence of acids: Fmoc-D-Leu-OH, Fmoc-D-Glu(*t*-Bu)-OH, *N*-Fmoc-(3*R*,4*S*)-4-(N$_3$)Agl-*R*-Val-OH (prepared as previously described in reference 15), Fmoc-D-Tyr(*t*-Bu)-OH, and Boc-D-Arg(Pmc)-OH. For the coupling of *N*-Fmoc-(3*R*,4*S*)-β-N$_3$-Agl-*R*-Val-OH only a stoichiometric quantity of dipeptide acid was used; for Fmoc-D-Tyr(*t*-Bu)-OH, coupling was repeated twice at higher reaction concentration. Synthetic progress was monitored using a combination of the Kaiser test and LC-MS analyses on TFA-cleaved resin aliquots, which were concentrated and dissolved in mixtures of water and MeCN. The completed peptide sequence **4.8c** with 80% crude purity was cleaved from the resin by treatment with TFA/H$_2$O/TES (3 mL, 95/2.5/2.5, v/v/v) with shaking for 3 h. The liquid phase was removed by filtration and collected. The resin was repeatedly (2x) washed with TFA and the combined liquid phases were concentrated in vacuo. The residue was dissolved in a minimal volume of acetonitrile, precipitated with ice-cold diethyl ether, and centrifuged with 7000 RPM. The supernatant was removed by decantation and the precipitate was collected. The precipitation and collection processes were repeated on the supernatant. The combined white solid precipitate was dissolved in water (5 mL), freeze-dried to give a white powder (80% crude purity), and purified using method A with UV detection at 214 nm. Fractions containing pure peptide were combined and lyophilized to afford peptide [(3*R*,4*S*)-β-N$_3$-Agl³]-**4.1** (**4.2c**, 9 mg, 22% yield of >95% purity): LCMS, 10-90%/10 min MeOH (0.1% FA) in water (0.1% FA), RT 8.3 min, and 10-90%/10 min MeCN (0.1% FA) in water (0.1% FA), RT 5.8 min; HRMS (ESI$^+$) calcd m/z for C$_{38}$H$_{60}$N$_{14}$O$_{10}$ [M+H]$^+$, 873.4690 found 873.4680.

[(3*S*, 4*S*)-4-(NCS)Agl³]-4.1 (4.2d)
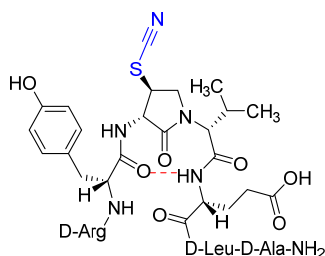
Employing the representative procedure described for peptide **4.2c** and *N*-Fmoc-(3*R*,4*S*)-4-(NCS)Agl-*R*-Val-OH (prepared as previously described in reference 15, [(3*S*,4*S*)-4-(NCS)Agl³]-**4.1** (**4.2d**) was synthesized and purified using method A with UV detection at 214 nm (3 mg, 3% yield of >95% purity); LCMS, 10-90%/10 min MeOH (0.1% FA) in water (0.1% FA), RT 8.3 min, and 10-90%/10 min MeCN (0.1% FA) in water (0.1% FA), RT 5.8 min; HRMS (ESI⁺) calcd m/z for $C_{39}H_{60}N_{12}O_{10}S$ [M+H]⁺, 889.4349 found 889.4342.

[(3*S*, 4*S*)-4-(MeS)Agl³]-4.1 (4.2e)
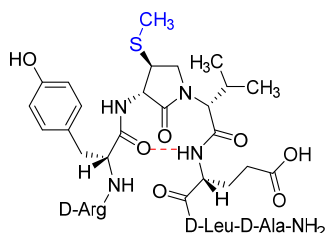
Employing the representative procedure described for peptide **4.2c**, and *N*-Fmoc-(3*R*,4*S*)-4-(MeS)Agl-*R*-Val-OH (prepared as previously described in reference 15, [(3*S*,4*S*)- 4-(MeS)Agl³]-**4.1** (**4.2e**) was synthesized and purified using method A with UV detection at 214 nm (4.5 mg, 10% yield of >95% purity); LCMS 10-90%/10 min MeOH (0.1% FA) in water (0.1% FA), RT 8.7 min, and 10-90%/10 min MeCN (0.1% FA) in water (0.1% FA), RT 5.9 min; HRMS (ESI⁺) calcd m/z for $C_{39}H_{63}N_{11}O_{10}S$ [M+H]⁺, 878.4553 found 878.4559.

[(3*R*,4*S*)-4-(PhthNO)Agl³]-4.1 (4.2f)

Chapter 4
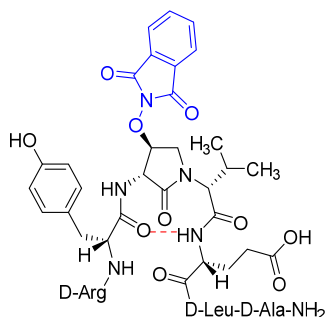
Employing the representative procedure described for peptide **4.2c**, [(3*R*, 4*S*)-4-(PhthNO)Agl[3]]-**4.1** (**4.2f**) was synthesized and purified using method A with UV detection at 214 nm (5.5 mg, 11% yield of >95% purity); LCMS 30-60%/10 min MeOH (0.1% FA) in water (0.1% FA), RT 8.8 min, and 5-60%/10 min MeCN (0.1% FA) in water (0.1% FA), RT 7.3 min; HRMS (ESI[+]) calcd m/z for $C_{46}H_{64}N_{12}O_{13}$ [M+H][+], 993.4789 found 993.4786.

[(3*R*,4*S*)-4-(H₂NO)Agl[3]]-4.1 (4.2g)
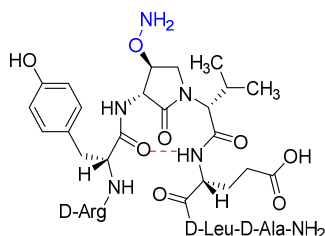
In a 10-mL plastic filtration tube equipped with a polyethylene filter, Boc-D-Arg(Pmc)-D-Tyr(*t*-Bu)-(3*R*,4*S*)-4-(PhthNO)Agl-D-Val-D-Glu(*t*-Bu)-D-Leu-D-Ala-Rink amide resin **4.8f** (100 mg, 50.0 µmol) was swollen in MeOH/DCM (1/1, v/v, 4 mL), treated with hydrazine monohydrate (73 µL, 1.50 mmol), and agitated for 5h at rt using an automated shaker.[19] The resin was filtered, washed with DMF (3 × 10 mL) and DCM (3 × 10 mL), dried under vacuum, and stored in the fridge. Resin **4.8g** was cleaved and the crude peptide was recovered as described for peptide **4.2c**; LCMS analysis indicated 38% crude purity. Purification using method A with UV detection at 280 nm and collection of the pure fractions afforded [(3*R*,4*S*)-4-(H₂NO)Agl[3]]-**4.1** (**4.2g**, 2.2 mg, 5% yield of >95% purity); LCMS 10-90%/10 min MeOH (0.1% FA) in water (0.1% FA), RT 6.6 min, and 10-90%/10 min MeCN (0.1% FA) in water (0.1% FA), RT 5.2 min; HRMS (ESI[+]) calcd m/z for $C_{38}H_{62}N_{12}O_{11}$ [M+H][+], 863.4661 found 863.4687.

[(3*R*,4*S*)-4-(H₂N)Agl[3]]-4.1 (4.2h)
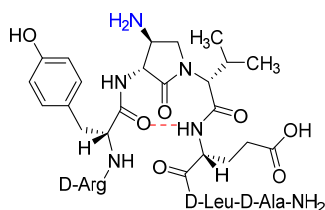
In a 10-mL plastic filtration tube equipped with a polyethylene filter, Boc-D-Arg(Pmc)-D-Tyr(*t*-Bu)-(3*R*,4*S*)-4-(N₃)Agl-D-Val-D-Glu(*t*-Bu)-D-Leu-D-Ala-Rink amide resin **4.8c** (100 mg, 50.0 µmol) was swollen in THF/H₂O (9/1, v/v, 4 mL), treated with tris(2-

Chapter 4

carboxyethyl)phosphine hydrochloride (40 µL, 150 µmol), and agitated for 4h at rt on an automated shaker.[20] The resin was filtered, washed with DMF (3 × 10 mL), MeOH (3 × 10 mL), THF (3 × 10 mL), and DCM (3 × 10 mL), dried under vacuum, and stored in the fridge. Resin **4.8h** was cleaved and the crude peptide was recovered as described for peptide **4.2c**; LCMS analysis indicated 70% crude purity. Purification using method A with UV detection at 280 nm, and collection and free-drying of the pure fractions afforded [(3*R*,4*S*)-4-(H$_2$N)Agl^3]-**4.1** (**4.2h**, 7.6 mg, 18% yield of >95% purity): LCMS 10-90%/10 min MeOH (0.1% FA) in water (0.1% FA), RT 5.8 min, and 50-90%/10 min MeCN (0.1% FA) in water (0.1% FA), RT 1.0 min; HRMS (ESI$^+$) calcd m/z for C$_{38}$H$_{62}$N$_{12}$O$_{10}$ [M+H]$^+$, 847.4785 found 847.4780.

[(3*R*,4*S*)-4-(AcHN)Agl^3]-4.1 (4.2i)
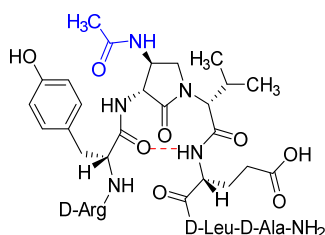
A 10-mL plastic filtration tube equipped with a polyethylene filter was charged with Boc-D-Arg(Pmc)-D-Tyr(*t*-Bu)-(3*R*,4*S*)-4-(H$_2$N)Agl-D-Val-D-Glu(*t*-Bu)-D-Leu-D-Ala-Rink amide resin **4.8h** (100 mg, 50.0 µmol), which was swollen in anhydrous DMF (2.00 mL) at rt, treated with acetic anhydride (14 µL, 150 µmol) followed by DIEA (52 µL, 300 µmol), and agitated at rt for 3 h. Water (0.5 mL) was added to the tube, which was agitated for 30 min. The resin was filtered, washed with DMF (3 × 10 mL) and DCM (3 × 10 mL), dried under vacuum, and stored in the fridge. Resin **4.9i** was cleaved and the crude peptide was recovered as described for peptide **4.2c**; LCMS analysis indicated 41% crude purity. Purification using method A with UV detection at 214 nm, and collection and free-drying of the pure fractions afforded [(3*R*,4*S*)-4-(AcHN)Agl^3]-**4.1** (**4.2i**, 4 mg, 9% yield of >95% purity); LCMS 10-90%/10 min MeOH (0.1% FA) in water (0.1% FA), RT 7.5 min, and 10-90%/10 min MeCN (0.1% FA) in water (0.1% FA), RT 5.9 min; HRMS (ESI$^+$) calcd m/z for C$_{40}$H$_{64}$N$_{12}$O$_{11}$ [M+H]$^+$, 890.4850 found 890.4867.

[(3*R*,4*S*)-4-(H$_2$N(C=O)HN)Agl^3]-4.1 (4.2j)
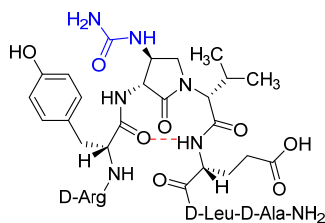
A 10-mL plastic filtration tube equipped with a polyethylene filter was charged with Boc-D-Arg(Pmc)-D-Tyr(*t*-Bu)-(3*R*,4*S*)-4-(H$_2$N)Agl-D-Val-D-Glu(*t*-Bu)-D-Leu-D-Ala-Rink amide resin **4.8h** (100 mg, 50.0 µmol), which was swollen in THF (2.00 mL) at rt, treated with potassium cyanate (10 mg, 150 µmol) followed by AcOH (8 µL,150 µmol) and H$_2$O (0.1 mL), and agitated at rt for 4 h on an automated shaker. The resin was filtered, washed with DMF (3 × 10 mL) and DCM (3 × 10 mL), dried under vacuum, and stored in the fridge. Resin **4.9j** was cleaved and the crude peptide was recovered as described for peptide **4.2c**; LCMS analysis indicated 57% purity. Purification using method A with UV detection at 214 nm, and collection and free-drying of the pure fractions afforded [(3*R*,4*S*)-4-(H$_2$N(C=O)HN)Agl^3]-**4.1** (**4.2j**, 4 mg, 8% yield of >95% purity); LCMS 10-90%/10 min MeOH (0.1% FA) in water (0.1% FA), RT 7.3 min, and 10-90%/10 min MeCN (0.1% FA) in water (0.1% FA), RT 5.1 min; HRMS (ESI$^+$) calcd m/z for C$_{39}$H$_{63}$N$_{13}$O$_{11}$ [M+H]$^+$, 890.4843 found 890.4841.

[(3*R*,4*S*)-4-(H$_2$N(C=NH)HN)Agl^3]-4.1 (4.2k)
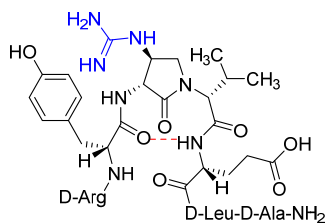
A 10-mL plastic filtration tube equipped with a polyethylene filter was charged with Boc-D-Arg(Pmc)-D-Tyr(*t*-Bu)-(3*R*,4*S*)-4-(H$_2$N)Agl-D-Val-D-Glu(*t*-Bu)-D-Leu-D-Ala-Rink amide resin **4.8h** (100 mg, 50.0 µmol), and washed with DMF (× 6), DCM (× 6), dry DCM (× 3) and dry DMF (× 6). The resin was swollen in dry DMF (4 mL), treated with 1,3-bis(*tert*-butoxycarbonyl)-2-methyl-2-thiopseudourea (22 µL, 75 µmol) and triethylamine (63 µL, 450 µmol), stirred for 5 min, treated with HgCl$_2$ (40 mg, 150 µmol) in dry DMF (0.5 mL), and agitated for 2 h, at rt. The resin was washed with DMF (× 6), and DCM (× 6), dried under vacuum, and stored in the fridge. Resin **4.9k** was cleaved and the crude

Chapter 4

peptide was recovered as described for peptide **4.2c**; LCMS analysis indicated 62% purity. Purification using method A with UV detection at 280 nm, and collection and free-drying of the pure fractions afforded [(3*R*,4*S*)-4-(H₂N(C=NH)HN)Agl³]-**4.1** (**4.2k**, 4 mg, 9% yield of >95% purity); LCMS 10-90%/10 min MeOH (0.1% FA) in water (0.1% FA), RT 5.9 min, and 5-60%/10 min MeCN (0.1% FA) in water (0.1% FA), RT 4.6 min; HRMS (ESI⁺) calcd m/z for $C_{39}H_{64}N_{14}O_{10}$ [M+H]⁺, 889.5003 found 889.5006.

[(3*R*,4*S*)-4-(4'-Phenyltriazolyl)Agl³]-4.1 (4.2l)
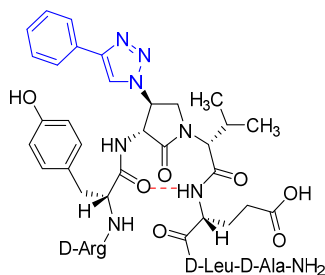
In a 10-mL plastic filtration tube equipped with a polyethylene filter, Fmoc-D-Arg(Pmc)-D-Tyr(*t*-Bu)-(3*R*,4*S*)-4-(N₃)Agl-D-Val-D-Glu(*t*-Bu)-D-Leu-D-Ala-Rink amide resin **4.8c** (100 mg, 50.0 µmol) was swollen in anhydrous DCM (2 mL), treated with copper(I)iodide (14 mg, 75.0 µmol) and DIEA (26 µL, 150 µmol), followed by phenylacetylene (20 µL, 180 µmol) and acetic acid (9 µL, 150 µmol), and shaken at rt for 18 h,[21] filtered and washed with DMF (× 3), DCM (× 3). Resin **4.10l** was cleaved and the crude peptide was recovered as described for peptide **4.2c**; LCMS analysis indicated 74% purity. Purification using method A with UV detection at 254 nm, and collection and free-drying of the pure fractions afforded [(3*R*,4*S*)-4-(4'-phenyltriazolyl)Agl³]- **4.1** (**4.2l**, 8 mg, 17% yield of >95% purity): LCMS 10-90%/10 min MeOH (0.1% FA) in water (0.1% FA), RT 9.6 min, and 10-90%/10 min MeCN (0.1% FA) water (0.1% FA), RT 6.5 min; HRMS (ESI⁺) calcd m/z for $C_{46}H_{66}N_{14}O_{10}$ [M+H]⁺, 975.5159 found 975.5147.

[(3*R*,4*S*)-4-(4'-*p*-Methylphenyltriazolyl)Agl³]-4.1 (4.2m)
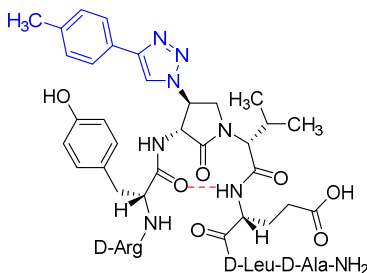
Chapter 4

Employing the representative procedures described for the synthesis of peptide **4.2l**, using resin **4.8c** (100 mg, 50.0 µmol) and 4-ethynyltoluene (22.8 µL, 180 µmol), peptide **4.2m**, was synthesized and indicated to be of 71% purity by LCMS analysis. Purification using method C with UV detection at 254 nm, and collection and free-drying of the pure fractions afforded [(3*R*,4*S*)-4-(4'-*p*-Methylphenyltriazolyl)Agl³]-**4.1** (**4.2m**, 7 mg, 16% yield of >95% purity); LCMS 30-90%/10 min MeOH (0.1% FA) in water (0.1% FA), RT 9.5 min, and 20-40%/10 min MeCN (0.1% FA) in water (0.1% FA), RT 6.5 min; HRMS (ESI⁺) calcd m/z for $C_{47}H_{68}N_{14}O_{10}$ [M+H]⁺, 989.5316 found 989.5307.

[(3*R*,4*S*)-4-(4'-*m*-Aminophenyltriazolyl)Agl³]-4.1 (4.2n)
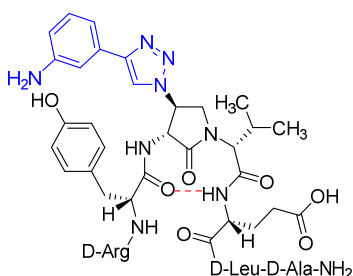
Employing the representative procedures described for the synthesis of peptide **4.2l**, using resin **4.8c** (100 mg, 50.0 µmol) and 3-ethynylaniline (20.3 mL, 180 µmol), peptide **4.2n**, was synthesized and indicated to be of 69% purity by LCMS analysis. Purification using method D with UV detection at 254 nm, and collection and free-drying of the pure fractions afforded [(3*R*,4*S*)-4-(4'-*m*-aminophenyltriazolyl)Agl³]-**4.1** (**4.2n**, 6 mg, 12% yield of >95% purity); LCMS 5-60%/10 min MeOH (0.1% FA) in water (0.1% FA), RT 7.9 min, and 5-60%/10 min MeCN (0.1% FA) in water (0.1% FA), RT 6.1 min; HRMS (ESI⁺) calcd m/z for $C_{46}H_{67}N_{15}O_{10}$ [M+H]⁺, 990.5268 found 990.5259.

[(3*R*,4*S*)-4-(4'-(1,1-dimethyl)aminomethyltriazolyl)Agl³]-4.1 (4.2o)
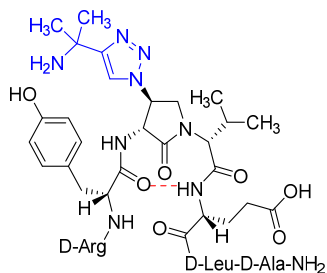
Employing the representative procedures described for the synthesis of peptide **4.2l**, using resin **4.8c** (100 mg, 50.0 µmol) and 1,1-dimethylpropargylamine (90% remainder H₂O,

15.0 µL, 180 µmol), peptide **4.2o** was synthesized and indicated to be of 73% purity by LCMS analysis. Purification using method B with UV detection at 214 nm, and collection and free-drying of the pure fractions afforded [(3*R*,4*S*)-4-(4'-(1,1-dimethyl)amino-methyltriazolyl)Agl^3]-**4.1** (**4.2o**, 6 mg, 13% yield of >95% purity); LCMS 10-90%/10 min MeOH (0.1% FA) in water (0.1% FA), RT 6.3 min, and 5-60%/10 min MeCN (0.1% FA) in water (0.1% FA), RT 4.9 min; HRMS (ESI$^+$) calcd m/z for $C_{43}H_{69}N_{15}O_{10}$ [M+H]$^+$, 956.5425 found 956.5408.

[(3*R*,4*S*)-4-(4'-Aminomethyltriazolyl)Agl^3]-4.1 (4.2p)
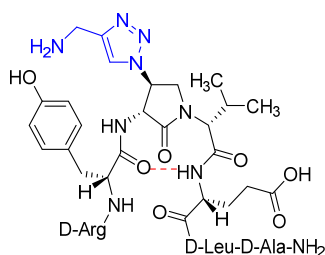
Employing the representative procedures described for the synthesis of peptide **4.2l**, using resin **4.8c** (100 mg, 50.0 µmol) and propargylamine (12 µL, 180 µmol), peptide **4.2p** was synthesized and indicated to be of 53% purity by LCMS analysis. Purification using method E with UV detection at 254 nm, and collection and free-drying of the pure fractions afforded [(3*R*,4*S*)-4-(4'-aminomethyltriazolyl)Agl^3]-**4.1** (**4.2p**, 4 mg, 8% yield of >95% purity); LCMS 5-60%/10 min MeOH (0.1% FA) in water (0.1% FA), RT 7.9 min, and 5-60%/10 min MeCN (0.1% FA) in water (0.1% FA), RT 6.1 min; HRMS (ESI$^+$) calcd m/z for $C_{41}H_{65}N_{15}O_{10}$ [M+H]$^+$, 928.5039 found 928.5029.

[(3*R*,4*S*)-4-(4'-Hydroxymethyltriazolyl)Agl^3]-4.1 (4.2q)
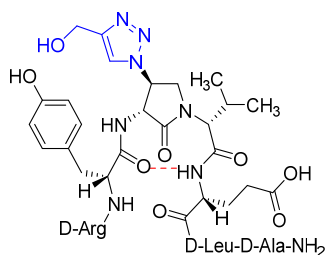
Employing the representative procedures described for the synthesis of peptide **4.2l**, using resin **4.8c** (100 mg, 50.0 µmol) and propargyl alcohol (7 µL, 180 µmol), peptide**4. 2q** was synthesized and indicated to be of 64% purity by LCMS analysis. Purification using method F with UV detection at 280 nm, and collection and free-drying of the pure fractions

afforded [(3*R*,4*S*)-4-(4'-hydroxymethyltriazolyl)Agl^3]-**4.1** (**4.2q**, 5 mg, 10% yield of >95% purity); LCMS 5-60%/10 min MeOH (0.1% FA) in water (0.1% FA), RT 7.2 min, and 5-60%/10 min MeCN (0.1% FA) in water (0.1% FA), RT 5.73 min; HRMS (ESI$^+$) calcd m/z for $C_{41}H_{64}N_{14}O_{11}$ [M+H]$^+$, 929.4930 found 929.4952.

Oxygen-induced retinopathy rodent model experiments were preformed identically to those described in reference 16, and described in brief below.

Animals

Two-day-old (P2) Sprague Dawley rat pups and their mothers were ordered from Charles River (Raleigh, SC, USA) and acclimatized for 3 days in standard conditions. All procedures and protocols involving the use of the rats were approved by the Animal Care Committee of the research center of the Hôpital Maisonneuve-Rosemont and are in accordance with the Statement for the Use of Animals in Ophthalmic and Vision Research approved by the Association for Research in Vision and Ophthalmology (ARVO), and guidelines established by the Canadian Council on Animal Care.

Oxygen-induced retinopathy in Sprague Dawley rats

The 80% oxygen model of retinopathy was conducted as previously described in reference 16. Briefly, litters of P5 pups and their mothers were kept in a controlled 80% oxygen environment until P10. The pups were injected intraperitoneally twice daily with PBS vehicle (20µL per injection), peptide **4.1** or derivatives (titrated to a daily dose of 2mg/kg/day). Control litters were kept under normal air atmosphere and standard conditions. On P10, pups were euthanized by decapitation under 2% isoflurane anesthesia. Eyes were enucleated and fixed in 4% paraformaldehyde, then stored at 4 °C in PBS until further processing.

Retinal Flatmount and Immunohistochemistry

The fixed eyes were dissected, and the obtained retinas were incubated with antibodies and mounted onto slides as previously described in reference 16. Briefly, the cornea and lens were removed from the eyes, and the retina gently removed from the underlying sclera-choroid-retinal pigmented epithelium (RPE) complex. Retinas were treated for 1h with blocking solution [1% bovine serum albumin (BSA), 1% normal goat serum, 0.1% Triton X-100 and 0.05% Tween-20 in PBS], and then incubated overnight with lectin and Iba-1 primary antibody, followed by Alexa-594-conjugated secondary

antibody for 2h. Retinas were then mounted onto microscope slides under coverslips with anti-fade mounting medium.

Microscopy

Retinal flatmounts were imaged using the Zeiss AxioImager Z2 and the MosaiX feature of the AxioVision software as previously described in reference 16. Representative images after Iba-1 staining were taken using a laser scanning confocal microscope (Olympus IX81 with Fluoview FV1000 Scanhead) using the Fluoview Software at 30X magnification.

Quantification and Data Analysis

The FIJI software was used to the quantify the area of vaso-obliteration in each retina, expressed as a percentage of the area of the whole retina. The number of Iba-1-positive cells was counted using the cell counter plug-in in FIJI, and the average of cell counts in 4 fields per retina was calculated. Data was analyzed using GraphPad Prism 7 with one-way ANOVA and the Dunnett's test for multiple comparisons. Results were treated as significant when p was less than 0.05 and expressed as mean $\pm$ SEM.

Results and discussion

Chemical Synthesis

Cyclic sulfamidate **4.4** is a valuable intermediate for the synthesis of β-substituted-Agl residues.[22] Previously sulfamidate **4.4** reacted as electrophile in nucleophilic ring opening reactions with sodium azide and potassium thiocyanide in routes to prepare Fmoc-(3*R*,4*S*)-β-substituted-Agl-(*R*)-Val-OH analogs **4.3c-e** with β-azido, thiocyano and methylthio ether substituents, respectively (Figure 1).[15, 17] Employing sulfamidate **4.4** in a similar protocol with the sodium salt of hydroxyphthalimide as nucleophile in a 1:2 DMF/DCM mixture has now provided Fmoc-(3*R*,4*S*)-β-phthalimidooxy-Agl-(*R*)-Val-O*t*-Bu (**4.5f**) in 78% yield (Scheme 4.1). *tert*-Butyl ester **4.5f** was quantitatively converted to acid **4.3f** using a 1:1 trifluoroacetic acid/DCM solution.
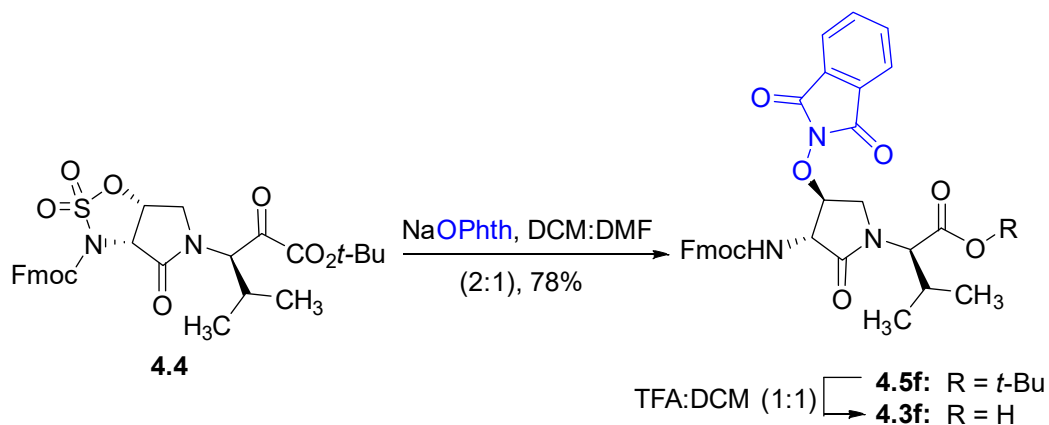
Scheme 4.1. Synthesis of dipeptide **4.3f** by ring opening of cyclic sulfamidate **4.4**

Dipeptide acids **4.3c-f** were respectively coupled to H-D-Glu(*t*-Bu)-D-Leu-D-Ala-NH-Rink amide resin **4.6** using *O*-(benzotriazol-1-yl)-*N,N,N′,N′*-tetramethyluronium hexafluorophosphate (HBTU), and *N,N*-diisopropylethylamine (DIEA) in DMF to provide pentapeptide resins **4.7c-f**. Peptide elongation by removals of Fmoc protection with 20% piperidine in DMF, and sequential couplings of Fmoc-D-Try(*t*-Bu)-OH and *N*-Boc-D-Arg(Pmc)-OH using HBTU and DIEA in DMF gave respectively protected heptapeptide resins **4.8c-f**. Treatment of *O*-alkyl hydroxy phthalimide resin **4.8f** with hydrazine monohydrate in a 1:1 MeOH/DCM mixture provided *O*-alkyl hydroxamine **4.8g** (Scheme 4.2). Note, *O*-alkyl hydroxamine **4.8g** offers potential for the synthesis of oxime ligation conjugates.[19, 23] Resin cleavage was performed using a cocktail of 95:2.5:2.5 TFA/H₂O/TES to furnish peptides **4.2c-g** in 38–80% crude purities. Purification by HPLC provided peptides **4.2c-g** in 3-22% overall yields (Table 4.1).
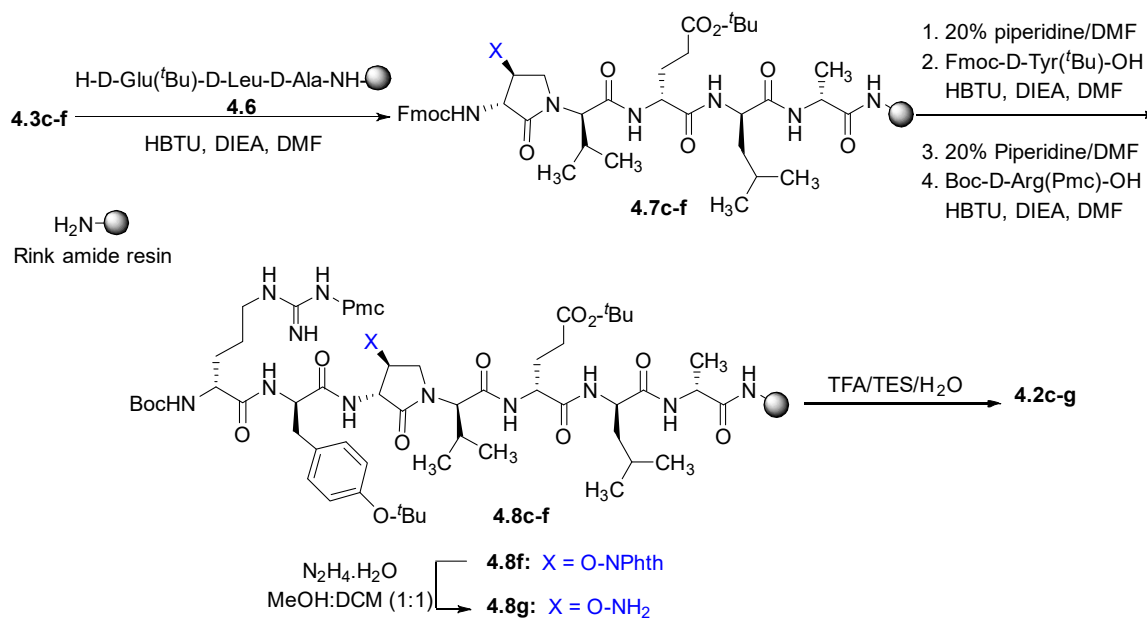
Scheme 4.2. Solid-phase synthesis of peptide **4.2c-g**

Amino resin **4.8h** was synthesized by reduction of azido resin **4.8c** using tris(2-carboxyethyl)phosphine hydrochloride (TCEP) in a 9:1 THF:H$_2$O mixture (Scheme 4.3). Amine **4.8h** was then employed in the synthesis of acetamide, urea and guanidine peptides **4.8i-k**. Acetamide **4.8i** was prepared by acylation of amine **4.8h** using acetic anhydride and DIEA in DMF. Urea **4.8j** was obtained from treating amine **4.8h** with a solution of potassium cyanate and acetic acid in a 20:1 THF:H$_2$O mixture.[24] Guanidine **4.9k** was prepared by reacting amine resin **4.8h** with 1,3-bis(*tert*-butoxycarbonyl)-2-methyl-2-thiopseudourea, triethylamine and mercuric chloride in DMF. Resin cleavage and removal of the Boc and *tert*-butyl protection groups were concomitantly accomplished using a cocktail of 95:2.5:2.5 TFA/H$_2$O/TES to furnish peptides **4.2h-k** in 41–70% crude purities. Purification by HPLC provided peptides **4.2h-k** in 8-18% overall yields (Table 4.1).
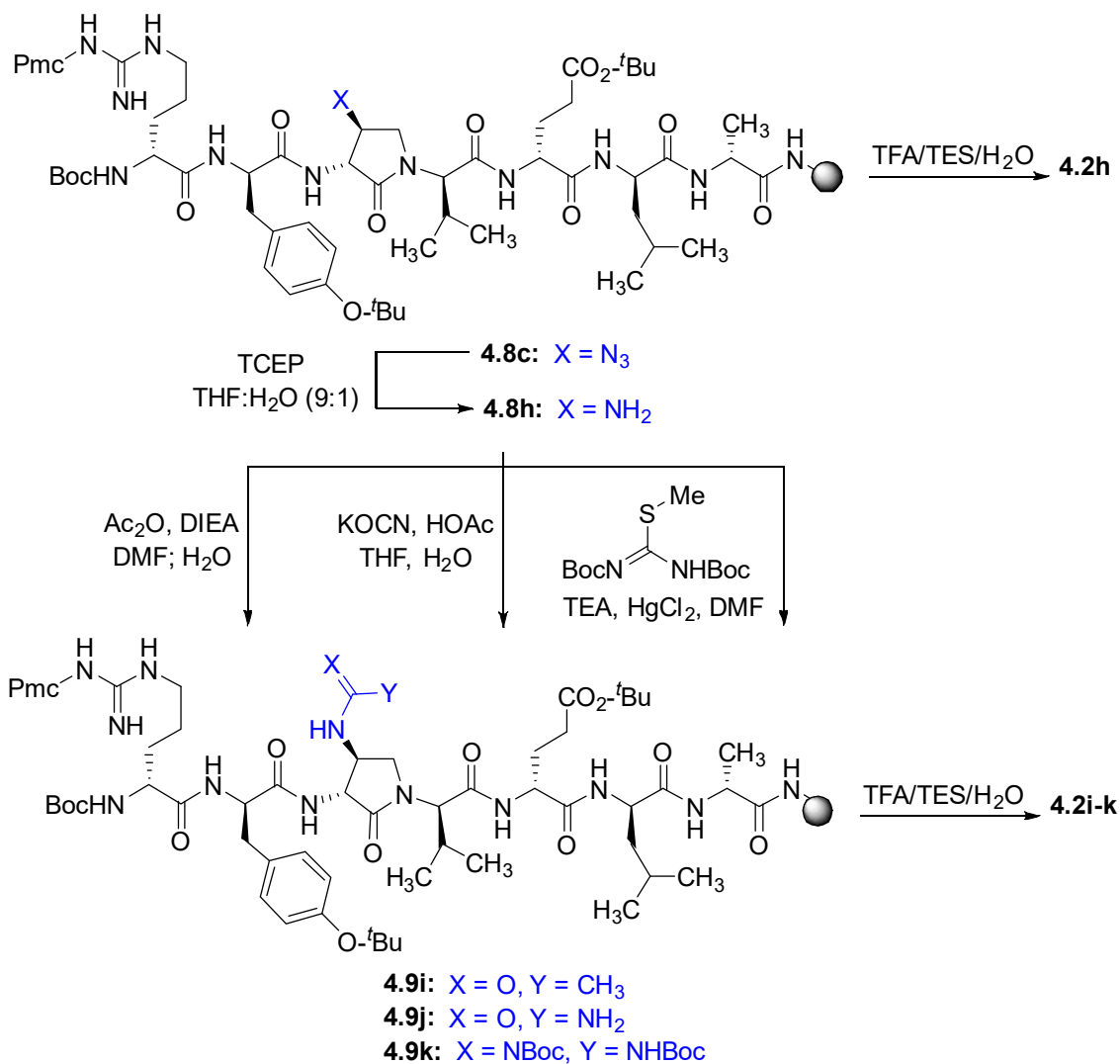
Scheme 4.3. Solid-phase synthesis of peptides **4.2h-k**.

Azide **4.8c** was also employed in CuAAC chemistry to provide 4-substituted-1,2,3-triazoles **4.8l-q** using a set of alkynes: phenylacetylene, 4-ethynyltoluene, 3-ethynylaniline, 1,1-dimethylpropargylamine, propargylamine and propargylalcohol (Scheme 4.4). Alkynes were selected to study potential for aromatic, salt bridge and hydrogen bond interactions with the receptor. In the CuAAC reaction, azide **4.8c** was treated with the corresponding alkyne, copper(I)iodide and DIEA in DCM to provide regioselectively the 4-substituted-1,2,3-triazole **4.8l-q**.[21] As described above, resin cleavage and removal of protection were concomitantly accomplished using a TFA/H$_2$O/TES cocktail to furnish peptides **4.2l-q** in 53-74% crude purities. After purification by HPLC, peptides **4.2l-q** were isolated in 8-17% overall yields (Table 4.1).
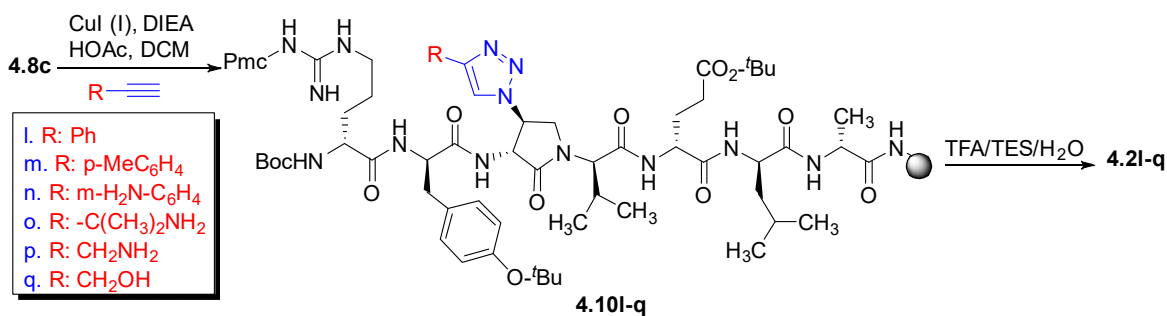
Scheme 4.4. CuAAC chemistry on resin **4.8c** provides access to triazole derivatives **4.2l-q**

Table 4.1. Retention times, purities, yields, and mass spectrometric data for peptides **2c-q**
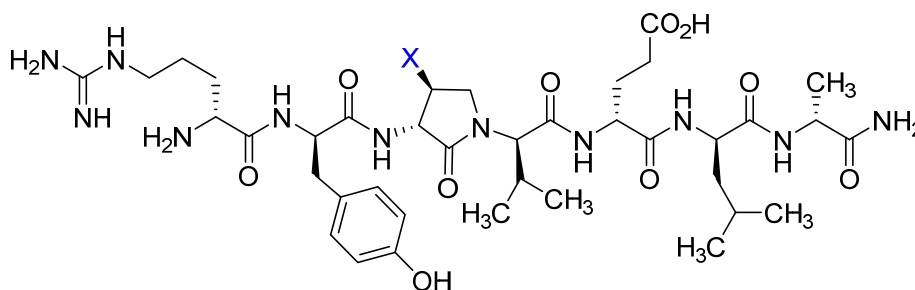
4.2 -**X**	RT (min)		crude purity %	final purity %	yield % (>95 % in MeOH)	HRMS [M+1]	
	MeOH	MeCN				m/z (calcd)	m/z (obsd)
c -N$_3$	8.3[a]	5.8[a]	80	>99	22	873.4690	873.4680
d -SCN	8.3[a]	5.8[a]	38	>96	3	889.4349	889.4342
e -SMe	8.7[a]	5.9[a]	46	>99	10	878.4553	878.4559
f -ONPhth	8.8[c]	7.3[d]	48	>96	11	993.4789	993.4786
g -ONH$_2$	6.6[a]	5.2[a]	38	>97	5	863.4661	863.4687
h -NH$_2$	5.8[a]	1.0[b]	70	>99	18	847.4785	847.4780
i -NH(C=O)Me	7.5[a]	5.9[a]	41	>99	9	890.4850	890.4867
j -NH(C=O)NH$_2$	7.3[a]	5.1[a]	57	>99	8	890.4843	890.4841
k -NH(C=N)NH$_2$	5.9[a]	4.6[d]	62	>98	9	889.5003	889.5006
l -4-(Ph)triazolyl	9.6[a]	6.5[a]	74	>99	17	975.5159	975.5147
m -4-(p-MeC$_6$H$_4$)-triazolyl	9.5[e]	6.5[f]	71	>97	16	989.5316	989.5307
n -4-(m-H$_2$NC$_6$H$_4$)-triazolyl	7.9[d]	6.1[d]	69	>96	12	990.5268	990.5259

o	-4-($H_2N(H_3C)_2C$)-triazolyl	6.3[d]	4.9[d]	73	>98	13	956.5425	956.5408
p	-4-(H_2NH_2C)-triazolyl	7.9[d]	6.1[d]	53	>97	8	928.5039	928.5029
q	-4-(HOH_2C)-triazolyl	7.2[d]	5.7[d]	64	>97	10	929.4930	929.4952

Isolated purity ascertained by LC-MS analysis using gradients **X-Y**% MeOH (0.1% FA) or MeCN (0.1% FA) in H_2O (0.1% FA) over 10 min. a) 10-90%, b) 50-90%, c) 30−60%, d) 5-60%, e) 30−90%, f) 20-40%.

Circular dichroism spectra

The impact of the β-substituent on the conformation of (3*R*,4*S*)-β-substituted-Agl[3] peptides **4.2c-q** was examined in water by CD spectroscopy and the curve shapes of the spectra were compared with that of [(3*R*,4*S*)-Hgl[3]]-**4.1** (**4.2b**). Previously **4.2b** exhibited negative and positive maximum, that were respectively at 198-207 and 221-227 nm indicative of a *β*-turn conformation in water, trifluoroethanol (TFE), MeOH and hexafluoroisopropanol (HFIP), with the greatest ellipticity seen in 5% TFE in water. In general, peptides **4.2**, all exhibited curve shapes indicative of *β*-turn conformer with slightly different ellipticity (Figure 4.2 and supporting information). Notably, thiocyanide **4.2d** exhibited a similar curve shifted to higher wavelengths at 215 and 230 nm (Figure 4.2). On the other hand, no curve shape was obtained from measuring the CD spectrum of 4-hydroxymethyltriazolyl peptide **4.2q** (supporting information). The similar curve shapes illustrated in the spectra of peptides **4.2b-p** indicated that changes of the β-substituent had little influence on the peptide conformation, which was significantly affected by the presence and configuration of the γ-lactam ring.[16]
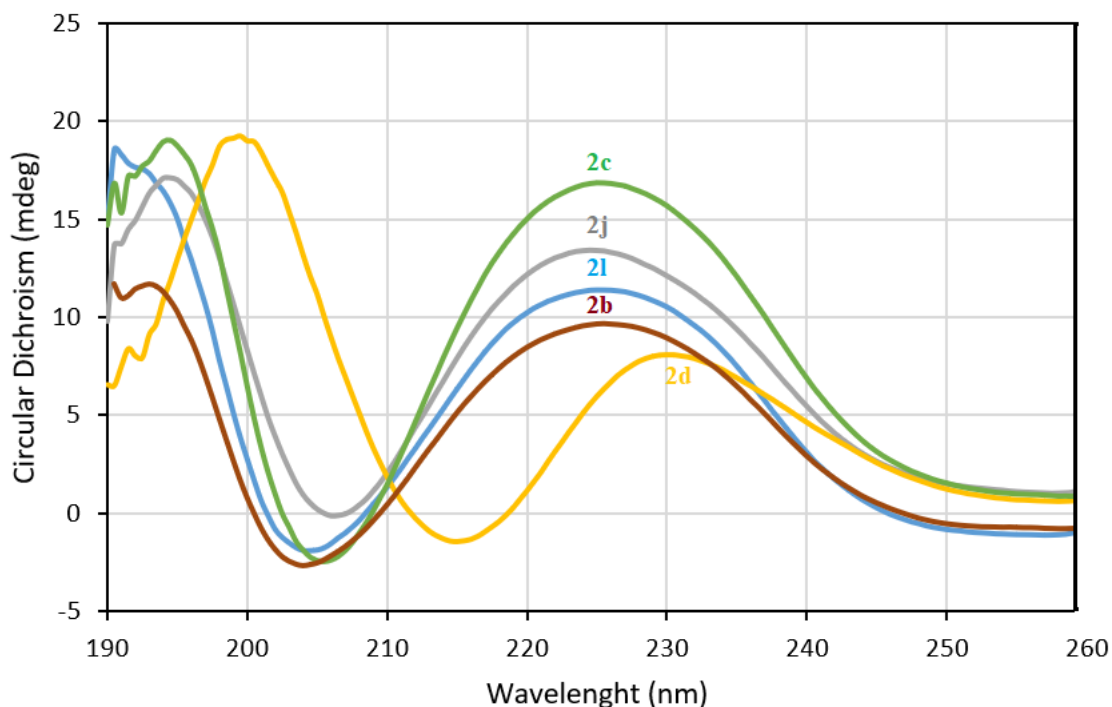
Figure 4.2. The molar ellipticity circular dichroism spectra of **4.2b-d**, **4.2j** and **4.2l**

Biology

Employing a series of *in vitro* screens performed as previously described in reference 16 with results to be described in due time, a set of six (3*R*,4*S*)-β-substituted-Agl[3] peptides (e.g., **4.2c**, **4.2d**, **4.2f**, **4.2l**, **4.2n**, **4.2q**) was selected for examination *in vivo* in a rodent model of oxygen-induced retinopathy (OIR). From days 5 to 10 of life, rat pups were exposed to 80% oxygen, which usually resulted in ~30% vaso-obliteration of the retinal capillaries that extend radially from the optic nerve (vehicle, Figures 4.3A and 4.3B). As previously reported,[16] peptide **4.1** diminished the extent of vaso-obliteration from ~30% to ~20% (p<0.0001). Among the six peptides, five, thiocyanide **4.2d**, *N*-oxyphthalimide **4.2f**, 4-phenyltriazole **4.2l**, 4-*m*-aminophenyltriazole **4.2n**, and 4-hydroxymethyltriazole **4.2q**, all exhibited efficacy in the OIR model and reduced vaso-obliteration from ~30% to ~20% (p<0.0001). Although thiocyanide **4.2d** and 4-phenyltriazole **4.2l** exhibited tendencies to have a stronger protective effect than peptide **4.1**, there was no statistically significant difference between the three peptides. On the other hand, [(3*R*, 4*S*)-4-(N$_3$)Agl[3]]-**4.1** (**4.2c**) had no protective effect against vaso-obliteration and was indistinguishable from the vehicle-treated group.

In the context of OIR, microglia have been previously shown to be mediators of vaso-obliteration.[25] The ramified and branched morphology of inactive microglia has also been observed to change to an amoeboid state with retracted limbs upon microglia activation.[26] Microglial activation and density was thus ascertained by histochemical staining for the Iba-1 marker. The active amoeboid state was observed in retina under hypoxia treated with vehicle or azide **4.2c** (Figure 4.4A and 4.4B). Pups raised under normal oxygen exhibited ramified and branched microglia in their retina. Furthermore, pups exposed to hypoxia, but treated with peptide **4.1** and analogs **4.2**, which diminished vaso-obliteration, possessed retina which exhibited similarly ramified and branched microglia. In summary, five $(3R,4S)$-β-substituted-Agl^3 peptides acted like peptide **4.1** and exhibited protection against vaso-obliteration in the hyperoxic phase of OIR, due in part to mitigation of microglial activation.
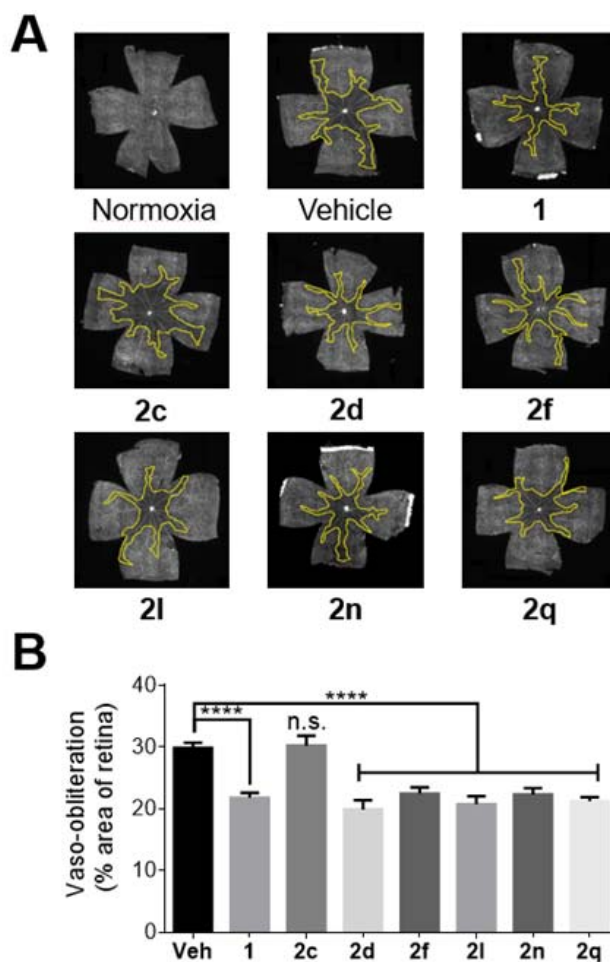
Figure 4.3. The preventive effects of peptide 4.2 against vaso-obliteration in an OIR model. (A) Representative retinal flatmounts stained with FITC-conjugated *Bandeiraea simplicifolia* lectin at 10X magnification. Yellow lines indicate the central area of vaso-obliteration extending from the optic nerve in the centre of the retina. **(B)** Quantification of area of vaso-obliteration performed using ImageJ, expressed as a percentage of the total retinal area: n = 5-7 of peptide 2, n = 10-12 for vehicle and peptide 1; Veh vehicle; ****p<0.0001 relative to the vehicle group, n.s. p>0.05 relative to vehicle group and not statistically significant.
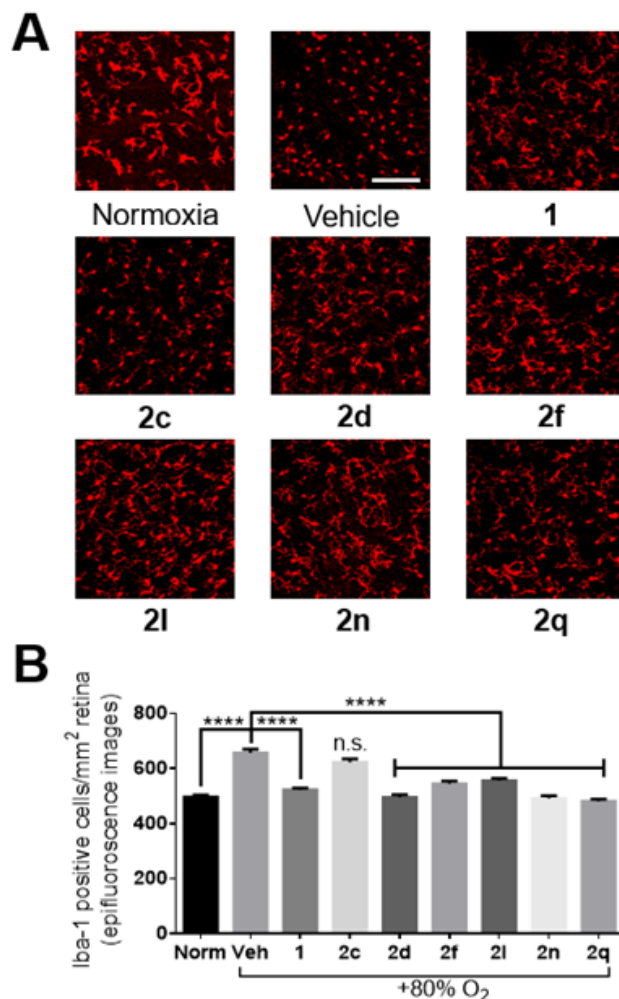
Figure 4.4. The effects of peptides 4.1 and 4.2 on retinal microglial activation and density. (A) Representative confocal images of retinal microglia at 30X magnification: scale bar 100 μm. **(B)** Epifluorescence microscopy images at 20X magnification of retinal microglial density quantified using ImageJ: 4 images per retina were taken at a distance halfway between the optic nerve and the edge of the retina; n = 5-7 for peptides **4.1** and **4.2**; n = 10-12 for normoxia and vehicle; Norm normoxia, Veh vehicle; ****$p<0.0001$ relative to the vehicle group, n.s. $p>0.05$ relative to vehicle group and not statistically significant.

Conclusion

Effective solid-phase methods have been developed for the synthesis of (3R,4S)-β-substituted-Agl peptides have been developed employing *N*-Fmoc protected β-substituted-Agl dipeptide building blocks. Applying the methods to replace the D-threonine residue in the IL-1R allosteric modulator peptide **4.1**, fifteen (3R,4S)-β-substituted-Agl[3] analogs were

synthesized. Notably, [(3R, 4S)-4-(N_3)Agl^3]-**4.1** (**4.2c**) proved a valuable intermediate for the synthesis of diverse analogs by way of azide reduction and CuAAC chemistry. Although the results of *in vitro* examinations and *in vivo* evaluation in a model of PTB have yet to be completed, the results on a subset of analogs in an OIR model of ROP have identified five analogs with similar activity as the parent peptide **4.4.1**. Determining structure activity relationships from the animal model is subjective at best, due in part to the similarities in activity of the five and the potential for activity to be affected by pharmacokinetic properties. Unlike, azide **4.2c**; however, thiocyanide **4.2d**, *N*-oxyphthalimide **4.2f**, 4-phenyltriazole **4.2l**, 4-*m*-aminophenyltriazole **4.2n**, and 4-hydroxymethyltriazole **4.2q**, all have relatively dispersed electron density and potential to serve in hydrogen-bond interactions like the alcohol of the D-threonine residue and [(3R, 4S)-4-Hgl^3]-**4.1** (**4.2b**). Moreover, four of the five analogs exhibited CD curve shapes that were like that of **2b** and indicative of β-turn structure. In summary, these five compounds merit further investigation as potential leads for the treatment of ROP. Moreover, this study has provided useful tools for elucidating the structure and conformation-activity relationships responsible for peptide biology.

Abbreviations

Boc, *tert*-butyloxycarbonyl; Fmoc, fluorenylmethyloxycarbonyl; DMF, dimethylformamide; FA, formic acid; TFA, trifluoroacetic acid; TLC, thin-layer chromatography; copper-catalyzed azide alkyne cycloadditions, CuAAC; the IL-1 receptor, IL-1R; Agl, α-amino-γ-lactam; Hgl, β-hydroxy-α-amino-γ-lactam; PTB, preterm birth; ROP, retinopathy of prematurity; TCEP, tris(2-carboxyethyl)phosphine hydrochloride; DMF, dimethylformamide; DIEA, *N*, *N*-Diisopropylethylamine.

Author contributions

AG wrote the manuscript, synthesized and purified compounds, and conducted circular dichroism analyses. CC wrote the manuscript and conducted *in vivo* and *in vitro* experiments. CQ edited the manuscript and conducted *in vitro* experiments. XH edited the manuscript and conducted in vivo experiments. SC and WL supervised the progress of the project, edited, and proofread the manuscript. All authors have read the final manuscript and agree to be accountable for the content of this work.

Funding

Acknowledgments

Author information

Corresponding Author

*E-mail: william.lubell@umontreal.ca. Phone: 514-343-7339. Fax: 202-513-8788.

ORCID

Azade Geranurimi: 0000-0002-6866-1089

William.D. Lubell: 0000-0002-3080-2712

Notes

The authors declare no competing financial interest.

Supplementary material

The Supplementary Material for this manuscript can be found online at:

References

1. Gabay, C.; Lamacchia, C.; Palmer, G., IL-1 pathways in inflammation and human diseases. *Nat. Rev. Rheumatol.* **2010,** *6*, 232-241.

2. Dinarello, C. A., Interleukin-1. *Cytokine & growth factor reviews* **1997,** *8*, 253-265.

3. Krumm, B.; Xiang, Y.; Deng, J., Structural biology of the IL-1 superfamily: Key cytokines in the regulation of immune and inflammatory responses. *Protein Science* **2014,** *23*, 526-538.

4. Roy, P. K.; Rashid, F.; Bragg, J.; Ibdah, J. A., Role of the JNK signal transduction pathway in inflammatory bowel disease. *World journal of gastroenterology: WJG* **2008,** *14*, 200.

5.   Amano, M.; Nakayama, M.; Kaibuchi, K., Rho-kinase/ROCK: a key regulator of the cytoskeleton and cell polarity. *Cytoskeleton* **2010,** *67*, 545-554.

6.   Opal, S. M.; Fisher, C. J.; Dhainaut, J.-F. A.; Vincent, J.-L.; Brase, R.; Lowry, S. F.; Sadoff, J. C.; Slotman, G. J.; Levy, H.; Balk, R. A., Confirmatory interleukin-1 receptor antagonist trial in severe sepsis: a phase III, randomized, doubleblind, placebo-controlled, multicenter trial. *Critical care medicine* **1997,** *25*, 1115-1124.

7.   Roerink, M. E.; Van der Schaaf, M. E.; Dinarello, C. A.; Knoop, H.; Van der Meer, J. W., Interleukin-1 as a mediator of fatigue in disease: a narrative review. *J. Neuroinflammation* **2017,** *14*, 16.

8.   Chemtob, S.; Quiniou, C.; Lubell, W. D.; Beauchamp, M.; Hansford, K. A., Interleukin-1 receptor antagonists, compositions, and methods of treatment. US20050122989, **2005**.

9.   Quiniou, C.; Sapieha, P.; Lahaie, I.; Hou, X.; Brault, S.; Beauchamp, M.; Leduc, M.; Rihakova, L.; Joyal, J.-S.; Nadeau, S., Development of a novel noncompetitive antagonist of IL-1 receptor. *J. Immunol.* **2008,** *180*, 6977-6987.

10.   Jamieson, A. G.; Boutard, N.; Beauregard, K.; Bodas, M. S.; Ong, H.; Quiniou, C.; Chemtob, S.; Lubell, W. D., Positional scanning for peptide secondary structure by systematic solid-phase synthesis of amino lactam peptides. *J. Am. Chem. Soc.* **2009,** *131*, 7917-7927.

11.   Ronga, L.; Jamieson, A. G.; Beauregard, K.; Quiniou, C.; Chemtob, S.; Lubell, W. D., Insertion of multiple α-amino γ-lactam (Agl) residues into a peptide sequence by solid-phase synthesis on synphase lanterns. *Peptide Science: Original Research on Biomolecules* **2010,** *94*, 183-191.

12.   Freidinger, R. M., Design and synthesis of novel bioactive peptides and peptidomimetics. *J. Med. Chem.* **2003,** *46*, 5553-5566.

13.   Freidinger, R. M.; Veber, D. F.; Perlow, D. S.; Saperstein, R., Bioactive conformation of luteinizing hormone-releasing hormone: evidence from a conformationally constrained analog. *Science* **1980,** *210*, 656-658.

14.   St-Cyr, D. J.; Jamieson, A. G.; Lubell, W. D., α-Amino-β-hydroxy-γ-lactam for constraining peptide Ser and Thr residue conformation. *Org. Lett.* **2010,** *12* , 1652-1655.

15.   Geranurimi, A.; Lubell, W. D., Diversity-oriented syntheses of β-substituted α-amino γ-lactam peptide mimics with constrained backbone and side chain residues. *Org. Lett.* **2018,** *20*, 6126-6129.

16.   Geranurimi, A.; Cheng, C. W.; Quiniou, C.; Zhu, T.; Hou, X.; Rivera, J. C.; St-Cyr, D. J.; Beauregard, K.; Bernard-Gauthier, V.; Chemtob, S., Probing Anti-inflammatory Properties Independent of NF-κB Through Conformational Constraint of Peptide-Based Interleukin-1 Receptor Biased Ligands. *Frontiers in chemistry* **2019,** *7*, Article 23.

17.   Gulea, M.; Hammerschmidt, F.; Marchand, P.; Masson, S.; Pisljagic, V.; Wuggenig, F., Synthesis of chiral, nonracemic α-sulfanylphosphonates and derivatives. *Tetrahedron: Asymmetry* **2003,** *14*, 1829-1836.

18.   Lubell, W.; Blankenship, J.; Fridkin, G.; Kaul, R., Peptides. Science of Synthesis 21.11, Chemistry of Amides. Thieme: Stuttgart, Germany: 2005, 713-809.

19.   Villadsen, K.; Martos-Maldonado, M. C.; Jensen, K. J.; Thygesen, M. B., Chemoselective reactions for the synthesis of glycoconjugates from unprotected carbohydrates. *ChemBioChem* **2017,** *18*, 574-612.

20.   Pandey, A. K.; Naduthambi, D.; Thomas, K. M.; Zondlo, N. J., Proline editing: a general and practical approach to the synthesis of functionally and structurally diverse peptides. Analysis of steric versus stereoelectronic effects of 4-substituted prolines on conformation within peptides. *J. Am. Chem. Soc.* **2013,** *135*, 4333-4363.

21.   Shao, C.; Wang, X.; Zhang, Q.; Luo, S.; Zhao, J.; Hu, Y., Acid–base jointly promoted copper (I)-catalyzed azide–alkyne cycloaddition. *J. Org. Chem.* **2011,** *76*, 6832-6836.

22.   Meléndez, R. E.; Lubell, W. D., Synthesis and reactivity of cyclic sulfamidites and sulfamidates. *Tetrahedron* **2003,** *15*, 2581-2616.

23.   Guthrie, Q. A.; Proulx, C., Oxime Ligation via in situ Oxidation of N-Phenylglycinyl Peptides. *Org. Lett.* **2018,** *20* , 2564-2567.

24.   Wertheim, E., Derivatives of Dulcin. *J. Am. Chem. Soc.* **1931,** *53*, 200-203.

25.   Rivera, J. C.; Sitaras, N.; Noueihed, B.; Hamel, D.; Madaan, A.; Zhou, T.; Honoré, J.-C.; Quiniou, C.; Joyal, J.-S.; Hardy, P., Microglia and interleukin-1β in ischemic retinopathy elicit microvascular degeneration through neuronal semaphorin-3A. *Arter. Thromb. Vasc. Biol.* **2013,** *33*, 1881-1891.

26.   Donat, C. K.; Scott, G.; Gentleman, S. M.; Sastre, M., Microglial activation in traumatic brain injury. *Frontiers in aging neuroscience* **2017,** *9*, 208.

Chapter 4

Chapter 5: Perspectives and Conclusions

I performed the synthesis and characterization of the dipeptide analogs using cyclopropyl amino acid components, which were synthesized and characterized by Ms. Emmanuelle Allouche.

Perspectives

Towards application of lactams and cyclopropyl amino acids to constrain peptide conformation

The utility of lactam constraint for studying biologically active peptide conformation has been demonstrated using the IL-1R modulator 101.10. Notably, [(3*R*,4*S*)-Hgl³]-101.10 exhibited a CD curve shape indicative of a *β*-turn and identical *in vitro* and *in vivo* activity as the parent peptide. The effectiveness of [(3*R*,4*S*)-Hgl³]-101.10 has indicated a likely active conformer of the parent peptide, and given a lead compound for the development of other β-substituted Agl derivatives of 101.10 showing promising *in vivo* activity.

Considering the relevance of valine configuration in the 101.10 analogs, constraint about this residue may offer another promising means to explore ligand activity. Employing [(3*R*,4*S*)-Hgl³]-101.10 as a lead compound, sets of constrained valine analogs have been pursued employing 1-aminocyclopropane-1-carboxylic acid (Acc, **5.1**) and the different enantiomers of 1-amino-2,2-dimethylcyclopropane-1-carboxylic acid [(2,2-diMe)Acc, **5.2**].

α,α-Disubstituted amino acids are α-amino acids in which the hydrogen atom at the α-position is replaced with an alkyl substituent. They have demonstrated utility as peptide constraints that restrict residues ϕ and ψ torsion angles,[1] as observed by X-ray crystallography and circular dichroism spectroscopy.[2-3] The α,α-disubstituted amino acid, Acc has been shown to induce a semi-extended conformation, and to adopt ϕ and ψ backbone torsion angles (90° and 0°) characterized by relatively larger and smaller values than those in a regular 3_{10}-helix and the related amino acids with larger ring sizes.[4-5] Addition of substituents at one of the β-carbons of Acc has been shown to favor a distorted helical conformation.[6]

Cyclopropyl amino acids **5.1** and **5.2** were synthesized according to literature procedures commencing respectively from dimethyl cyclopropane dicarboxylate and serine,[7,8] and converted to their respective esters **5.3** and **5.4**. Reactions of **5.3** and **5.4** with oxiranyl glycine **5.5** were pursued to provide the corresponding dipeptides **5.6** and **5.7** (Scheme 5.1).

Initially, *tert*-butyl esters **5.3a** and **5.4a** were respectively reacted with *N*-(Fmoc)-(2*R*,3*R*)oxiranylglycine **5.5** and a catalytic amount of benzoic acid in TFE to provide Fmoc-(3*R*,4*S*)-Hgl-Acc-O*t*Bu (**5.6a**) and Fmoc-(3*R*,4*S*)-Hgl-(2,2-diMe)Acc-O*t*Bu (**5.7a**), the latter was observed to be a ratio of 4:3 (*R*):(*S*)-**5.7a** or (*S*):(*R*)-**5.7a** (Scheme 5.1). Attempts failed however to remove the *tert*-butyl ester from dipeptides **5.6a** and **5.7a** using a variety of conditions: TFA in

DCM, ZnBr$_2$[9], NaOH in MeOH,[10] as well as silica gel and silica gel combined with AcOH under microwave heating.[11] In all cases, product was destroyed and no carboxylic acid or ester were recovered. Subsequently, benzyl ester **5.6b** was synthesized,[12] and reacted as described above with *N*-(Fmoc)-(2*R*,3*R*)oxiranylglycine **5.5** to provide Fmoc-(3*R*,4*S*)-Hgl-Acc-OBn (**5.6b**). Hydrogenolysis of benzyl ester **5.6b** using 10% palladium-on-carbon in EtOH under a balloon of hydrogen afforded Fmoc-(3*R*,4*S*)-Hgl-Acc-OH (**5.8**) in 54 % yield.
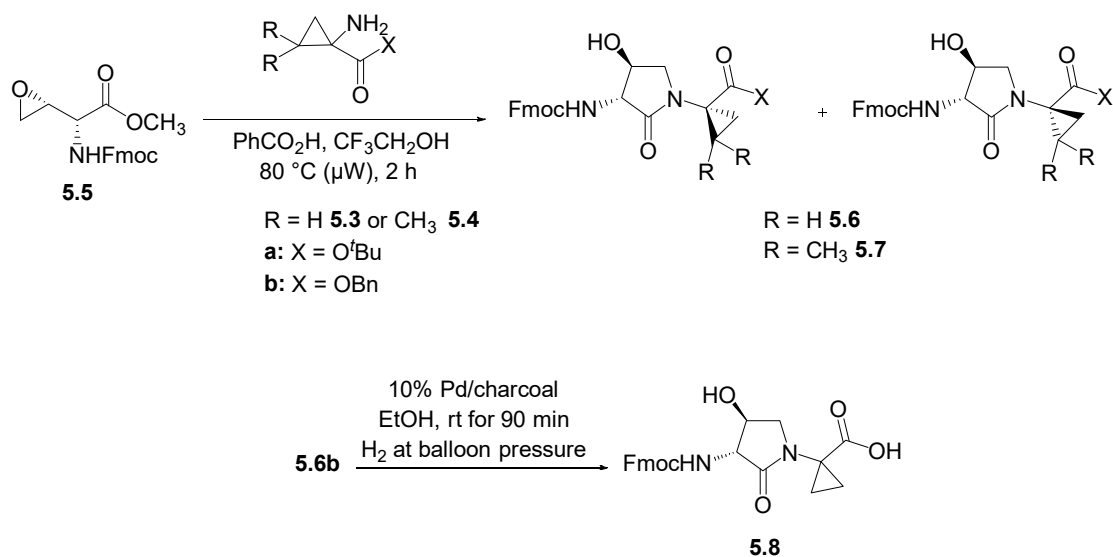
Scheme 5.1. Synthesis of Fmoc-(3*R*,4*S*)-Hgl-Acc-O^{t}Bu (**5.6a**), Fmoc-(3*R*,4*S*)-Hgl-Acc-OBn (**5.6b**), Fmoc-(3*R*,4*S*)-Hgl-Acc-OH (**5.8**) and Fmoc-(3*R*,4*S*)-Hgl-(*R*)- and (*S*)-(2,2-diMe)Acc-O^{t}Bu [(*R*)- and (*S*)-**5.7a**]

Previously, the combination of Agl and Acc residues was used to study the tripeptide dopamine modulator H-Pro-Leu-Gly-NH$_2$ (**5.9**).[3] Although replacement of Ley with (*S*)-Agl gave constrained peptide H-Pro-Agl-Gly-NH$_2$ (**5.10**) that modulates dopaminergic neurotransmission with 1,000 to 10,000 times greater potency than the parent peptide **5.9** in a set of pharmacological assays, combining the Agl and Acc residues in H-Pro-Agl-Acc-NH$_2$ (**5.11**) provided a significantly less potent yet active analog. The X-ray structure of Cbz-Pro-Agl-Acc-NH$_2$ was obtained and exhibited dihedral angles which matched closely to those of an ideal type II *β*-turn.[3] Considering the success in using the Agl-Acc dipeptide to induce *β*-turn geometry and obtain an biologically active H-Pro-Leu-Gly-NH$_2$ analog, incorporation of Fmoc-(3*R*,4*S*)-Hgl-Acc-OH (**5.8**) and (2,2-diMe)Acc counterparts into 101.10 merit further study in the future.

Experimental

Fmoc-(3*R*,4*S*)-Hgl-Acc-O*t*Bu (5.6a)
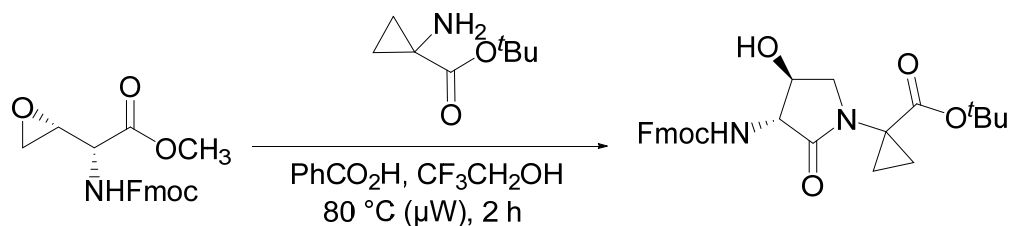
In a 20-mL screw cap vial, *tert*-butyl 1-aminocyclopropane-1-carboxylate (**5.3**, 3 eq, 230 mg, 1.46 mmol), (2*R*,3*R*)-methyl *N*-(Fmoc)oxiranyl glycinate (**5.5**, 1 eq, 172 mg, 0.5 mmol) and benzoic acid (0.3 eq, 18 mg, 0.15 mmol) were dissolved in 2,2,2-trifluoroethanol (5 ml). The vial was sealed and heated under microwave irradiation (50 W) at 80 °C for 2 h. The resulting homogeneous brown solution was concentrated in vacuum and the residue was purified by column chromatography using a step gradient of 1 to 4% THF in DCM to yield lactam **5.6a** (200 mg, 86%); R_f = 0.1 (40% EtOAc in hexane); $[\alpha]_D^{20}$ 17.7° (*c* 1, CHCl₃); ¹H NMR (500 MHz, CDCl₃) δ 7.80 (d, *J* = 7.5 Hz, 2H), 7.62 (d, *J* = 7.5 Hz, 2H), 7.44 (t, *J* = 7.4 Hz, 2H), 7.35 (td, *J* = 7.4, 0.9 Hz, 2H), 5.75 (s, 1H), 4.46 (dd, *J* = 7.0, 3.2 Hz, 2H), 4.36 (q, *J* = 8.1 Hz, 1H), 4.26 (t, *J* = 7.0 Hz, 1H), 4.08 (dd, *J* = 8.0, 1.6 Hz, 1H), 3.60 (t, *J* = 8.7 Hz, 1H), 3.39 (t, *J* = 8.8 Hz, 1H), 1.57 (d, *J* = 3.0 Hz, 1H), 1.47 (s, 9H), 1.46 (s, 1H), 1.28 (dd, *J* = 8.7, 4.1 Hz, 1H), 1.10-1.13 (m, 1H); ¹³C NMR (126 MHz, CDCl₃) δ 170.1, 169.7, 158.1, 143.5, 141.3, 127.9, 127.1, 125.0, 120.1, 82.2, 73.2, 67.7, 61.1, 51.0, 47.0, 36.7, 28.0, 16.9, 15.9; [M+Na]⁺ calcd for $C_{27}H_{30}N_2O_6Na^+$ 501.1996 found 501.2004.

Fmoc-(3*R*,4*S*)-Hgl-(*R*)- and (*S*)-(2,2-diMe)Acc-O*t*Bu [(*R*)- and (*S*)-5.7a]
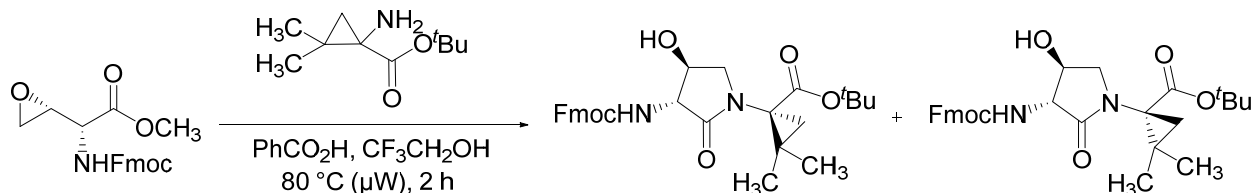
Lactams (***R***)-**5.7a** and (***S***)-**5.7a** were synthesized and purified using the representative protocol for the synthesis of Hgl-Acc dipeptide **5.6a** described above using *tert*-butyl 1-amino-2,2-dimethylcyclopropane-1-carboxylate (**5.4**, 3 eq, 410 mg, 2.2 mmol). First to elute was a yellow oil (130 mg, 35%); Rf = 0.24 (3% THF in DCM); $[\alpha]_D^{20}$ 26° (*c* 1, CHCl₃); ¹H NMR (500 MHz, CDCl₃) δ 7.77 (d, *J* = 7.5 Hz, 2H), 7.65 – 7.59 (m, 2H), 7.41 (t, *J* = 7.4 Hz, 2H), 7.32 (td, *J* = 7.4,

2.6 Hz, 2H), 5.62 (d, J = 9.5 Hz, 1H), 4.45 (dd, J = 10.5, 7.1 Hz, 1H), 4.36 (td, J = 10.3, 4.5 Hz, 2H), 4.26 (t, J = 7.2 Hz, 1H), 4.08 (d, J = 9.2 Hz, 1H), 3.78 (s, 2H), 2.95 (dd, J = 12.2, 3.6 Hz, 1H), 2.51 (dd, J = 12.3, 10.3 Hz, 1H), 1.46 (s, 9H), 1.32 (d, J = 4.8 Hz, 1H), 1.25 (s, 3H), 1.15 (s, 3H); ^{13}C NMR (126 MHz, CDCl₃) δ 173.2, 171.3, 156.7, 143.9, 143.7, 141.3, 127.7, 127.1, 125.5, 125.2, 120.0, 81.6, 69.9, 67.3, 55.9, 52.7, 50.4, 50.2, 47.1, 30.3, 28.4, 28.2, 25.9, 21.6, 20.4. Second to elute was a white solid (166 mg, 45%); Rf = 0.16 (3% THF in DCM); mp 125-127; $[\alpha]_D^{20}$ –33° (c 0.8, CHCl₃); ^{1}H NMR (500 MHz, CDCl₃) δ 7.77 (d, J = 7.5 Hz, 2H), 7.65-7.60 (m, 2H), 7.41 (t, J = 7.4 Hz, 2H), 7.32 (td, J = 7.4, 2.2 Hz, 2H), 5.64 (d, J = 9.5 Hz, 1H), 4.45 (dd, J = 10.4, 7.2 Hz, 1H), 4.36 (ddd, J = 18.1, 10.0, 4.5 Hz, 2H), 4.26 (t, J = 7.2 Hz, 1H), 4.10 (d, J = 9.1 Hz, 1H), 3.78 (s, 2H), 2.95 (dd, J = 12.3, 3.4 Hz, 1H), 2.55 (t, J = 11 Hz, 1H), 1.46 (s, 9H), 1.26 (s, 3H), 1.15 (s, 3H); ^{13}C NMR (126 MHz, CDCl₃) δ 172.5, 171.6, 156.6, 143.8, 141.3, 127.7, 127.1, 125.5, 125.1, 120.0, 81.3, 69.2, 67.3, 56.4, 52.7, 50.4, 49.9, 47.1, 30.3, 28.2, 26.7, 25.7, 21.6, 20.4.

Fmoc-(3R,4S)-Hgl-Acc-OBn (5.6b)
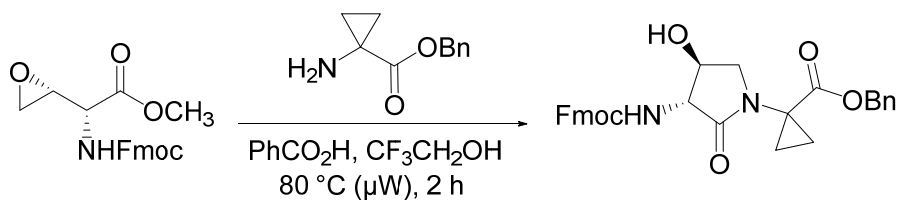
Lactams **5.6b** was synthesized and purified using the representative protocol for the synthesis of Hgl-Acc dipeptide **5.6a** described above using a 10-mL screw cap vial and benzyl 1-aminocyclopropane-1-carboxylate (1 eq, 290 mg, 1.52 mmol). Evaporation of the collected fractions gave **5.6b** (130 mg, 52 %) as red oil: R_f = 0.28 (4% THF in DCM); $[\alpha]_D^{20}$ 50° (c 1, CHCl₃);

Fmoc-(3R,4S)-Hgl-Acc-OH (5.8)
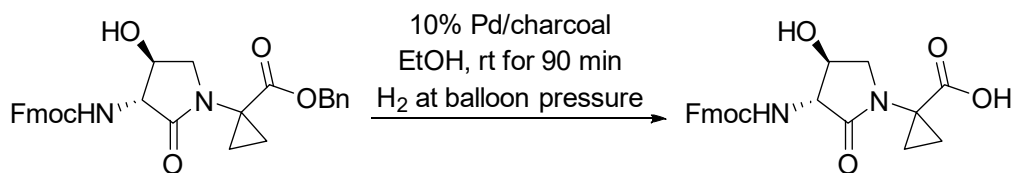
To a solution of Fmoc-(3R,4S)-Hgl-ACC-Bn (90 mg, 176 umol) in EtOH (2 mL), palladium-on-carbon (10 wt %, 18 mg, 17 µmol) was added, and the mixture was stirred under a balloon of hydrogen for 2 h. The reaction mixture was filtered through Celite™ and the filter cake was washed with 5 mL of ethanol and 2 mL of DCM. The filtrate and washings were combined and

concentrated under reduced pressure to a residue, that was purified by column chromatography using a step gradient of 0 to 5% acetic acid in EtOAc. Evaporation of the collected fractions gave **5.8** as white solid (40 mg, 54%): Rf = 0.2 (10% MeOH in DCM); mp: 185-190; ^{1}H NMR (500 MHz, DMSO) δ 7.91 (d, J = 7.5 Hz, 2H), 7.74 (d, J = 7.3 Hz, 2H), 7.68 (d, J = 9.0 Hz, 1H), 7.43 (t, J = 7.5 Hz, 2H), 7.34 (t, J = 7.4 Hz, 2H), 4.38 – 4.20 (m, 3H), 4.10 (dd, J = 16.6, 8.0 Hz, 1H), 3.92 (t, J = 8.8 Hz, 1H), 3.39 (t, J = 8.2 Hz, 2H), 3.18 (t, J = 8.4 Hz, 1H), 1.91 (s, 1H), 1.40 – 0.94 (m, 5H); ^{13}C NMR (126 MHz, DMSO) δ 171.2, 156.7, 144.4, 144.3, 141.21, 128.1, 127.6, 125.7, 120.6, 69.5, 66.1, 60.7, 51.4, 47.1, 36.6, 16.7, 14.4; [M+H]$^+$ calcd for $C_{23}H_{23}N_2O_6^+$ 423.1551 found 423.1552.

Conclusion

The influences of side chain function and conformation on peptide activity have been explored by the synthesis and application of β-substituted α-amino-γ-lactam (Agl) analogs. Methods employing Mitsunobu chemistry and cyclic sulfamidate nucleophilic ring opening have been developed to prepare stereoselectively Agl peptide mimics with various β-substituents, including constrained Cys, Ser, Thr, Dap, Dab, His, and Met residues.[13] The importance of the central D-threonine residue of the allosteric IL-1R modulator peptide 101.10 has been elucidated using such protocols, which revealed the relevance of the conformation and hydroxyl group function for the biased signaling mechanism of action.

Initially, the D-Thr-D-Val dipeptide of 101.10 was replaced by all stereoisomers of the Agl- and Hgl-Val dipeptide counterparts.[14,15] Circular dichroism (CD) spectroscopy demonstrated that the conformation of the lactam peptide analogs in solution were contingent on the configurations of the Agl, Hgl, and Val residues.[16] In contrast to the parent peptide, which exhibited a random coil CD spectrum, the D-Agl-D-Val and D-Hgl-D-Val analogs exhibited curve shapes indicative of β-turns, which were likely induced by the lactam residues. Examination of the activity of the analogs of the IL-1R allosteric modulator was performed in comparison to 101.10 using *in vitro* assays on RAW- and HEK-Blue cells. Moreover, the *in vivo* activity of the lactam analogs was compared to 101.10 in murine models of PTB and OIR. Notably, 101.10 and the Agl and Hgl analogs, all did not inhibit NF-κB signaling. Instead, contingent on structure and configuration, the lactam analogs exhibited varying degrees of inhibitory activity compared to 101.10 in blocking pathways featuring p38, JNK and ROCK2 kinase phosphorylation and expression of IL-1β, IL-6 and COX2. Depending on their *in vivo* activity, the lactams exhibited

varying degrees of efficacy in models of PTB and ROP. Among them [(3*R*,4*S*)-Hgl³]-101.10 exhibited identical *in vitro* and *in vivo* activity as 101.10 indicating that a *β*-turn conformation may be important for biological activity. Other derivatives exhibit different biased signaling effects and became a toolkit for studying the influences of different kinases with regards to effects on inflammatory responses and indications involving chronic inflammation.

The lactam analog, [(3*R*,4*S*)-Hgl³]-101.10 became an important lead to develop new compounds that can modulate the immune system selectively while maintaining immuno-vigilance. In this context, a library of fifteen novel (3*R*,4*S*)-β-substituted-Agl³ analogs of 101.10 were synthesized using solid-phase methods employing β-substituted Agl dipeptide building blocks that were made in solution. Employing the (3*R*,4*S*)-β-azido-Agl³ analog # in solid-phase chemistry entailing azide reduction and amine acylation, as well as CuAAC chemistry a series of amide, urea and guanidine, and triazole derivatives were synthesized. The latter analogs are currently being tested in *in vitro* assays, as well as an *in vivo* PTB model system. Certain (3*R*,4*S*)-β-substituted-Agl³ analogs have already exhibited promising activity in an *in vivo* model of ROP. In conclusion, this thesis has unveiled important methods for the restriction of peptide backbone and side chain residues to study structure activity relationships responsible for biological activity. Employing the methods on the IL-1R allosteric modulator has furnished a promising series of labor delaying agents that can improve neonatal outcomes in part due to their ability to reduce inflammation without compromising immune vigilance.

References

1.   Toniolo, C., Structure of conformationally constrained peptides: from model compounds to bioactive peptides. *Biopolymers: Original Research on Biomolecules* **1989,** *28*, 247-257.

2.   Tanaka, M., Design and synthesis of chiral α, α-disubstituted amino acids and conformational study of their oligopeptides. *Chemical and pharmaceutical bulletin* **2007,** *55*, 349-358.

3.   Evans, M. C.; Pradhan, A.; Venkatraman, S.; Ojala, W. H.; Gleason, W. B.; Mishra, R. K.; Johnson, R. L., Synthesis and dopamine receptor modulating activity of novel peptidomimetics of L-prolyl-L-leucyl-glycinamide featuring α, α-disubstituted amino acids. *J. Med. Chem.* **1999,** *42*, 1441-1447.

4.   Benedetti, E.; Di Blasio, B.; Pavone, V.; Pedone, C.; Santini, A.; Barone, V.; Fraternali, F.; Lelj, F.; Bavoso, A.; Crisma, M., Structural versatility of peptides containing Cα, α-dialkylated

glycines. An X-ray diffraction study of six 1-aminocyclopropane-1-carboxylic acid rich peptides. *International journal of biological macromolecules* **1989,** *11*, 353-360.

5.   Benedetti, E.; Di Blasio, B.; Pavone, V.; Pedone, C.; Santini, A.; Crisma, M.; Valle, G.; Toniolo, C., Structural versatility of peptides from Cα, αdialkylated glycines: Linear Ac3c homo-oligopeptides. *Biopolymers: Original Research on Biomolecules* **1989,** *28*, 175-184.

6.   Brackmann, F.; de Meijere, A., Natural occurrence, syntheses, and applications of cyclopropyl-group-containing α-amino acids. 1. 1-Aminocyclopropanecarboxylic acid and other 2, 3-methanoamino acids. *Chemical reviews* **2007,** *107*, 4493-4537.

7.   Lopez-Tapia, F.; Brotherton-Pleiss, C.; Yue, P.; Murakami, H.; Costa Araujo, A. C.; Reis dos Santos, B.; Ichinotsubo, E.; Rabkin, A.; Shah, R.; Lantz, M., Linker variation and structure-activity relationship analyses of carboxylic acid-based small molecule STAT3 inhibitors. *ACS medicinal chemistry letters* **2018,** *9*, 250-255.

8.   Rothman, D. M.; Vazquez, M. E.; Vogel, E. M.; Imperiali, B., Caged phospho-amino acid building blocks for solid-phase peptide synthesis. *J. Org. Chem.* **2003,** *68*, 6795-6798.

9.   Kaul, R.; Brouillette, Y.; Sajjadi, Z.; Hansford, K. A.; Lubell, W. D., Selective *tert*-butyl ester deprotection in the presence of acid labile protecting groups with use of ZnBr2. *J. Org. Chem.* **2004,** *69*, 6131-6133.

10.   Ricci, L.; Sernissi, L.; Scarpi, D.; Bianchini, F.; Contini, A.; Occhiato, E. G., Synthesis and conformational analysis of peptides embodying 2, 3-methanopipecolic acids. *Org. Biomol. Chem.* **2017,** *15*, 6826-6836.

11.   Park, D.-H.; Park, J.-H., Solvent-free cleavage of tert-butyl esters under microwave conditions. *Bulletin of the Korean Chemical Society* **2009,** *30*, 230-232.

12.   Bender, D. M.; Peterson, J. A.; McCarthy, J. R.; Gunaydin, H.; Takano, Y.; Houk, K., Cyclopropanecarboxylic acid esters as potential prodrugs with enhanced hydrolytic stability. *Org. Lett.* **2008,** *10*, 509-511.

13.   Geranurimi, A.; Lubell, W. D., Diversity-oriented syntheses of β-substituted α-amino γ-lactam peptide mimics with constrained backbone and side chain residues. *Org. Lett.* **2018,** *20*, 6126-6129.

14.   Freidinger, R. M.; Veber, D. F.; Perlow, D. S.; Saperstein, R., Bioactive conformation of luteinizing hormone-releasing hormone: evidence from a conformationally constrained analog. *Science* **1980,** *210*, 656-658.

15.   St-Cyr, D. J.; Maris, T.; Lubell, W. D., Crystal-state structure analysis of β-hydroxy-γ-lactam constrained Ser/Thr peptidomimetics. *Heterocycles* **2010,** *82*, 729-737.

16.   Geranurimi, A.; Cheng, C. W.; Quiniou, C.; Zhu, T.; Hou, X.; Rivera, J. C.; St-Cyr, D. J.; Beauregard, K.; Bernard-Gauthier, V.; Chemtob, S., Probing anti-inflammatory properties independent of NF-κB through conformational constraint of peptide-based interleukin-1 receptor biased ligands. *Frontiers in chemistry* **2019,** *7*.

Chapter 5

Annex 1: Supporting information of Article 1

Probing anti-inflammatory properties independent of NF-κB through conformational constraint of peptide-based interleukin-1β receptor biased ligands

Azade Geranurimi, Colin WH Cheng, Christiane Quiniou, Xin Hou, Tang Zhu, Daniel St-Cyr, Kim Beauregard, Vadim Bernard-Gauthier, Sylvain Chemtob, William D. Lubell[*]

* Correspondence: Prof. William D. Lubell, *william.lubell@umontreal.ca*

H-D-Arg-D-Tyr-(*R*)-Agl-(*S*)-Val-D-Glu-D-Leu-D-Ala-NH₂ [(3*R*)-Agl³-(*S*)-Val]- 2.1 [(3*R*, 2'*S*)-2.5]

Employing the representative procedure described for peptide (3*R*)-**2.5**, (3*R*,2'*S*)-**2.5** was synthesized (13 mg, 16% yield of >95% purity); LCMS [10-90% MeOH (0.1% FA) in water (0.1% FA) over 14 min; RT 7.6 min] and [10-90% MeCN (0.1% FA) in water (0.1% FA) over 14 min; RT 5.3 min]; HRMS (ESI⁺) calcd m/z for $C_{38}H_{62}N_{11}O_{10}$ [M+H]⁺, 832.4676 found 832.4687.

H-D-Arg-D-Tyr-(*S*)-Agl-D-Val-D-Glu-D-Leu-D-Ala-NH₂ [(3*S*)-Agl³]-2.1 [(3*S*)-2.5]

Employing the representative procedure described for peptide (3*R*)-**2.5**, (3*S*)-**2.5** was synthesized (12 mg, 15% yield of >95% purity); LCMS [10-90% MeOH (0.1% FA) in water (0.1% FA) over 14 min; RT 8 min] and [10-90% MeCN (0.1% FA) in water (0.1% FA) over 14 min; RT 5.4 min]; HRMS (ESI⁺) calcd m/z for $C_{38}H_{62}N_{11}O_{10}$ [M+H]⁺, 832.4676 found 832.4680.

H-D-Arg-D-Tyr-(*S*)-Agl-(*S*)-Val-D-Glu-D-Leu-D-Ala-NH₂ [(3*S*)-Agl³-(*S*)-Val]-2.1 [(3*S*, 2'*S*)-2.5]

Employing the representative procedure described for peptide (3*R*)-**2.5**, (3*S*,2'*S*)-**2.5** was synthesized (11 mg, 13% yield of >95% purity); LCMS [10-90% MeOH (0.1% FA) in water (0.1% FA) over 14 min; RT 7.9 min] and [10-90% MeCN (0.1% FA) in water (0.1% FA) over 14 min; RT 5.5 min]; HRMS (ESI⁺) calcd m/z for $C_{38}H_{62}N_{11}O_{10}$ [M+H]⁺, 832.4676 found 832.4692.

H-D-Arg-D-Tyr-(3*R*,4*R*)-Hgl-D-Val-D-Glu-D-Leu-D-Ala-NH₂ [(3*R*, 4*R*)-Hgl³]-2.1 [(3*R*, 4*R*)-2.6]

Employing the representative procedure described for peptide (3*R*)-**2.5**, (3*R*,4*R*)-**2.6** was synthesized (7 mg, 8% yield of >95% purity); LCMS [10-90% MeOH (0.1% FA) in water (0.1% FA) over 14 min; RT 7.8 min] and [10-90% MeCN (0.1% FA) in water (0.1% FA) over 14 min; RT 5.4 min]; HRMS (ESI$^+$) calcd m/z for $C_{38}H_{63}N_{11}O_{11}$ [M+2H]$^{+2}$, 424.7349 found 424.73556 and calcd m/z for $C_{38}H_{62}N_{11}O_{11}$ [M+H]$^+$, 848.4625 found 848.4525.

H-D-Arg-D-Tyr-(3*R*,4*S*)-Hgl-D-Val-D-Glu-D-Leu-D-Ala-NH₂ [(3*R*, 4*S*)-Hgl³]-2.1 [(3*R*, 4*S*)-2.6]

Employing the representative procedure described for peptide (3*R*)-**2.5**, (3*R*,4*S*)-**2.6** was synthesized (12 mg, 14% yield of >95% purity); LCMS [10-90% MeOH (0.1% FA) in water (0.1% FA) over 14 min; RT 7.5 min] and [10-90% MeCN (0.1% FA) in water (0.1% FA) over 14 min; RT 5.2 min]; HRMS (ESI$^+$) calcd m/z for $C_{38}H_{63}N_{11}O_{11}$ [M+2H]$^{+2}$, 424.7349 found 424.7342 and calcd m/z for $C_{38}H_{62}N_{11}O_{11}$ [M+H]$^+$, 848.4625 found 848.4573.

H-D-Arg-D-Tyr-(3*R*,4*R*)-Hgl-(*S*)-Val-D-Glu-D-Leu-D-Ala-NH₂ [(3*R*, 4*R*)-Hgl³-(*S*)-Val]-2.1 [(3*R*, 4*R*, 2'*S*)-2.6]

Employing the representative procedure described for peptide (3*R*)-**2.5**, (3*R*,4*R*,2'*S*)-**2.6** was synthesized (11 mg, 13% yield of >95% purity); LCMS [10-90% MeOH (0.1% FA) in water (0.1% FA) over 14 min; RT 6.8 min] and [10-90% MeCN (0.1% FA) in water (0.1% FA) over 14 min; RT 4.9 min]; HRMS (ESI$^+$) calcd m/z for $C_{38}H_{63}N_{11}O_{11}$ [M+2H]$^{+2}$, 424.7349 found 424.7358 and calcd m/z for $C_{38}H_{62}N_{11}O_{11}$ [M+H]$^+$, 848.4625 found 848.4629.

H-D-Arg-D-Tyr-(3*R*,4*S*)-Hgl-(*S*)-Val-D-Glu-D-Leu-D-Ala-NH₂ [(3*R*, 4*S*)-Hgl³-(*S*)-Val]-2.1 [(3*R*, 4*S*, 2'*S*)-2.6]

Employing the representative procedure described for peptide (3*R*)-**2.5**, (3*R*,4*S*,2'*S*)-**2.6** was synthesized (11 mg, 13% yield of >95% purity); LCMS [10-90% MeOH (0.1% FA) in water (0.1% FA) over14 min; RT 6.9 min] and [10-90% MeCN (0.1% FA) in water (0.1% FA) over 14 min; RT 4.9 min]; HRMS (ESI$^+$) calcd m/z for $C_{38}H_{63}N_{11}O_{11}$ [M+2H]$^{+2}$, 424.7349 found 424.7352 and calcd m/z for $C_{38}H_{62}N_{11}O_{11}$ [M+H]$^+$, 848.4625 found 848.4629.

H-D-Arg-D-Tyr-(3*S*,4*R*)-Hgl-D-Val-D-Glu-D-Leu-D-Ala-NH₂ [(3*S*, 4*R*)-Hgl³]-2.1 [(3*S*, 4*R*)-2.6]

Employing the representative procedure described for peptide (3*R*)-**2.5**, (3*S*,4*R*)-**2.6** was synthesized (9 mg, 11% yield of >95% purity) as a white solid; LCMS [10-90% MeOH (0.1% FA)

in water (0.1% FA) over 14 min; RT 7.8 min] and [10-90% MeCN (0.1% FA) in water (0.1% FA) over 14 min; RT 5.4 min]; HRMS (ESI$^+$) calcd m/z for C$_{38}$H$_{63}$N$_{11}$O$_{11}$ [M+2H]$^{+2}$, 424.7349 found 424.7340 and calcd m/z for C$_{38}$H$_{62}$N$_{11}$O$_{11}$ [M+H]$^+$, 848.4625 found 848.4625.

H-D-Arg-D-Tyr-(3*S*,4*S*)-Hgl-D-Val-D-Glu-D-Leu-D-Ala-NH$_2$ [(3*S*, 4*S*)-Hgl^3]-2.1 [(3*S*, 4*S*)-2.6]

Employing the representative procedure described for peptide (3*R*)-**2.5**, (3*S*,4*S*)-**2.6** was synthesized (8 mg, 9% yield of >95% purity); LCMS [10-90% MeOH (0.1% FA) in water (0.1% FA) over 14 min; RT 7.3 min] and [10-90% MeCN (0.1% FA) in water (0.1% FA) over 14 min; RT 5.2 min]; HRMS (ESI$^+$) calcd m/z for C$_{38}$H$_{63}$N$_{11}$O$_{11}$ [M+2H]$^{+2}$, 424.7349 found 424.7356 and calcd m/z for C$_{38}$H$_{62}$N$_{11}$O$_{11}$ [M+H]$^+$, 848.4625 found 848.4627.

H-D-Arg-D-Tyr-(3*S*,4*R*)-Hgl-(*S*)-Val-D-Glu-D-Leu-D-Ala-NH$_2$ [(3*S*, 4*R*)-Hgl^3-(*S*)-Val]-2.1 [(3*S*, 4*R*, 2'*S*)-2.6]

Employing the representative procedure described for peptide (3*R*)-**2.5**, (3*S*,4*R*,2'*S*)-**2.6** was synthesized (10 mg, 12% yield of >95% purity); LCMS [10-90% MeOH (0.1% FA) in water (0.1% FA) over 14 min; RT 7 min] and [10-90% MeCN (0.1% FA) in water (0.1% FA) over 14 min; RT 4.9 min]; HRMS (ESI$^+$) calcd m/z for C$_{38}$H$_{63}$N$_{11}$O$_{11}$ [M+2H]$^{+2}$, 424.7349 found 424.7353 and calcd m/z for C$_{38}$H$_{62}$N$_{11}$O$_{11}$ [M+H]$^+$, 848.4625 found 848.4618.

H-D-Arg-D-Tyr-(3*S*,4*S*)-Hgl-(*S*)-Val-D-Glu-D-Leu-D-Ala-NH$_2$ [(3*S*, 4*S*)-Hgl^3-(*S*)-Val]-2.1 [(3*S*, 4*S*, 2'*S*)-2.6]

Employing the representative procedure described for peptide (3*R*)-**2.5**, (3*S*,4*S*,2'*S*)-**2.6** was synthesized (10 mg, 12% yield of >95% purity); LCMS [10-90% MeOH (0.1% FA) in water (0.1% FA) over 14 min; RT 6.6 min] and [10-90% MeCN (0.1% FA) in water (0.1% FA) over 14 min; RT 5.2 min]; HRMS (ESI$^+$) calcd m/z for C$_{38}$H$_{63}$N$_{11}$O$_{11}$ (M+2H)$^{+2}$, 424.7349 found 424.7371 and calcd m/z for C$_{38}$H$_{62}$N$_{11}$O$_{11}$ (M+H)$^+$, 848.4625 found 848.4635.

(3*R*, 2'*S*)-2-[3-*N*-(Fmoc)amino-2-oxopyrrolidin-1-yl]-3-methylbutanoic acid [(3*R*, 2'*S*)-2.7]
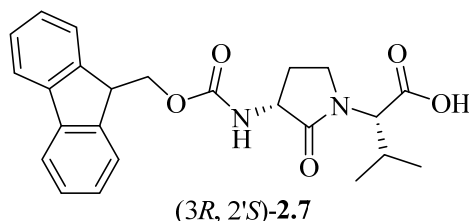
(3*R*, 2'*S*)-**2.7**

Employing the representative procedure described for the synthesis of (3*R*,2'*R*)-carbamate (3*R*,2'*R*)-**2.7**, (3*R*,2'*S*)-acid (3*R*,2'*S*)-**2.14** (51 mg, 0.209 mmol) was converted to (3*R* 2'*S*)-

carbamate (3*R*,2'*S*)-**2.7** (75 mg, 0.178 mmol, 85%): R$_f$ = 0.17 (10% MeOH:DCM); [α]$_D^{25}$ –43.2°
(*c* 0.5, MeOH); ^{1}H NMR (300 MHz, MeOD) δ 7.80 (d, *J* = 7.3, 2H), 7.68 (d, *J* = 7.4, 2H), 7.39 (t,
J = 7.1, 2H), 7.31 (td, *J* = 7.4, 1.2, 2H), 5.57 (d, *J* = 5.6, 1H); 4.48-4.14 (m, 5H), 3.57-3.42 (m,
2H), 2.54-2.33 (m, 1H), 2.33-2.10 (m, 1H), 2.09-1.90 (m, 1H), 1.40-1.23 (m, 1H), 1.05 (d, *J* = 6.6,
3H), 0.95 (d, *J* = 6.6, 3H); ^{13}C NMR (75 MHz, MeOD) δ 173.9, 171.4, 157.1 143.9, 141.2, 127.3,
126.7, 124.8, 119.5, 66.6, 60.9, 52.4, 40.7, 27.0, 25.7, 24.8, 18.5, 18.0; HRMS (ESI$^+$) calcd *m/z*
for $C_{24}H_{27}N_2O_5$ [M+H]$^+$, 423.1914 found 423.1906.

(3*S*, 2'*R*)-2-[3-*N*-(Fmoc)amino-2-oxopyrrolidin-1-yl]-3-methylbutanoic acid [(3*S*, 2'*R*)-2.7]
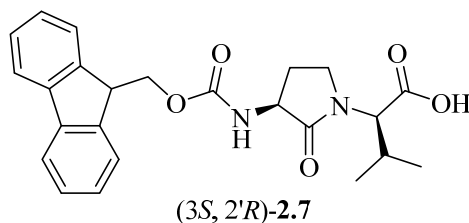
(3*S*, 2'*R*)-**2.7**

Employing the representative procedure described for the synthesis of (3*R*,2'*R*)-carbamate
(3*R*,2'*R*)-**2.7**, (3*S*,2'*R*)-acid (3*S*,2'*R*)-2.**14** (1 eq., 86 mg, 0.352 mmol) was converted to (3*S*,2'*R*)-
carbamate (3*S*,2'*R*)-**2.7** (100 mg, 0.237 mmol, 67%): [α]$_D^{25}$ 2.4° (*c* 0.67, MeOH).

(3*S*, 2'*S*)-2-[3-*N*-(Fmoc)amino-2-oxopyrrolidin-1-yl]-3-methylbutanoic acid [(3*S*, 2'*S*)-2.7]
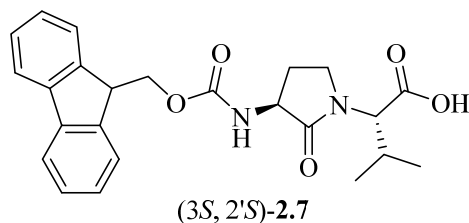
(3*S*, 2'*S*)-**2.7**

Employing the representative procedure described for the synthesis of (3*R*,2'*R*)-carbamate
(3*R*,2'*R*)-**2.7**, (3*S*,2'*S*)-acid (3*S*,2'*S*)-**2.14** (1 eq., 67 mg, 0.274 mmol) was converted to (3*S*,2'*S*)-
carbamate (3*S*,2'*S*)-**2.7** (81 mg, 0.192 mmol, 70%): [α]$_D^{25}$ –89.9° (*c* 0.76, MeOH).

***N*-Boc-(*R*)-Methionine [(*R*)-2.8]**

(*R*)-**2.8**

Annex 1: Supporting information of Article 1
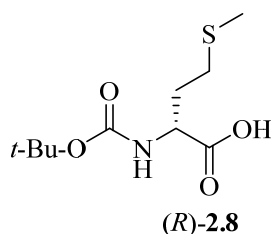
D-Met-OH (1 eq., 2 g, 13.4 mmol), was dissolved in a 1:1 mixture of dioxane (10 mL) and H_2O (10 mL). The addition of NaOH (2 eq., 2 M, 13.4 mL, 26.8 mmol) to this reaction mixture dissolved the reactant and afforded a miscible solution. The reaction mixture was then cooled to 0 °C and stirred for 15 min. Finally, (Boc)$_2$O (1.1 eq., 3.22 g, 3.15 mL, 14.7 mmol) was added, and the reaction mixture was stirred at 0 °C for 10 min. The ice bath was then removed, and the temperature of the reaction mixture warmed to rt with stirring for 18 h. On completion of the reaction, the reaction mixture was concentrated under reduced pressure. The aqueous layer was acidified with citric acid 0.5 N (pH 2 to 3) and extracted with EtOAc. The organic extractions were cobined, washed with brine, dried over Na_2SO_4, and concentrated under reduced pressure to provide *N*-Boc-D-methionine [(*R*)-**2.8**, 3.17 g, 12.7 mmol, 95%] as white solid[1]: mp 47-50 °C (Lit.[2] 50-51 °C); R$_f$ = 0.6 (10% EtOH in CHCl$_3$); [α] $_D^{20}$ 23° (*c* 1, MeOH) [Lit.[2] [α] $_D^{20}$ 22°, (*c* 1, MeOH)].

N-Boc-(S)-Methionine [(S)-2.8]

(*S*)-**2.8**
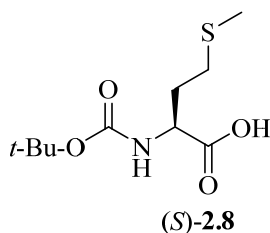
Employing the representative procedure described for the synthesis of *N*-Boc-D-methionine (*R*)-**2.8**, NaOH (2 eq., 2 M, 13.4 mL, 26.8 mmol) and (Boc)$_2$O (1.1 eq., 3.22 g, 3.15 mL, 14.7 mmol) were added to H-L-Met-OH (1 eq., 2 g, 13.4 mmol) respectively to yield *N*-Boc-L-methionine (*S*)-**2.8** (3.28 g, 13.1 mmol, 98%): [α] $_D^{20}$ –25° (*c* 1, MeOH) {Lit.[2] [α] $_D^{22}$ –22.8°, (*c* 1, MeOH)}.

(R)-N-(Boc)-Methioninyl-(S)-valine *tert*-butyl ester [(R, S)-2.10]
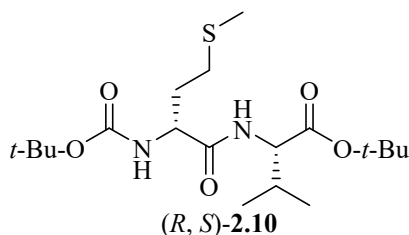
(*R*, *S*)-**2.10**

Employing the representative procedure described for the synthesis of (*R*,*R*)-dipeptide (*R*,*R*)-**2.10**, *N*-Boc-(*R*)-methionine (1 eq., 1 g, 4 mmol) and (*S*)-valine *tert*-butyl ester hydrochloride (*S*)-

2.9•HCl (1 eq., 840 mg, 4 mmol) were coupled to give (*R,S*)-dipeptide (*R,S*)-**2.10** as light yellow oil (1.13 g, 2.8 mmol, 70%): R_f = 0.3 (20% EtOAc in hexane); [α] $_D^{25}$ 13.7° (*c* 1.9, CHCl$_3$); ^{1}H NMR (300 MHz, CDCl$_3$) δ 6.67 (d, *J* = 8.3, 1H), 5.23 (d, *J* = 7.2, 1H), 4.39 (dd, *J* = 8.7, 4.4, 1H), 4.36-4.22 (m, 1H), 2.63-2.47 (m, 2H), 2.22-2.04 (m, 4H), 1.90 (tt, *J* = 7.6, 3.9, 1H), 1.44 (s, 9H), 1.43 (s, 9H), 0.92 (d, *J* = 6.9, 3H), 0.88 (d, *J* = 6.9, 3H); ^{13}C NMR (75 MHz, CDCl$_3$) δ 171.4, 170.8, 155.6, 82.1, 80.2, 57.5, 53.9, 31.8, 31.5, 30.3, 28.4, 28.1, 19.0, 17.6, 15.4; HRMS (ESI$^+$) calcd *m/z* for C$_{19}$H$_{36}$N$_2$O$_5$S [M+H]$^+$, 405.2418 found 405.2424.

(*S*)-*N*-(Boc)-Methioninyl-(*R*)-valine *tert*-butyl ester [(*S, R*)-2.10]
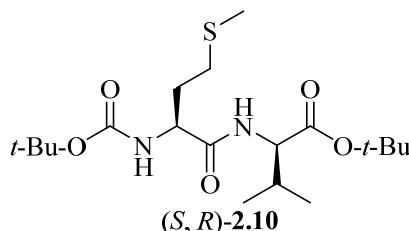
(*S, R*)-**2.10**

Employing the representative procedure described for the synthesis of (*R,R*)-dipeptide (*R,R*)-**2.10**, *N*-Boc-(*S*)-methionine (1 eq., 1 g, 4 mmol) and (*R*)-valine *tert*-butyl ester hydrochloride (*R*)-**2.9** HCl (1 eq., 840 mg, 4 mmol) were coupled to give (*S,R*)-dipeptide (*S,R*)-**2.10** as light yellow oil (1.22 g, 3.01 mmol, 75%): [α] $_D^{25}$ –23.3° (*c* 3.7, CHCl$_3$).

(*S*)-*N*-(Boc)-Methioninyl-(*S*)-valine *tert*-butyl ester [(*S, S*)-2.10]
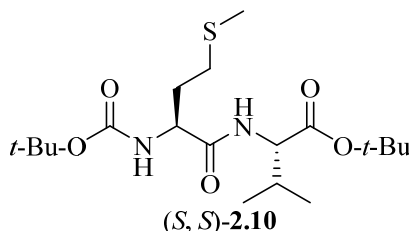
(*S, S*)-**2.10**

Employing the representative procedure described for the synthesis of (*R,R*)-dipeptide (*R,R*)-**2.10**, *N*-Boc-(*S*)-methionine (*S*)-**2.8** (1 eq., 1 g, 4 mmol) and (*S*)-valine *tert*-butyl ester hydrochloride (*S*)-**2.9** HCl (1 eq., 840 mg, 4 mmol) were coupled to give (*S,S*)-dipeptide (*S,S*)-**2.10** (1.33 g, 3.28 mmol, 82%): [α] $_D^{25}$ 13.0° (*c* 1, CHCl$_3$).

N-Boc-(*R*)-Methioninyl-(*S*)-valine *tert*-butyl ester methylsulfonium iodide [(*R, S*)-2.11]
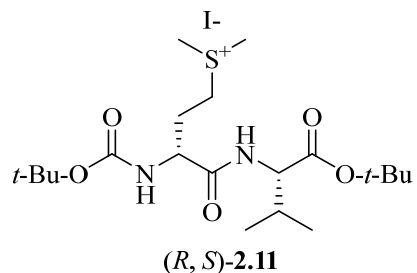
Annex 1: Supporting information of Article 1

(*R*, *S*)-**2.11**

Employing the representative procedure described for the synthesis of (*R*,*R*)-methylsulfonium iodide (*R*,*R*)-**2.11**, (*R*,*S*)-dipeptide (*R*,*S*)-**2.10** (1 g, 2.47 mmol) was converted to (*R*,*S*)-methylsulfonium iodide (*R*,*S*)-**2.11** as light yellow foam (1.065 g, 1.95 mmol, 79%): R_f = 0.18 (5% MeOH in DCM); $[\alpha]_D^{25}$ 14° (*c* 1, MeOH); ^{1}H NMR (300 MHz, CDCl$_3$) δ 7.52-7.36 (br s, 1H), 6.00 (d, *J* = 7.3, 1H), 4.54-4.43 (br s, 1H), 4.27 (dd, *J* = 8.3, 5.1, 1H), 3.95-3.82 (m, 1H), 3.78-3.60 (br s, 1H), 3.31 (s, 3H), 3.23 (s, 3H), 2.60-2.52 (m, 1H), 2.31-2.16 (m, 2H), 1.44 (dd, *J* = 5.9, 2.4, 18H), 0.95 (dd, *J* = 6.8, 4.6, 6H); HRMS (ESI$^+$) calcd *m/z* for C$_{20}$H$_{39}$N$_2$O$_5$S [M]$^+$, 419.2574 found 419.2573.

N-Boc-(*S*)-Methioninyl-(*R*)-valine *tert*-butyl ester methylsulfonium iodide [(*S*, *R*)-2.11]
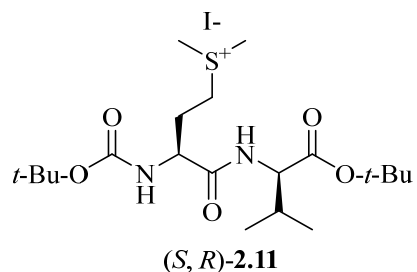
(*S*, *R*)-**2.11**

Employing the representative procedure described for the synthesis of (*R*,*R*)-methylsulfonium iodide (*R*,*R*)-**2.11**, (*S*,*R*)-dipeptide (*S*,*R*)-**2.10** (1 g, 2.47 mmol) was converted to (*S*,*R*)-methylsulfonium iodide (*S*,*R*)-**2.11** as light yellow foam (1.187 g, 2.17 mmol, 88%): $[\alpha]_D^{25}$ −31° (*c* 1, MeOH).

N-Boc-(*S*)-Methioninyl-(*S*)-valine *tert*-butyl ester methylsulfonium iodide [(*S*, *S*)-2.11]
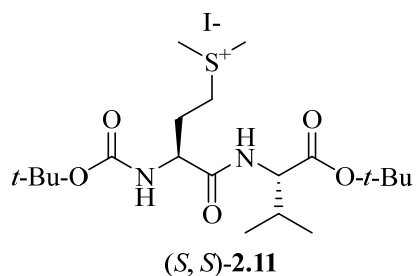
(*S*, *S*)-**2.11**

Annex 1: Supporting information of Article 1

Employing the representative procedure described for the synthesis of (*R,R*)-methylsulfonium iodide (*R,R*)-**2.11**, (*S,S*)-dipeptide (*S,S*)-**2.10** (1 g, 2.47 mmol) was converted to (*S,S*)-methylsulfonium iodide (*S,S*)-**2.11** as yellow gummy foam (670 mg, 1.23 mmol, 99%): [α] $_D^{25}$ –28° (*c* 1, MeOH).

N-Fmoc-(3R, 4R, 2'R)-Hgl-Val-OH [(3R, 4R, 2'R)-2.12]
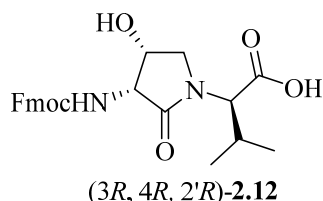
(3*R*, 4*R*, 2'*R*)-**2.12**

Employing the previously described procedure,[3] (3*R*,4*R*,2'*R*)-ester (3*R*,4*R*,2'*R*)-**2.19** (133 mg, 0.269 mmol) was converted into (3*R*,4*R*,2'*R*)-acid (3*R*,4*R*,2'*R*)-**2.12** (113 mg, 0.258 mmol, 96%): R_f = 0.08 (10% MeOH in DCM); [α]$_D^{20}$ 14.8 (*c* 1.3, MeOH); HRMS (ESI$^+$) calcd m/z for $C_{24}H_{27}N_2O_6$ [M+H]$^+$, 439.1864 found 439.1868.

N-Fmoc-(3R, 4S, 2'R)-Hgl-Val-OH [(3R, 4S, 2'R)-2.12]
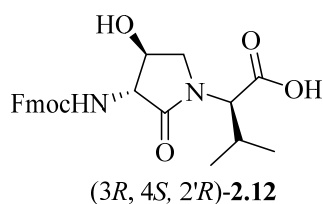
(3*R*, 4*S*, 2'*R*)-**2.12**

Employing the previously described procedure,[3] (3*R*,4*S*,2'*R*)-ester (3*R*,4*S*,2'*R*)-**2.19** (450 mg, 0.91 mmol) was converted into (3*R*,4*S*,2'*R*)-acid (3*R*,4*S*,2'*R*)-**2.12** (379 mg, 0.86 mmol, 95 %): R_f = 0.16 (5% THF in DCM); HRMS (ESI$^+$) calcd m/z for $C_{24}H_{27}N_2O_6$ [M+H]$^+$, 439.1864 found 439.1861.

N-Fmoc-(3R, 4R, 2'S)-Hgl-Val-OH [(3R, 4R, 2'S)-2.12]
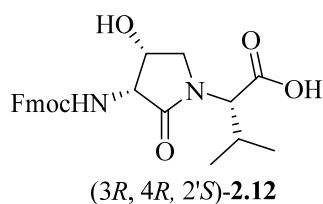
(3*R*, 4*R*, 2'*S*)-**2.12**

Employing the previously described procedure,[3] (3*R*,4*R*,2'*S*)-ester (3*R*,4*R*,2'*S*)-**2.19** (220 mg, 0.445 mmol) was converted into (3*R*,4*R*,2'*S*)-acid (3*R*,4*R*,2'*S*)-**2.12** (181 mg, 0.414 mmol, 93 %): R_f = 0.07 (10% MeOH in DCM); ^{1}H NMR (300 MHz, MeOD) δ 7.82 (d, *J* = 7.3, 2H), 7.73 (dd, *J*

= 7.1, 3.4, 2H), 7.41 (t, J = 7.3, 2H), 7.34 (td, J = 7.3, 0.9, 2H), 4.52 (d, J = 4.9, 1H), 4.44 (dd, J = 7.1, 3.2, 2H), 4.39 (d, J = 5.2, 1H), 4.35 (d, J = 3.3, 1H), 4.29 (dd, J = 14.0, 7.0, 1H), 3.75 (dd, J = 11.4, 3.6, 1H), 3.41 (d, J = 11.4, 1H), 2.31-2.14 (m, 1H), 1.07 (d, J = 6.6, 3H), 0.99 (d, J = 6.7, 3H); ^{13}C NMR (75 MHz, MeOD) δ 172.5, 171.4, 157.6, 143.7, 141.2, 127.4, 126.8, 124.9, 119.5, 69.1, 67.1, 65.7, 60.5, 56.7, 50.3, 27.0, 20.9, 18.4, 17.7; HRMS (ESI$^+$) calcd m/z for $C_{24}H_{27}N_2O_6$ [M+H]$^+$, 439.1864 found 439.1871.

_N_-Fmoc-(3_R_, 4_S_, 2'_S_)-Hgl-Val-OH [(3_R_, 4_S_, 2'_S_)-2.12]
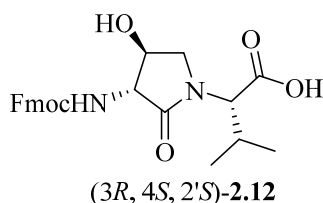
(3_R_, 4_S_, 2'_S_)-**2.12**

Employing the previously described procedure,[3] (3_R_,4_S_,2'_S_)-ester (3_R_,4_S_,2'_S_)-**2.19** (220 mg, 0.445 mmol) was converted into (3_R_,4_S_,2'_S_)-acid (3_R_,4_S_,2'_S_)-**2.12** (150 mg, 0.342 mmol, 77%): R_f = 0.1 (5% THF in DCM); HRMS (ESI$^+$) calcd m/z for $C_{24}H_{27}N_2O_6$ [M+H]$^+$, 439.1864 found 439.1853.

_N_-Fmoc-(3_S_, 4_R_, 2'_R_)-Hgl-Val-OH [(3_S_, 4_R_, 2'_R_)-2.12]
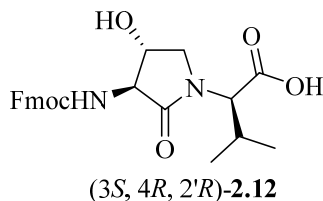
(3_S_, 4_R_, 2'_R_)-**2.12**

Employing the previously described procedure,[3] (3_S_,4_R_,2'_R_)-ester (3_S_,4_R_,2'_R_)-**2.19** (120 mg, 0.243 mmol) was converted into (3_S_,4_R_,2'_R_)-acid (3_S_,4_R_,2'_R_)-**2.12** (85.1 mg, 0.194 mmol, 80%).

_N_-Fmoc-(3_S_, 4_S_, 2'_R_)-Hgl-Val-OH [(3_S_, 4_S_, 2'_R_)-2.12]
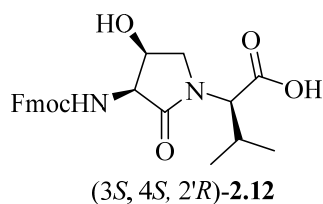
(3_S_, 4_S, 2'_R_)-**2.12**

Employing the previously described procedure,[3] (3_S_,4_S_,2'_R_)-ester (3_S_,4_S_,2'_R_)-**2.19** (145 mg, 0.293 mmol) was converted into (3_S_,4_S_,2'_R_)-acid (3_S_,4_S_,2'_R_)-**2.12** (106 mg, 0.243 mmol, 83 %).

_N_-Fmoc-(3_S_, 4_R_, 2'_S_)-Hgl-Val-OH [(3_S_, 4_R_, 2'_S_)-2.12]

Annex 1: Supporting information of Article 1
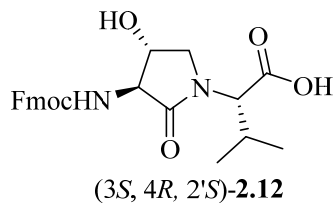
(3*S*, 4*R*, 2'*S*)-**2.12**

Employing the previously described procedure,[3] (3*S*,4*R*,2'*S*)-ester (3*S*,4*R*,2'*S*)-**2.19** (250 mg, 0.505 mmolwas converted to (3*S*,4*R*,2'*S*)-acid (3*S*,4*R*,2'*S*)-2.**12** (160 mg, 0.365 mmol, 72%).

N-Fmoc-(3*S*, 4*S*, 2'*S*)-Hgl-Val-OH [(3*S*, 4*S*, 2'*S*)-2.12]
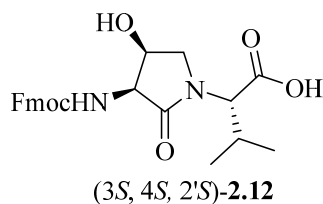
(3*S*, 4*S*, 2'*S*)-**2.12**

Employing the previously described procedure,[3] (3*S*,4*S*,2'*S*)-ester (3*S*,4*S*,2'*S*)-**2.19** (80 mg, 0.162 mmol) was converted into (3*S*,4*S*,2'*S*)-acid 3*S*,4*S*,2'*S*)-**2.12** (62.4 mg, 0.142 mmol, 88%).

(3*R*, 2'*S*)-*tert*-Butyl 2-[3-(Boc)amino-2-oxopyrrolidin-1-yl]-3-methylbutanoate [(3*R*, 2'*S*)-2.13]
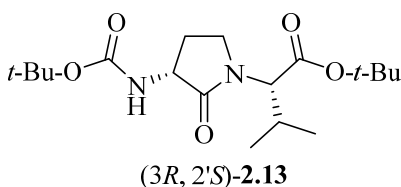
(3*R*, 2'*S*)-**2.13**

Employing the representative procedure described for the synthesis of (3*R*,2'*R*)-lactam (3*R*,2'*R*)-**2.13**, (*R*,*S*)-methylsulfonium iodide (*R*,*S*)-**2.11** (274 mg, 0.501 mmol) was converted to (3*R*,2'*S*)-lactam (3*R*,2'*S*)-**2.13** (109 mg, 0.306 mmol, 61%): R_f = 0.30 (30% EtOAc in Hexane); [α] $_D^{25}$ − 83.7° (*c* 1, CHCl$_3$); ^{1}H NMR (300 MHz, CDCl$_3$) δ 5.12 (s, 1H), 4.32 (d, *J* = 10.1, 1H), 4.26-4.09 (m, 1H), 3.50-3.29 (m, 2H), 2.77-2.58 (m, 1H), 2.17 (ddt, *J* = 13.4, 10.3, 6.7, 1H), 1.86-1.67 (m, 1H), 1.44 (s, 18H), 1.00 (d, *J* = 6.6, 3H), 0.86 (d, *J* = 6.7, 3H); ^{13}C NMR (75 MHz, CDCl$_3$) δ 173.1, 169.4, 156.0, 82.2, 80.0, 61.4, 52.9, 41.4, 29.2, 28.5, 28.2, 27.6, 19.5, 19.2; HRMS (ESI[+]) calcd *m/z* for C$_{18}$H$_{33}$N$_2$O$_5$ [M+H][+], 357.2384 found 357.2394.

(3*S*, 2'*R*)-*tert*-Butyl 2-[3-(Boc)amino-2-oxopyrrolidin-1-yl]-3-methylbutanoate [(3*S*, 2'*R*)-2.13]
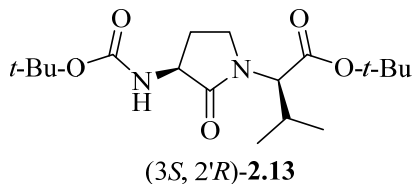
(3*S*, 2'*R*)-**2.13**

Employing the representative procedure described for the synthesis of (3*R*,2'*R*)-lactam (3*R*,2'*R*)-**2.13**, (*S*,*R*)-methylsulfonium iodide (*S*,*R*)-**2.11** (1 eq., 450 mg, 0.8 mmol) was converted (3*S*,2'*R*)-lactam (3*S*,2'*R*)-**2.13** (181 mg, 0.511 mmol, 62%): [α] $_D^{25}$ 53.1° (*c* 1.2, CHCl$_3$).

(3*S*, 2'*S*)-*tert*-Butyl 2-[3-(Boc)amino-2-oxopyrrolidin-1-yl]-3-methylbutanoate [(3*S*, 2'*S*)-2.13]
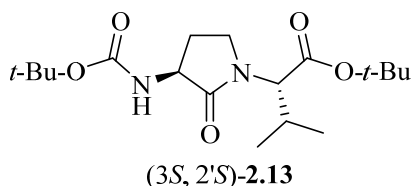
(3*S*, 2'*S*)-**2.13**

Employing the representative procedure described for the synthesis of (3*R*,2'*R*)-lactam (3*R*,2'*R*)-**2.13**, (*S*,*S*)-methylsulfonium iodide (*S*,*S*)-**2.11** (1 eq., 158 mg, 0.3 mmol) was converted to (3*S*,2'*S*)-lactam (3*S*,2'*S*)-**2.13** (65 mg, 0.182 mmol, 63%): [α] $_D^{25}$ –39.7° (*c* 1, CHCl$_3$).

(3*R*, 2'*S*)-2-[3-amino-2-oxopyrrolidin-1-yl]-3-methylbutanoate trifluoroacetate [(3*R*, 2'*S*)-2.14]
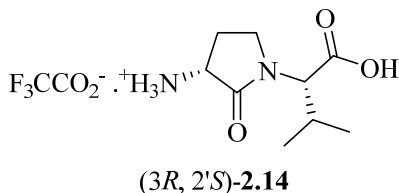
(3*R*, 2'*S*)-**2.14**

Employing the representative procedure described for the synthesis of (3*R*,2'*R*)-trifluoroacetate (3*R*,2'*R*)-**2.14**, (3*R* 2'*S*)-lactam (3*R*,2'*S*)-**2.13** (74 mg, 0.208 mmol) was converted to a white precipitate, (3*R*,2'*S*)-trifluoroacetate (3*R*,2'*S*)-**2.14** (62 mg, 0.197 mmol, 95%): R$_f$ = 0.12 (1:9:90 Et$_3$N:MeOH:DCM); [α]$_D^{25}$ –69.5° (*c* 0.42, MeOH); ^{1}H NMR (300 MHz, MeOD) δ 4.31 (d, *J* = 10.1, 1H), 4.10 (dd, *J* = 11.1, 8.5, 1H), 3.65-3.45 (m, 2H), 2.67-2.52 (m, 1H), 2.35-2.17 (m, 1H), 2.11-1.91 (m, 1H), 1.07 (d, *J* = 6.6, 3H), 0.95 (d, *J* = 6.7, 3H); ^{13}C NMR (75 MHz, MeOD) δ 171.0, 170.0, 61.0, 50.6, 41.2, 27.1, 24.5, 18.4 18.0; HRMS (ESI$^+$) calcd *m/z* for C$_9$H$_{17}$N$_2$O$_3$ [M+H]$^+$, 201.1234 found 201.1225.

(3*S*, 2'*R*)-2-[3-amino-2-oxopyrrolidin-1-yl]-3-methylbutanoate trifluoroacetate [(3*S*, 2'*R*)-2.14]
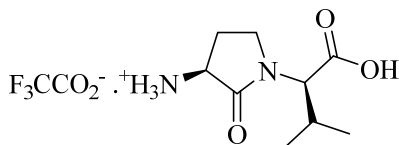
(3*S*, 2'*R*)-**2.14**

Employing the representative procedure described for the synthesis of (3*R*,2'*R*)-trifluoroacetate (3*R*,2'*R*)-**2.14**, (3*S*,2'*R*)-lactam (3*S*,2'*R*)-**2.13** (115 mg, 0.323 mmol) was converted to a white precipitate, (3*S*,2'*R*)-trifluoroacetate (3*S*,2'*R*)-**2.14** (97 mg, 0.309 mmol, 96%): [α]$_D^{25}$ 8.0º (*c* 0.8, MeOH).

(3*S*, 2'*S*)-2-[3-amino-2-oxopyrrolidin-1-yl]-3-methylbutanoate trifluoroacetate [(3*S*, 2'*S*)-2.14]
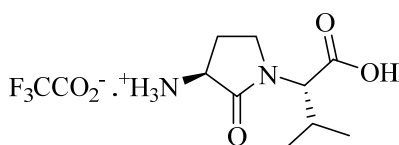
(3*S*, 2'*S*)-**2.14**

Employing the representative procedure described for the synthesis of (3*R*,2'*R*)-trifluoroacetate (3*R*,2'*R*)-**2.14**, (3*S*,2'*S*)-lactam (3*S*,2'*S*)-**2.13** (1 eq., 100 mg, 0.281 mmol) was converted to (3*S*,2'*S*)-trifluoroacetate (3*S*,2'*S*)-**2.14** (80 mg, 0.255 mmol, 91%): [α]$_D^{25}$ –69.2º (*c* 1, MeOH).

***N*-Fmoc-(*R*)-methionine methyl ester [(*R*)-2.15]**
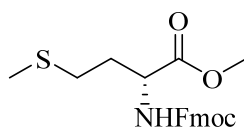
(*R*)-**2.15**

Employing the previously described procedure,[4] (*R*)-Met-OMe•HCl (1 eq., 7.5 g, 37.6 mmol, prepared from (*R*)-methionine as previously described)[5] was converted to *N*-Fmoc-(*R*)-Met-OMe (*R*)-**2.15** as light yellow solid (14.5 g, 37.6 mmol, 100 %) that was used without further purification: R$_f$ = 0.32 (20% EtOAc in hexane); mp 93 °C (Lit.[6] 88-89 °C); [α]$_D^{20}$ –12° (*c* 1, CHCl₃); ¹H NMR (300 MHz, CDCl₃) δ 7.77 (d, *J* = 7.7, 2H), 7.60 (d, *J* = 6.6, 2H), 7.41 (t, *J* = 7.5, 2H), 7.32 (tt, *J* = 7.4, 1.1, 2H), 5.46 (d, *J* = 8.2, 1H), 4.51 (dd, *J* = 12.9, 7.7, 1H), 4.42 (d, *J* = 7.0, 2H), 4.23 (t, *J* = 6.8, 1H), 3.76 (s, 3H), 2.53 (t, *J* = 7.3, 2H), 2.26-1.90 (m, 5H); ¹³C NMR (75

MHz, CDCl₃) δ 172.5, 155.9, 143.8, 141.3, 127.7, 127.1, 125.0, 120.0, 67.0, 53.1, 52.6, 47.2, 31.9, 29.9, 15.5.

N-Fmoc-(S)-methionine methyl ester [(S)-2.15]
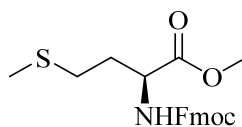
(S)-**2.15**

Employing the previously described procedure,[4] (S)-Met-OMe•HCl (1 eq., 7.5 g, 37.6 mmol) was converted to N-Fmoc-(S)-Met-OMe (S)-**2.15** as light yellow solid (14.5 g, 37.6 mmol, 100 %) that was used without further purification: [α] $_D^{20}$ 18° (c 1, CHCl₃).

N-Fmoc-(R)-Methionine sulfoxide methyl ester [(R)-2.16]
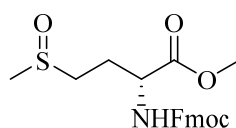
(R)-**2.16**

Employing the previously described procedure,[4] (R)-Fmoc-Met-OMe (1 eq., 12 g, 31.1 mmol) was converted to sulfoxide (R)-**2.16** as yellow sticky oil (10 g, 24.9 mmol, 80 %): R_f = 0.28 (3% MeOH in DCM); [α] $_D^{20}$ –25° (c 1, CHCl₃); ¹H NMR (300 MHz, CDCl₃) δ 7.77 (d, J = 7.5, 2H), 7.65-7.54 (br, 2H), 7.41 (t, J = 7.5, 2H), 7.32 (tt, J = 7.4, 1.3, 2H), 5.77 (d, J = 8.3, 0.5H), 5.68 (d, J = 7.5, 0.5H), 4.58-4.47 (m, 1H), 4.42 (d, J = 7.4, 2H), 4.22 (t, J = 6.8, 1H), 3.78 (s, 3H), 2.88-2.62 (m, 2H), 2.57 (s, 3H), 2.51-2.31 (m, 1H), 2.30-2.08 (m, 1H); ¹³C NMR (75 MHz, CDCl₃) δ 171.7, 156.2, 143.6, 141. 3, 127.8, 127.1, 125.1, 120.0, 67.1, 60.4, 52.8, 50.1, 47.1, 38.6, 25.8.

N-Fmoc-(S)-Methionine sulfoxide methyl ester [(S)-2.16]
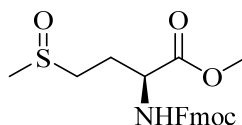
(S)-**2.16**

Employing the previously described procedure,[4] N-Fmoc-(S)-Met-OMe (S)-**2.15** (1 eq., 14.5 g, 37.6 mmol) was converted to a 1:1 mixture of diasteromers of sulfoxide (S)-**2.16** as white foam (11.6 g, 28.9 mmol, 77 %): [α] $_D^{20}$ 44° (c 0.8, CHCl₃).

N-Fmoc-(2R)-Vinylglycine- methyl ester [(R)-2.17]
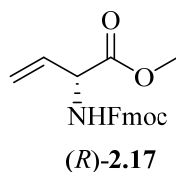
(*R*)-**2.17**

Employing the previously described procedure,[7] using a longer reaction time, 2 h, *N*-Fmoc-(*R*)-Met-sulfoxide-OMe (*R*)-**2.16** (1 eq., 35 mg, 87.2 mol) was transformed into vinylglycine (*R*)-**2.17** (24 mg, 0.074 mmol, 84 %); R_f = 0.34 (20% EtOAc in hexane); $[\alpha]_D^{25}$ –28 (c 0.7, CHCl₃); ¹H NMR (300 MHz, CDCl₃) δ 7.77 (d, *J* = 7.5, 2H), 7.61 (d, *J* = 6.9, 2H), 7.41 (t, *J* = 7.4, 2H), 7.32 (t, *J* = 7.4, 2H), 6.00-5.82 (m, 1H), 5.51 (d, *J* = 7.7, 1H), 5.32 (dd, *J* = 18.9, 13.9, 2H), 4.96 (s, 1H), 4.43 (d, *J* = 7.0, 2H), 4.24 (t, *J* = 6.9, 1H), 3.79 (s, 3H); ¹³C NMR (75 MHz, CDCl₃) δ 170.9, 155.6, 143.8, 141.3, 132.3, 127.7, 127.1, 125.1, 120.0, 117.8, 67.1, 56.1, 52.8, 47.2.

N-Fmoc-(2S)-Vinylglycine- methyl ester [(S)-2.17]
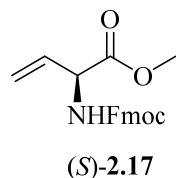
(*S*)-**2.17**

Employing the previously described procedure,[7] using a longer reaction time, 2 h, *N*-Fmoc-(*S*)-Met-sulfoxide-OMe (*S*)-**2.16** (1 eq., 35 mg, 87.2 mol) was converted to vinylglycine (*S*)-**2.17** (25 mg, 0.074 mmol, 85 %): $[\alpha]_D^{20}$ 3° (c 0.5, CHCl₃) {Lit.[8] $[\alpha]_D^{20}$ 2.6° (c 5.5, CHCl₃)}.

N-Fmoc-(2S)-Vinylglycine methyl ester [(S)-2.17]
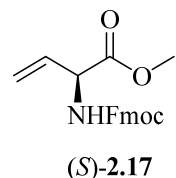
(*S*)-**2.17**

Employing the previously described procedure,[9] *N*-Fmoc-(*S*)-Met-sulfoxide-OMe (*S*)-**2.16** (1 eq., 5.36 g, 13.4 mmol) was converted to vinylglycine (*S*)-**2.17** (3.15 g, 9.35 mmol, 70 %): $[\alpha]_D^{20}$ 3° (c 0.5, CHCl₃) {Lit.[8] $[\alpha]_D^{20}$ 2.6° (c 5.5, CHCl₃)}.

(2R, 2'R)- and (2R, 2'S)-Methyl 2-(oxiranyl)-N-(Fmoc)glycinate [(2R, 2'R)-2.18 and (2R, 2'S)-2.18]

(2R, 2'R)-**2.18**   (2R, 2'S)-**2.18**
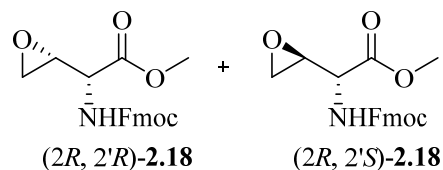
A solution of vinylglycine (*R*)-**2.17** (1 eq., 100 mg, 0.296 mmol) in toluene (4 mL) was treated with *m*-CPBA (77%, 5 eq., 332 mg, 1.48 mmol), heated to 80 °C using microwave irradiation for 2 h, cooled using an ice bath and treated with 30 mL of saturated Na_2SO_3. The phases were separated. The organic layer was washed with Na_2SO_3, saturated $NaHCO_3$ and brine, and the washing sequences were repeated. After drying the organic layer over Na_2SO_4, the volatiles were evaporated to a residue that was purified by column chromatography eluting with a step gradient of 5-20% EtOAc in toluene, which after evaporation furnished three fractions [(20 mg, 0.06 mmol, 19 %), (52.4 mg, 0.15 mmol, 50 %), and (3 mg, 0.009 mmol, 3 %)] with 9:1, 2.7:1, and 1:9 ratios of (2*R*,2'*R*) to (2*R*,2'*S*) assessed by NMR analysis comparing the relative intensities of the peaks at 3.48 and 3.24 ppm respectively, providing a combined (75.4 mg, 0.213 mmol, 71 %) of oxiranylglycine (2*R*,2'*R*)-**2.18** and (2*R*,2'*S*)-**2.18** with ratio of 3:1.

Oxiranylglycine (2*R*,2'*R*)-**2.18**; R_f = 0.23 (15% EtOAc in toluene); [α] $_D^{20}$ –5.4° (*c* 0.8, $CHCl_3$); ^{1}H NMR (500 MHz, $CDCl_3$) δ 7.77 (d, *J* = 7.6, 2H), 7.60 (t, *J* = 6.6, 2H), 7.41 (t, *J* = 7.5, 2H), 7.32 (tdd, *J* = 7.4, 3.5, 1.0, 2H), 5.32 (d, *J* = 8.8, 1H), 4.73 (dd, *J* = 8.9, 1.6, 1H), 4.43 (d, *J* = 7.0, 2H), 4.22 (t, *J* = 6.9, 1H), 3.83 (s, 3H), 3.48 (s, 1H), 2.79 (t, *J* = 4.2, 1H), 2.62 (dd, *J* = 4.1, 2.5, 1H); ^{13}C NMR (126 MHz, $CDCl_3$) δ 170.1, 156.2, 143.7, 143.5, 141.3(2C), 127.7 (2C), 127.1 (2C), 125.0 (2C), 120.0 (2C), 67.2, 53.0 (2C), 51.1, 47.1, 43.8; HRMS (ESI[+]) calcd *m/z* for $C_{20}H_{20}NO_5$ [M+H][+], 354.1336 found 354.1330.

Oxiranylglycine (2*R*,2'*S*)-**2.18**; R_f = 0.21 (15% EtOAc in toluene); [α] $_D^{20}$ –31.2° (*c* 0.8, $CHCl_3$); ^{1}H NMR (500 MHz, $CDCl_3$) δ 7.77 (d, *J* = 7.6, 2H), 7.60 (d, *J* = 7.5, 2H), 7.41 (td, *J* = 7.7, 2.8, 2H), 7.32 (td, *J* = 7.4, 1.1, 2H), 5.64 (d, *J* = 7.5, 1H), 4.53 (dd, *J* = 7.6, 5.0, 1H), 4.42 (d, *J* = 6.9, 2H), 4.23 (t, *J* = 6.8, 1H), 3.82 (s, 3H), 3.25 (s, 1H), 2.82 (d, *J* = 2.5, 2H); ^{13}C NMR (126 MHz, $CDCl_3$) δ 169.7, 155.8, 143.7, 143.6, 141.2 (2C), 128.2 (2C), 127.7, 127.0, 125.0 (2C), 120.0 (2C), 67.3, 54.7, 52.9, 51.4, 47.0, 45.0; HRMS (ESI[+]) calcd *m/z* for $C_{20}H_{20}NO_5$ [M+H][+], 354.1336 found 354.1330.

(2*S*, 2'*S*)- and (2*S*, 2'*R*)-Methyl 2-(oxiranyl)-*N*-(Fmoc)glycinate [(2*S*, 2'*S*)-2.18 and (2*S*, 2'*R*)-2.18]

Annex 1: Supporting information of Article 1
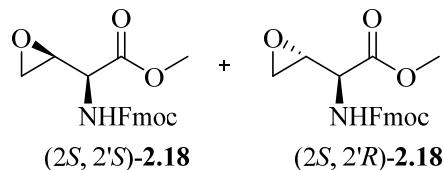
(2*S*, 2'*S*)-**2.18**   (2*S*, 2'*R*)-**2.18**

Employing the representative procedure described for oxiranylglycines (2*R*,2'*R*)- and (2*R*,2'*S*)-**2.18**, vinylglycine (*S*)-**2.17** (1 eq., 100 mg, 0.296 mmol) was converted to oxiranylglycine (2*S*,2'*S*)-**2.18**; $[\alpha]_D^{20}$ −18.3° (*c* 1.1, CHCl$_3$) and (2*S*,2'*R*)-**2.18**; $[\alpha]_D^{20}$ −10.9° (*c* 1.2, CHCl$_3$) (75.4 mg, 0.213 mmol, 73 %) with ratio of 3:1.

N-Fmoc-(3*R*, 4*S*, 2'*R*)-Hgl-Val-*t*Bu [(3*R*, 4*S*, 2'*R*)-2.19]
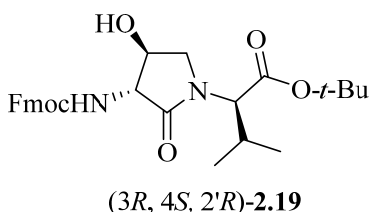
(3*R*, 4*S*, 2'*R*)-**2.19**

Employing the previously described procedure,[3] (2*R*,2'*R*)-oxiranylglycine (2*R*,2'*R*)-**2.18** (1 eq., 500 mg, 1.41 mmol) was converted to (3*R*,4*S*,2'*R*)-lactam (3*R*,4*S*,2'*R*)-**2.19** (545 mg, 1.1 mmol, 78%): R$_f$ = 0.45 (3% THF in DCM); $[\alpha]_D^{20}$ 7.7° (*c* 2, CHCl$_3$); ^{1}H NMR (500 MHz, CDCl$_3$) δ 7.77 (dd, *J* = 7.6, 0.5, 2H), 7.59 (d, *J* = 7.5, 2H), 7.41 (t, *J* = 7.5, 2H), 7.33 (td, *J* = 7.5, 1.1, 2H), 5.76 (s, 1H), 5.01 (s, 1H), 4.44 (d, *J* = 1.8, 1H), 4.43 (dd, *J* = 5.0, 3.9, 2H), 4.34 (q, *J* = 8.1, 1H), 4.23 (t, *J* = 7.0, 1H), 4.12 (dd, *J* = 8.1, 1.8, 1H), 4.02 (dd, *J* = 9.5, 8.0, 1H), 3.23 (dd, *J* = 9.4, 8.3, 1H), 2.27-2.16 (m, 1H), 1.47 (s, 9H), 1.01 (d, *J* = 6.7, 3H), 0.95 (d, *J* = 6.8, 3H); ^{13}C NMR (126 MHz, CDCl$_3$) δ 169.4, 168.6, 158.1, 143.5, 141.3, 127.9, 127.1, 125.0, 120.1, 82.4, 73.6, 67.7, 61.1, 60.8, 47.5, 47.0, 28.1, 27.5, 19.3, 19.0; HRMS (ESI[+]) calcd *m/z* for C$_{28}$H$_{35}$N$_2$O$_6^+$ [M+H]$^+$, 495.2490 found 495.2496.

N-Fmoc-(3*R*, 4*S*, 2'*S*)-Hgl-Val-*t*Bu [(3*R*, 4*S*, 2'*S*)-2.19]

(3*R*, 4*S*, 2'*S*)-**2.19**
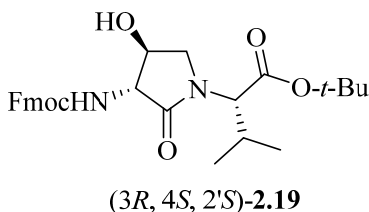
Employing the previously described procedure,[3] (2*R*,2'*R*)-oxiranylglycine (2*R*,2'*R*)-**2.18** (1 eq., 225 mg, 0.637 mmol) was converted to (3*R*,4*S*,2'*S*)-lactam (3*R*,4*S*,2'*S*)-**7** (258 mg, 0.522 mmol,

82%): R_f = 0.39 (3% THF in DCM); $[\alpha]_D^{20}$ –44.1° (*c* 1.2, CHCl₃); ¹H NMR (500 MHz, CDCl₃) δ 7.77 (dd, *J* = 7.6, 0.7, 2H), 7.59 (dd, *J* = 7.5, 0.6, 2H), 7.41 (td, *J* = 7.5, 0.6, 2H), 7.33 (td, *J* = 7.4, 0.9, 2H), 5.75 (s, 1H), 5.02 (s, 1H), 4.44 (d, *J* = 7.0, 2H), 4.33 (d, *J* = 10.2, 1H), 4.28 (t, *J* = 8.1, 1H), 4.23 (t, *J* = 6.9, 1H), 4.09 (dd, *J* = 8.1, 1.7, 1H), 3.67 (dd, *J* = 10.2, 7.9, 1H), 3.37 (dd, *J* = 10.2, 8.5, 1H), 2.22-2.12 (m, 1H), 1.47 (s, 9H), 1.02 (d, *J* = 6.6, 3H), 0.86 (d, *J* = 6.7, 3H); ¹³C NMR (126 MHz, CDCl₃) δ 169.4, 168.6, 158.1, 143.5, 141.3, 127.9, 127.1, 125.0, 120.1, 82.4, 73.6, 67.7, 61.1, 60.8, 47.5, 47.0, 28.1, 27.5, 19.3, 19.0; HRMS (ESI⁺) calcd *m/z* for $C_{28}H_{35}N_2O_6^+$ [M+H]⁺, 495.2490 found 495.2480.

N-Fmoc-(3S, 4R, 2'R)-Hgl-Val-tBu [(3S, 4R, 2'R)-2.19]
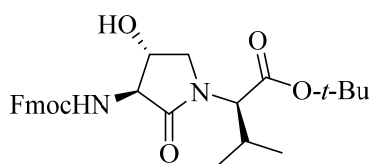
(3*S*, 4*R*, 2'*R*)-**2.19**

Employing the previously described procedure,[3] (2*S*,2'*S*)-oxiranylglycine (2*S*,2'*S*)-**2.18** (1 eq., 150 mg, 0.424 mmol) was converted to (3*S*,4*R*,2'*R*)-lactam (3*S*,4*R*,2'*R*)-**7** (151 mg, 0.305 mmol, 72%): R_f = 0.37 (3% THF in DCM); $[\alpha]_D^{20}$ 37.9° (*c* 1.3, CHCl₃); ¹H NMR (500 MHz, CDCl₃) δ 7.77 (d, *J* = 7.5, 2H), 7.59 (d, *J* = 7.5, 2H), 7.41 (t, *J* = 7.5, 2H), 7.33 (td, *J* = 7.4, 0.7, 2H), 5.77 (s, 1H), 5.02 (s, 1H), 4.44 (d, *J* = 7.0, 2H), 4.33 (d, *J* = 10.2, 1H), 4.28 (t, *J* = 8.1, 1H), 4.23 (t, *J* = 6.9, 1H), 4.09 (dd, *J* = 8.1, 1.6, 1H), 3.67 (dd, *J* = 10.2, 7.9, 1H), 3.37 (dd, *J* = 10.1, 8.5, 1H), 2.24-2.11 (m, 1H), 1.47 (s, 9H), 1.02 (d, *J* = 6.6, 3H), 0.86 (d, *J* = 6.7, 3H); ¹³C NMR (75 MHz, CDCl₃) δ 169.4, 168.6, 158.1, 143.5, 141.3, 127.8, 127.1, 125.0, 120.1, 82.4, 73.6, 67.7, 61.0, 60.8, 47.5, 47.0, 28.0, 27.5, 19.3, 19.0; HRMS (ESI⁺) calcd *m/z* for $C_{28}H_{35}N_2O_6^+$ [M+H]⁺, 495.2490 found 495.2499.

N-Fmoc-(3S, 4R, 2'S)-Hgl-Val-tBu [(3S, 4R, 2'S)-2.19]
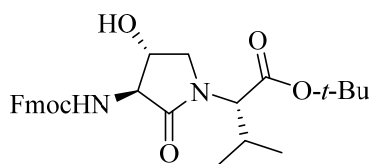
(3*S*, 4*R*, 2'*S*)-**2.19**

Employing the previously described procedure,[3] (2*S*,2'*S*)-oxiranylglycine (2*S*,2'*S*)-**2.18** (1 eq., 220 mg, 0.623 mmol) was converted to (3*S*,4*R*,2'*S*)-lactam [(3*S*,4*R*,2'*S*)-**2.19**] (258 mg, 0.523 mmol, 84%): R_f = 0.44 (3% THF in DCM); $[\alpha]_D^{20}$ –18.9° (*c* 1.3, CHCl₃); ¹H NMR (500 MHz, CDCl₃) δ

7.77 (d, J = 7.6, 2H), 7.59 (d, J = 7.5, 2H), 7.41 (t, J = 7.5, 2H), 7.33 (td, J = 7.5, 1.0, 2H), 5.74 (s, 1H), 5.01 (s, 1H), 4.45-4.40 (m, 3H), 4.34 (q, J = 8.2, 1H), 4.23 (t, J = 7.0, 1H), 4.12 (dd, J = 8.1, 1.7, 1H), 4.02 (dd, J = 9.5, 8.0, 1H), 3.23 (dd, J = 9.4, 8.3, 1H), 2.27-2.17 (m, 1H), 1.47 (s, 9H), 1.01 (d, J = 6.7, 3H), 0.95 (d, J = 6.8, 3H); ^{13}C NMR (126 MHz, CDCl$_3$) δ 169.7, 169.1, 158.2, 143.6, 141.5, 128.0, 127.3, 125.1, 120.2, 82.4, 73.8, 67.8, 60.6, 60.5, 48.2, 47.1, 29.0, 28.2, 19.5, 19.4; HRMS (ESI[+]) calcd m/z for C$_{28}$H$_{35}$N$_2$O$_6$ [M+H][+], 495.2490 found 495.2493.

_N_-Fmoc-(3_R_, 4_R_, 2'_R_)-Hgl-Val-_t_Bu [(3_R_, 4_R_, 2'_R_)-2.19]
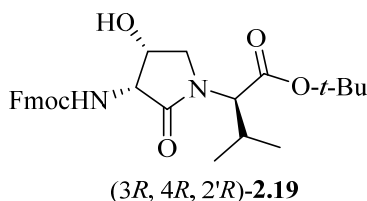
(3_R_, 4_R_, 2'_R_)-**2.19**

Employing the previously described procedure,[3] (3_R_,4_R_,2'_R_)-benzoate (3_R_,4_R_,2'_R_)-**2.20** (50 mg, 0.078 mmol) was converted to (3_R_,4_R_,2'_R_)-alcohol (3_R_,4_R_,2'_R_)-**2.19** (23 mg, 0.047 mmol, 60%): R$_f$ = 0.18 (3% THF in DCM); [α]$_D^{20}$ 10.9° (c 1.2, CHCl$_3$), ^{1}H NMR (400 MHz, DMSO) δ 7.89 (d, J = 7.5, 2H), 7.81 (t, J = 7.4, 2H), 7.42 (t, J = 7.4, 2H), 7.37 (d, J = 9.1, 1H), 7.33 (t, J = 7.4, 2H), 5.33 (d, J = 4.2, 1H), 4.43 (dd, J = 9.1, 5.1, 1H), 4.31-4.19 (m, 4H), 4.11 (d, J = 10.4, 1H), 3.52 (dd, J = 10.5, 3.6, 1H), 3.44 (d, J = 10.5, 1H), 2.08-1.96 (m, 1H), 1.42 (s, 9H), 0.90 (d, J = 6.6, 3H), 0.79 (d, J = 6.6, 3H); ^{13}C NMR (75 MHz, CDCl$_3$) δ 169.9, 143.8, 141.3, 127.7, 127.1, 125.7, 119.9, 82.7, 67.6, 67.5, 60.5, 57.2, 50.6, 47.1, 28.7, 28.0, 19.4, 19.3; HRMS (ESI[+]) calcd m/z for C$_{28}$H$_{35}$N$_2$O$_6$[+] [M+H][+], 495.2490 found 495.2502.

_N_-Fmoc-(3_R_, 4_R_, 2'_S_)-Hgl-Val-_t_Bu [(3_R_, 4_R_, 2'_S_)-2.19]
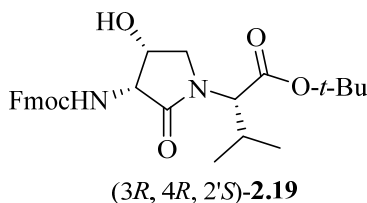
(3_R_, 4_R_, 2'_S_)-**2.19**

Employing the procedure described in reference[3] (3_R_,4_R_,2'_S_)-benzoate (3_R_,4_R_,2'_S_)-**2.20** (425 mg, 0.66 mmol) was converted to (3_R_,4_R_,2'_S_)-alcohol (3_R_,4_R_,2'_S_)-**2.19** (220 mg, 0.44 mmol, 67%): R$_f$ = 0.22 (3% THF in DCM); [α]$_D^{20}$ −45.5° (c 1.4, CHCl$_3$); ^{1}H NMR (300 MHz, DMSO) δ 7.89 (d, J = 7.5, 2H), 7.81 (dd, J = 7.3, 4.2, 2H), 7.42 (t, J = 7.2, 2H), 7.33 (m, 3H), 5.43 (d, J = 3.7, 1H), 4.36 (dd, J = 9.0, 4.8, 1H), 4.32-4.17 (m, 4H), 4.09 (d, J = 10.5, 1H), 3.54 (dd, J = 10.8, 3.5,

1H), 3.18 (d, J = 10.8, 1H), 2.15-1.98 (m, 1H), 1.41 (s, 9H), 0.93 (d, J = 6.6, 3H), 0.84 (d, J = 6.6, 3H); ^{13}C NMR (75 MHz, CDCl$_3$) δ 170.4, 169.4, 156.7, 143.7, 141.4, 127.8, 127.2, 125.0, 120.0, 82.2, 70.1, 66.5, 61.0, 57.5, 49.8, 47.2, 28.0, 27.7, 19.2, 18.7; HRMS (ESI$^+$) calcd m/z for C$_{28}$H$_{35}$N$_2$O$_6$ [M+H]$^+$, 495.2490 found 495.2494.

N-Fmoc-(3S, 4S, 2'R)-Hgl-Val-tBu [(3S, 4S, 2'R)-2.19]
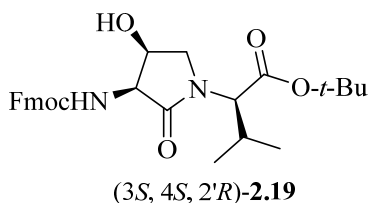
(3S, 4S, 2'R)-**2.19**

Employing the previously described procedure,[3] (3S,4S,2'R)-benzoate (3S,4S,2'R)-**2.20** (245 mg, 0.38 mmol) was converted to (3S,4S,2'R)-alcohol (3S,4S,2'R)-**2.19** (180 mg, 0.36 mmol, 96%): R$_f$ = 0.25 (3% THF in DCM); [α]$_D^{20}$ 30.6° (c 1.5, CHCl$_3$); ^{1}H NMR (300 MHz, DMSO) δ 7.89 (d, J = 7.5, 2H), 7.81 (dd, J = 7.2, 4.2, 2H), 7.42 (t, J = 7.3, 2H), 7.37-7.27 (m, 3H), 5.43 (d, J = 3.8, 1H), 4.36 (dd, J = 8.9, 5.0, 1H), 4.31-4.18 (m, 4H), 4.09 (d, J = 10.4, 1H), 3.54 (dd, J = 10.9, 3.4, 1H), 3.18 (d, J = 11.0, 1H), 2.15-1.95 (m, 1H), 1.41 (s, 9H), 0.93 (d, J = 6.6, 3H), 0.84 (d, J = 6.6, 3H); ^{13}C NMR (75 MHz, CDCl$_3$) δ 170.4, 169.4, 143.7, 141.4, 141.3, 127.8, 127.2, 125.0, 120.0, 82.2, 70.1, 66.5, 61.0, 57.5, 49.8, 47.1, 28.0, 27.7, 19.2, 18.7; HRMS (ESI$^+$) calcd m/z for C$_{28}$H$_{35}$N$_2$O$_6$ [M+H]$^+$, 495.2490 found 495.2500.

N-Fmoc-(3S, 4S, 2'S)-Hgl-Val-tBu [(3S, 4S, 2'S)-2.19]
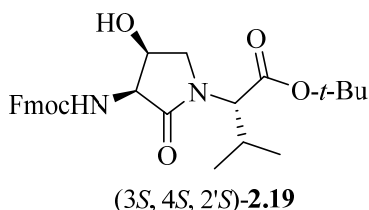
(3S, 4S, 2'S)-**2.19**

Employing the previously described procedure,[3] (3S,4S,2'S)-benzoate (3S,4S,2'S)-**2.20** (1 eq., 160 mg, 0.249 mmol) was converted to (3S,4S,2'S)-alcohol (3S,4S,2'S)-**2.19** (94 mg, 0.19 mmol, 76%): R$_f$ = 0.17 (3% THF in DCM); [α]$_D^{20}$ –13.7° (c 0.8, CHCl$_3$); ^{1}H NMR (300 MHz, DMSO) δ 7.89 (d, J = 7.5, 2H), 7.80 (m, 2H), 7.46-7.28 (m, 5H), 5.32 (d, J = 4.2, 1H), 4.42 (dd, J = 9.2, 5.0, 1H), 4.29-4.17 (m, 4H), 4.11 (d, J = 10.4, 1H), 3.51 (dd, J = 10.1, 3.3, 1H), 3.43 (d, J = 10.3, 1H), 2.11-1.93 (m, 1H), 1.42 (s, 9H), 0.90 (d, J = 6.6, 3H), 0.78 (d, J = 6.6, 3H); ^{13}C NMR (75 MHz, CDCl$_3$) δ 170.1, 156.8, 144.0, 143.8, 141.4, 127.9, 127.3, 125.3, 120.0, 82.9, 67.8, 67.5, 60.6, 57.3, 50.7,

47.3, 28.9, 28.1, 19.6, 19.5; HRMS (ESI$^+$) calcd m/z for $C_{28}H_{35}N_2O_6$ [M+H]$^+$, 495.2490 found 495.2492.

(3*R*,4*R*,2'*R*)-*tert*-Butyl 2-[3-(Fmoc)amino-4-*p*-nitrobenzoyloxy-2-oxopyrrolidin-1-yl]-3-methylbutanoate [(3*R*, 4*R*, 2'*R*)-2.20]
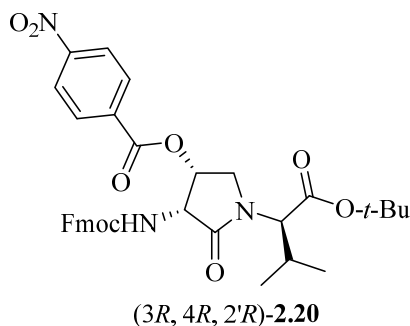
(3*R*, 4*R*, 2'*R*)-**2.20**

Employing the previously described procedure,[3] (3*R*,4*S*,2'*R*)-alcohol (3*R*,4*S*,2'*R*)-**2.19** (65 mg, 0.131 mmol) was transformed into (3*R*,4*R*,2'*R*)-benzoate (3*R*,4*R*,2'*R*)-**2.20** (58.4 mg, 0.0907 mmol, 69%): R$_f$ = 0.22 (30% EtOAc in hexane); [α]$_D^{20}$ –93.9° (*c* 0.2, CHCl$_3$); ^{1}H NMR (300 MHz, CDCl$_3$) δ 8.22 (d, *J* = 8.8, 2H), 8.12 (d, *J* = 8.7, 2H), 7.71 (t, *J* = 7.8, 2H), 7.50 (dd, *J* = 19.8, 7.5, 2H), 7.42-7.29 (m, 2H), 7.24-7.13 (m, 2H), 5.83 (m, 1H), 5.49 (d, *J* = 6.1, 1H), 4.72 (m, 1H), 4.50-4.39 (m, 2H), 4.33 (dd, *J* = 10.5, 7.2, 1H), 4.18 (d, *J* = 7.2, 1H), 4.13 (d, *J* = 5.8, 1H), 3.74 (dd, *J* = 12.1, 3.3, 1H), 2.27-2.08 (m, 1H), 1.36 (s, 9H), 1.01 (d, *J* = 6.7, 3H), 0.93 (d, *J* = 6.7, 3H); ^{13}C NMR (75 MHz, CDCl$_3$) δ 170.0, 169.2, 163.7, 156.2, 150.7, 143.6, 141.3, 134.8, 130.9, 127.7, 127.0, 124.9, 123.5, 120.0, 82.2, 70.4, 67.4, 60.7, 54.9, 48.0, 47.0, 28.9, 27.9, 19.4, 19.2; HRMS (ESI$^+$) calcd m/z for $C_{35}H_{38}N_3O_9$ [M+H]$^+$, 644.2603 found 644.2634.

(3*R*,4*R*,2'S)-*tert*-Butyl 2-[3-(Fmoc)amino-4-*p*-nitrobenzoyloxy-2-oxopyrrolidin-1-yl]-3-methylbutanoate [(3*R*, 4*R*, 2'S)-2.20]
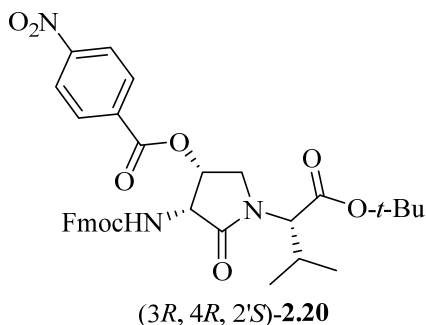
(3*R*, 4*R*, 2'*S*)-**2.20**

Employing the previously described procedure,[3] (3*R*,4*S*,2'*S*)-alcohol (3*R*,4*S*,2'*S*)-**2.19** (233 mg, 0.47 mmol) was transformed into (3*R*,4*R*,2'*S*)-benzoate (3*R*,4*R*,2'*S*)-**2.20** (269 mg, 0.42 mmol,

89%): R_f = 0.31 (30% EtOAc in hexane); [α] $_D^{20}$ –39.4° (*c* 2.5, CHCl₃); ¹H NMR (300 MHz, CDCl₃) δ 8.24 (d, *J* = 8.9, 2H), 8.12 (d, *J* = 8.8, 2H), 7.69 (t, *J* = 8.1, 2H), 7.48 (dd, *J* = 25.2, 7.5, 2H), 7.39-7.28 (m, 2H), 7.24-7.10 (m, 2H), 5.91 (d, *J* = 6.3, 1H), 5.86 (m, 1H), 4.70 (m, 1H), 4.43 (dd, *J* = 10.2, 6.4, 2H), 4.29 (dd, *J* = 10.6, 7.2, 1H), 4.14 (t, *J* = 6.8, 1H), 4.00 (dd, *J* = 12.7, 3.6, 1H), 3.63 (d, *J* = 12.9, 1H), 2.19-2.05 (m, 1H), 1.47 (s, 9H), 1.00 (d, *J* = 6.6, 3H), 0.85 (d, *J* = 6.7, 3H); ¹³C NMR (75 MHz, CDCl₃) δ 170.0, 168.9, 163.6, 156.4, 150.8, 143.6, 141.2, 134.5, 130.8, 127.7, 127.0, 124.9, 123.7, 119.9, 82.6, 70.2, 67.3, 61.1, 55.3, 48.1, 47.0, 28.0, 27.6, 19.1, 18.7; HRMS (ESI⁺) calcd *m/z* for $C_{35}H_{38}N_3O_9^+$ [M+H]⁺, 644.2603 found 644.2592.

(3*S*,4*S*,2'*R*)-*tert*-Butyl   2-[3-(Fmoc)amino-4-*p*-nitrobenzoyloxy-2-oxopyrrolidin-1-yl]-3-methylbutanoate [(3*S*, 4*S*, 2'*R*)-2.20]
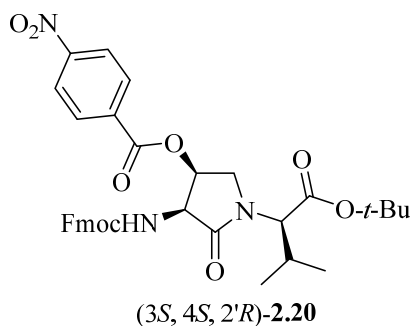
(3*S*, 4*S*, 2'*R*)-**2.20**

Employing the previously described procedure,[3] (3*S*,4*R*,2'*R*)-alcohol (3*S*,4*R*,2'*R*)-**2.19** (233 mg, 0.471 mmol) was transformed into (3*S*,4*S*,2'*R*)-benzoate (3*S*,4*S*,2'*R*)-**2.20** (260 mg, 0.404 mmol, 86%): R_f = 0.29 (30% EtOAc in hexane); [α] $_D^{20}$ 50.2° (*c* 1.3, CHCl₃); ¹H NMR (300 MHz, CDCl₃) δ 8.25 (d, *J* = 8.8, 2H), 8.11 (d, *J* = 8.7, 2H), 7.70 (t, *J* = 8.2, 2H), 7.49 (dd, *J* = 24.3, 7.5, 2H), 7.41-7.28 (m, 2H), 7.25-7.11 (m, 2H), 5.88 (t, *J* = 4.6, 1H), 5.69 (d, *J* = 6.2, 1H), 4.69 (t, *J* = 5.4, 1H), 4.42 (d, *J* = 9.6, 2H), 4.31 (dd, *J* = 10.6, 7.1, 1H), 4.15 (t, *J* = 6.8, 1H), 4.00 (dd, *J* = 13.0, 3.4, 1H), 3.64 (d, *J* = 12.7, 1H), 2.22-2.05 (m, 1H), 1.48 (s, 9H), 1.01 (d, *J* = 6.5, 3H), 0.86 (d, *J* = 6.7, 3H); ¹³C NMR (75 MHz, CDCl₃) δ 170.1, 168.9, 163.5, 156.1, 150.8, 143.6, 141.3, 134.4, 130.8, 127.7, 126.9, 124.9, 123.7, 119.9, 82.7, 70.3, 67.3, 61.1, 55.3, 48.1, 47.0, 28.1, 27.6, 19.1, 18.7; HRMS (ESI⁺) calcd *m/z* for $C_{35}H_{38}N_3O_9$ [M+H]⁺, 644.2603 found 644.2603.

(3*S*,4*S*,2'*S*)-*tert*-Butyl   2-[3-(Fmoc)amino-4-*p*-nitrobenzoyloxy-2-oxopyrrolidin-1-yl]-3-methylbutanoate [(3*S*, 4*S*, 2'*S*)-2.20]

Annex 1: Supporting information of Article 1
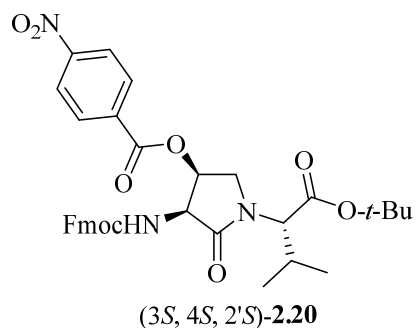
(3*S*, 4*S*, 2'*S*)-**2.20**

Employing the previously described procedure,[3] (3*S*,4*R*,2'*S*)-alcohol (3*S*,4*R*,2'*S*)-**2.19** (1 eq., 200 mg, 0.4 mmol) was converted to (3*S*,4*S*,2'*S*)-benzoate (3*S*,4*S* 2'*S*)-**2.20** (200 mg, 0.3 mmol, 77%): R$_f$ = 0.25 (30% EtOAc in hexane); [α] $_D^{20}$ 40.7° (*c* 1.1, CHCl$_3$); ^{1}H NMR (300 MHz, CDCl$_3$) δ 8.22 (dt, *J* = 8.8, 2.0, 2H), 8.12 (d, *J* = 8.8, 2H), 7.71 (t, *J* = 7.7, 2H), 7.50 (dd, *J* = 19.7, 7.6, 2H), 7.43-7.28 (m, 2H), 7.25-7.11 (m, 2H), 5.83 (m, 1H), 5.51 (d, *J* = 5.9, 1H), 4.74 (m, 1H), 4.44 (m, 2H), 4.34 (dd, *J* = 10.7, 6.9, 1H), 4.18 (d, *J* = 6.7, 1H), 4.13 (d, *J* = 3.4, 1H), 3.74 (dd, *J* = 12.4, 3.3, 1H), 2.30-2.04 (m, 1H), 1.36 (s, 9H), 1.01 (d, *J* = 6.7, 3H), 0.94 (d, *J* = 6.7, 3H); ^{13}C NMR (75 MHz, CDCl$_3$) δ 170.1, 169.2, 167.0, 163.7, 156.2, 150.7, 143.6, 141.3, 134.8, 131.0, 127.7, 127.0, 124.9, 123.6, 120.0, 82.2, 70.4, 67.4, 60.7, 55.0, 48.0, 47.0, 28.9, 27.9, 19.4, 19.2; HRMS (ESI$^+$) calcd *m/z* for C$_{35}$H$_{38}$N$_3$O$_9$ [M+H]$^+$, 644.2603 found 644.2599.

References

1. (a) Dola, V. R.; Soni, A.; Agarwal, P.; Ahmad, H.; Raju, K. S. R.; Rashid, M.; Wahajuddin, M.; Srivastava, K.; Haq, W.; Dwivedi, A., *Antimicrob. Agents Chemother.* **2017,** *61*, e01152-16; (b) Pícha, J.; Vaněk, V.; Buděšínský, M.; Mládková, J.; Garrow, T. A.; Jiráček, J., *European J. Med. Chem.* **2013,** *65*, 256-275.

2. Keller, O.; Keller, W. E.; Look, G. V.; Wersin, G., *Org. Synth.* **2003,** *63*, 160-170.

3. Geranurimi, A.; Lubell, W. D., *Org. Lett.* **2018,** *20*, 6126-6129..

4. Sicherl, F.; Cupido, T.; Albericio, F., *Chem. Commun.* **2010,** *46*, 1266-1268.

5. (a) Carrasco, M.; Jones, R. J.; Kamel, S.; Rapoport, H.; Truong, T., *Org. Synth.* **1992**, 29-29; (b) Lumbroso, A.; Coeffard, V.; Le Grognec, E.; Beaudet, I.; Quintard, J.-P., *Tetrahedron Lett.* **2010,** *51*, 3226-3228.

6. Buglioni, L.; Bizet, V.; Bolm, C., *Advanced Synthesis & Catalysis* **2014,** *356*, 2209-2213.

7. Lamborelle, N.; Simon, J. F.; Luxen, A.; Monbaliu, J.-C. M., *Org. Biomol. Chem.* **2015,** *13*, 11602-11606.

Annex 1: Supporting information of Article 1

8. Organ, M. G.; Xu, J.; N'Zemba, B., *Tetrahedron Lett.* **2002,** *43*, 8177-8180.

9. St-Cyr, D. J.; Jamieson, A. G.; Lubell, W. D., *Org. Lett.* **2010,** *12*, 1652-1655.

Annex 1: Supporting information of Article 1

^{1}H NMR (300 MHz, MeOD) **(R, R)-2.7**
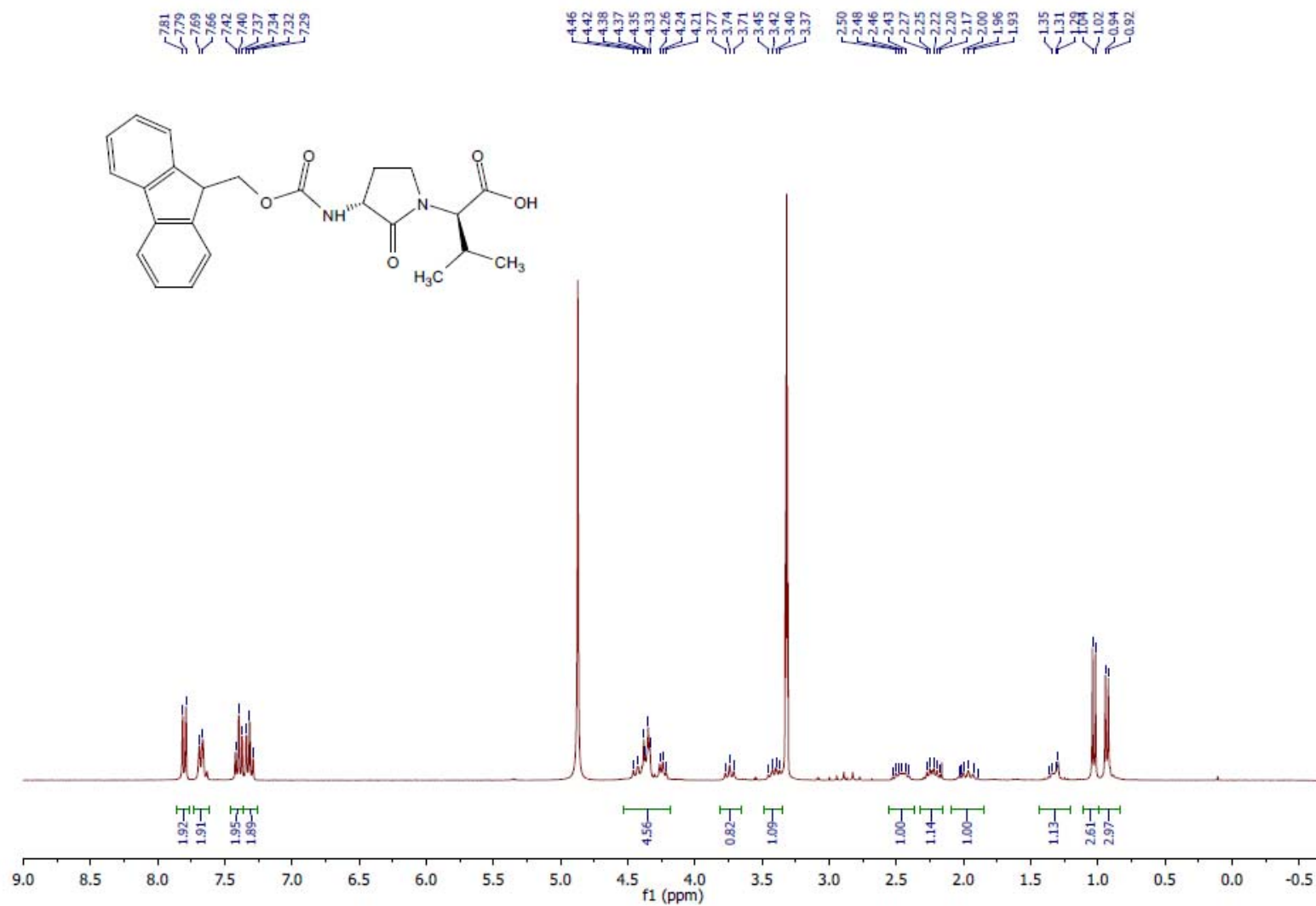
^{13}C NMR (75 MHz, MeOD) **(*R, R*)-2.7**
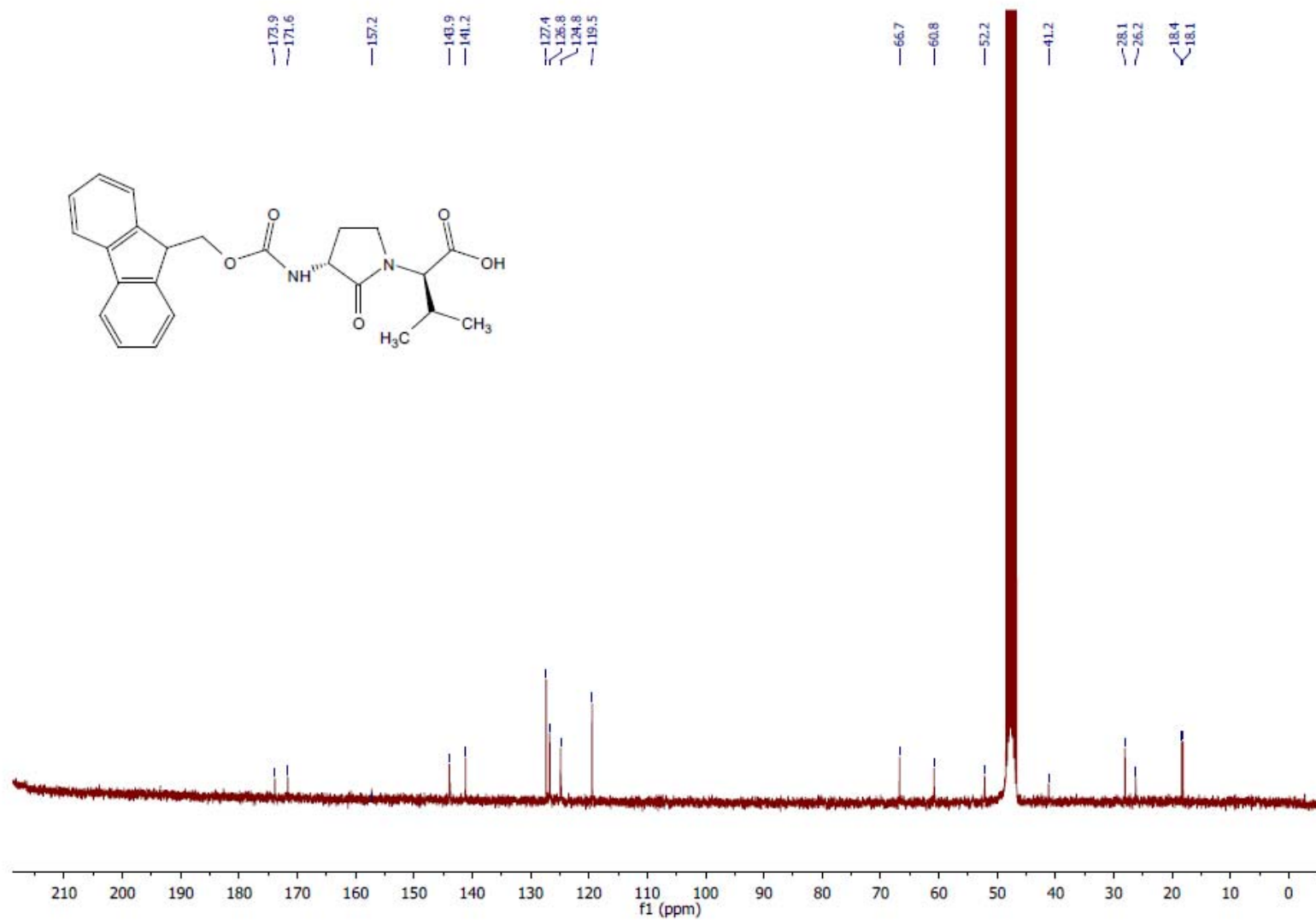
^{1}H NMR (300 MHz, MeOD) **(*R*, *S*)-2.7**
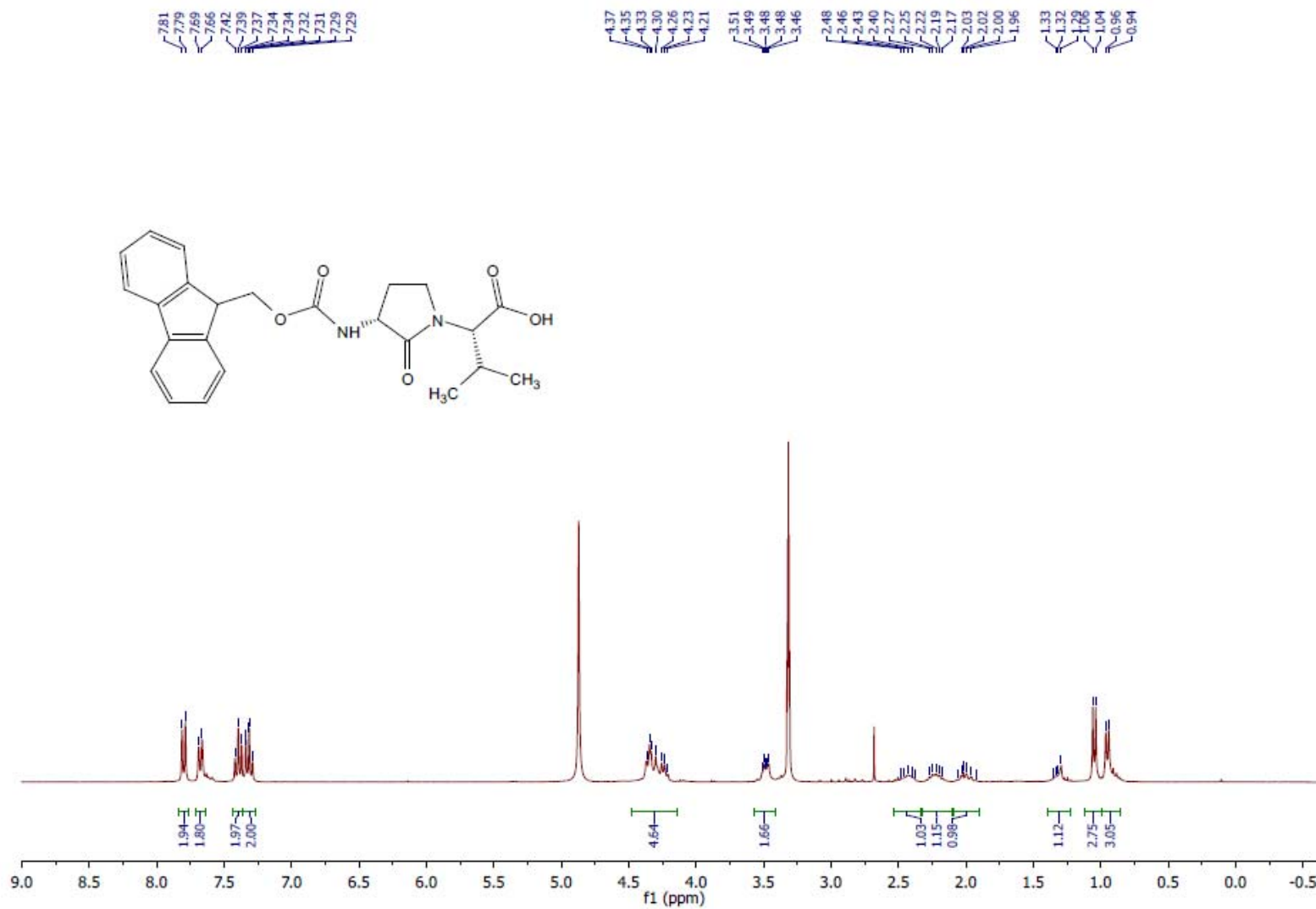
^{13}C NMR (75 MHz, MeOD) (*R, S*)-2.7
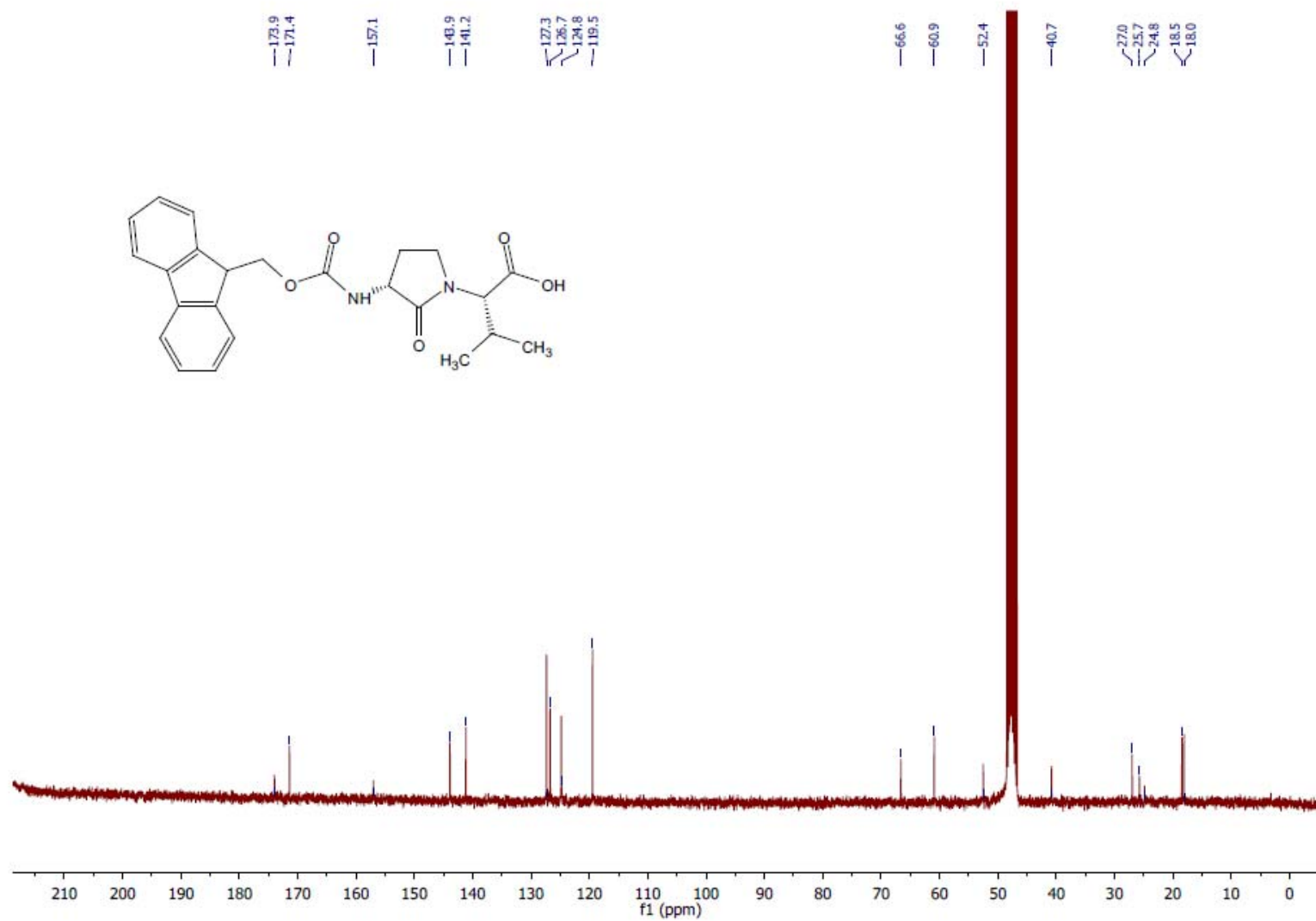
^{1}H NMR (300 MHz, CDCl$_3$) **(R, R)-2.10**
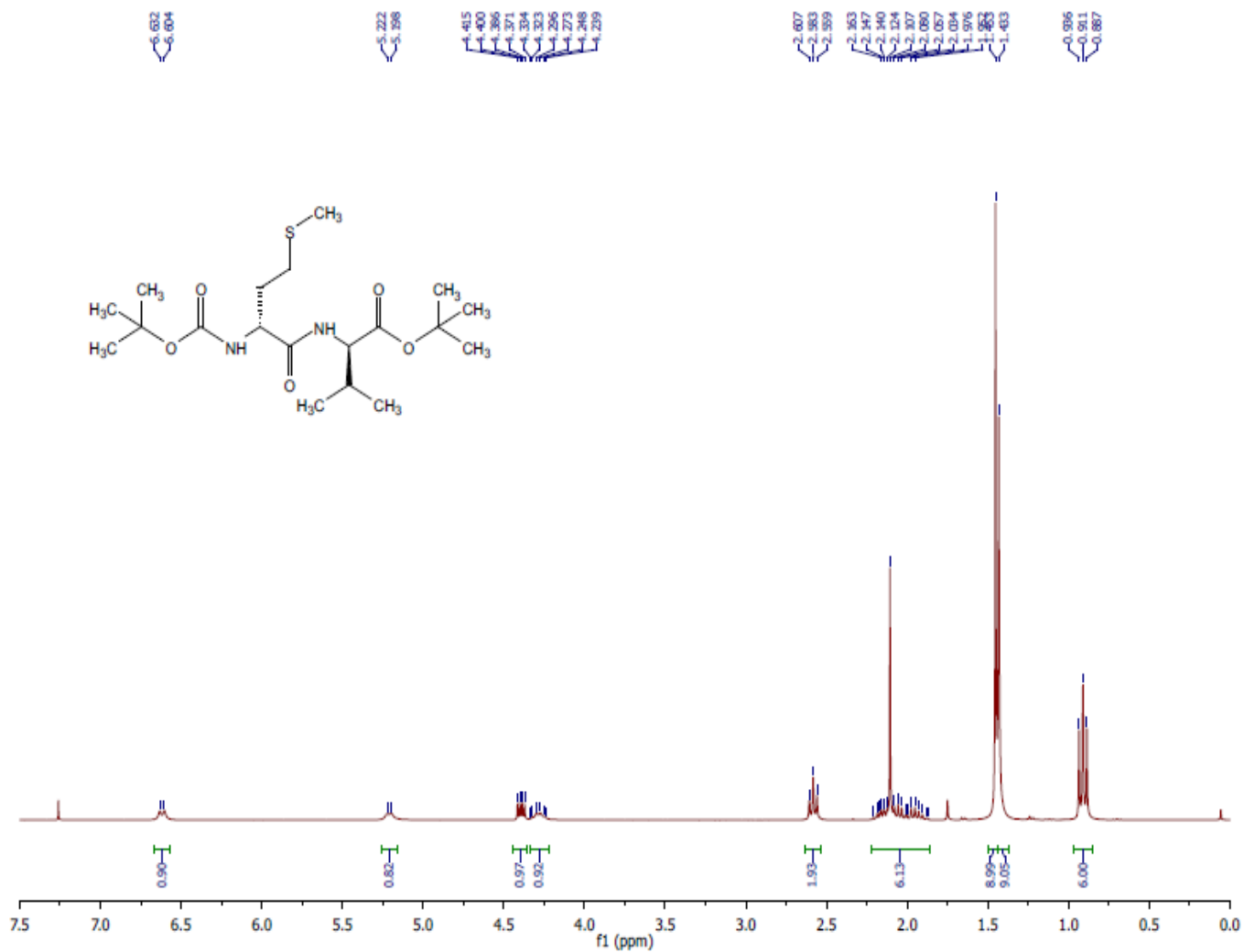
^{13}C NMR (75 MHz, CDCl$_3$) **(*R, R*)-2.10**
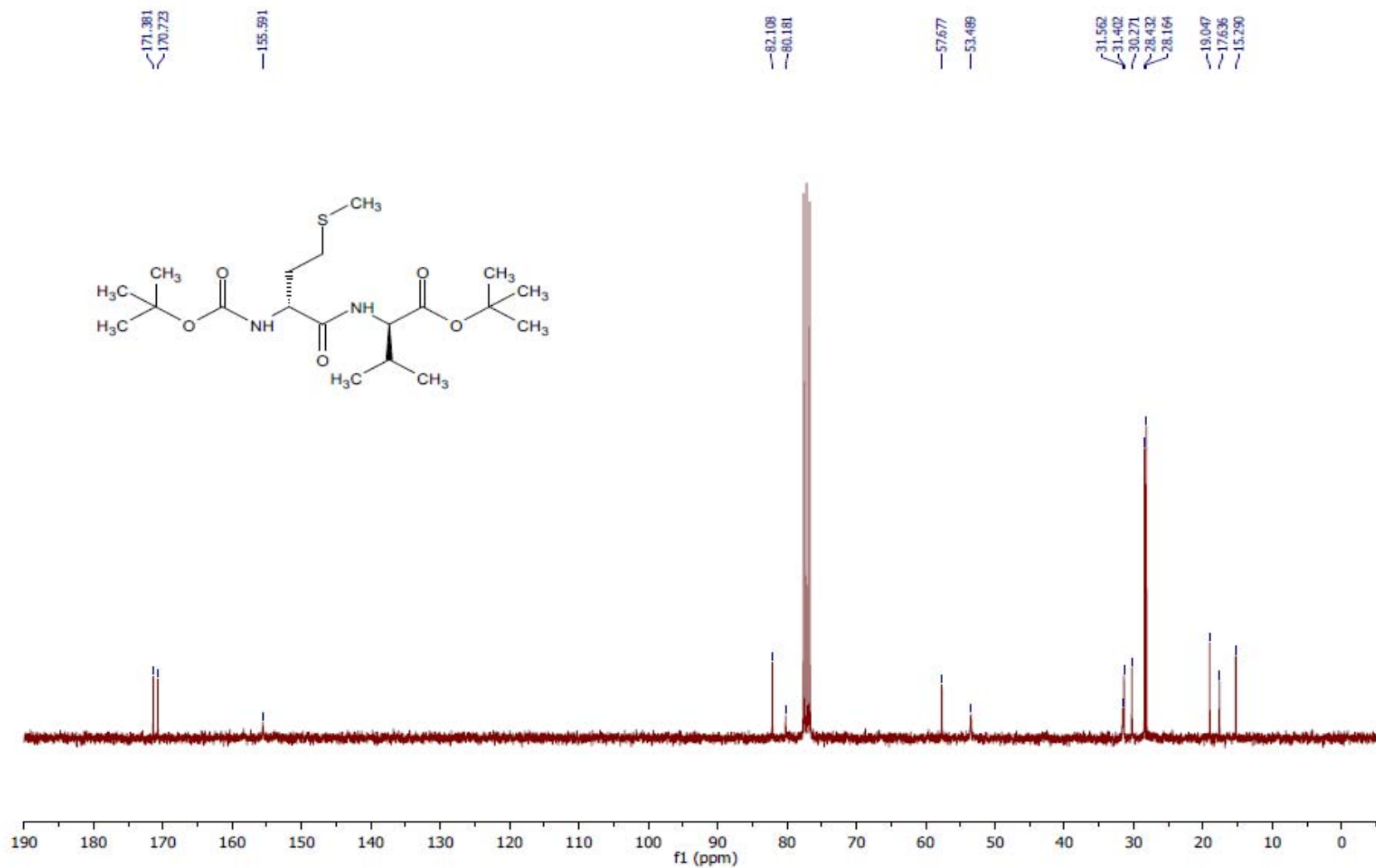
^{1}H NMR (300 MHz, CDCl$_3$) **(*R*, *S*)-2.10**
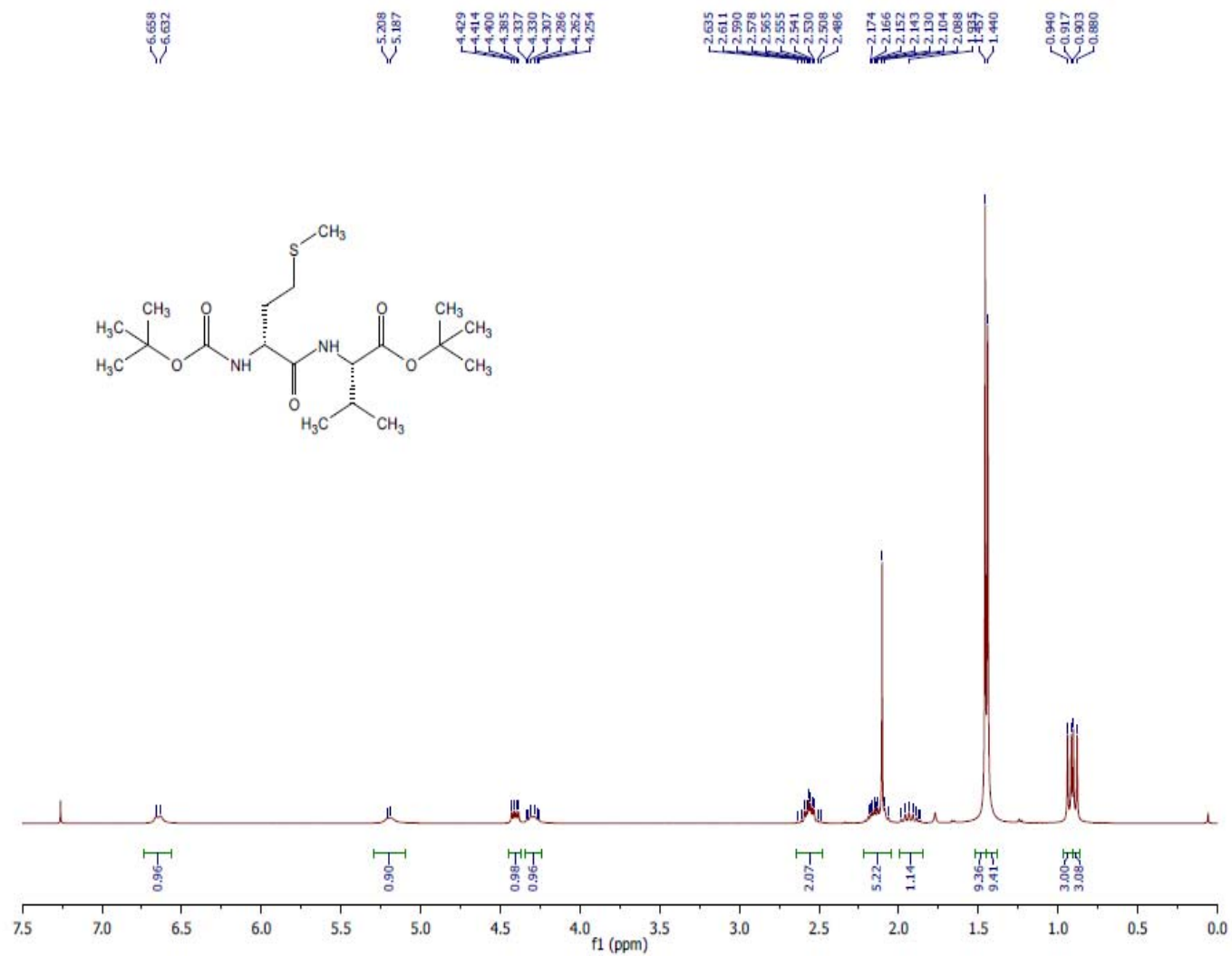
^{13}C NMR (75 MHz, CDCl$_3$) (*R, S*)-2.10
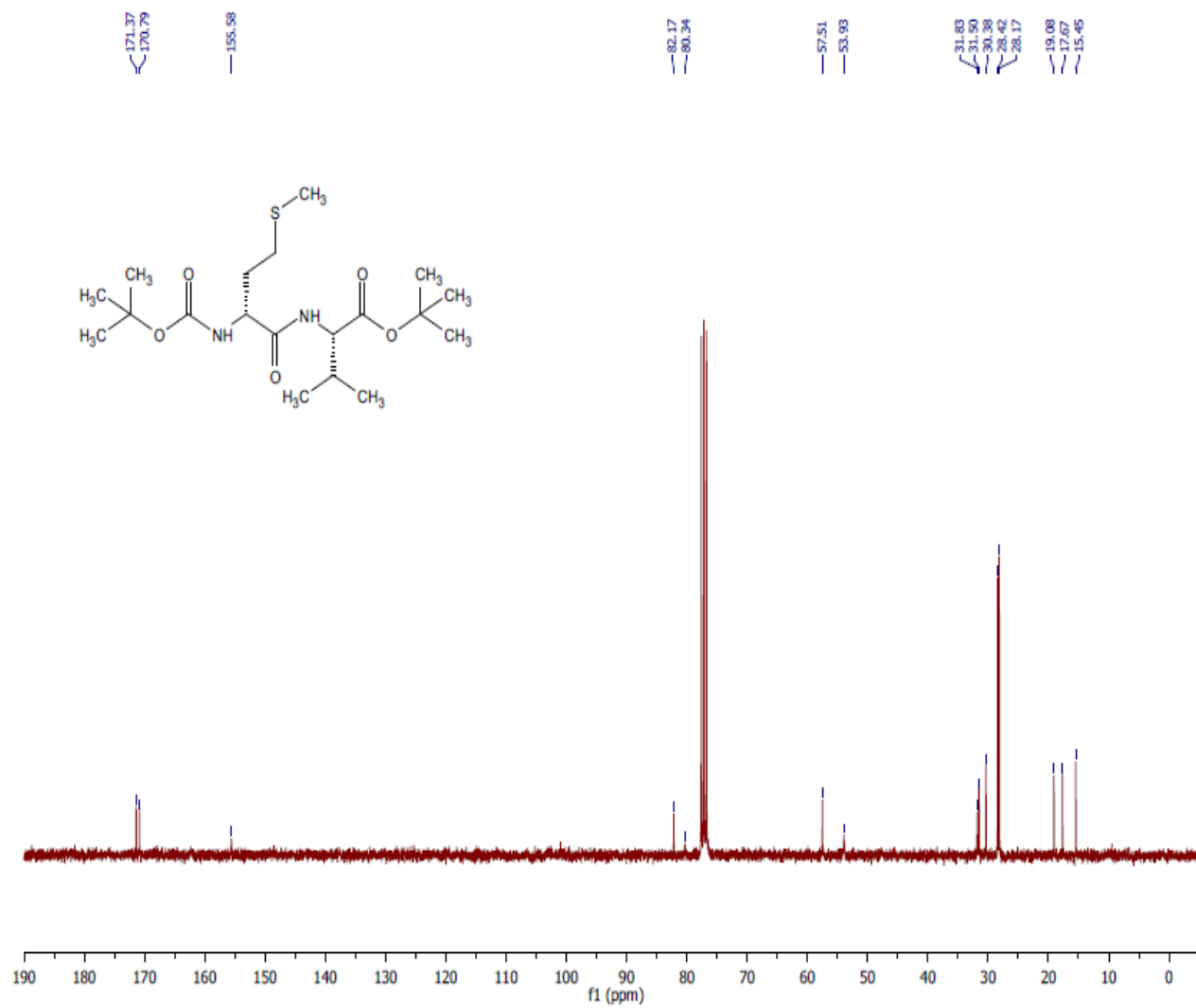
^{1}H NMR (300 MHz, CDCl$_3$) **(R, R)-2.11**

Annex 1: Supporting information of Article 1

^{1}H NMR (300 MHz, CDCl$_3$) **(*R*, *S*)-2.11**

Annex 1: Supporting information of Article 1
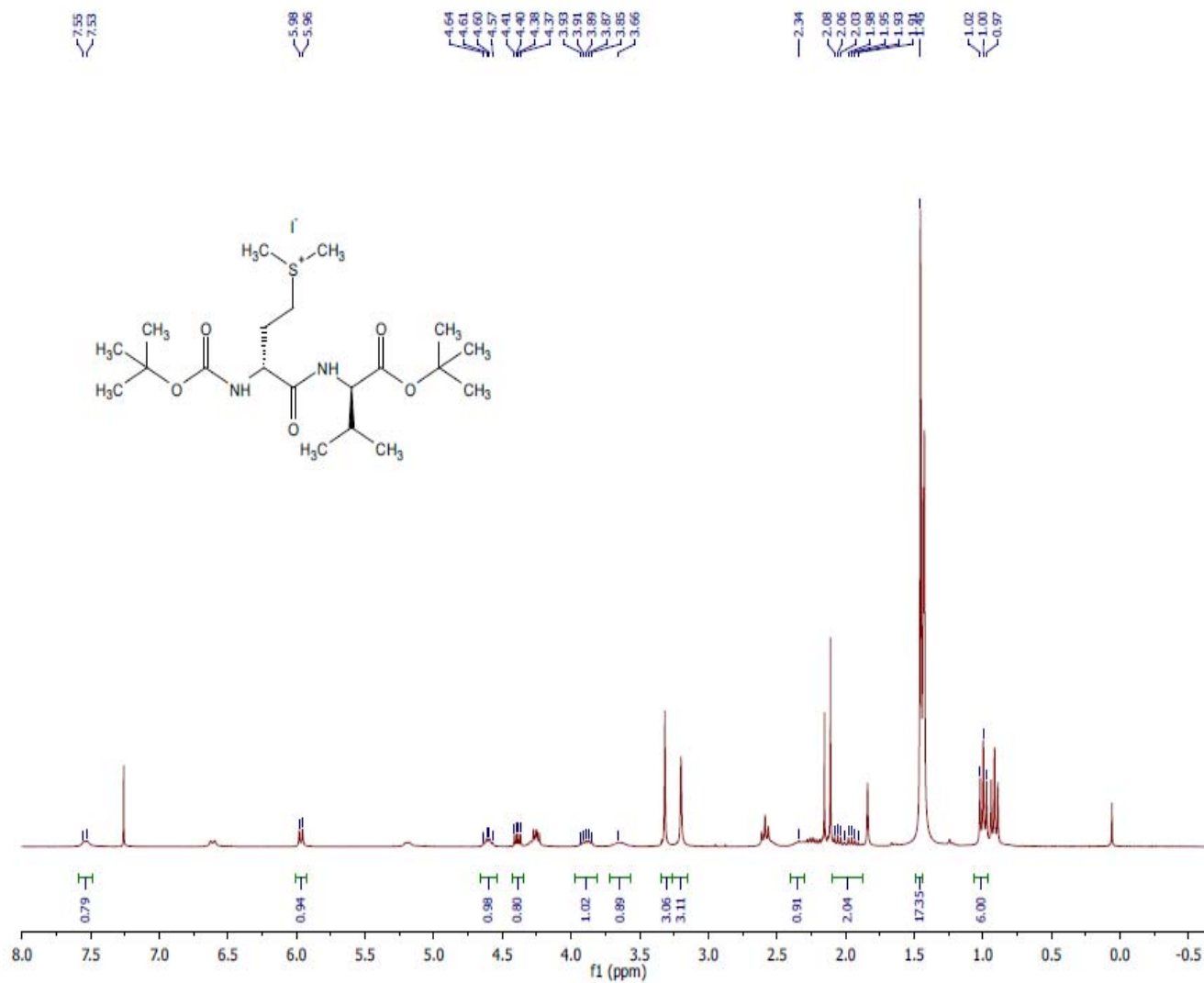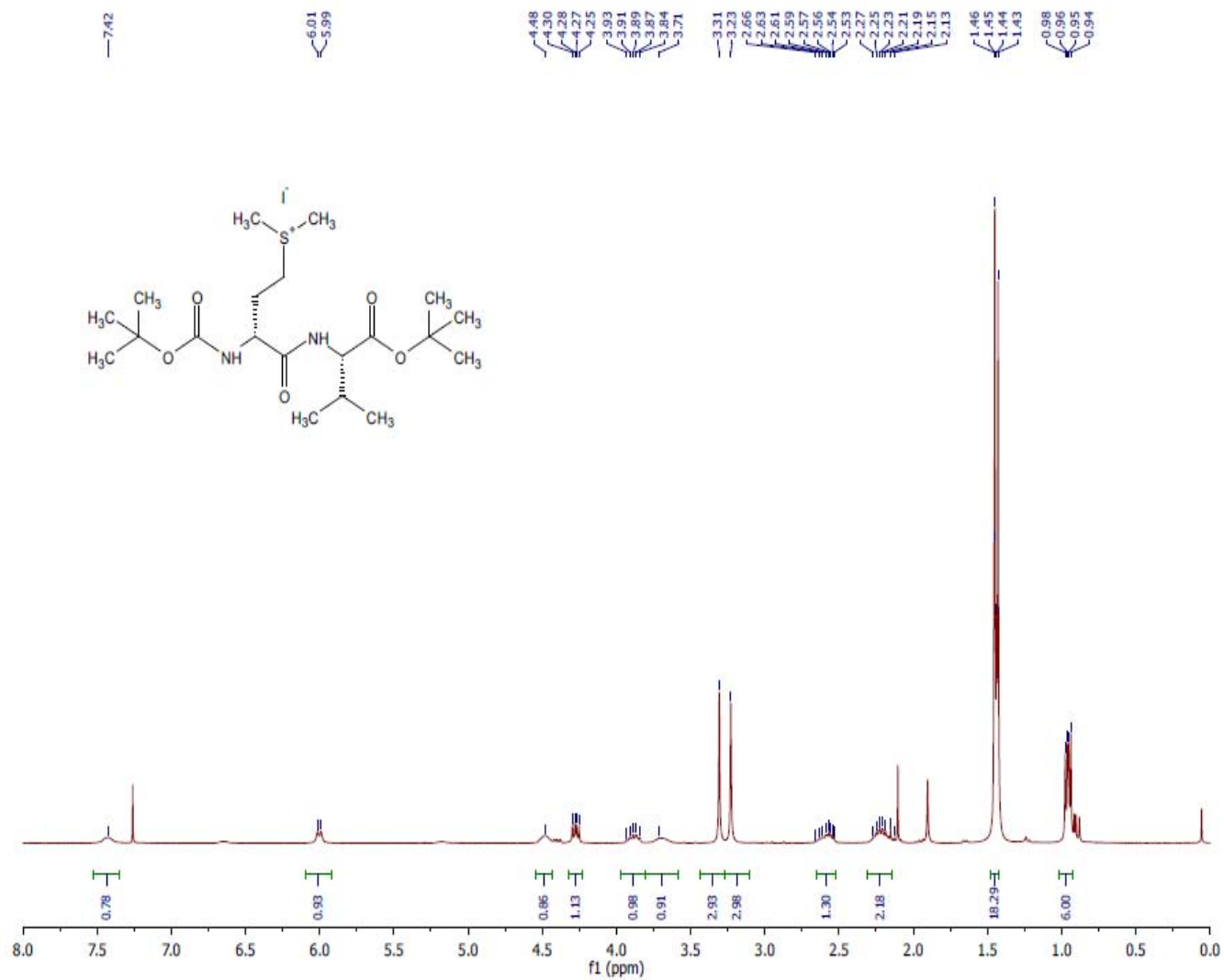
^{1}H NMR (300 MHzMeOD) [(**3R, 4R, 2'S**)-2.12]

7.83
7.81
7.74
7.73
7.72
7.71
7.44
7.41
7.39
7.36
7.34
7.34
7.31
7.31

4.53
4.52
4.46
4.45
4.43
4.42
4.40
4.38
4.36
4.35
4.33
4.30
4.28
4.26

3.76
3.73
3.43
3.43
3.39
3.34

2.29
2.26
2.24
2.23
2.22
2.21
2.19
2.16

1.08
1.06
1.00
0.98

2.13
1.84

2.22
2.17

1.00
1.60
1.08
0.99
1.45

0.93

0.90

1.09

3.23
3.31

f1 (ppm)

Annex 1: Supporting information of Article 1
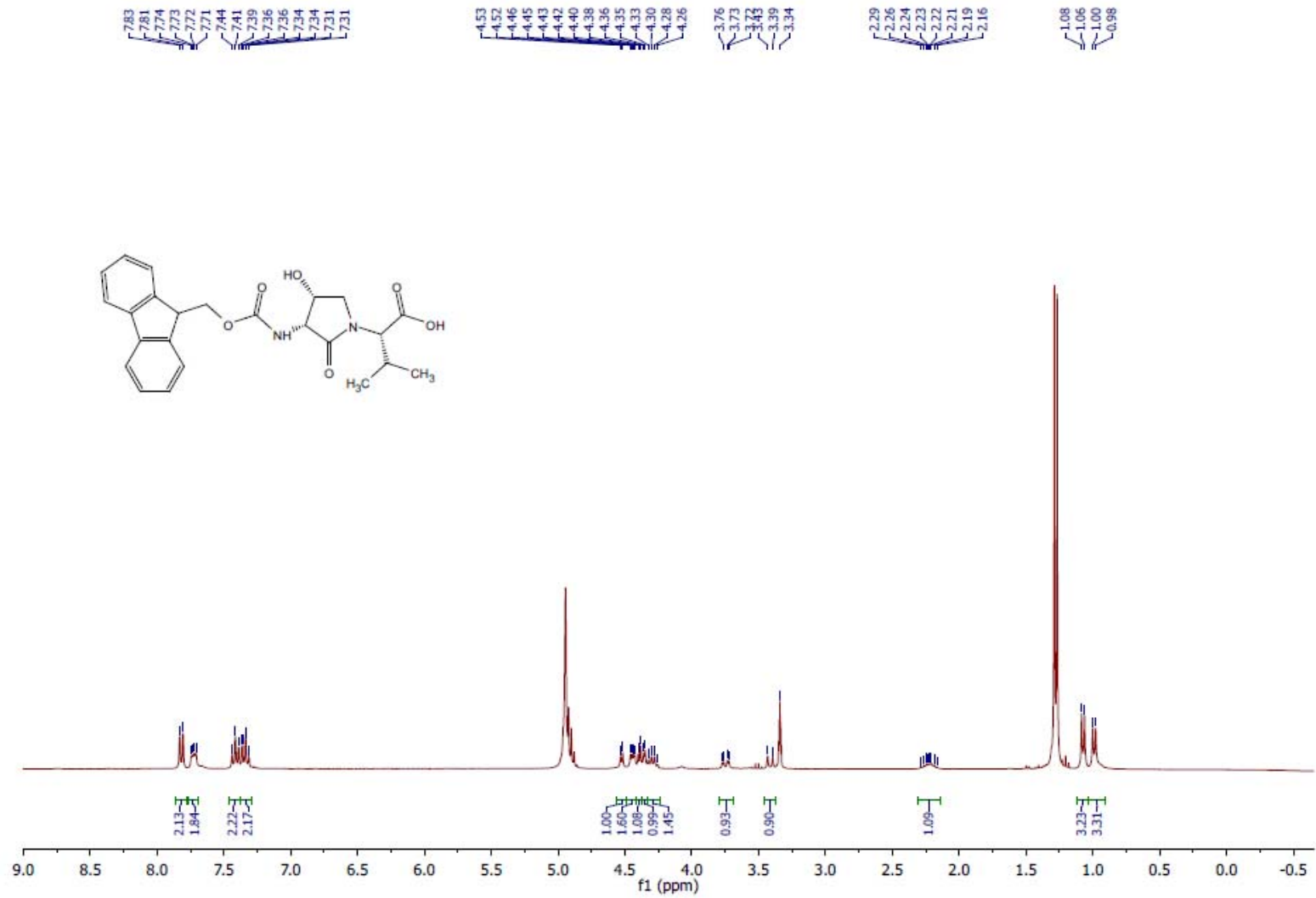
^{13}C NMR (75 MHz, MeOD) [(3*R*, 4*R*, 2'*S*)-2.12]

Annex 1: Supporting information of Article 1
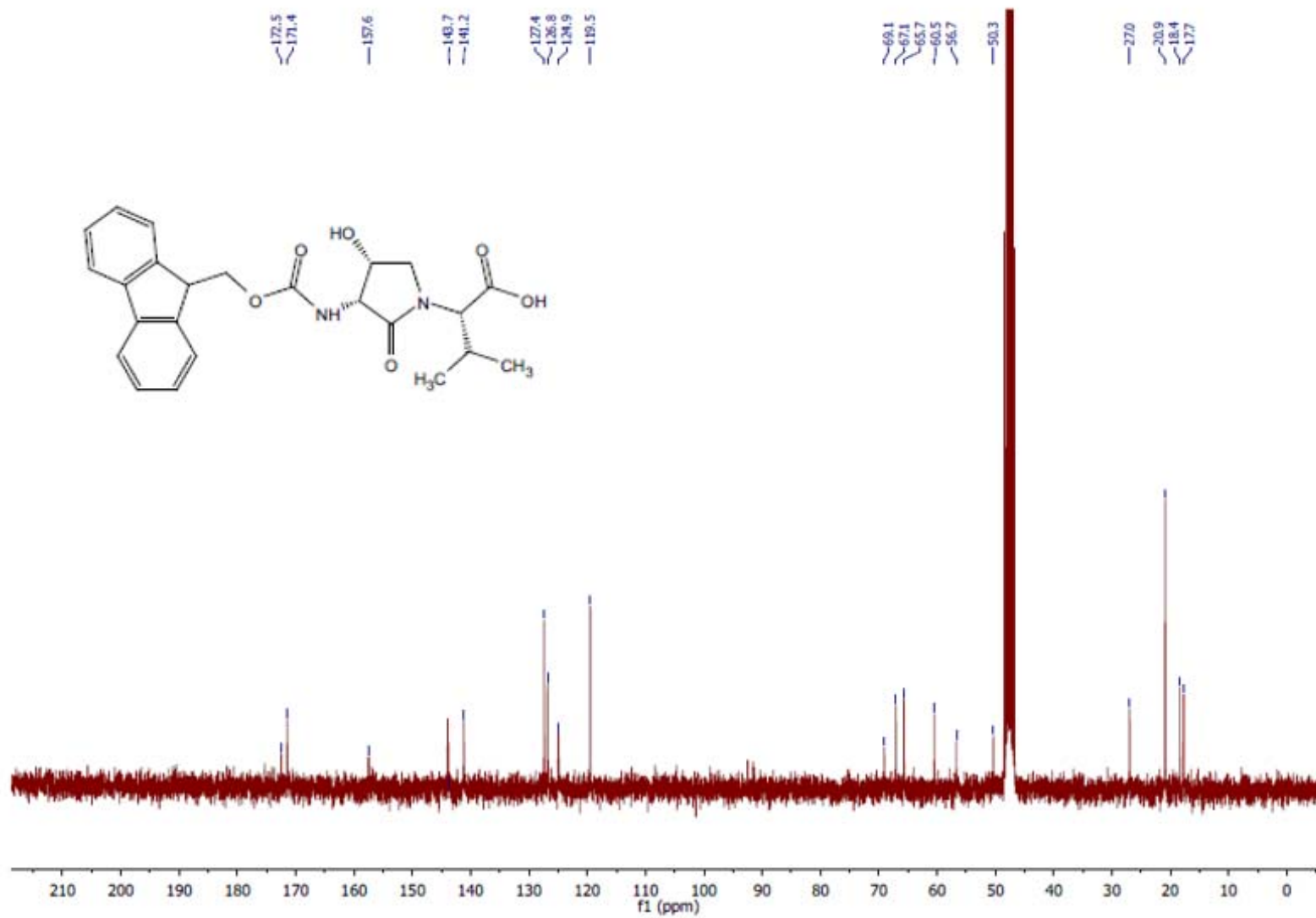
^{1}H NMR (300 MHz, CDCl$_3$) **(R, R)-2.13**
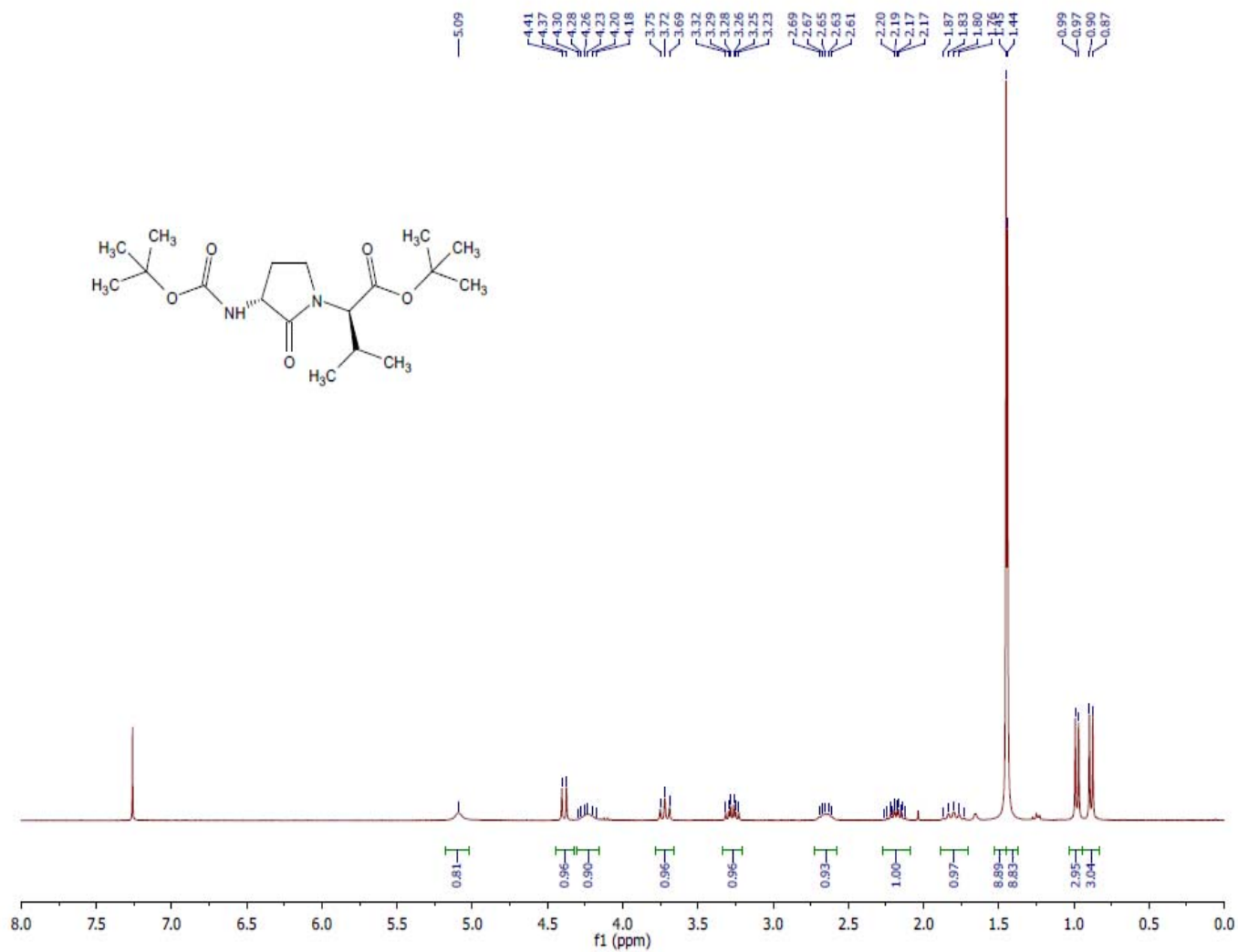
^{13}C NMR (75 MHz, CDCl$_3$) (**R, R**)-2.13

^{1}H NMR (300 MHz, CDCl$_3$) **(*R*, *S*)-2.13**

Annex 1: Supporting information of Article 1
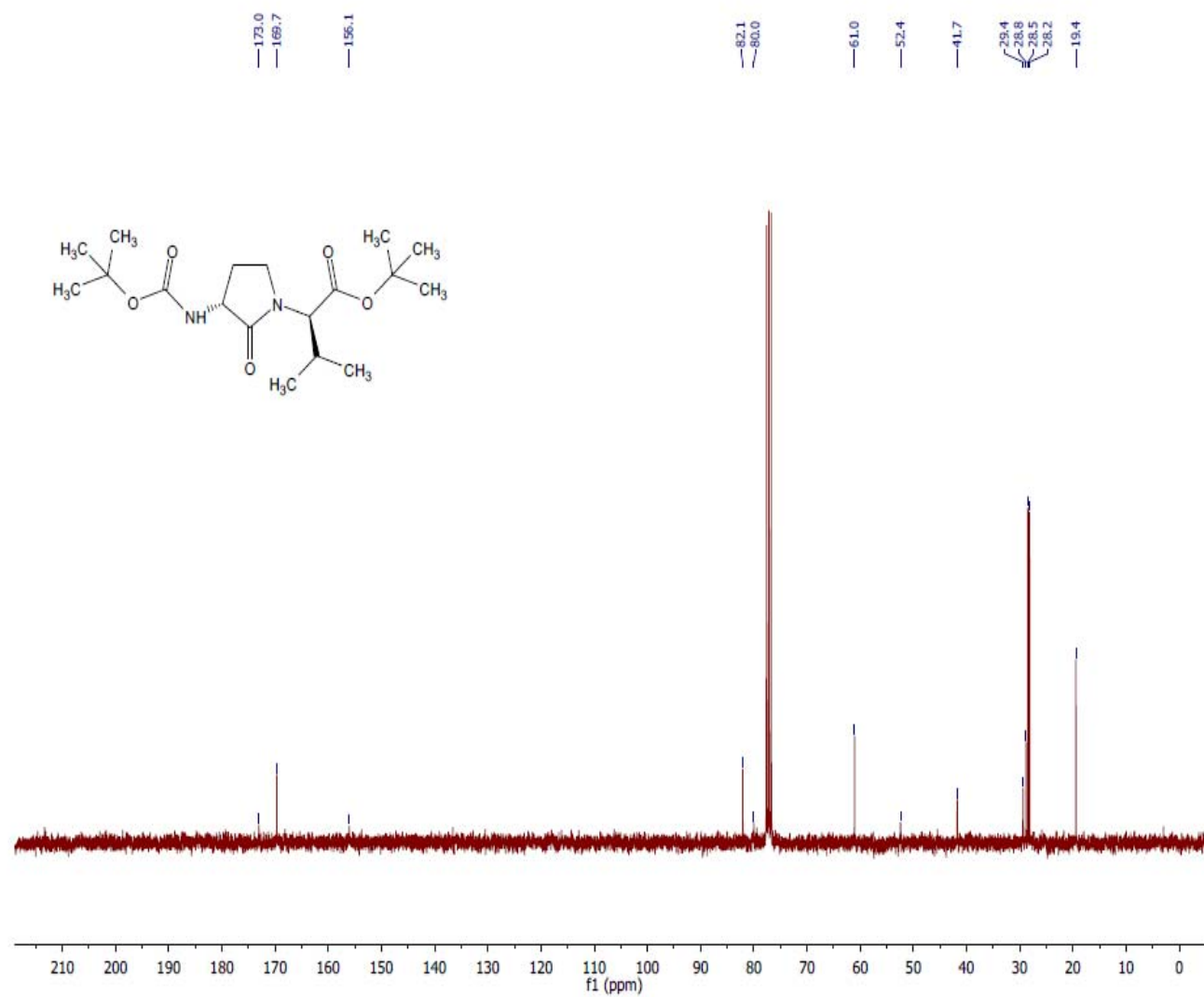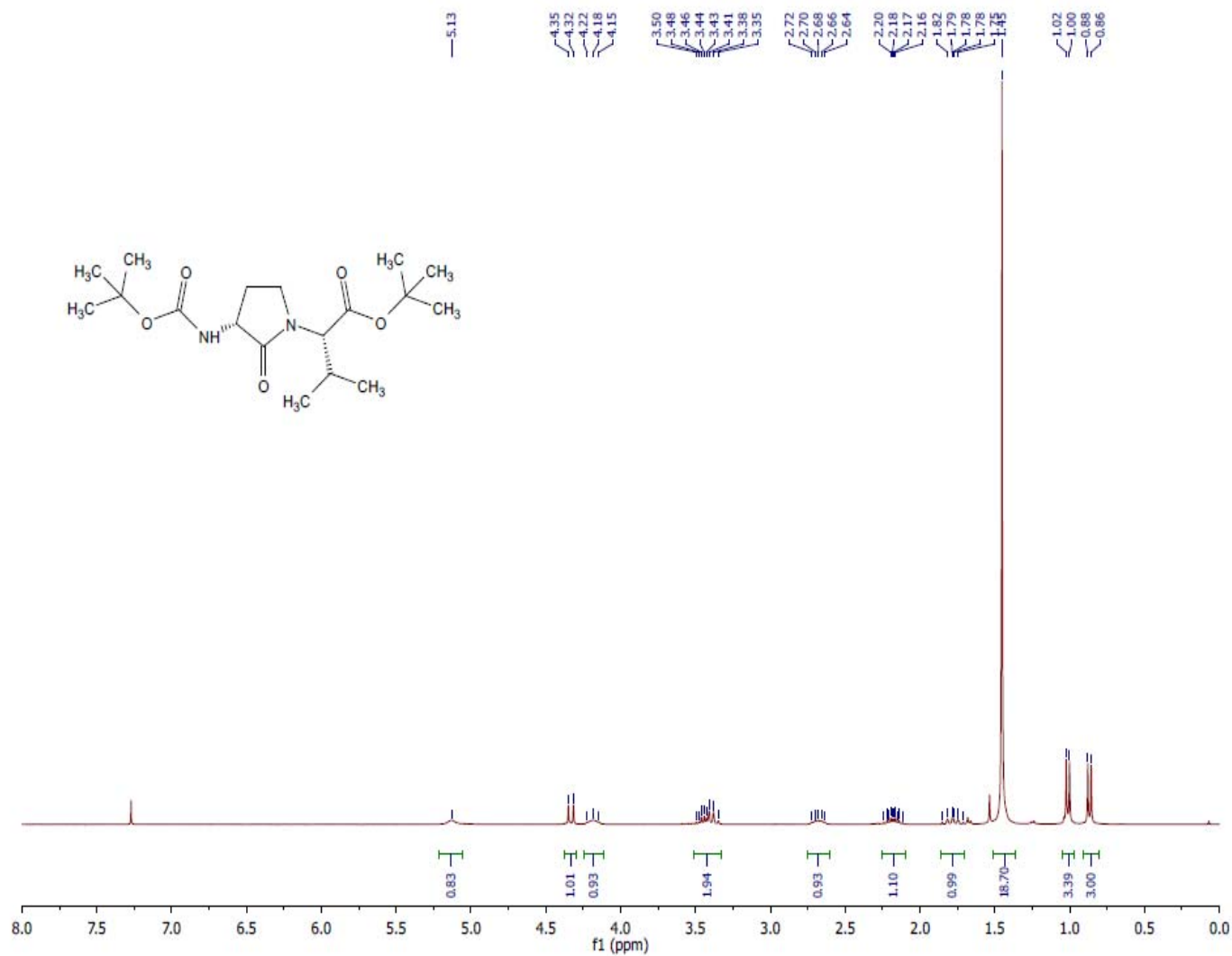
^{13}C NMR (75 MHz, CDCl$_3$) **(*R*, *S*)-2.13**
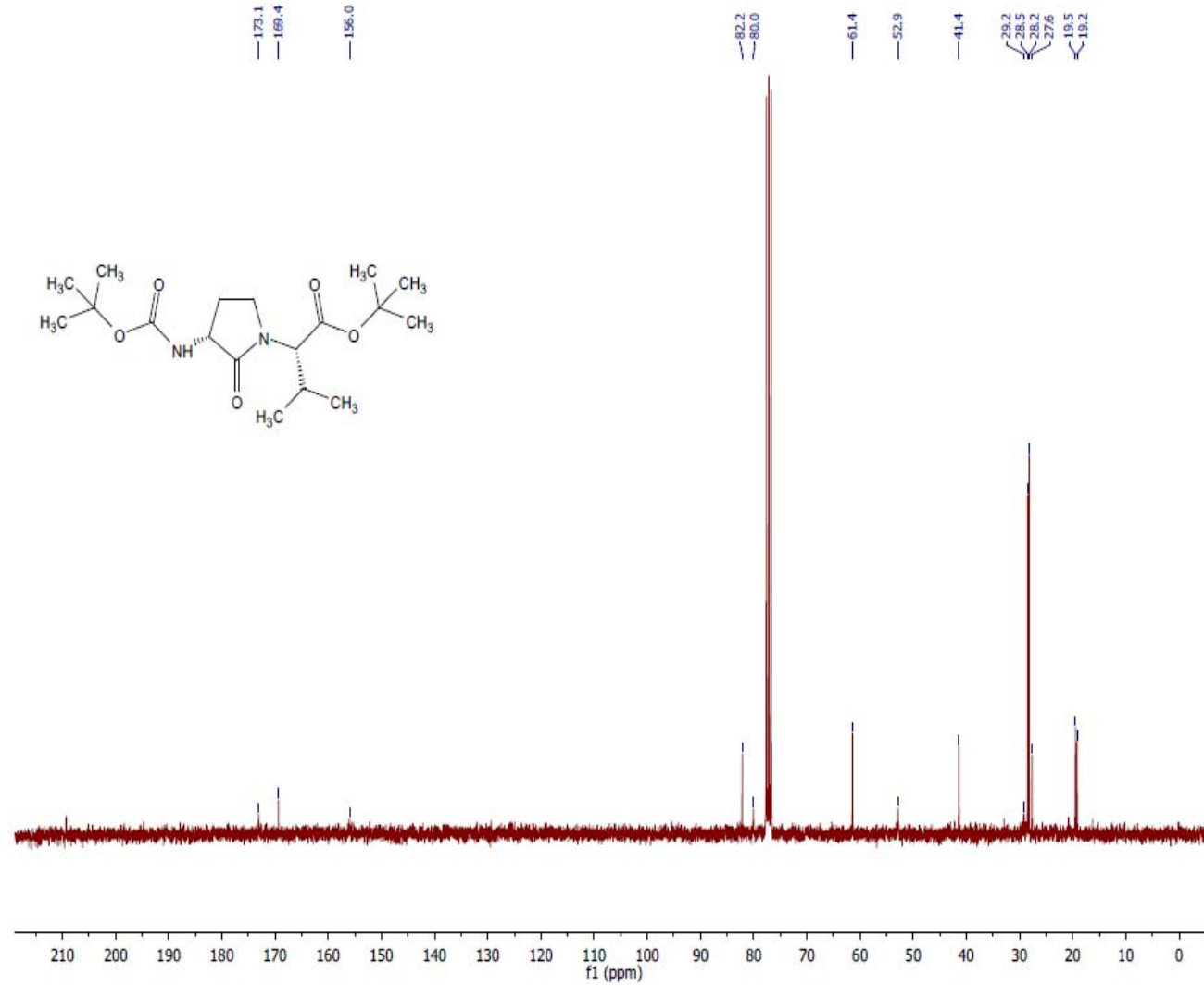
^{1}H NMR (300 MHz, MeOD) (*R, R*)-2.14
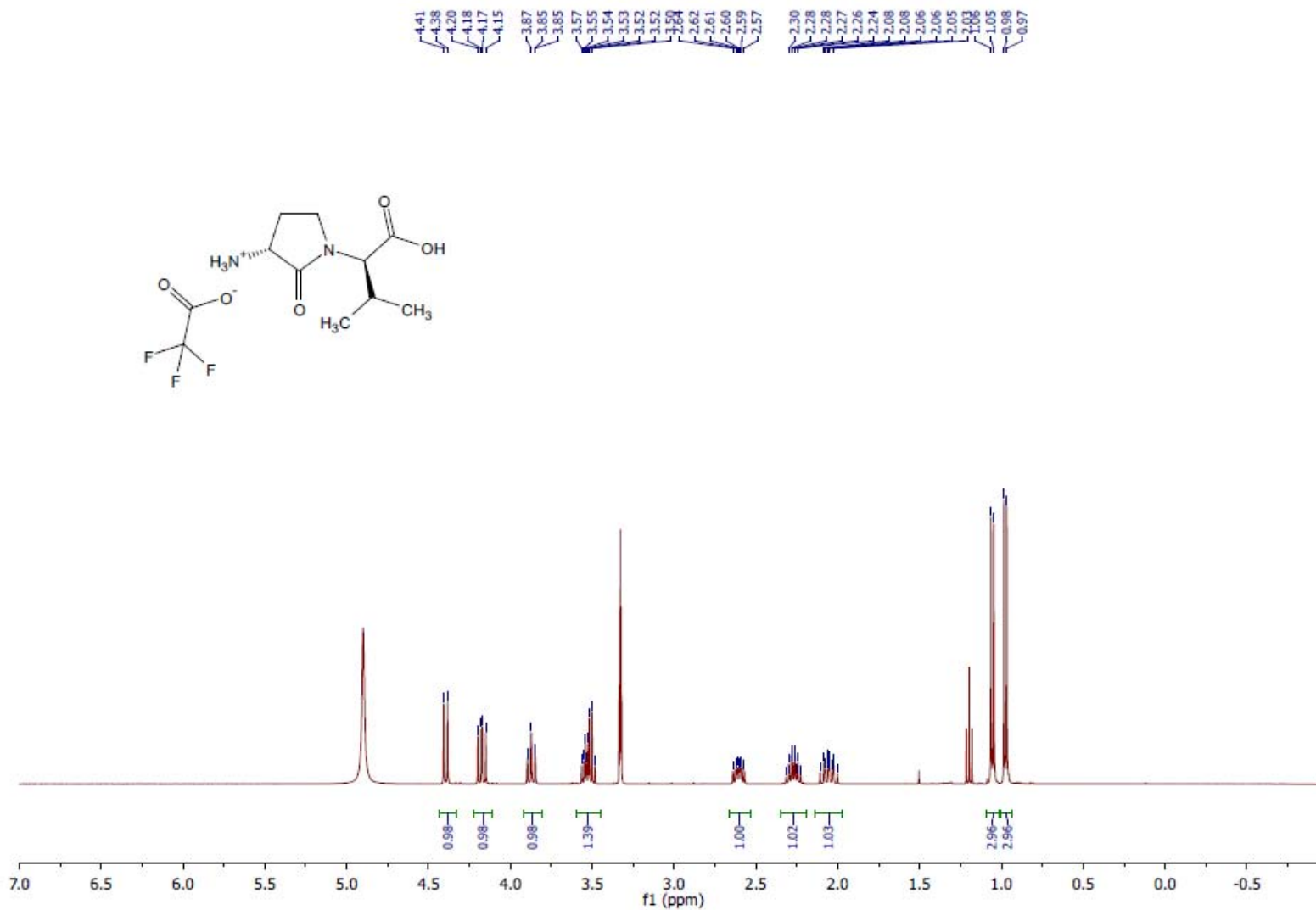
¹³C NMR (75 MHz, MeOD) **(*R, R*)-2.14**
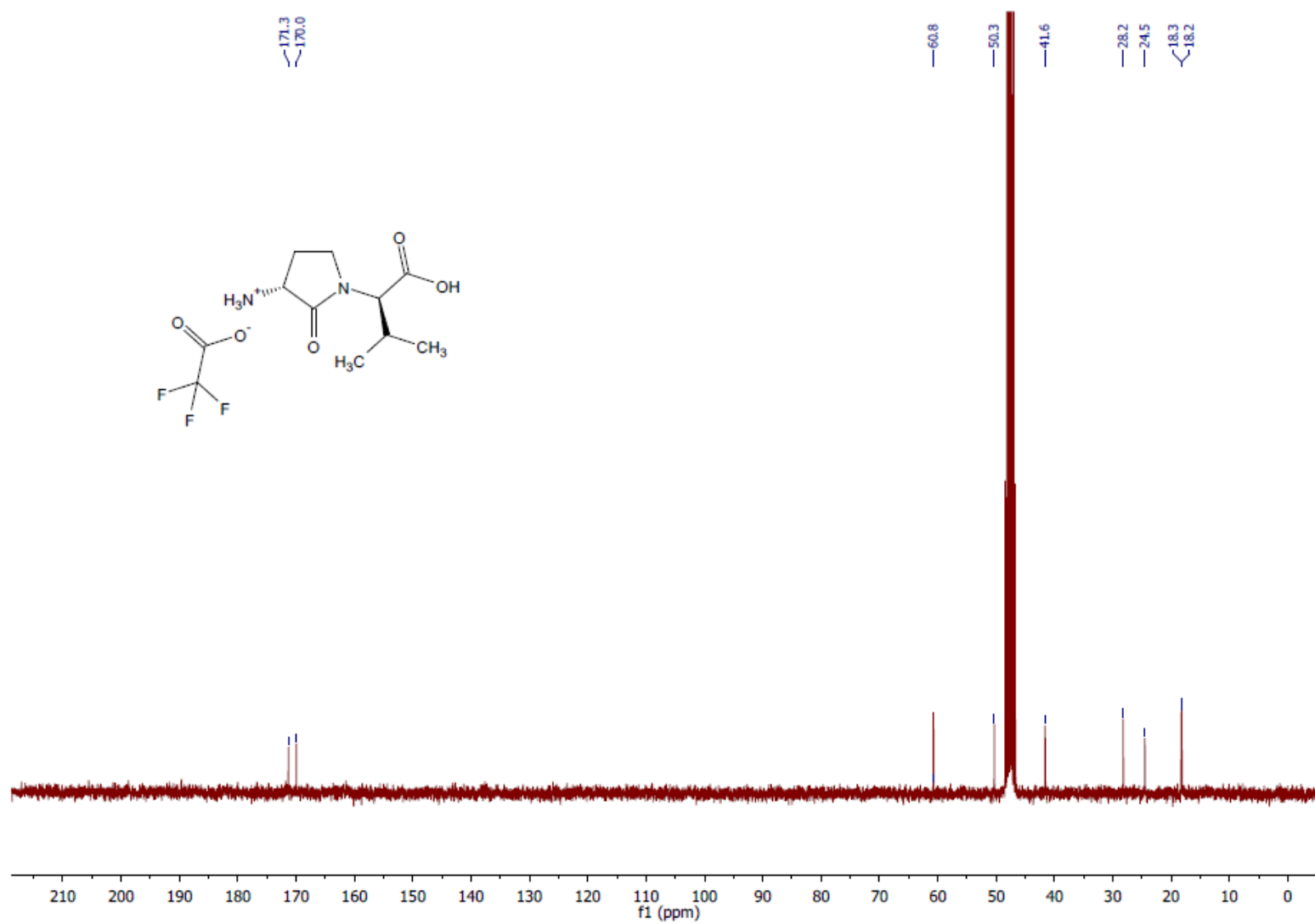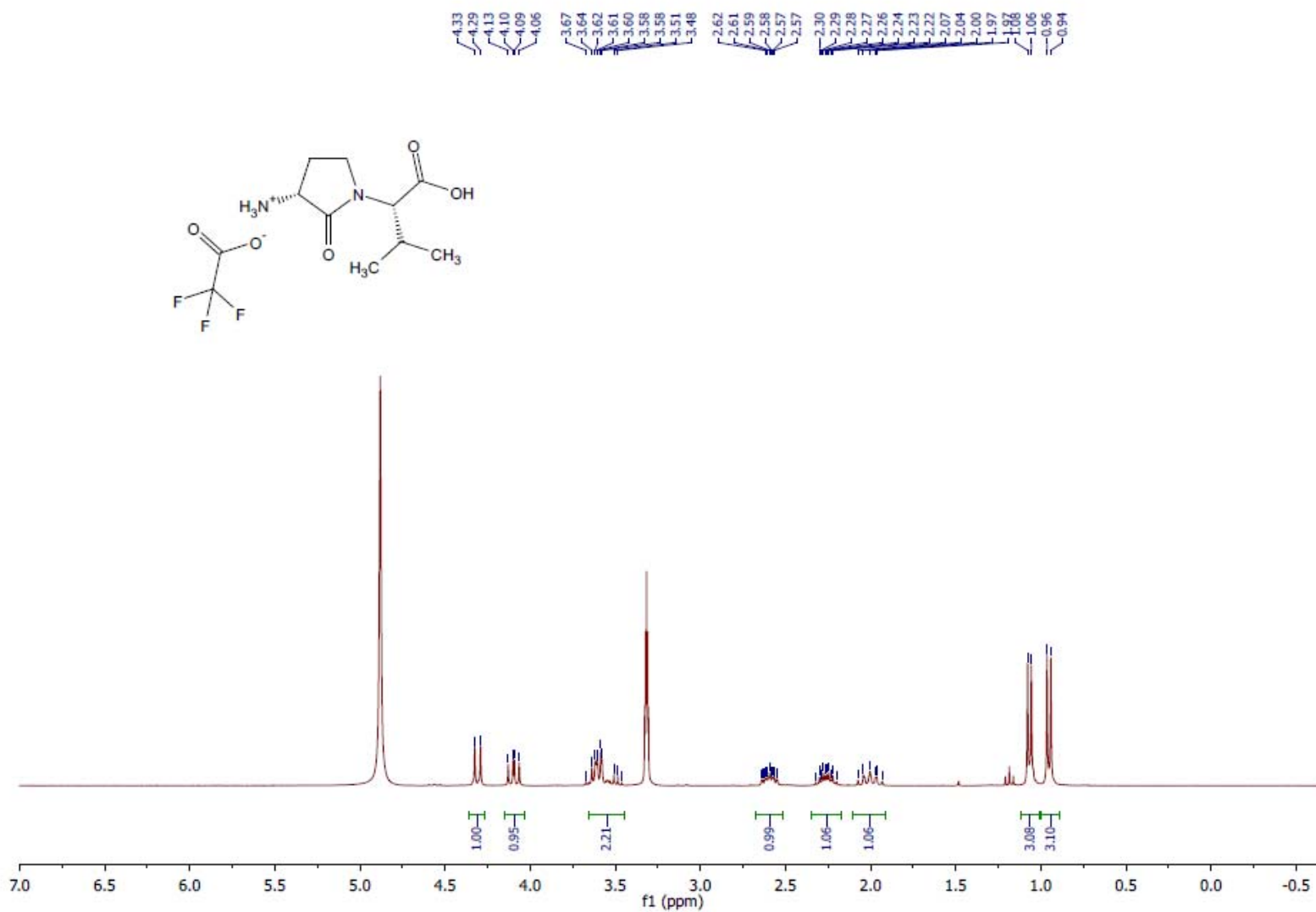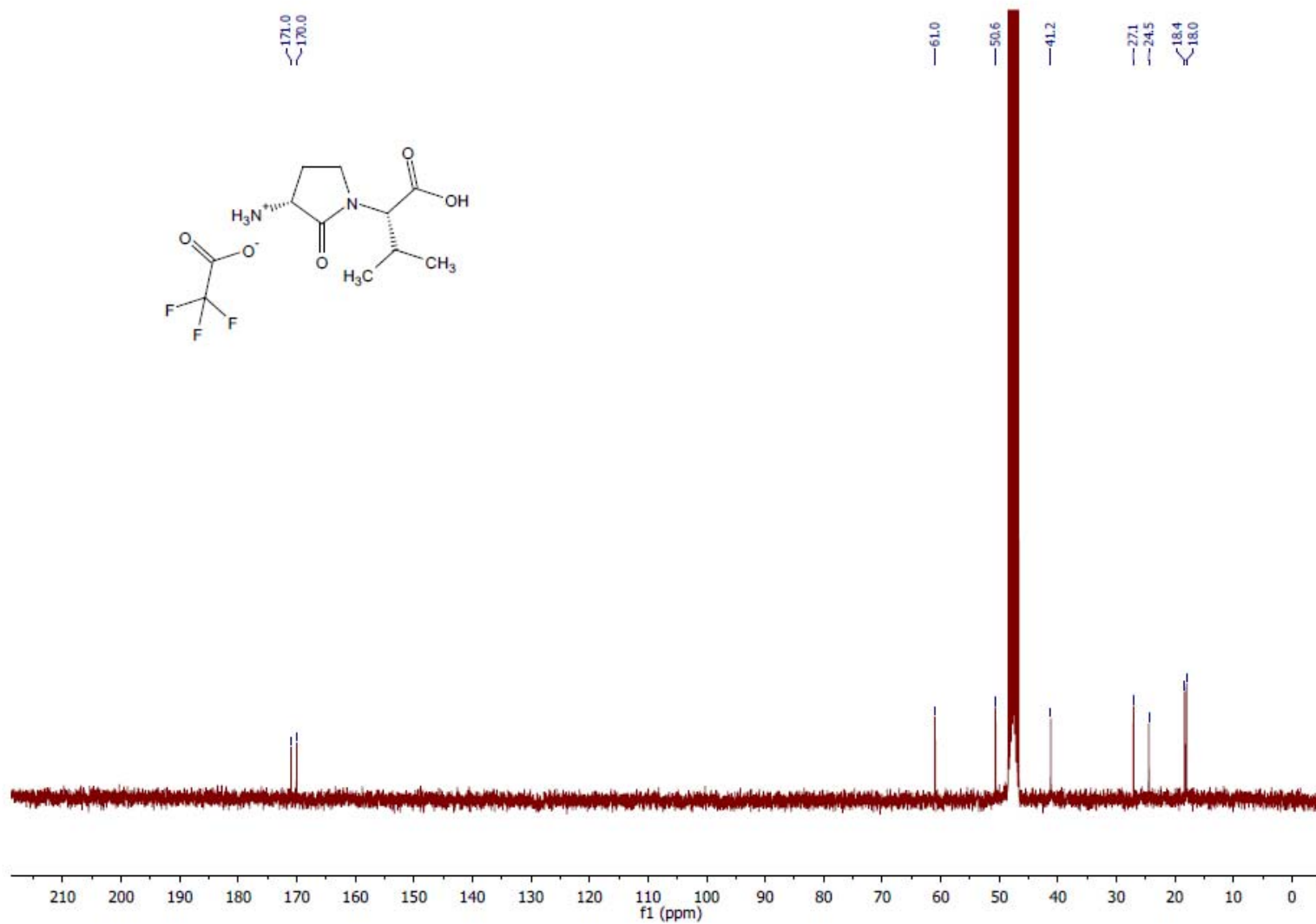
Annex 1: Supporting information of Article 1

^{1}H NMR (300 MHz, MeOD) **(*R*, *S*)-2.14**

Annex 1: Supporting information of Article 1

^{13}C NMR (75 MHz, MeOD) **(*R*, *S*)-2.14**

Annex 1: Supporting information of Article 1

^{1}H NMR (300 MHz, CDCl$_3$) **(*R*)-2.15**

Annex 1: Supporting information of Article 1

^{13}C NMR (75 MHz, CDCl$_3$) (*R*)-2.15

Annex 1: Supporting information of Article 1

^{1}H NMR (300 MHz, CDCl$_3$) (*R*)-2.16

Annex 1: Supporting information of Article 1
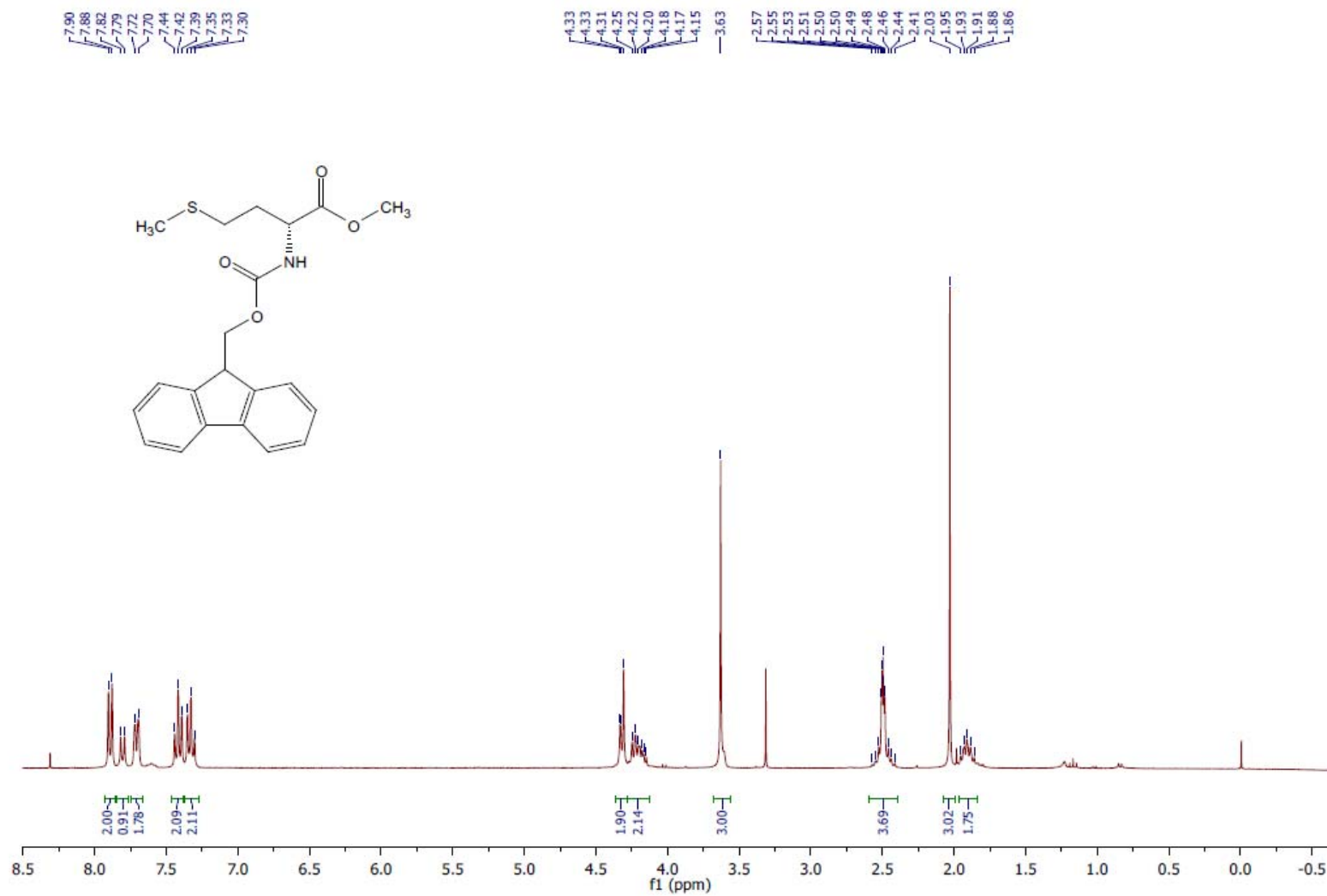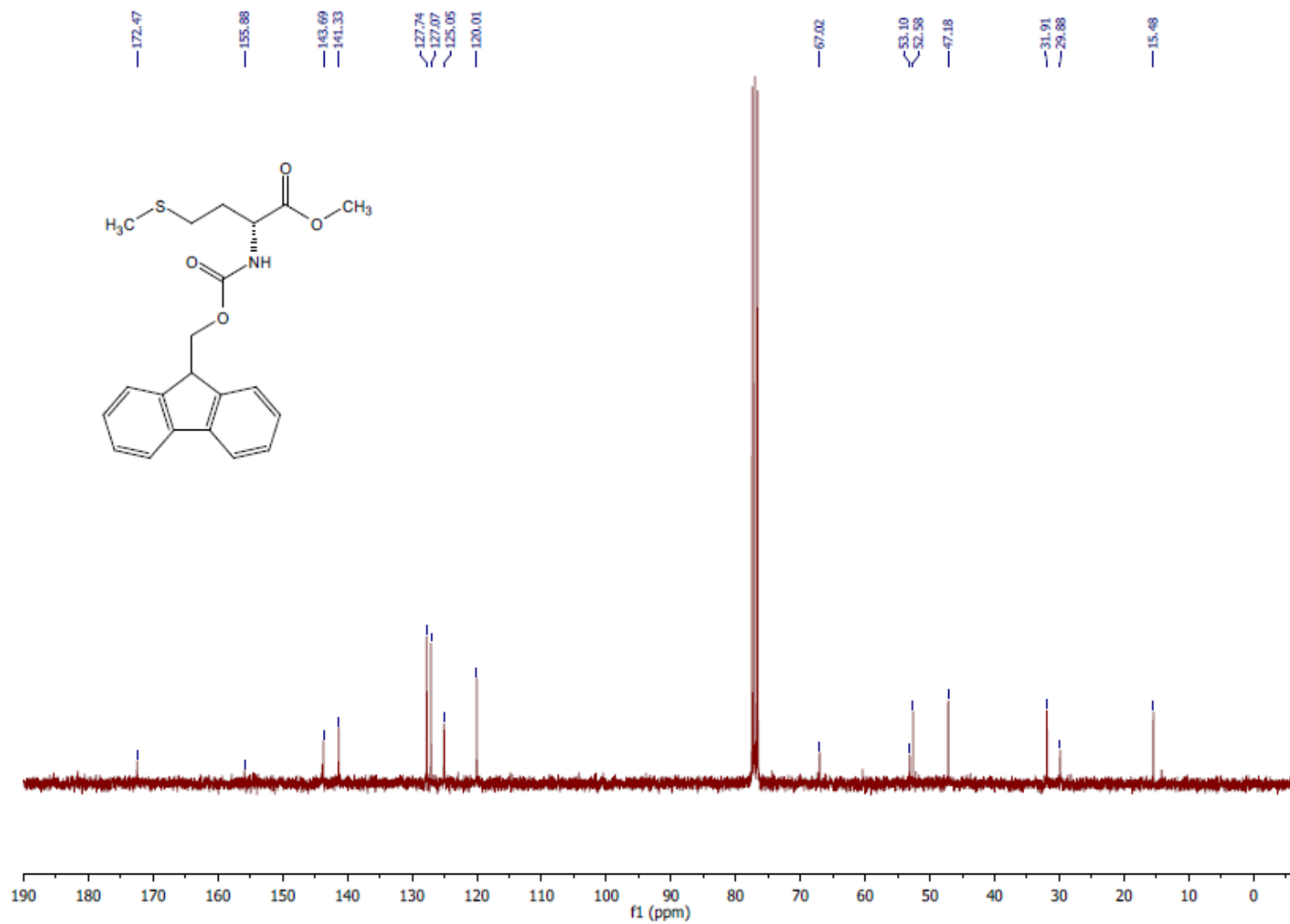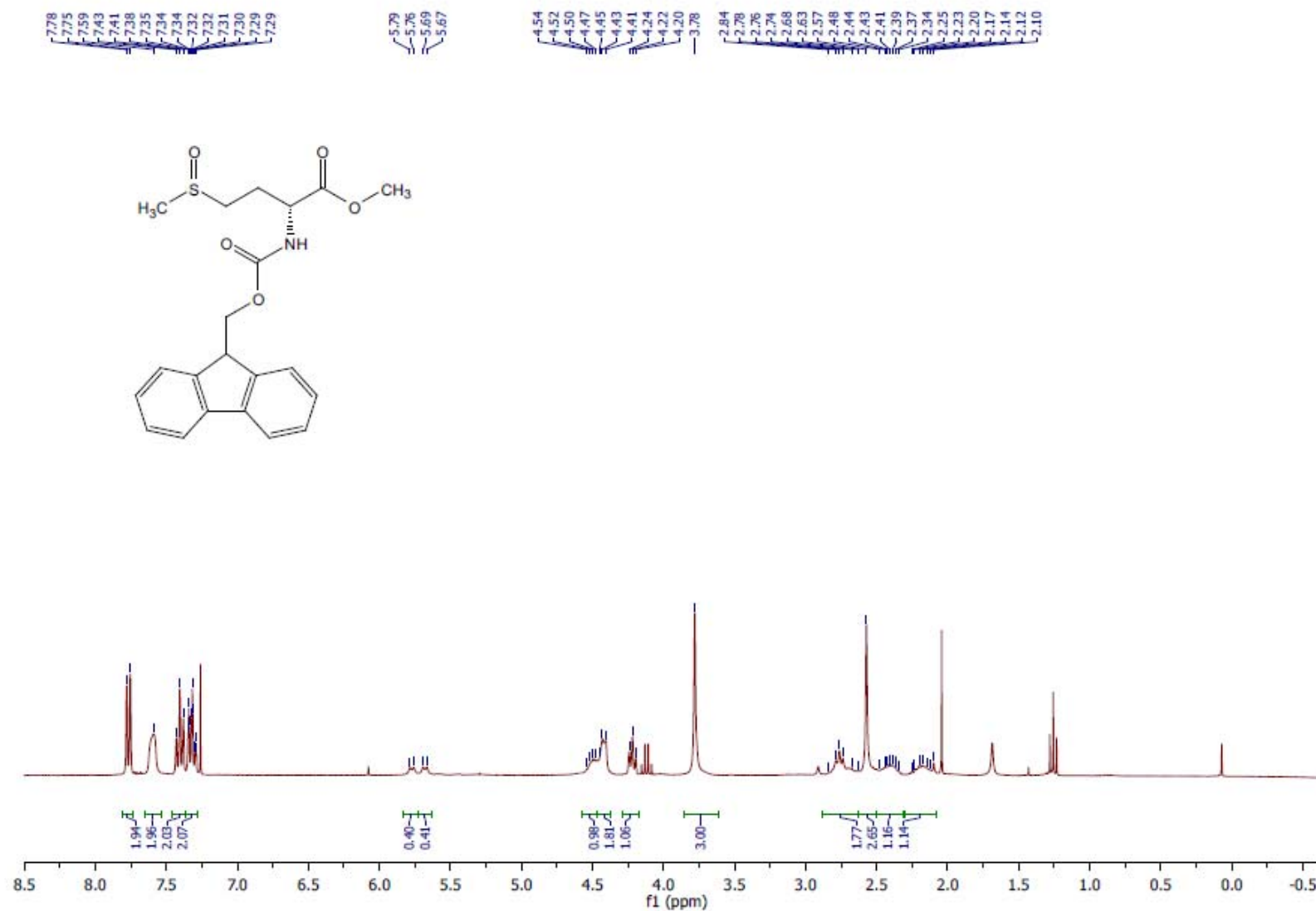
^{13}C NMR (75 MHz, CDCl$_3$) **(R)-2.16**
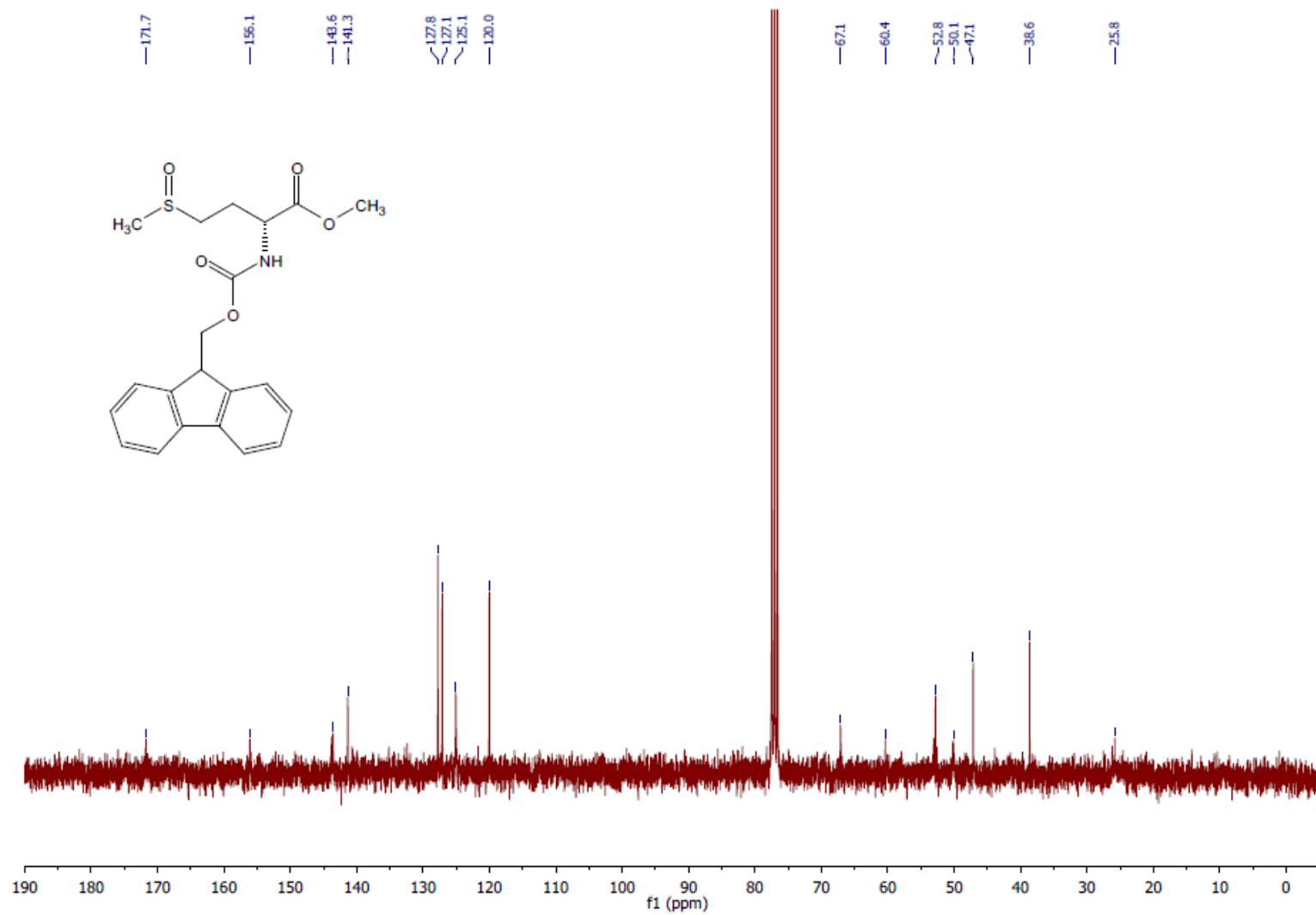
^{1}H NMR (300 MHz, CDCl$_3$) (*R*)-2.17
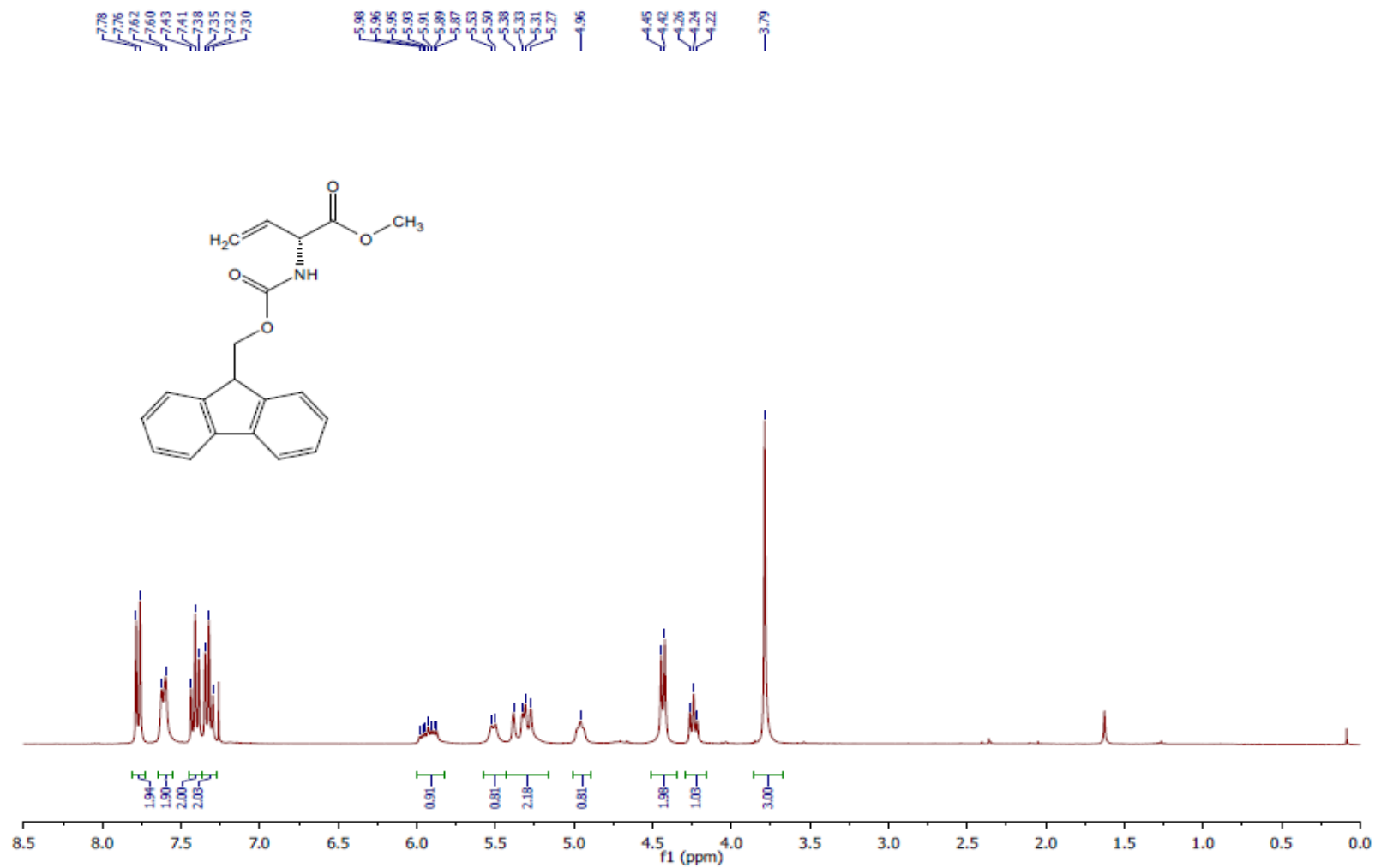
^{13}C NMR (75 MHz, CDCl$_3$) **(R)-2.17**
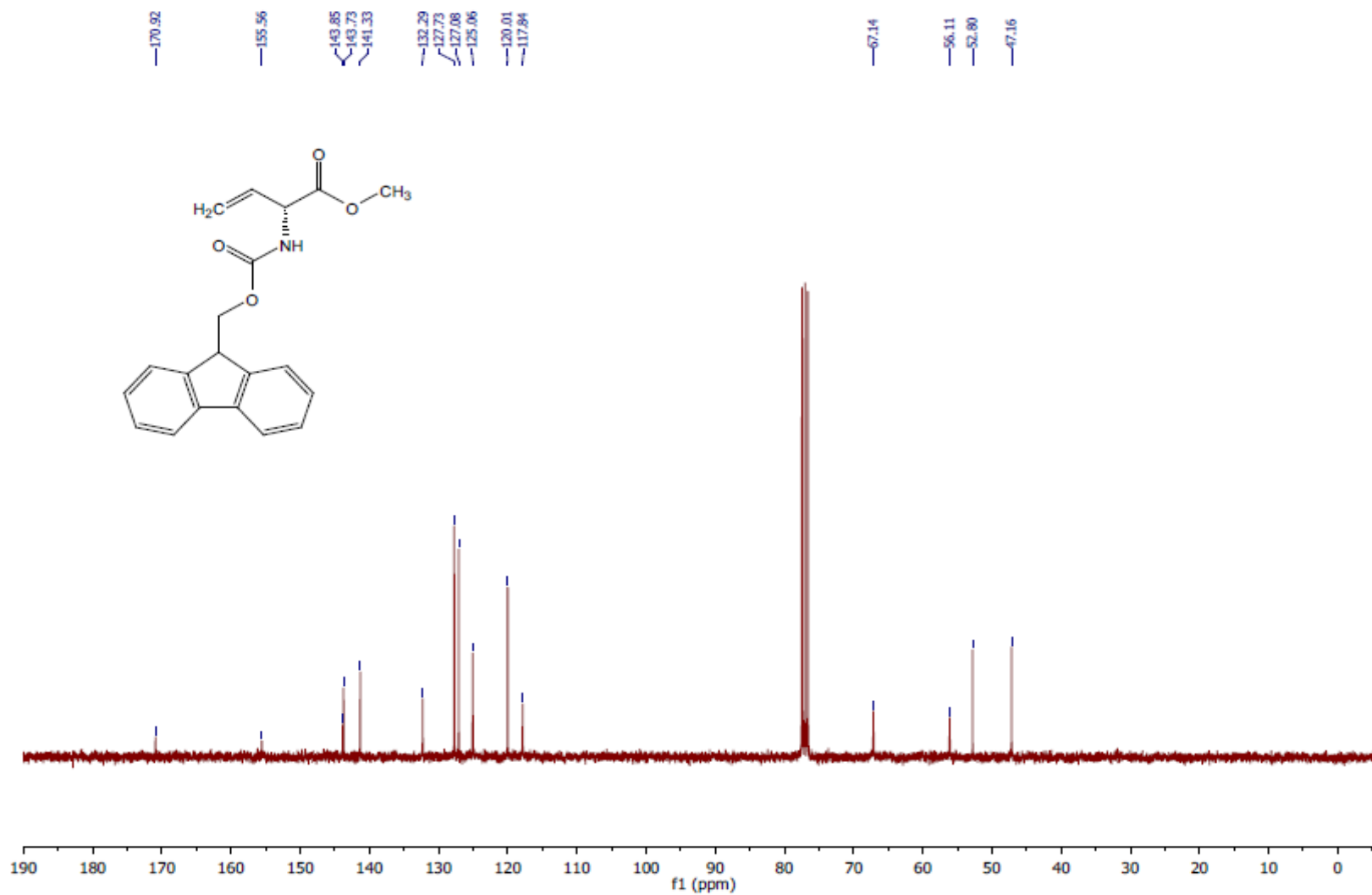
^{1}H NMR (500 MHz, CDCl$_3$) **(*R*, *R*)-2.18**
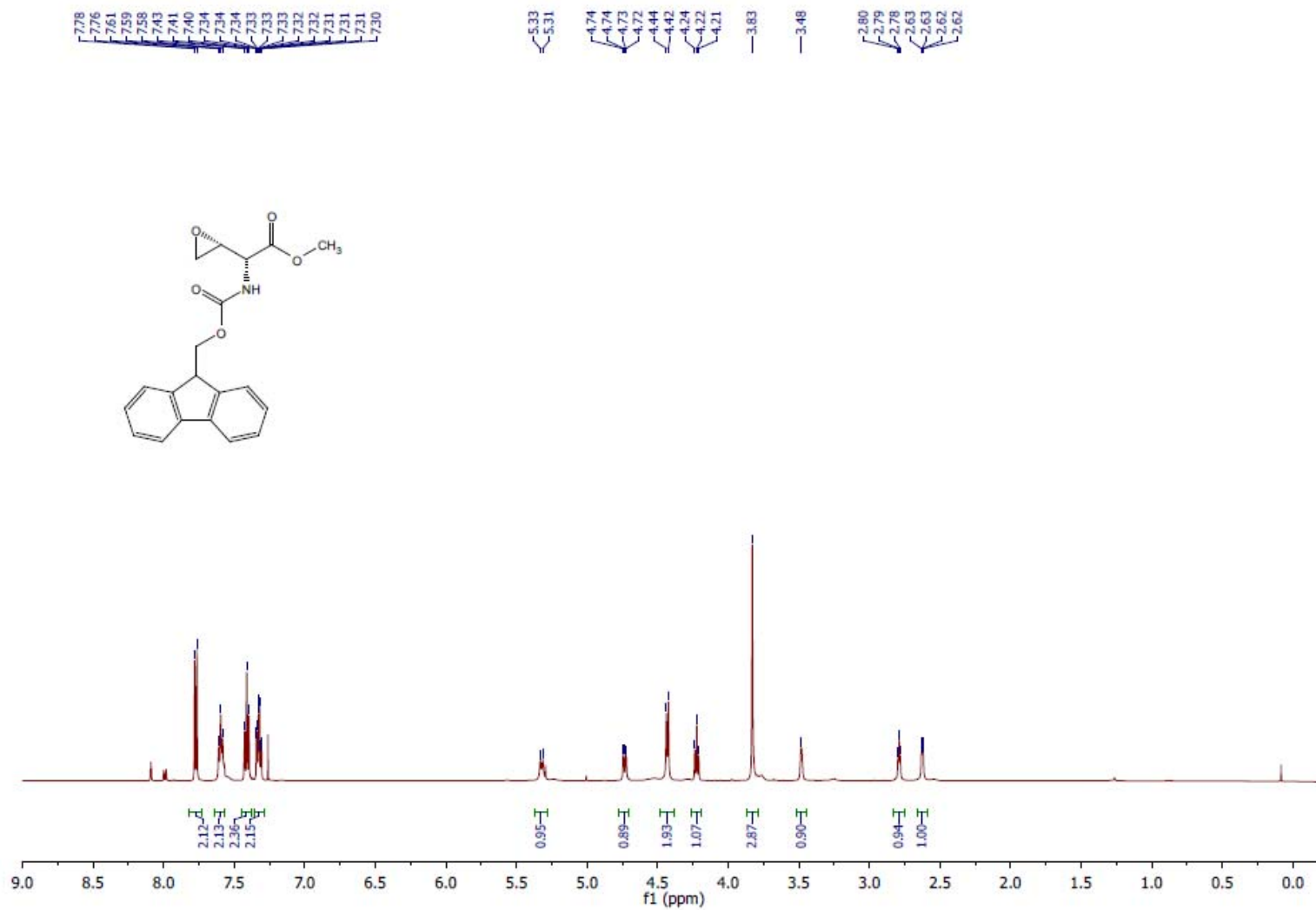
^{13}C NMR (126 MHz, CDCl$_3$) (*R, R*)-2.18
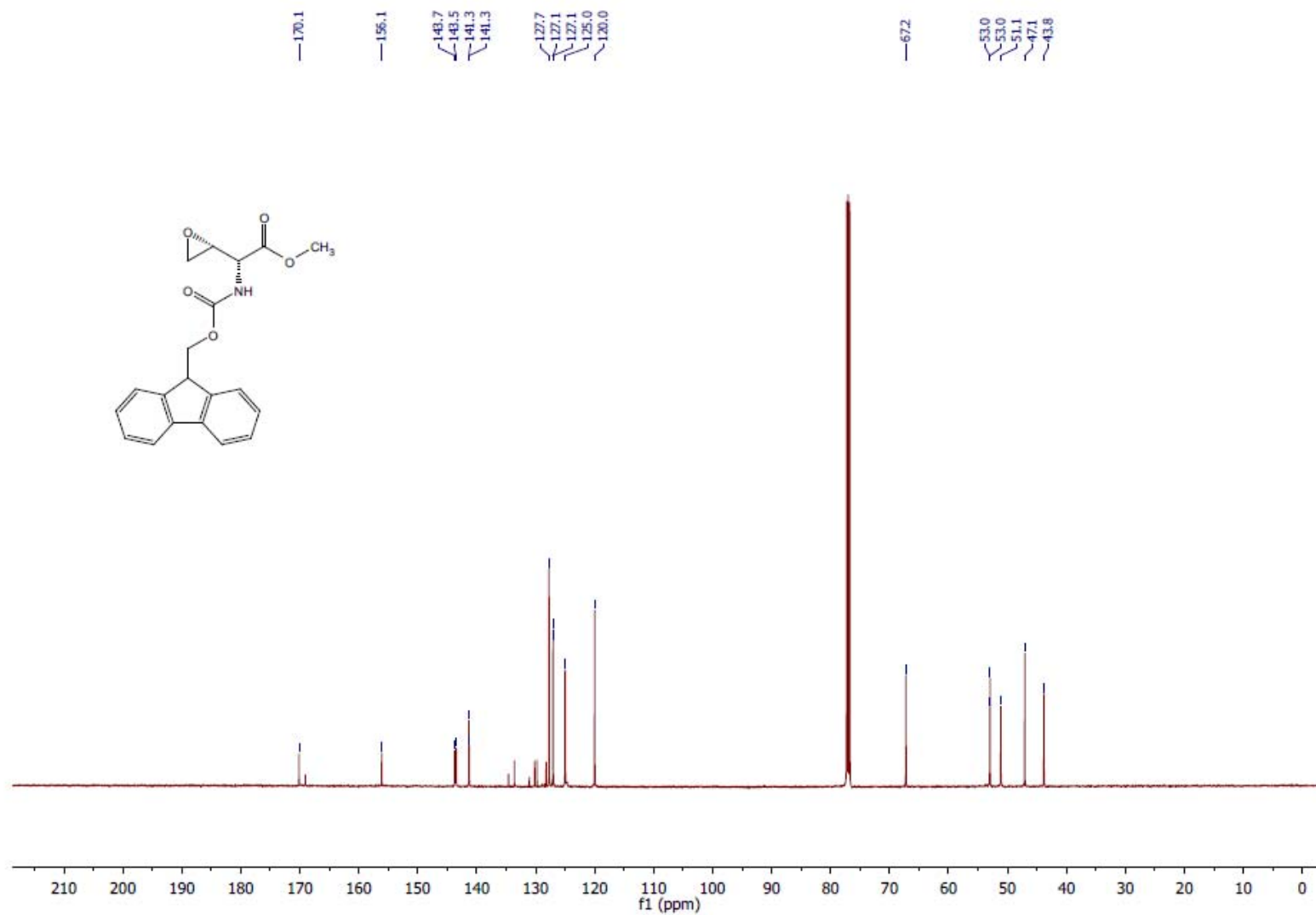
^{1}H NMR (500 MHz, CDCl$_3$) **(R, S)-2.18**
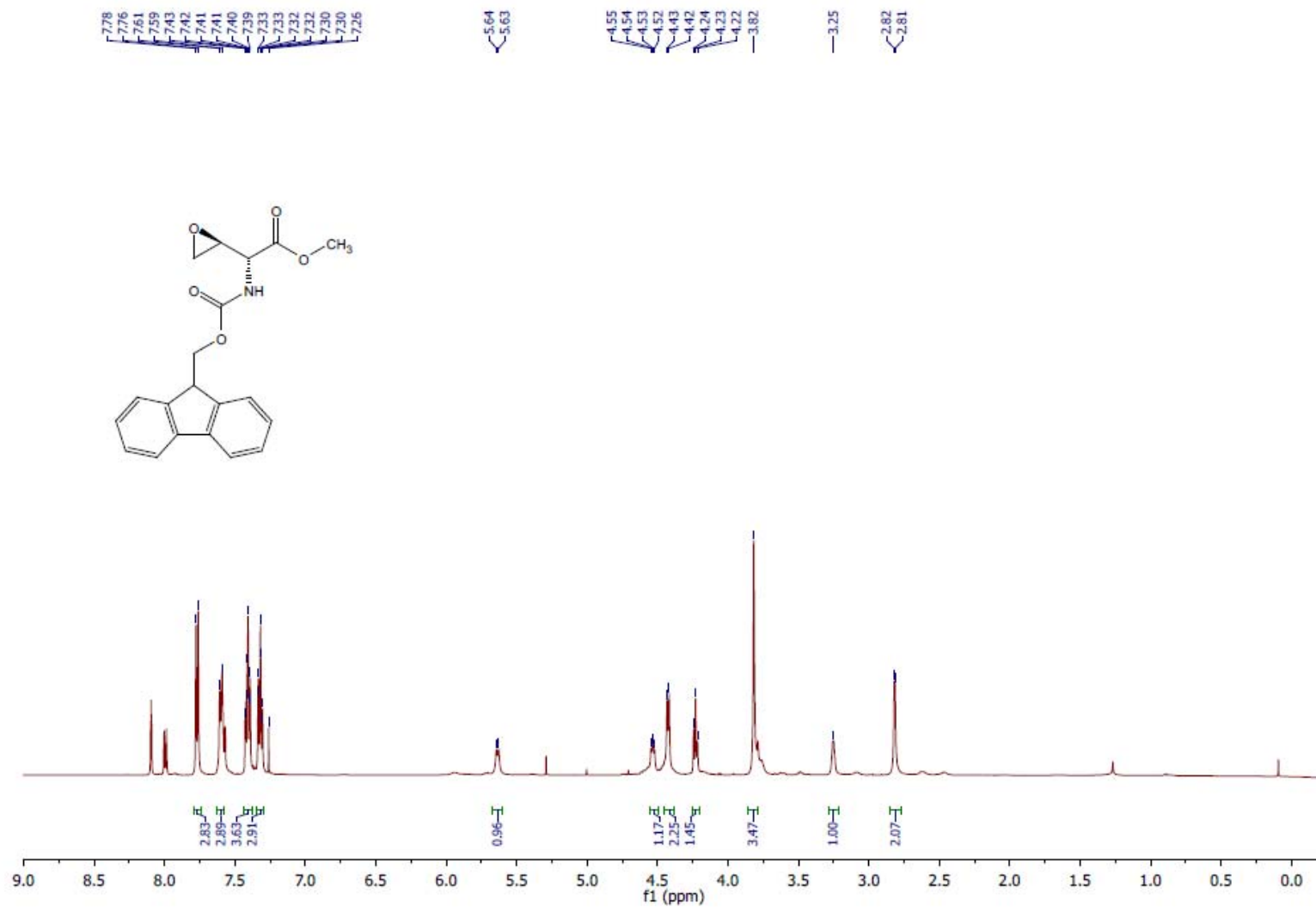
^{13}C NMR (126 MHz, CDCl$_3$) **(R, S)-2.18**

Annex 1: Supporting information of Article 1
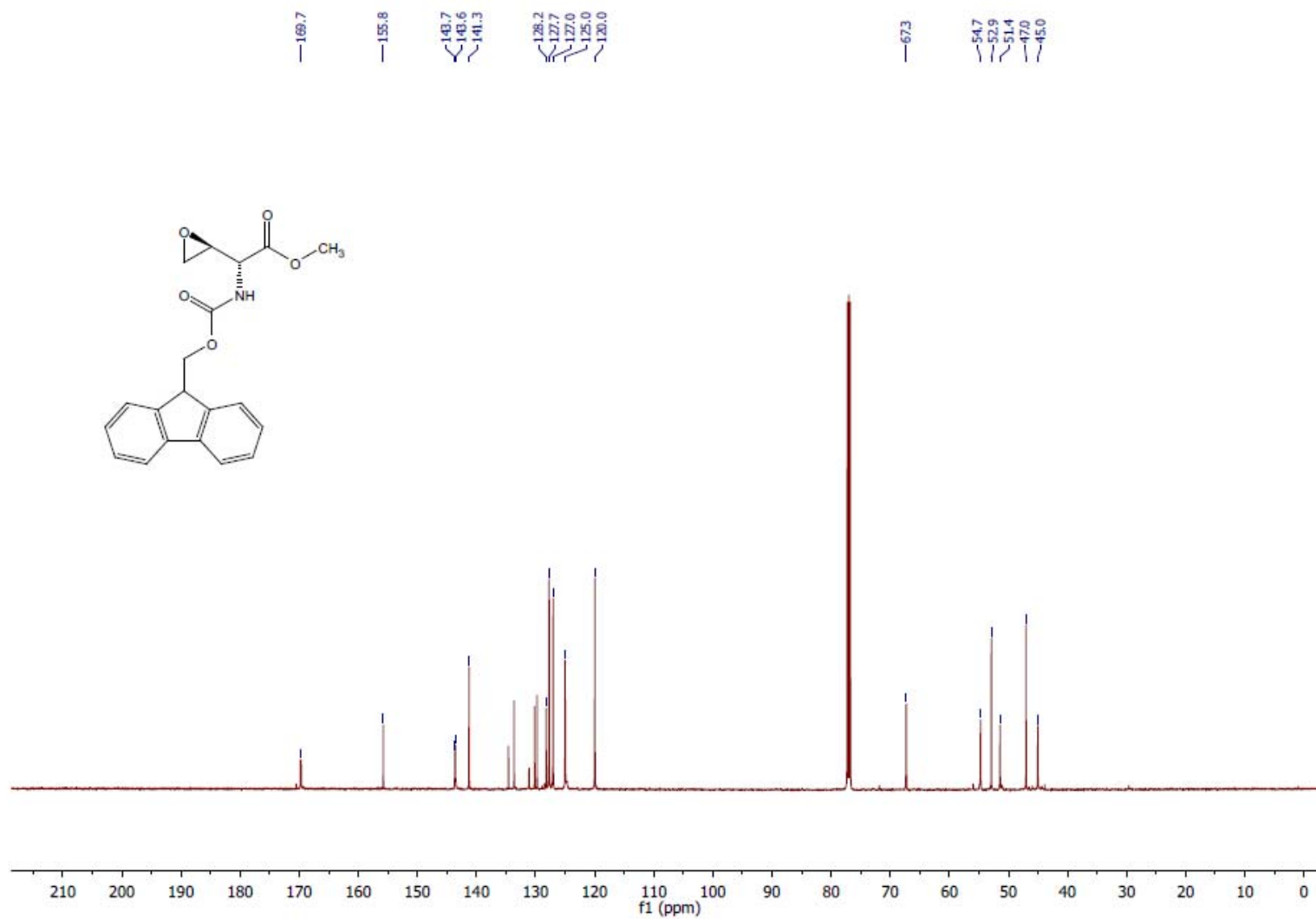
^{1}H NMR (500 MHz, CDCl$_3$) **[(3*R*, 4*S*, 2'*R*)-2.19]**
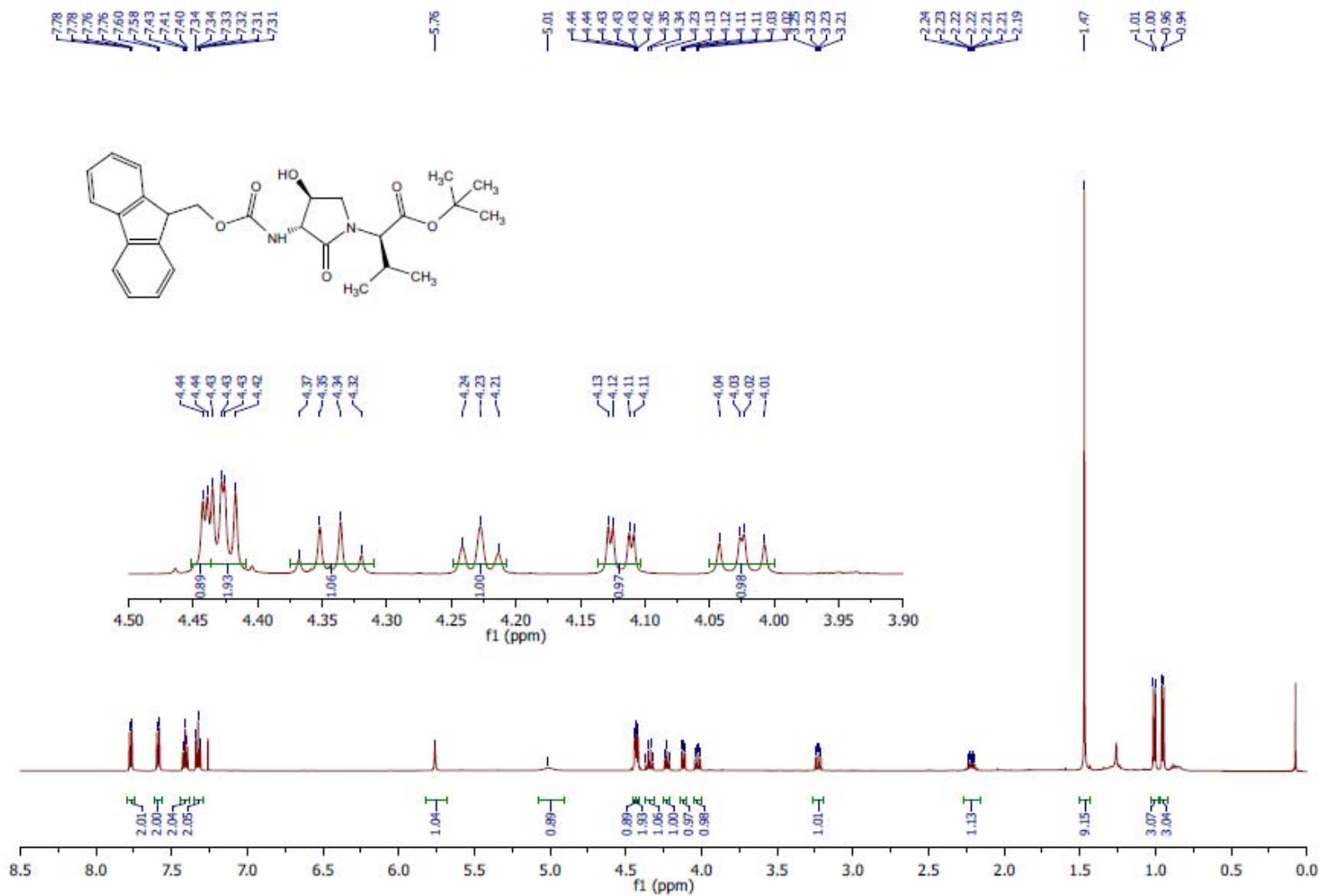
^{13}C NMR (126 MHz, CDCl$_3$) **[(3*R*, 4*S*, 2'*R*)-2.19]**

Annex 1: Supporting information of Article 1

^{1}H NMR (500 MHz, CDCl$_3$) **[(3R, 4S, 2'S)-2.19]**

Annex 1: Supporting information of Article 1

^{13}C NMR (126 MHz, CDCl$_3$) **[(3*R*, 4*S*, 2'*S*)-2.19]**

Annex 1: Supporting information of Article 1
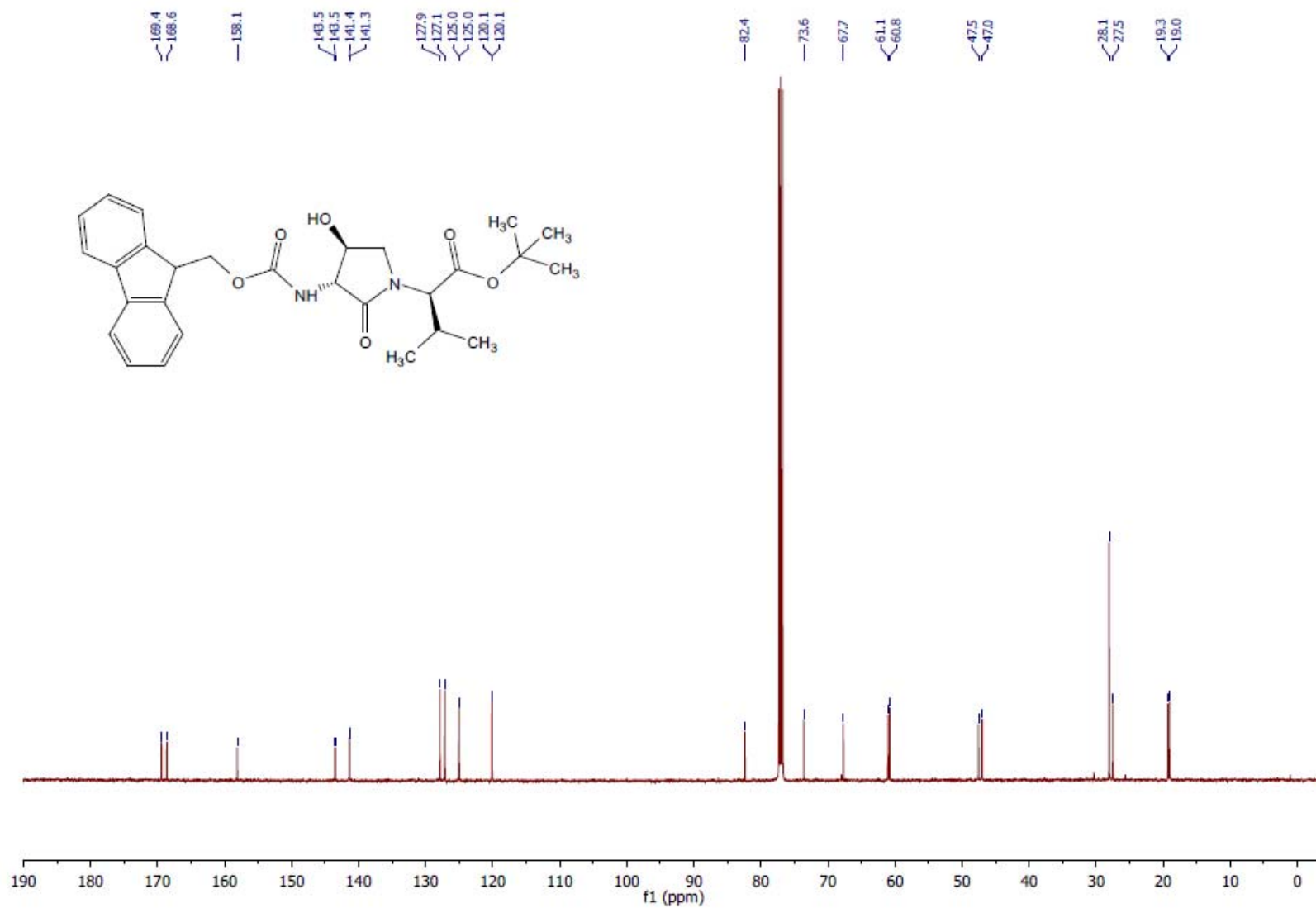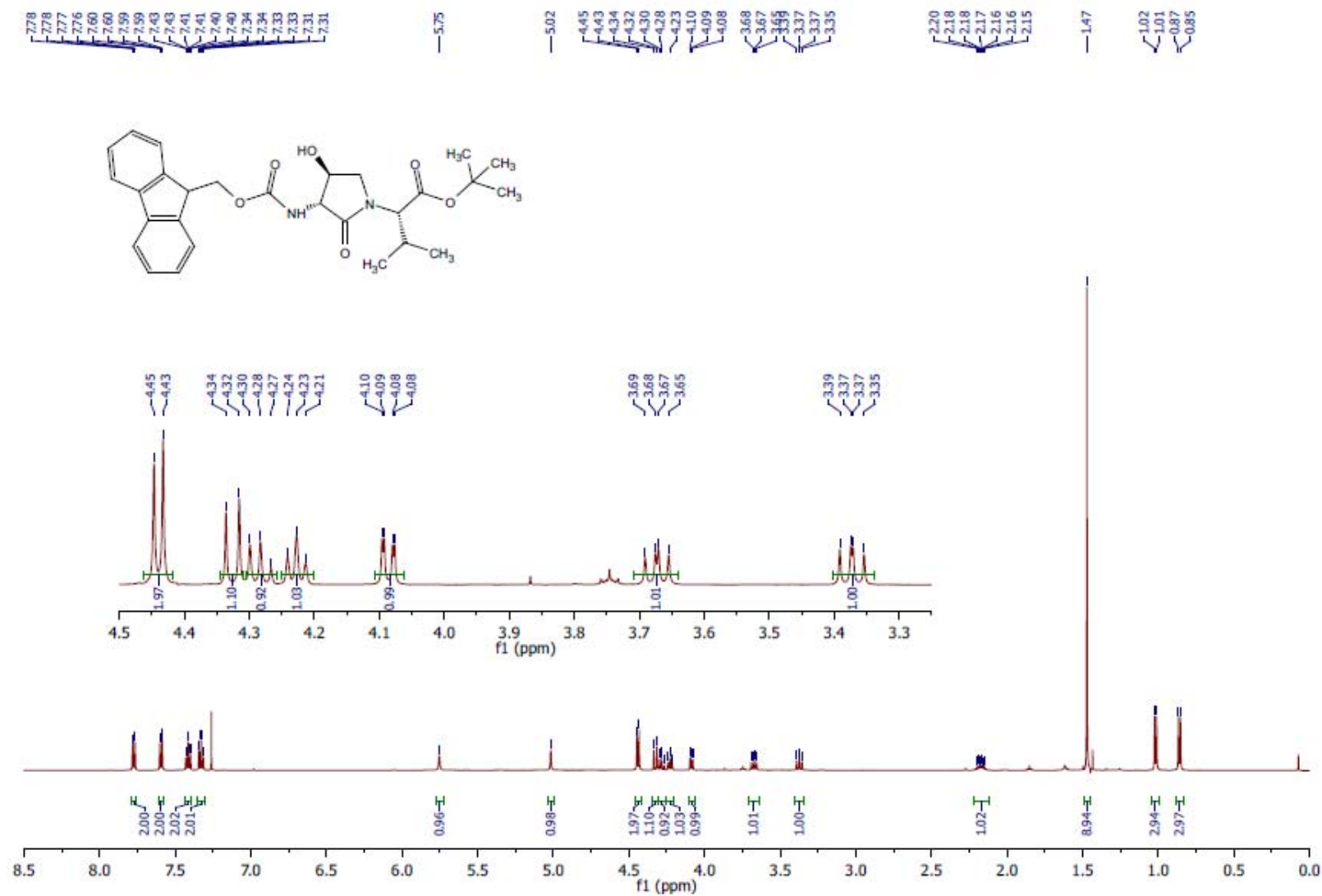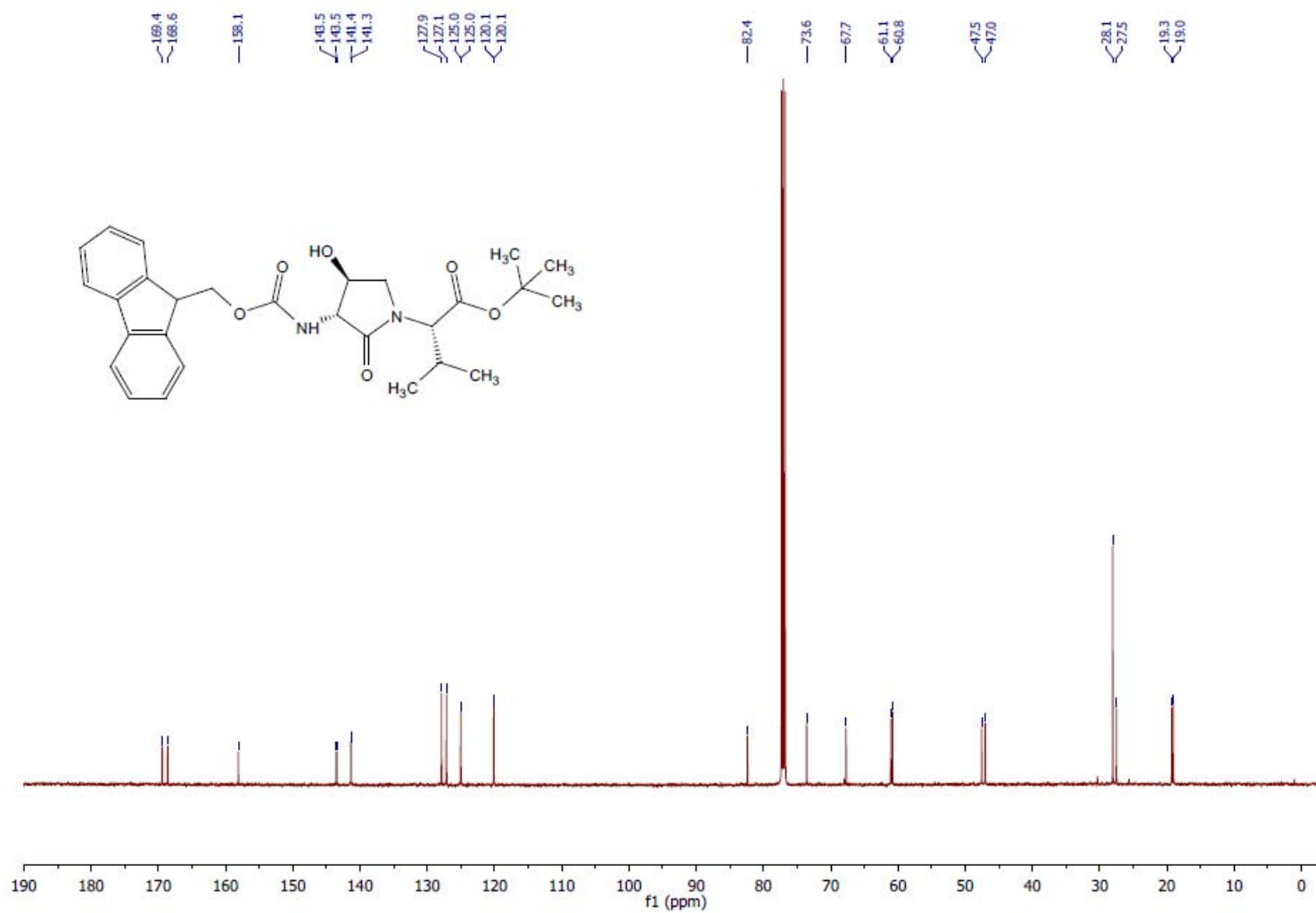
^{1}H NMR (500 MHz, CDCl$_3$) **[(3*S*, 4*R*, 2'*R*)-2.19]**

^{13}C NMR (75 MHz, CDCl$_3$) **[(3*S*, 4*R*, 2'*R*)-2.19]**

169.4
168.6
158.1
143.5
141.3
127.9
127.1
125.0
120.1
82.4
73.6
67.7
61.0
60.8
47.5
47.0
28.0
27.5
19.3
19.0

190 180 170 160 150 140 130 120 110 100 90 80 70 60 50 40 30 20 10 0
f1 (ppm)

Annex 1: Supporting information of Article 1

^{1}H NMR (500 MHz, CDCl$_3$) **[(3*S*, 4*R*, 2'*S*)-2.19]**
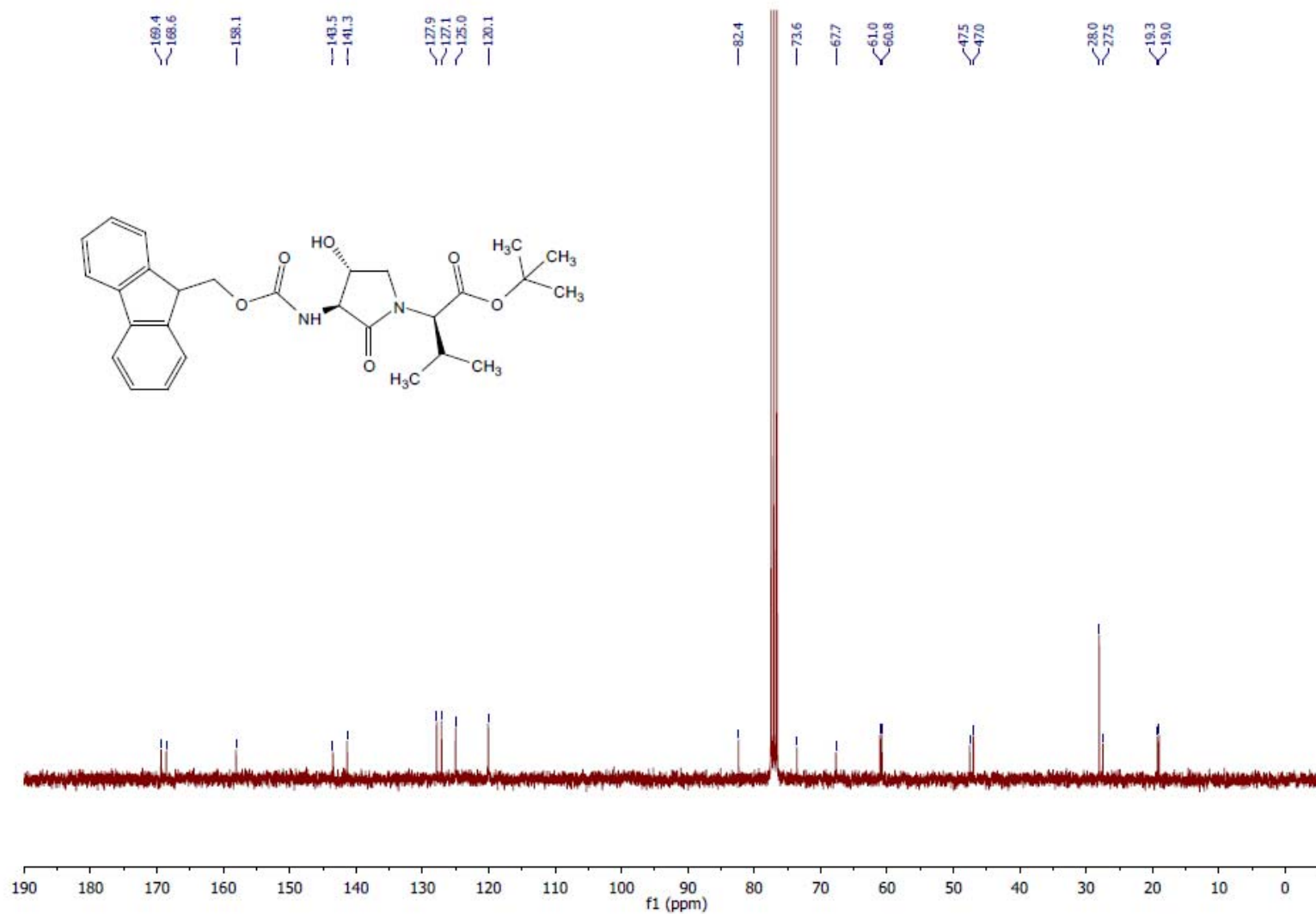
Annex 1: Supporting information of Article 1
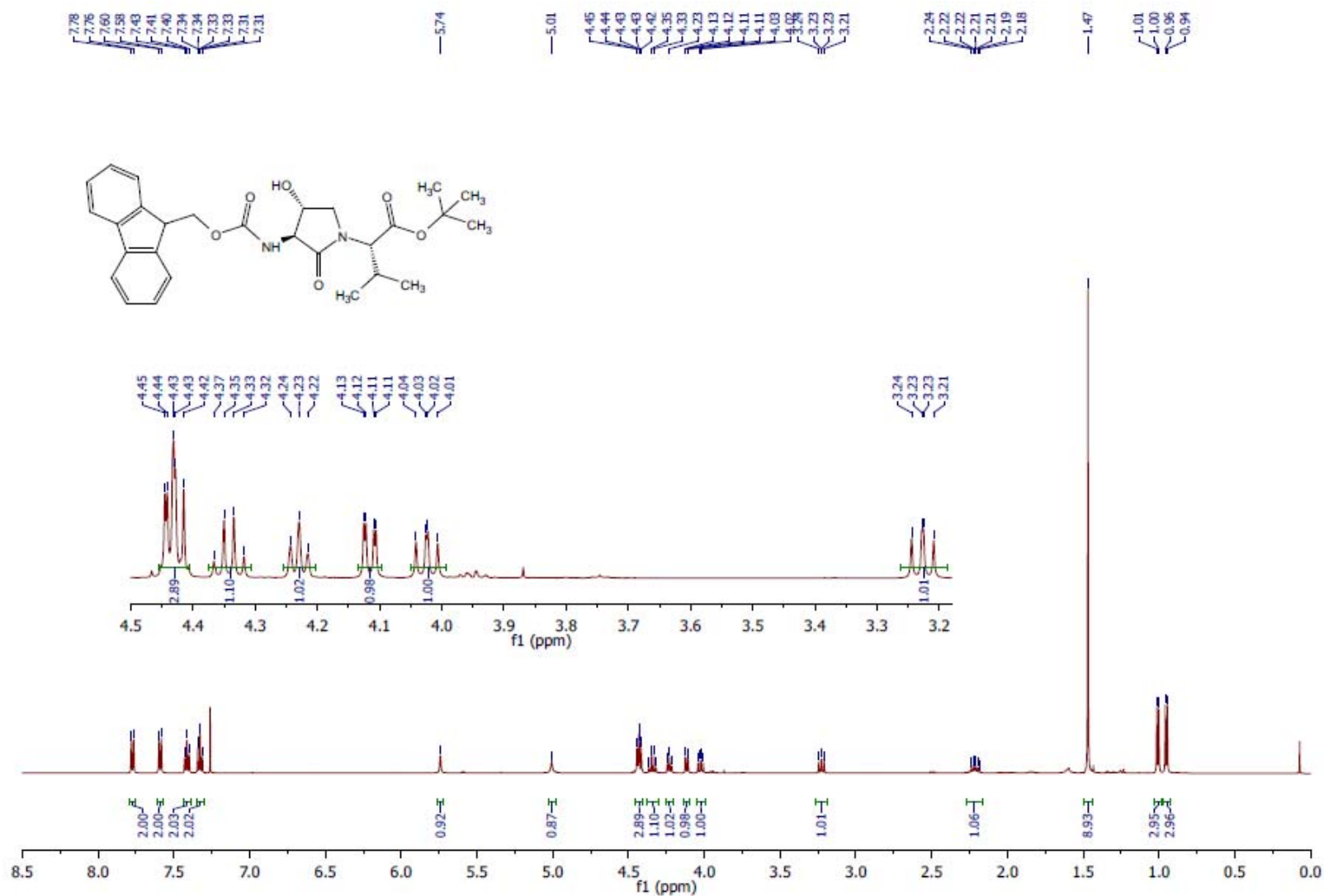
^{13}C NMR (126 MHz, CDCl$_3$) **[(3S, 4R, 2'S)-2.19]**

Annex 1: Supporting information of Article 1
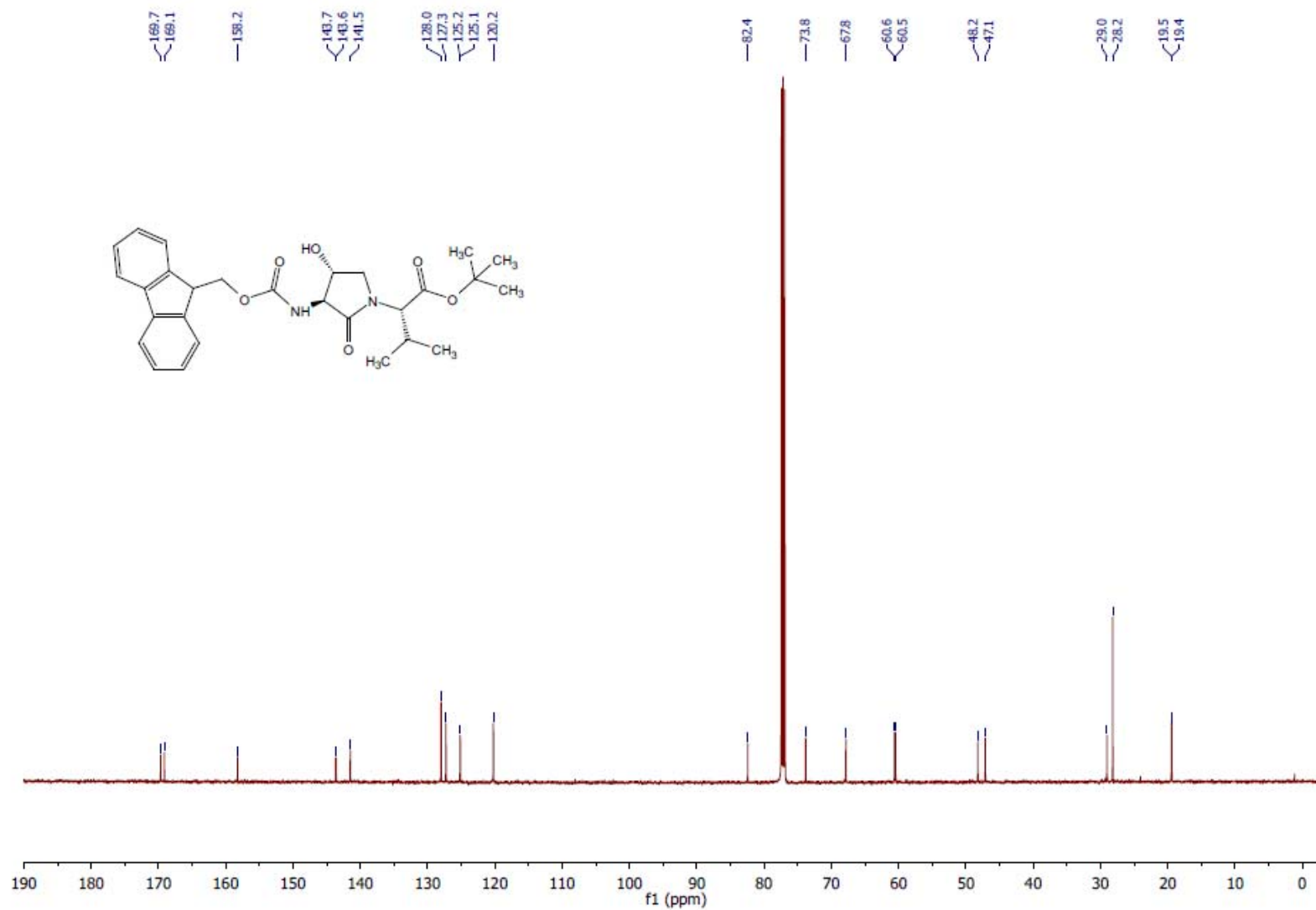
^{1}H NMR (400 MHz, DMSO) [(3*R*, 4*R*, 2'*R*)-2.19]

Annex 1: Supporting information of Article 1

¹³C NMR (75 MHz, CDCl₃) **[(3R, 4R, 2'R)-2.19]**
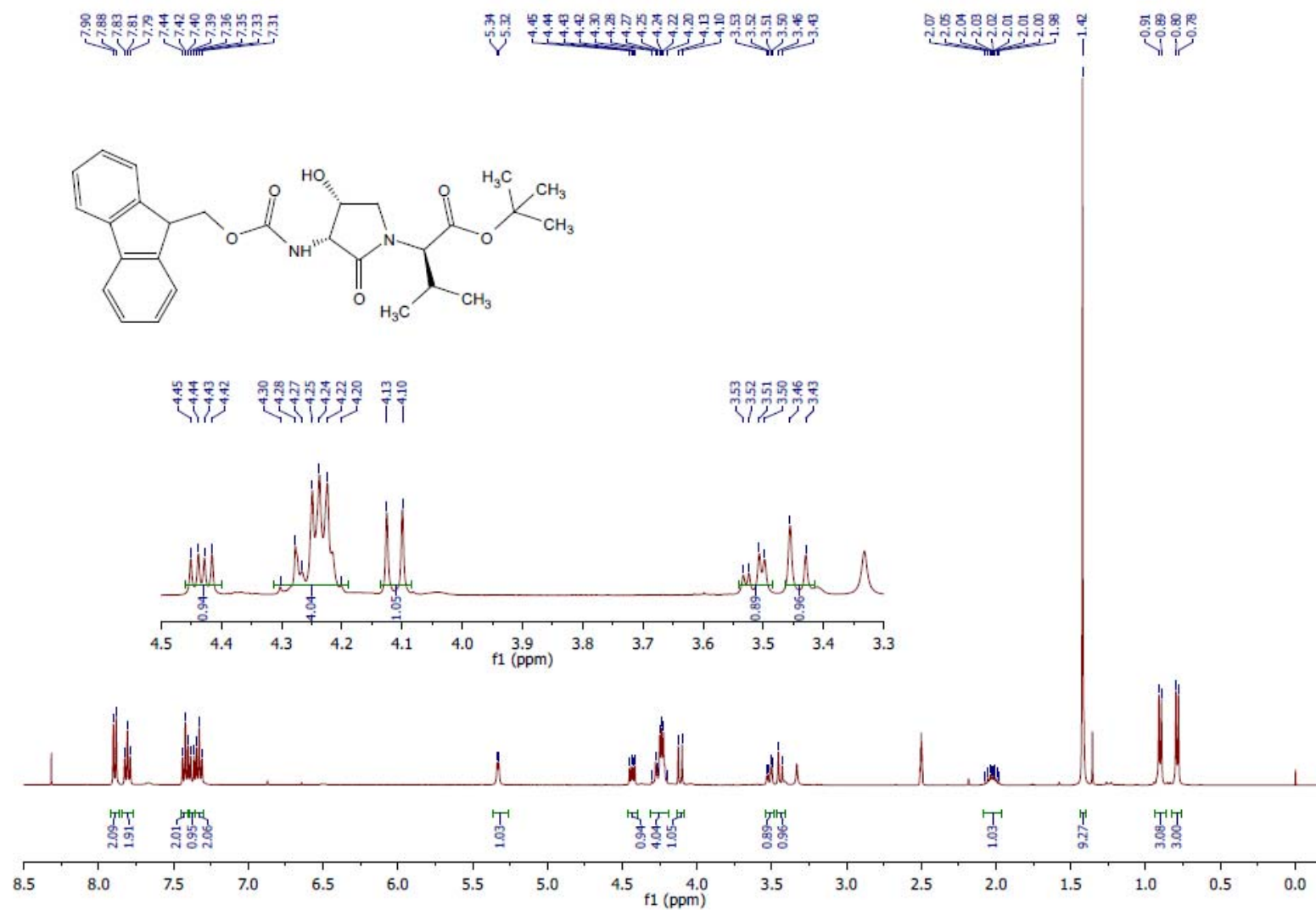
Annex 1: Supporting information of Article 1

¹H NMR (300 MHz, DMSO) **[(3R, 4R, 2'S)-2.19]**
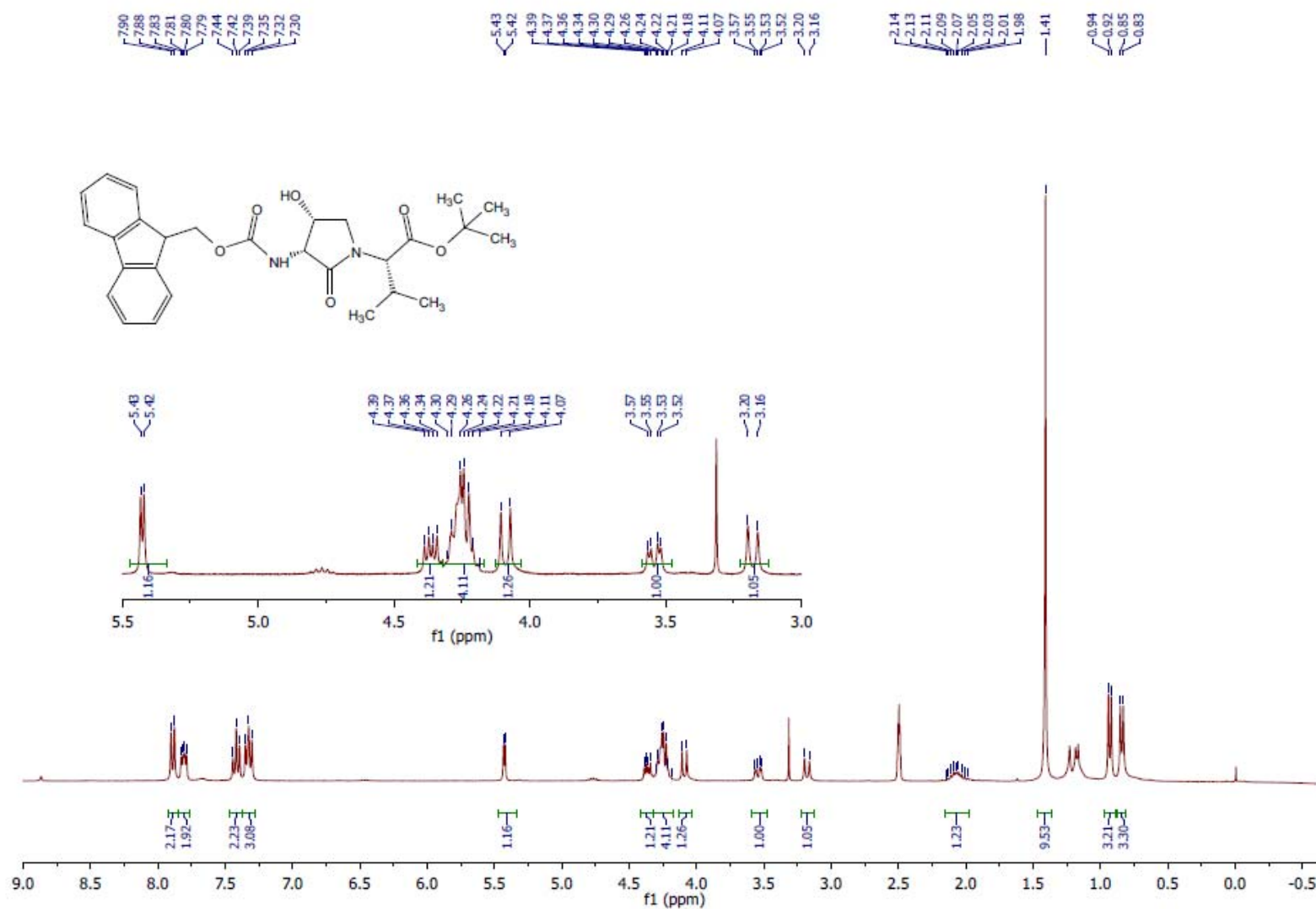
^{13}C NMR (75 MHz, CDCl$_3$) **[(3*R*, 4*R*, 2'*S*)-2.19]**
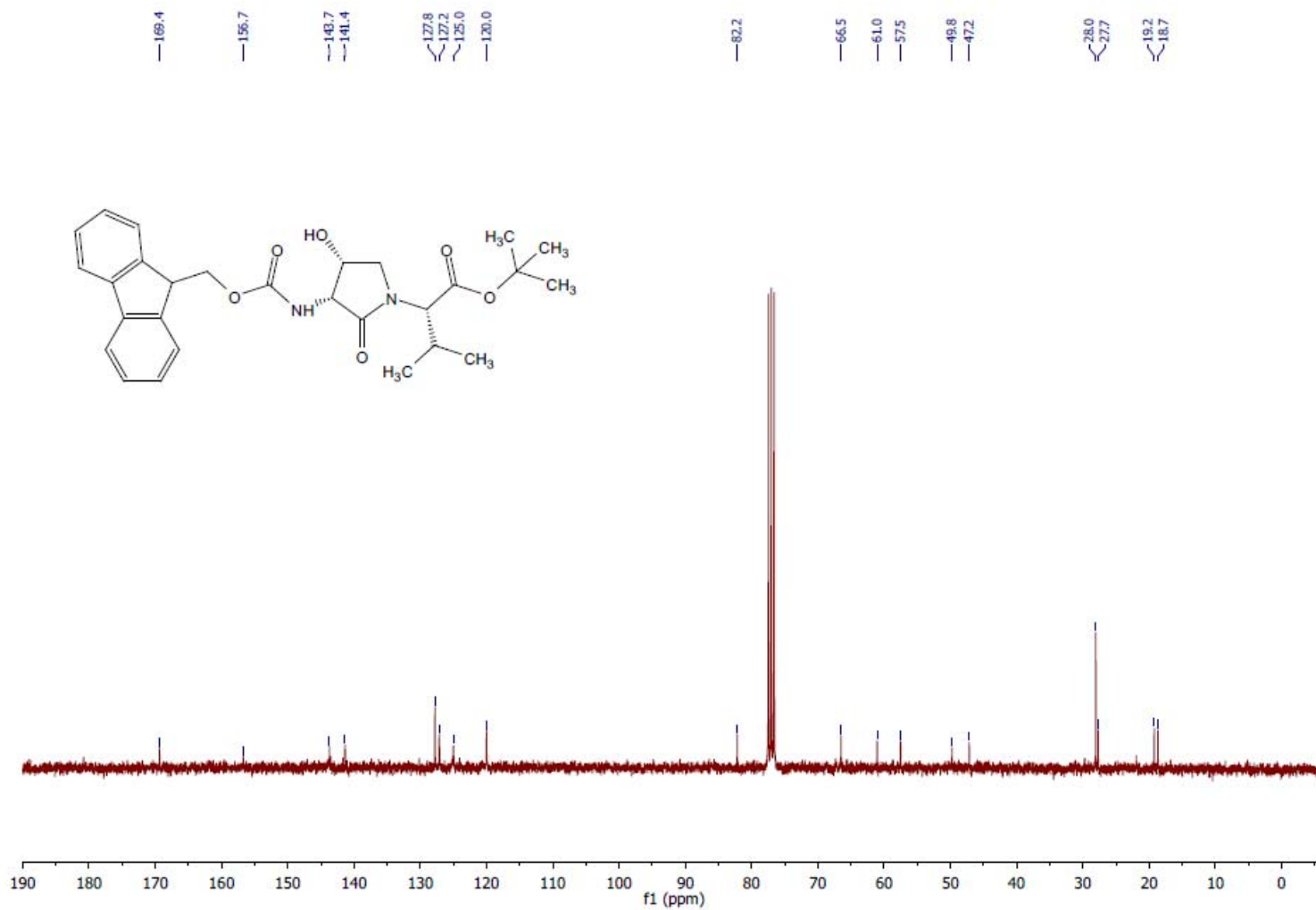
169.4
156.7
143.7
141.4
127.8
127.2
125.0
120.0
82.2
66.5
61.0
57.5
49.8
47.2
28.0
27.7
19.2
18.7
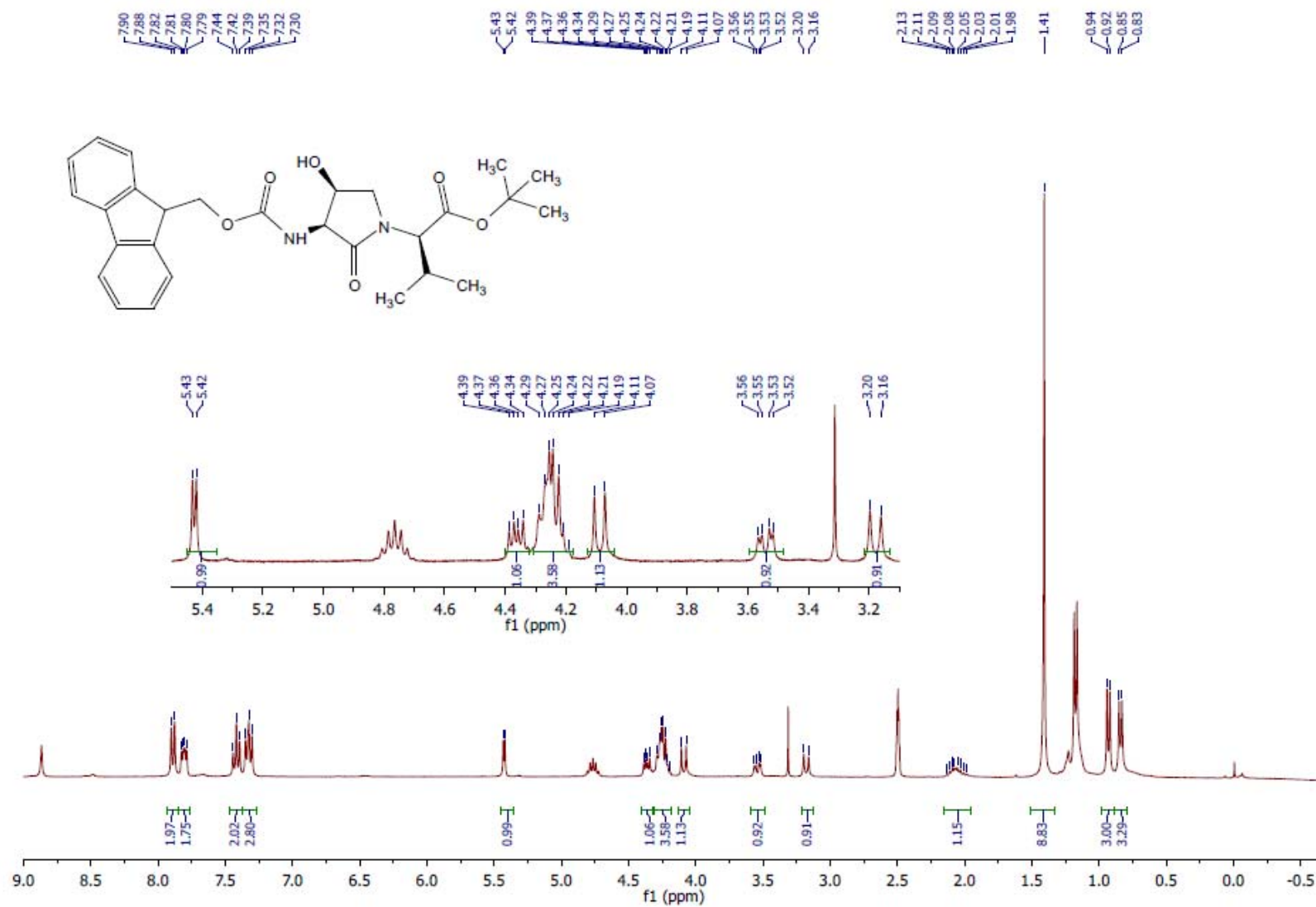
Annex 1: Supporting information of Article 1

^{1}H NMR (300 MHz, CDCl$_3$) **[(3*S*, 4*S*, 2'*R*)-2.19]**

Annex 1: Supporting information of Article 1

^{13}C NMR (75 MHz, CDCl$_3$) **[(3*S*, 4*S*, 2'*R*)-2.19]**

Annex 1: Supporting information of Article 1
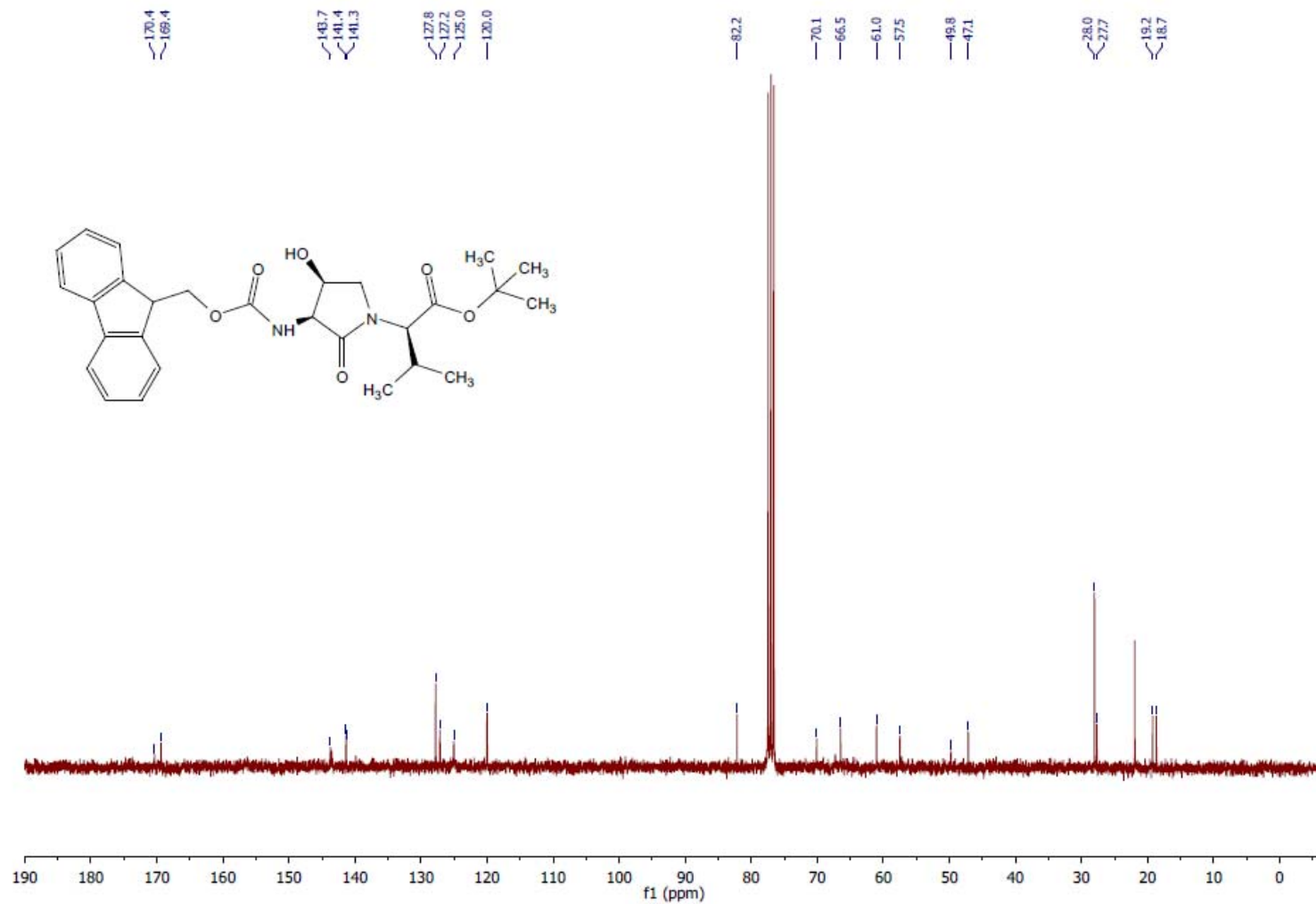
^{1}H NMR (300 MHz, DMSO) **[(3*S*, 4*S*, 2'*S*)-2.19]**
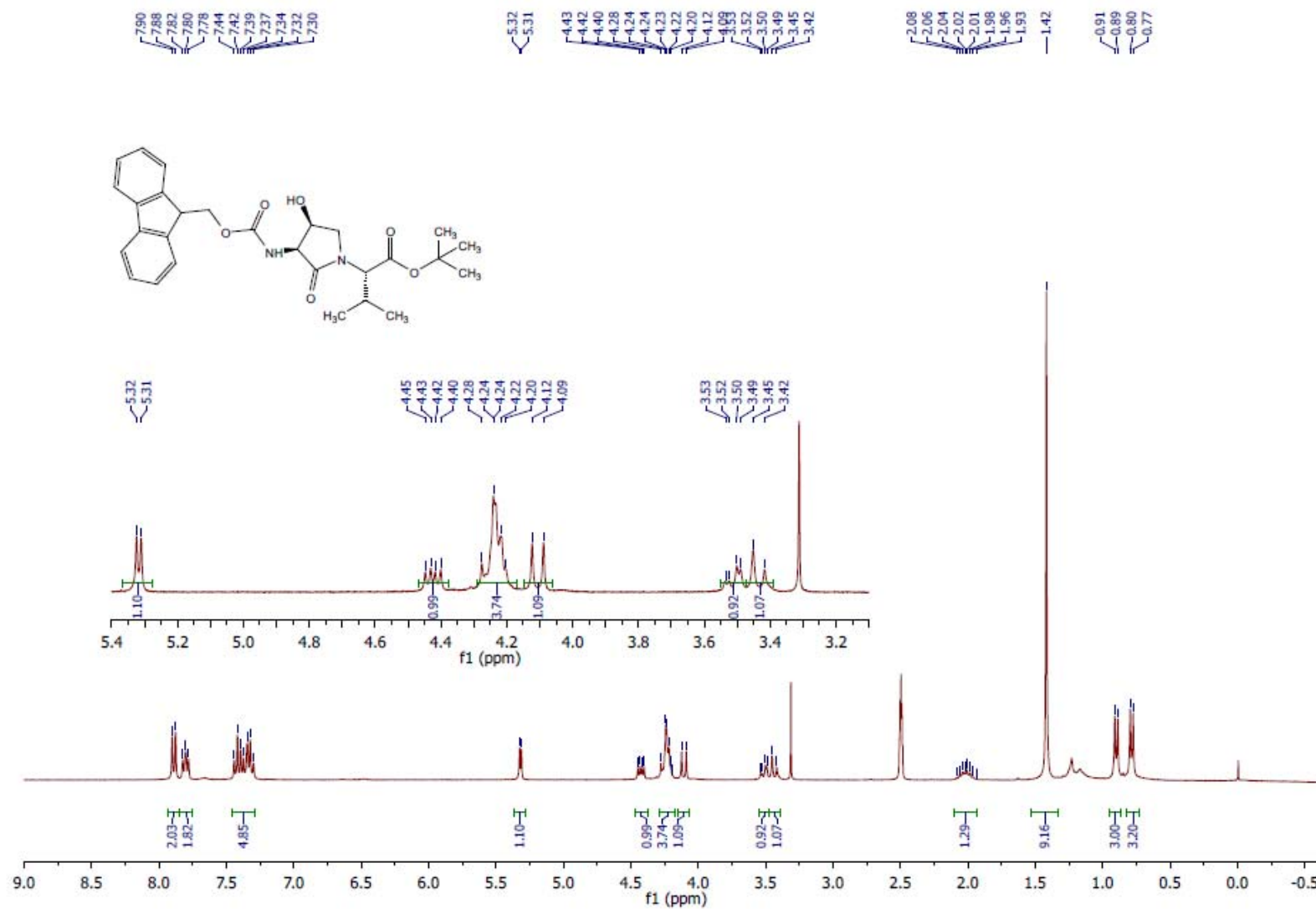
^{13}C NMR (75 MHz, CDCl$_3$) **[(3S, 4S, 2'S)-2.19]**

Annex 1: Supporting information of Article 1

^{1}H NMR (300 MHz, CDCl$_3$) **[(3*R*, 4*R*, 2'*R*-2.20]**
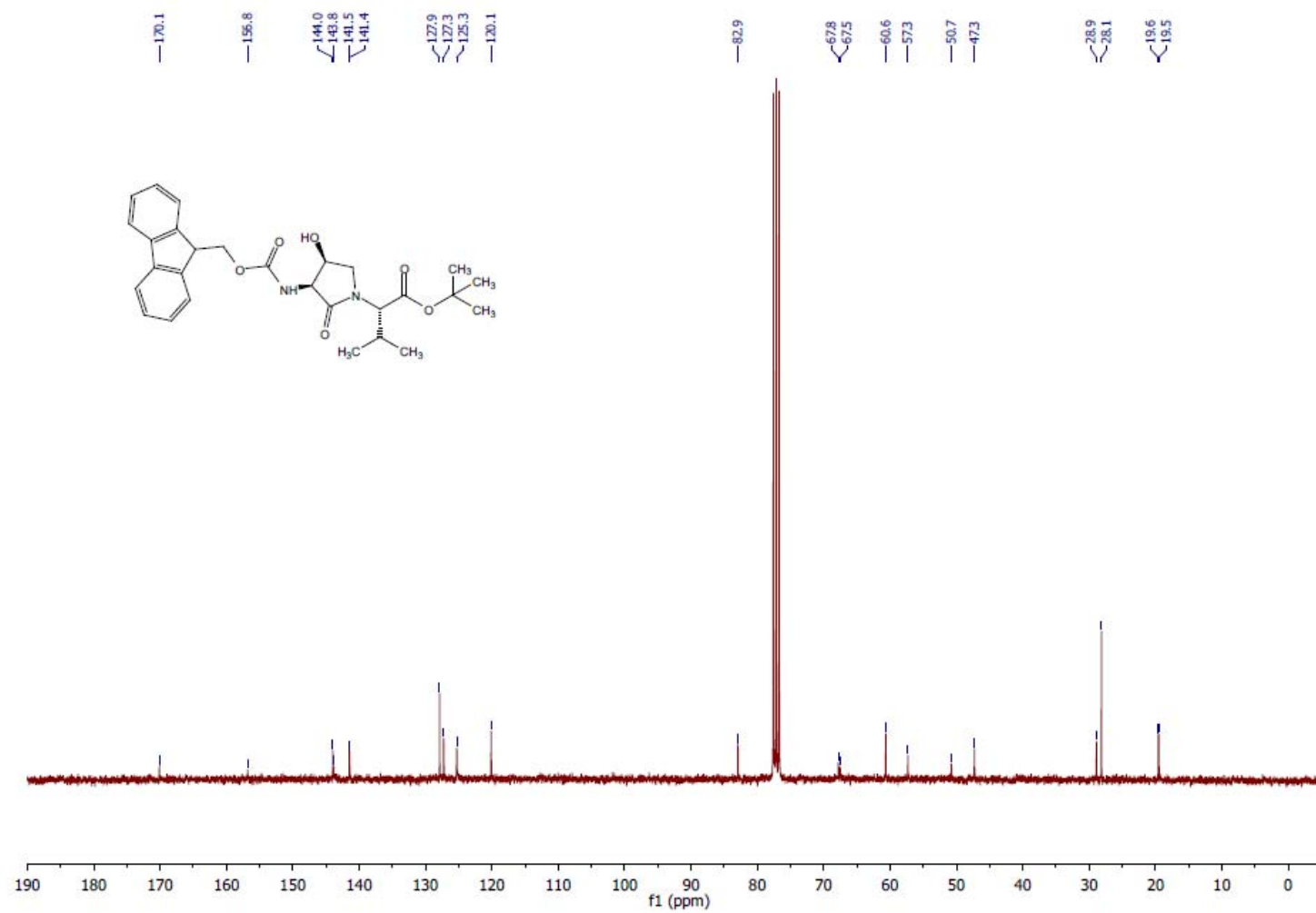
Annex 1: Supporting information of Article 1
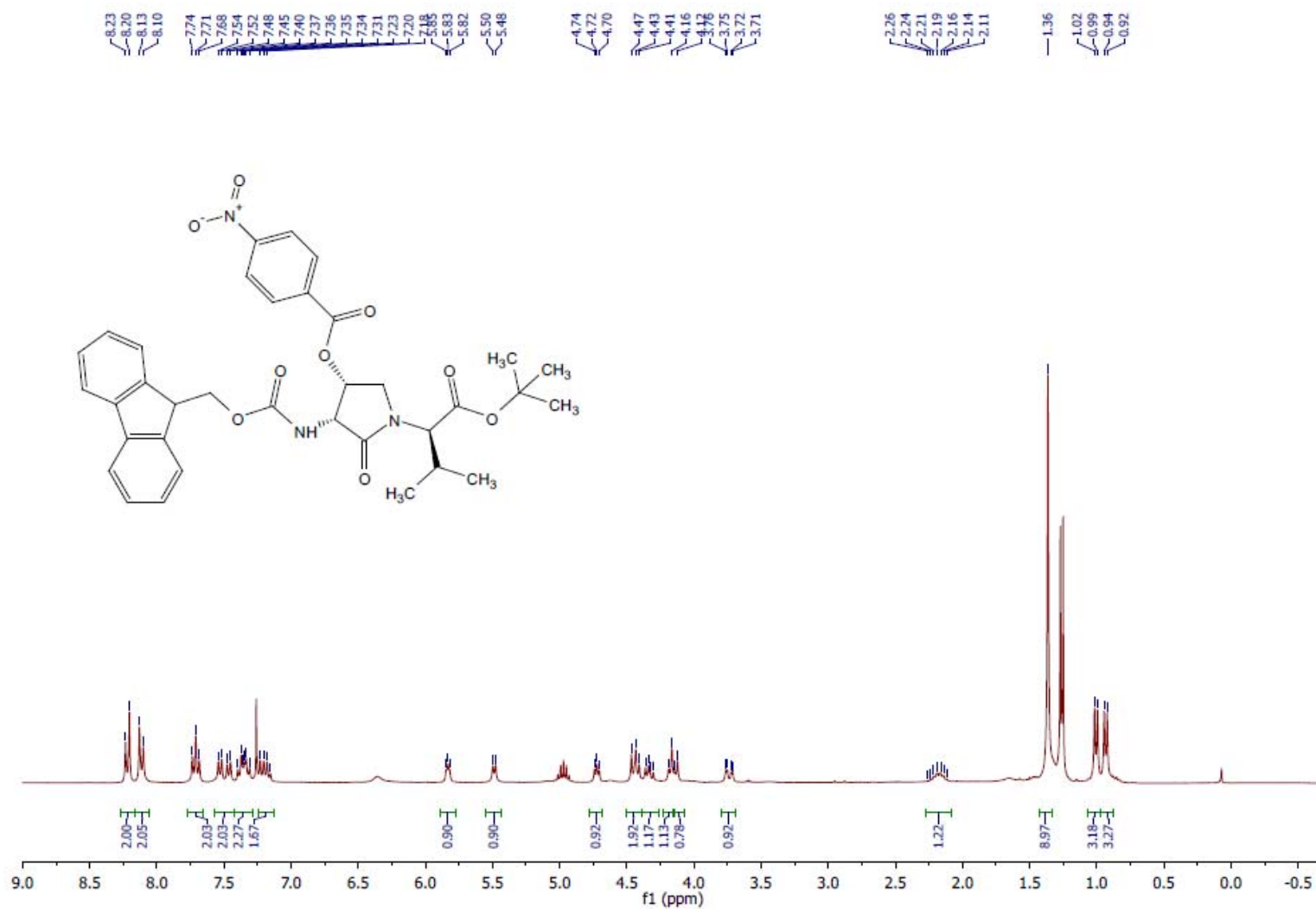
^{13}C NMR (75 MHz, CDCl$_3$) **[(3*R*, 4*R*, 2'*R*)-2.20]**

^{1}H NMR (300 MHz, CDCl$_3$) [(3*R*, 4*R*, 2'*S*)-2.20]

Annex 1: Supporting information of Article 1
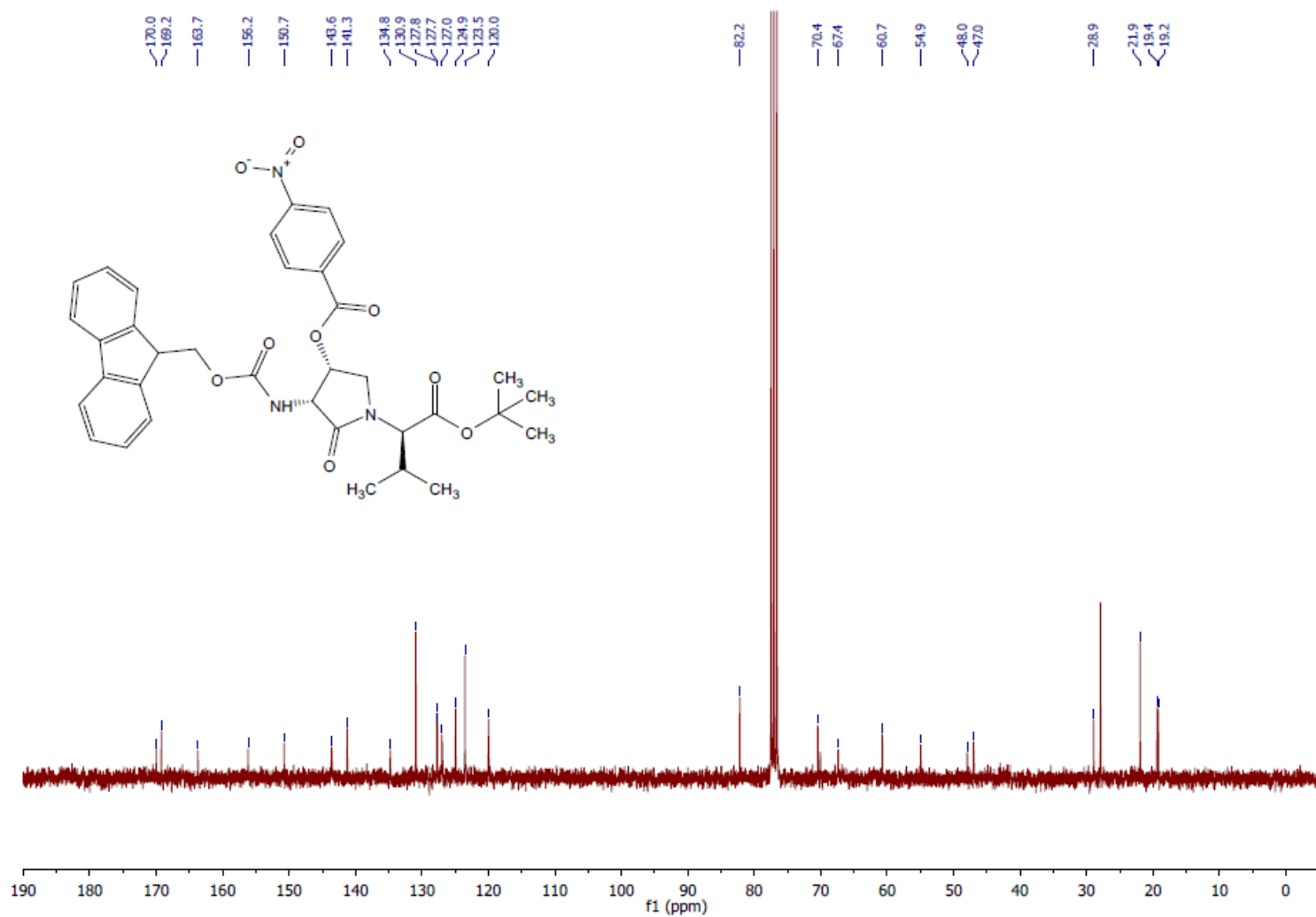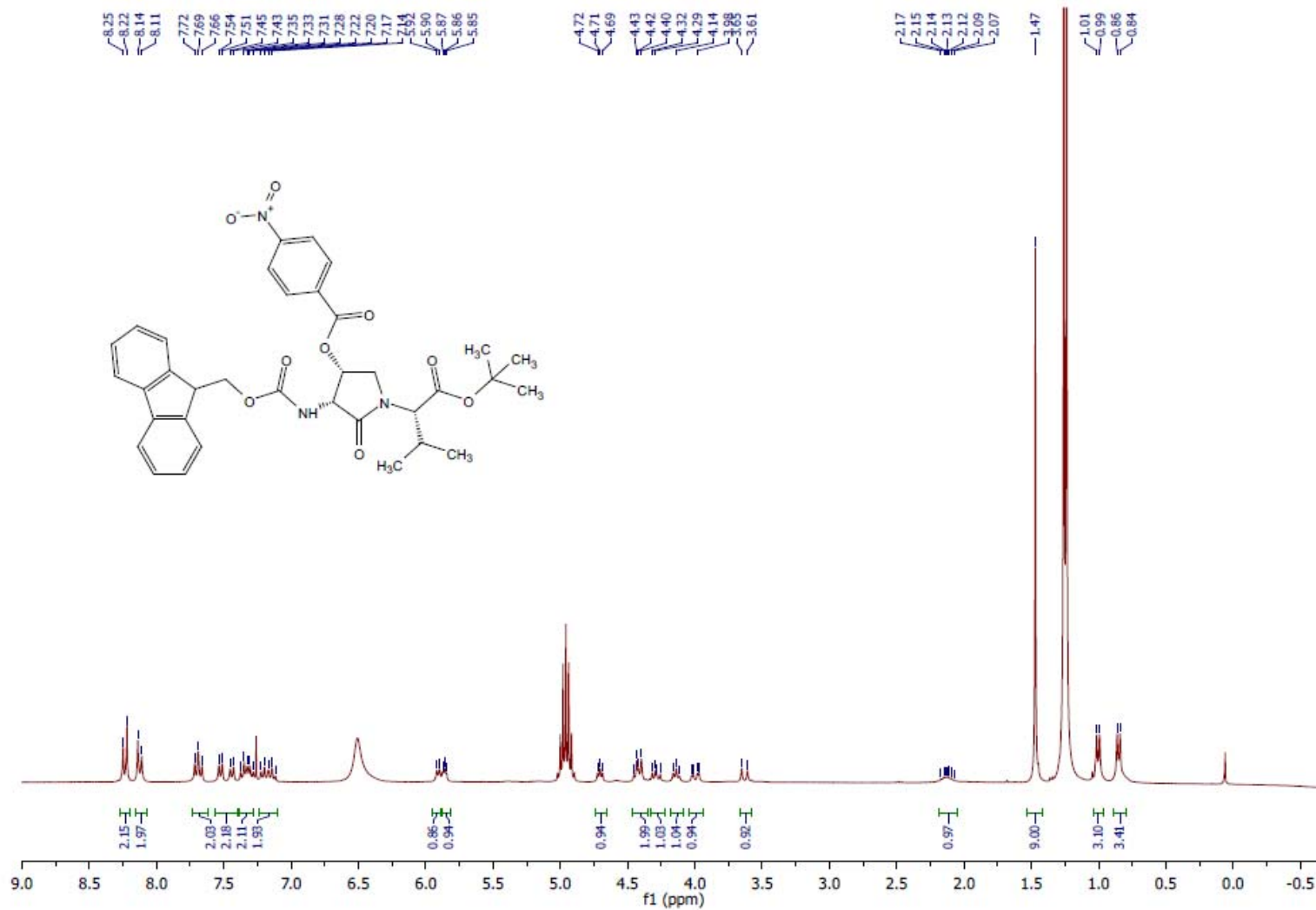
^{13}C NMR (75 MHz, CDCl$_3$) [(3*R*, 4*R*, 2'*S*)-2.20
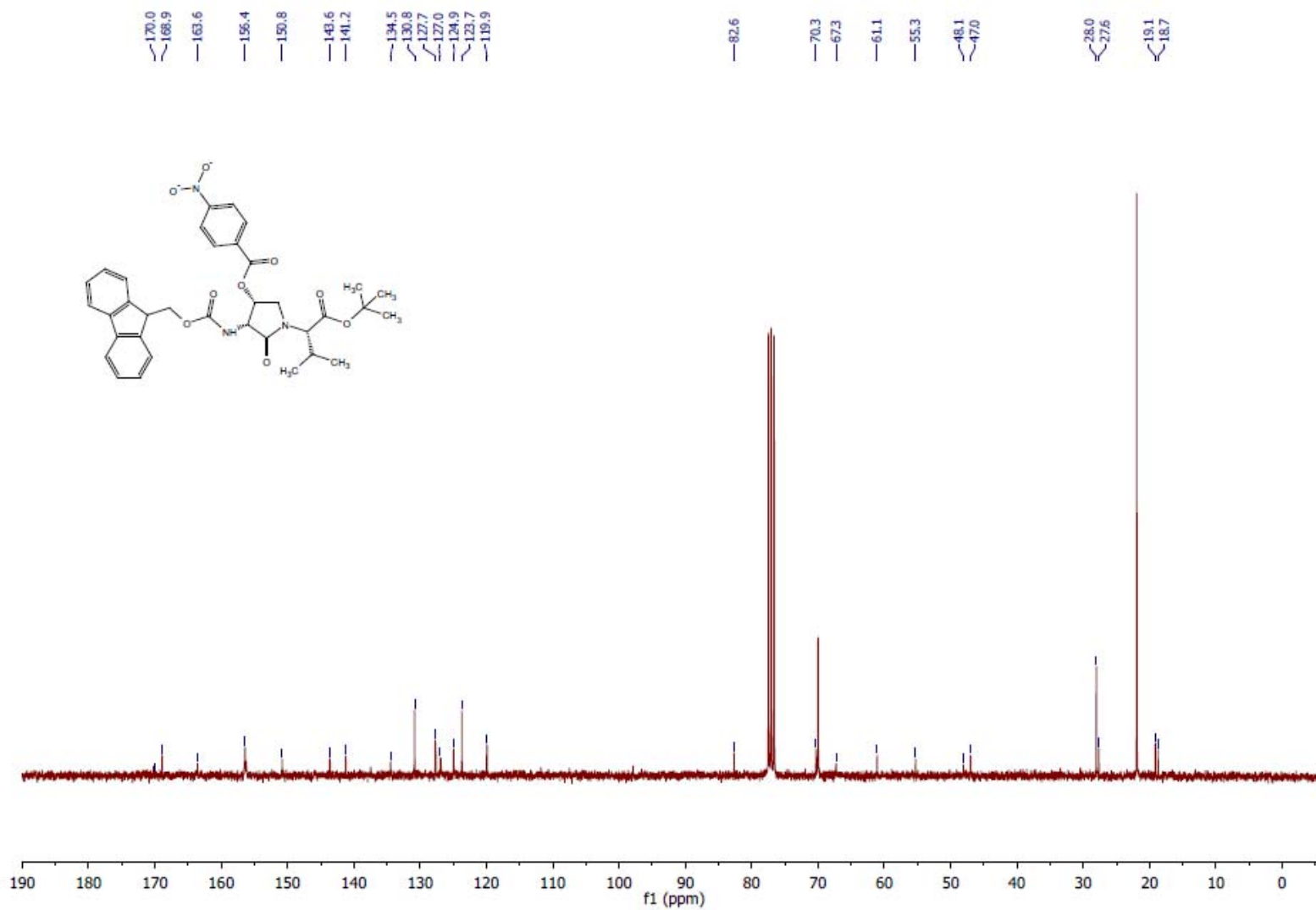
^{1}H NMR (300 MHz, CDCl$_3$) [(3*S*, 4*S*, 2'*R*)-2.20]

^{13}C NMR (75 MHz, CDCl$_3$) **[(3S, 4S, 2'R)-2.20]**

Annex 1: Supporting information of Article 1

^{1}H NMR (300 MHz, CDCl$_3$) [(3*S*, 4*S*, 2'*S*)-2.20]

Annex 1: Supporting information of Article 1
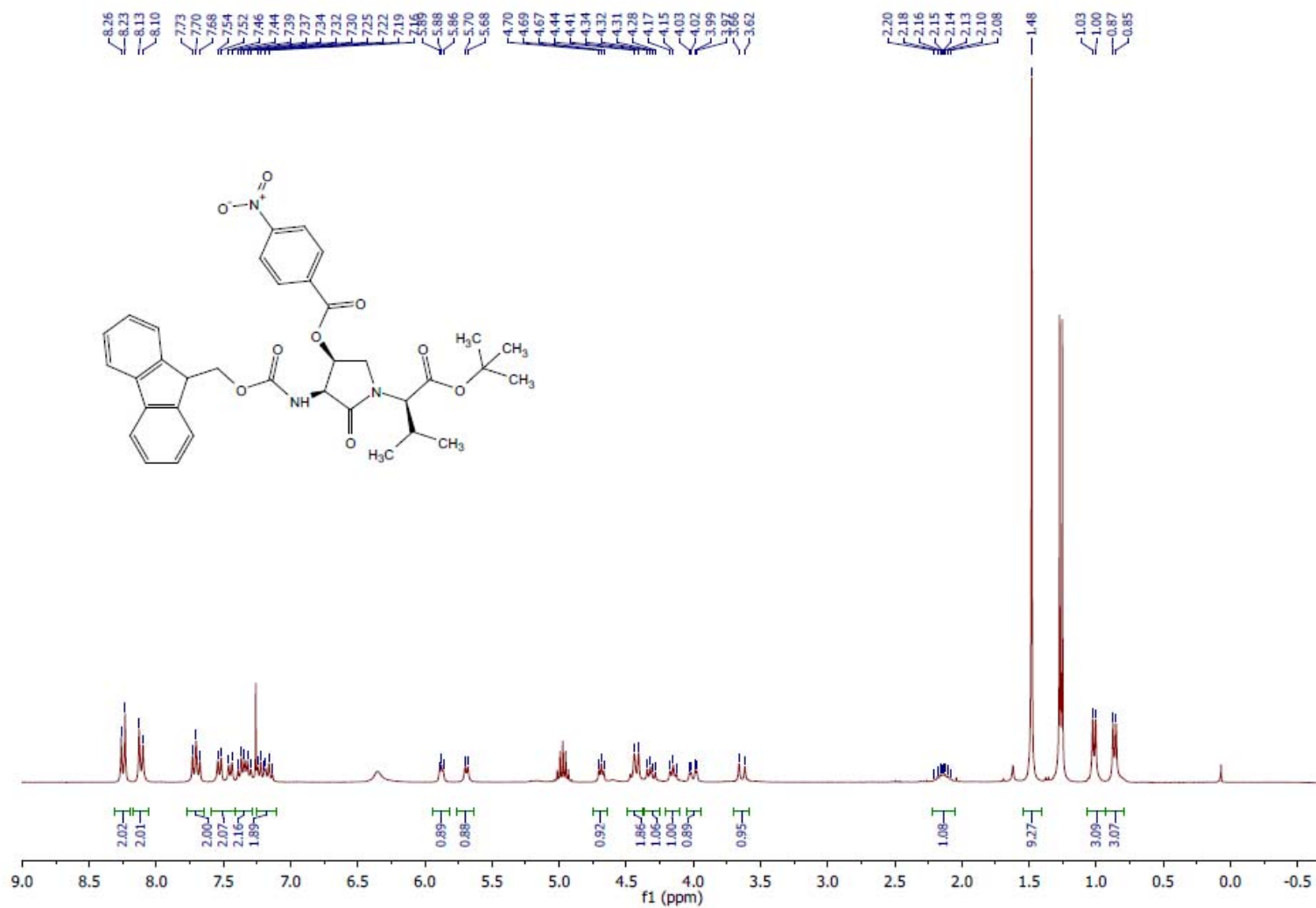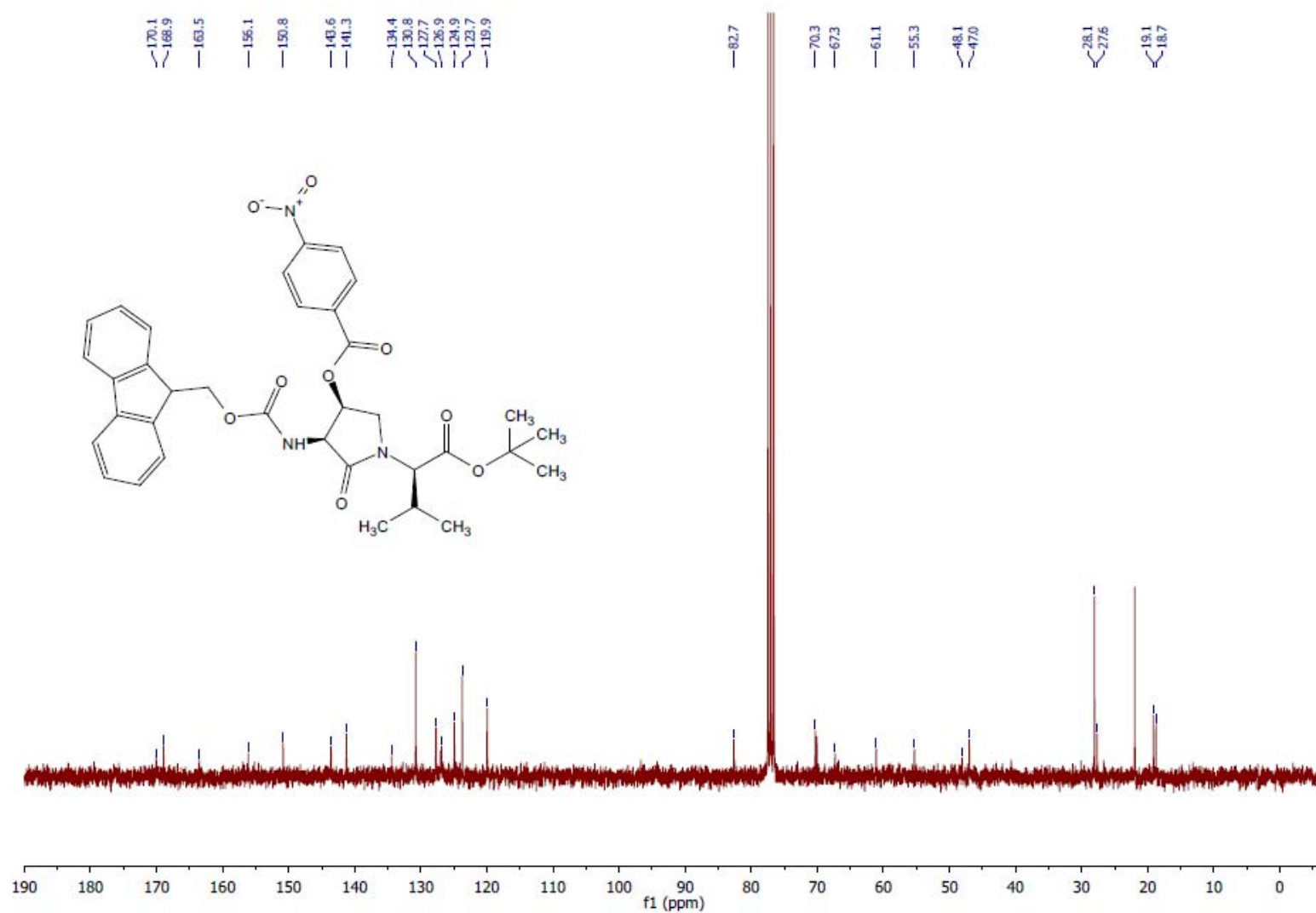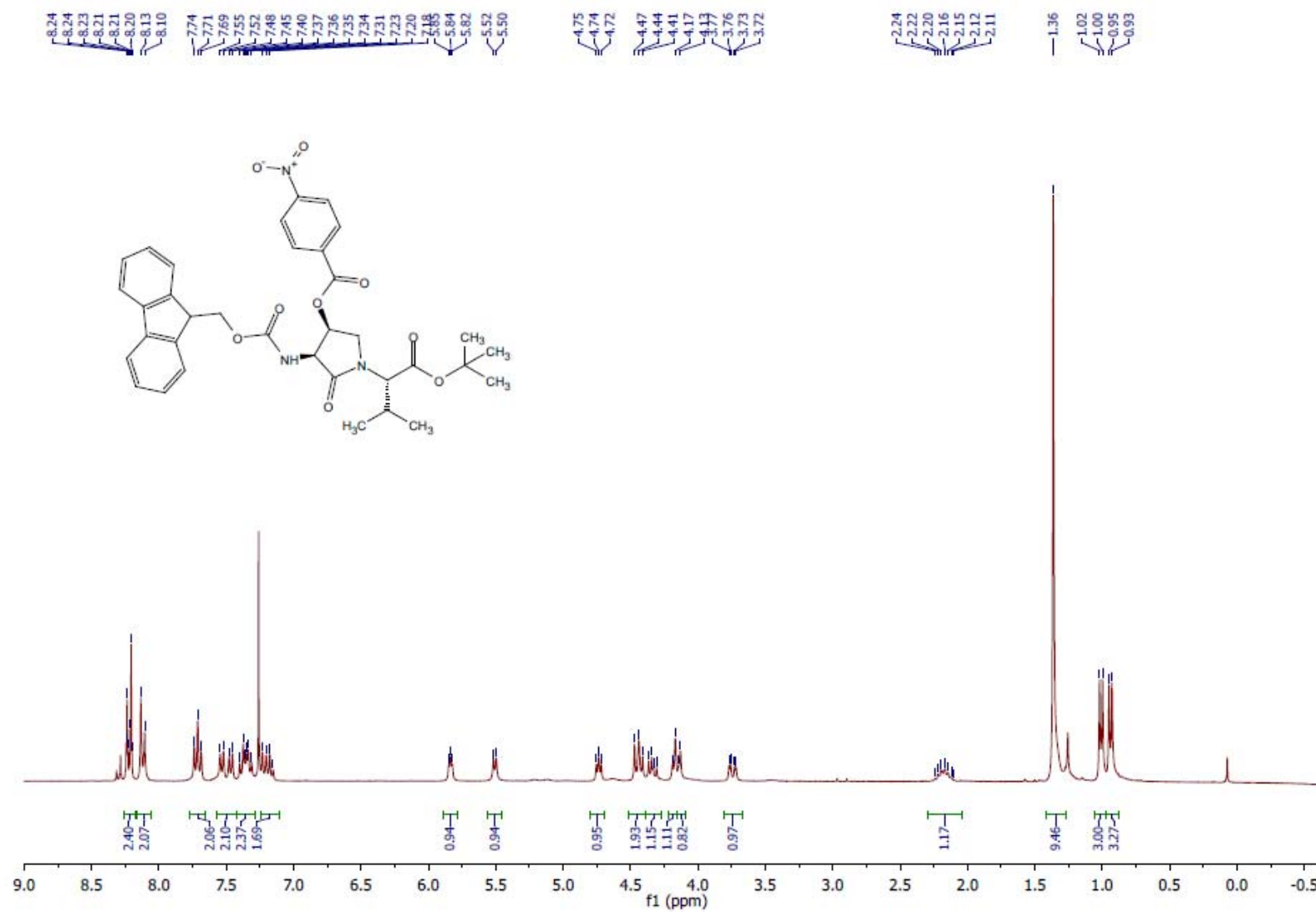
^{13}C NMR (75 MHz, CDCl$_3$) **[(3S, 4S, 2'S)-2.20]**
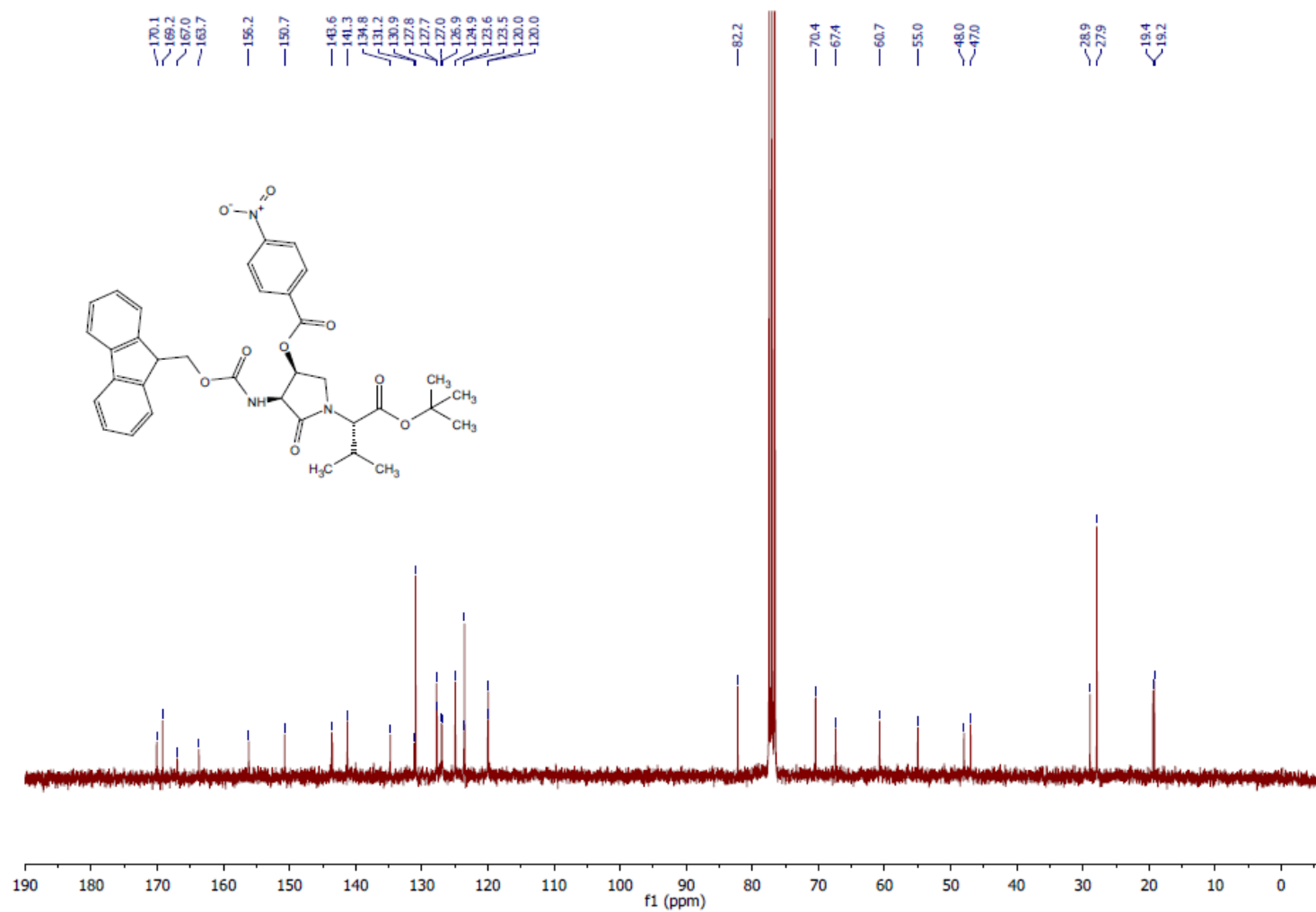
[(3R)-AgI³]-101.10 [(3R, 2'R)-2.5]

[(3R, 2'R)-2.5] LCMS chromatogram [10-90% MeOH (0.1% FA)/water (0.1% FA), 14 min]; RT = 8 on a Sunfire C18 analytical column (100Å, 3.5 μm, 4.6 mm X 100 mm).
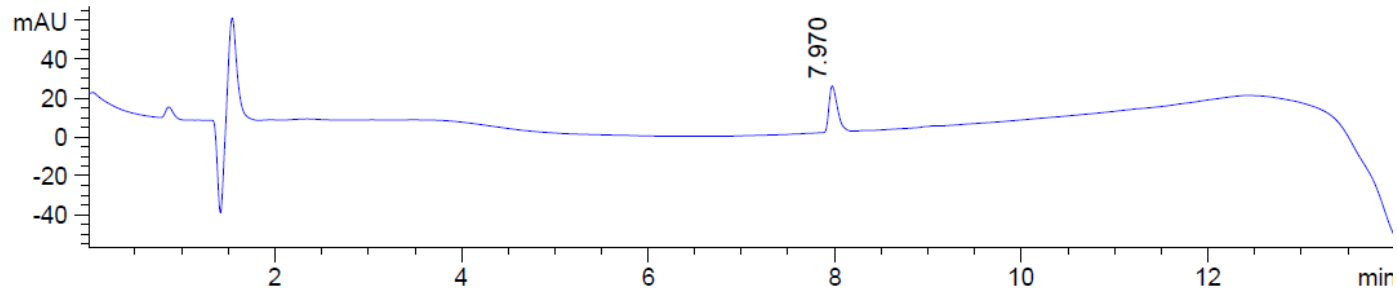
[(3R, 2'R)-2.5] LCMS chromatogram [10-90% MeCN (0.1% FA)/water (0.1% FA), 14 min]; RT = 5.6 on a Sunfire C18 analytical column (100Å, 3.5 μm, 4.6 mm X 100 mm).

Annex 1: Supporting information of Article 1
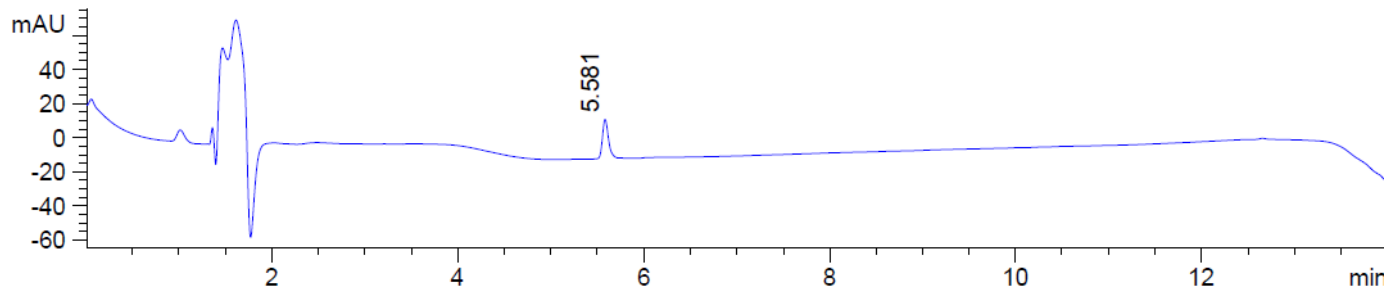
[(3R)-Agl³-L-Val]-2.1 [(3R, 2'S)-2.5]
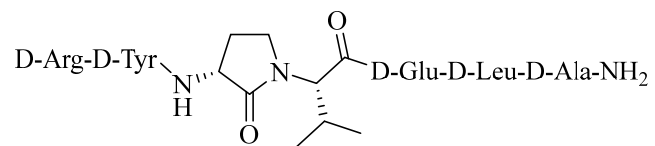
[(3R, 2'S)-2.5] LCMS chromatogram [10-90% MeOH (0.1% FA)/water (0.1% FA), 14 min]; RT = 7.6 on a Sunfire C18 analytical column (100Å, 3.5 μm, 4.6 mm X 100 mm).
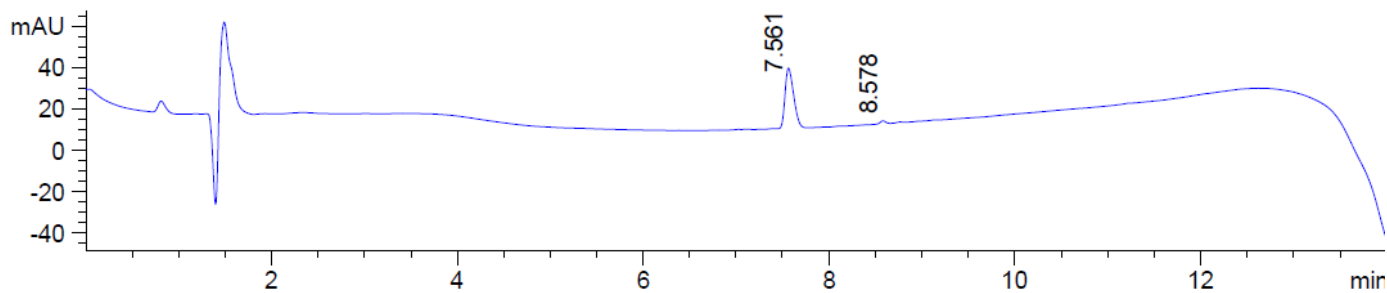
[(3R, 2'S)-2.5] LCMS chromatogram [10-90% MeCN (0.1% FA)/water (0.1% FA), 14 min]; RT = 5.3 on a Sunfire C18 analytical column (100Å, 3.5 μm, 4.6 mm X 100 mm).
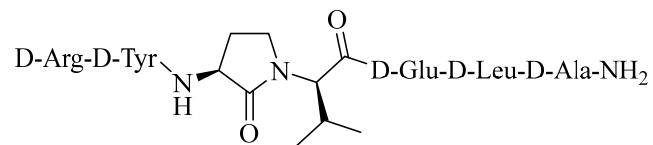
Annex 1: Supporting information of Article 1

[(3*S*)-AgI³]-2.1 [(3*S*, 2'*R*)-2.5]

[(3*S*, 2'*R*)-2.5] LCMS chromatogram [10-90% MeOH (0.1% FA)/water (0.1% FA), 14 min]; RT = 8 on a Sunfire C18 analytical column (100Å, 3.5 μm, 4.6 mm X 100 mm).

[(3*S*, 2'*R*)-2.5] LCMS chromatogram [10-90% MeCN (0.1% FA)/water (0.1% FA), 14 min]; RT = 5.4 on a Sunfire C18 analytical column (100Å, 3.5 μm, 4.6 mm X 100 mm).

Annex 1: Supporting information of Article 1
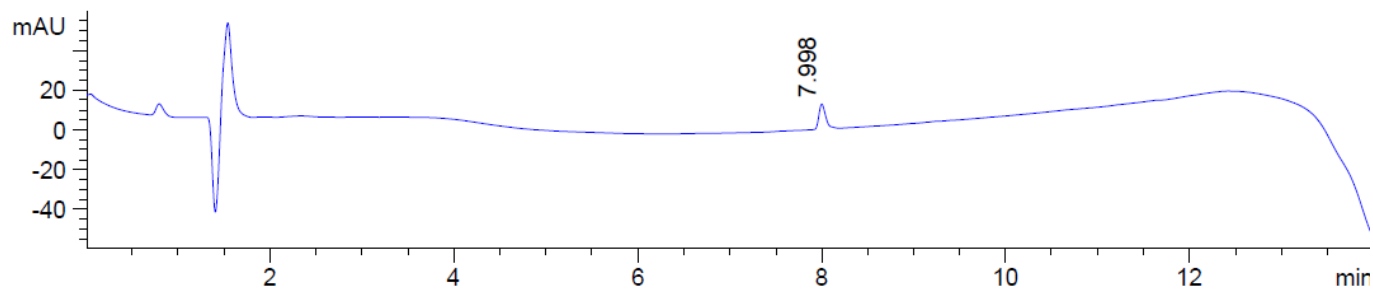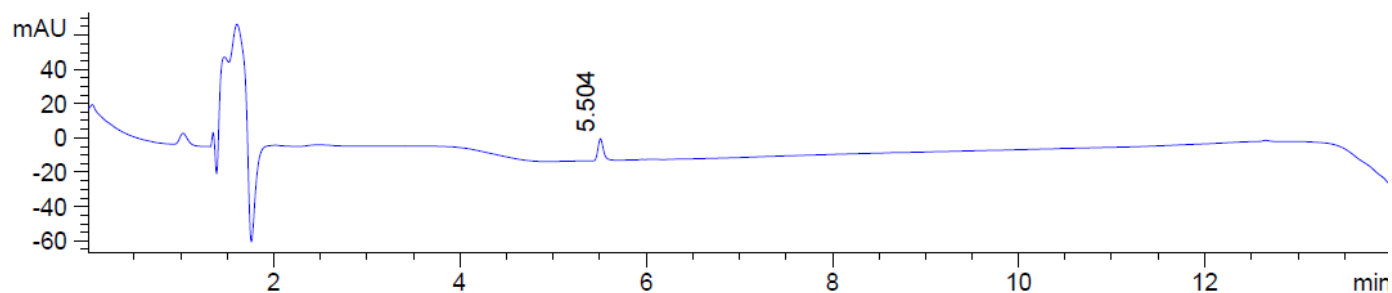
[(3*S*)-AgI³-L-Val]-2.1 [(3*S*, 2'*S*)-2.5]
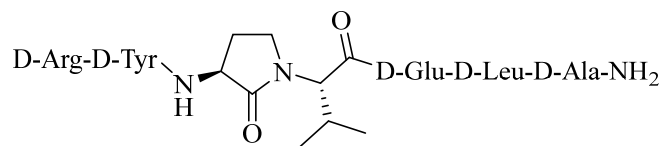
[(3*S*, 2'*S*)-2.5] LCMS chromatogram [10-90% MeOH (0.1% FA)/water (0.1% FA), 10 min]; RT = 7.9 on a Sunfire C18 analytical column (100Å, 3.5 μm, 4.6 mm X 100 mm).
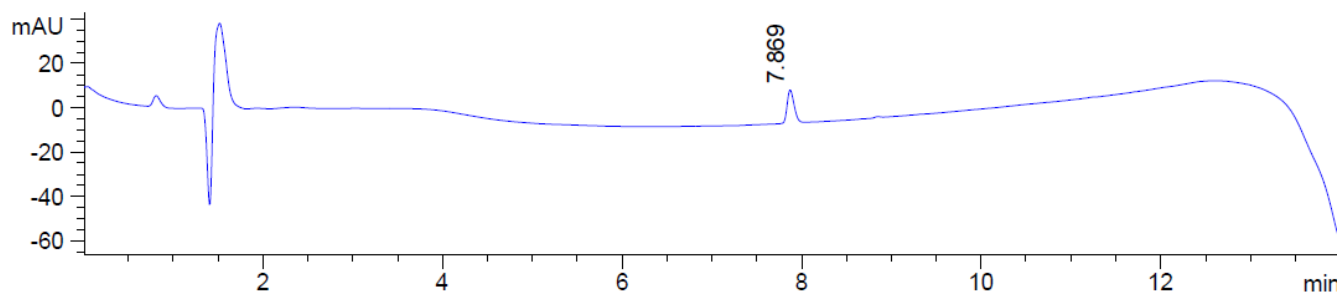
[(3*S*, 2'*S*)-2.5] LCMS chromatogram [10-90% MeCN (0.1% FA)/water (0.1% FA), 14 min]; RT = 5.5 on a Sunfire C18 analytical column (100Å, 3.5 μm, 4.6 mm X 100 mm).
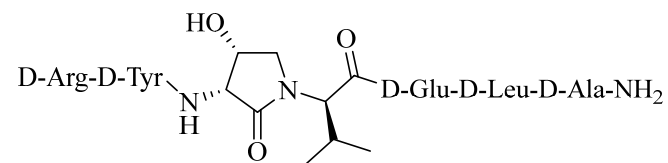
Annex 1: Supporting information of Article 1

[(3*R*, 4*R*)-Hgl³]-2.1 [(3*R*, 4*R*, 2'*R*)-2.6]

[(3*R*, 4*R*, 2'*R*)-2.6] LCMS chromatogram [10-90% MeOH (0.1% FA)/water (0.1% FA), 14 min]; RT = 7.8 on a Sunfire C18 analytical column (100Å, 3.5 µm, 4.6 mm X 100 mm).

[(3*R*, 4*R*, 2'*R*)-2.6] LCMS chromatogram [10-90% MeCN (0.1% FA)/water (0.1% FA), 14 min]; RT = 5.4 on a Sunfire C18 analytical column (100Å, 3.5 µm, 4.6 mm X 100 mm).

Annex 1: Supporting information of Article 1
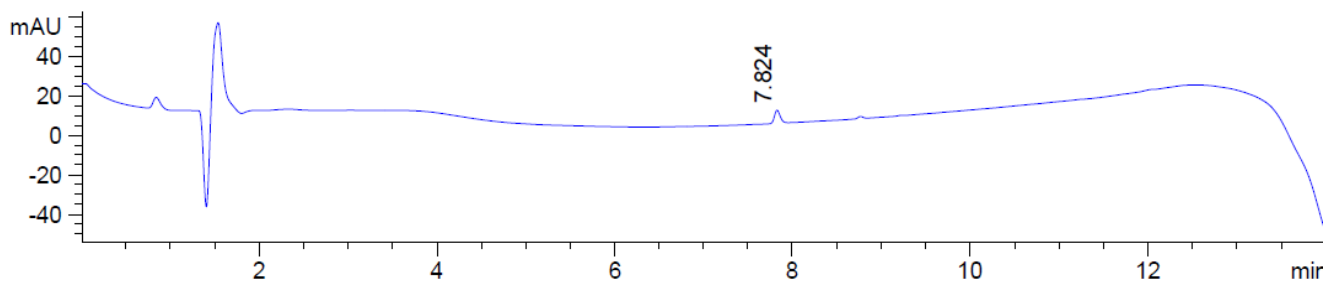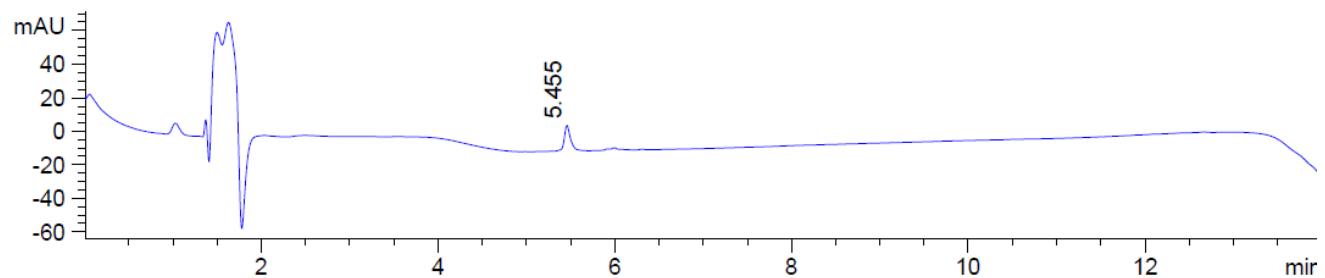
[(3*R*, 4*S*)-Hgl³]-2.1 [(3*R*, 4*S*, 2'*R*)-2.6]
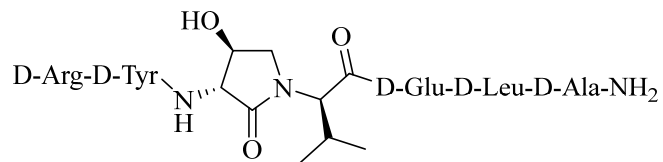
[(3*R*, 4*S*, 2'*R*)-2.6] LCMS chromatogram [10-90% MeOH (0.1% FA)/water (0.1% FA), 14 min]; RT = 7.5 on a Sunfire C18 analytical column (100Å, 3.5 µm, 4.6 mm X 100 mm).
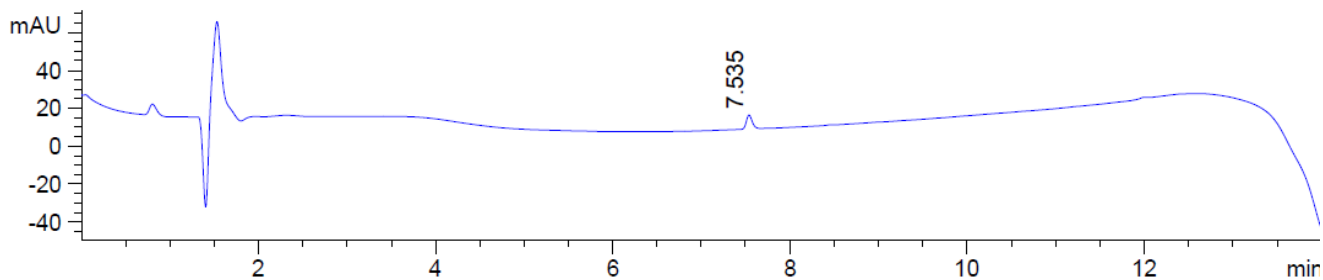
[(3*R*, 4*S*, 2'*R*)-2.6] LCMS chromatogram [10-90% MeCN (0.1% FA)/water (0.1% FA), 14 min]; RT = 5.2 on a Sunfire C18 analytical column (100Å, 3.5 µm, 4.6 mm X 100 mm).

Annex 1: Supporting information of Article 1
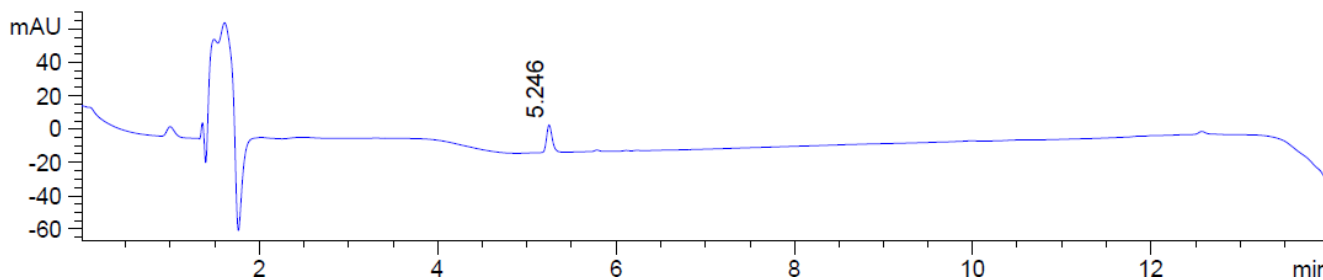
[(3*R*, 4*R*)-Hgl³-(*S*)-Val]-2.1 [(3*R*, 4*R*, 2'*S*)-2.6]
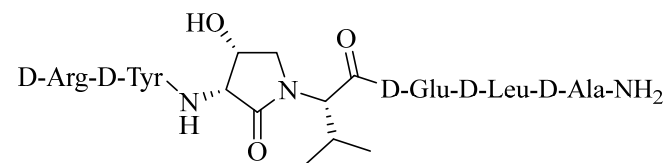
[(3*R*, 4*R*, 2'*S*)-2.6] LCMS chromatogram [10-90% MeOH (0.1% FA)/water (0.1% FA), 14 min]; RT = 6.8 on a Sunfire C18 analytical column (100Å, 3.5 μm, 4.6 mm X 100 mm).
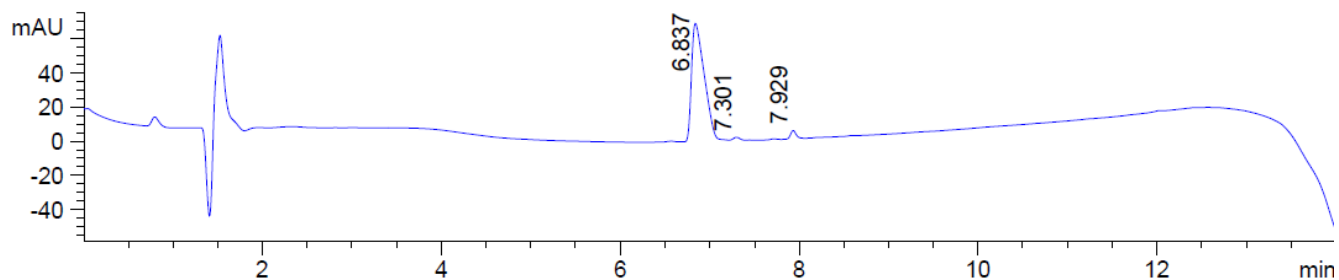
[(3*R*, 4*R*, 2'*S*)-2.6] LCMS chromatogram [10-90% MeCN (0.1% FA)/water (0.1% FA), 14 min]; RT = 4.9 on a Sunfire C18 analytical column (100Å, 3.5 μm, 4.6 mm X 100 mm).

Annex 1: Supporting information of Article 1
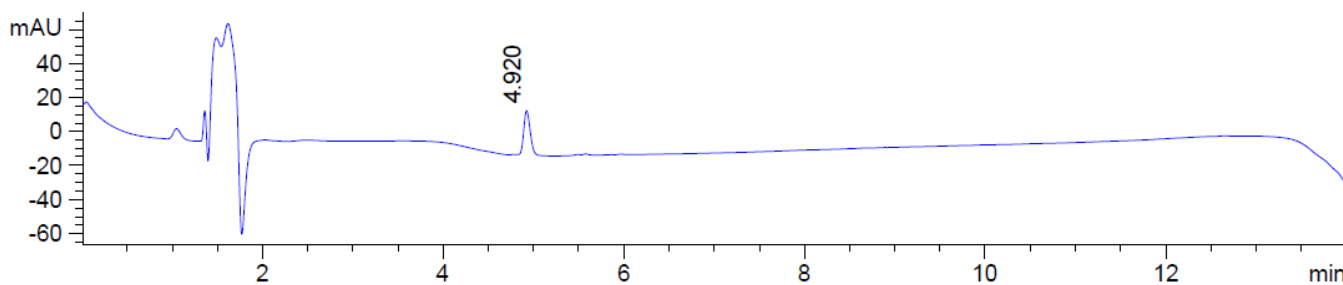
[(3*R*, 4*S*)-Hgl³-(*S*)-Val]-2.1 [(3*R*, 4*S*, 2'*S*)-2.6]
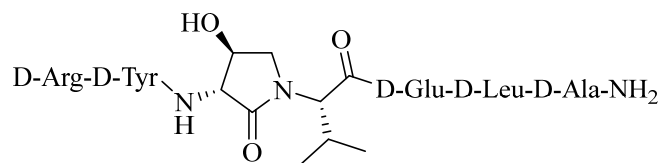
[(3*R*, 4*S*, 2'*S*)-2.6] LCMS chromatogram [10-90% MeOH (0.1% FA)/water (0.1% FA), 14 min]; RT = 6.9 on a Sunfire C18 analytical column (100Å, 3.5 µm, 4.6 mm X 100 mm).
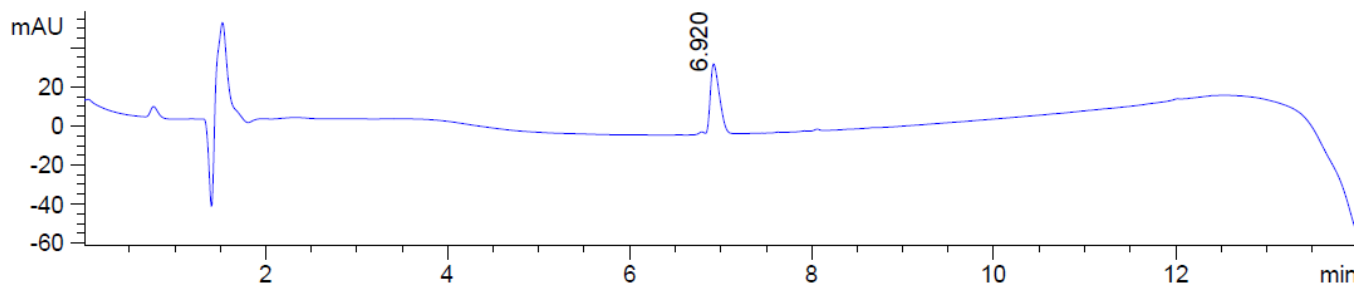
[(3*R*, 4*S*, 2'*S*)-2.6] LCMS chromatogram [10-90% MeCN (0.1% FA)/water (0.1% FA), 14 min]; RT = 4.9 on a Sunfire C18 analytical column (100Å, 3.5 µm, 4.6 mm X 100 mm).

Annex 1: Supporting information of Article 1
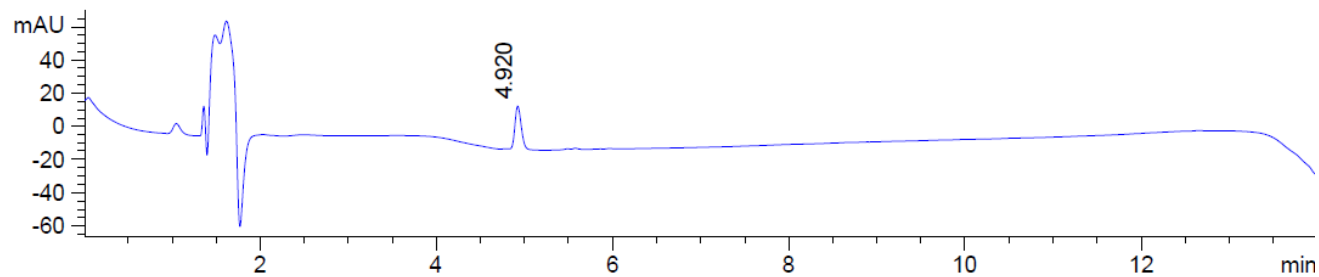
[(3S, 4R)-Hgl³]-2.1 [(3S, 4R, 2'R)-2.6]
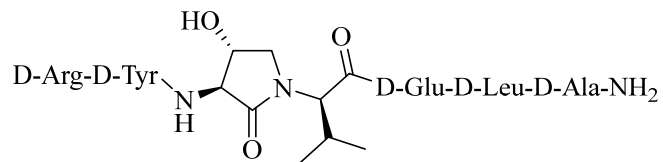
[(3S, 4R, 2'R)-2.6] LCMS chromatogram [10-90% MeOH (0.1% FA)/water (0.1% FA), 14 min]; RT = 7.8 on a Sunfire C18 analytical column (100Å, 3.5 μm, 4.6 mm X 100 mm).

[(3S, 4R, 2'R)-2.6] LCMS chromatogram [10-90% MeCN (0.1% FA)/water (0.1% FA), 14 min]; RT = 5.4 on a Sunfire C18 analytical column (100Å, 3.5 μm, 4.6 mm X 100 mm).

Annex 1: Supporting information of Article 1
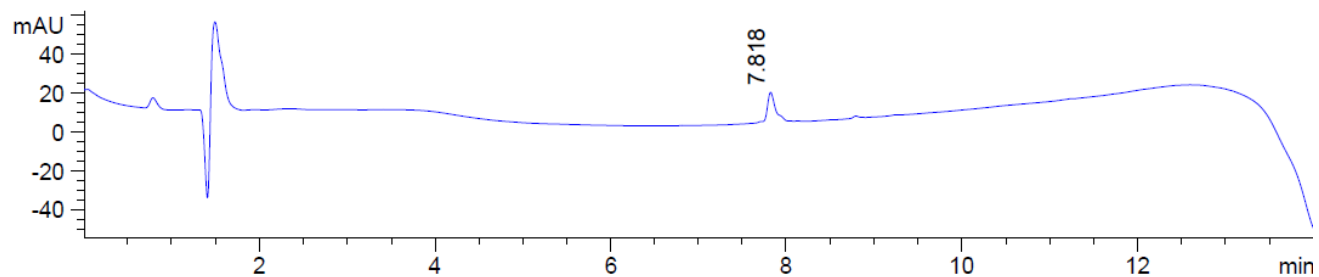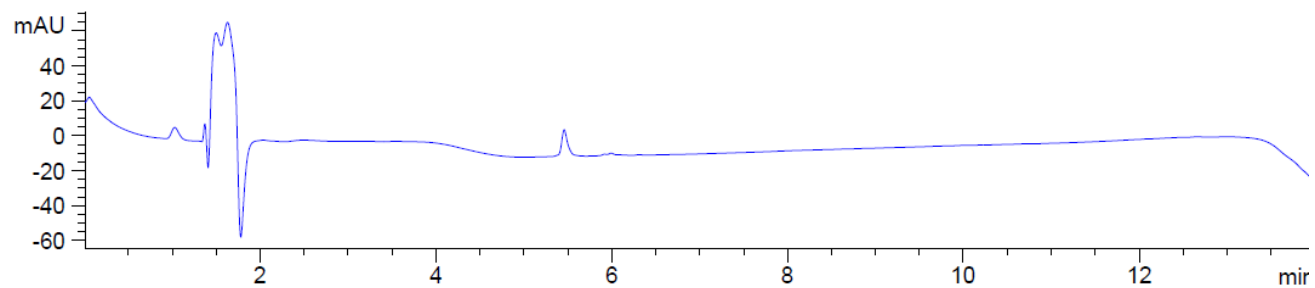
[(3*S*, 4*S*)-Hgl³]-2.1 [(3*S*, 4*S*, 2'*R*)-2.6]
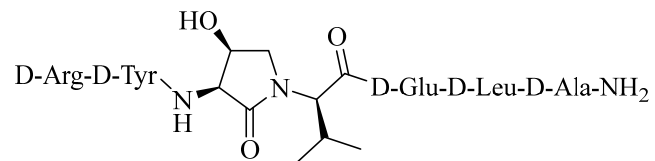
[(3*S*, 4*S*, 2'*R*)-2.6] LCMS chromatogram [10-90% MeOH (0.1% FA)/water (0.1% FA), 14 min]; RT = 7.3 on a Sunfire C18 analytical column (100Å, 3.5 μm, 4.6 mm X 100 mm).
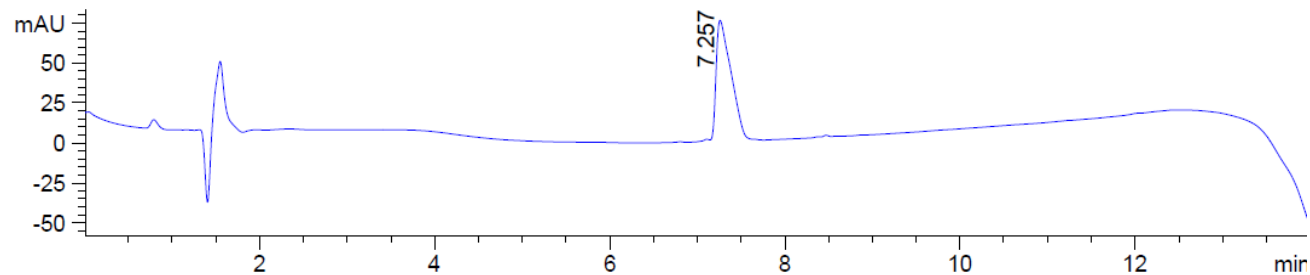
[(3*S*, 4*S*, 2'*R*)-2.6] LCMS chromatogram [10-90% MeCN (0.1% FA)/water (0.1% FA), 14 min]; RT = 5.2 on a Sunfire C18 analytical column (100Å, 3.5 μm, 4.6 mm X 100 mm).

Annex 1: Supporting information of Article 1

[(3S, 4R)-Hgl³-(S)-Val]-2.1 [(3S, 4R, 2'S)-2.6]

HO — D-Arg-D-Tyr — N(H) — ... — N — ... — D-Glu-D-Leu-D-Ala-NH₂
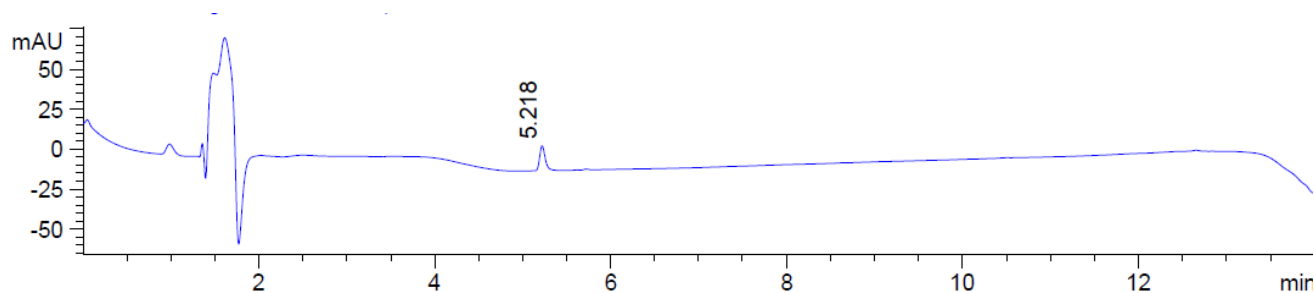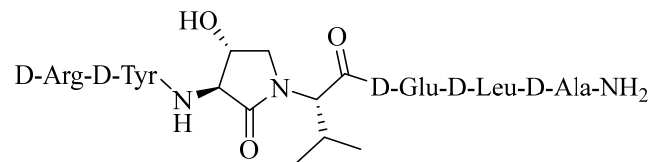
[(3S, 4R, 2'S)-2.6] LCMS chromatogram [10-90% MeOH (0.1% FA)/water (0.1% FA), 14 min]; RT = 7 on a Sunfire C18 analytical column (100Å, 3.5 µm, 4.6 mm X 100 mm).
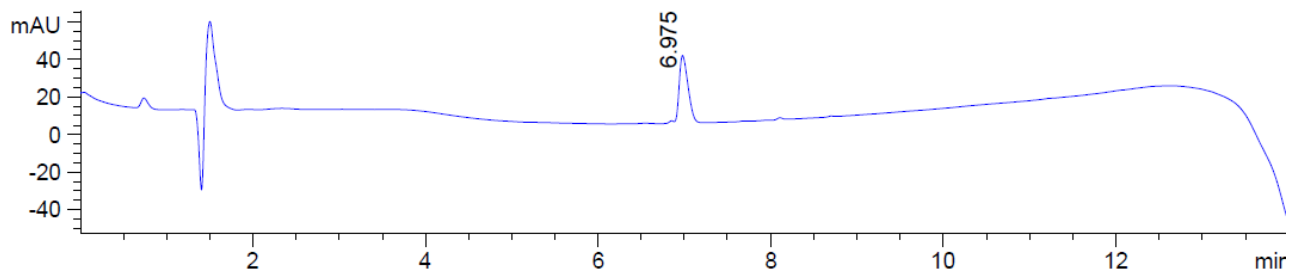
[(3S, 4R, 2'S)-2.6] LCMS chromatogram [10-90% MeCN (0.1% FA)/water (0.1% FA), 14 min]; RT = 4.9 on a Sunfire C18 analytical column (100Å, 3.5 µm, 4.6 mm X 100 mm).

Annex 1: Supporting information of Article 1
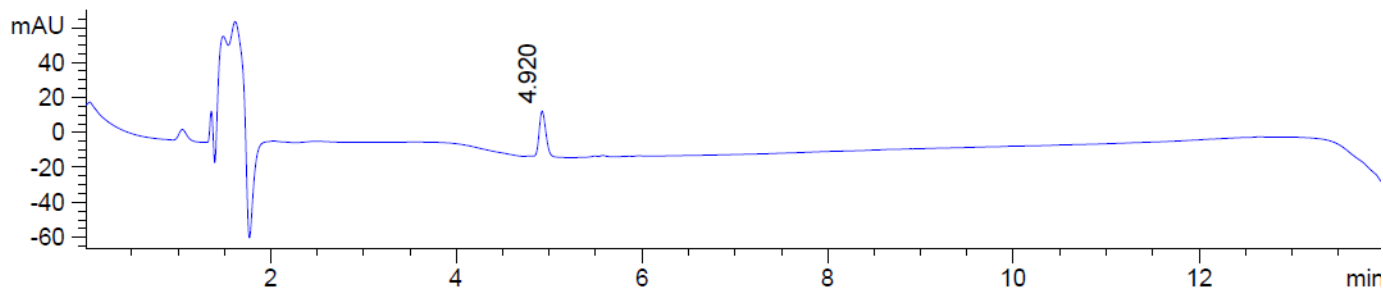
[(3*S*, 4*S*)-Hgl³-(*S*)-Val]-2.1 [(3*S*, 4*S*, 2'*S*)-2.6]
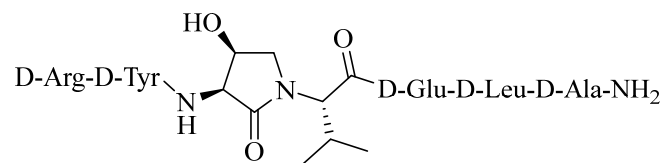
[(3*S*, 4*S*, 2'*S*)-2.6] LCMS chromatogram [10-90% MeOH (0.1% FA)/water (0.1% FA), 14 min]; RT = 6.6 on a Sunfire C18 analytical column (100Å, 3.5 μm, 4.6 mm X 100 mm).
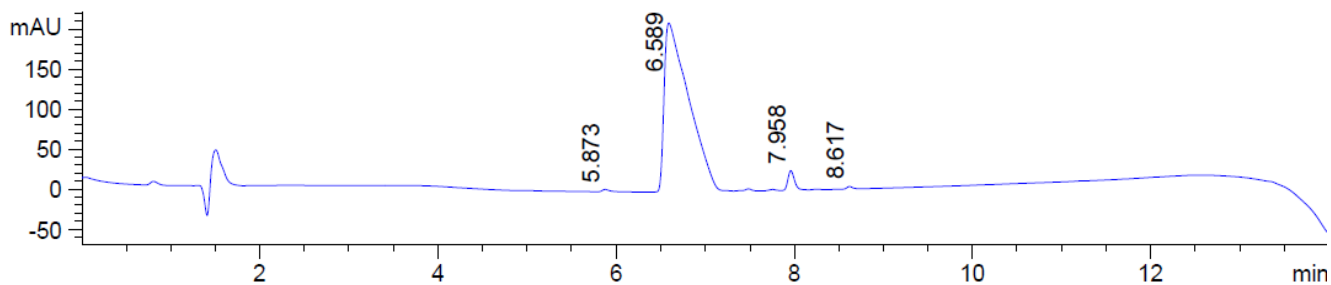
[(3*S*, 4*S*, 2'*S*)-2.6] LCMS chromatogram [10-90% MeCN (0.1% FA)/water (0.1% FA), 14 min]; RT = 5.2 on a Sunfire C18 analytical column (100Å, 3.5 μm, 4.6 mm X 100 mm).

Annex 1: Supporting information of Article 1
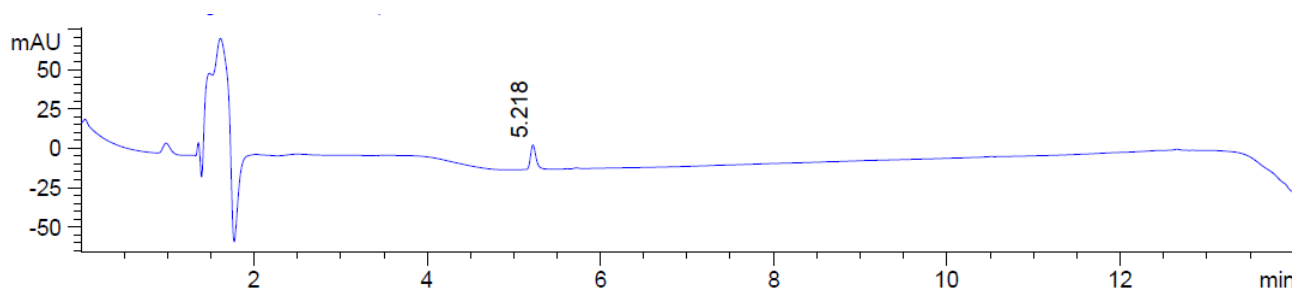
Annex 2: Supporting information of Article 2

Diversity-oriented syntheses of β-substituted α-amino γ-lactam peptide mimics with constrained backbone and side chain residues

Azade Geranurimi and William D. Lubell*

Département de Chimie, Université de Montréal, C.P. 6128, Succursale Centre-Ville, Montréal, Québec H3C 3J7, Canada

E-mail: william.lubell@umontreal.ca

Experimental section

General Methods: Unless otherwise specified, all non-aqueous reactions were performed under an inert argon atmosphere. All glassware was dried with a flame under flushing argon gas or stored in the oven, and let cool under an inert atmosphere prior to use. Anhydrous solvents (THF, DCM, MeCN, MeOH, toluene and DMF) were obtained by passage through solvent filtration systems (Glass Contour, Irvine, CA) and solvents were transferred by syringe. Reaction mixture solutions (after aqueous workup) were dried over anhydrous $MgSO_4$ or Na_2SO_4, filtered, and rotary-evaporated under reduced pressure. The syntheses under microwave conditions were performed on a 0-400 W Biotage® Robot Eight & Robot Sixty microwave synthesizer. Column chromatography was performed on 230-400 mesh silica gel, and thin-layer chromatography was performed on an alumina plates coated with silica gel (Merck 60 F_{254} plates). Visualization of the developed chromatogram was performed by UV absorbance or staining with iodine or potassium permanganate solutions. Melting points were obtained on a Buchi melting point B-540 apparatus and are uncorrected. Specific rotations, $[\alpha]^D$ values, were calculated from optical rotations measured at 20 °C and 25 °C in $CHCl_3$ or MeOH at the specified concentrations (c in g/100 mL) using a 0.5 dm cell length (l) on a Anton Paar Polarimeter, MCP 200 at 589 nm, using the general formula: $[\alpha]^D_{25} = (100 \times \alpha)/(1 \times c)$. Accurate mass measurements were performed on an LC-MSD instrument in electrospray ionization (ESI-TOF) mode at the Université de Montréal Mass Spectrometry facility. Sodium adducts $[M + Na]^+$ were used for empirical formula confirmation. Nuclear magnetic resonance spectra (^1H, ^{13}C, COSY) were recorded on Bruker 300, 400, 500 and 700 MHz spectrometers. ^1H NMR spectra were referenced to $CDCl_3$ (7.26 ppm), CD_3OD (3.31

ppm), C_6D_6 (7.16 ppm) or DMSO-d_6 (2.50 ppm) and ^{13}C NMR spectra were measured in CDCl$_3$ (77.16 ppm), CD$_3$OD (49.0 ppm), C_6D_6 (128.39 ppm) or DMSO-d_6 (39.52 ppm) as specified below. Coupling constant J values were measured in Hertz (Hz) and chemical shift values in parts per million (ppm). Infrared spectra were recorded in the neat on a Perkin Elmer Spectrometer FT-IR instrument, and are reported in reciprocal centimeters (cm^{-1}).

Reagents: D-Val-O-*t*-Bu,[1] and potassium thiobenzoate[2] were synthesized as previously described. Unless specified otherwise, commercially available reagents were purchased from Aldrich, A & C American Chemicals Ltd., Fluka and Advanced Chemtech™ and used without further purification, including PPh$_3$, DIAD, *p*-nitrobenzoic acid, NaN$_3$, thiobenzoic acid, 15-crown-5, benzoic acid, DEAD, diphenyl phosphoryl azide, CuI, DIEA, phenylacetylene, HOAc, HOBt, ethyl (hydroxyimino)cyanoacetate (oxyma), *N*-hydroxyphthalimide, thiophenol, thionyl chloride, imidazole, ruthenium (III) chloride hydrate and sodium periodate.

***tert*-Butyl (3*R*, 4*S*, 2'*R*)-2-[3-(Fmoc)amino-4-hydroxy-2-oxopyrrolidin-1-yl]-3-methylbutanoate [(4*S*)-3.17]**
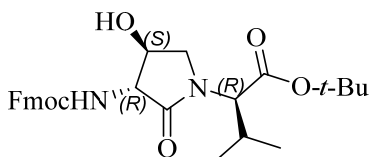
(4*S*)-3.17

In a 20-mL screw cap vial, D-Val-O-*t*-Bu (3.3 equiv, 571 mg, 3.3 mmol), (2*R*, 3*R*)-oxirane (3*R*)-**3.13** (1 equiv, 353 mg, 1 mmol, prepared from D-methionine according to reference[1] and benzoic acid (0.3 equiv, 36.6 mg, 0.3 mmol) were dissolved in THF (3 mL). The vial was sealed and heated under microwave irradiation (50 W) at 80 °C for 2 h. The resulting homogeneous brown solution was concentrated in vacuum and the residue was purified by column chromatography using a step gradient of 1 to 6% THF in DCM to yield (3*R*, 4*S*, 2'*R*)-lactam (4*S*)-**3.17** (440 mg, 0.89 mmol, 89%): R$_f$ = 0.44 (3% THF in DCM); [α] $_D^{20}$ 7.7° (*c* 2, CHCl$_3$); ^{1}H NMR (500 MHz, CDCl$_3$) δ 7.77 (dd, *J* = 7.6, 0.5, 2H), 7.59 (d, *J* = 7.5, 2H), 7.41 (t, *J* = 7.5, 2H), 7.33 (td, *J* = 7.5, 1.1, 2H), 5.76 (s, 1H), 5.01 (s, 1H), 4.44 (d, *J* = 1.8, 1H), 4.43 (dd, *J* = 5.0, 3.9, 2H), 4.34 (q, *J* = 8.1, 1H), 4.23 (t, *J* = 7.0, 1H), 4.12 (dd, *J* = 8.1, 1.8, 1H), 4.02 (dd, *J* = 9.5, 8.0, 1H), 3.23 (dd, *J* = 9.4, 8.3, 1H), 2.27-2.16 (m, 1H), 1.47 (s, 9H), 1.01 (d, *J* = 6.7, 3H), 0.95 (d, *J* = 6.8, 3H); ^{13}C NMR (126 MHz, CDCl$_3$) δ 169.4, 168.6, 158.1, 143.5 (2), 141.3 (2), 127.9 (2), 127.1 (2), 125.0 (2), 120.1 (2), 82.4,

73.6, 67.7, 61.1, 60.8, 47.5, 47.0, 28.1 (3), 27.5, 19.3, 19.0; HRMS (ESI-TOF) m/z [M + H]$^+$ calcd for $C_{28}H_{35}N_2O_6^+$ 495.2490, found 495.2496.

tert-Butyl (3*R*, 4*R*, 2'*R*)-2-[3-(Fmoc)amino-4-hydroxy-2-oxopyrrolidin-1-yl]-3-methylbutanoate [(4*R*)-**3.17**] was prepared using the same protocol with (2*R*, 3*S*)-oxirane (3*S*)-**3.13** in 85% yield and gave identical characterization as that described below.

tert-Butyl (3*R*, 4*R*, 2'*R*)-2-[3-(Fmoc)amino-4-hydroxy-2-oxopyrrolidin-1-yl]-3-methylbutanoate [(4*R*)-3.17]

(4*R*)-3.17
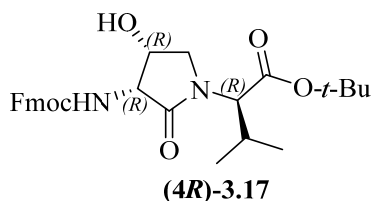
A solution of (3*R*, 4*R*, 2'*R*)-benzoate (4*R*)-**3.24a** (1 equiv, 160 mg, 0.249 mmol) and NaN$_3$ (3.7 equiv, 60 mg, 323 µL, 0.92 mmol) in dry MeOH (10 mL) was stirred for 24 h at 40 °C. The volatiles were evaporated, and the residue was purified by column chromatography on silica gel using a step gradient of 0 to 50% EtOAc in hexane. Evaporation of the collected fractions gave (3*R*, 4*R*, 2'*R*)-Hgl (4*R*)-**3.17** as a light yellow oil (94 mg, 0.19 mmol, 75%): R$_f$ = 0.18 (3% THF in DCM); [α]$_D^{20}$ 10.9° (*c* 1.2, CHCl$_3$); ^{1}H NMR (400 MHz, DMSO) δ 7.89 (d, *J* = 7.5, 2H), 7.81 (t, *J* = 7.4, 2H), 7.42 (t, *J* = 7.4, 2H), 7.37 (d, *J* = 9.1, 1H), 7.33 (t, *J* = 7.4, 2H), 5.33 (d, *J* = 4.2, 1H), 4.43 (dd, *J* = 9.1, 5.1, 1H), 4.31-4.19 (m, 4H), 4.11 (d, *J* = 10.4, 1H), 3.52 (dd, *J* = 10.5, 3.6, 1H), 3.44 (d, *J* = 10.5, 1H), 2.08-1.96 (m, 1H), 1.42 (s, 9H), 0.90 (d, *J* = 6.6, 3H), 0.79 (d, *J* = 6.6, 3H); ^{13}C NMR (75 MHz, CDCl$_3$) δ 169.9, 143.8, 143.7, 141.3, 141.3, 127.7, 127.1, 125.2, 119.9, 82.7, 67.6, 67.4, 60.5, 57.2, 50.6, 47.1, 28.7, 28.0, 19.4, 19.3; HRMS (ESI-TOF) m/z [M + H]$^+$ calcd for $C_{28}H_{35}N_2O_6^+$ 495.2490, found 495.2502.

tert-Butyl (3*R*, 4*R*, 2'*R*)-2-[3-(Fmoc)amino-4-*p*-nitrobenzoyloxy-2-oxopyrrolidin-1-yl]-3-methylbutanoate [(4*R*)-3.24a]
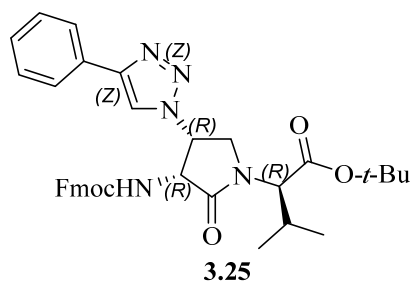
Annex 2: Supporting information of Article 2

(4*R*)-3.24a
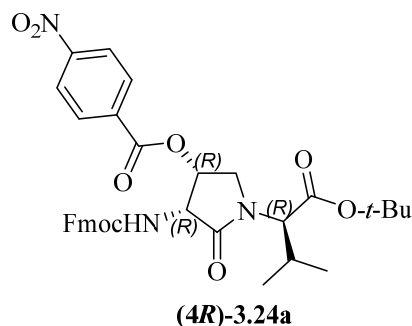
A solution of (4*S*)-Hgl (4*S*)-**3.17** (1 equiv, 200 mg, 0.404 mmol), *p*-nitrobenzoic acid (2 equiv, 135 mg, 0.809 mmol) and PPh$_3$ (2.2 equiv, 233 mg, 0.89 mmol) in dry THF (9 mL) was treated dropwise with DIAD (2.2 equiv, 179 mg, 0.176 mL, 0.89 mmol) and stirred for 24 h. The volatiles were evaporated on a rotary evaporator. The residue was partitioned between saturated NaHCO$_3$ (15 mL) and EtOAc (15 mL). The aqueous phase was separated and extracted with EtOAc (3 x 10 mL). The combined organic layers were washed with water, dried over MgSO$_4$, and evaporated to a residue that was purified by column chromatography on silica gel using 10% EtOAc in hexane as eluent. Evaporation of the collected fractions provided (4*R*)-ester (4*R*)-**3.24a** as white foam (208 mg, 0.324 mmol, 80% yield): R$_f$ = 0.22 (30% EtOAc in hexane); [α]$_D^{20}$ –93.9° (*c* 0.2, CHCl$_3$); ^{1}H NMR (300 MHz, CDCl$_3$) δ 8.22 (d, *J* = 8.8, 2H), 8.12 (d, *J* = 8.7, 2H), 7.71 (t, *J* = 7.8, 2H), 7.50 (dd, *J* = 19.8, 7.5, 2H), 7.42-7.29 (m, 2H), 7.24-7.13 (m, 2H), 5.83 (t, *J* = 3.9, 1H), 5.49 (d, *J* = 6.1, 1H), 4.72 (t, *J* = 4.95, 1H), 4.50-4.39 (m, 2H), 4.33 (dd, *J* = 10.5, 7.2, 1H), 4.18 (d, *J* = 7.2, 1H), 4.13 (d, *J* = 5.8, 1H), 3.74 (dd, *J* = 12.1, 3.3, 1H), 2.27-2.08 (m, 1H), 1.36 (s, 9H), 1.01 (d, *J* = 6.7, 3H), 0.93 (d, *J* = 6.7, 3H); ^{13}C NMR (75 MHz, CDCl$_3$) δ 170.0, 169.2, 163.7, 156.2, 150.7, 143.6, 141.3, 134.8, 130.9, 127.7, 127.0, 124.9, 123.5, 120.0, 82.2, 70.4, 67.4, 60.7, 54.9, 48.0, 47.0, 28.9, 27.9, 19.4, 19.2; HRMS (ESI-TOF) m/z [M + H]$^+$ calcd for C$_{35}$H$_{38}$N$_3$O$_9^+$ 644.2603, found 644.2634, as well as dehydrolactam **3.21** (31 mg, 0.065 mmol, 16%); R$_f$ = 0.56 (30% EtOAc in hexane); [α]$_D^{25}$ 33.2° (*c* 1, CHCl$_3$); ^{1}H NMR (400 MHz, C$_6$D$_6$) δ 7.65 (d, *J* = 7.5, 2H), 7.44 (d, *J* = 7.5, 2H), 7.30 (t, *J* = 7.5, 2H), 7.20 (t, *J* = 7.4, 2H), 6.92 (s, 1H), 4.85 (d, *J* = 9.8, 1H), 4.33 (d, *J* = 6.4, 2H), 4.19 (dd, *J* = 19.2, 1.9, 1H), 4.09 (t, *J* = 7.0, 1H), 3.54 (dd, *J* = 19.3, 2.2, 1H), 2.19-2.03 (m, 1H), 1.37 (s, 9H), 0.96 (d, *J* = 6.7, 3H), 0.77 (d, *J* = 6.6, 3H); ^{13}C NMR (75 MHz, CDCl$_3$) δ 169.9, 167.0, 153.4, 143.6, 141.5, 129.9, 128.0, 127.3, 125.1, 120.2, 115.2, 82.3, 67.6, 61.2, 47.4, 47.0, 29.6, 28.2, 19.5, 19.3; HRMS (ESI-TOF) m/z [M + H]$^+$ calcd for C$_{28}$H$_{33}$N$_2$O$_5^+$ 477.2384, found 477.2397.

tert-Butyl (3S, 4R, 2'R)-2-[3-(Fmoc)amino-4-benzoylsulfanyl-2-oxopyrrolidin-1-yl]-3-methylbutanoate [(4R)-3.24b]

[(4R)-3.24b]
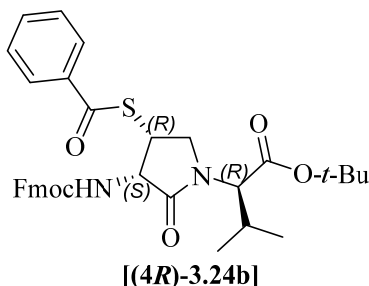
A solution of PPh$_3$ (2.2 equiv, 215 mg, 0.823 mmol) in THF (2.5 mL) at 0 °C was treated slowly with DIAD (2.2 equiv, 166 mg, 0.163 mL, 0.823 mmol), stirred for 30 min, treated with (4S)-Hgl (4S)-**3.17** (1 equiv, 185 mg, 0.374 mmol) followed by thiobenzoic acid (2 equiv, 103 mg, 884 µL, 0.748 mmol), stirred for 1h and let warm with stirring for 20 h. The volatiles were evaporated on a rotary evaporator. The residue was partitioned between saturated NaHCO$_3$ (10 mL) and EtOAc (10 mL). The aqueous phase was separated and extracted with EtOAc (3 x 5 mL). The combined organic layers were washed with water, dried over MgSO$_4$ and evaporated to a residue that was purified by column chromatography on silica gel using 0 to 20% EtOAc in hexanes. Evaporation of the collected fractions gave (4R)-thioester (4R)-**3.24b** as a light yellow foam (163 mg, 0.266 mmol, 71 % yield): R$_f$ = 0.35 (30% EtOAc in hexane); [α]$_D$^{25} 164° (c 1, CHCl$_3$); ^{1}H NMR (500 MHz, CDCl$_3$) δ 7.91 (dd, J = 8.4, 1.2, 2H), 7.73 (dd, J = 7.4, 3.2, 2H), 7.62-7.52 (m, 3H), 7.44 (t, J = 7.7, 2H), 7.35 (dd, J = 16.0, 7.9, 2H), 7.24 (dd, J = 7.5, 1.0, 1H), 7.23-7.18 (m, 1H), 5.55 (d, J = 5.4, 1H), 4.85 (t, J=5.7 1H), 4.76 (t, J = 6.3, 1H), 4.45 (dd, J = 10.4, 7.2, 1H), 4.39 (d, J = 9.8, 1H), 4.31 (t, J = 9.0, 1H), 4.21 (t, J = 7.1, 1H), 4.14 (dd, J = 11.4, 4.3, 1H), 3.58 (d, J = 12.0, 1H), 2.20-2.08 (m, 1H), 1.47 (s, 9H), 1.02 (d, J = 6.6, 3H), 0.95 (d, J = 6.6, 3H); ^{13}C NMR (126 MHz, CDCl$_3$) δ 190.0, 170.6, 168.9, 156.1, 143.7, 141.3, 136.5, 133.9, 128.8, 127.7, 127.4, 127.1, 125.2, 120.0, 82.4, 67.4, 61.5, 54.8, 49.4, 47.0, 43.9, 28.1, 27.8, 19.4, 19.2; HRMS (ESI-TOF) m/z [M + H]$^+$ calcd for C$_{35}$H$_{39}$N$_2$O$_6$S$^+$ 615.2523, found 615.2535, as well as dehydrolactam **3.21** (36 mg, 0.075 mmol, 20%).

tert-Butyl (3R, 4R, 2'R)-2-[3-(Fmoc)amino-4-benzoyloxy-2-oxopyrrolidin-1-yl]-3-methylbutanoate [(4R)-3.24c]

Annex 2: Supporting information of Article 2
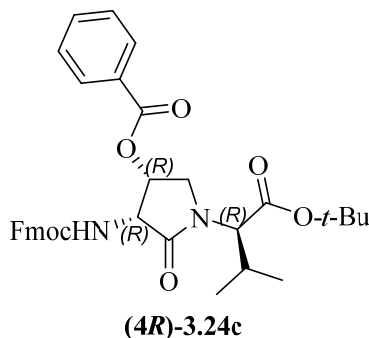
(4R)-3.24c

As described for the synthesis of β-substituted lactam (4R)-**3.24b**, DIAD (2.2 equiv, 63 mg, 620 µL, 0.3 mmol) was premixed for 30 min with PPh$_3$ (2.2 equiv, 81.7 mg, 0.3 mmol) in THF (3 mL) at 0 °C, treated slowly with (4S)-Hgl (4S)-**3.17** (1 equiv, 70 mg, 0.14 mmol) and benzoic acid (2 equiv, 34.6 mg, 0.000283 mol), stirred for 1h at 0 °C and let warm with stirring for 20 h. Purification by column chromatography on silica gel using 0 to 20% EtOAc in hexanes gave (4R)-ester (4R)-**3.24c** as white foam (58 mg, 0.096 mmol, 68%); R$_f$ = 0.27 (30% EtOAc in hexane); [α]$_D^{25}$ 14.9° (c 1, CHCl$_3$); ^{1}H NMR (700 MHz, CDCl$_3$) δ 8.01 (d, J = 7.3, 2H), 7.72 (dd, J = 15.7, 7.5, 2H), 7.62 (t, J = 7.4, 1H), 7.55 (d, J = 7.5, 1H), 7.51 (d, J = 7.5, 1H), 7.47 (t, J = 7.8, 2H), 7.38 (t, J = 7.5, 1H), 7.35 (t, J = 7.5, 1H), 7.25-7.19 (m, 2H), 5.87-5.83 (t, J = 4.5, 1H), 5.51 (d, J = 6.8, 1H), 4.75 (dd, J = 6.7, 5.2, 1H), 4.49-4.43 (m, 2H), 4.32 (dd, J = 10.7, 7.4, 1H), 4.21 (t, J = 7.2, 1H), 3.98 (dd, J = 12.7, 3.6, 1H), 3.65 (d, J = 12.7, 1H), 2.16 (qd, J = 13.3, 6.6, 1H), 1.50 (s, 9H), 1.04 (d, J = 6.6, 3H), 0.91 (d, J = 6.7, 3H); ^{13}C NMR (176 MHz, CDCl$_3$) δ 170.3, 169.0, 165.3, 156.1, 143.7, 141.2, 133.6, 129.7, 128.6, 127.6, 127.0, 125.5, 125.1, 119.9, 82.5, 69.3, 67.4, 61.1, 55.2, 48.2, 47.0, 30.3, 28.1, 27.6, 19.2, 18.7; HRMS (ESI-TOF) m/z [M + H]$^+$ calcd for C$_{35}$H$_{39}$N$_2$O$_7^+$ 599.2733, found 599.2734, as well as dehydrolactam **3.21** (13 mg, 0.027 mmol, 19%), and 6% recovered (4S)-**3.17**.

***tert*-Butyl (3*R*, 4*R*, 2'*R*)-2-[3-(Fmoc)amino-4-benzotriazole-*N*-oxy-2-oxopyrrolidin-1-yl]-3-methylbutanoate [(4R)-3.24d]**
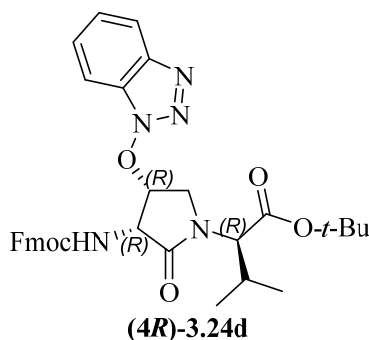
(4R)-3.24d

As described for the synthesis of β-substituted lactam (4R)-**3.24b**, DIAD (2.2 equiv, 90 mg, 88 μL, 0.46 mmol) was premixed for 30 min with PPh$_3$ (2.2 equiv, 116 mg, 0.445 mmol) in THF (2 mL) at 0 °C, treated slowly with (4S)-Hgl (4S)-**3.17** (1 equiv, 100 mg, 0.202 mmol) and HOBt (2 equiv, 55 mg, 0.4 mmol), stirred for 1h at 0 °C and let warm with stirring for 40 h. Purification by column chromatography on silica gel using 20 to 35% EtOAc in hexane provided (4R)-oxy benzotriazole (4R)-**3.24d** as a colorless oil that became a white foam under vacuum (87 mg, 0.14 mmol, 70% yield): R$_f$ = 0.41 (40% EtOAc in hexane); [α]$_D^{25}$ –13° (c 1, CHCl$_3$); ^{1}H NMR (300 MHz, CDCl$_3$) δ 7.99 (m, 1H), 7.76 (d, J = 7.5, 2H), 7.68-7.55 (m, 3H), 7.45-7.27 (m, 6H), 5.74 (d, J = 6.1, 1H), 5.45-5.38 (m, 1H), 4.74 (t, J = 5.7, 1H), 4.58 (d, J = 12.6, 1H), 4.52-4.41 (m, 2H), 4.39-4.30 (m, 1H), 4.24 (t, J = 7.2, 1H), 3.64 (dd, J = 12.6, 3.5, 1H), 2.29-2.16 (m, 1H), 1.53 (s, 9H), 1.03 (d, J = 6.6, 3H), 0.91 (d, J = 6.7, 3H); ^{13}C NMR (75 MHz, CDCl$_3$) δ 169.0, 168.6, 156.3, 143.7, 143.5, 143.3, 141.3, 128.4, 127.8, 127.5, 127.1, 125.2, 125.1, 124.9, 120.2, 120.0, 108.8, 83.1, 82.7, 67.8, 61.6, 54.8, 47.3, 47.0, 28.7, 28.0, 19.2; HRMS (ESI-TOF) m/z [M + H]$^+$ calcd for C$_{34}$H$_{38}$N$_5$O$_6^+$ 612.2817, found, 612.2843; HRMS (ESI-TOF) m/z [M + Na]$^+$ calcd for C$_{34}$H$_{37}$N$_5$O$_6$Na$^+$ 634.2636, found 634.2664, as well as dehydrolactam **3.21** (14 mg, 0.03 mmol, 15%), and 7% recovered (4S)-**3.17**.

***tert*-Butyl (3R, 4R, 2'R)-2-[3-(Fmoc)amino-4-{1-cyano-2-ethoxy-2-oxoethylidene-aminoxy}-2-oxopyrrolidin-1-yl]-3-methylbutanoate [(4R)-3.24e]**
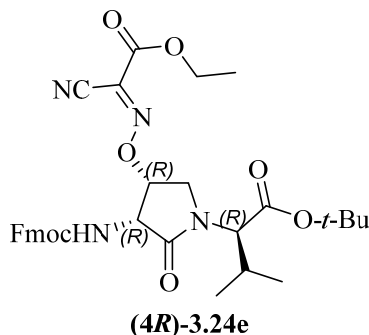
(4*R*)-3.24e

As described for the synthesis of β-substituted lactam (4*R*)-**3.24b**, DIAD (2.2 equiv, 63 mg, 62 µL, 0.31 mmol) was premixed for 30 min with PPh₃ (2.2 equiv, 82 mg, 0.31 mmol) in THF (1 mL) at 0 °C, treated slowly with (4*S*)-Hgl (4*S*)-**3.17** (1 equiv, 70 mg, 0.14 mmol) and ethyl (hydroxyimino)cyanoacetate (2 equiv, 40 mg, 0.28 mmol), stirred for 1h at 0 °C and let warm with stirring. After 18 h, TLC showed significant amounts of unreacted (4*S*)-**3.17** in the reaction mixture which was cooled to 0 °C, treated with another premixed solution of DIAD (2.2 equiv, 62 µL) and PPh₃ (2.2 equiv, 82 mg) in THF (1 mL), and allowed to warm to rt with stirring for another 20 h. Purification by column chromatography on silica gel using 4% THF in DCM gave (4*R*)-oxime (4*R*)-**3.24e** as white foam (50 mg, 0.08 mmol, 57%); R_f = 0.43 (4% THF in DCM); [α] $_D^{25}$ –20.4° (*c* 1, MeOH); ^{1}H NMR (300 MHz, CDCl₃) δ 7.75 (d, *J* = 7.5, 2H), 7.59 (t, *J* = 7.3, 2H), 7.39 (t, *J* = 7.4, 2H), 7.31 (td, *J* = 7.4, 1.1, 2H), 5.49 (d, *J* = 6.6, 1H), 5.38 (t, *J* = 4.1, 1H), 4.75 (dd, *J* = 6.5, 5.1, 1H), 4.46-4.12 (m, 7H), 3.67 (dd, *J* = 12.5, 3.6, 1H), 2.09-2.21 (m, 1H), 1.45 (s, 9H), 1.31 (t, *J* = 7.1, 3H), 1.00 (d, *J* = 6.6, 3H), 0.90 (d, *J* = 6.7, 3H); ^{13}C NMR (75 MHz, CDCl₃) δ 169.1, 169.0, 157.1, 156.2, 143.7, 141.2, 127.7, 127.2, 127.1, 125.2, 120.0, 107.2, 82.4, 81.5, 67.8, 63.7, 60.9, 54.9, 47.2, 46.9 28.6, 28.0, 19.2, 19.1, 13.9; HRMS (ESI-TOF) m/z [M + H]$^+$ calcd for C₃₃H₃₉N₄O₈$^+$ 619.2762, found 619.2784; HRMS (ESI-TOF) m/z [M + Na]$^+$ calcd for C₃₃H₃₈N₄O₈Na$^+$ 641.2582, found 641.2599, as well as dehydrolactam **3.21** (16 mg, 0.033 mmol, 23 %), and 17% recovered (4*S*)-**3.17**.

tert-**Butyl (3*S*, 4*R*, 2'*R*)-2-[3-(Fmoc)amino-4-thiophenyl-2-oxopyrrolidin-1-yl]-3-methylbutanoate [(4*R*)-3.24f]**
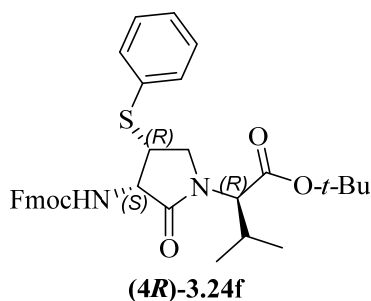
(4*R*)-3.24f

As described for the synthesis of β-substituted lactam (4*R*)-**3.24b**, DIAD (2.2 equiv, 63 mg, 62 µL, 0.31 mmol) was premixed for 30 min with PPh₃ (2.2 equiv, 82 mg, 0.311 mmol) in THF (1 mL) at 0 °C, treated slowly with (4*S*)-Hgl (4*S*)-**3.17** (1 equiv, 70 mg, 0.14 mmol) and thiophenol (2 equiv, 31 mg, 29 µL, 0.28 mmol), stirred for 1h at 0 °C and let warm with stirring. After 18 h, TLC showed significant amounts of unreacted (4*S*)-**3.17** in the reaction mixture which was cooled to 0 °C, treated with another premixed solution of DIAD (2.2 equiv, 62 µL) and PPh₃ (2.2 equiv, 82 mg) in THF (1 mL), and allowed to warm to rt with stirring for another 20 h. Purification by column chromatography on silica gel using 0 to 60% EtOAc in hexane gave (4*R*)-thioether (4*R*)-**3.24f** as white foam (40.7 mg, 0.0694 mmol, 49%); R_f = 0.33 (30% THF in DCM); [α] $_D^{25}$ 186° (*c* 1, CHCl₃); ¹H NMR (300 MHz, CDCl₃) δ 7.76 (d, *J* = 7.5, 2H), 7.58 (t, *J* = 7.5, 2H), 7.40 (t, *J* = 7.6, 4H), 7.30 (tt, *J* = 7.4, 1.4, 2H), 7.25-7.13 (m, 3H), 5.58 (d, *J* = 6.1, 1H), 4.74 (t, *J* = 6.3, 1H), 4.37 (dd, *J* = 10.7, 4.9, 2H), 4.28-4.12 (m, 3H), 3.91 (d, *J* = 11.3, 1H), 3.68 (dd, *J* = 11.3, 5.0, 1H), 2.12 (qd, *J* = 13.3, 6.5, 1H), 1.51 (s, 9H), 0.99 (d, *J* = 6.6, 3H), 0.88 (d, *J* = 6.7, 3H); ¹³C NMR (75 MHz, CDCl₃) δ 170.1, 168.8, 156.1, 143.8, 141.3, 133.7, 131.7, 129.1, 127.7, 127.3, 127.1, 125.3, 119.9, 82.3, 67.5, 61.5, 56.2, 47.4, 47.0, 30.3, 28.5, 28.1, 19.1; HRMS (ESI⁺) calcd *m/z* for C₃₄H₃₉N₂O₅S⁺ [M+H]⁺, 587.5274 found 587.2582; HRMS (ESI-TOF) m/z [M + Na]⁺ calcd for C₃₄H₃₈N₂O₅SNa⁺ 609.2394, found 609.2402, as well as dehydrolactam **3.21** (18.9 mg, 0.0396 mmol, 28%), and 21% unreacted SM.

***tert*-Butyl (3*R*, 4*R*, 2'*R*)-2-[3-(Fmoc)amino-4-(1,3-dioxoisoindolin-2-yl)oxy)-2-oxopyrrolidin-1-yl]-3-methylbutanoate [(4*R*)-3.24g]**
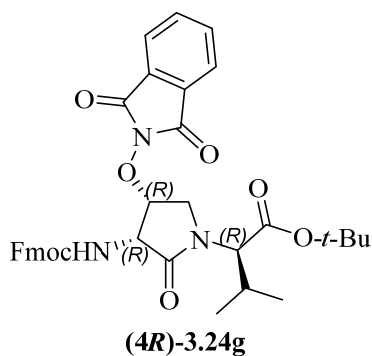
(4R)-3.24g

As described for the synthesis of β-substituted lactam (4R)-**3.24b**, DIAD (2.2 equiv, 63 mg, 0.0617 mL, 0.311 mmol) was premixed for 30 min with PPh$_3$ (2.2 equiv, 81.7 mg, 0.311 mmol) in DCM (2 mL) at 0 °C, treated slowly with (4S)-Hgl (4S)-**3.17** (1 equiv, 70 mg, 0.142 mmol) and *N*-hydroxyphthalimide (2 equiv, 46.2 mg, 0.283 mmol), stirred for 1 h at 0 °C and let warm with stirring for 24 h. Purification by column chromatography on silica gel using 4% THF in DCM provided (4R)-phthalimide (4R)-**3.24g** as white foam (46 mg, 0.072 mmol, 51%): R$_f$ = 0.26 (40% EtOAc in hexane); [α]$_D^{25}$ –9.4° (*c* 1, CHCl$_3$); ^{1}H NMR (300 MHz, CDCl$_3$) δ 7.88-7.65 (m, 8H), 7.41 (t, *J* = 7.1, 2H), 7.33 (t, *J* = 6.9, 2H), 6.53 (d, *J* = 8.6, 1H), 5.00 (t, *J* = 4.5, 1H), 4.77 (dd, *J* = 8.6, 5.1, 1H), 4.51-4.43 (m, 1H), 4.43-4.30 (m, 2H), 4.27-4.15 (m, 2H), 3.73 (dd, *J* = 12.5, 4.3, 1H), 2.29-2.11 (m, 1H), 1.41 (s, 9H), 1.02 (d, *J* = 6.6, 3H), 0.92 (d, *J* = 6.8, 3H); ^{13}C NMR (75 MHz, CDCl$_3$) δ 169.4, 168.9, 163.8, 156.7, 144.0, 143.8, 141.2, 134.7, 128.8, 127.7,127.6, 127.1, 127.0, 125.6, 125.5, 123.8, 119.8, 82.1, 67.7, 61.0, 55.0, 47.4, 47.0, 28.7, 28.0, 21.9, 19.3; HRMS (ESI-TOF) m/z [M + H]$^+$ calcd for C$_{36}$H$_{38}$N$_3$O$_8^+$ 640.2653, found 640.2624; HRMS (ESI-TOF) m/z [M + Na]$^+$ calcd for C$_{36}$H$_{37}$N$_3$O$_8$Na$^+$ 662.2473, found 662.2449, as well as dehydrolactam **3.21** (17 mg, 0.035 mmol, 25 %).

***tert*-Butyl (3*S*, 4*R*, 2'*R*)-2-[3-(Fmoc)amino-4-thiol-2-oxopyrrolidin-1-yl]-3-methylbutanoate [(4R)-3.24h]**
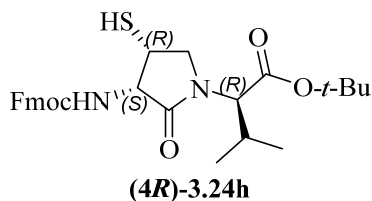
(4R)-3.24h

A solution of (3*S*, 4*R*, 2'*R*)-thioester (4R)-**3.24b** (1 equiv, 50 mg, 0.081 mmol), NaN$_3$ (3.7 equiv, 20 mg, 0.011 mL, 0.3 mmol) and 15-crown-5 (3.7 equiv, 66 mg, 60 μL, 0.3 mmol) in dry MeOH

(3 mL) was stirred at 40 °C for 24 h. The volatiles were removed using a rotary evaporator. The residue was purified by column chromatography using a step gradient of 10 to 50% EtOAc in hexane. Evaporation of the collected fractions gave (3*S*, 4*R*, 2'*R*)-thiol (4*R*)-**3.24h** (23 mg, 0.045 mmol, 55% yield): R_f = 0.14 (30% EtOAc in hexane); $[\alpha]_D^{25}$ 181.6° (*c* 0.25, CHCl$_3$); ^{1}H NMR (400 MHz, CDCl$_3$) δ 7.79 (d, *J* = 7.2, 2H), 7.67 (d, *J* = 7.9, 2H), 7.43 (t, *J* = 8.2, 2H), 7.34 (t, *J* = 7.5, 2H), 5.55 (s, 1H), 4.53 (s, 2H), 4.32 (s, 3H), 4.16 (s, 1H), 3.86 (s, 2H), 3.77-3.58 (br s, 1H), 2.12-1.87 (br s, 1H), 1.39 (s, 9H), 0.88 (s, 6H); ^{13}C NMR (75 MHz, CDCl$_3$) δ 170.0, 168.8, 156.1, 143.9, 141.3, 127.7, 127.1, 125.3, 120.0, 82.2, 67.7, 61.3, 55.9, 47.7, 47.0, 29.7, 27.9, 21.9, 19.2 (2); HRMS (ESI-TOF) m/z [M]$^+$ calcd for C$_{28}$H$_{34}$N$_2$O$_5$S 510.2290 found, 510.2299. **tert-Butyl (3*R*, 4*R*, 2'*R*)-2-[3-(Fmoc)amino-4-(aminoxy)-2-oxopyrrolidin-1-yl]-3-methylbutanoate [(4*R*)-3.24i]**
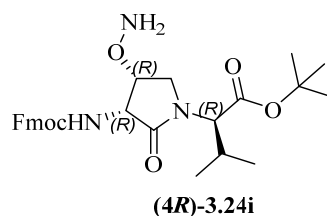
(4*R*)-3.24i

To a solution of (4*R*)-phthalimide (4*R*)-**3.24g** (1 equiv, 40 mg, 0.063 mmol) in a mixture of MeOH (0.5 mL) and DCM (0.5 mL), hydrazine monohydrate (10 equiv, 31 mg, 31 μL, 0.63 mmol) was added. The mixture was stirred at rt for 3 h, and concentrated to a residue, that was purified by column chromatography using 30% EtOAc in hexane. Evaporation of the collected fractions gave (4*R*)-*O*-alkylhydroxamine (4*R*)-**3.24i** as an oil (25 mg, 0.05 mmol, 78%): R_f = 0.28 (40% EtOAc in hexane); $[\alpha]_D^{25}$ 96° (*c* 1, CHCl$_3$); ^{1}H NMR (300 MHz, CDCl$_3$) δ 7.76 (d, *J* = 7.4, 2H), 7.62 (d, *J* = 7.4, 2H), 7.40 (t, *J* = 7.4, 2H), 7.32 (t, *J* = 7.4, 2H), 5.40 (s, 1H), 5.35 (d, *J* = 7.5, 1H), 4.55-4.40 (m, 3H), 4.35 (d, *J* = 10.2, 1H), 4.24 (t, *J* = 7.0, 1H), 3.73 (d, *J* = 12.3, 1H), 3.58 (dd, *J* = 12.1, 3.3, 1H), 2.28-2.08 (m, 1H), 1.46 (s, 9H), 1.25 (s, 2H), 1.02 (d, *J* = 6.6, 3H), 0.91 (d, *J* = 6.7, 3H); ^{13}C NMR (126 MHz, CDCl$_3$) δ 170.8, 169.4, 156.4, 143.9, 141.3, 127.7, 127.1, 125.2, 120.0, 82.2, 77.4, 67.3, 61.0, 55.4, 47.1, 46.3, 28.1, 27.6, 19.2, 18.6; HRMS (ESI-TOF) m/z [M + H]$^+$ calcd for C$_{28}$H$_{36}$N$_3$O$_6$$^+$ 510.2566 found, 510.2561.

***tert*-Butyl (3*R*, 4*R*, 2'*R*)-2-[3-(Fmoc)amino-4-azido-2-oxopyrrolidin-1-yl]-3-methylbutanoate [(4*R*)-3.24j]**

(4R)-3.24j

To an ice-cooled stirred solution of (4S)-Hgl (4S)-**3.17** (1 equiv, 200 mg, 0.40 mmol) and PPh₃ (2.2 equiv, 233 mg, 0.9 mmol) in dry THF (8 mL), DEAD (2.2 equiv, 154 mg, 0.14 mL, 0.9 mmol) was slowly added, followed by a dropwise addition of diphenyl phosphoryl azide (2 equiv, 222 mg, 174 μL, 0.81 mmol). The ice bath was removed. The reaction was let warm to rt. After 18 h, TLC showed incomplete conversion and the mixture was cooled to 0 °C and treated with a solution of PPh₃ (2.2 equiv, 233 mg) in dry THF (8 mL), followed by DEAD (2.2 equiv, 0.14 mL). The mixture was let warm to rt and stirred 20 h. The volatiles were evaporated. The residue was partitioned between saturated NaHCO₃ (15 mL) and EtOAc (15 mL). The aqueous phase was separated and extracted with EtOAc (3 x 10 mL). The combined organic layers were washed with water, dried over MgSO₄, and evaporated to a residue, that was purified by column chromatography using a step gradient of 0 to 20% EtOAc in hexane gave (4R)-azide (4R)-**3.24j** white foam (126 mg, 0.24 mmol, 60% yield): R_f = 0.4 (20% EtOAc in hexane); [α] $_D$ ^{25} –31.4° (c 1, CHCl₃); FT-IR (neat) vmax 2959, 2873, 1993, 1464, 1381, 882, 730 cm^{-1}; ^{1}H NMR (500 MHz, CDCl₃) δ 7.76 (d, J = 7.5, 2H), 7.62 (d, J = 7.4, 2H), 7.40 (t, J = 7.4, 2H), 7.32 (t, J = 6.9, 2H), 5.57 (d, J = 5.2, 1H), 4.60 (t, J = 4.6, 1H), 4.53-4.46 (m, 2H), 4.39-4.32 (m, 2H), 4.25 (t, J = 7.2, 1H), 3.78 (dd, J = 11.9, 4.0, 1H), 3.41 (d, J = 11.9, 1H), 2.18-2.09 (m, 1H), 1.46 (s, 9H), 1.03 (d, J = 6.6, 3H), 0.94 (d, J = 6.7, 3H); ^{13}C NMR (126 MHz, CDCl₃) δ 169.6, 169.2, 156.4, 143.7, 141.3, 127.8, 127.1, 125.2, 120.0, 82.45, 67.7, 61.1, 58.6, 56.6, 47.5, 47.1, 28.1, 27.9, 19.2, 18.80; HRMS (ESI-TOF) m/z [M + H]$^+$ calcd for C₂₈H₃₄N₅O₅$^+$ 520.2555, found 520.2551, HRMS (ESI-TOF) m/z [M + Na]$^+$ calcd for C₂₈H₃₃N₅O₅Na$^+$ 542.2374, found 542.2376, HRMS (ESI-TOF) m/z [M + K]$^+$ calcd for C₂₈H₃₃N₅O₅K$^+$ 558.2113, found 558.2109, as well as 10% recovered (4S)-**3.17**.

***tert*-Butyl (3R, 4R, 2'R)-2-[3-(Fmoc)amino-4-(4-phenyl-1H-1,2,3-triazol-1-yl)-2-oxopyrrolidin-1-yl]-3-methylbutanoate [3.25]**

3.25

A solution of CuI (0.5 equiv, 7 mg, 0.039 mmol) in DCM (0.3 mL) at rt was treated sequentially with DIEA (1 equiv, 10 mg, 12.7 μL, 0.077 mmol), phenylacetylene (1.2 equiv, 9.44 mg, 10.1 μL, 0.092 mmol), (4R)-azide (4R)-**3.24j** (1 equiv, 40 mg, 0.08 mmol) and acetic acid (1 equiv, 5 mg, 5 μL, 0.08 mmol), stirred 18 h, when no more alkyne was observed by TLC R_f = 0.85 (20% EtOAc in hexane). The volatiles were removed by rotary evaporation. The residue was partitioned between saturated sodium bicarbonate (2 mL) and EtOAc (2 mL). The aqueous phase was extracted with EtOAc (3 x 2 mL). The combined organic layers were washed with brine, water and brine, dried and evaporated to a residue that was purified by column chromatography using 30% EtOAc in hexane. Evaporation of the collected fractions gave (4R)-phenyltriazole **3.25** (38 mg, 0.06 mmol, 80%) as light yellow solid: R_f = 0.06 (20% EtOAc in hexane); $[\alpha]_D^{25}$ –24.8° (c 2, CHCl$_3$), ^{1}H NMR (400 MHz, CDCl$_3$) δ 7.78 (s, 1H), 7.75 (d, J = 7.2, 2H), 7.67 (d, J = 7.1, 2H), 7.37 (dd, J = 13.0, 6.8, 4H), 7.33-7.27 (m, 3H), 7.12 (dd, J = 15.5, 7.7, 2H), 5.48 (t, J = 6.7, 1H), 5.38 (d, J = 5.5, 1H), 4.82 (t, J = 6.4, 1H), 4.56 (d, J = 9.1, 1H), 4.37-4.19 (m, 3H), 4.10-4.00 (m, 2H), 2.20- 2.17 (m, 1H), 1.49 (s, 9H), 1.08 (dd, J = 8.5, 7.0, 6H); ^{13}C NMR (75 MHz, CDCl$_3$) δ 169.4, 169.2, 156.5, 147.5, 143.3, 141.1, 130.0, 128.8, 128.4, 127.7, 127.1, 125.7, 124.9, 121.2, 119.8, 82.5, 67.8, 61.8, 56.1, 55.8, 48.1, 46.7, 29.7, 28.4, 28.1, 19.7, 19.4; HRMS (ESI-TOF) m/z [M + H]$^+$ calcd for C$_{36}$H$_{40}$N$_5$O$_5^+$ 622.3024, found 622.3019.

(2S)- and (2R)-(9H-fluoren-9-yl)methyl-(3aR,6aR)-5-((R)-1-(tert-butoxy)-3-methyl-1-oxobutan-2-yl)-4-oxotetrahydropyrrolo[3,4-d][1,2,3]oxathiazole-3(3aH)-carboxylate 2-oxide [(2S)- and (2R)-3.23]

(2S)-3.23   **(2R)-3.23**

Annex 2: Supporting information of Article 2

A solution of (3*R*, 4*R*, 2'*R*)-Hgl (4*R*)-**3.17** (1 equiv, 650 mg, 1.31 mmol) in DCM (28 mL) was cooled to 0 °C, treated with imidazole (4 equiv, 357 mg, 5.26 mmol) followed by thionyl chloride (1.1 equiv, 171 mg, 0.105 mL, 1.45 mmol), stirred for 3 h, and diluted with water. The phases were separated. The aqueous phase was extracted with DCM. The combined organic fractions were washed with water, dried, filtered, evaporated to a residue that was used in the next step without further purification.

During purification by column chromatography eluting with 20 to 40% EtOAc in hexanes, first to elute was (2*S*)-sulfamidite (2*S*)-**3.23**: (170 mg, 0.315 mmol, 24%), R_f = 0.39 (40% EtOAc in hexane); [α] $_D^{25}$ 84.2° (c 1, CHCl₃); ¹H NMR (300 MHz, CDCl₃) δ 7.76 (d, *J* = 7.5, 2H), 7.67 (d, *J* = 7.2, 2H), 7.41 (t, *J* = 7.4, 2H), 7.33 (td, *J* = 7.4, 1.2, 2H), 5.81 (t, *J* = 4.9, 1H), 5.06 (br s, 1H), 4.63 (br s, 1H), 4.48 (br s, 1H), 4.41 (d, *J* = 9.6, 1H), 4.33 (t, *J* = 7.2, 1H), 4.20 (d, *J* = 12.7, 1H), 3.84 (dd, *J* = 12.7, 4.2, 1H), 2.17-2-11 (m, 1H), 1.47 (s, 9H), 1.02 (d, *J* = 6.7, 3H), 0.94 (d, *J* = 6.7, 3H); ¹³C NMR (75 MHz, CDCl₃) δ 168.7, 165.4, 151.4, 143.2, 141.3, 127.9, 127.3, 125.3, 120.0, 82.6, 69.9, 60.9, 46.8, 46.4, 39.0, 29.4, 28.5, 28.0, 19.3 (2); HRMS (ESI-TOF) m/z [M + H]⁺ calcd for $C_{28}H_{33}N_2O_7S^+$ 541.1953, found 541.1924. Next to elute was (2*R*)-sulfamidite (2*R*)-**3.23**: (333 mg, 0.618 mmol, 47%), R_f = 0.28 (40% EtOAc in hexane); [α] $_D^{25}$ 50.6° (c 1, CHCl₃); ¹H NMR (300 MHz, CDCl₃) δ 7.76 (d, *J* = 7.5, 2H), 7.62 (d, *J* = 7.4, 2H), 7.41 (td, *J* = 7.5, 0.6, 2H), 7.32 (tt, *J* = 7.4, 1.1, 2H), 5.43 (dd, *J* = 6.8, 5.3, 1H), 5.13 (d, *J* = 7.0, 1H), 4.66-4.56 (m, 1H), 4.55-4.44 (m, 1H), 4.40-4.30 (m, 2H), 4.26 (d, *J* = 12.6, 1H), 3.79 (dd, *J* = 12.6, 5.3, 1H), 2.25-2.08 (m, 1H), 1.47 (s, 9H), 1.01 (d, *J* = 6.6, 3H), 0.90 (d, *J* = 6.7, 3H); ¹³C NMR (75 MHz, CDCl₃) δ 168.4, 167.9, 151.4, 143.3, 141.3, 128.0, 127.3, 125.3, 120.0, 84.2, 82.6, 69.7, 61.4, 58.1, 49.0, 46.7, 27.9, 27.9, 19.1, 19.0; HRMS (ESI-TOF) m/z [M + H]⁺ calcd for $C_{28}H_{33}N_2O_7S^+$ 541.1953 found, 541.1926.

(9H-fluoren-9-yl)methyl (3a*R*,6a*R*)-5-((*R*)-1-(*tert*-butoxy)-3-methyl-1-oxobutan-2-yl)-4-oxotetrahydropyrrolo[3,4-d][1,2,3]oxathiazole-3(3aH)-carboxylate 2,2-dioxide [3.22]

3.22

Annex 2: Supporting information of Article 2

The residue prior to chromatography containing (2*R*)- and (2*S*)-**3.23** was dissolved in acetonitrile (40 mL), cooled to 0 °C, treated with ruthenium (III) chloride hydrate (2%, 5 mg, 0.026 mmol) followed by sodium periodate (1.5 equiv, 421 mg, 1.97 mmol). After stirring for 15 min, the reaction mixture was treated with water (33 mL), stirred for 6 h at 0 °C and diluted with ether. The phases were separated. The aqueous phase was extracted with ether. The combined organic fractions were washed with saturated aqueous sodium bicarbonate and brine, dried, filtered, evaporated and purified by column chromatography eluting with 20 to 40% EtOAc in hexanes to furnish sulfamidate **3.22** as colorless oil (327 mg, 0.589 mmol, 79% yield): $R_f = 0.34$ (40% EtOAc in hexane); $[\alpha]_D^{25}$ 97.5° (c 1, CHCl$_3$); ^{1}H NMR (300 MHz, CDCl$_3$) δ 7.80-7.58 (m, 4H), 7.41 (td, $J = 7.4, 0.6, 2H$), 7.33 (td, $J = 7.4, 0.7, 2H$), 5.45 (dd, $J = 5.6, 4.2, 1H$), 5.12 (d, $J = 5.7, 1H$), 4.58 (d, $J = 1.6, 1H$), 4.56 (s, 1H), 4.46-4.31 (m, 2H), 4.17 (d, $J = 13.0, 1H$), 3.78 (dd, $J = 13.1, 4.2, 1H$), 2.25-2.11 (m, 1H), 1.49 (s, 9H), 1.02 (d, $J = 6.6, 3H$), 0.92 (d, $J = 6.7, 3H$); ^{13}C NMR (75 MHz, CDCl$_3$) δ 168.3, 166.2, 149.8, 143.0, 141.3, 128.0, 127.4, 125.5, 120.0, 83.0, 75.4, 71.8, 70.9, 61.2, 58.8, 46.5, 28.1, 27.9, 19.2, 19.2; HRMS (ESI-TOF) m/z $[M + NH_4]^+$ calcd for C$_{28}$H$_{36}$N$_3$O$_8$S 574.2218 found, 574.2217.

tert-**Butyl (3*S*, 4*S*, 2'*R*)-2-[3-(Fmoc)amino-4-benzoylsulfanyl-2-oxopyrrolidin-1-yl]-3-methylbutanoate [(4*S*)-3.24b]**

(4*S*)-3.24b

A solution of sulfamidate **3.22** (1 equiv, 30 mg, 0.26 mL, 0.054 mmol) in DCM (1.5 mL) was treated with potassium thiobenzoate (3 equiv, 29 mg, 0.16 mmol), stirred at rt for 10 h, poured into 1 M NaH$_2$PO$_4$ and extracted with DCM. The combined organic phase was washed with brine, dried, filtered, evaporated and purified by column chromatography using a step gradient of 10 to 50% EtOAc in hexane. Evaporation of the collected fractions gave (4*S*)-thioester (4*S*)-**3.24b** (30 mg, 0.049 mmol, 90%): $R_f = 0.42$ (40% EtOAc in hexane); $[\alpha]_D^{25}$ –32.5° (c 1, CHCl$_3$); ^{1}H NMR (700 MHz, CDCl$_3$) δ 7.94 (d, $J = 7.6, 2H$), 7.74 (d, $J = 7.5, 2H$), 7.61-7.56 (m, 3H), 7.45 (t, $J =$

7.8, 2H), 7.36 (td, J = 7.4, 2.8, 2H), 7.30-7.26 (m, 2H), 5.36 (d, J = 7.0, 1H), 4.65-4.54 (m, 1H), 4.49 (d, J = 9.0, 1H), 4.38 (d, J = 7.2, 2H), 4.30 (t, J = 8.9, 1H), 4.23 (t, J = 7.0, 1H), 4.19-4.09 (m, 1H), 3.34 (t, J = 9.5, 1H), 2.25-2.18 (m, 1H), 1.52 (s, 9H), 1.02 (d, J = 6.7, 3H), 0.95 (d, J = 6.8, 3H); ^{13}C NMR (176 MHz, CDCl$_3$) δ 190.8, 170.3, 169.0, 156.4, 143.8, 141.3, 136.3, 133.9, 128.8, 127.7, 127.4, 127.1, 125.2, 119.9, 82.4, 67.5, 61.0, 56.1, 47.8, 47.1, 43.1, 29.7, 28.8, 28.1, 19.4; HRMS (ESI-TOF) m/z [M + H]$^+$ calcd for C$_{35}$H$_{39}$N$_2$O$_6$S$^+$ 615.2523, found 615.2532.

tert-Butyl (3R, 4S, 2'S)-2-[3-(Fmoc)amino-4-azido-2-oxopyrrolidin-1-yl]-3-methylbutanoate [(4S)-3.24j]

(4S)-3.24j

A solution of sulfamidate **3.22** (1 equiv, 37 mg, 0.26 mL, 0.067 mmol) in DCM (1.6 mL) and DMF (0.4 mL) was treated with sodium azide (3 equiv, 13 mg, 0.2 mmol), stirred at rt for 8 h, poured into 1 M NaH$_2$PO$_4$, and extracted with DCM. The combined organic phase was washed with brine, dried, filtered, evaporated and purified by column chromatography using a step gradient of 10-30% EtOAc in hexane. Evaporation of the collected fractions gave (4S)-azide (4S)-**3.24j** (28 mg, 0.053 mmol, 80% yield): Rf = 0.5 (30% EtOAc in hexane); [α] $_D$ ^{25} 12° (c 0.8, CHCl$_3$); FT-IR (neat) νmax 3334, 2942, 2831, 2108, 1701, 1449, 1114, 1022, 621 cm^{-1}; ^{1}H NMR (500 MHz, CDCl$_3$) δ 7.76 (d, J = 7.5, 2H), 7.60 (d, J = 7.5, 2H), 7.40 (t, J = 7.5, 2H), 7.32 (t, J = 7.5, 2H), 5.37 (s, 1H), 4.49-4.41 (m, 3H), 4.32 (t, J = 7.3, 1H), 4.25 (t, J = 6.9, 1H), 4.19-4.10 (m, 1H), 4.06 (t, J = 8.9, 1H), 3.13 (t, J = 8.7, 1H), 2.24-2.14 (m, 1H), 1.47 (s, 9H), 1.00 (d, J = 6.7, 3H), 0.93 (d, J = 6.8, 3H); ^{13}C NMR (126 MHz, CDCl$_3$) δ 169.6, 169.3, 156.3, 143.7, 141.3, 127.8, 127.1, 125.1, 120.0, 82.5, 67.5, 61.8, 60.5, 58.0, 47.1, 46.4, 28.9, 28.0, 19.3(2); HRMS (ESI-TOF) m/z [M + H]$^+$ calcd for C$_{28}$H$_{34}$N$_5$O$_5$$^+$ 520.2555, found 520.2551, HRMS (ESI-TOF) m/z [M + Na]$^+$ calcd for C$_{28}$H$_{33}$N$_5$O$_5$Na$^+$ 542.2374, found 542.2376, HRMS (ESI-TOF) m/z [M + K]$^+$ calcd for C$_{28}$H$_{33}$N$_5$O$_5$K$^+$ 558.2113, found 558.2109.
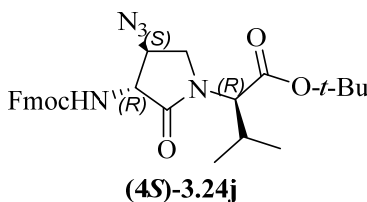
References

1. St-Cyr, D. J.; Jamieson, A. G.; Lubell, W. D., *Org. Lett.* **2010**, *12*, 1652-1655.

2. Dekamin, M. G.; Moghaddam, F. M.; Saeidian, H.; Mallakpour, S.,   *Monatsh.   Chem. /Chemical Monthly* **2006,** *137*, 1591-1595.

Annex 2: Supporting information of Article 2

¹H NMR (500 MHz, CDCl₃) **(4S)-3.17**

^{13}C NMR (126 MHz, CDCl$_3$) **(4S)-3.17**

Annex 2: Supporting information of Article 2
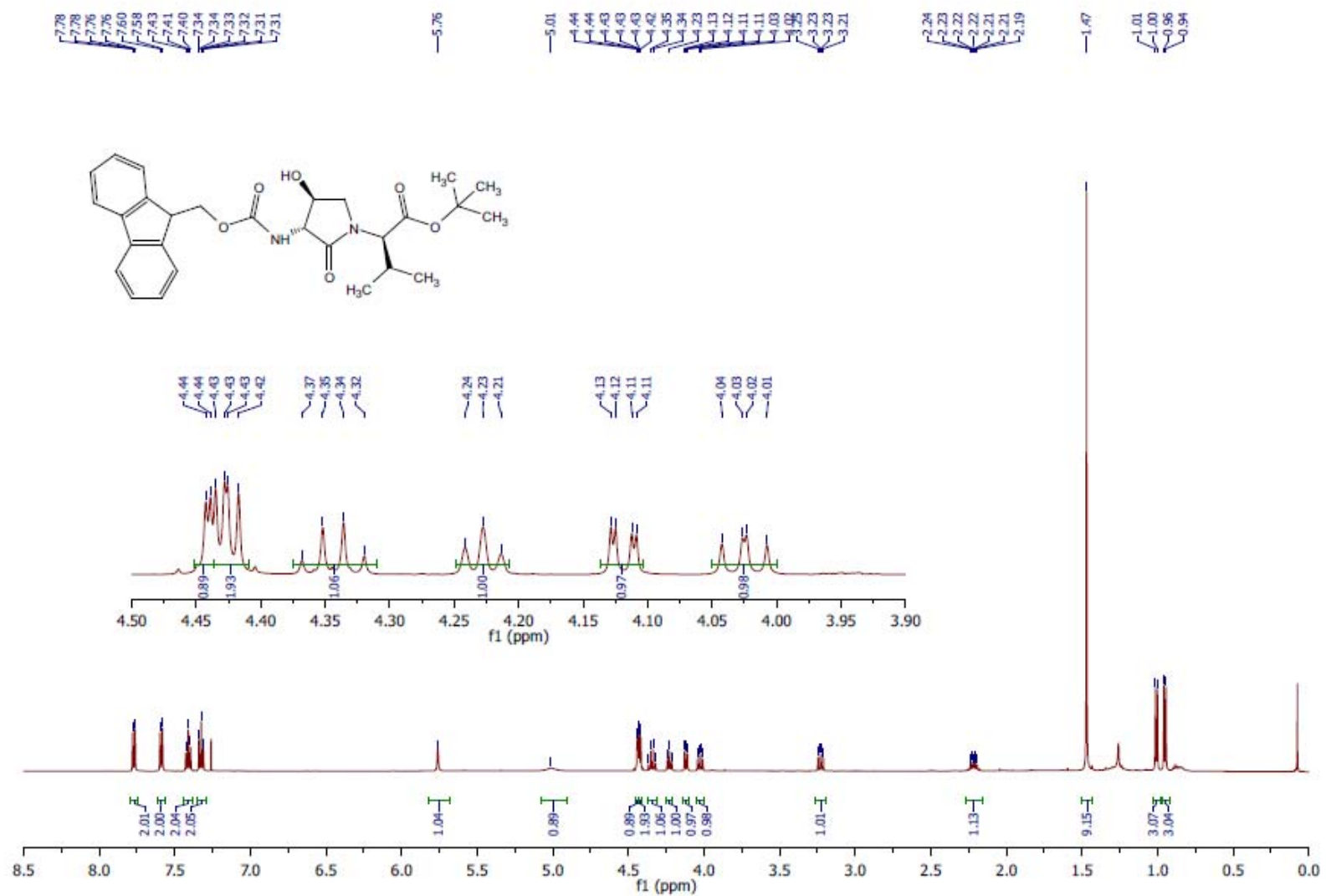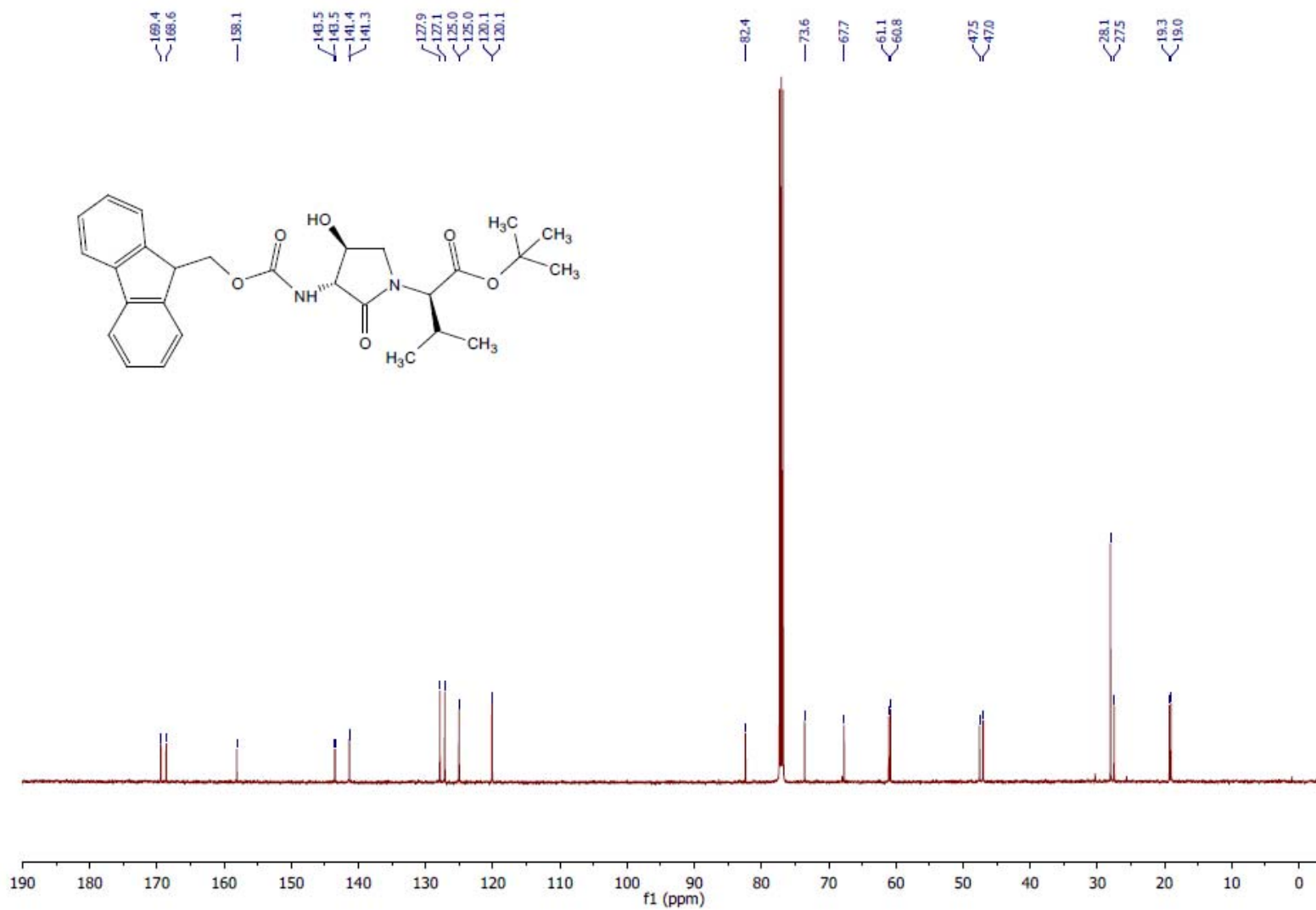
DEPT (126 MHz, CDCl₃) **(4*S*)-3.17**
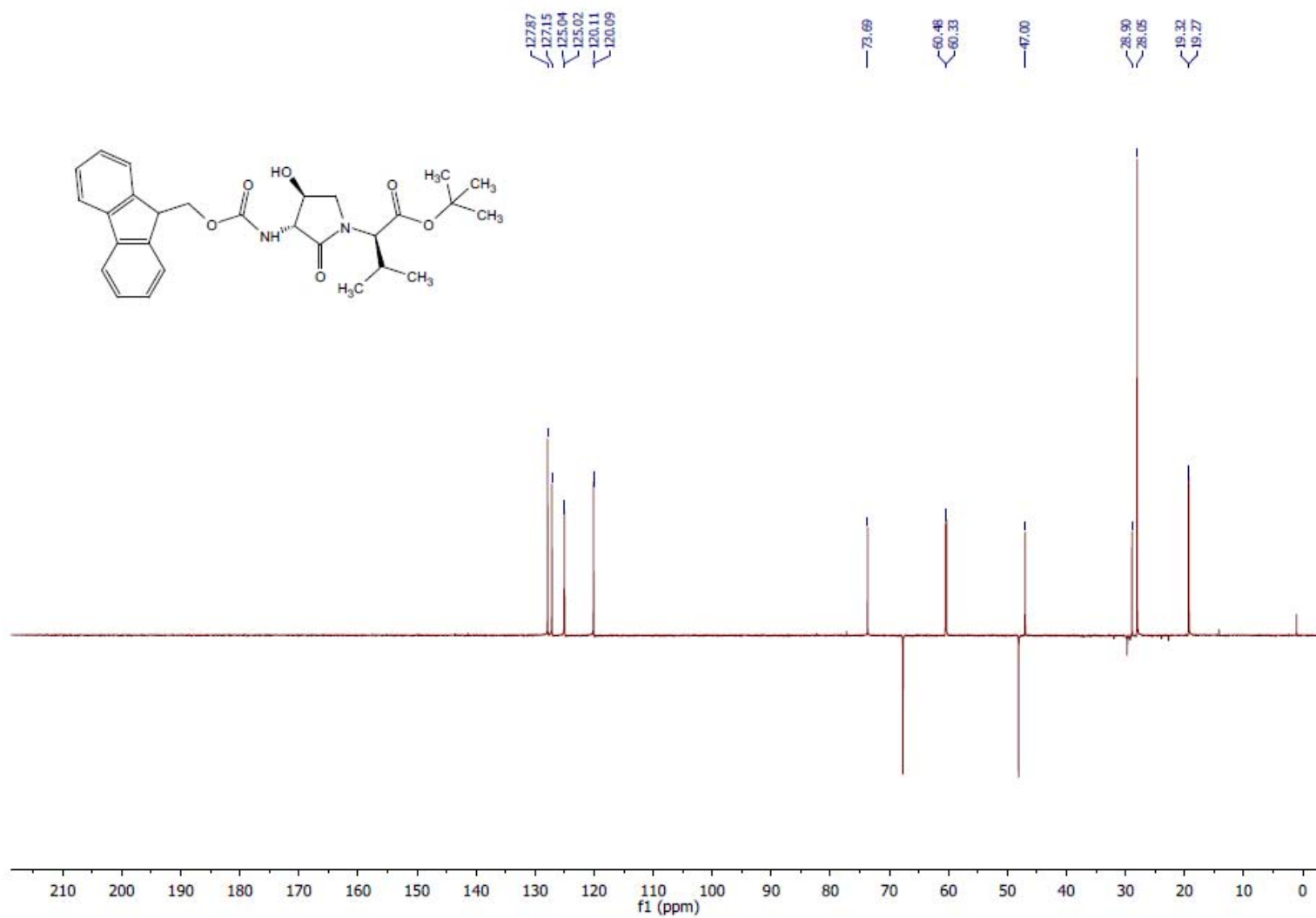
COSY (500 MHz, CDCl$_3$) **(4*S*)-3.17**

HSQC (126 MHz, CDCl₃) **(4*S*)-3.17**
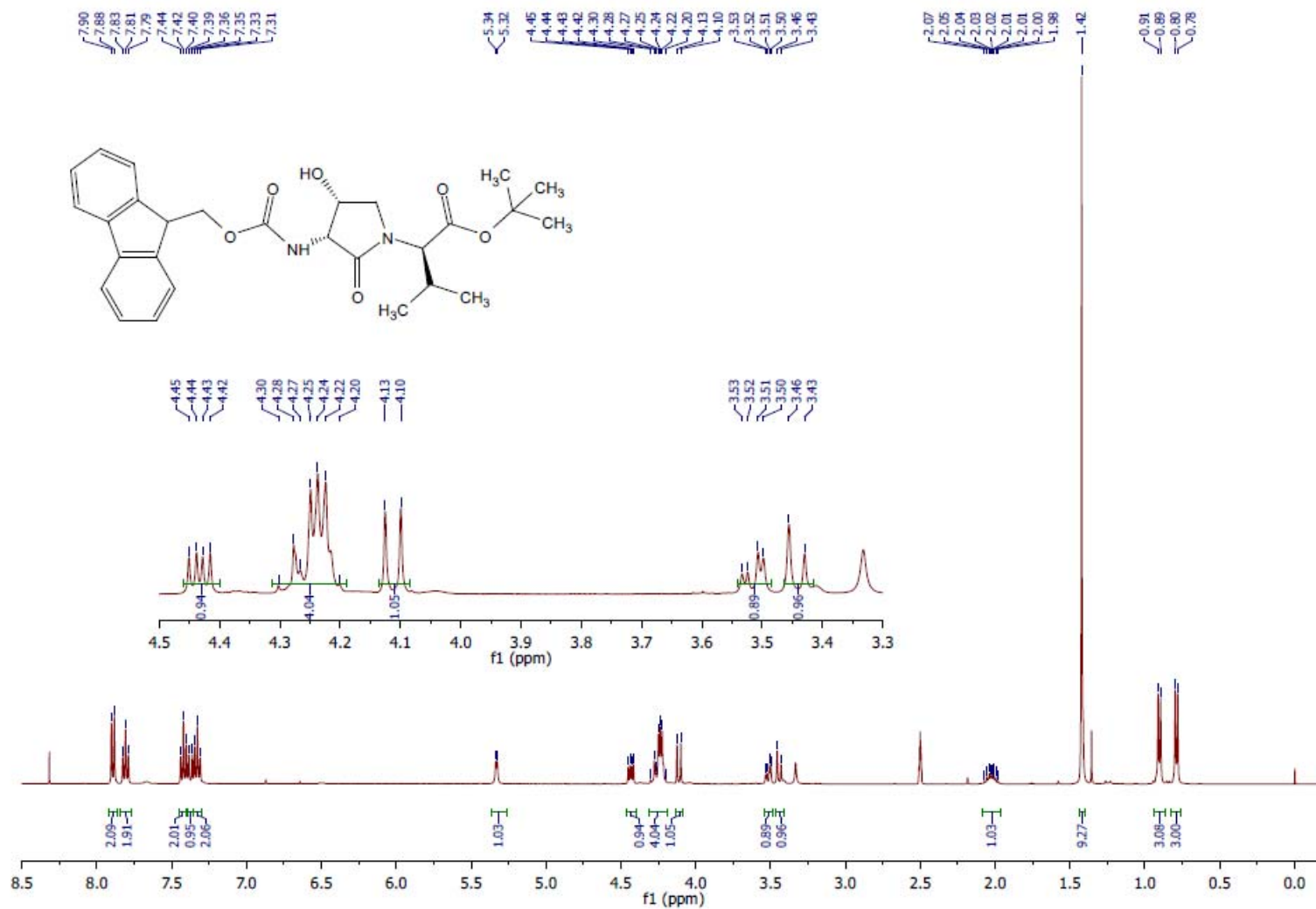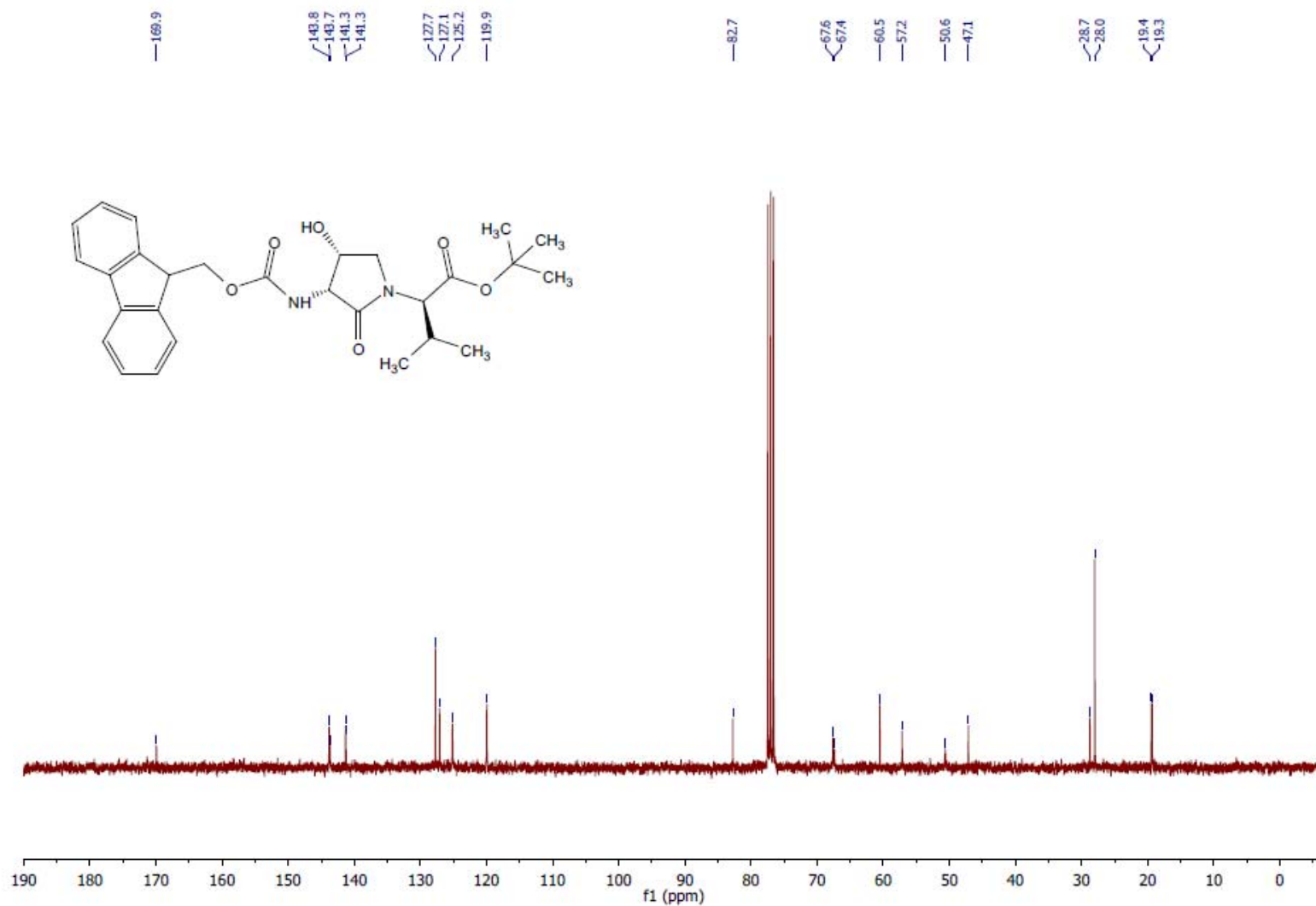
Annex 2: Supporting information of Article 2

¹H NMR (400 MHz, DMSO) **(4R)-3.17**

Annex 2: Supporting information of Article 2

¹³C NMR (75 MHz, CDCl₃) **(4R)-3.17**

^{13}C NMR (75 MHz, CDCl$_3$) **(4R)-3.17**

Annex 2: Supporting information of Article 2

DEPT (75 MHz, CDCl$_3$) **(4*R*)-3.17**

Annex 2: Supporting information of Article 2

COSY (400 MHz, DMSO) **(4R)-3.17**

Annex 2: Supporting information of Article 2

HSQC (75 MHz, CDCl₃) **(4R)-3.17**

Annex 2: Supporting information of Article 2

^{1}H NMR (300 MHz, CDCl$_3$) **(4R)-3.24a**
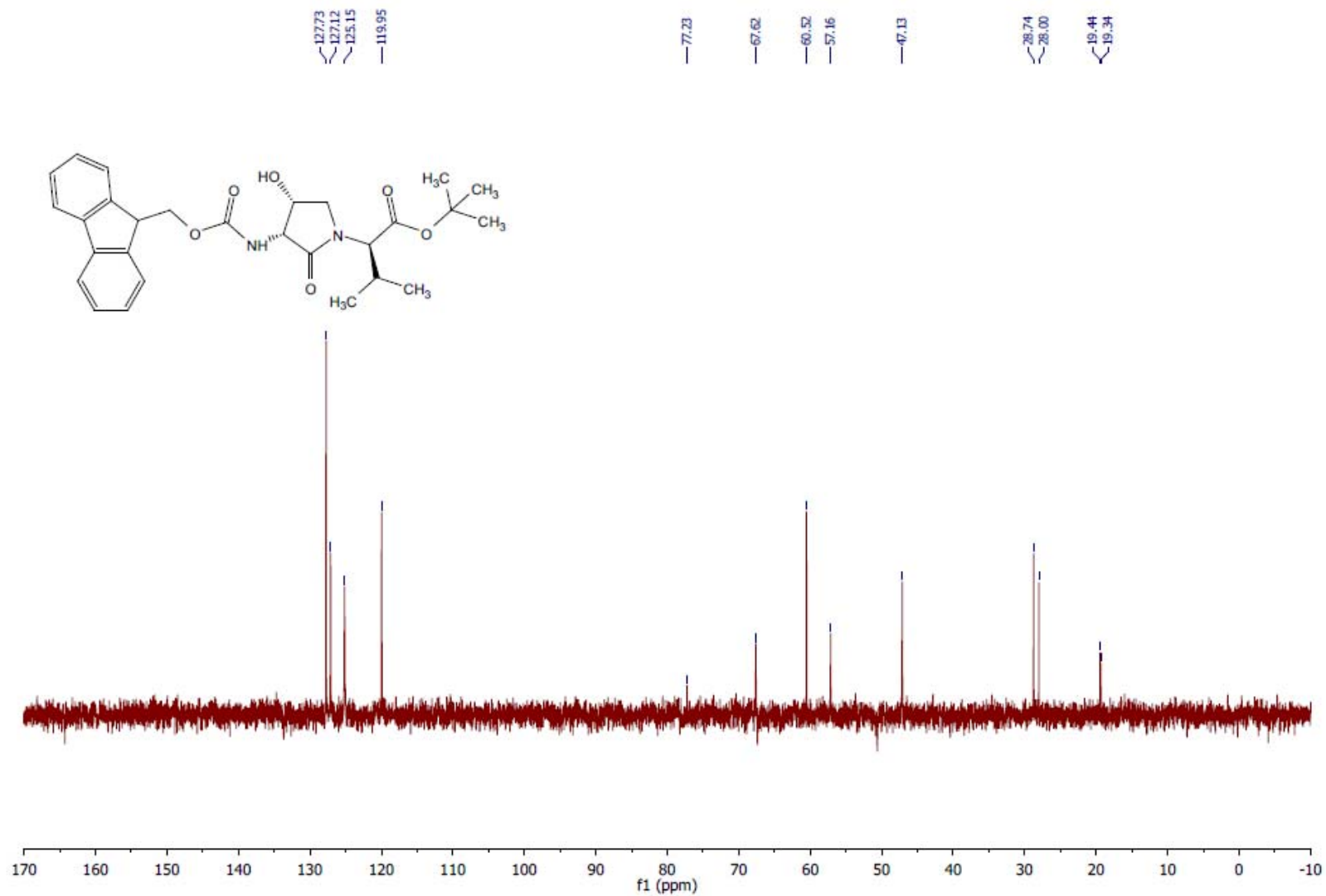
Annex 2: Supporting information of Article 2
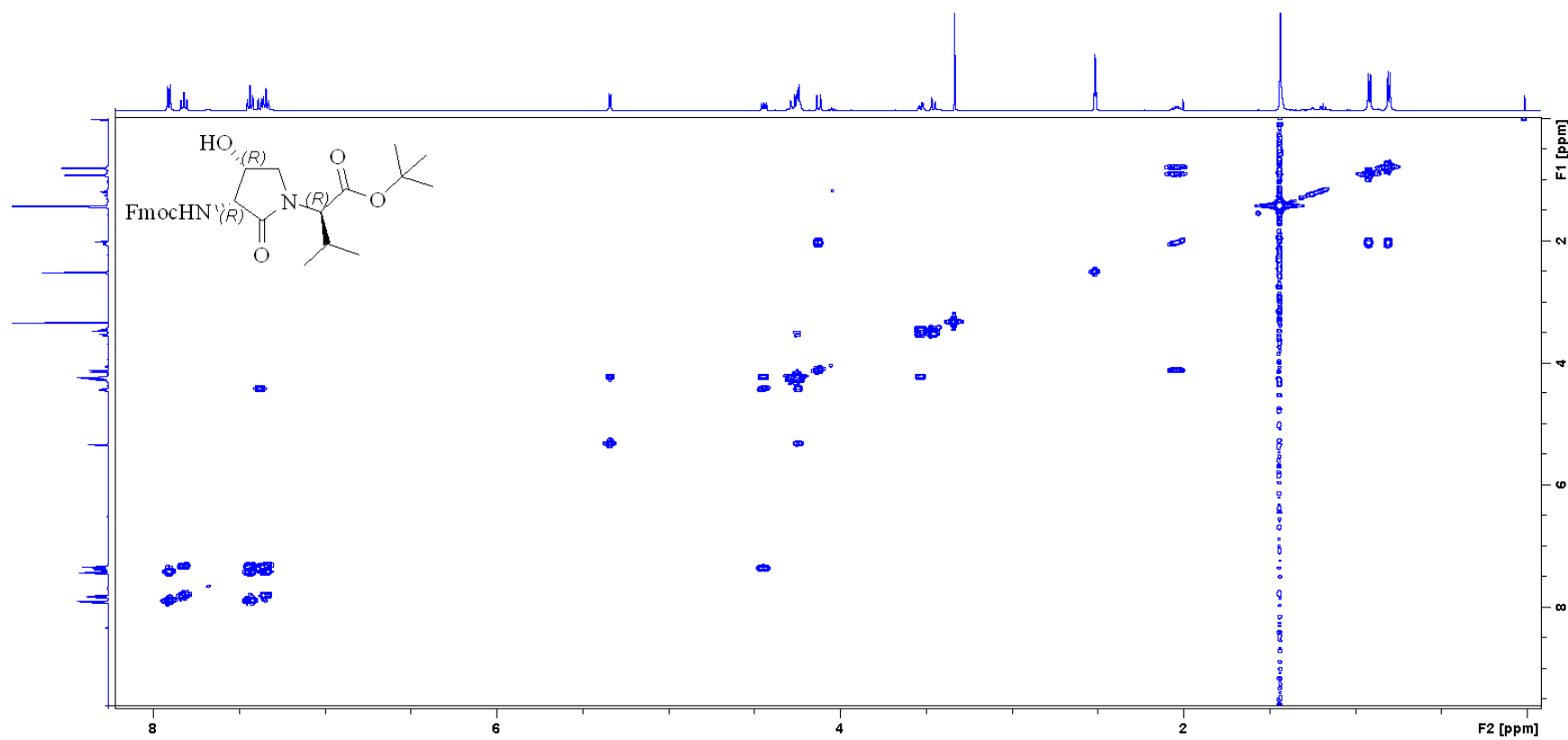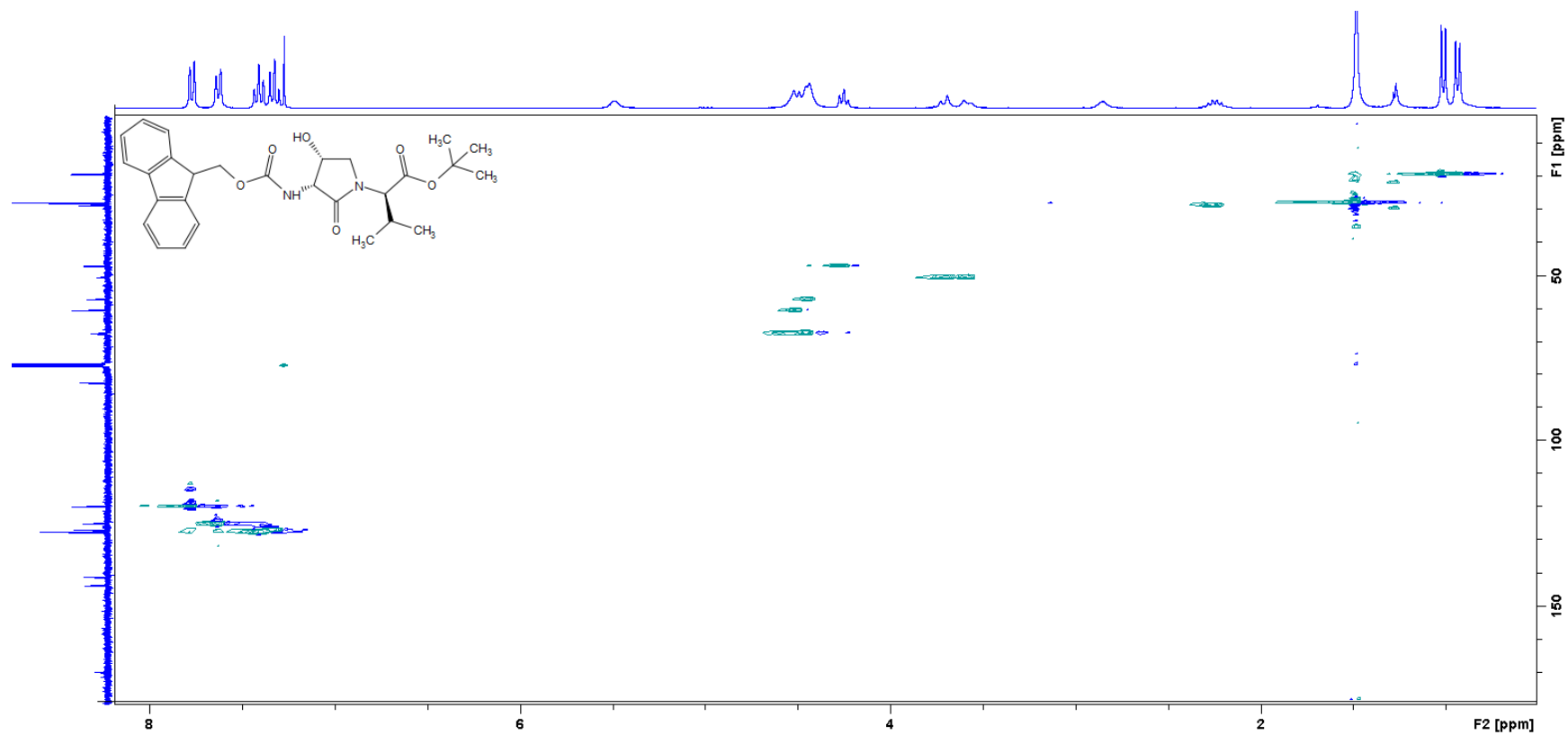
^{13}C NMR (75 MHz, CDCl$_3$) (4*R*)-3.24a

Annex 2: Supporting information of Article 2

DEPT (75 MHz, CDCl₃) **(4*R*)-3.24a**

Annex 2: Supporting information of Article 2
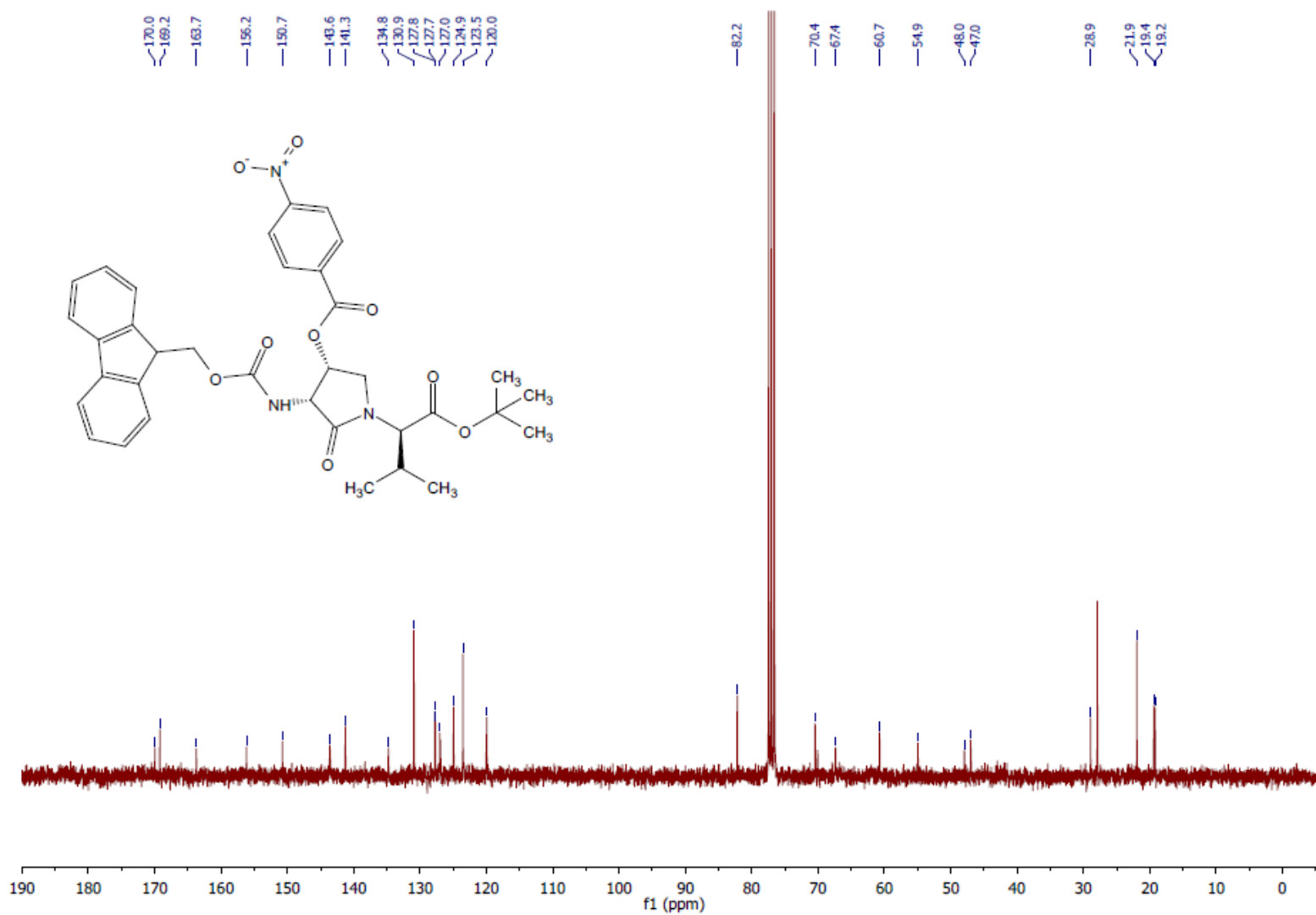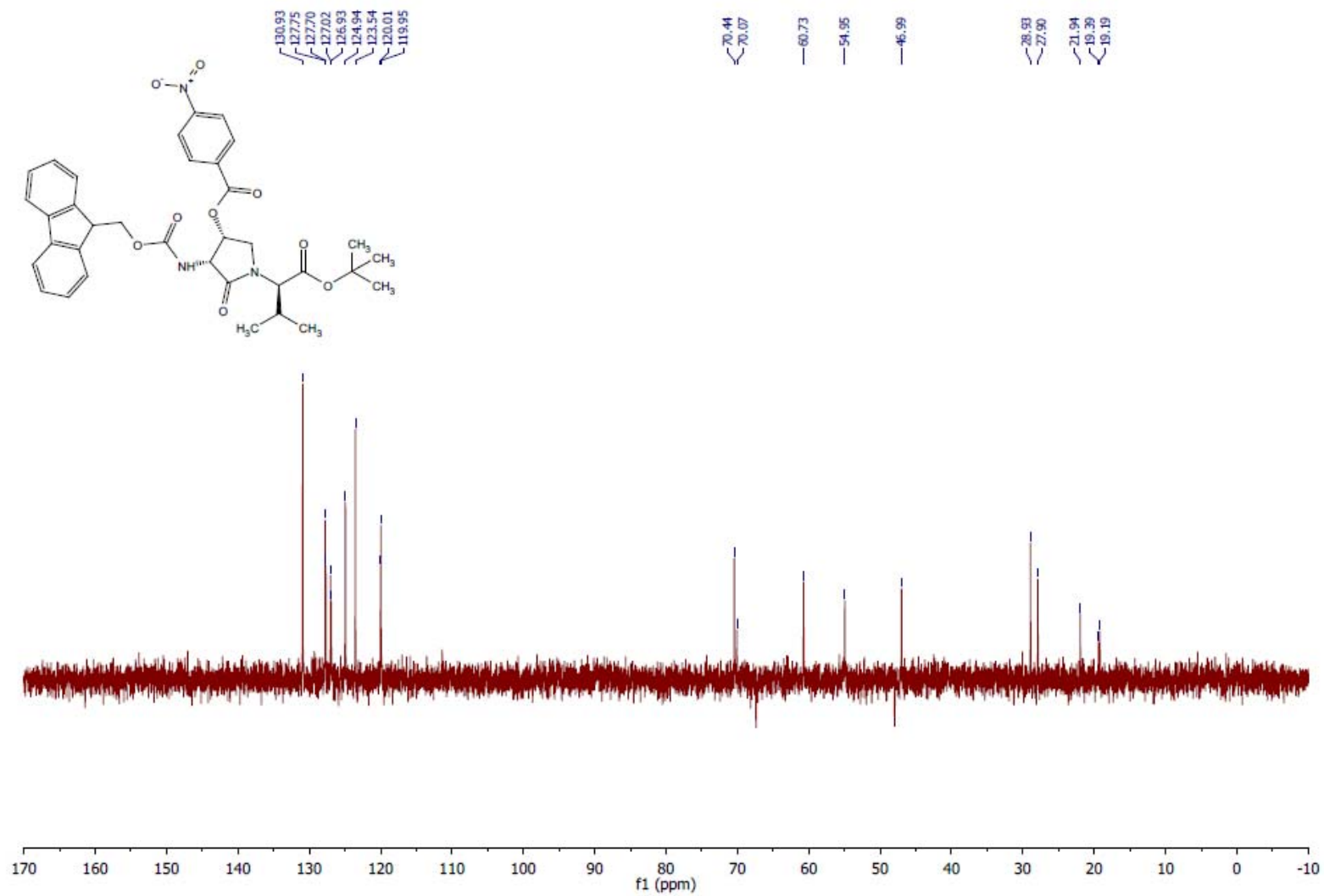
COSY (300 MHz, CDCl$_3$) **(4R)-3.24a**
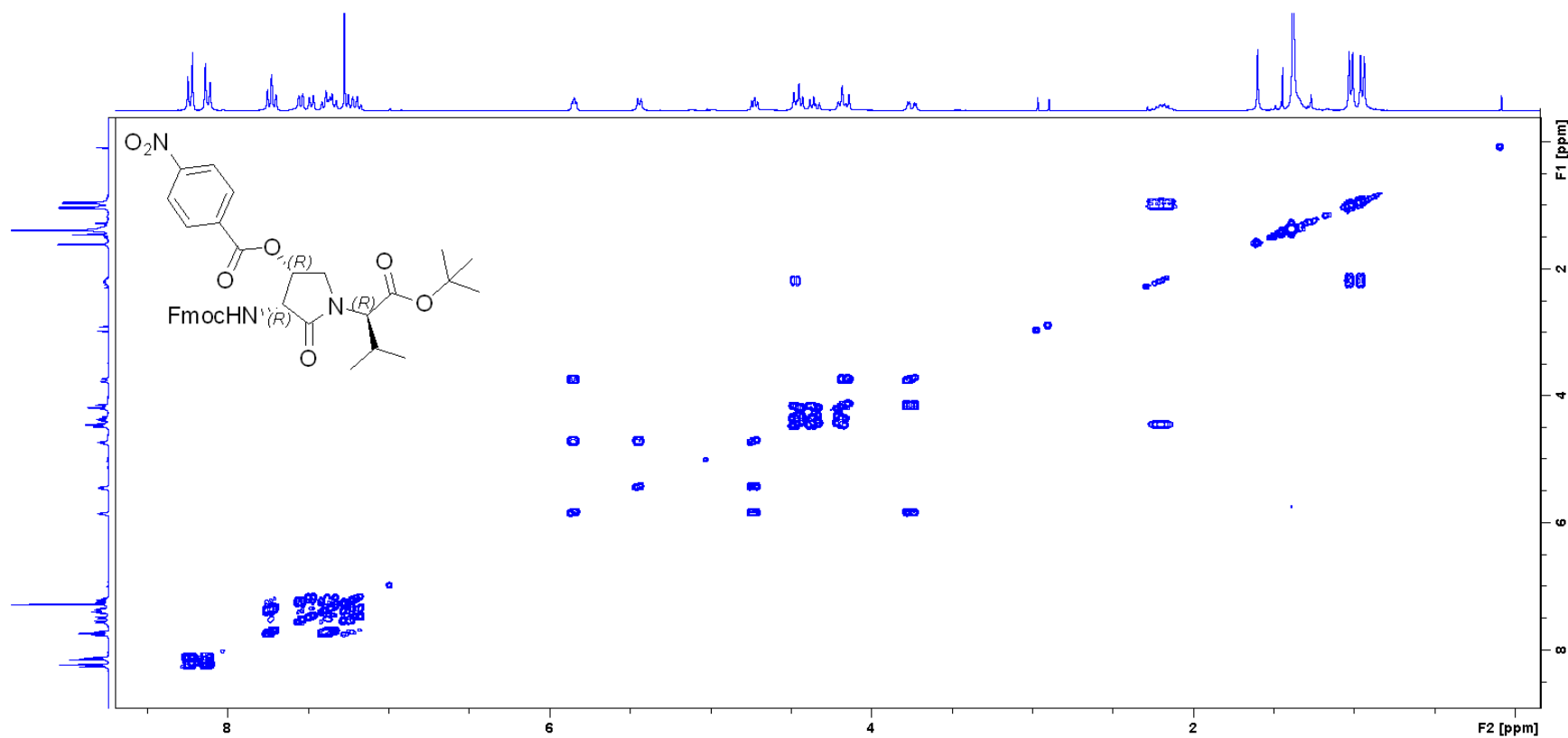
HSQC (75 MHz, CDCl₃) **(4R)-3.24a**
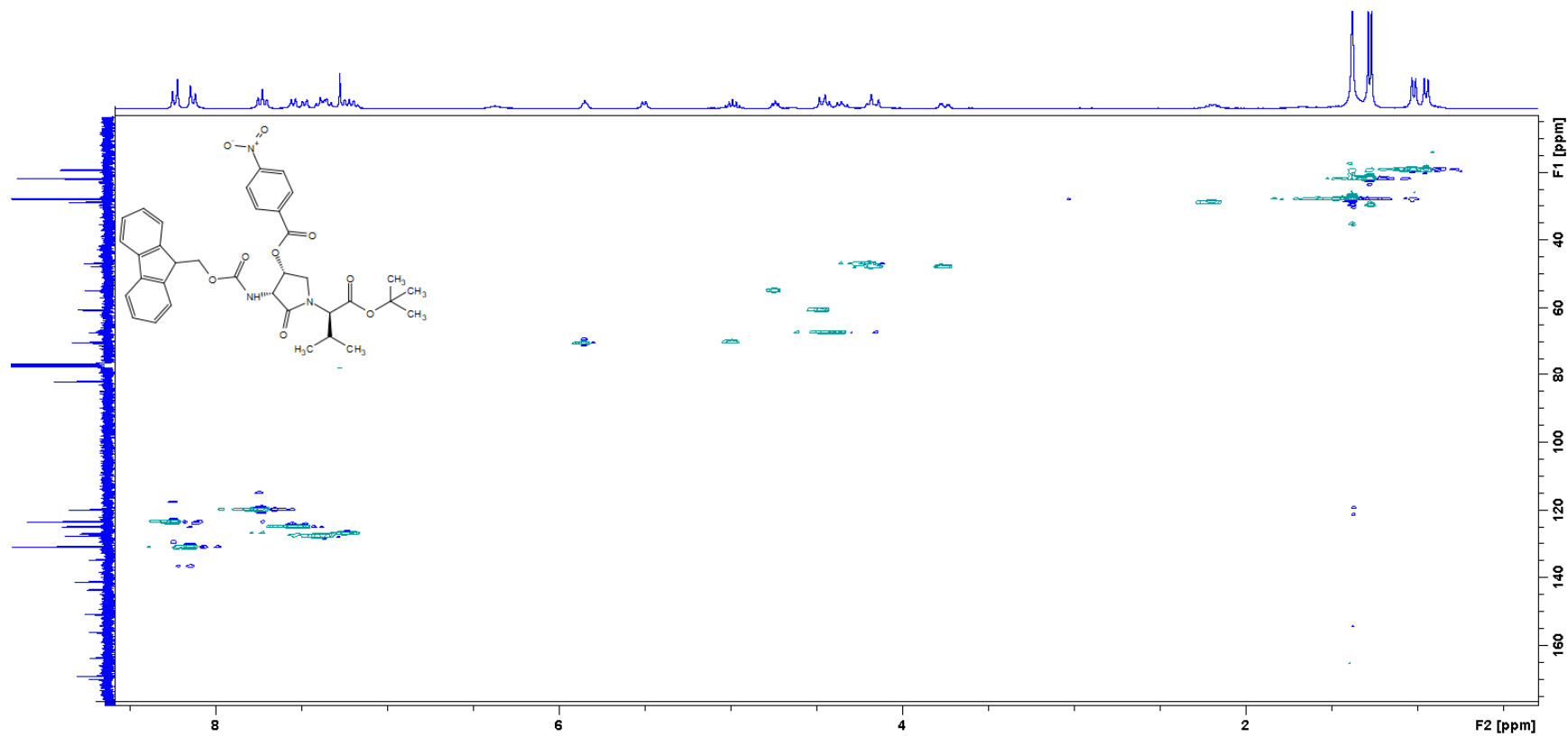
^{1}H NMR (400 MHz, C$_6$D$_6$) **3.21**
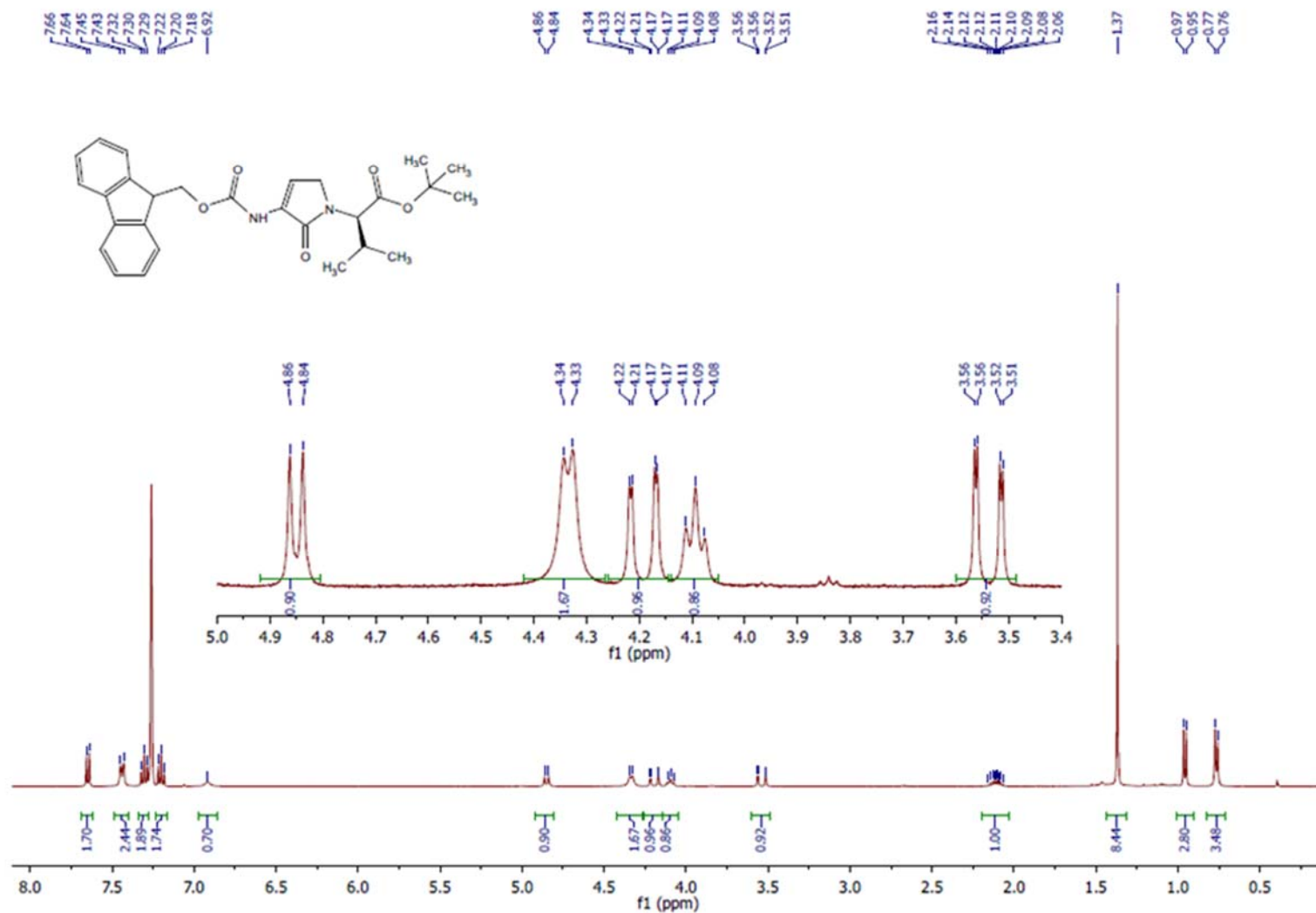
^{13}C NMR (75 MHz, CDCl$_3$) **3.21**

Annex 2: Supporting information of Article 2
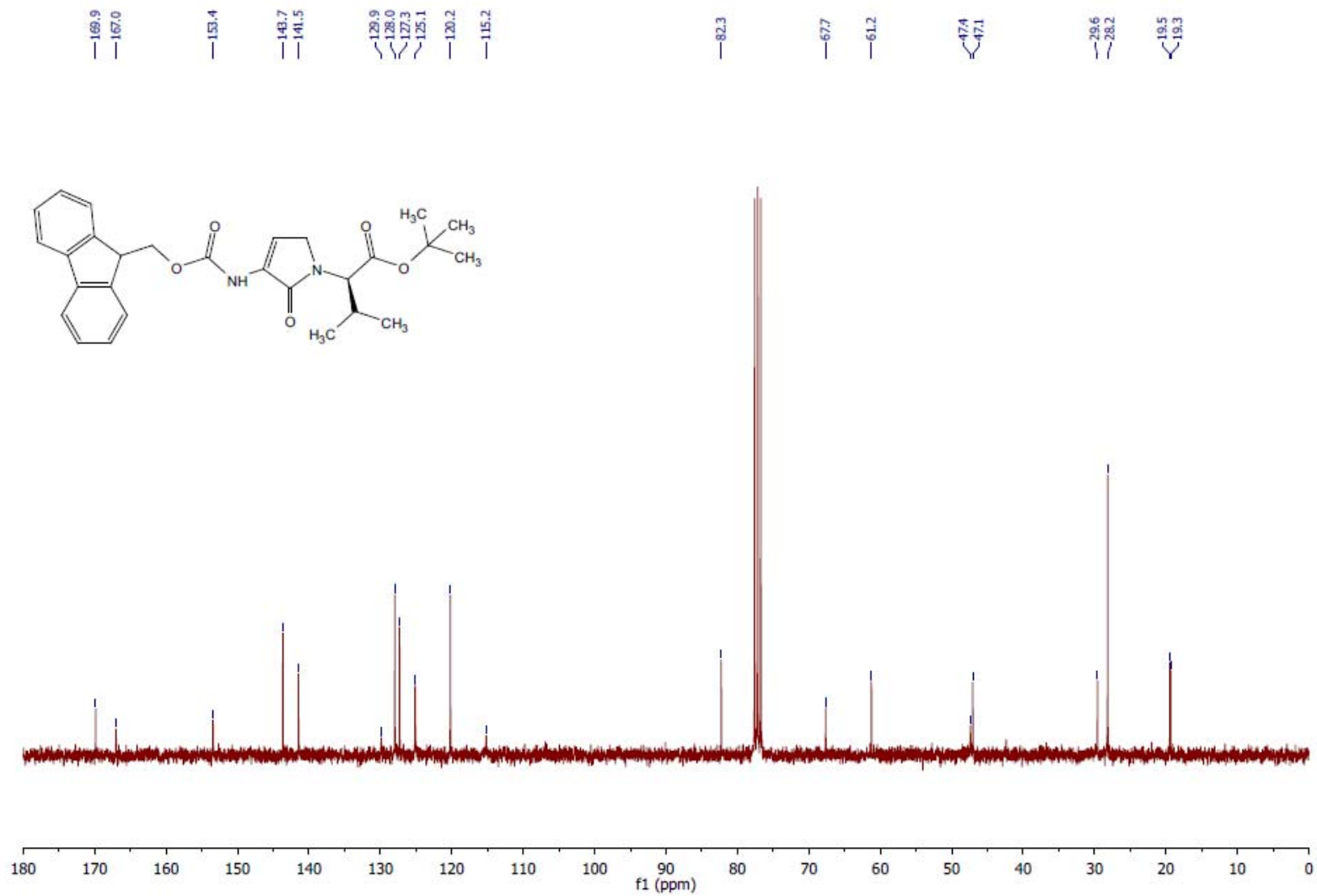
¹³C NMR (75 MHz, CDCl₃) **3.21**
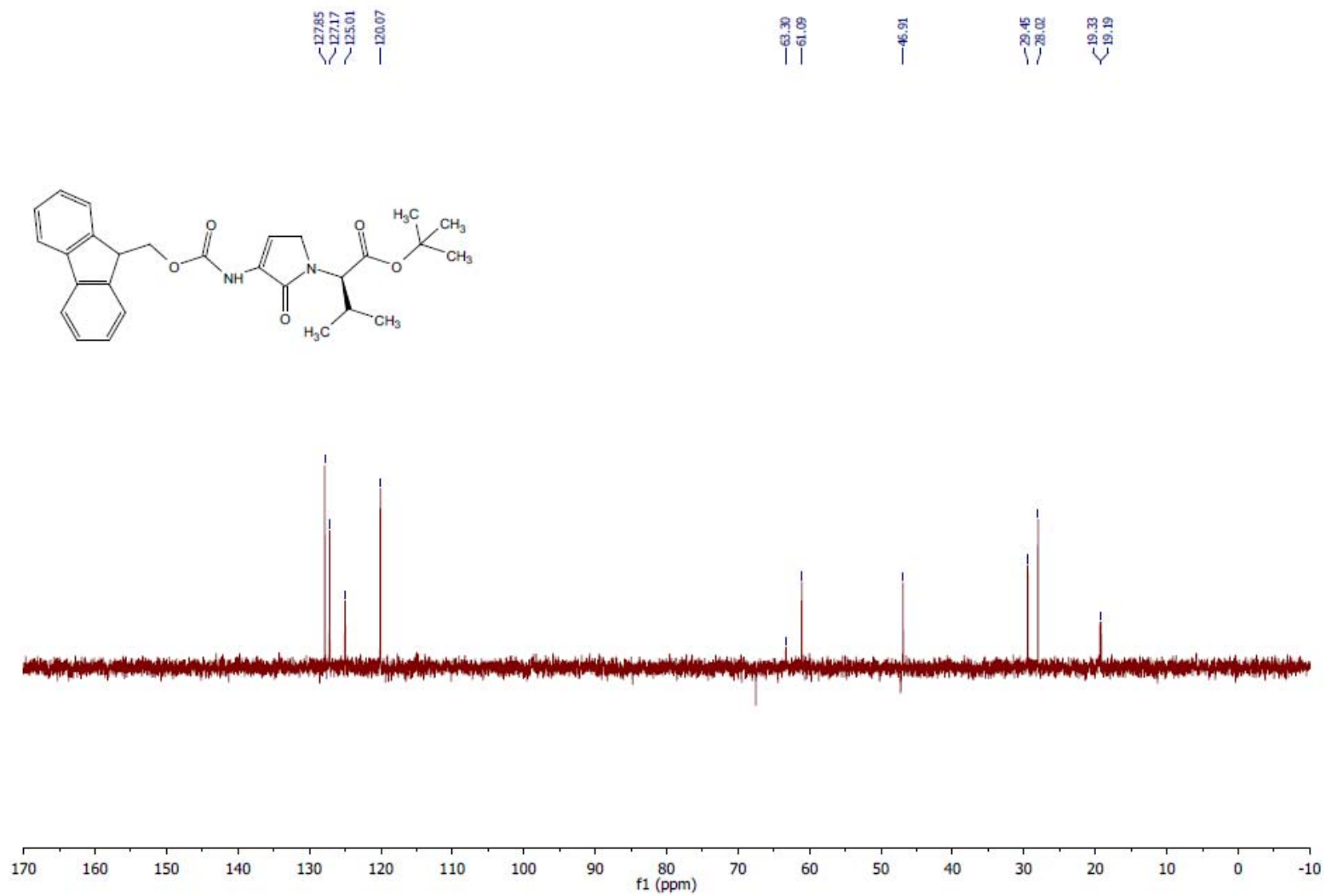
COSY (300 MHz, CDCl$_3$) **3.21**
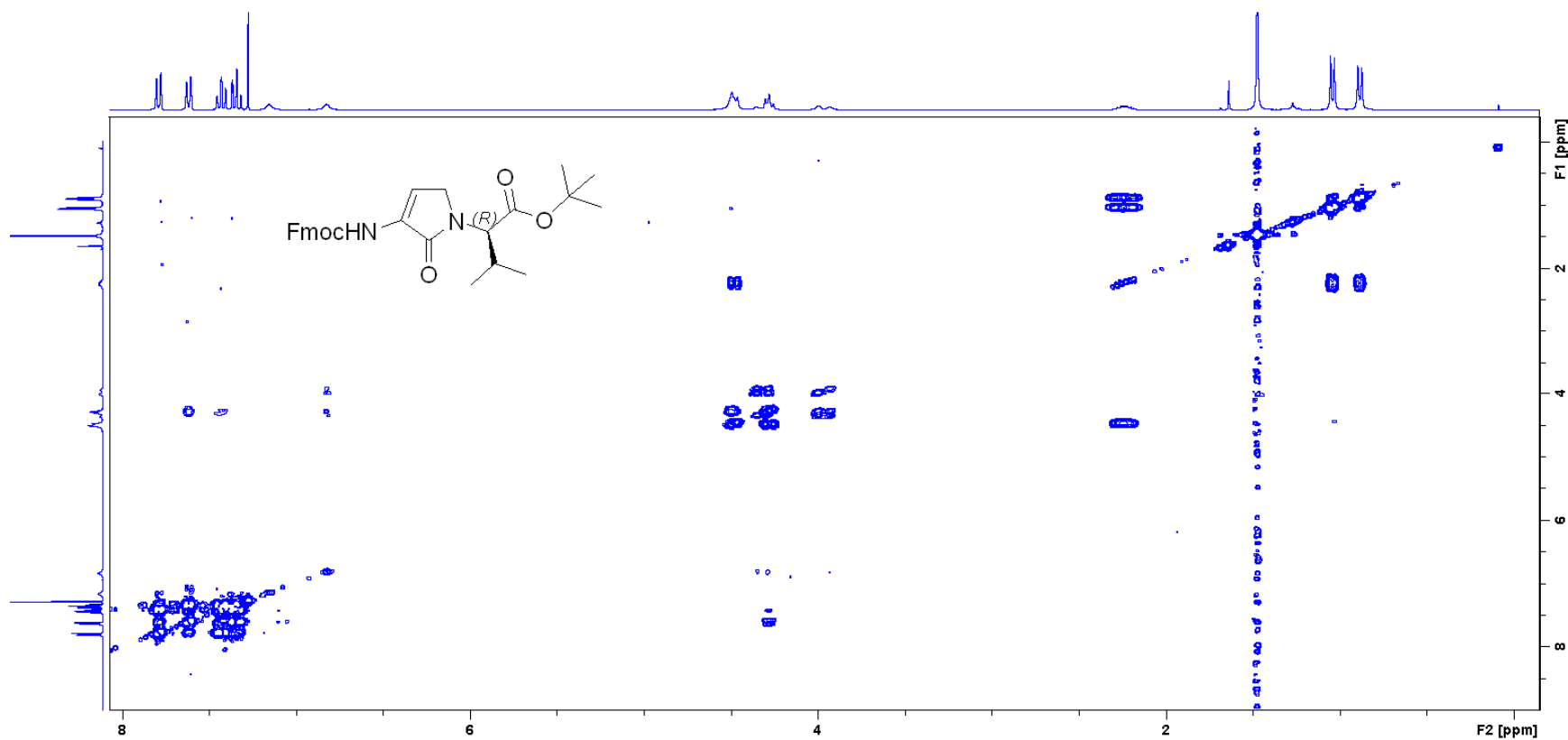
HSQC (75 MHz, CDCl₃) **3.21**
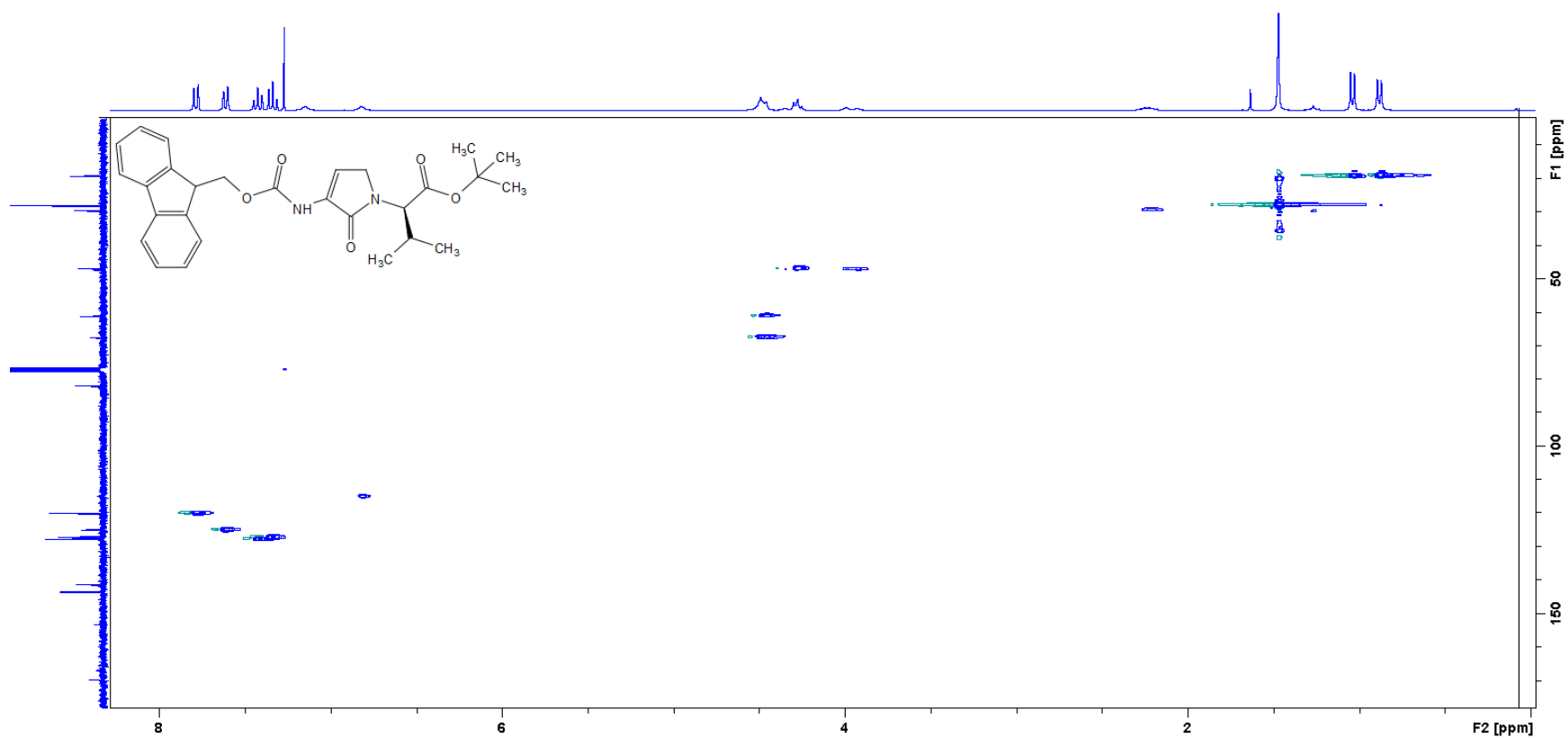
^{1}H NMR (500 MHz, CDCl$_3$) **(4*R*)-3.24b**
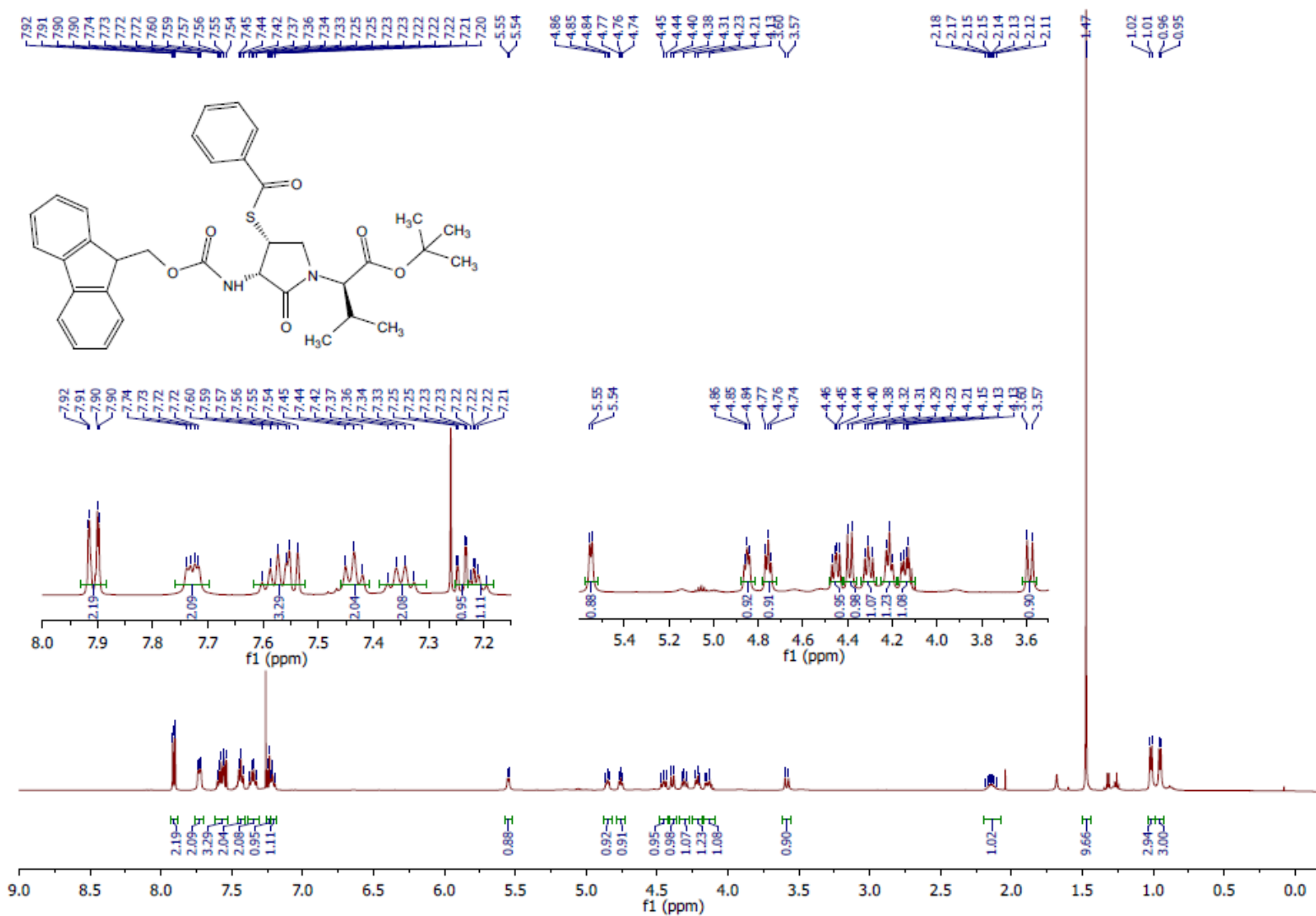
^{13}C NMR (126 MHz, CDCl$_3$) **(4*R*)-3.24b**
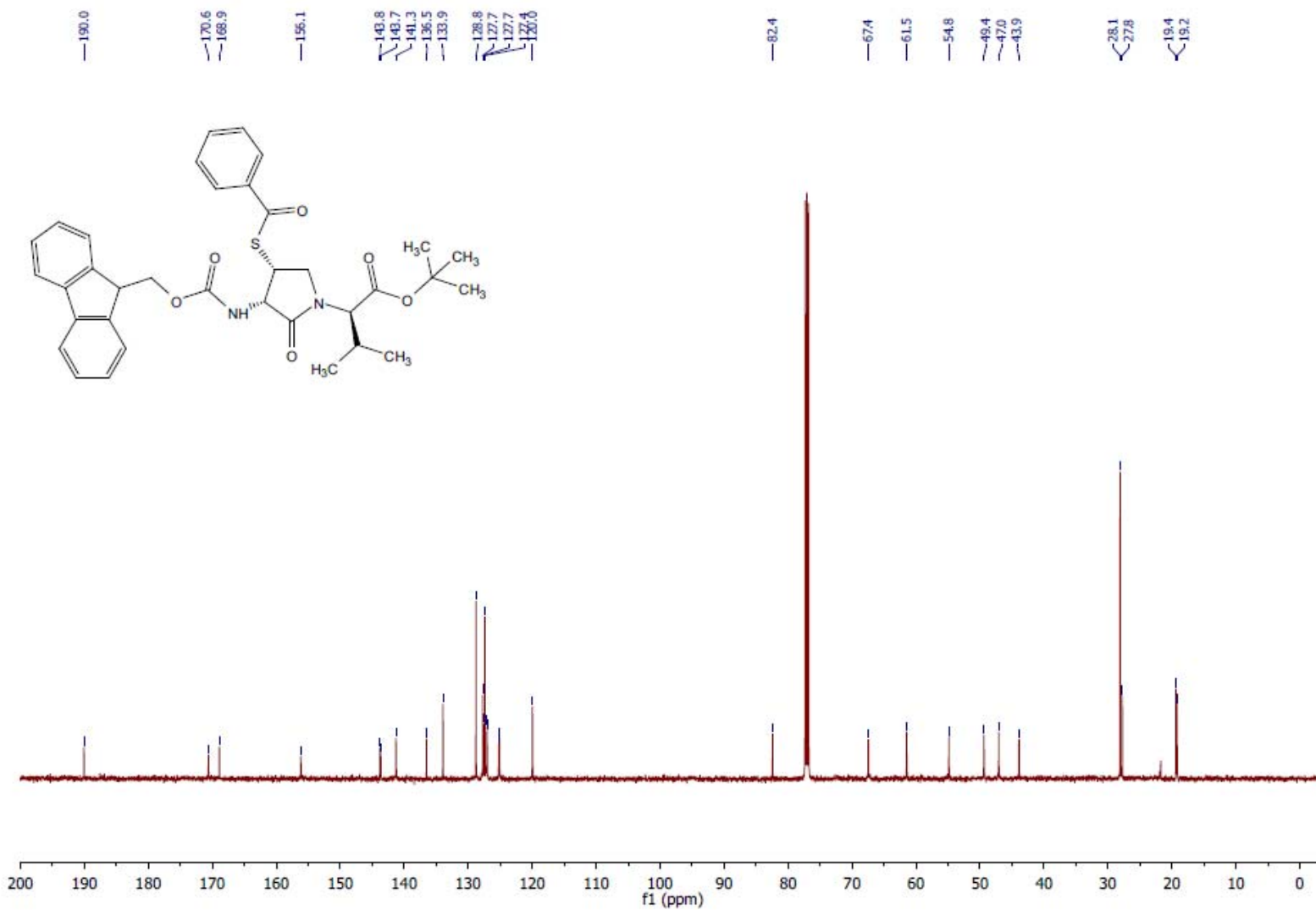
DEPT (126 MHz, CDCl₃) **(4*R*)-3.24b**
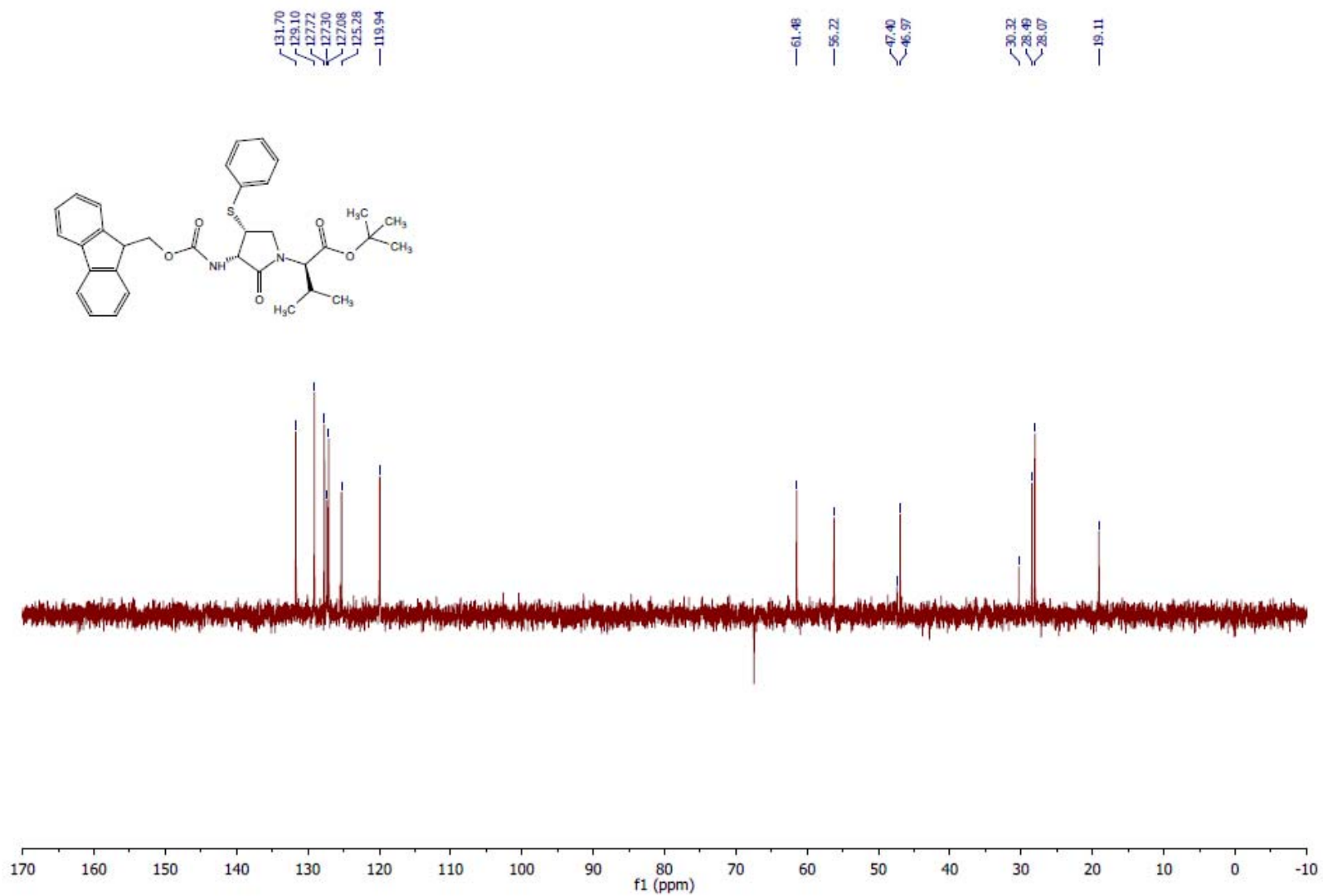
COSY (500 MHz, CDCl$_3$) **(4*R*)-3.24b**
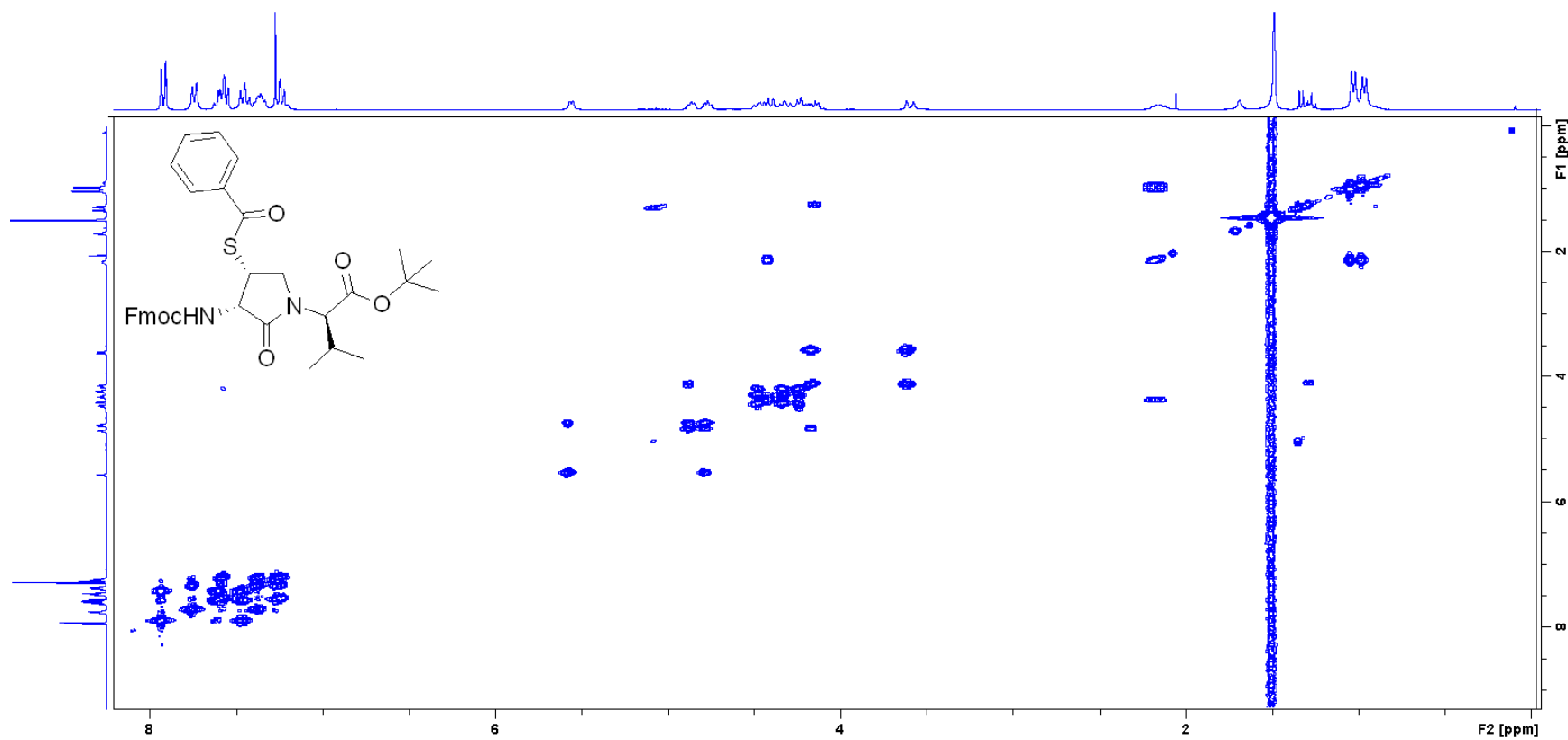
HSQC (126 MHz, CDCl$_3$) **(4*R*)-3.24b**

^{1}H NMR (700 MHz, CDCl$_3$) **(4R)-3.24c**

Annex 2: Supporting information of Article 2
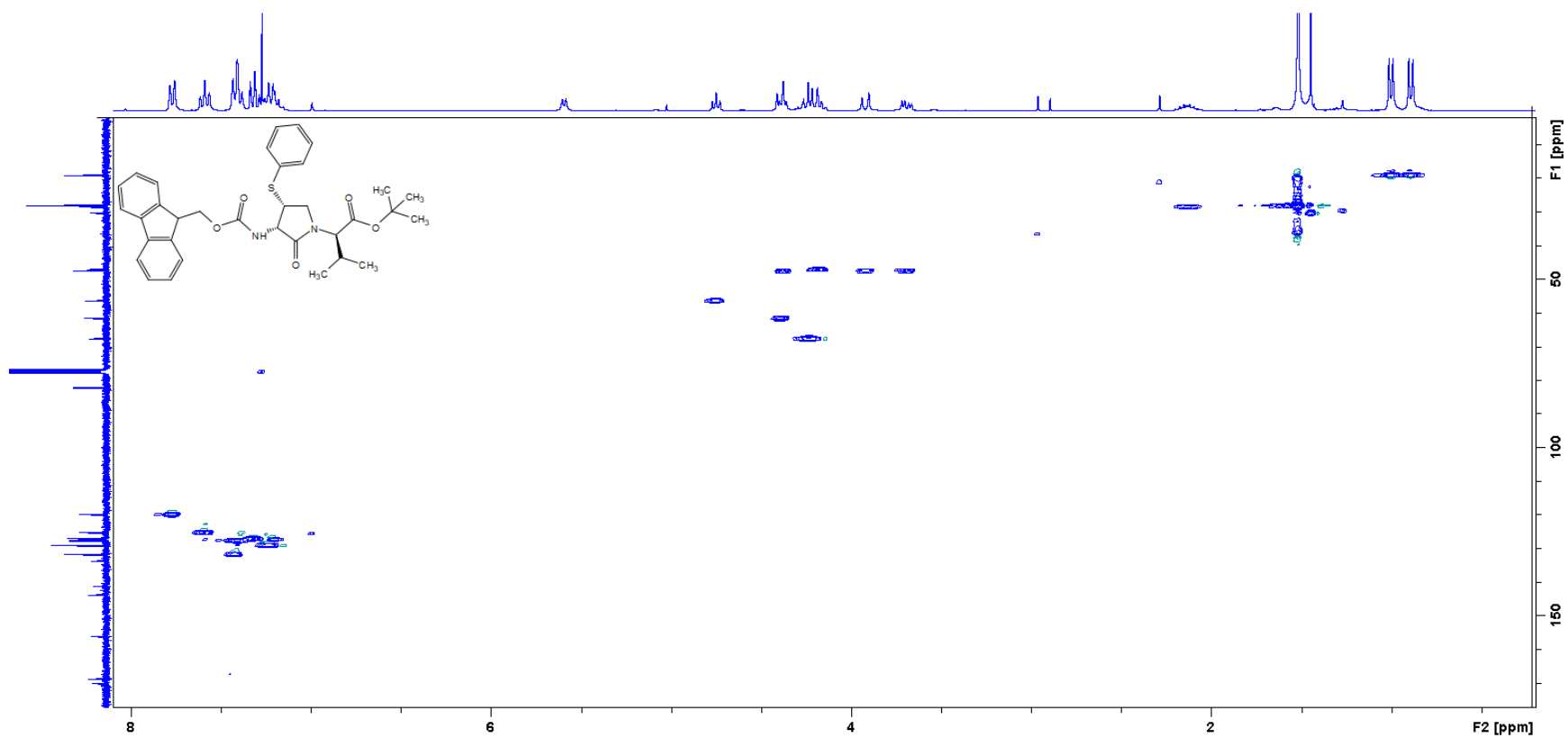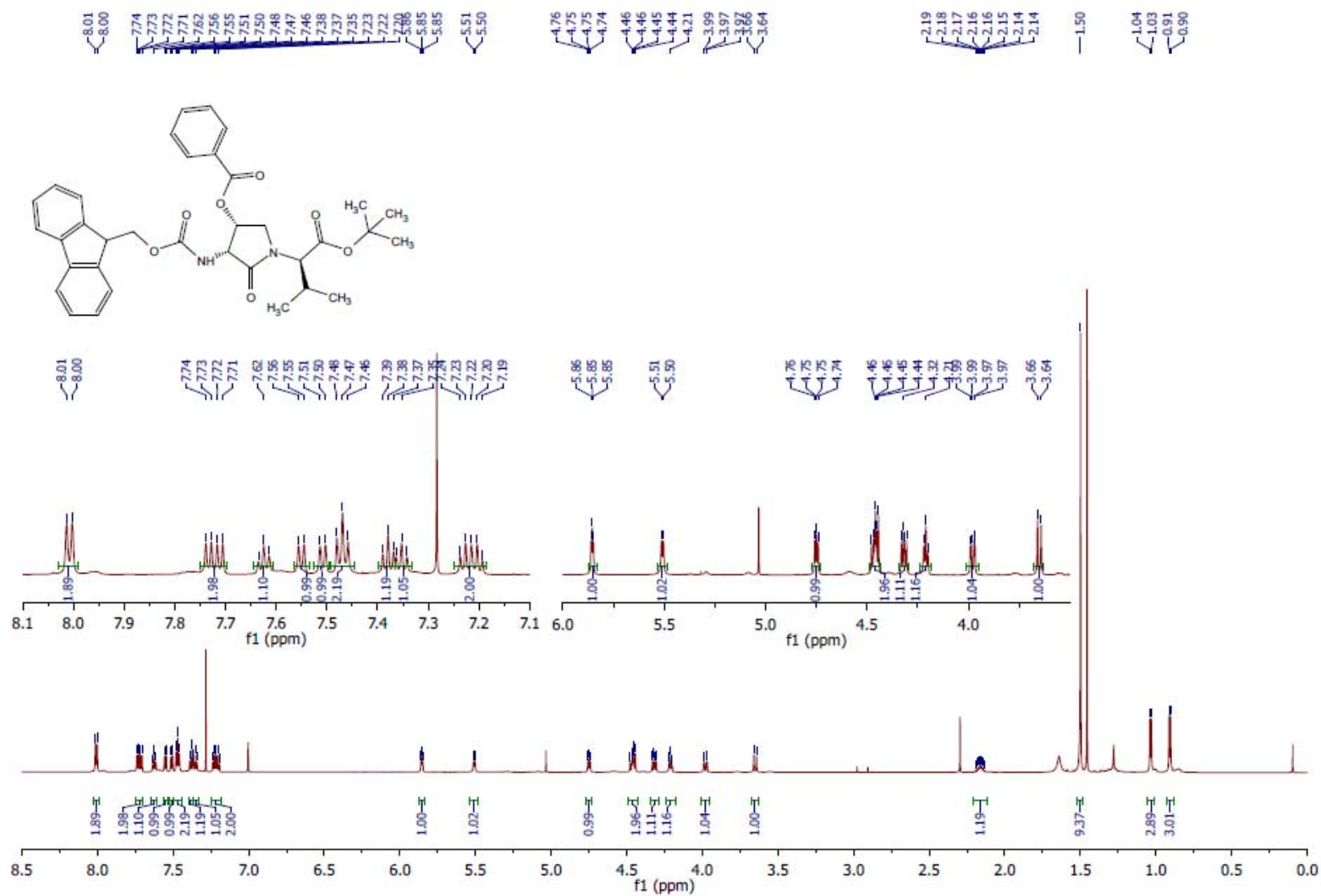
^{13}C NMR (176 MHz, CDCl$_3$) **(4R)-3.24c**

COSY (700 MHz, CDCl$_3$) **(4*R*)-3.24c**

Annex 2: Supporting information of Article 2
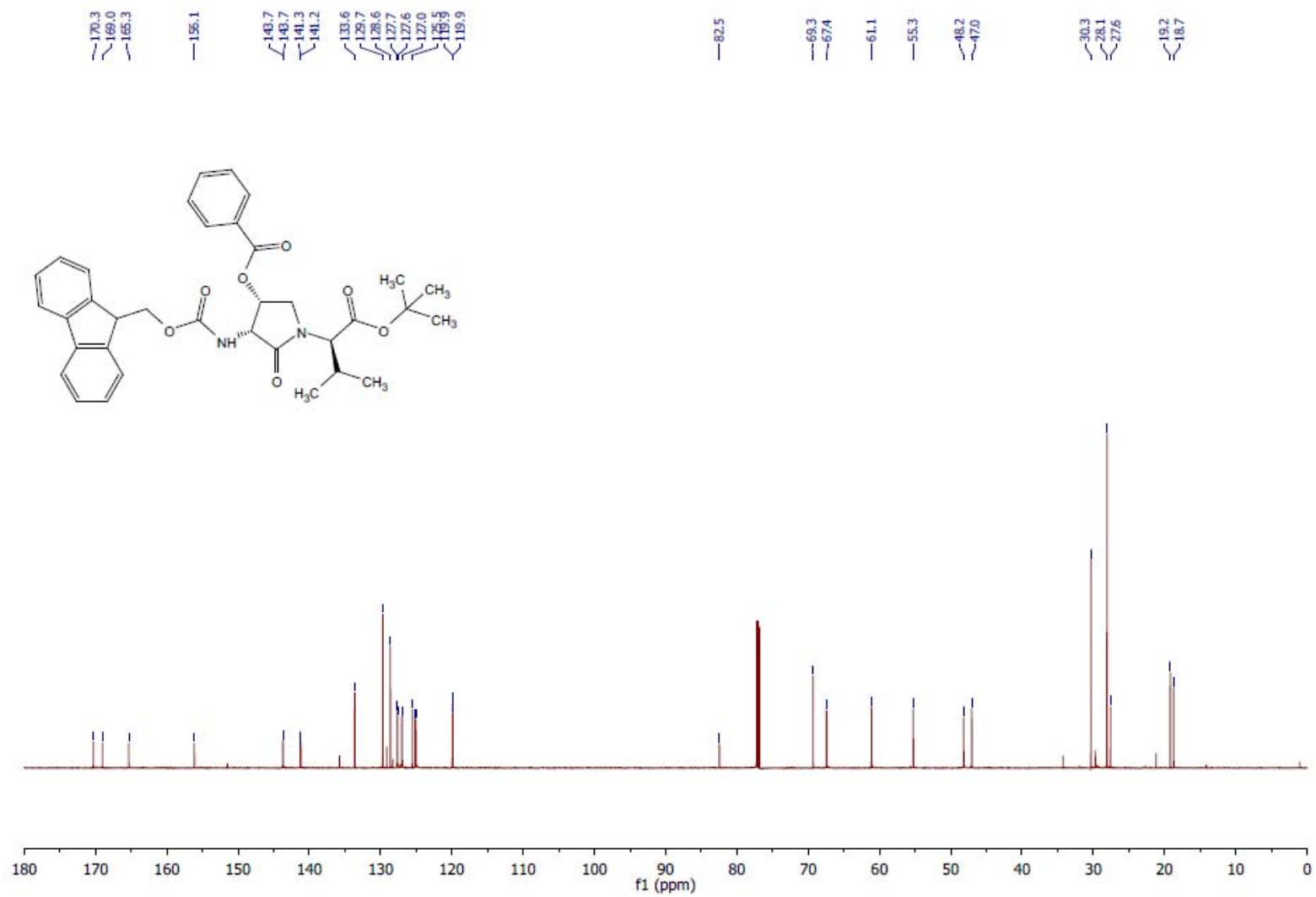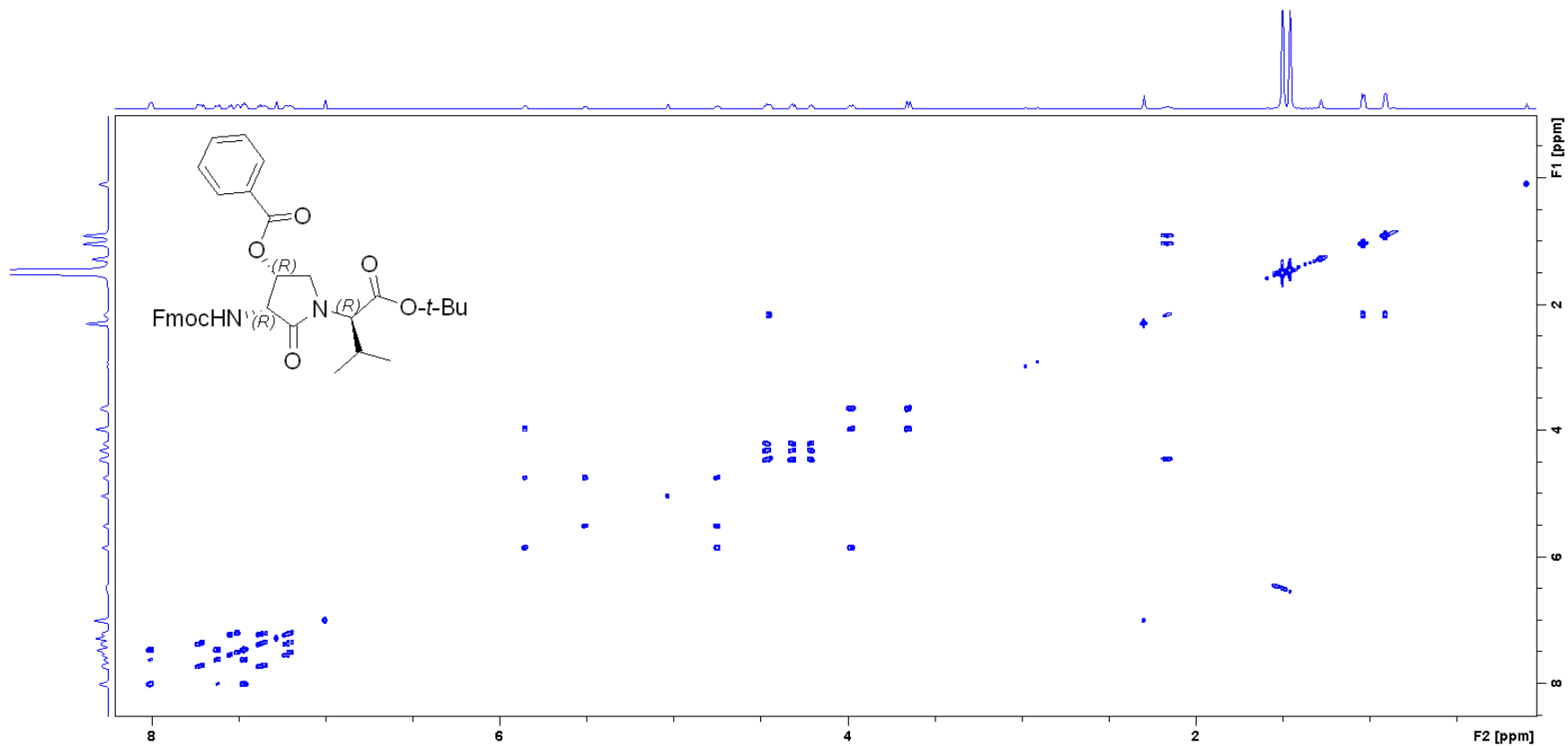
^{1}H NMR (300 MHz, CDCl$_3$) **(4R)-3.24d**
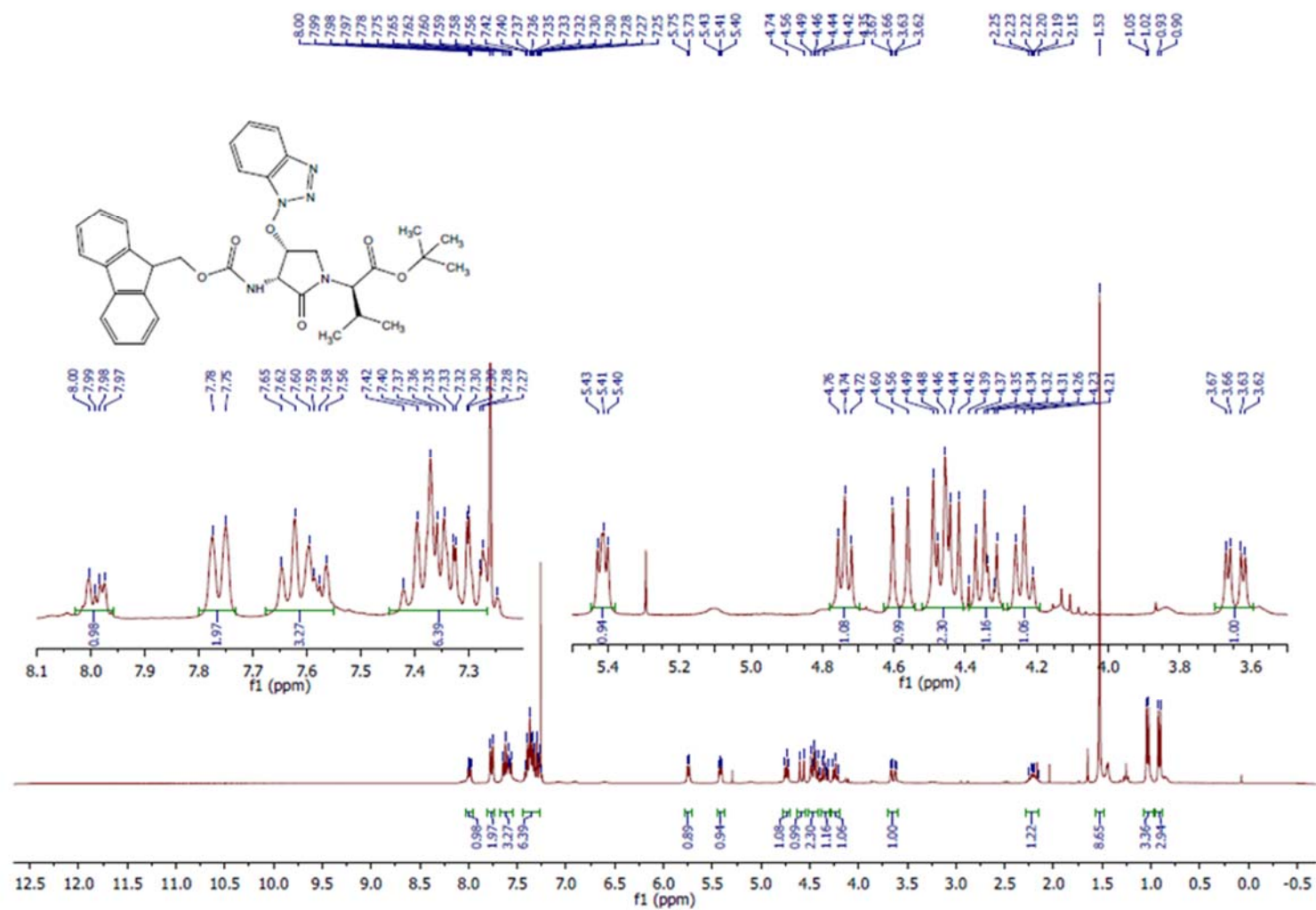
^{13}C NMR (75 MHz, CDCl$_3$) **(4R)-3.24d**
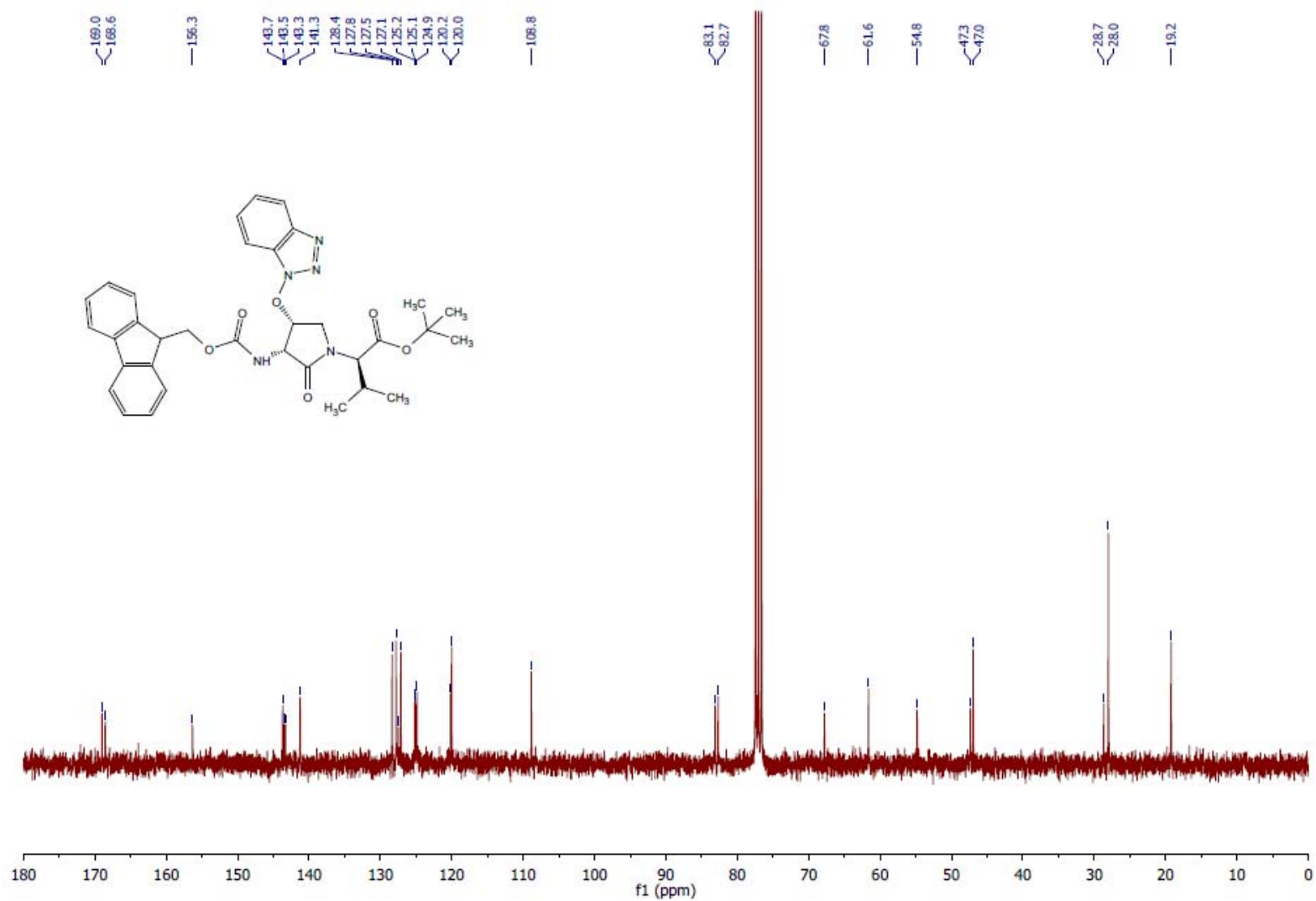
DEPT (75 MHz, CDCl₃) **(4R)-3.24d**
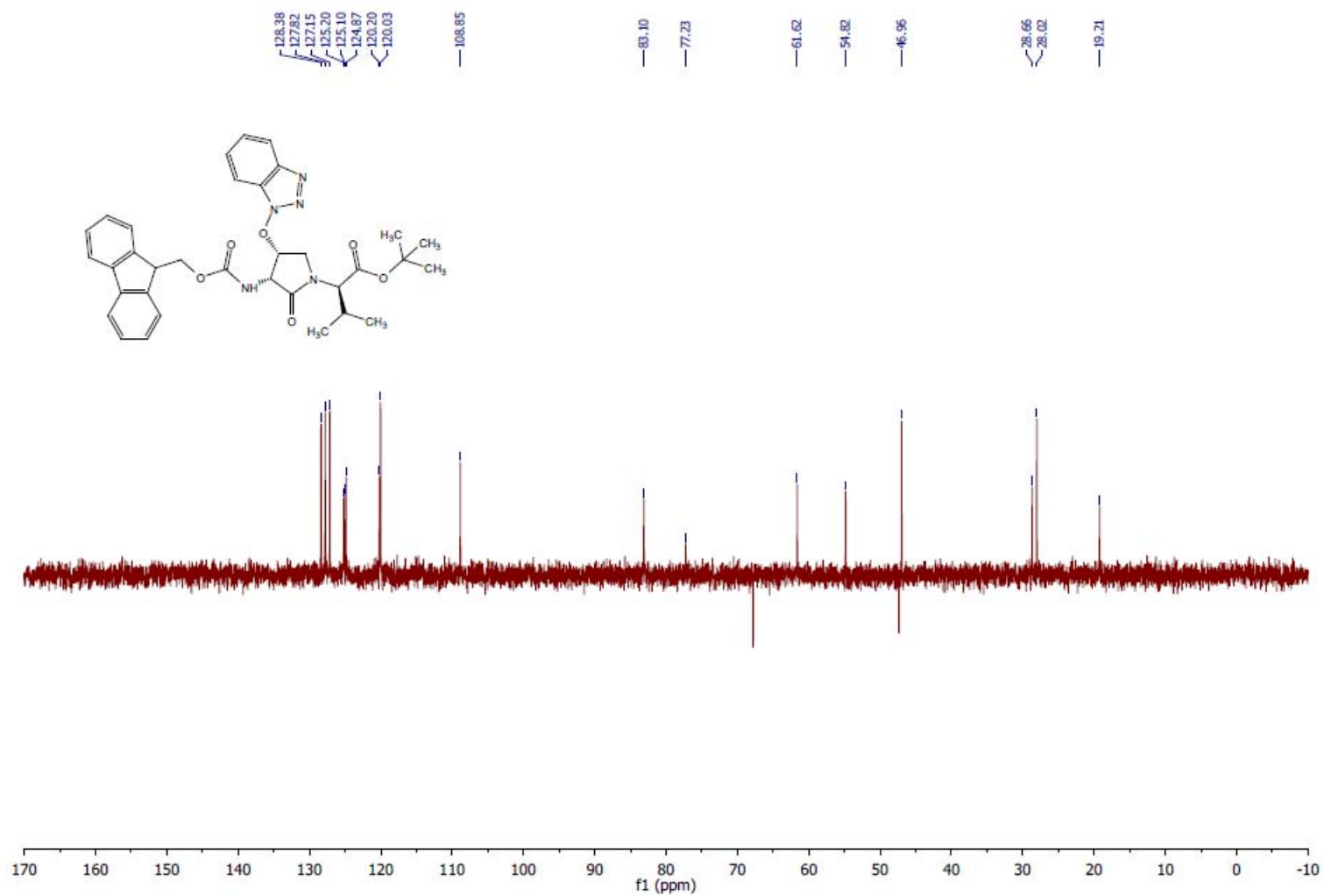
170   160   150   140   130   120   110   100   90   80   70   60   50   40   30   20   10   0   -10
f1 (ppm)

Annex 2: Supporting information of Article 2

COSY (300 MHz, CDCl₃) **(4*R*)-3.24d**

Annex 2: Supporting information of Article 2

HSQC (75 MHz, CDCl$_3$) **(4*R*)-3.24d**

Annex 2: Supporting information of Article 2

^{1}H NMR (300 MHz, CDCl$_3$) **(4R)-3.24e**

Annex 2: Supporting information of Article 2
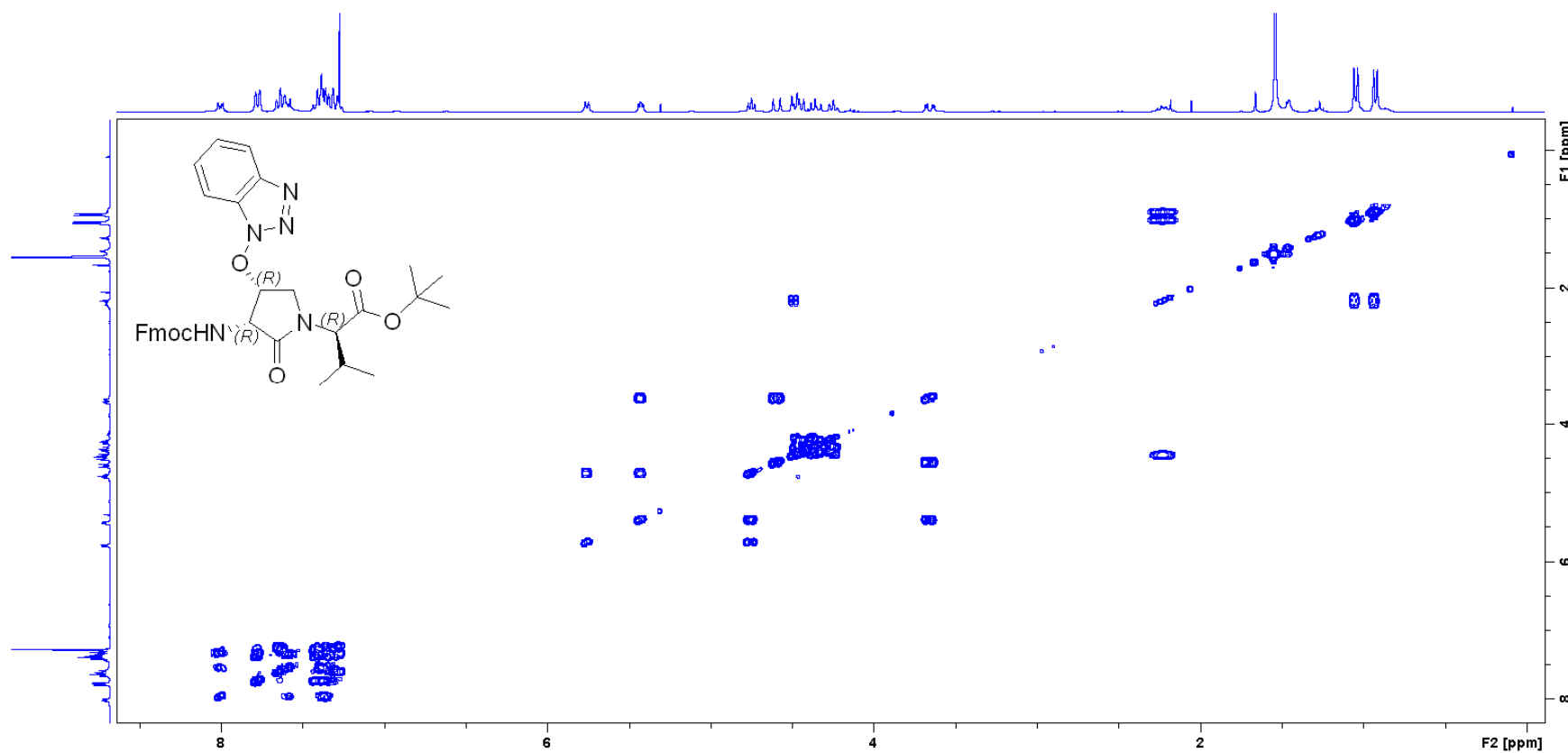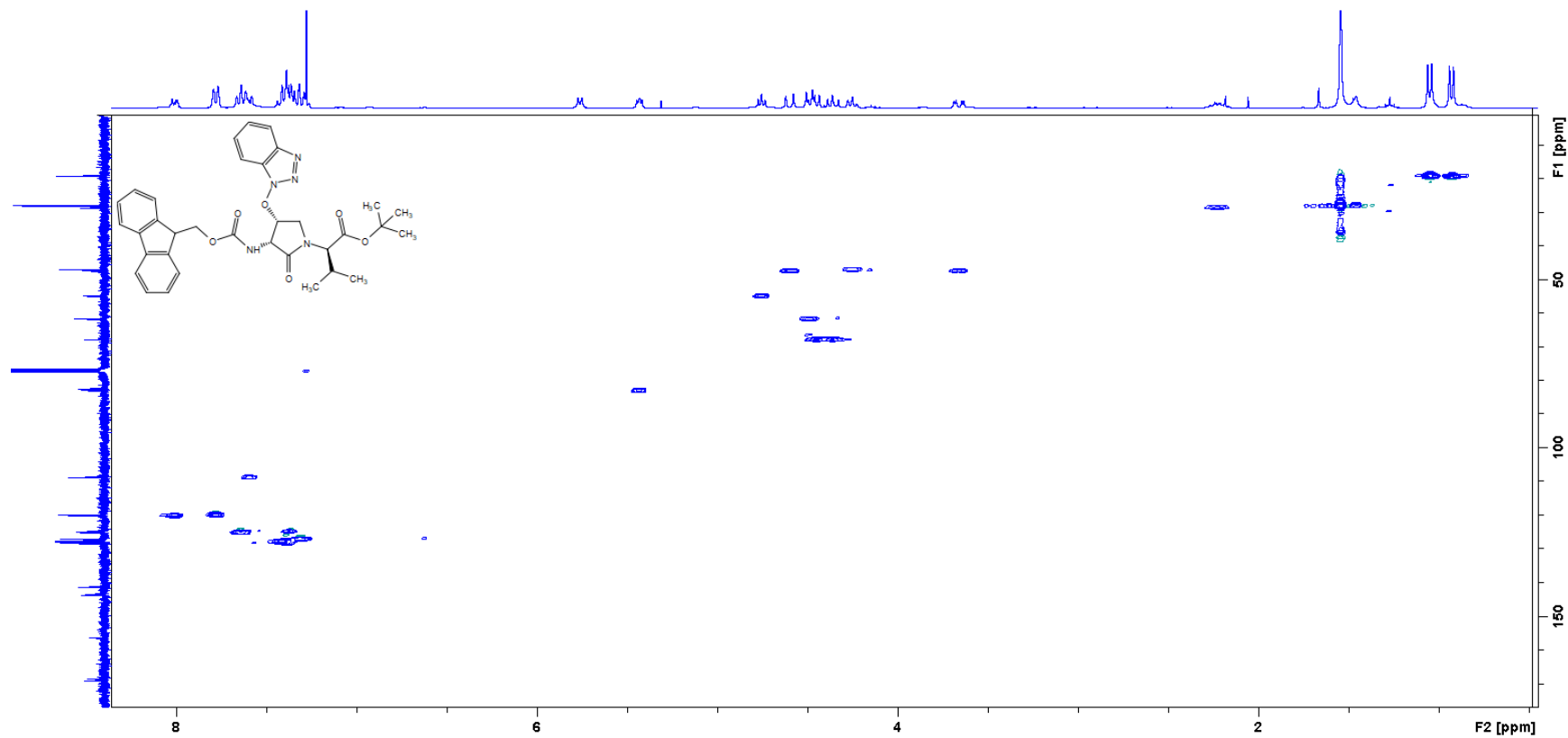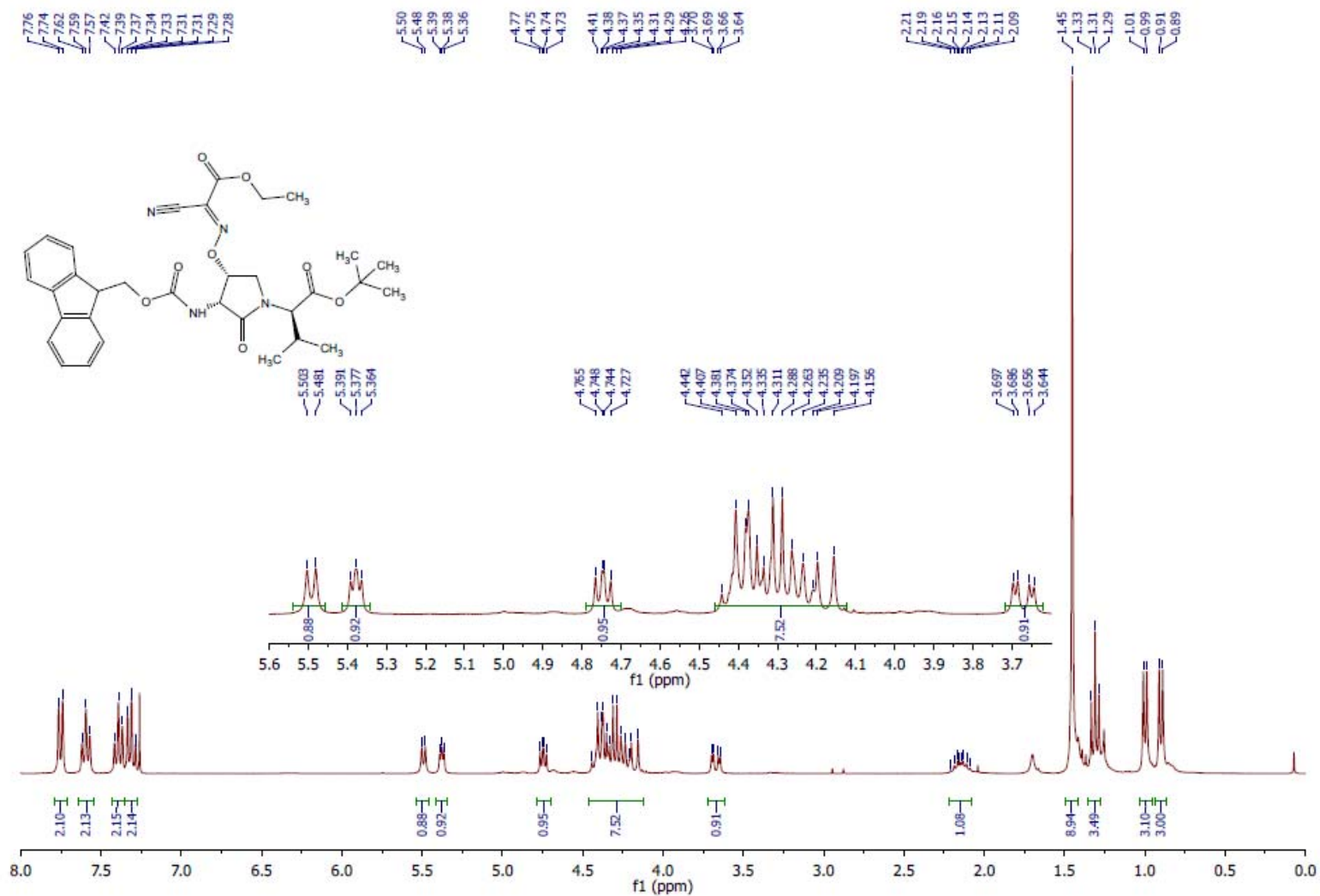
^{13}C NMR (75 MHz, CDCl$_3$) **(4*R*)-3.24e**
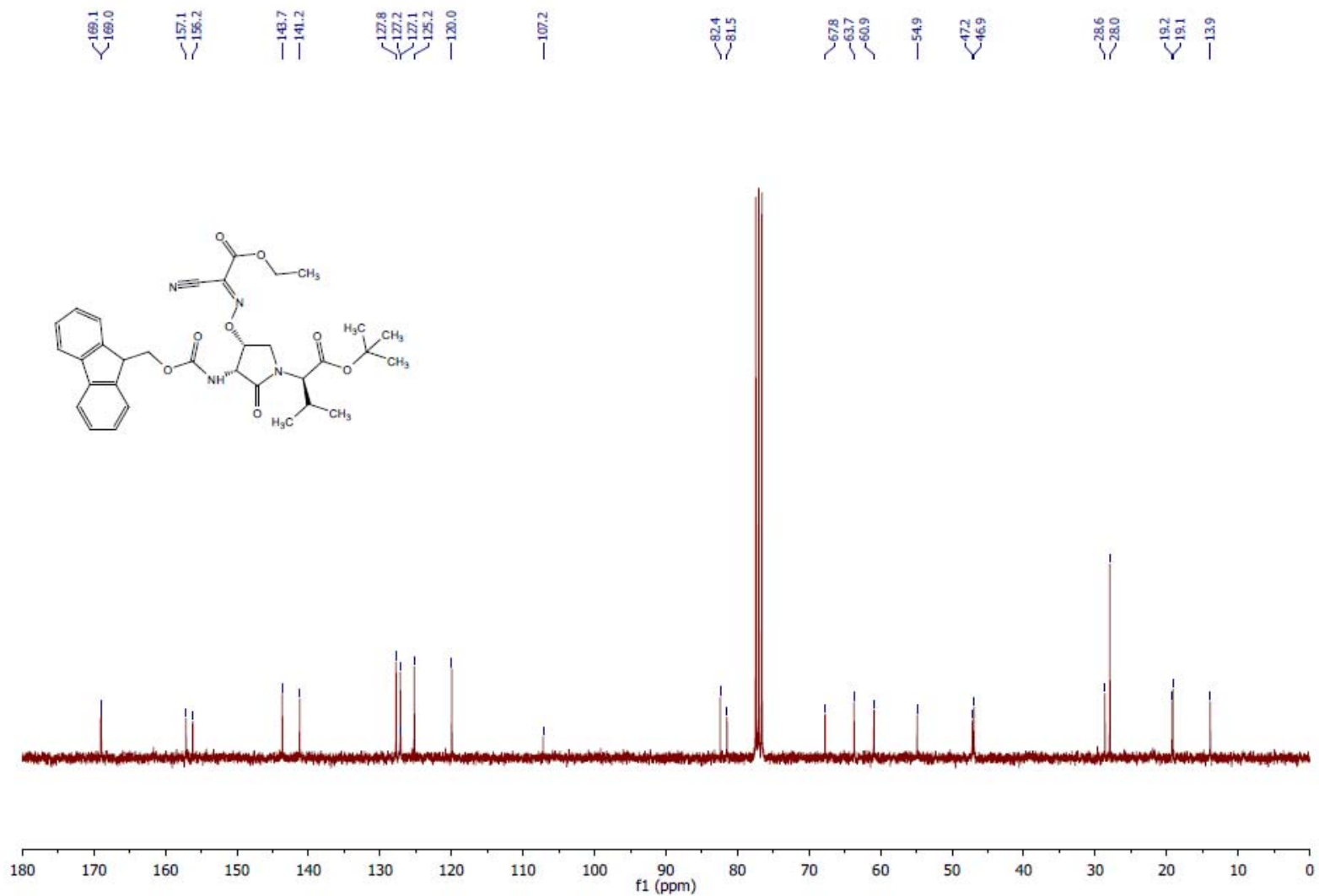
COSY (300 MHz, CDCl₃) **(4*R*)-3.24e**
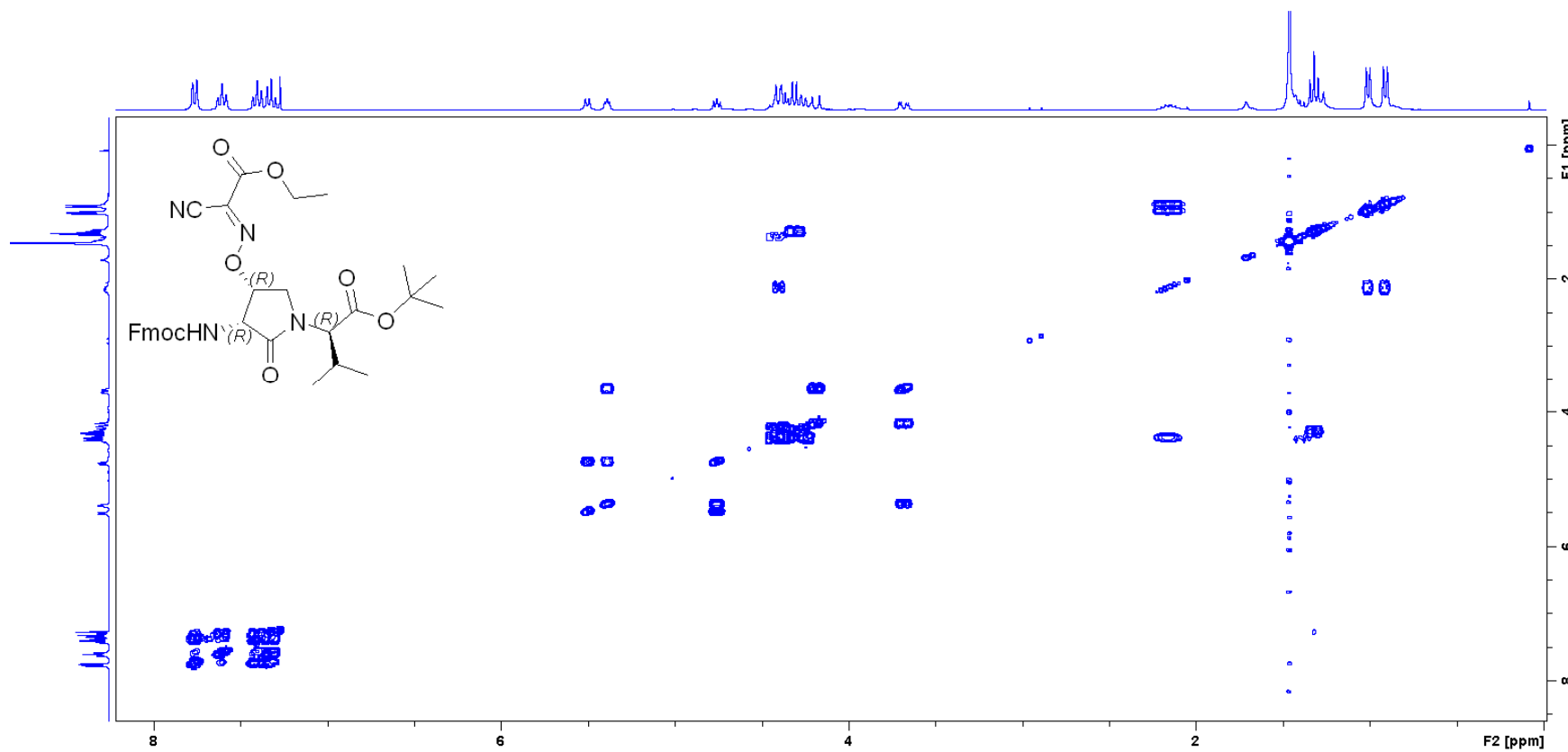
HSQC (75 MHz, CDCl₃) **(4*R*)-3.24e**
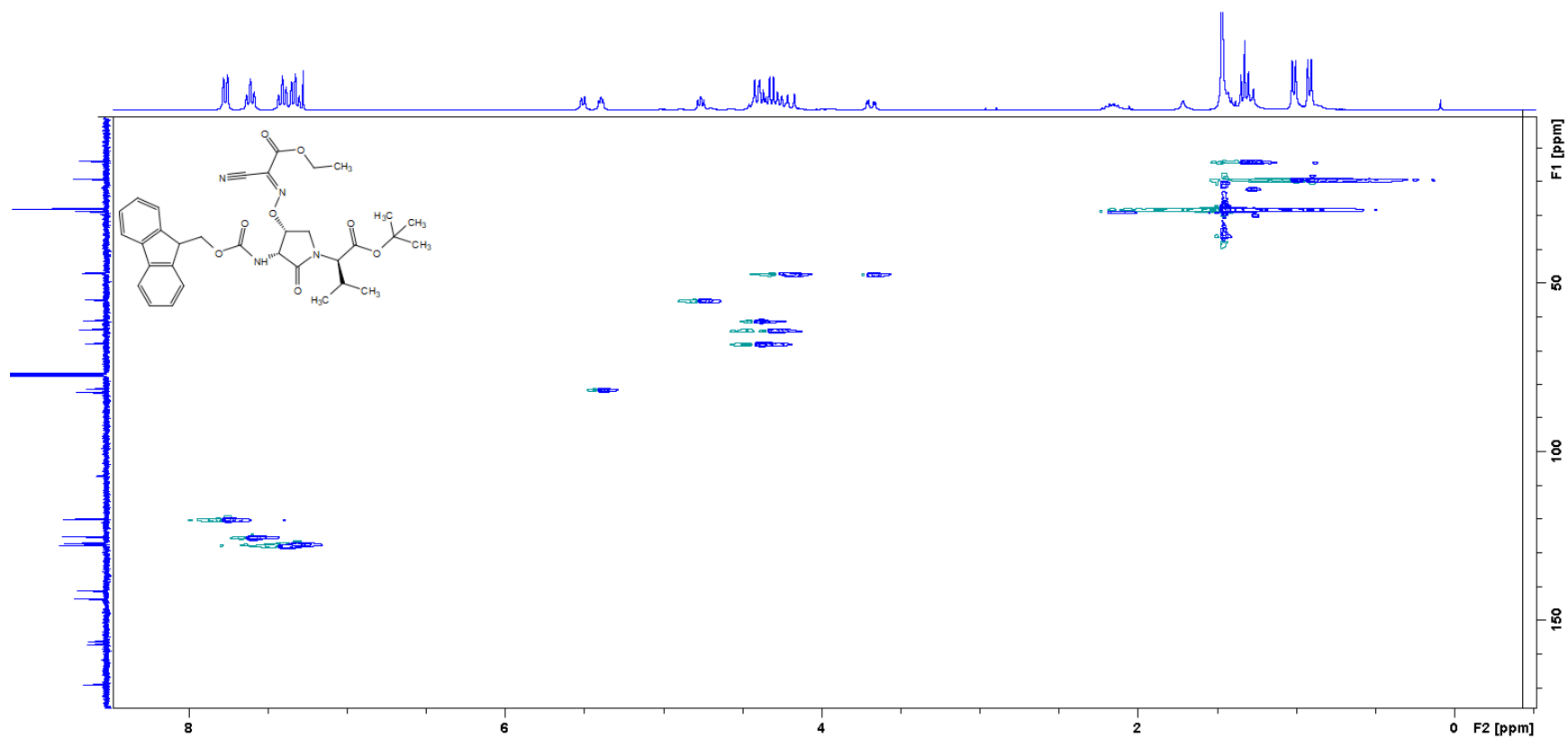
^{1}H NMR (300 MHz, CDCl$_3$) **(4R)-3.24f**
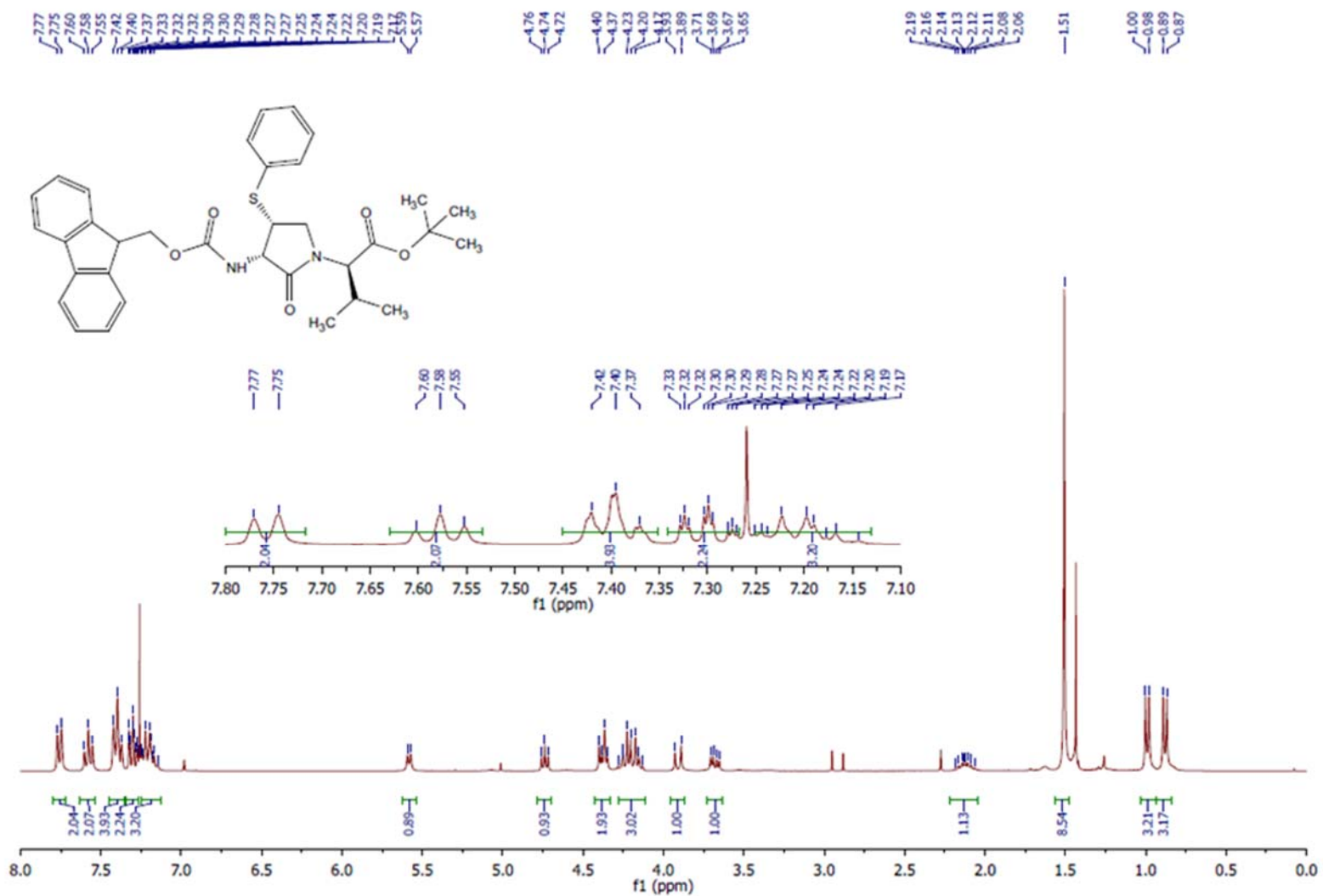
^{13}C NMR (75 MHz, CDCl$_3$) **(4*R*)-3.24f**
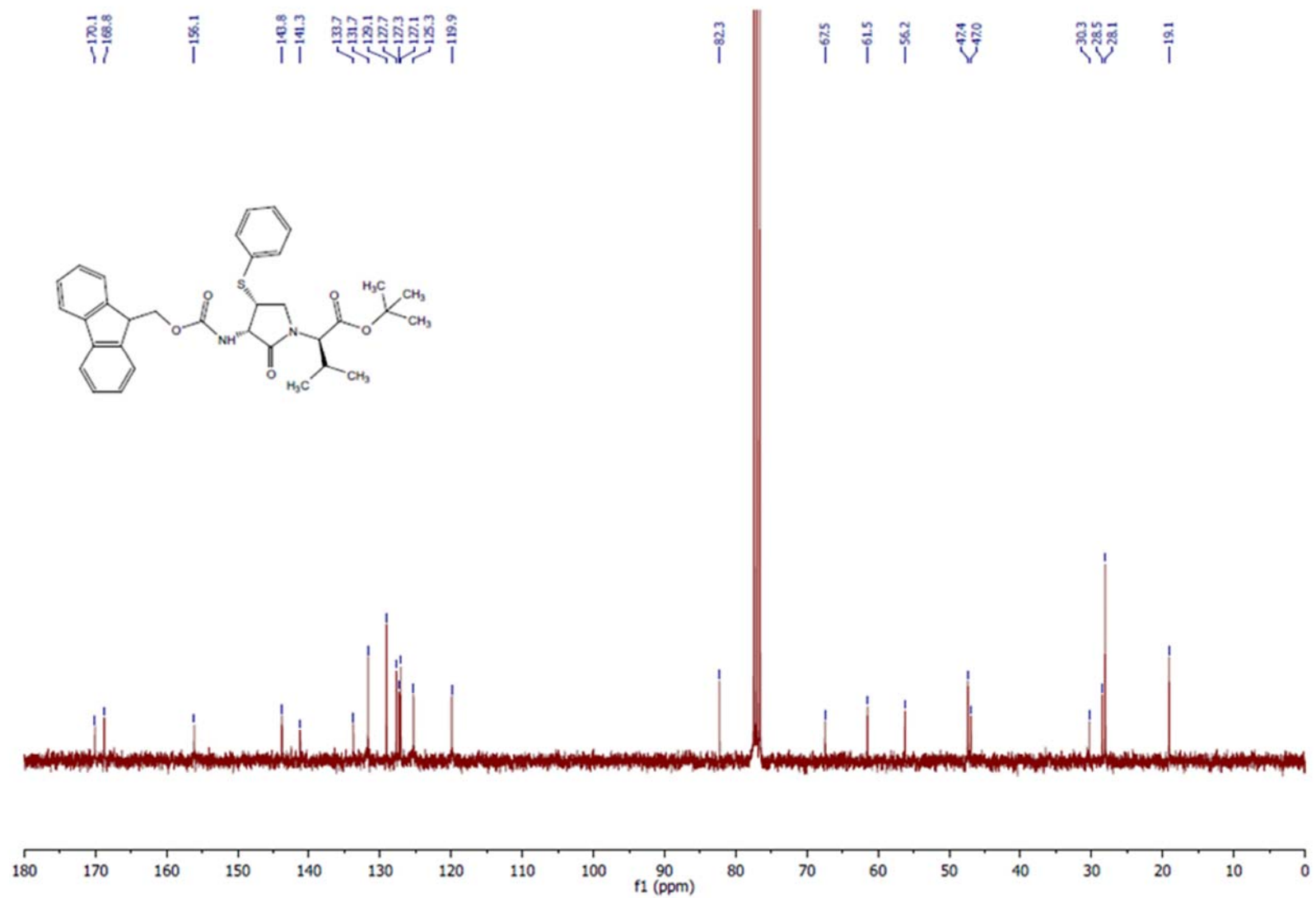
DEPT (75 MHz, CDCl₃) **(4*R*)-3.24f**
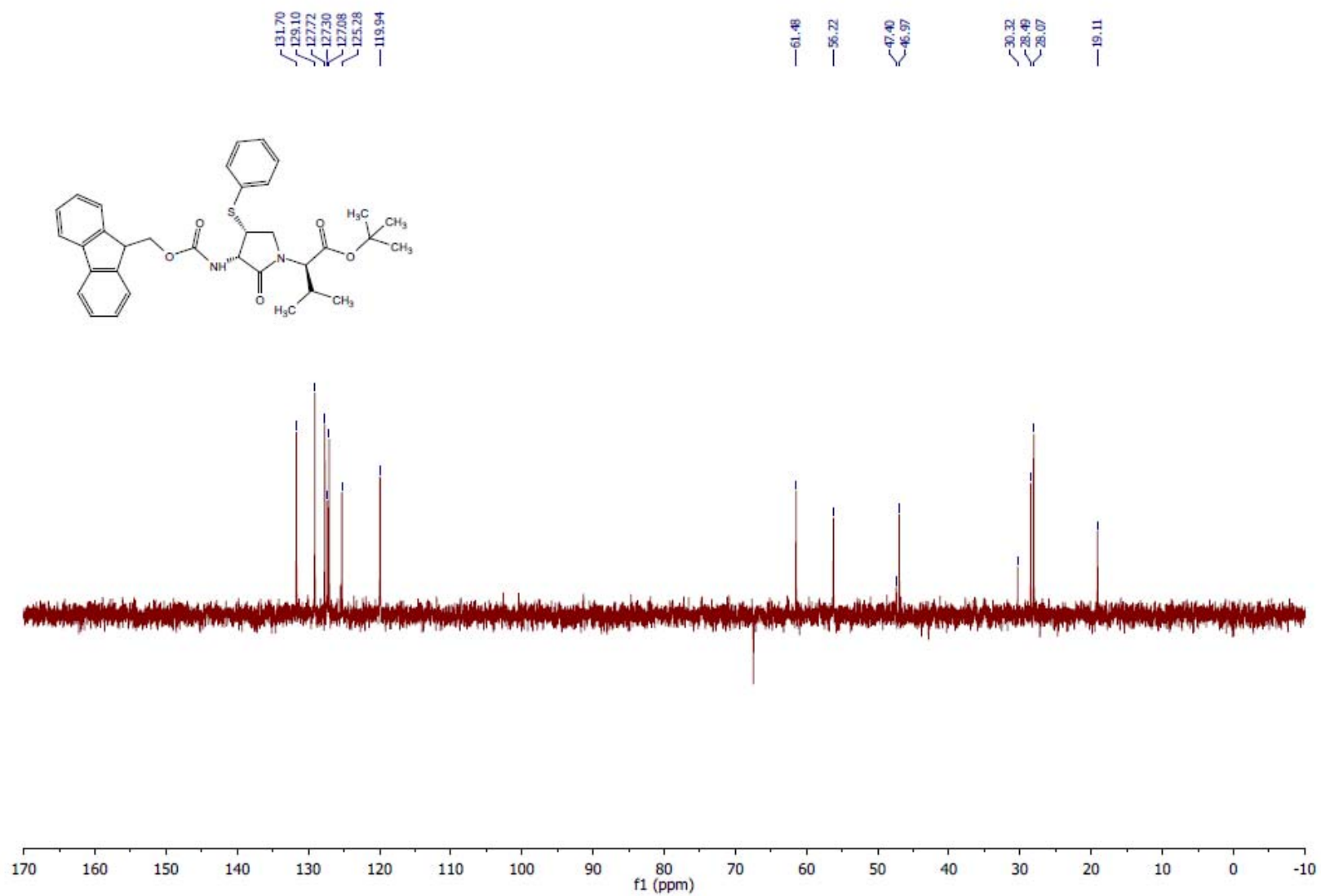
COSY (300 MHz, CDCl₃) **(4*R*)-3.24f**
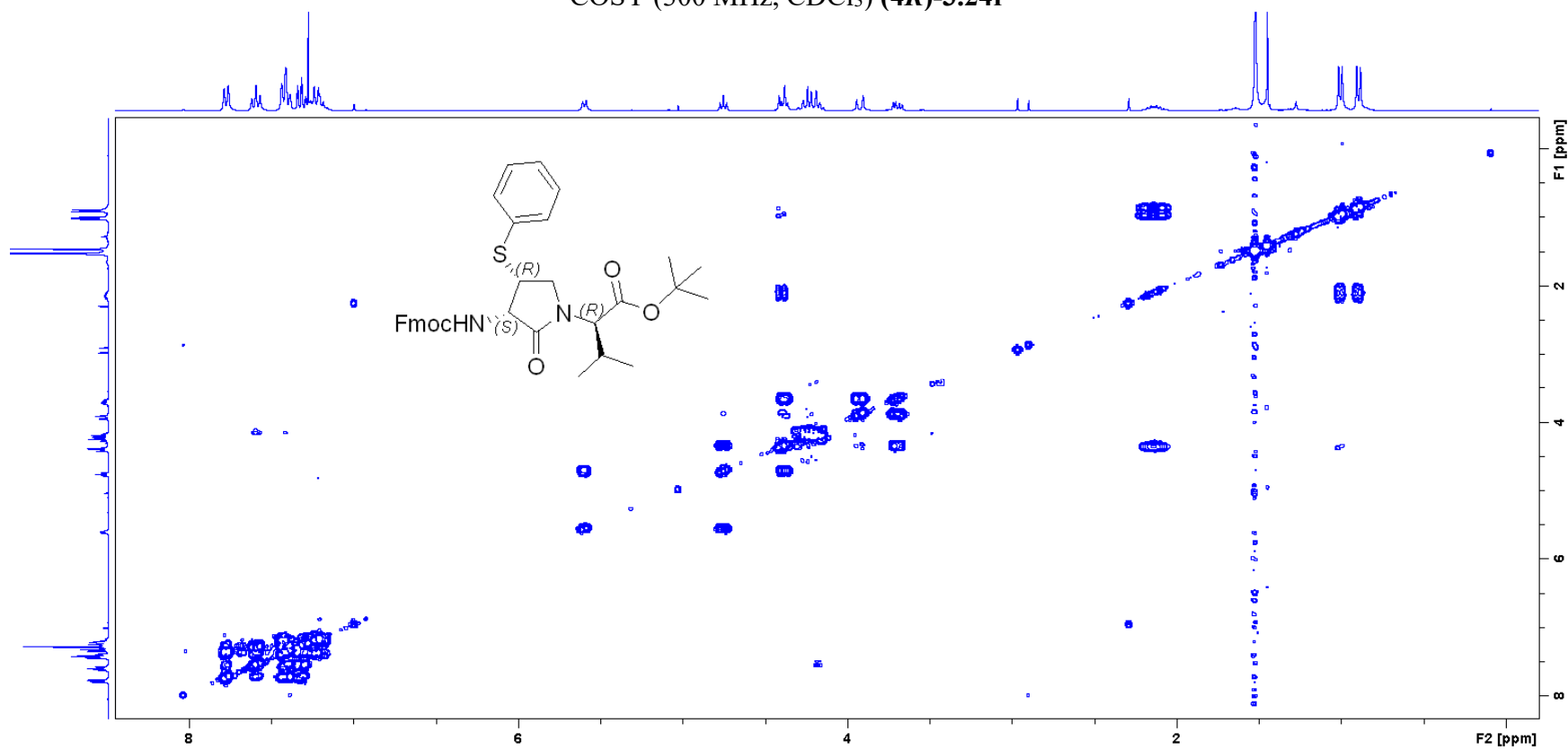
HSQC (75 MHz, CDCl₃) **(4*R*)-3.24f**
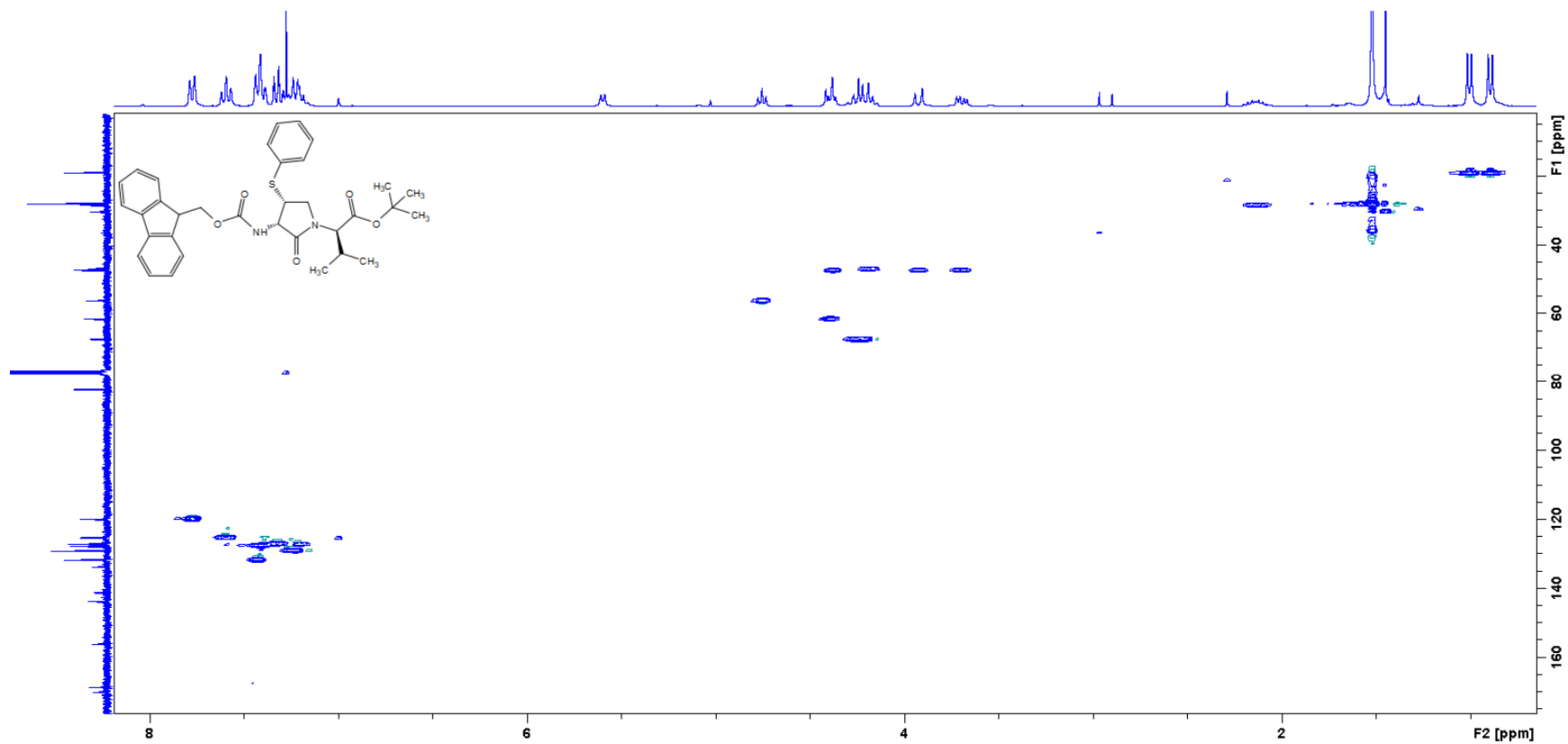
^{1}H NMR (300 MHz, CDCl$_3$) **(4R)-3.24g**

^{13}C NMR (75 MHz, CDCl$_3$) **(4R)-3.24g**

169.4
168.9
163.8
156.7
144.0
143.8
141.2
134.7
128.8
127.7
127.6
127.1
127.0
125.6
125.5
123.8
119.9
82.1
67.7
61.0
55.0
47.4
47.0
28.7
28.0
27.9
21.9
19.3
19.3

180　170　160　150　140　130　120　110　100　90　80　70　60　50　40　30　20　10　0
f1 (ppm)

Annex 2: Supporting information of Article 2

DEPT (75 MHz, CDCl₃) **(4R)-3.24g**

170 160 150 140 130 120 110 100 90 80 70 60 50 40 30 20 10 0 -10
f1 (ppm)

Annex 2: Supporting information of Article 2
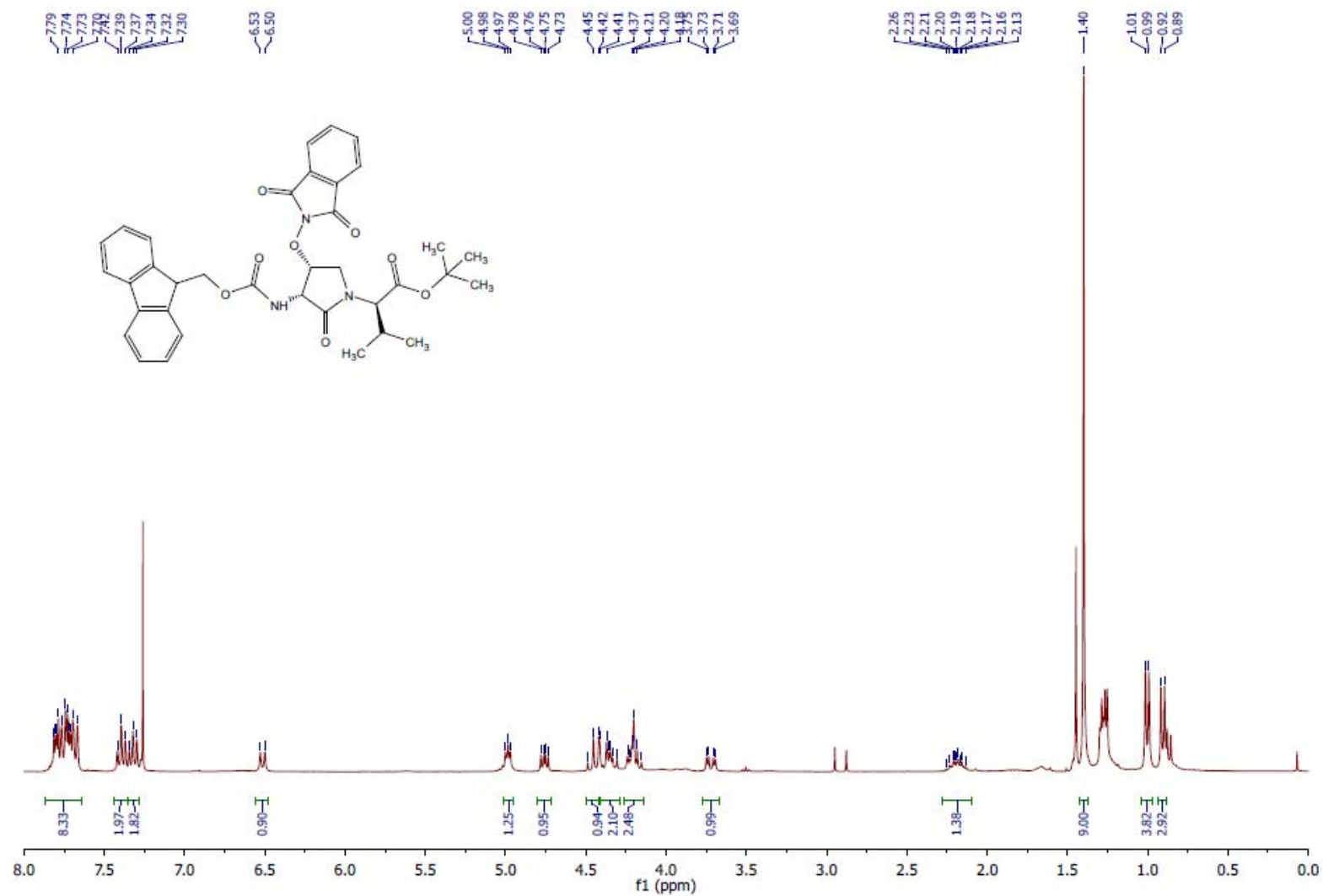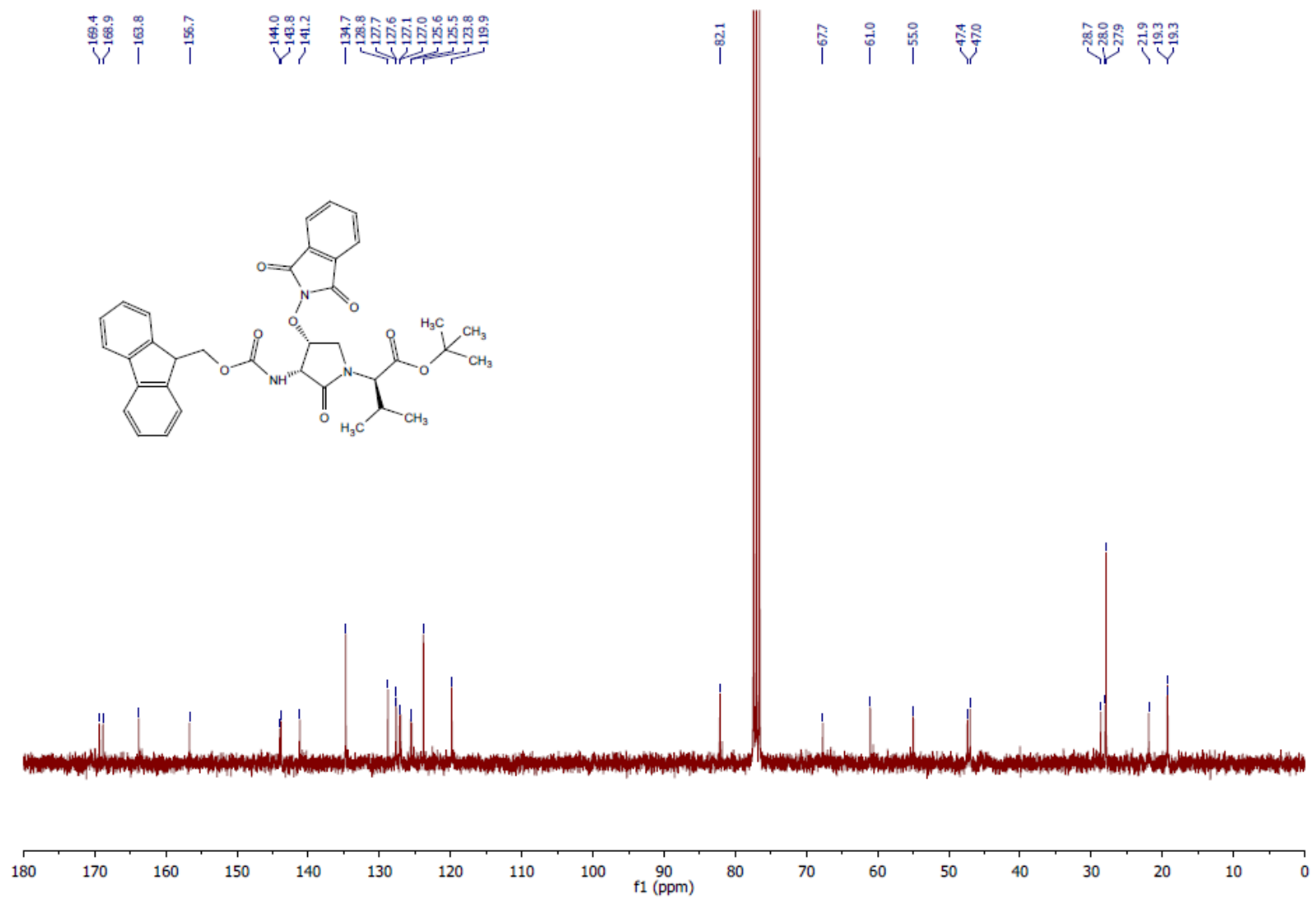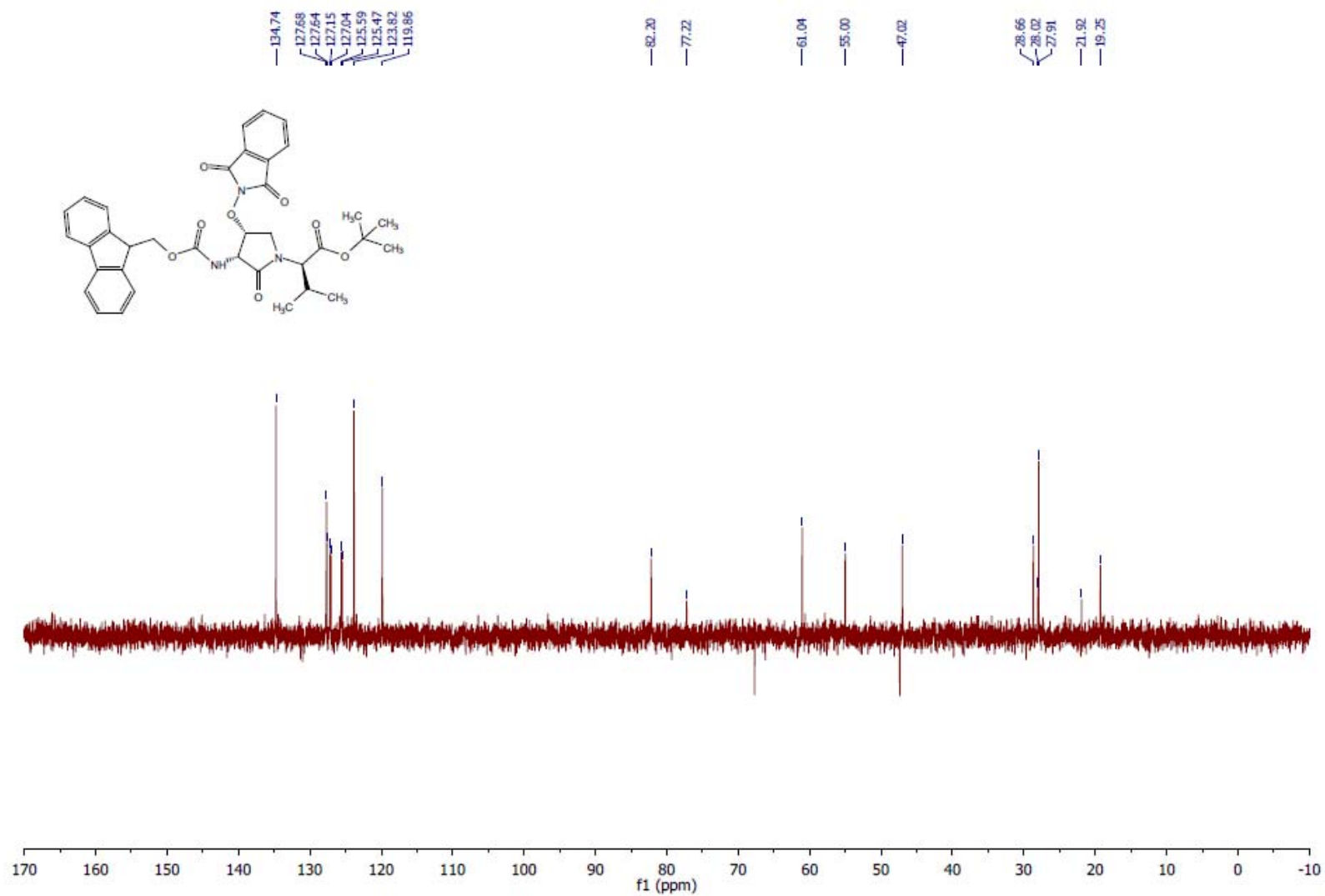
COSY NMR (300 MHz, CDCl$_3$) **(4R)-3.24g**
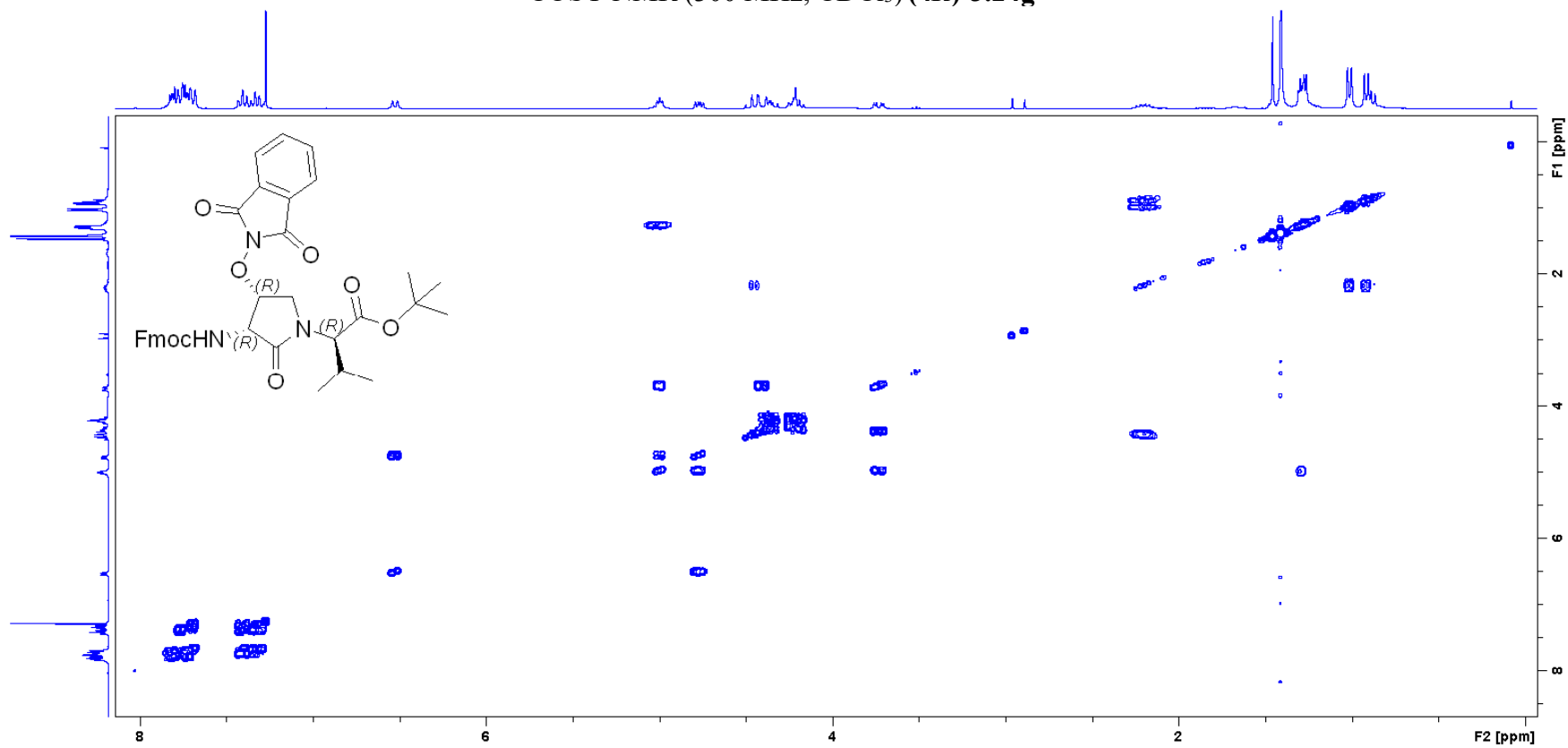
HSQC (75 MHz, CDCl₃) **(4*R*)-3.24g**
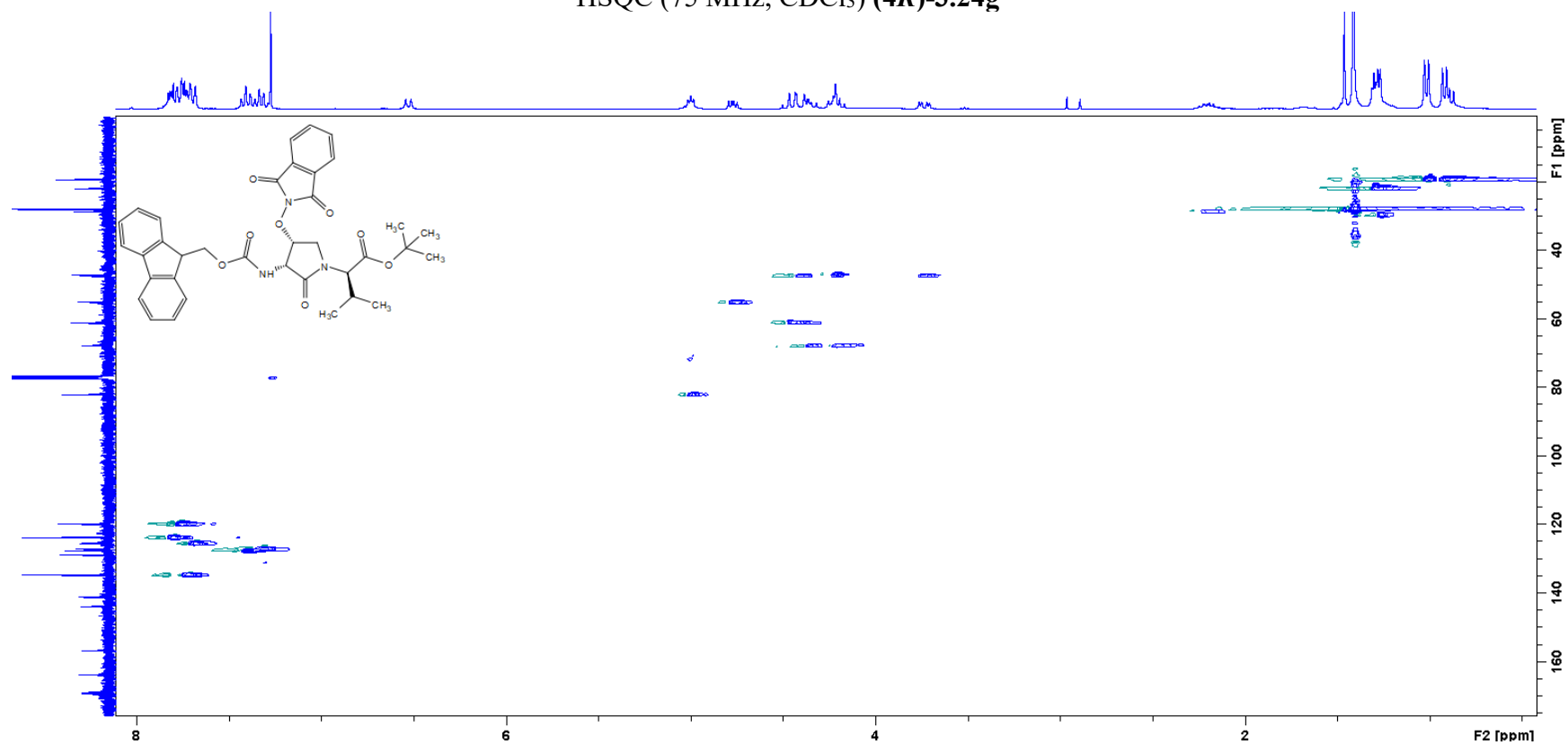
^{1}H NMR (400 MHz, CDCl$_3$) **(4R)-3.24h**

Annex 2: Supporting information of Article 2
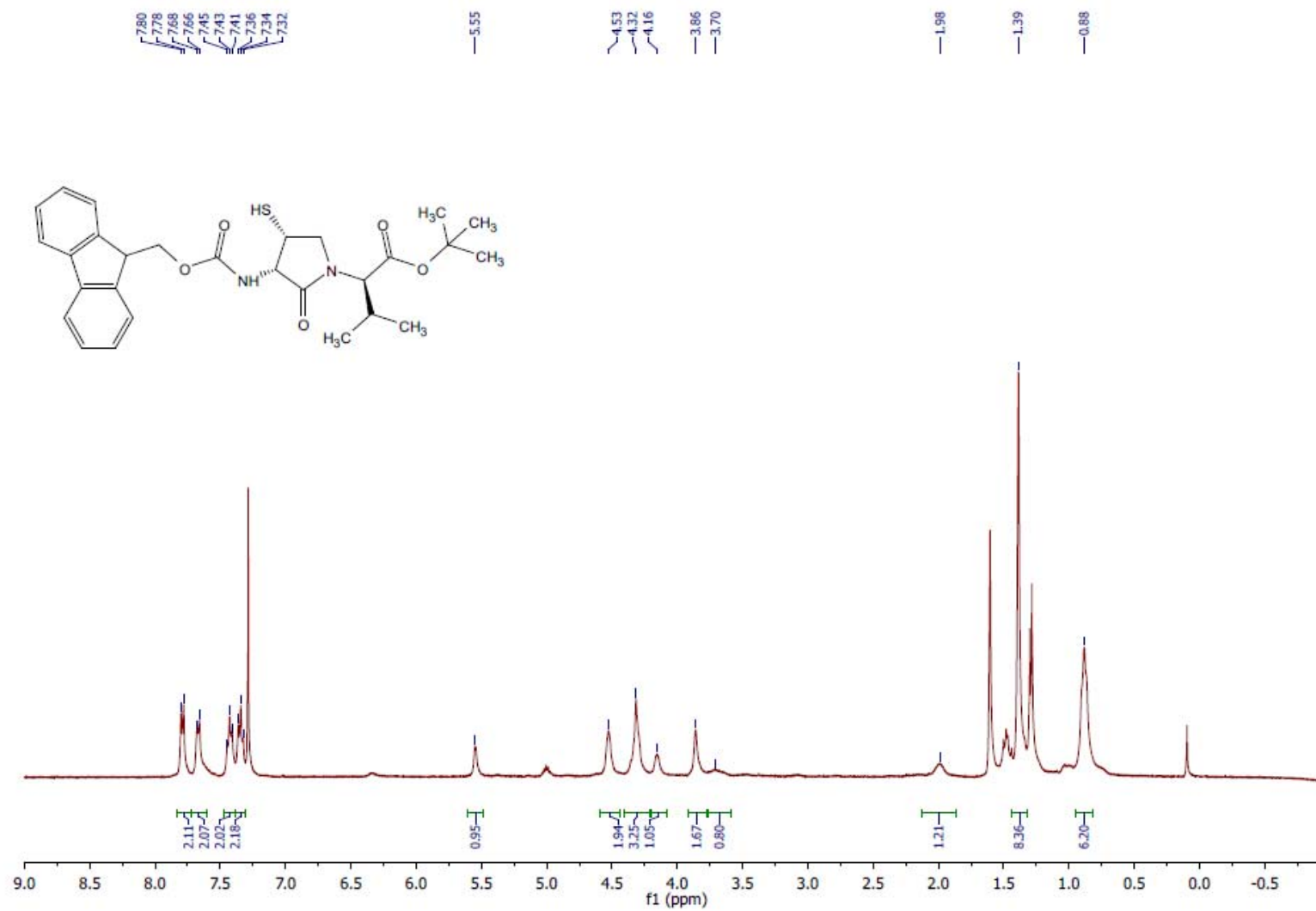
^{13}C NMR (75 MHz, CDCl$_3$) **(4R)-3.24h**

^{1}H NMR (300 MHz, CDCl$_3$) **(4R)-3.24i**

Annex 2: Supporting information of Article 2
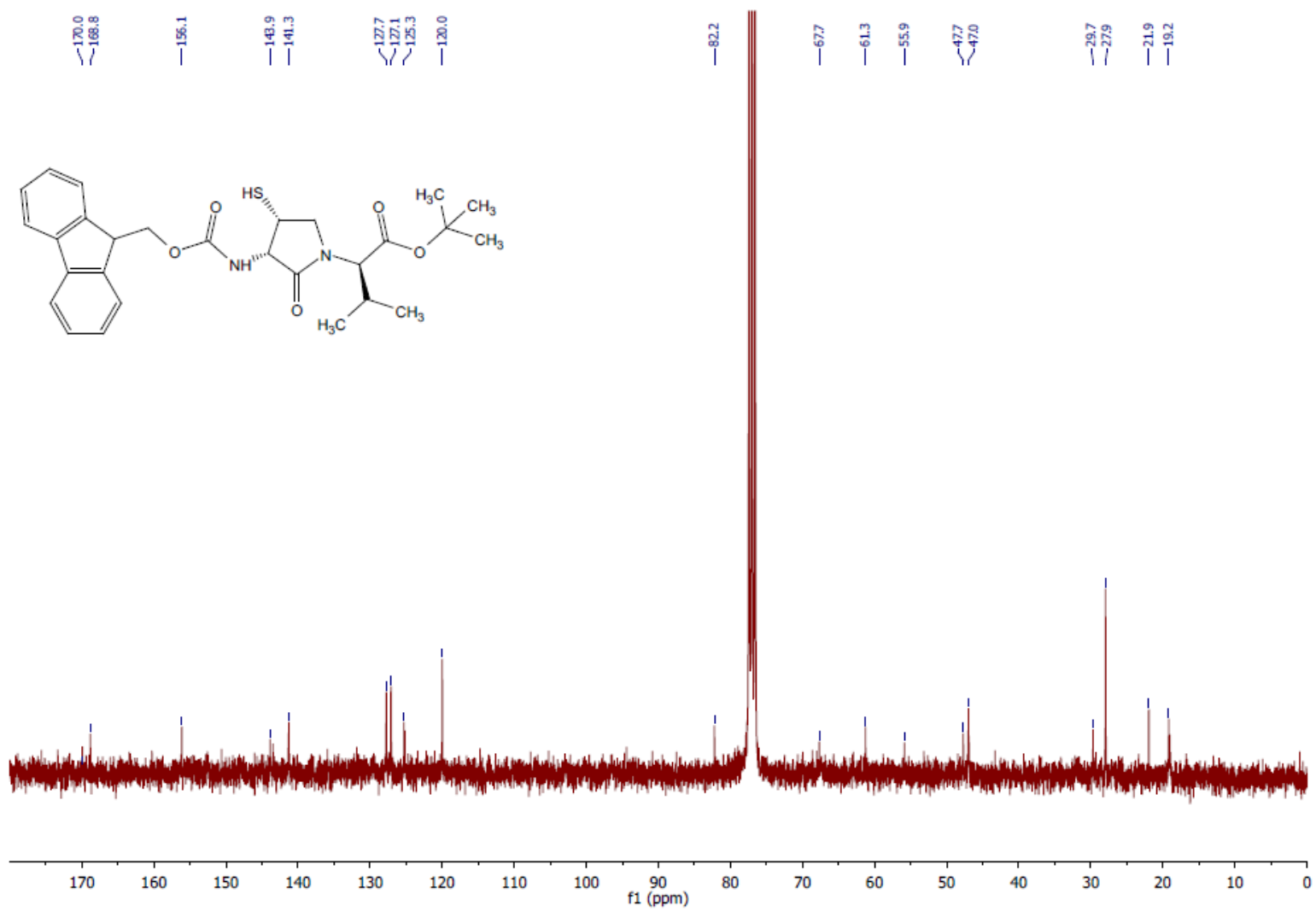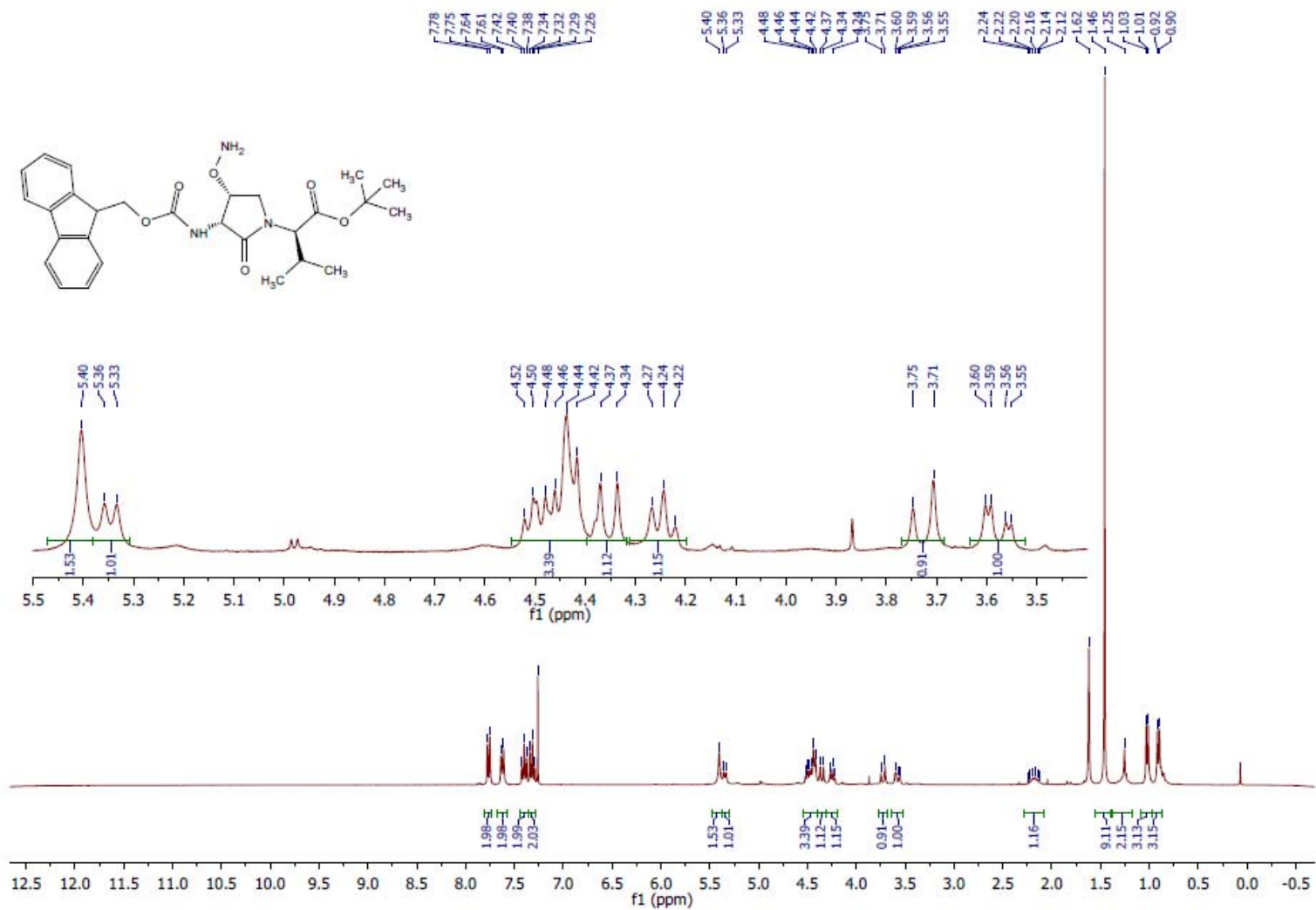
¹³C NMR (126 MHz, CDCl₃) **(4R)-3.24i**
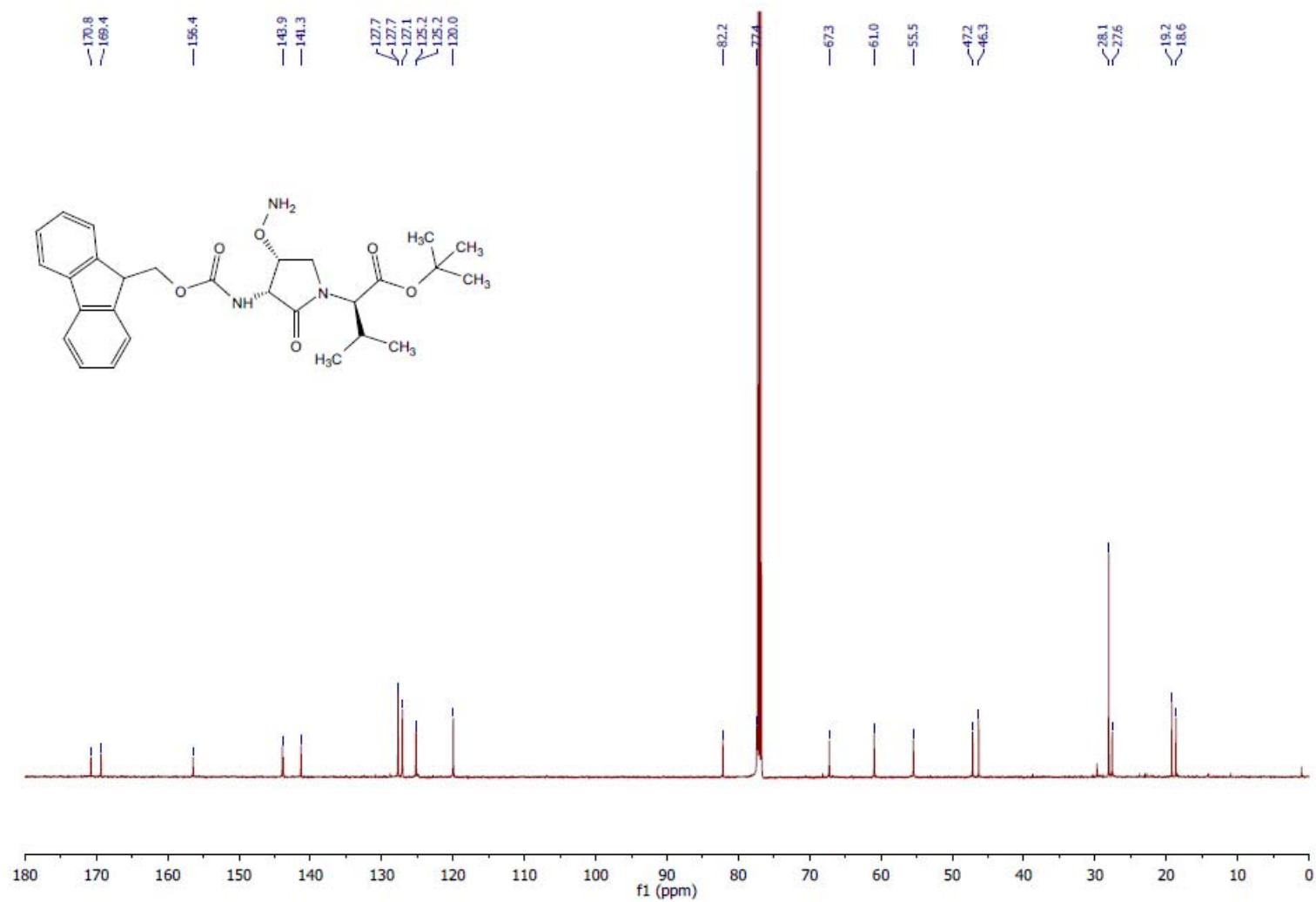
DEPT (126 MHz, CDCl₃) **(4R)-3.24i**

COSY (300 MHz, CDCl₃) **(4R)-3.24i**

Annex 2: Supporting information of Article 2

^{1}H NMR (500 MHz, CDCl$_3$) **(4R)-3.24j**

Annex 2: Supporting information of Article 2

^{13}C NMR (126 MHz, CDCl$_3$) **(4R)-3.24j**

f1 (ppm)

Annex 2: Supporting information of Article 2

DEPT (126 MHz, CDCl₃) **(4*R*)-3.24j**

COSY (500 MHz, CDCl$_3$) **(4*R*)-3.24j**

¹H NMR (400 MHz, CDCl₃) **3.25**

Annex 2: Supporting information of Article 2
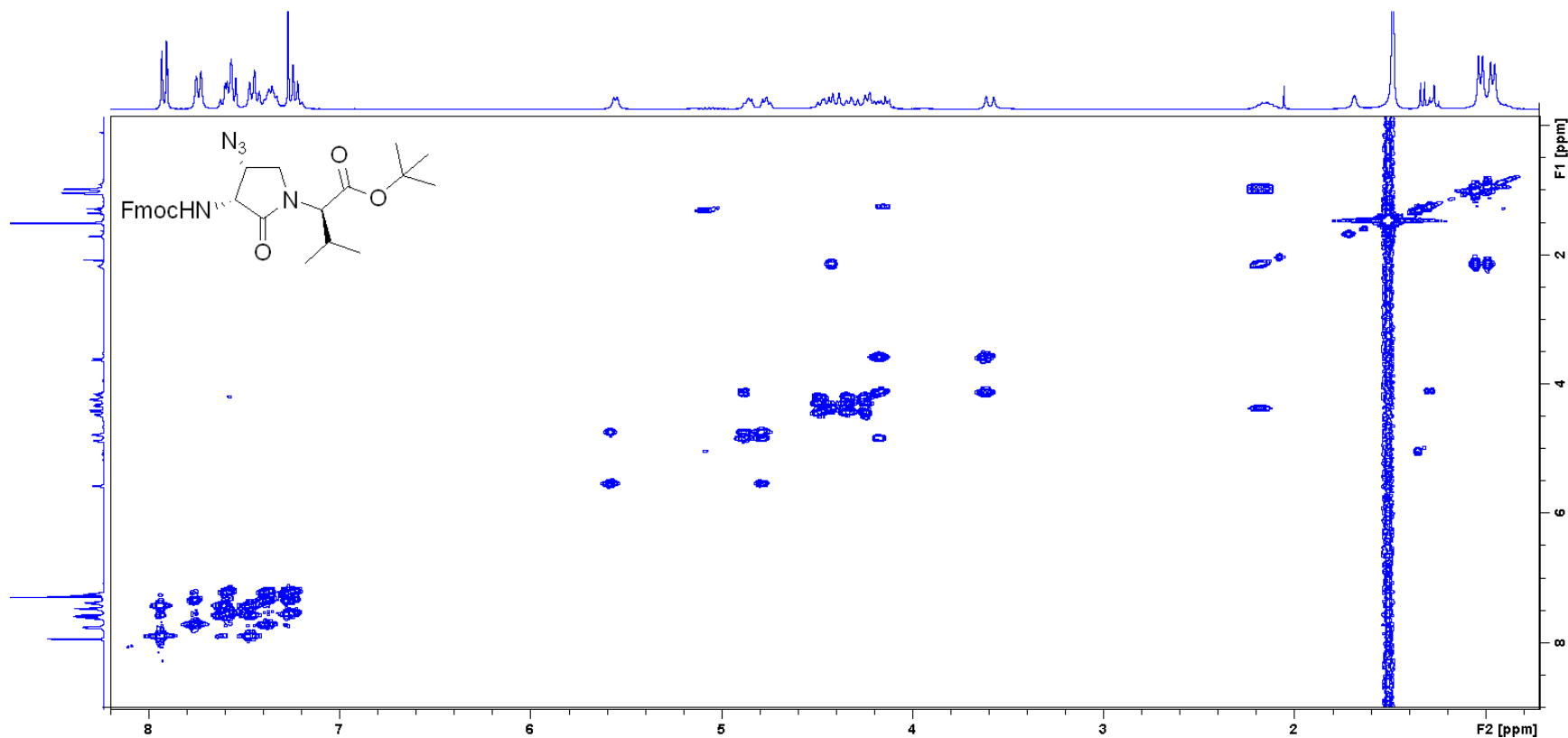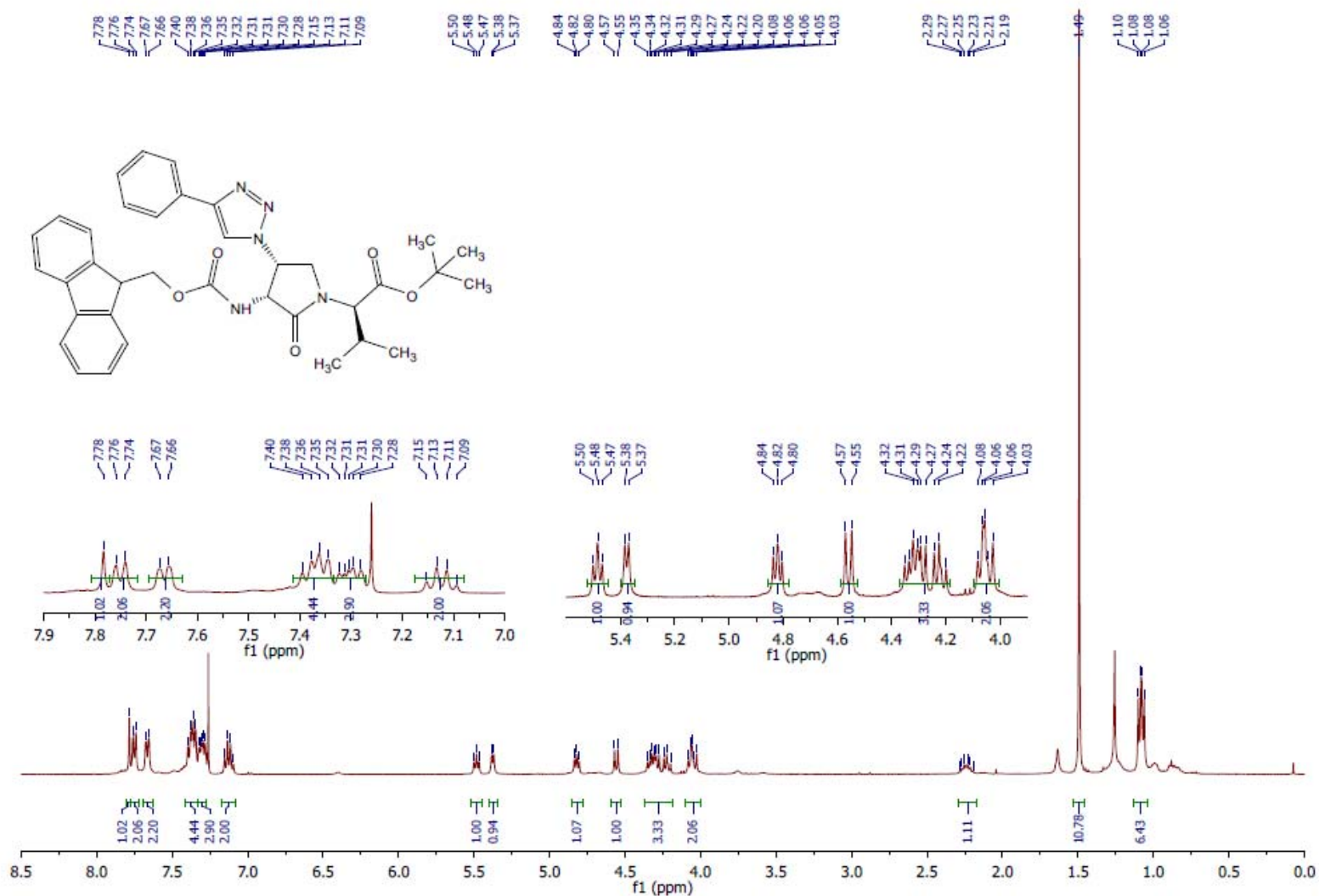
^{13}C NMR (75 MHz, CDCl$_3$) **3.25**

DEPT (75 MHz, CDCl₃) **3.25**

131.70
129.10
127.72
127.30
127.08
125.52
125.28
119.94

61.48
56.22
46.97
30.32
28.49
28.07
19.11

170 160 150 140 130 120 110 100 90 80 70 60 50 40 30 20 10 0 -10
f1 (ppm)

Annex 2: Supporting information of Article 2

COSY (400 MHz, CDCl$_3$) **3.25**

Annex 2: Supporting information of Article 2
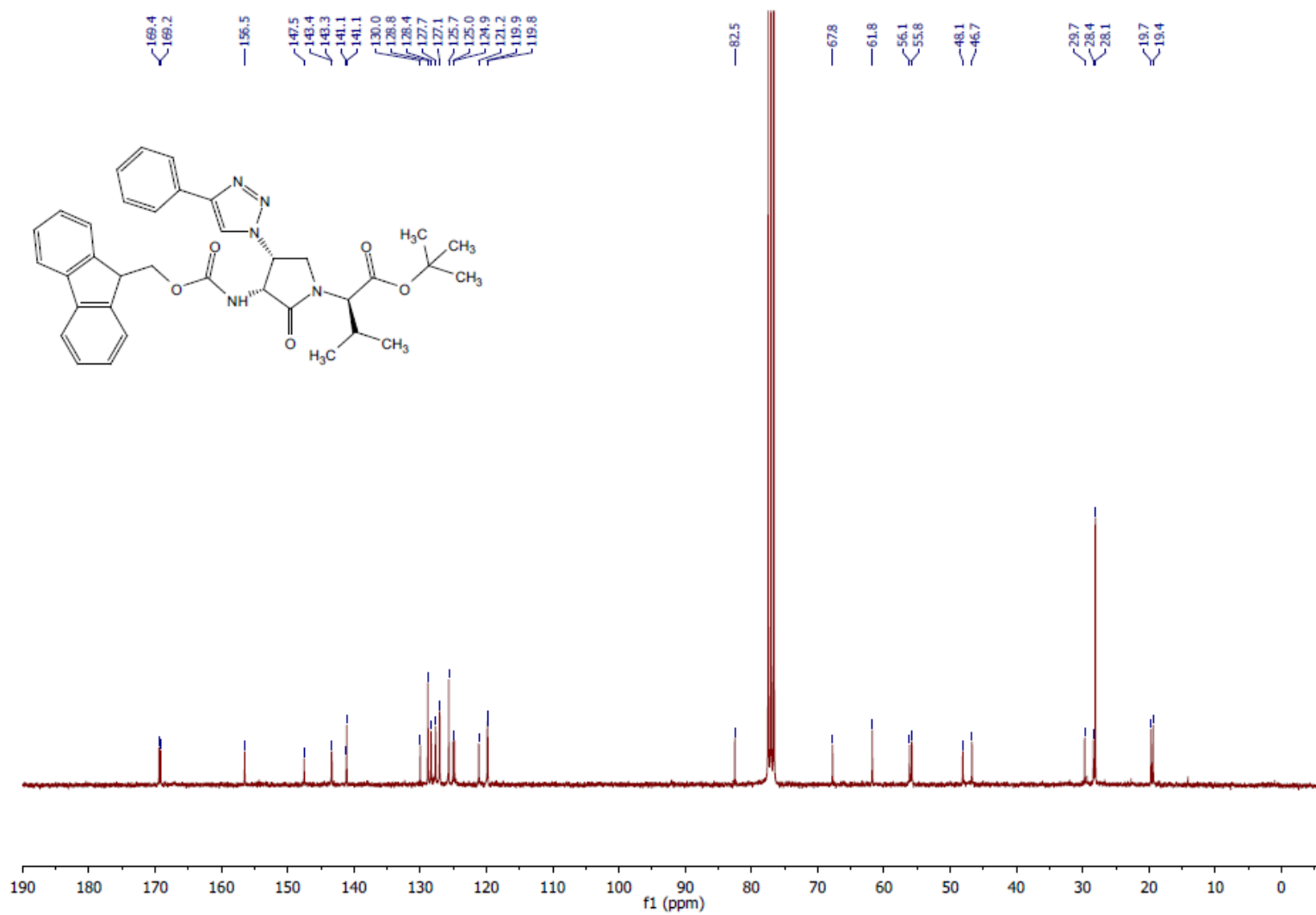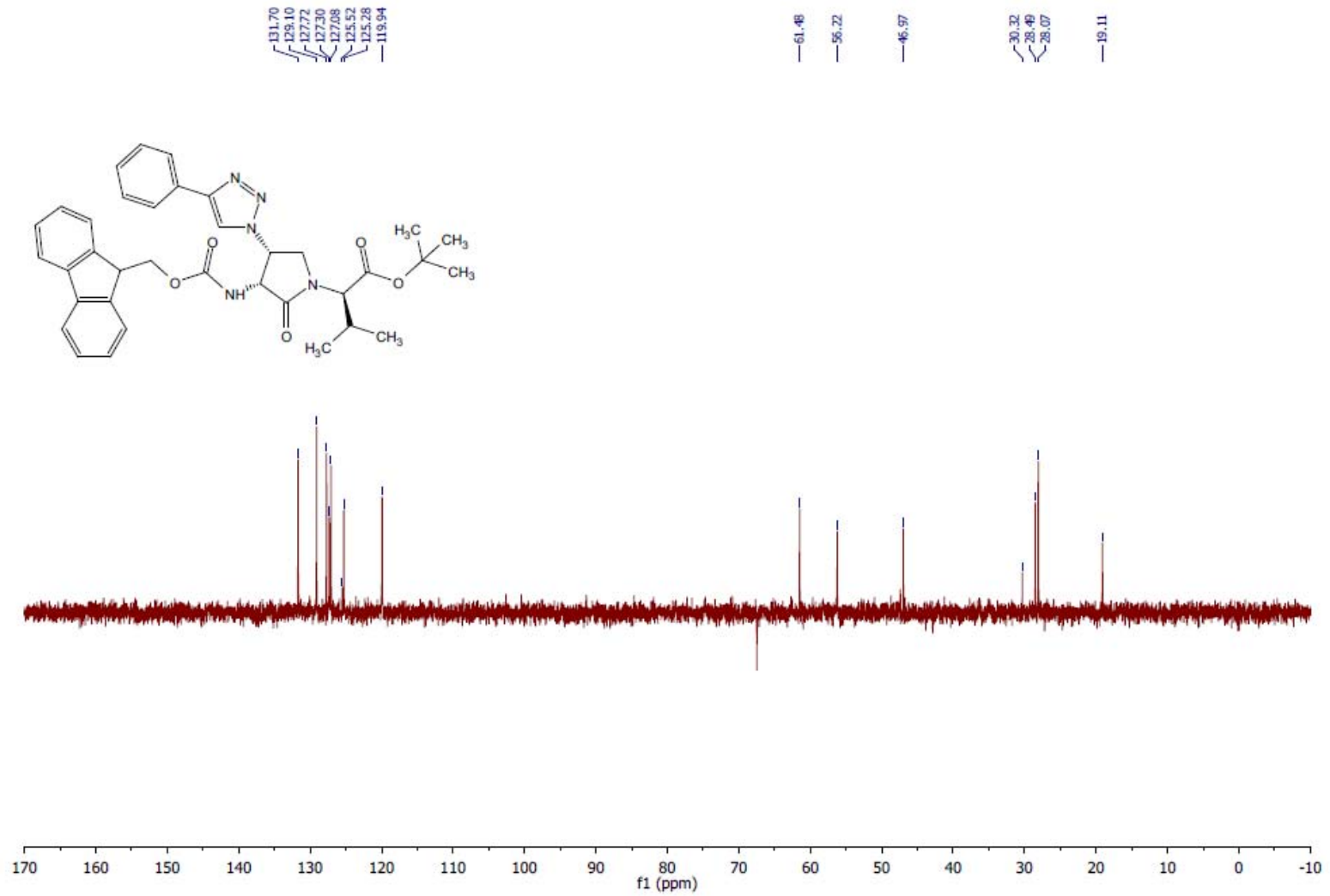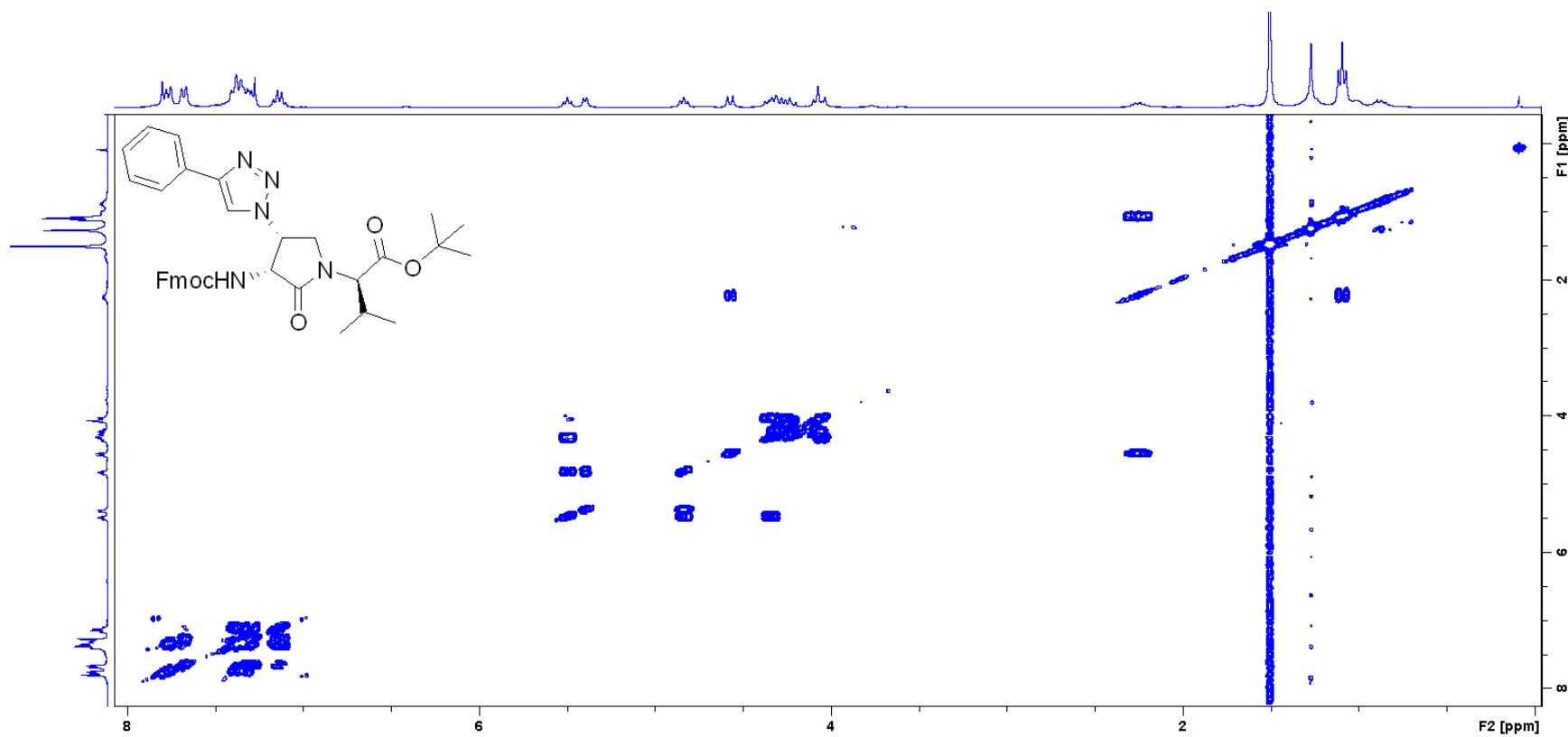
HSQC (75 MHz, CDCl₃) **3.25**
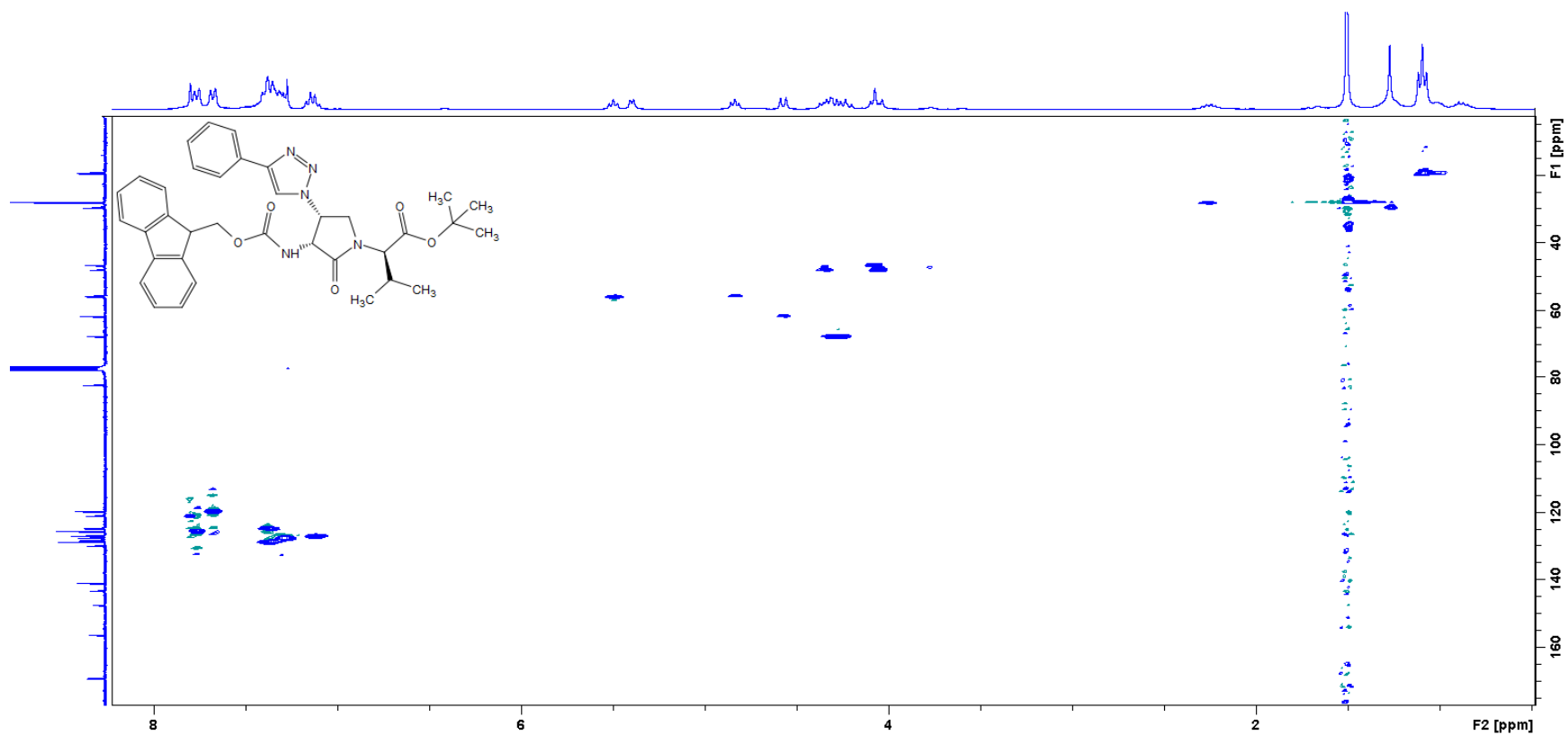
^{1}H NMR (300 MHz, CDCl$_3$) **(2*S*)-3.23**
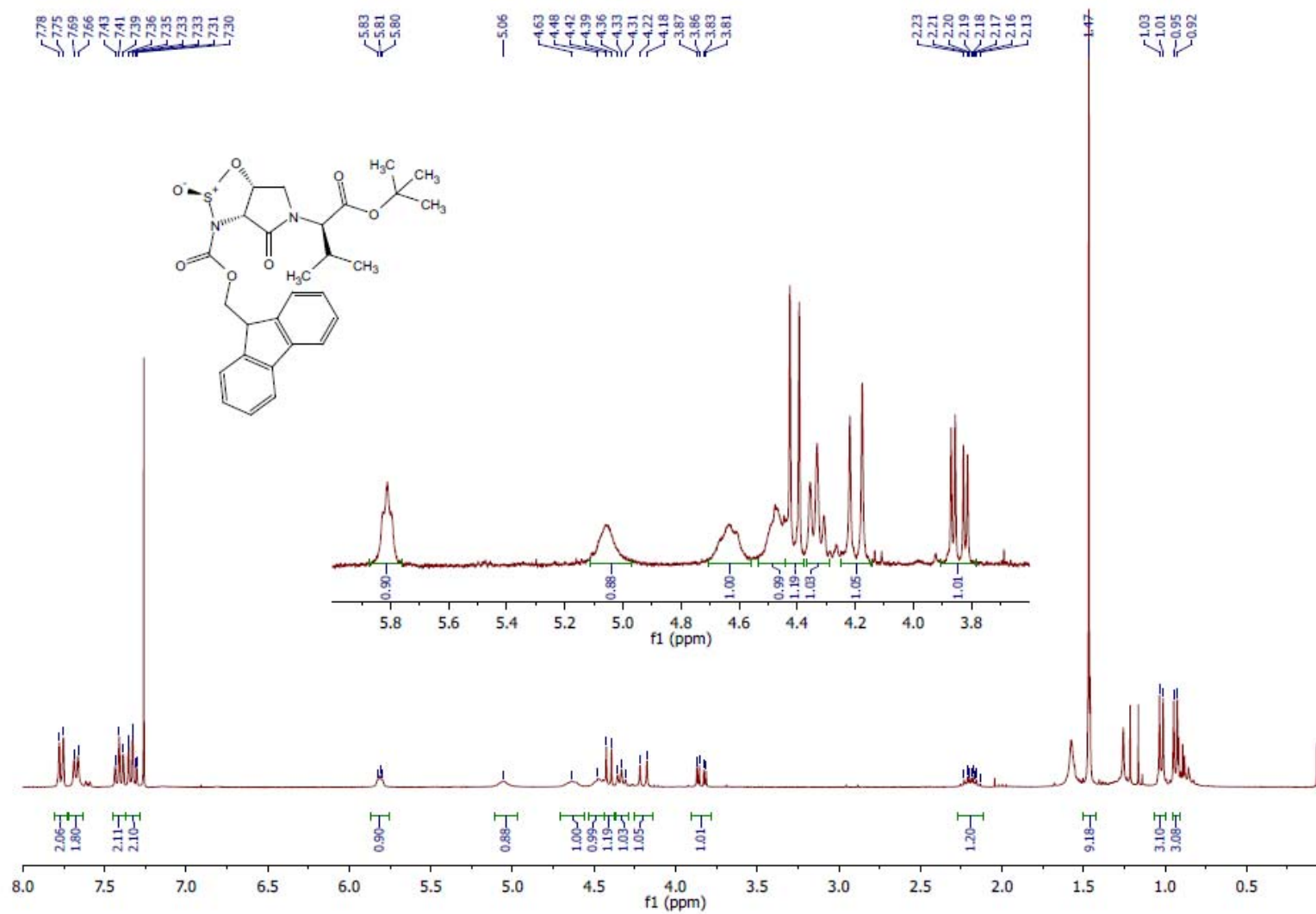
^{13}C NMR (75 MHz, CDCl$_3$) **(2*S*)-3.23**
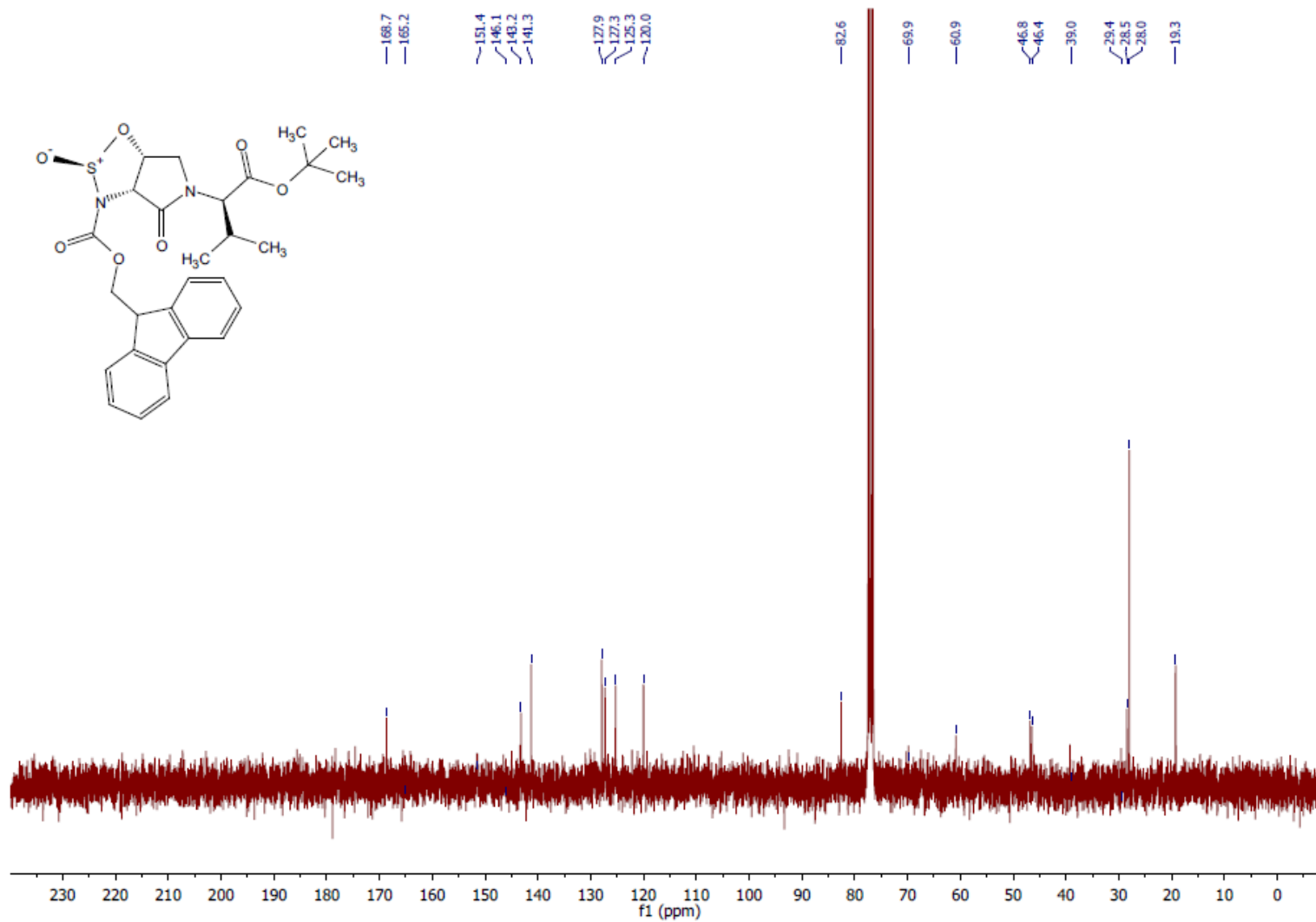
COSY (300 MHz, CDCl₃) **(2*S*)-3.23**
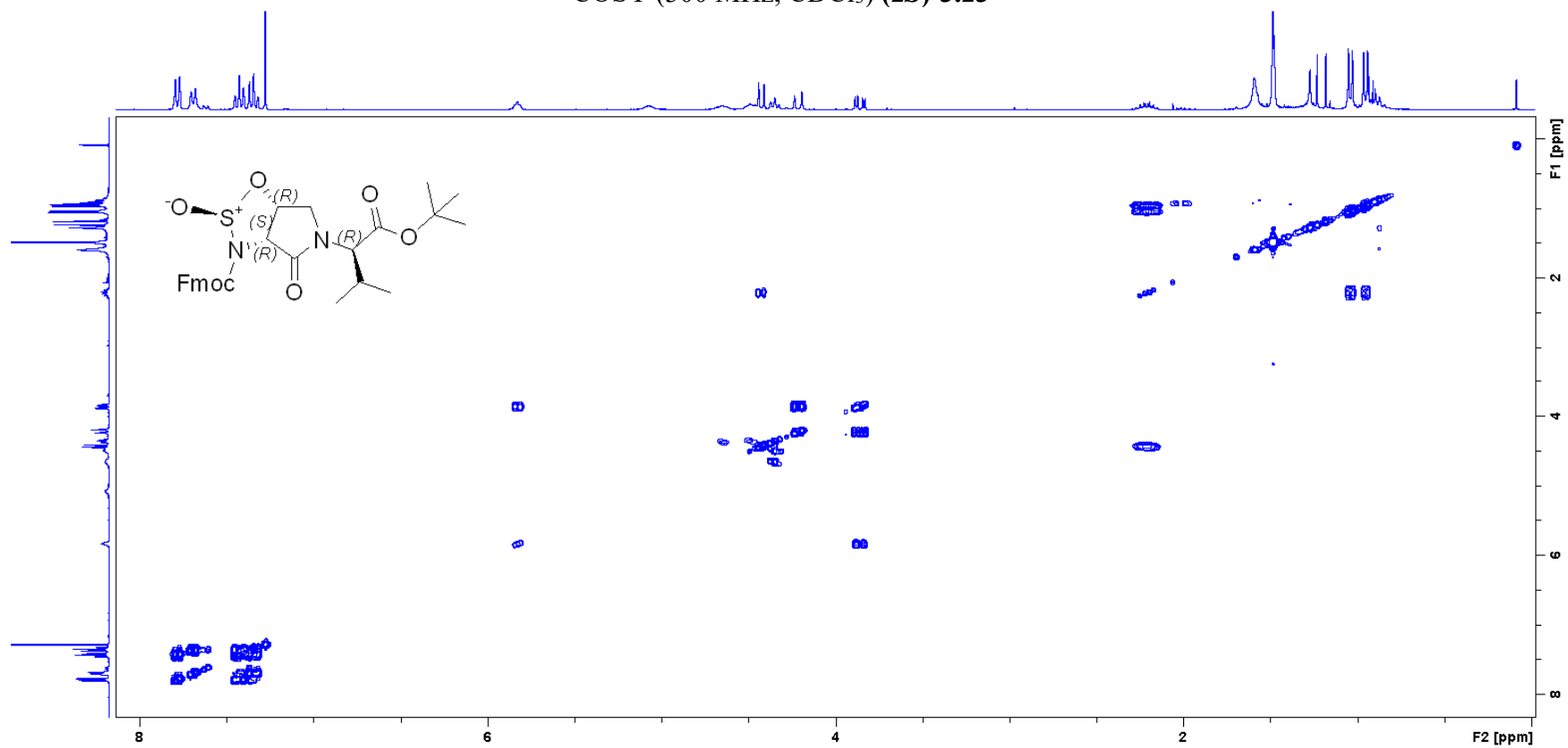
^{1}H NMR (300 MHz, CDCl$_3$) **(2R)-3.23**
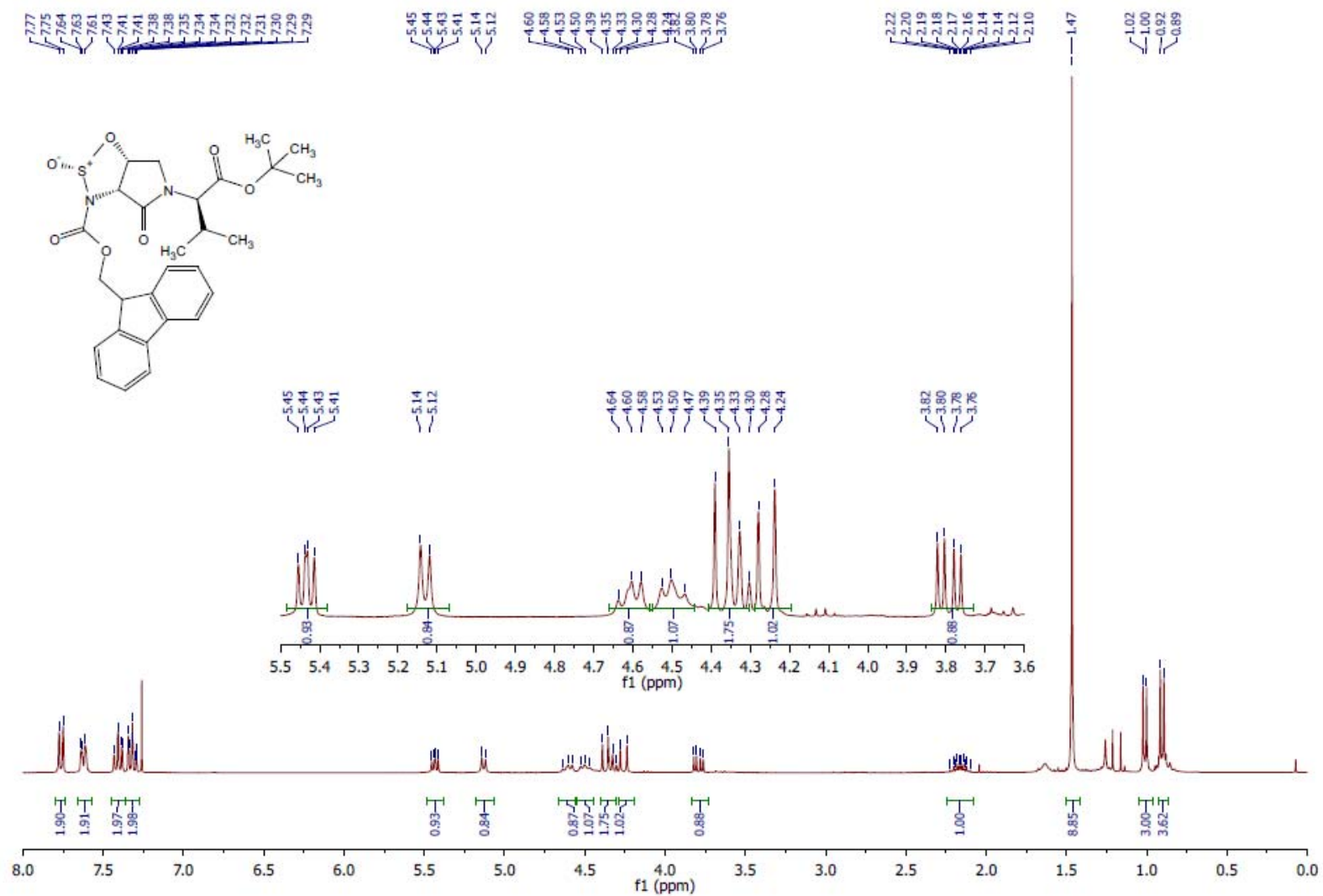
^{13}C NMR (75 MHz, CDCl$_3$) (2*R*)-3.23
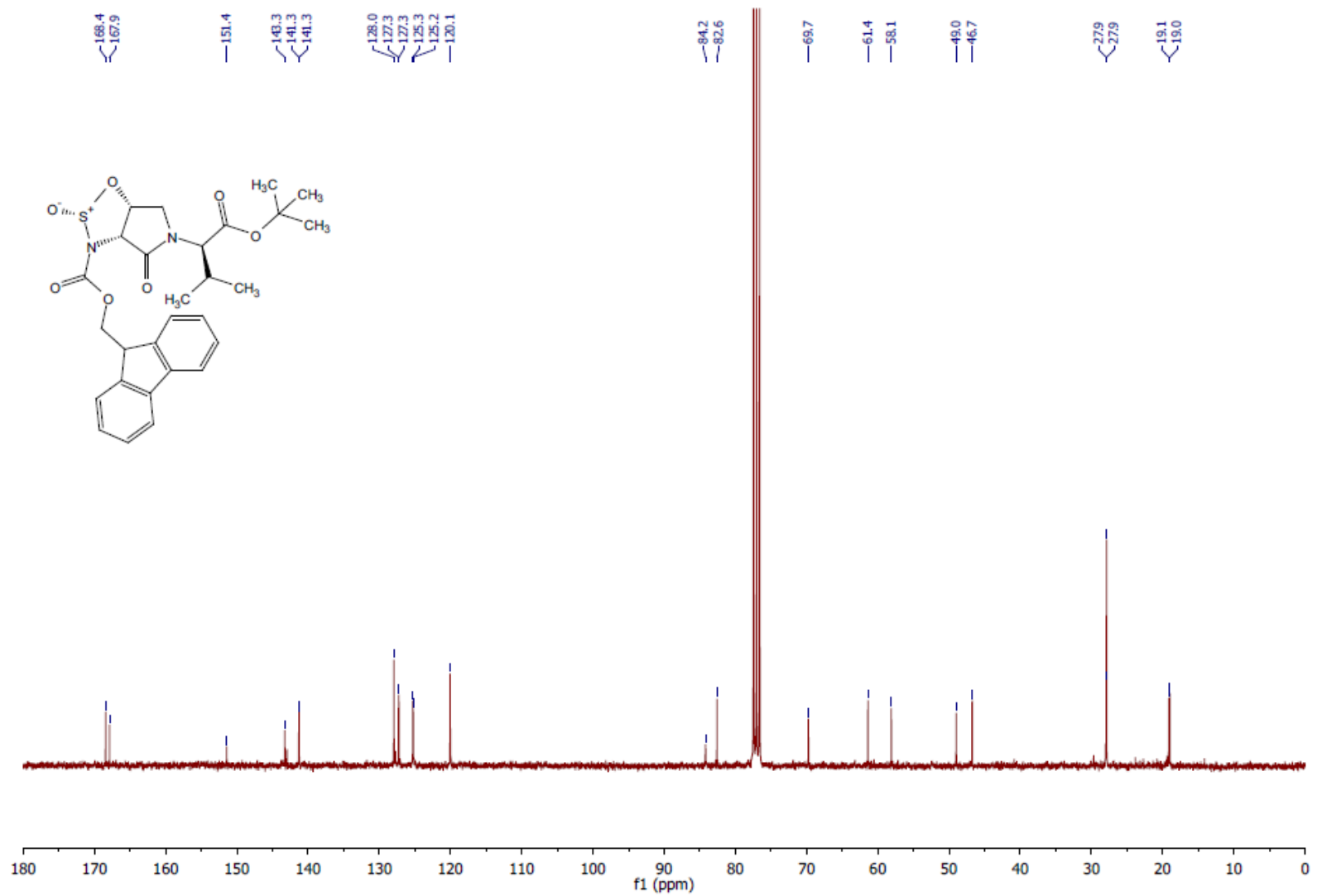
COSY (300 MHz, CDCl₃) **(2*R*)-3.23**
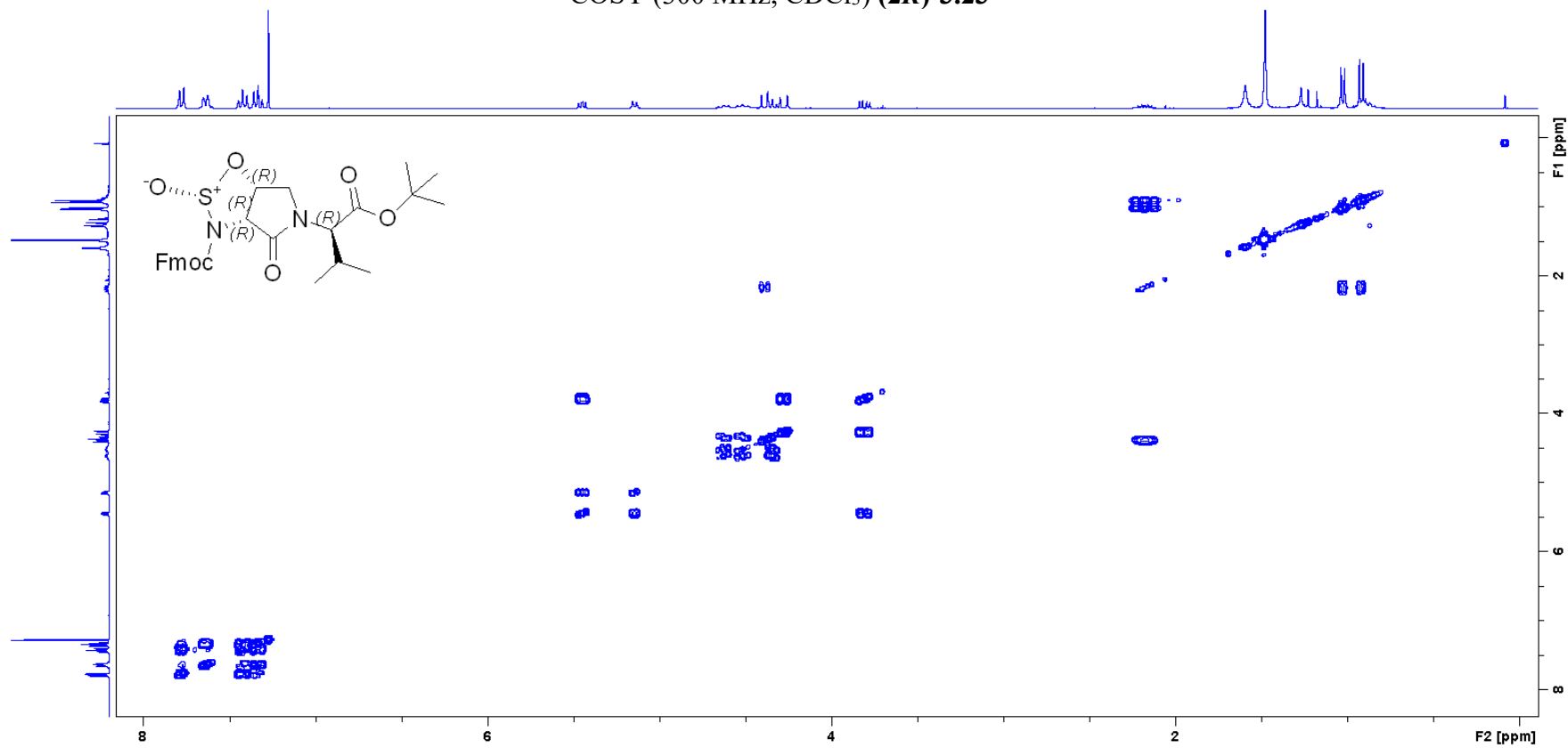
^{1}H NMR (300 MHz, CDCl$_3$) **3.22**

^{13}C NMR (75 MHz, CDCl$_3$) **3.22**

168.3, 166.2, 149.8, 143.0, 142.9, 141.3, 128.0, 127.4, 127.3, 125.5, 120.0, 83.0, 75.4, 71.8, 70.9, 61.2, 58.8, 46.5, 46.4, 28.1, 27.9, 19.2, 19.2

Annex 2: Supporting information of Article 2

COSY (300 MHz, CDCl$_3$) **3.22**

Annex 2: Supporting information of Article 2
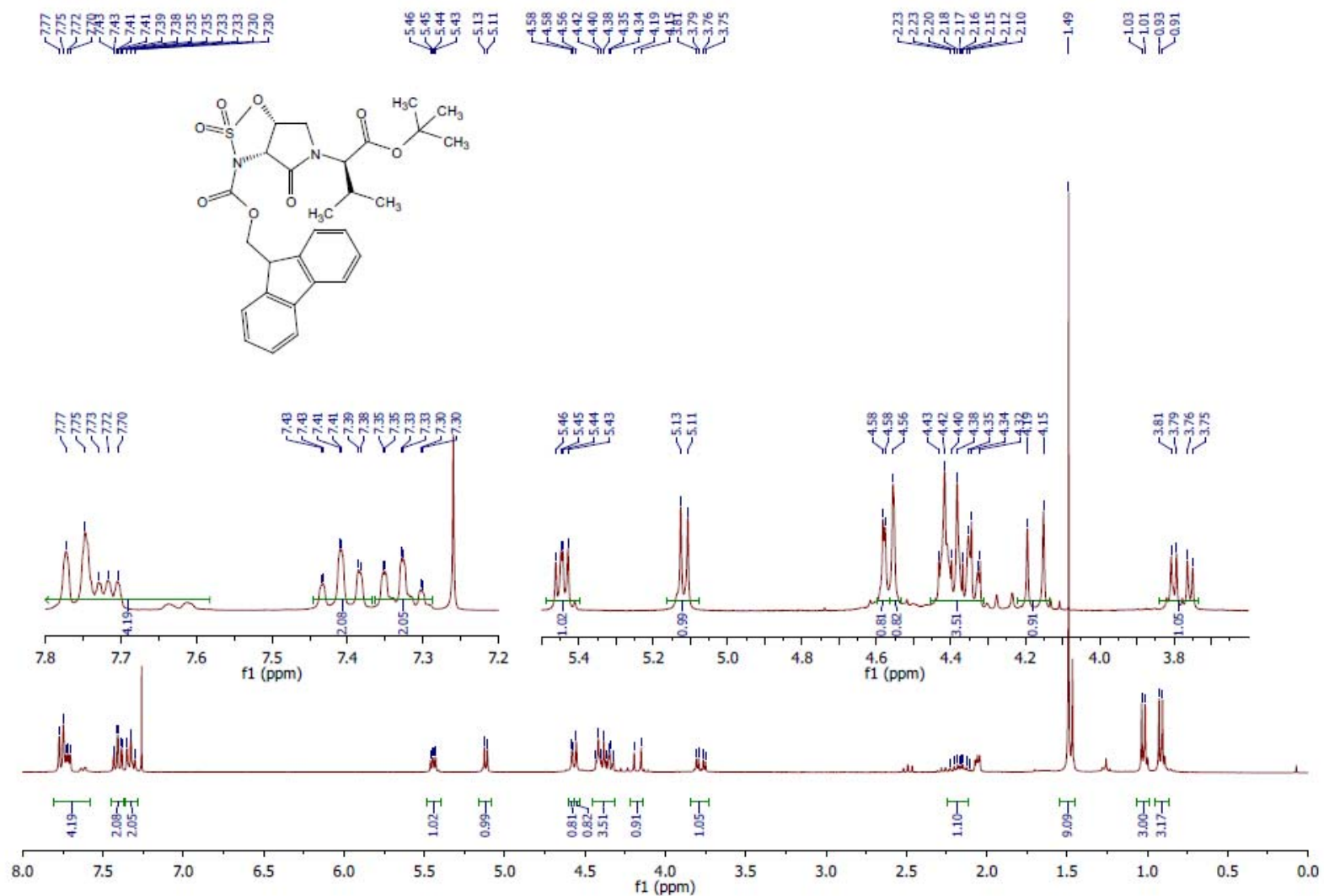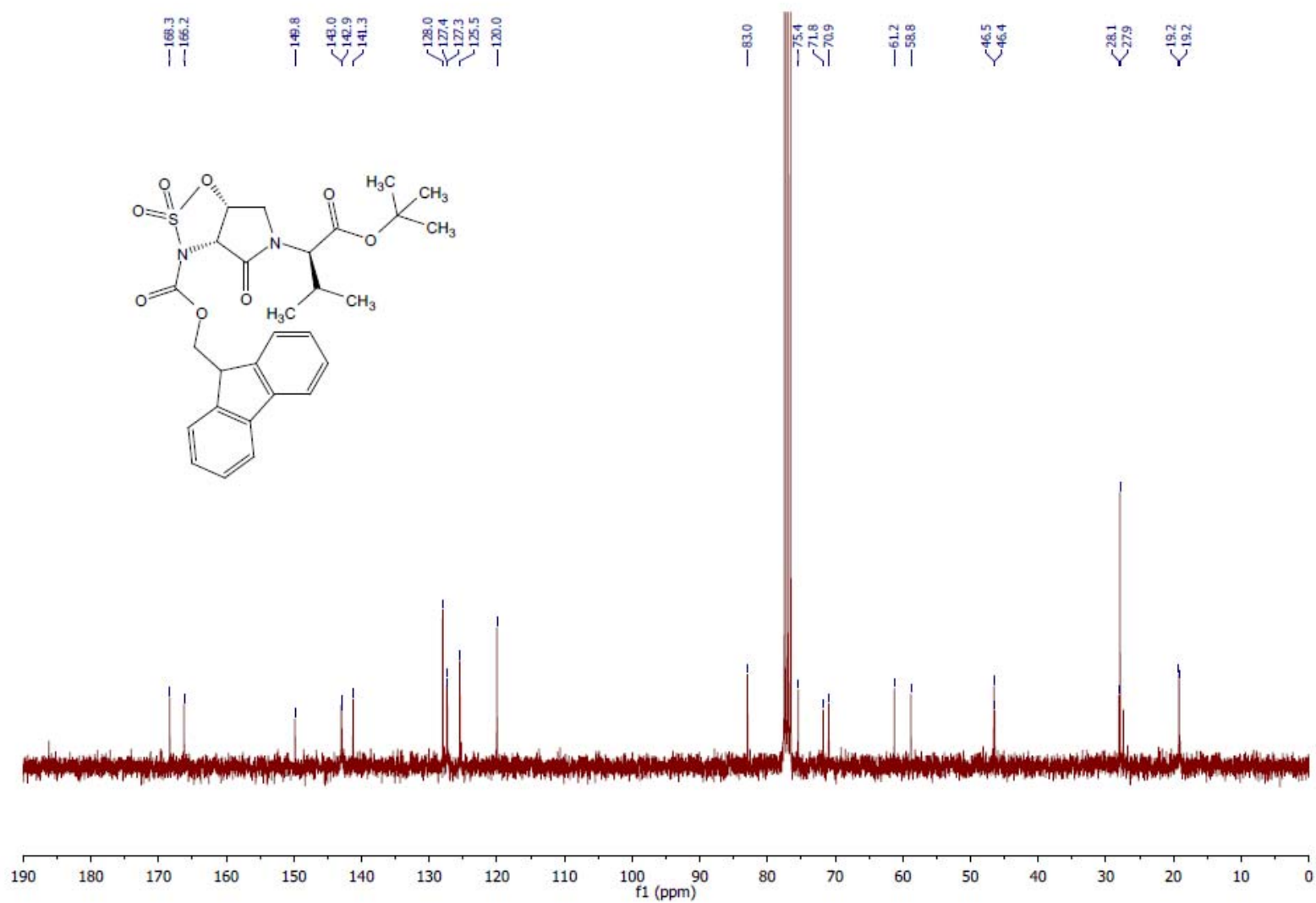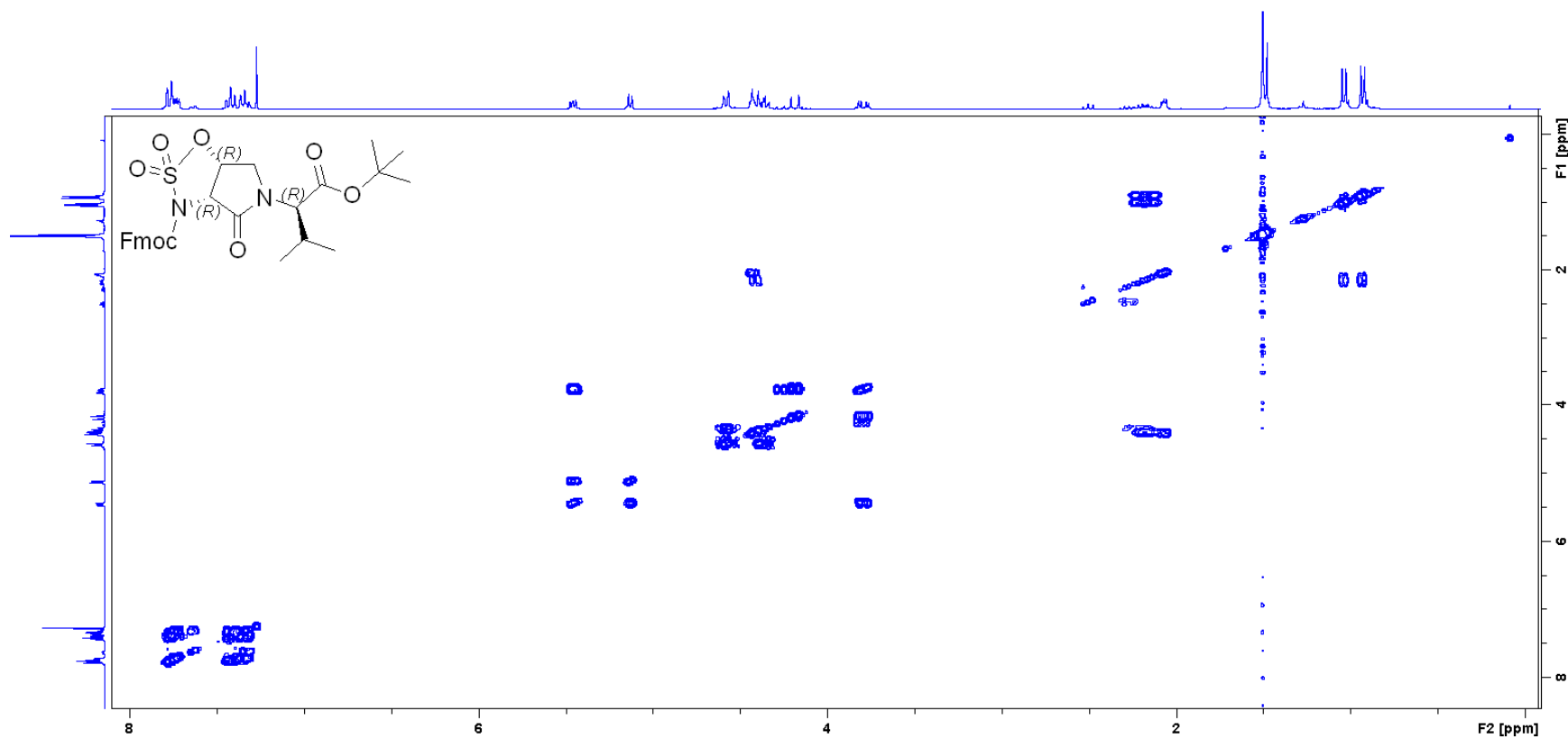
HSQC (75 MHz, CDCl₃) **3.22**
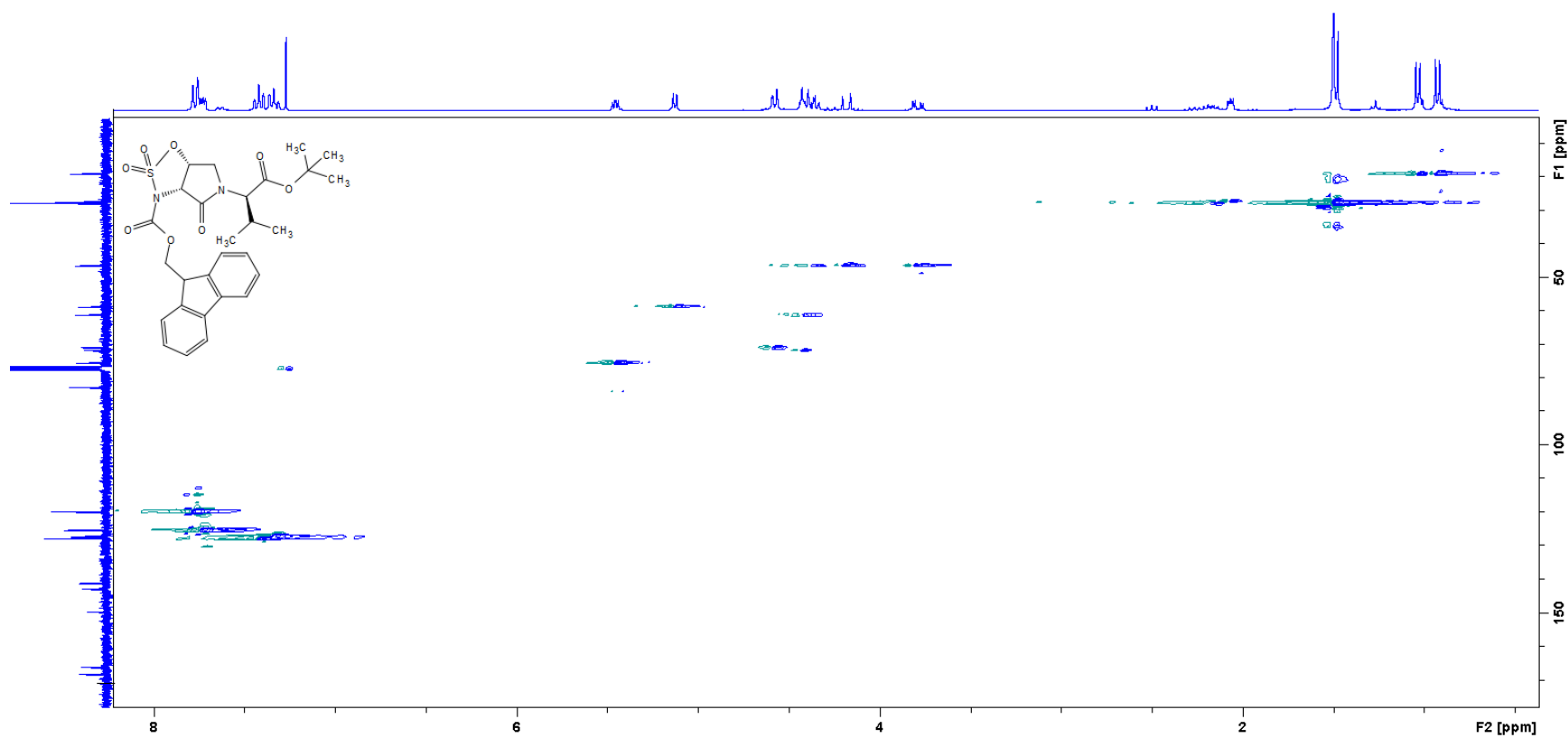
^{1}H NMR (700 MHz, CDCl$_3$) **(4S)-3.24b**
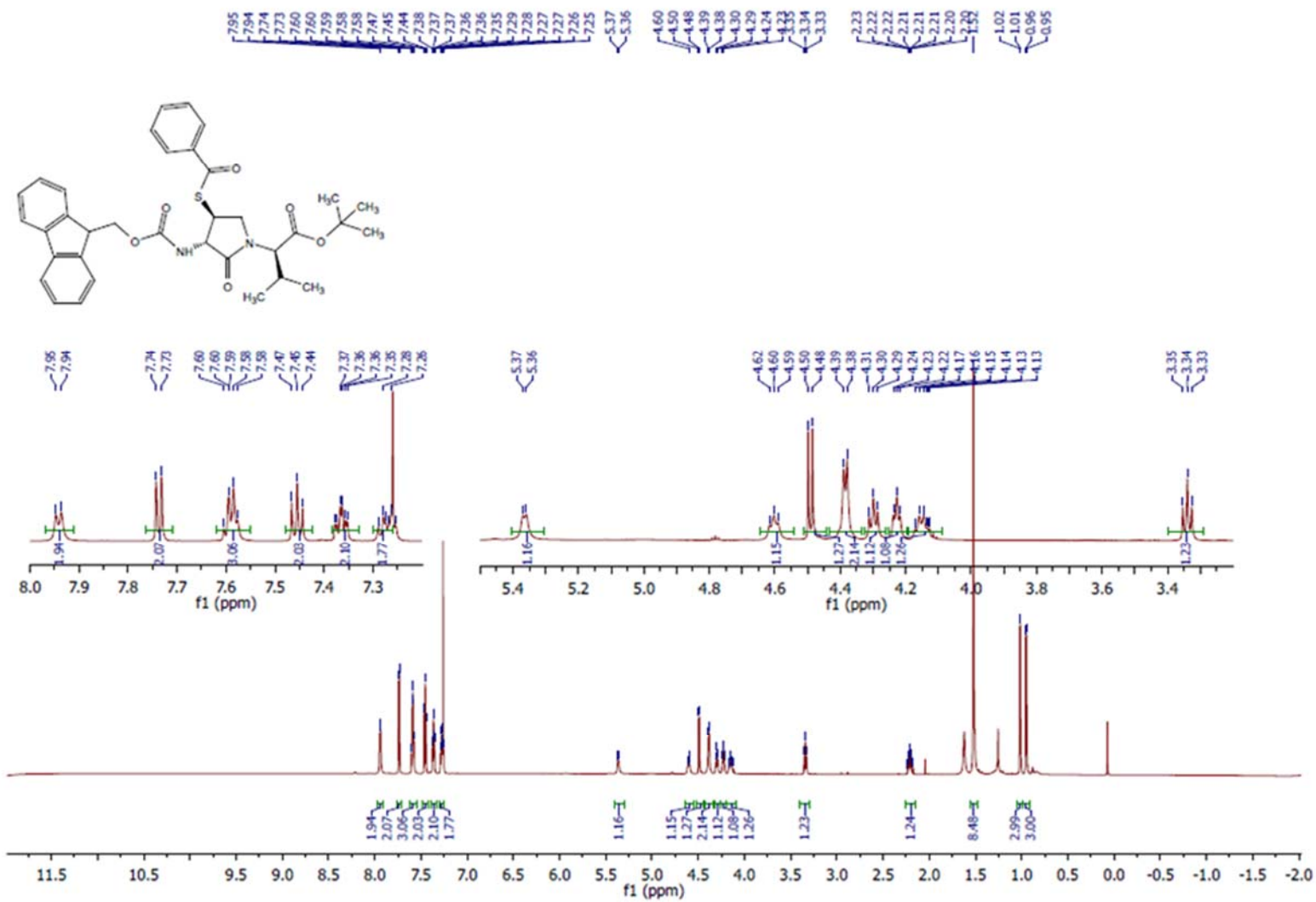
¹³C NMR (176 MHz, CDCl₃) **(4*S*)-3.24b**

COSY (700 MHz, CDCl₃) **(4*S*)-3.24b**
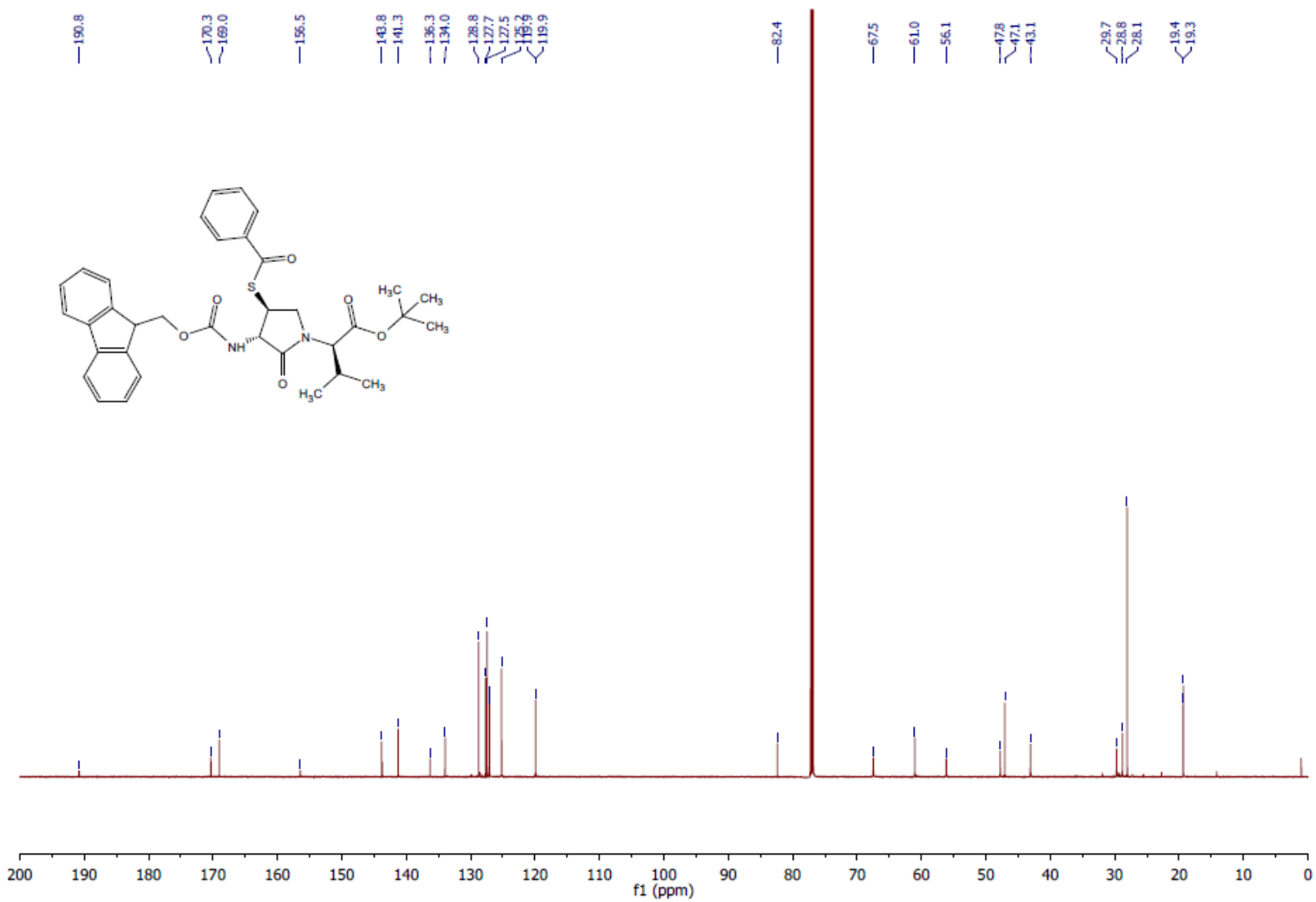
Annex 2: Supporting information of Article 2
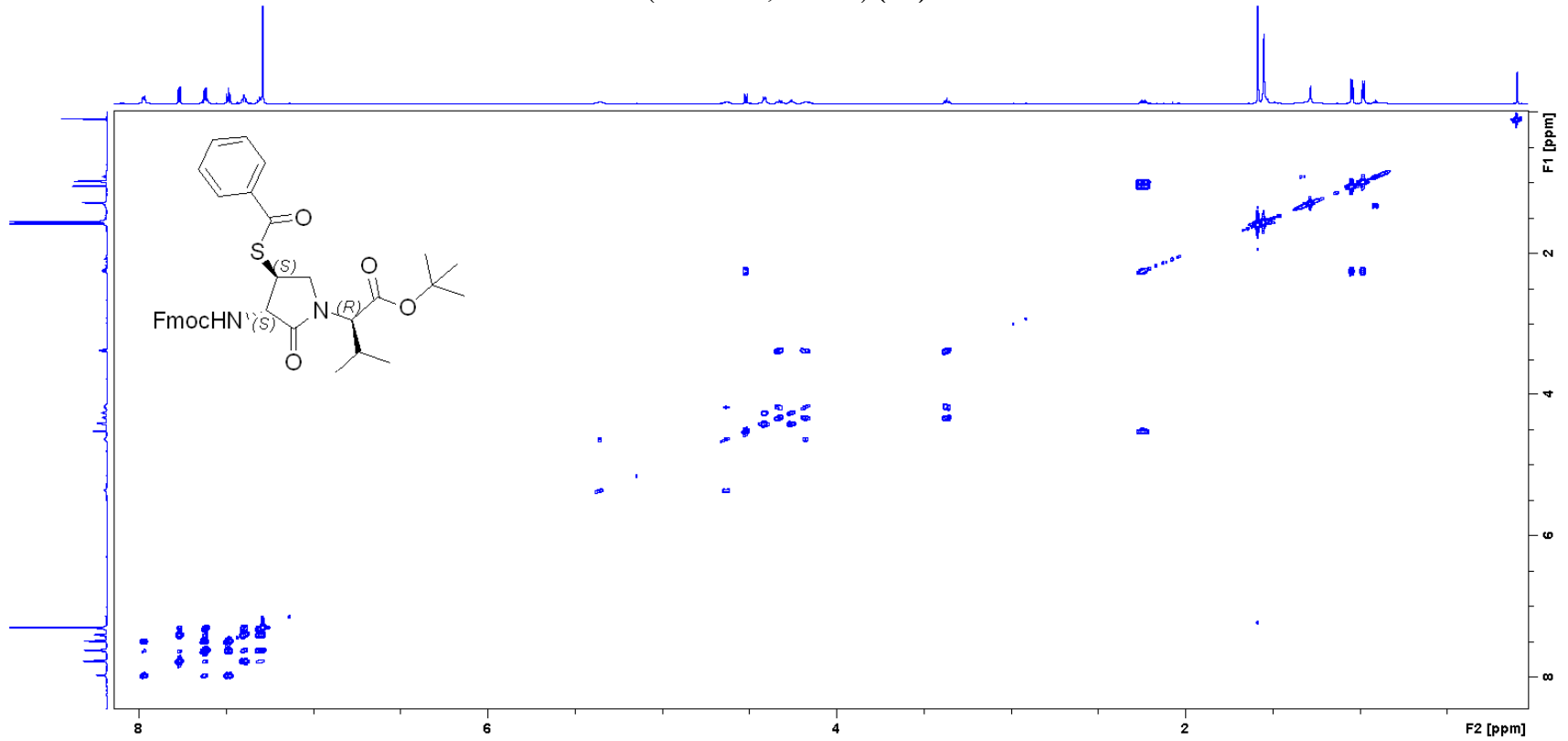
HSQC (176 MHz, CDCl₃) **(4*S*)-3.24b**
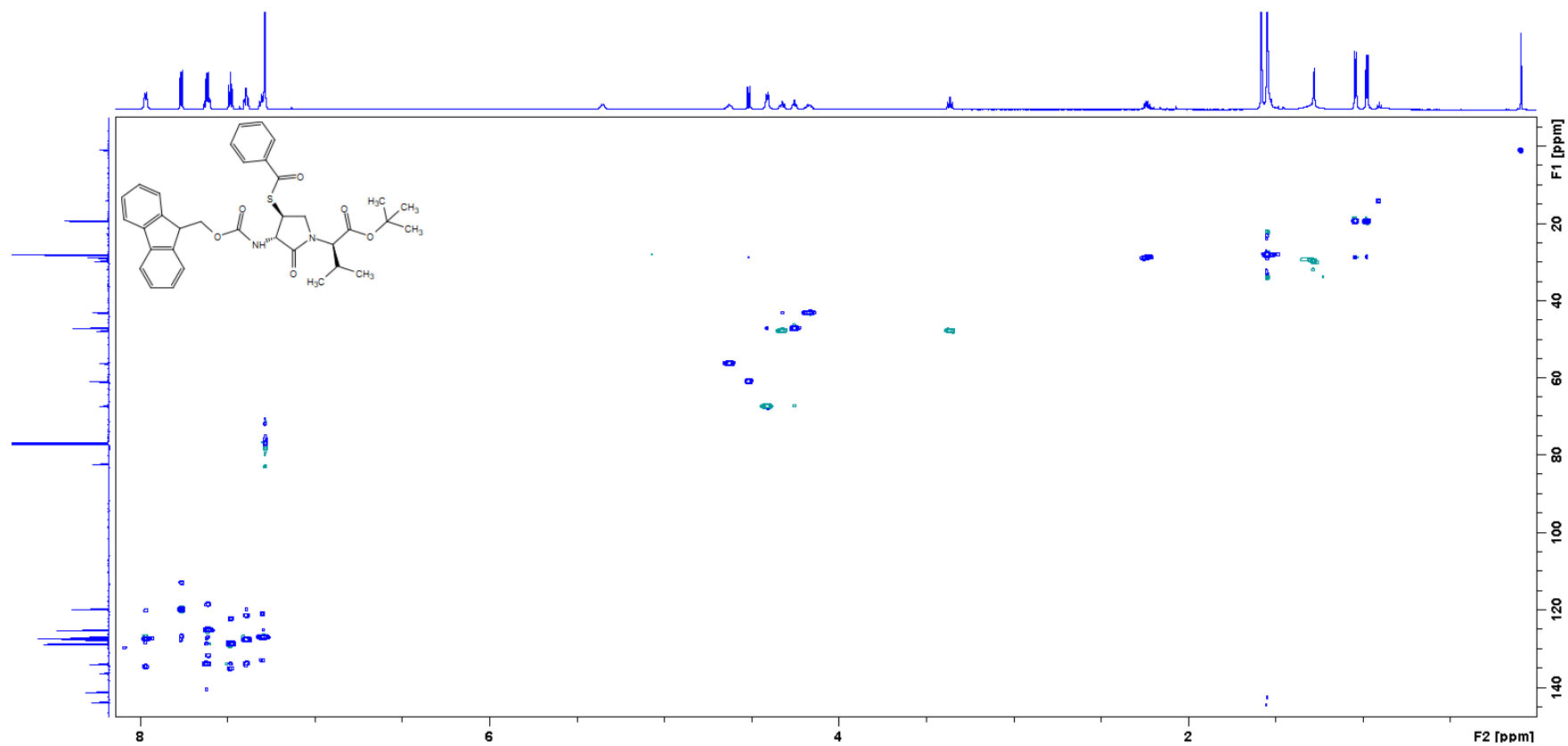
^{1}H NMR (500 MHz, CDCl$_3$) **(4R)-3.24j**
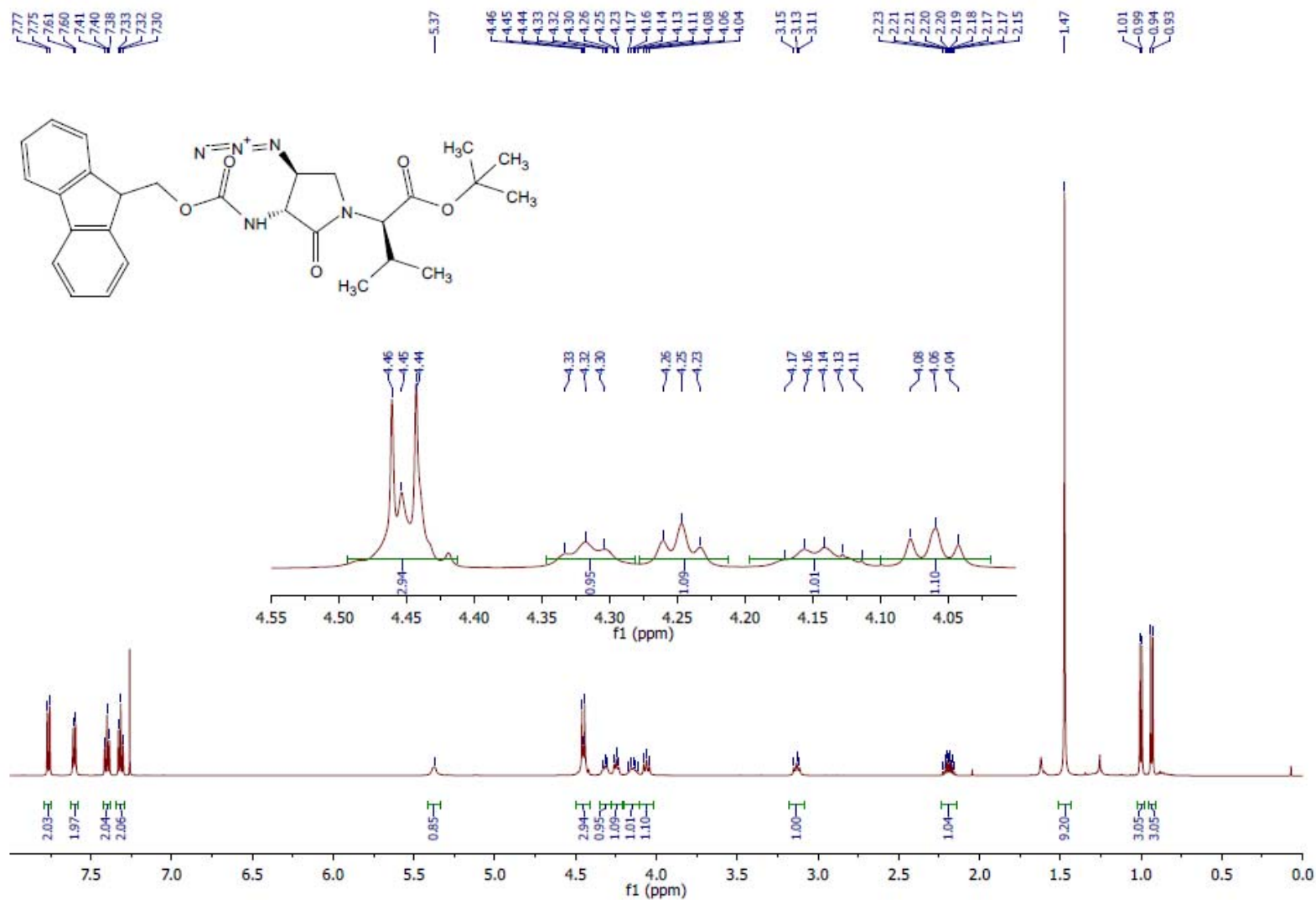
^{13}C NMR (126 MHz, CDCl$_3$) **(4R)-3.24j**

DEPT (126 MHz, CDCl$_3$) **(4*R*)-3.24j**

127.76
127.75
127.13
125.12
120.01

61.81
60.48
57.99

47.09

28.88
28.05

19.38
19.28

Annex 2: Supporting information of Article 2

COSY (500 MHz, CDCl₃) **(4*R*)-3.24j**
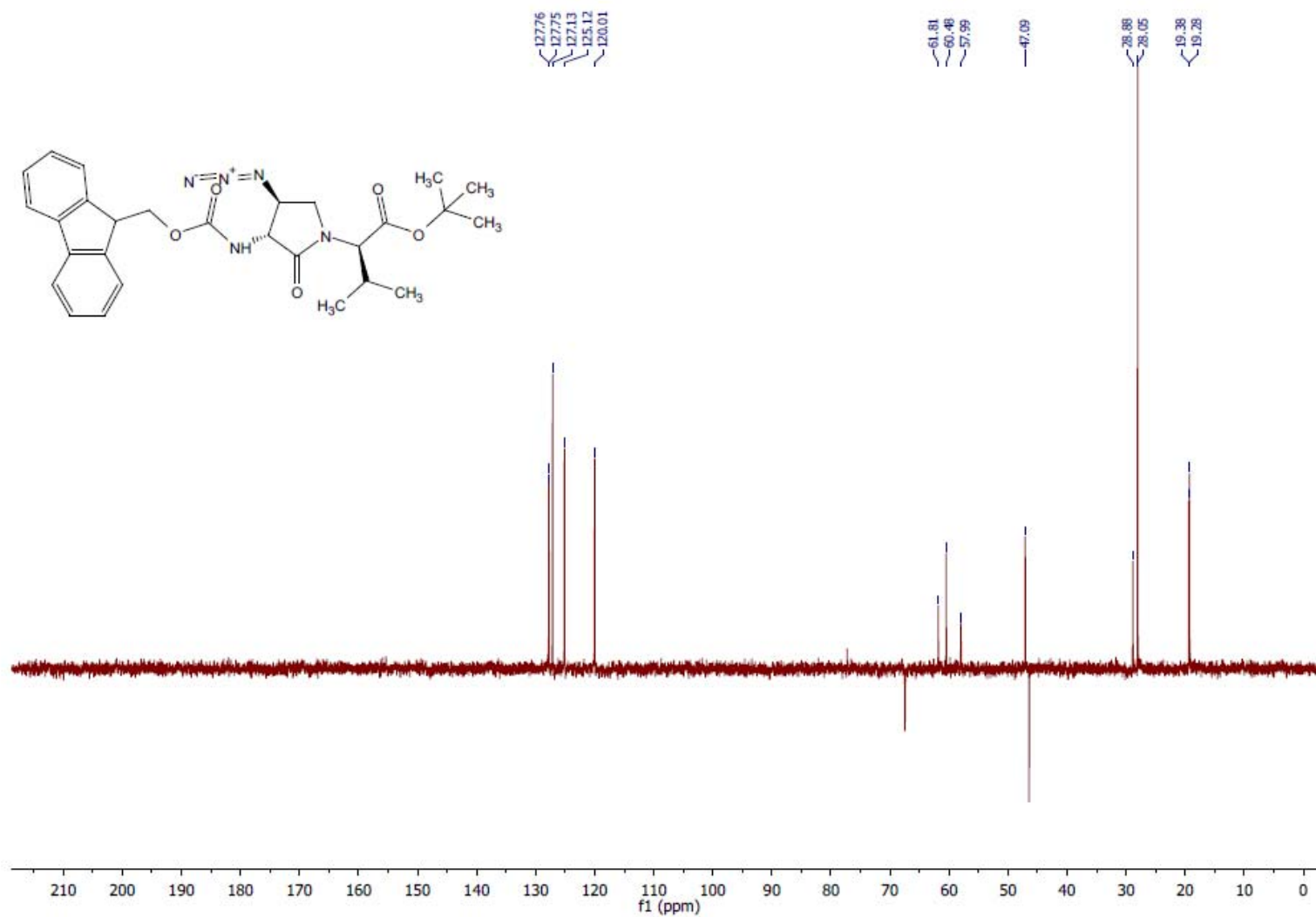
Annex 2: Supporting information of Article 2

HSQC (126 MHz, CDCl$_3$) **(4*R*)-3.24j**

Annex 3: Supporting information of Article 3

Solid-Phase Synthesis and Diversification of β-Substituted α-Amino-γ-Lactam Peptide Allosteric Modulators of the Interleukin-1 Receptor

Azade Geranurimi and William D. Lubell*

Département de Chimie, Université de Montréal, C.P. 6128, Succursale Centre-Ville, Montréal, Québec H3C 3J7, Canada

***Correspondence:** Prof. William D. Lubell, *william.lubell@umontreal.ca*

***tert*-Butyl (3*R*, 4*S*, 2'*S*)-2-[3-(Fmoc)amino-4-azido-2-oxopyrrolidin-1-yl]-3-methylbutanoate (4.5c)**

Was prepared as previously described (Geranurimi and Lubell 2018).

***tert*-Butyl (3*S*, 4*S*, 2'*R*)-2-[3-(Fmoc)amino-4-thiocyanato-2-oxopyrrolidin-1-yl]-3-methylbutanoate (4.5e)**

Was prepared as previously described (Geranurimi and Lubell 2018).

***tert*-Butyl (3*S*, 4*S*, 2'*R*)-2-[3-(Fmoc)amino-4-methylthio-2-oxopyrrolidin-1-yl]-3-methylbutanoate (4.5f)**

Was prepared as previously described (Geranurimi and Lubell 2018).

Annex 3: Supporting information of Article 3

[(3*R*, 4*S*)-β-N₃-AgI³]-101.10 (4.2c)

LCMS chromatogram [10-90% MeOH (0.1% FA)/water (0.1% FA), 14 min]; RT = 8.3 on a CE-C18, 3 x 50 mm, 2.7 um with a flow rate of 0.4 mL/min.
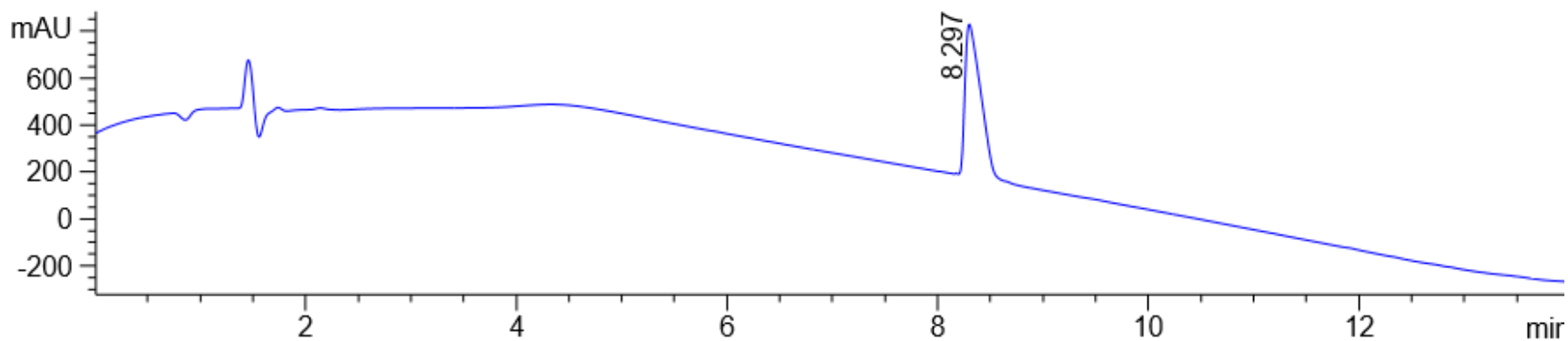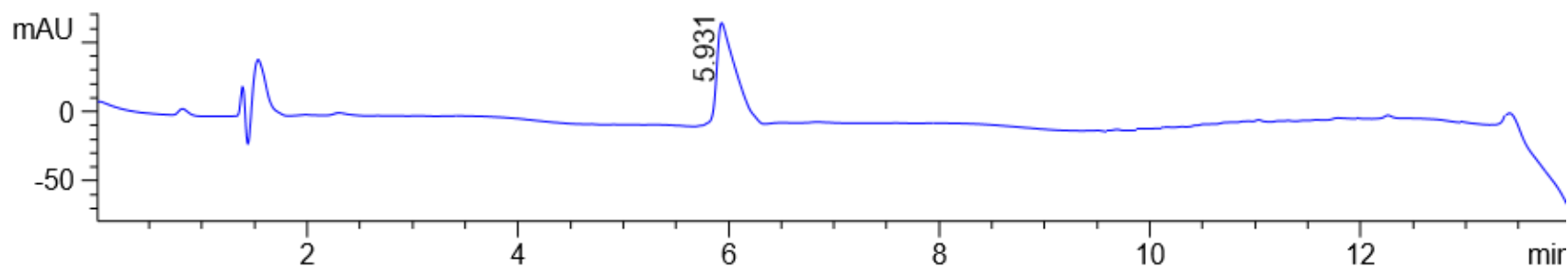

LCMS chromatogram [10-90% MeCN (0.1% FA)/water (0.1% FA), 14 min]; RT = 5.9 on a CE-C18, 3 x 50 mm, 2.7 um with a flow rate of 0.4 mL/min.


Annex 3: Supporting information of Article 3
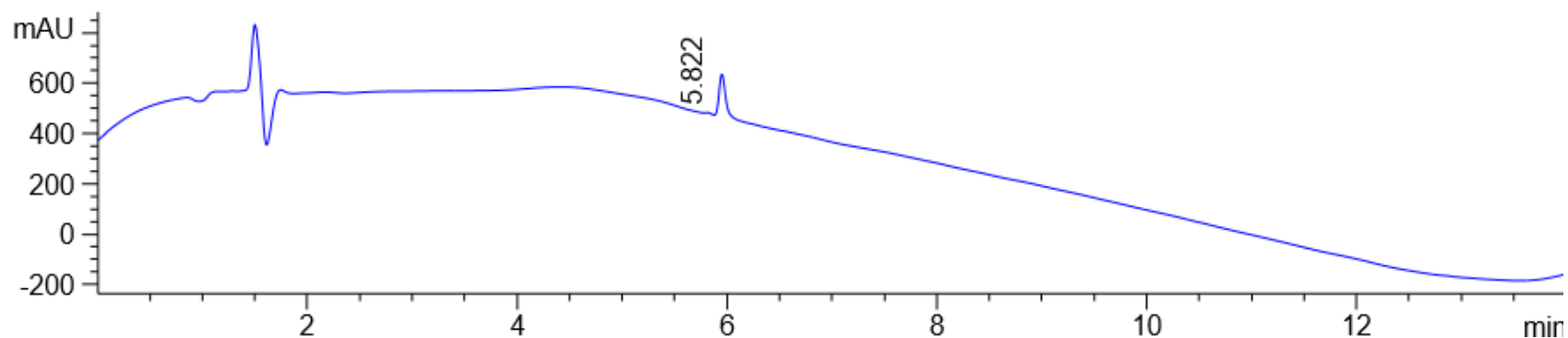
[(3S, 4S)-β-SCN-AgI³]-101.10 (4.2d)

LCMS chromatogram [10-90% MeOH (0.1% FA)/water (0.1% FA), 14 min]; RT = 8.3 on a Sunfire C18 analytical column (100Å, 3.5 µm, 4.6 mm X 100 mm).
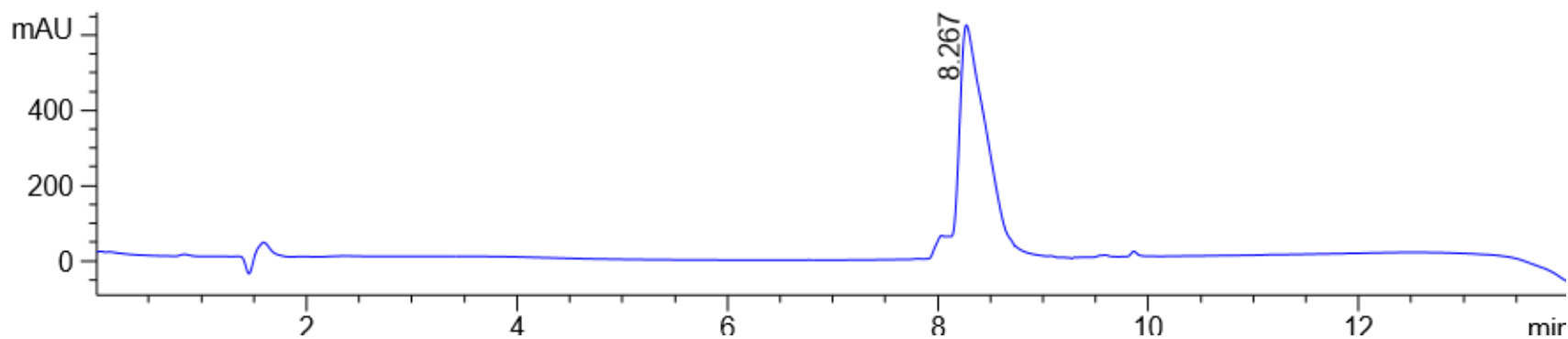
LCMS chromatogram [10-90% MeCN (0.1% FA)/water (0.1% FA), 14 min]; RT = 5.7 on a CE-C18, 3 x 50 mm, 2.7 um with a flow rate of 0.4 mL/min.

Annex 3: Supporting information of Article 3
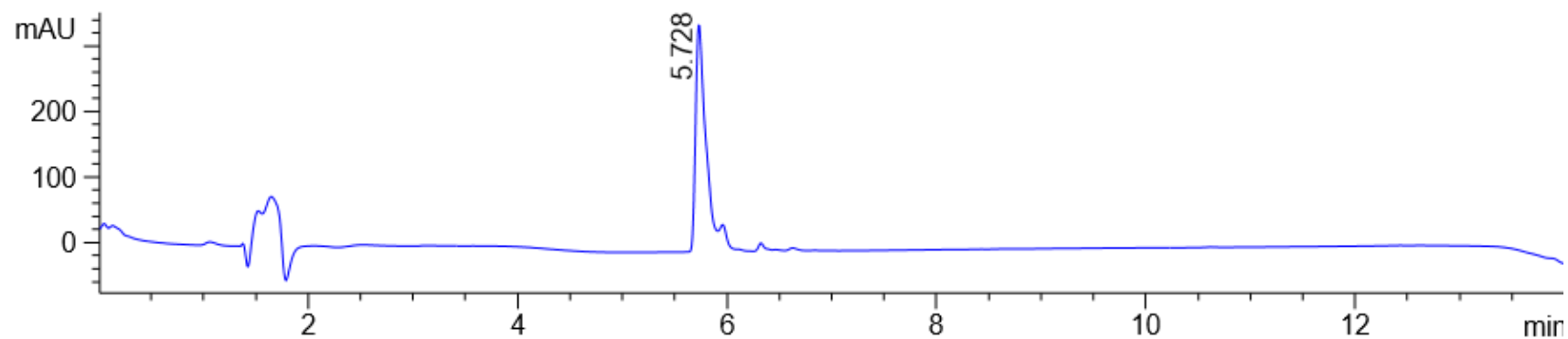
[(3*S*, 4*S*)-β-SMe-AgI³]-101.10 (4.2e)

LCMS chromatogram [10-90% MeOH (0.1% FA)/water (0.1% FA), 14 min]; RT = 8.7 on a CE-C18, 3 x 50 mm, 2.7 um with a flow rate of 0.4 mL/min.
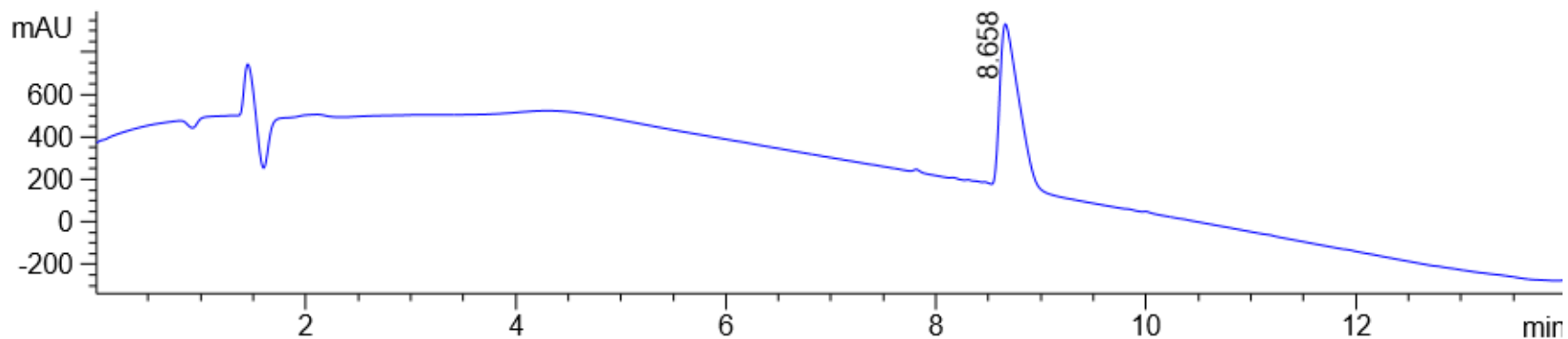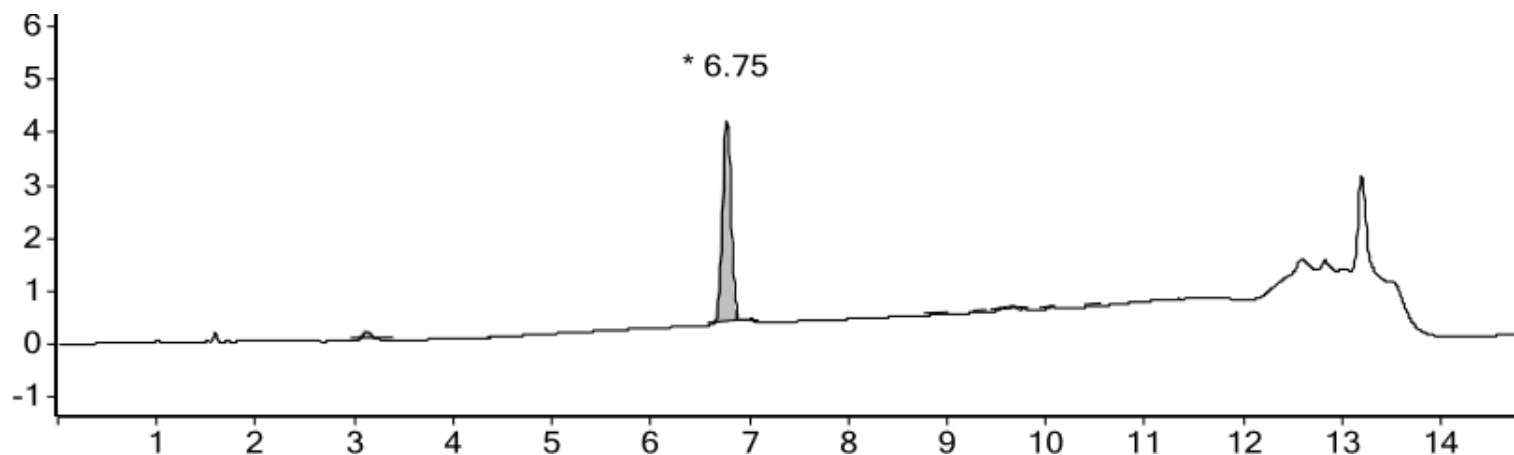

LCMS chromatogram [10-90% MeCN (0.1% FA)/water (0.1% FA), 14 min]; RT = 5.9 on a CE-C18, 3 x 50 mm, 2.7 um with a flow rate of 0.4 mL/min.


Annex 3: Supporting information of Article 3
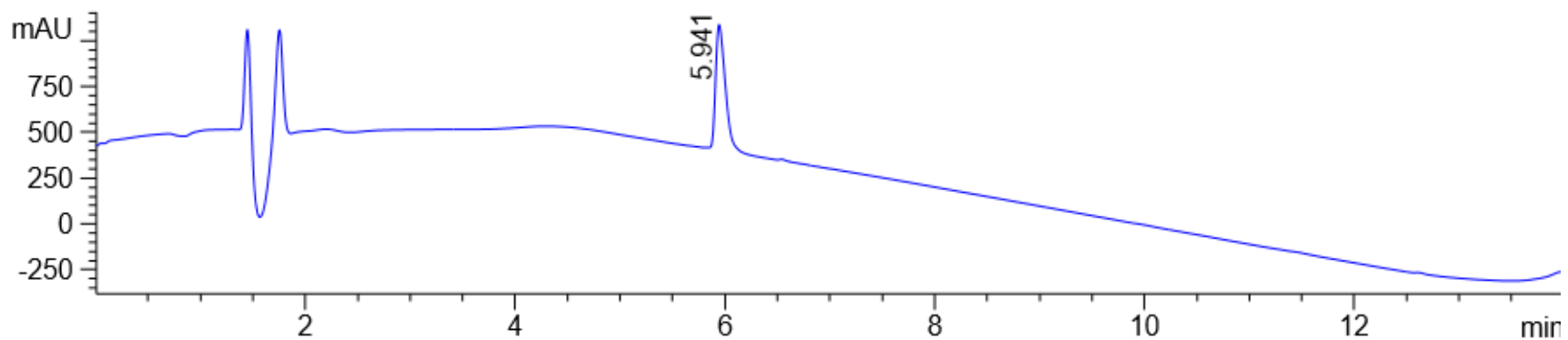
[(3*R*, 4*S*)-β-ONPhth-AgI³]-101.10 (4.2f)

LCMS chromatogram [30-60-90% MeOH (0.1% FA)/water (0.1% FA), 15 min]; RT = 8.8 on a CSH-C18, 4.6 X100 mm, 5 um, with a flow rate of 0.8 mL/min.
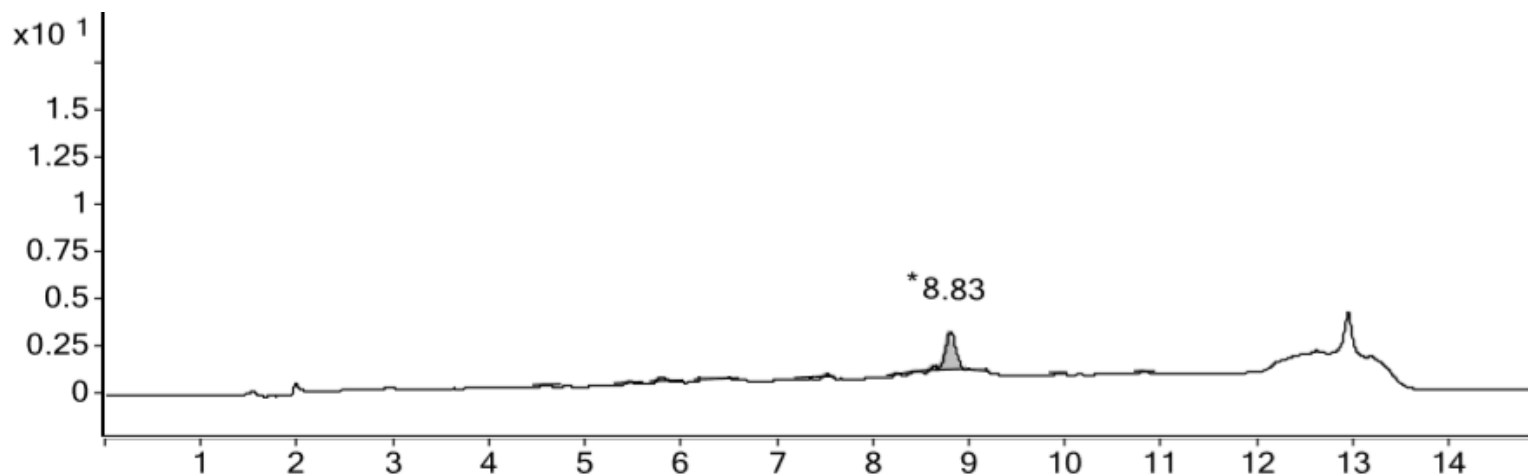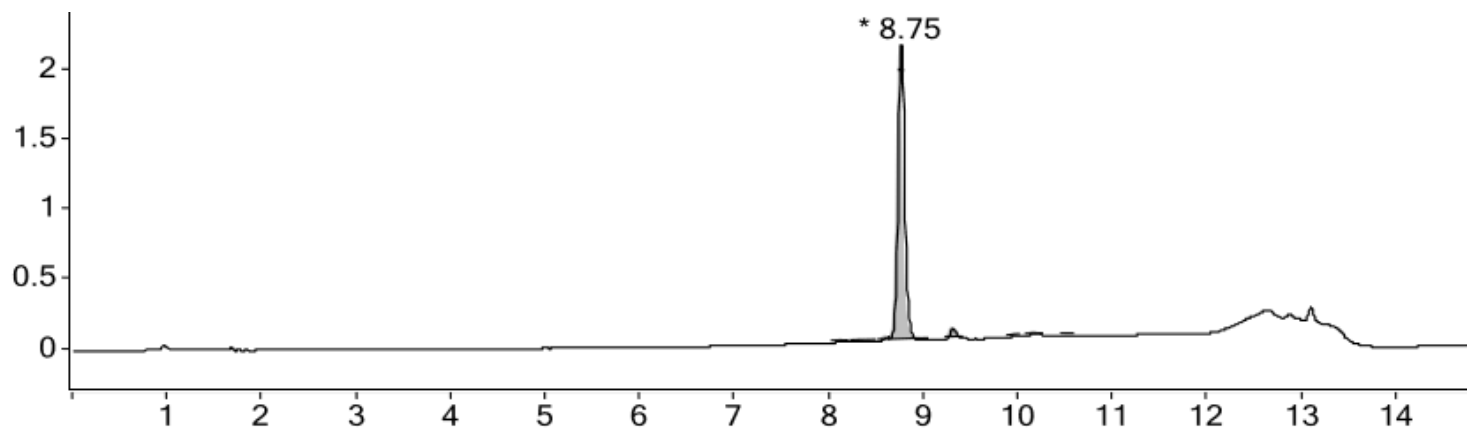

LCMS chromatogram [5-60-90% ACN (0.1% FA)/water (0.1% FA), 15 min]; RT = 8.8 on a CSH-C18, 4.6 X100 mm, 5 um, with a flow rate of 0.8 mL/min.


Annex 3: Supporting information of Article 3

Annex 3: Supporting information of Article 3
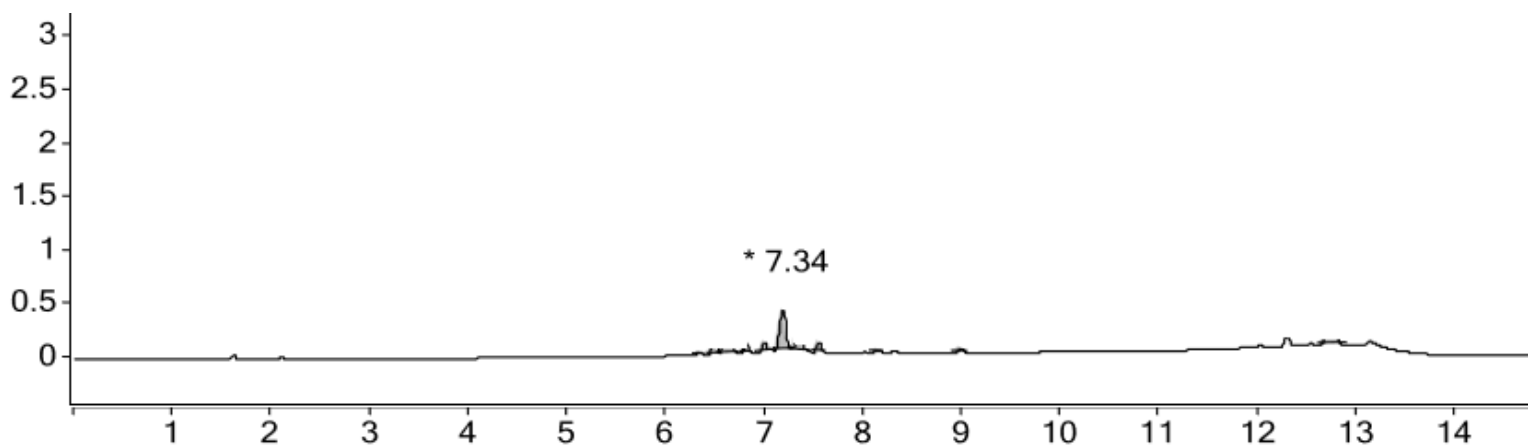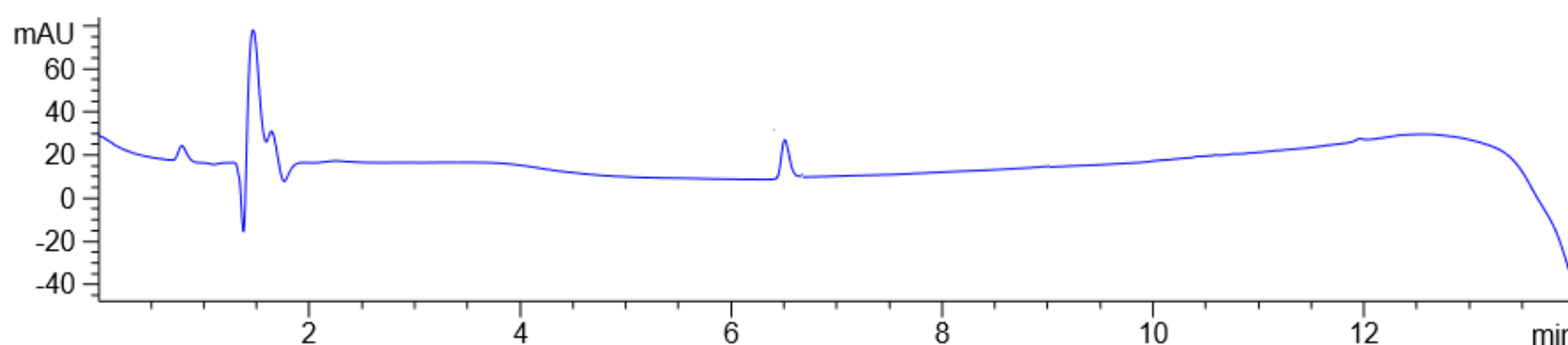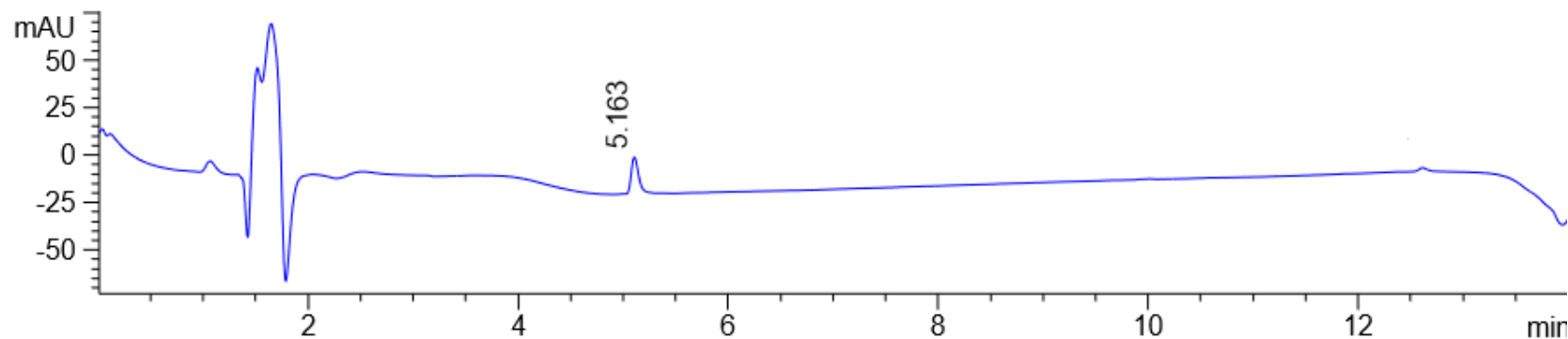
[(3*R*, 4*S*)-β-NH₂-AgI³]-101.10 (4.2h)

LCMS chromatogram [10-90% MeOH (0.1% FA)/water (0.1% FA), 14 min]; RT = 5.8 on a CE-C18, 3 x 50 mm, 2.7 um with a flow rate of 0.4 mL/min.
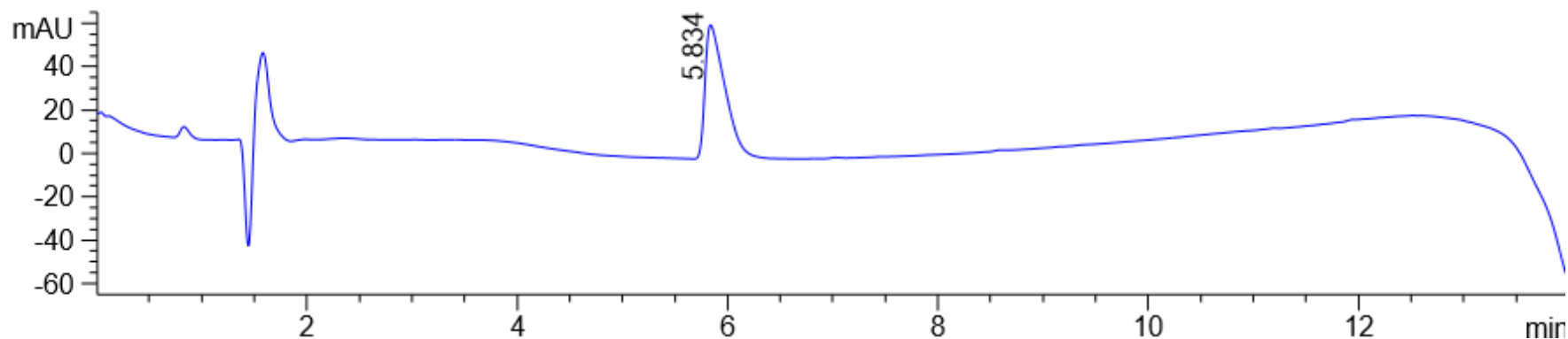
LCMS chromatogram [50-90% MeCN (0.1% FA)/water (0.1% FA), 14 min]; RT = 1.0 on a CE-C18, 3 x 50 mm, 2.7 um with a flow rate of 0.4 mL/min.

Annex 3: Supporting information of Article 3
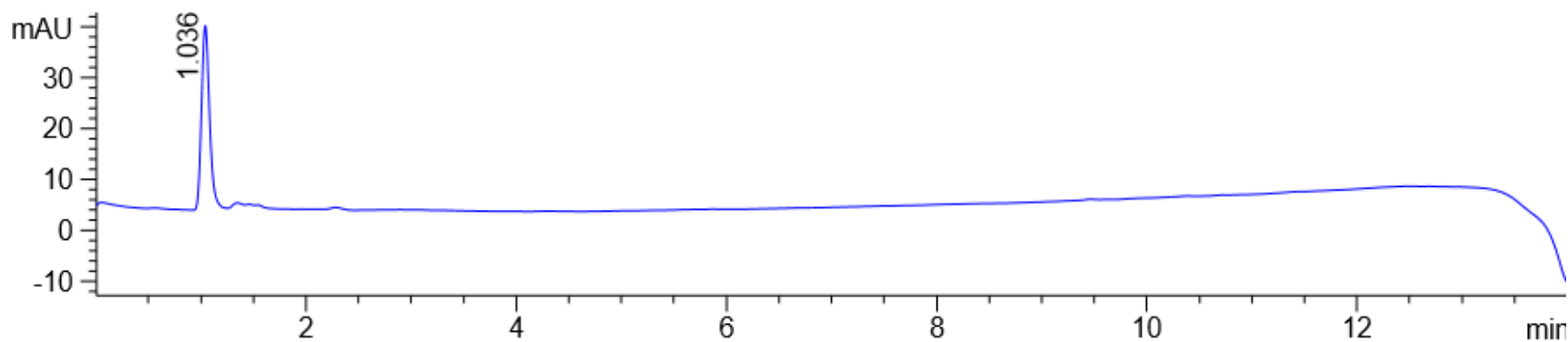
[(3*R*, 4*S*)-β-NH(C=O)Me-Agl³]-101.10 (4.2i)

LCMS chromatogram [10-90% MeOH (0.1% FA)/water (0.1% FA), 14 min]; RT = 7.5 on a CE-C18, 3 x 50 mm, 2.7 um with a flow rate of 0.4 mL/min.
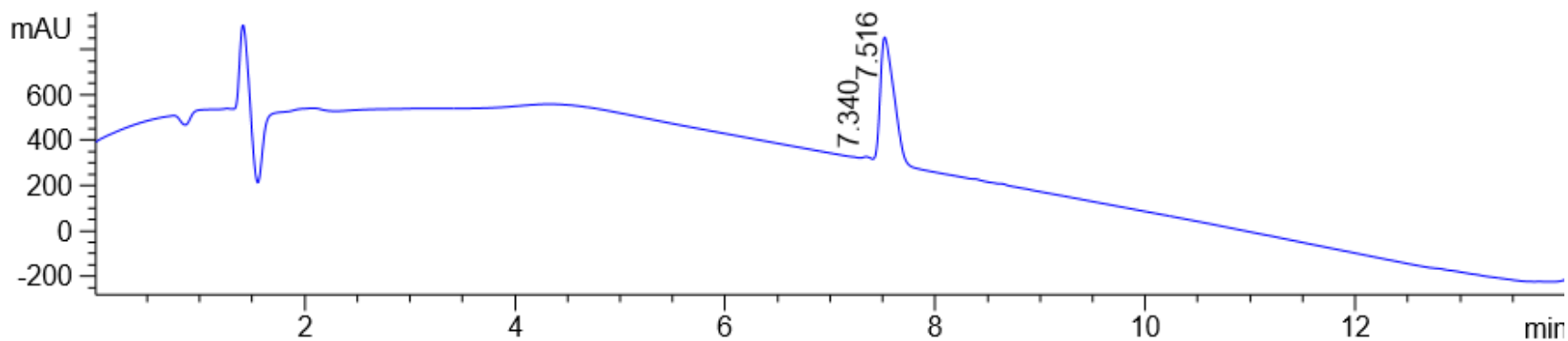
LCMS chromatogram [10-90% MeCN (0.1% FA)/water (0.1% FA), 14 min]; RT = 5.9 on a CE-C18, 3 x 50 mm, 2.7 um with a flow rate of 0.4 mL/min.


Annex 3: Supporting information of Article 3
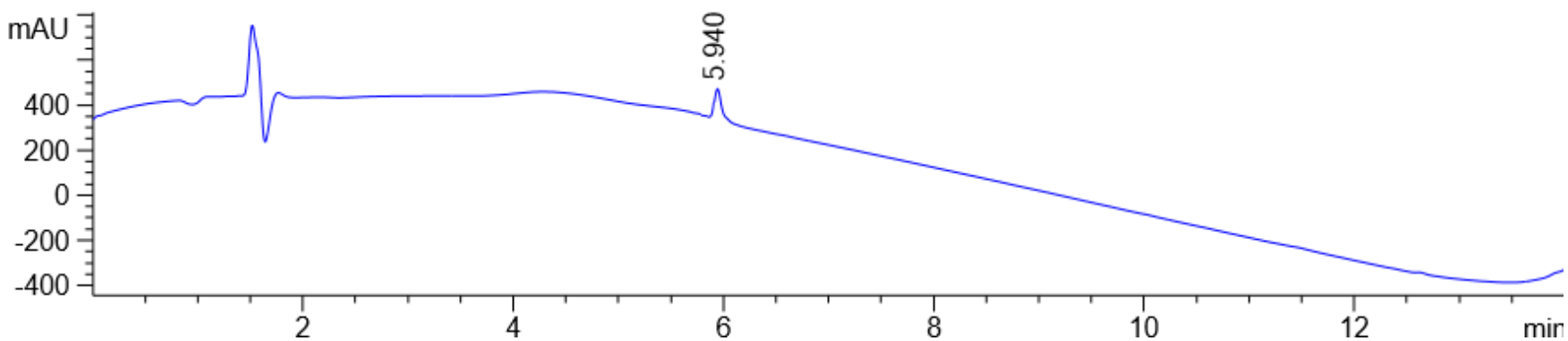
[(3*R*, 4*S*)-β-NH(C=O)NH₂-AgI³]-101.10 (4.2j)

LCMS chromatogram [10-90% MeOH (0.1% FA)/water (0.1% FA), 14 min]; RT = 7.3 on a CE-C18, 3 x 50 mm, 2.7 um with a flow rate of 0.4 mL/min.
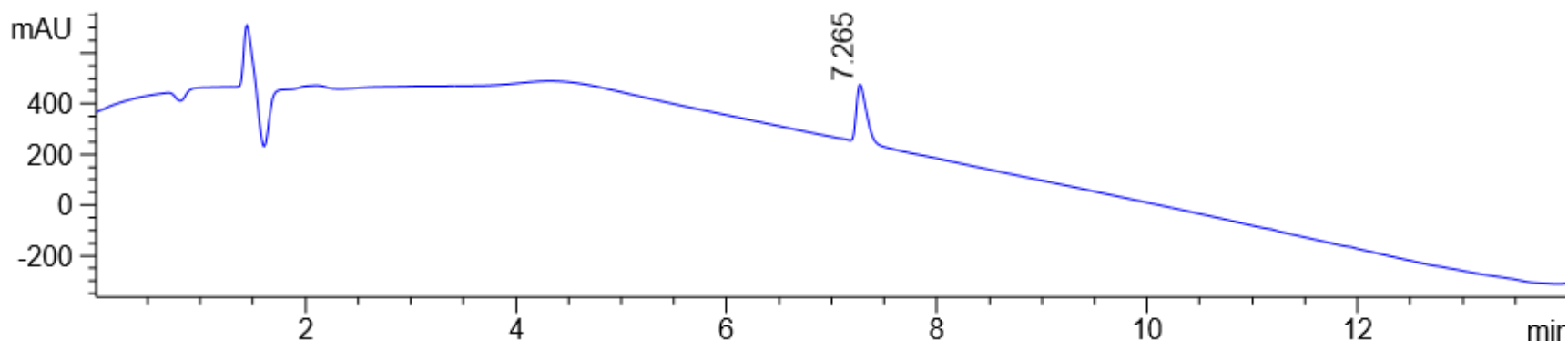
LCMS chromatogram [10-90% MeCN (0.1% FA)/water (0.1% FA), 14 min]; RT = 5.1 on a CE-C18, 3 x 50 mm, 2.7 um with a flow rate of 0.4 mL/min.

Annex 3: Supporting information of Article 3
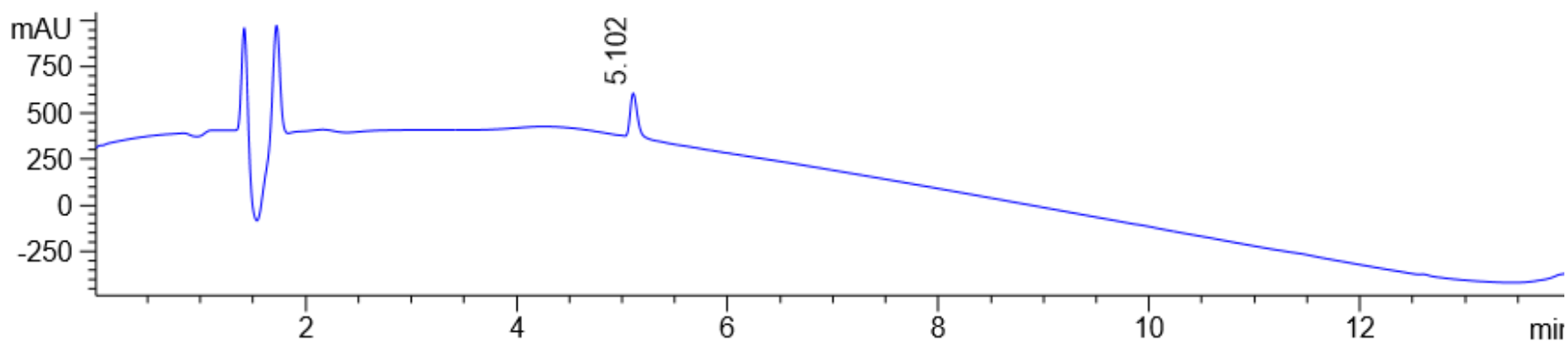
[(3*R*, 4*S*)-β-NH(C=N)NH₂-AgI³]-101.10 (4.2k)

LCMS chromatogram [10-90% MeOH (0.1% FA)/water (0.1% FA), 14 min]; RT = 5.9 on a CE-C18, 3 x 50 mm, 2.7 um with a flow rate of 0.4 mL/min.
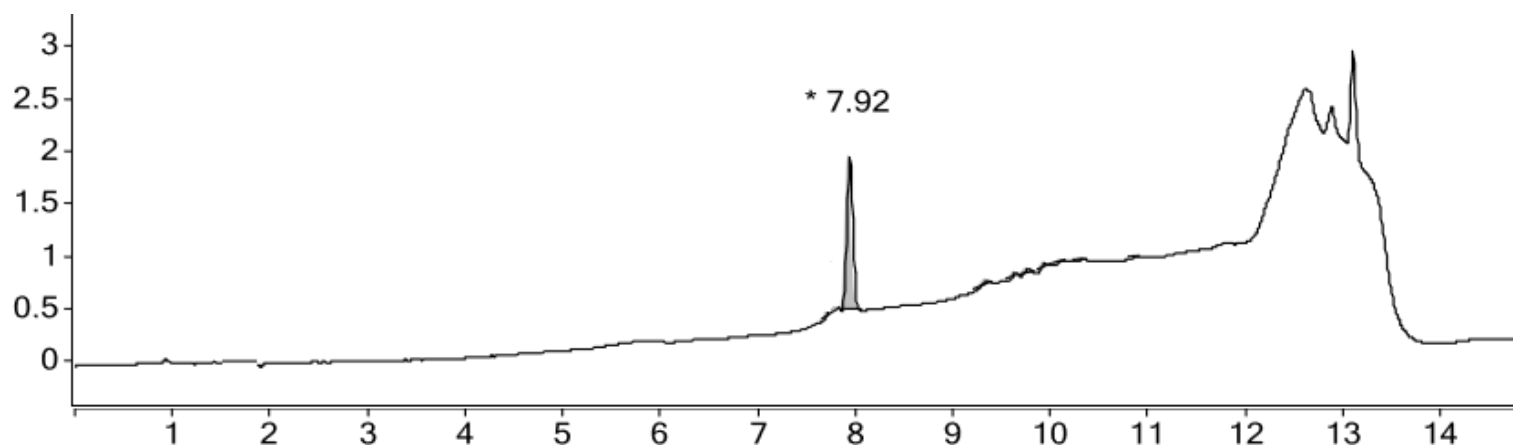

LCMS chromatogram [5-60-90% MeOH (0.1% FA)/water (0.1% FA), 15 min]; RT = 5.4 on a CSH C18, 4.6x100mm,5um, H₂O+0.1FA: MeOH

Annex 3: Supporting information of Article 3
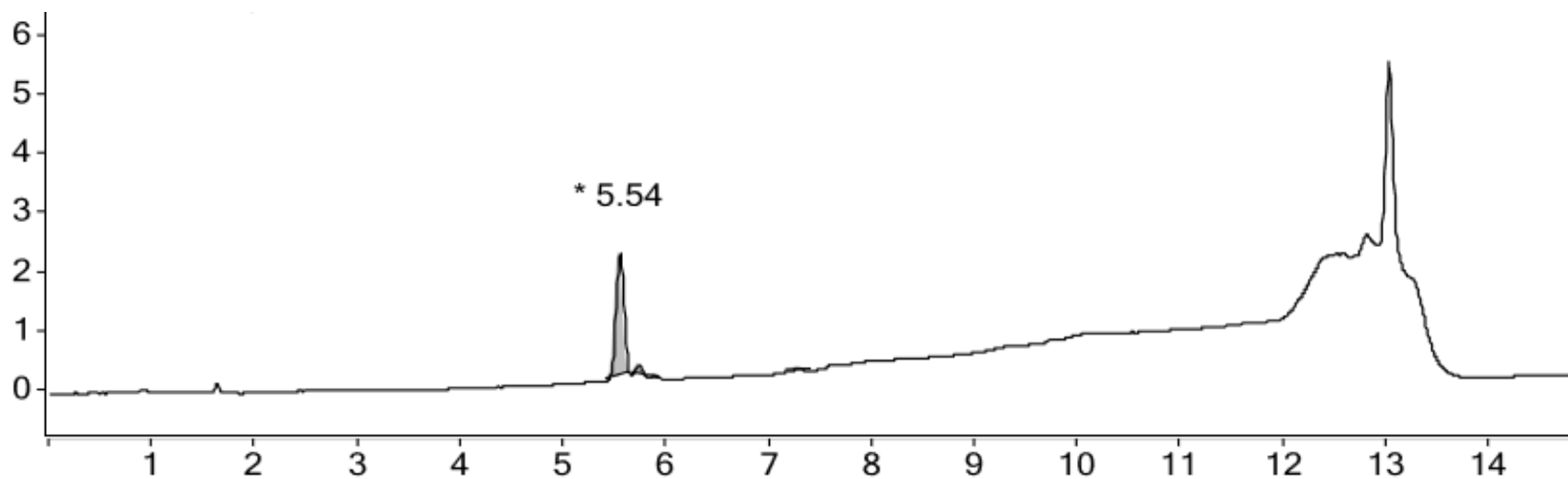
LCMS chromatogram [5-60-90% ACN (0.1% FA)/water (0.1% FA), 15 min]; RT = 4.6 on a CSH-C18, 4.6 X100 mm, 5 um, with a flow rate of 0.8 mL/min.
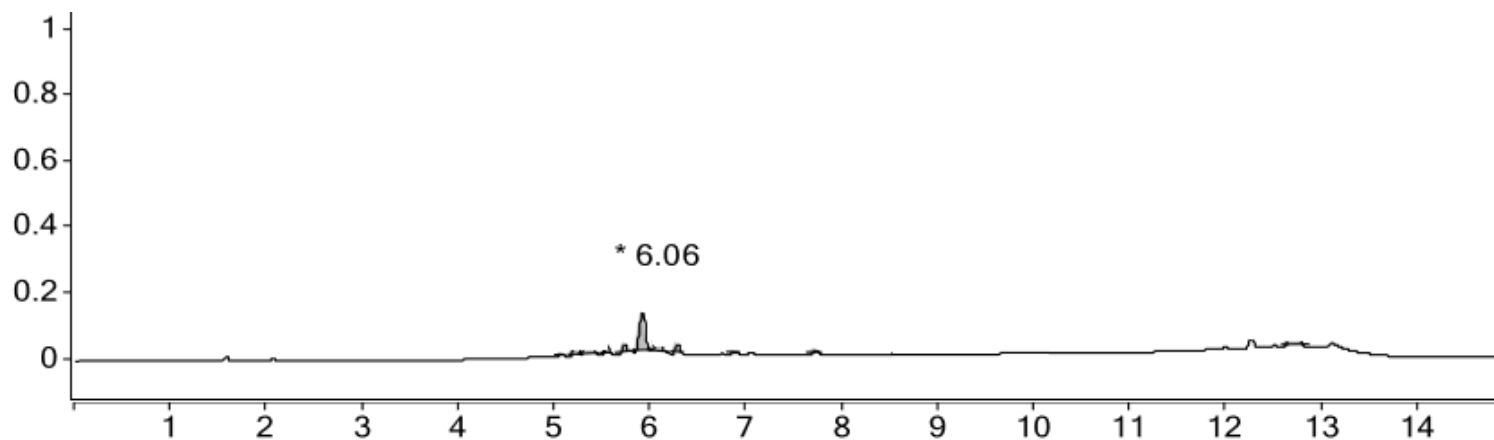
* 4.59

Annex 3: Supporting information of Article 3
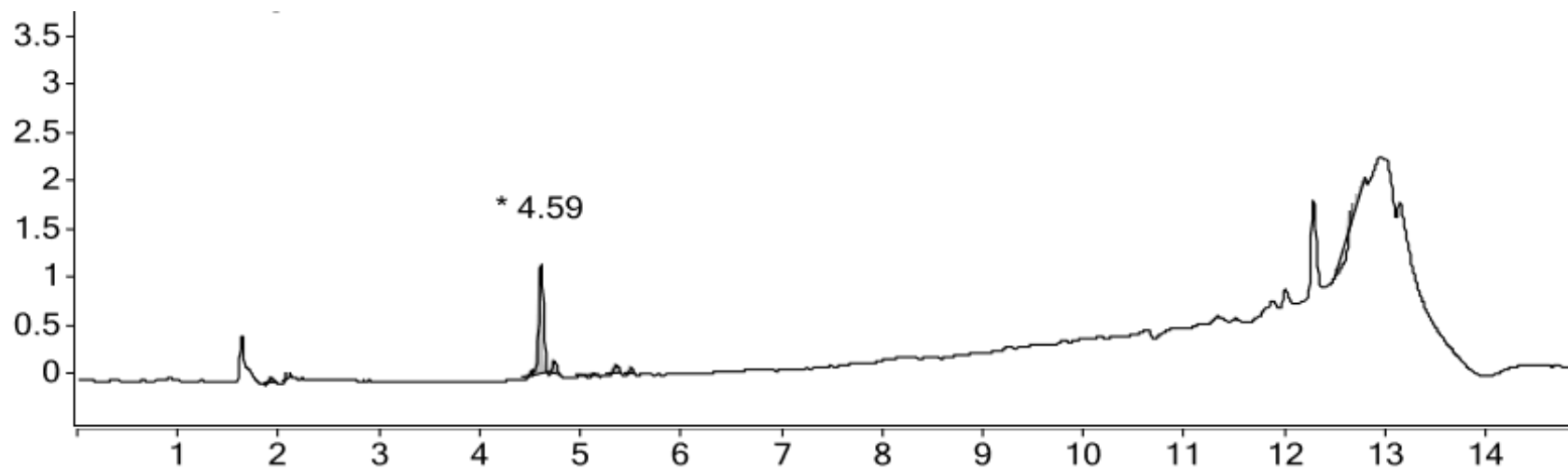
[(3*R*, 4*S*)-β-4-(Ph)triazolyl-Agl³]-101.10 (4.2l)

LCMS chromatogram [10-90% MeOH (0.1% FA)/water (0.1% FA), 14 min]; RT = 9.6 on a CE-C18, 3 x 50 mm, 2.7 um with a flow rate of 0.4 mL/min.
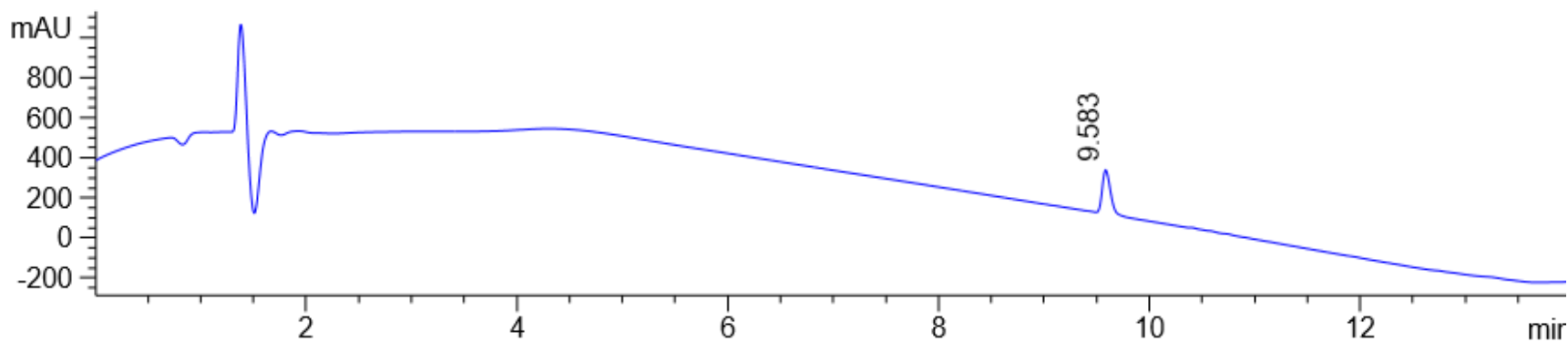
LCMS chromatogram [10-90% MeCN (0.1% FA)/water (0.1% FA), 14 min]; RT = 6.4 on a CE-C18, 3 x 50 mm, 2.7 um with a flow rate of 0.4 mL/min.

Annex 3: Supporting information of Article 3
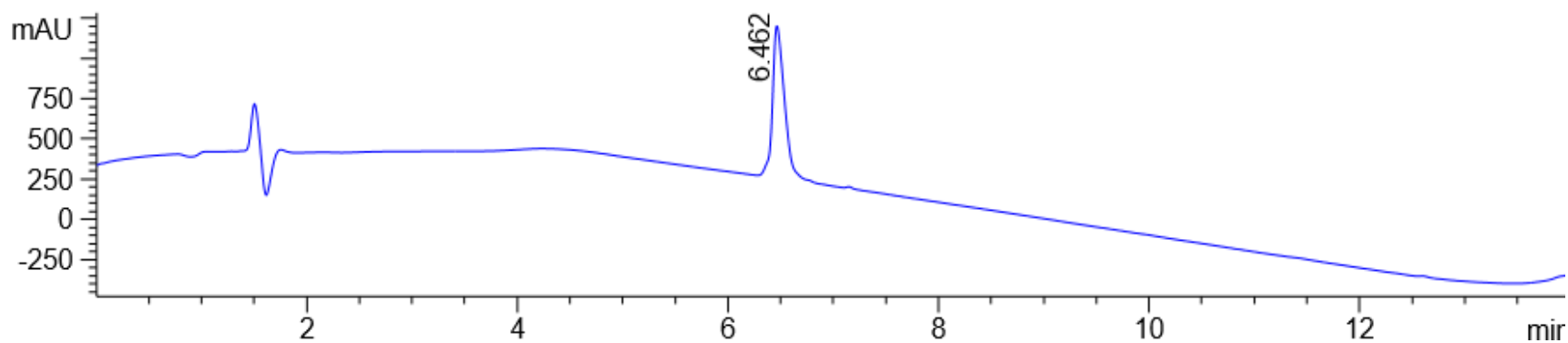
[(3R, 4S)-β-4-(p-MeC₆H₄)-triazolyl-AgI³]-101.10 (4.2m)

LCMS chromatogram [40-70-90% MeOH (0.1% FA)/water (0.1% FA), 15 min]; RT = 6.8 on a CSH-C18, 4.6 X100 mm, 5 um, with a flow rate of 0.8 mL/min.

LCMS chromatogram [20-40-90% ACN (0.1% FA)/water (0.1% FA), 15 min]; RT = 6.5 on a CSH-C18, 4.6 X100 mm, 5 um, with a flow rate of 0.8 mL/min.
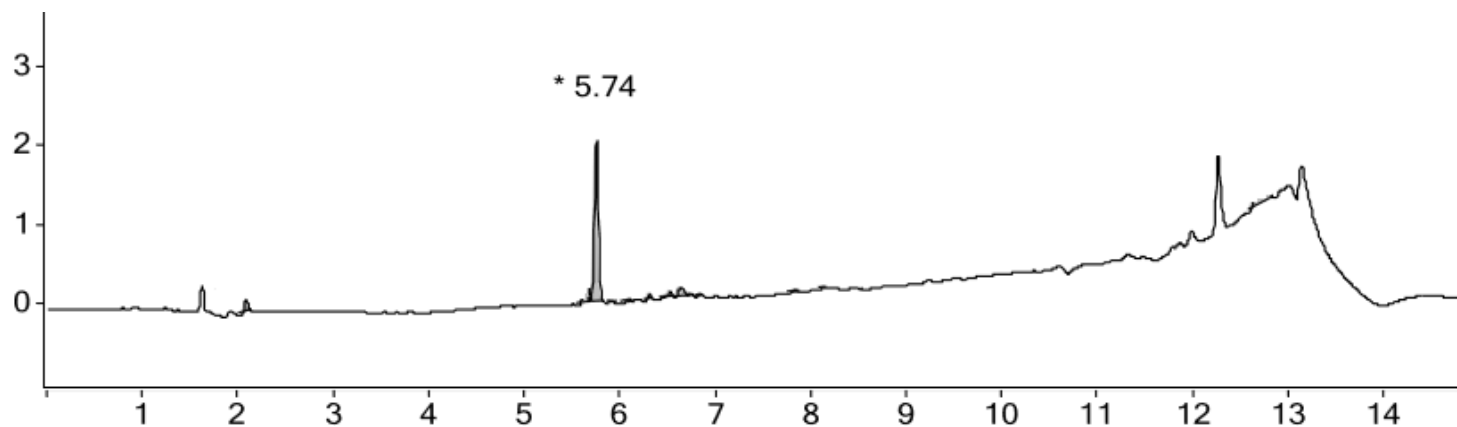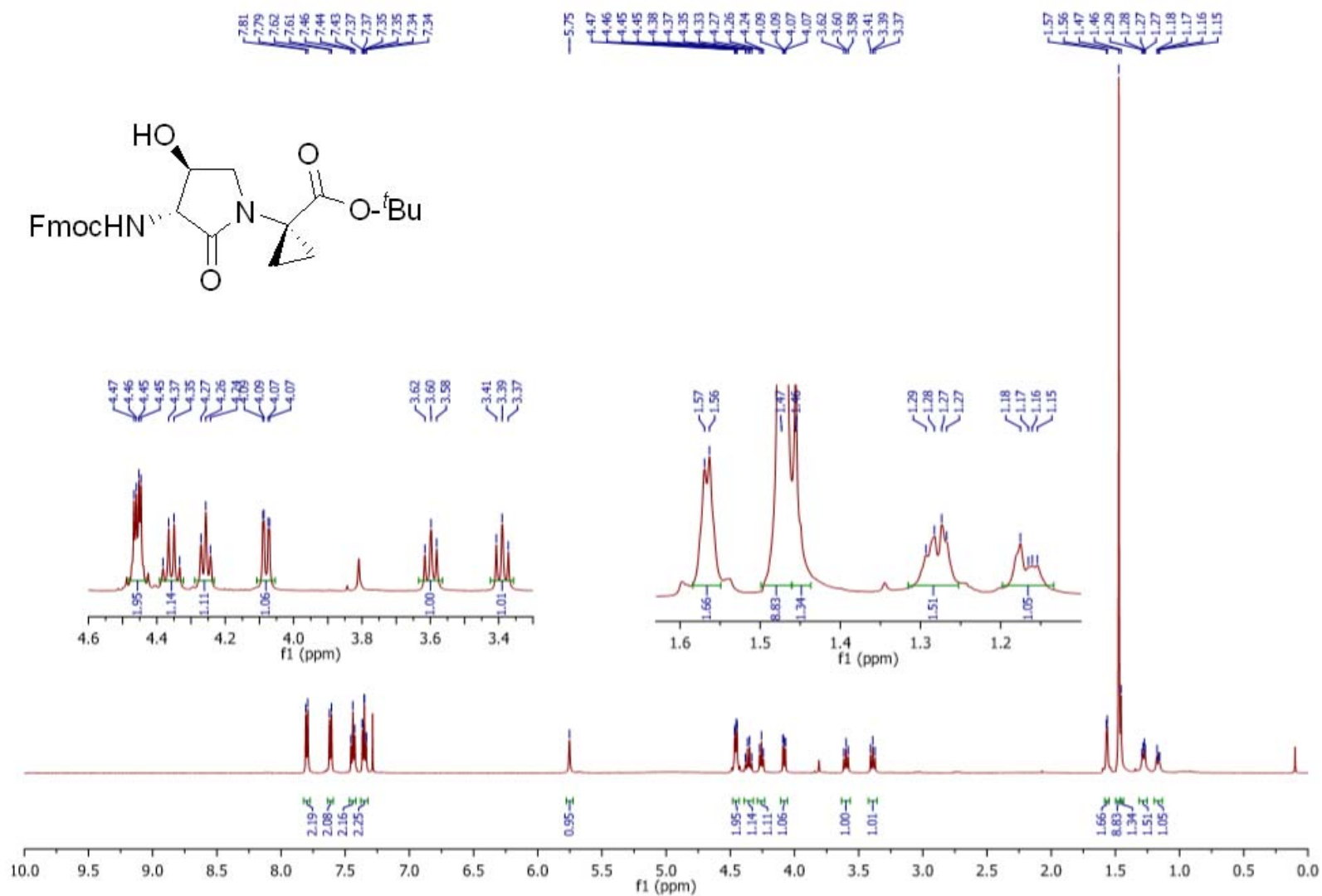

Annex 3: Supporting information of Article 3
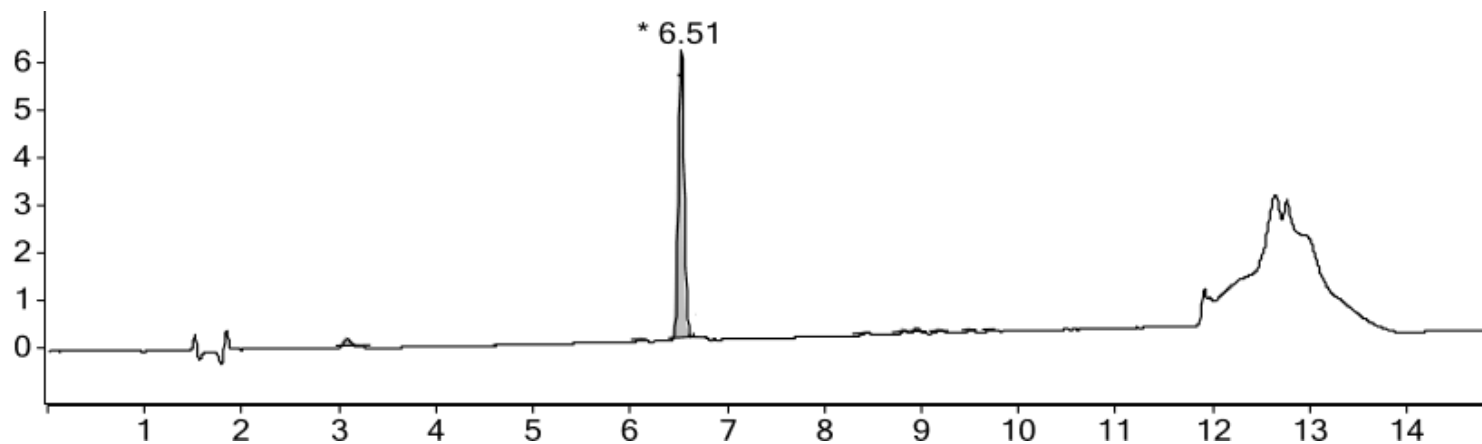
[(3R, 4S)-β-4-(m-H$_2$NC$_6$H$_4$)-triazolyl-Agl^3]-101.10 (4.2n)

LCMS chromatogram [5-60-90% MeOH (0.1% FA)/water (0.1% FA), 15 min]; RT = 8.8 on a CSH-C18, 4.6 X100 mm, 5 um, with a flow rate of 0.8 mL/min.


LCMS chromatogram [5-60-90% ACN (0.1% FA)/water (0.1% FA), 15 min]; RT = 6.1 on a CSH-C18, 4.6 X100 mm, 5 um, with a flow rate of 0.8 mL/min.
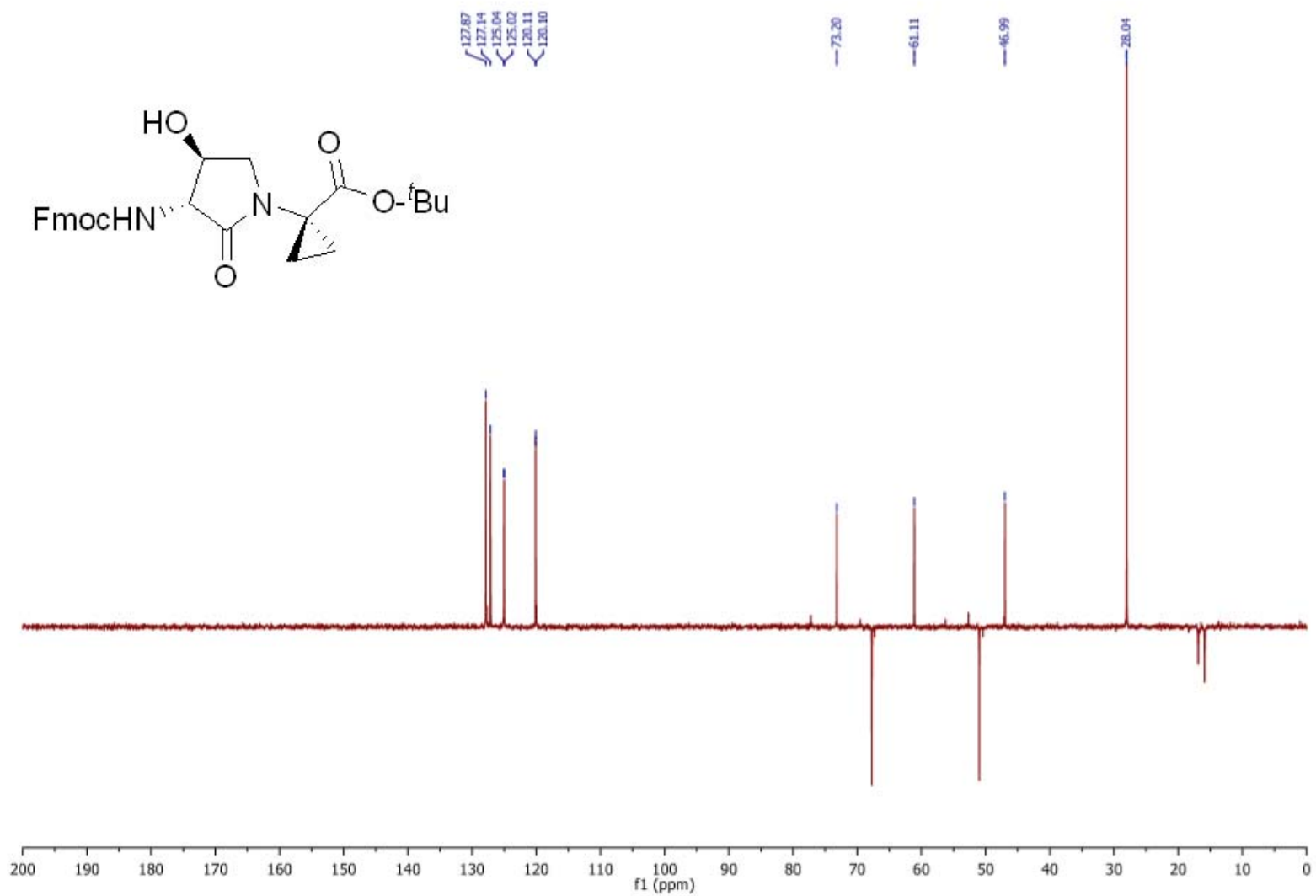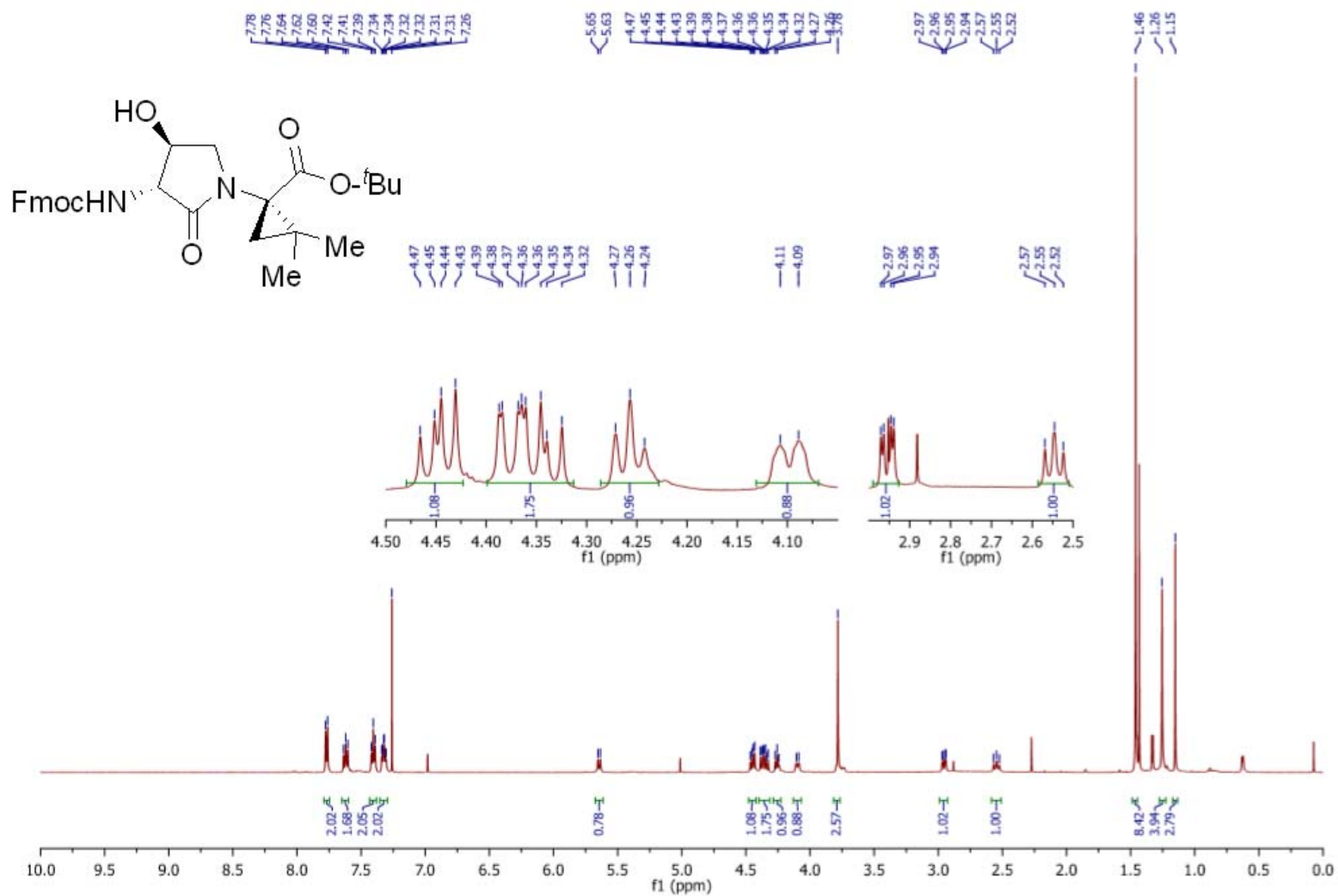

Annex 3: Supporting information of Article 3
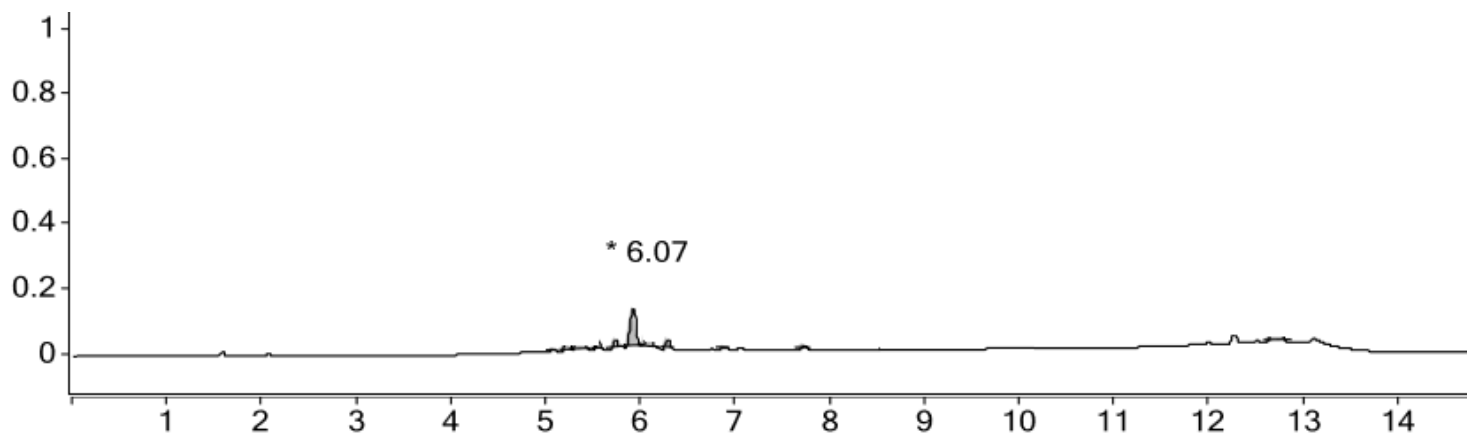
[(3*R*, 4*S*)-β-4-(H₂N(H₃C)₂C)-triazolyl-Agl³]-101.10 (4.2o)

LCMS chromatogram [5-60-90% MeOH (0.1% FA)/water (0.1% FA), 15 min]; RT = 6.3 on a CSH-C18, 4.6 X100 mm, 5 um, with a flow rate of 0.8 mL/min.
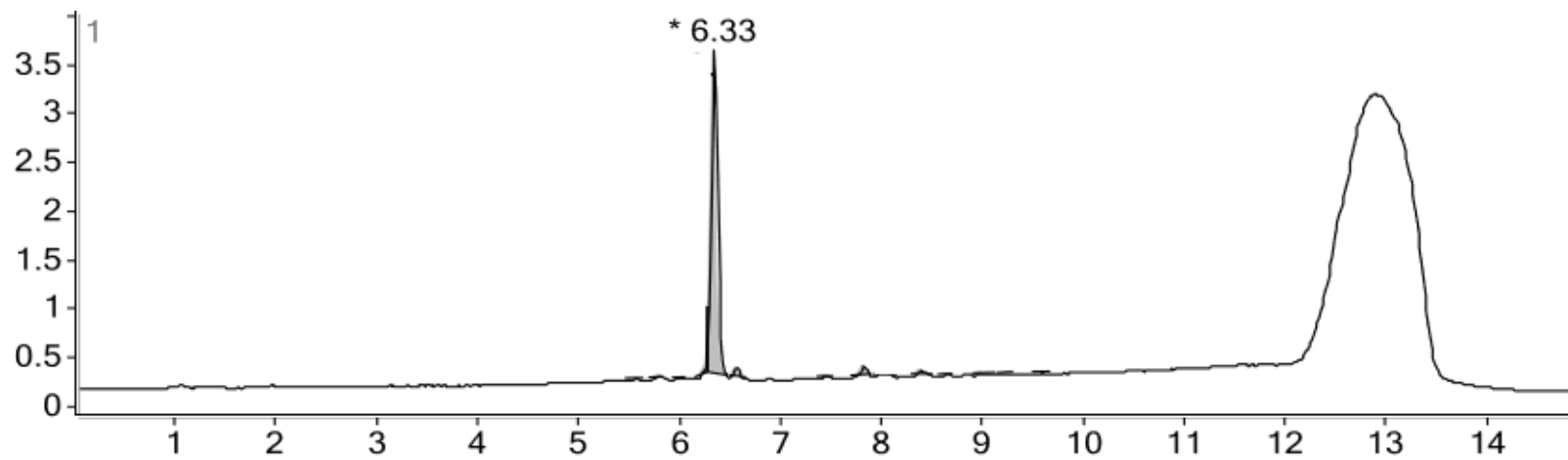
LCMS chromatogram [5-60-90% ACN (0.1% FA)/water (0.1% FA), 15 min]; RT = 4.9 on a CSH-C18, 4.6 X100 mm, 5 um, with a flow rate of 0.8 mL/min.

Annex 3: Supporting information of Article 3
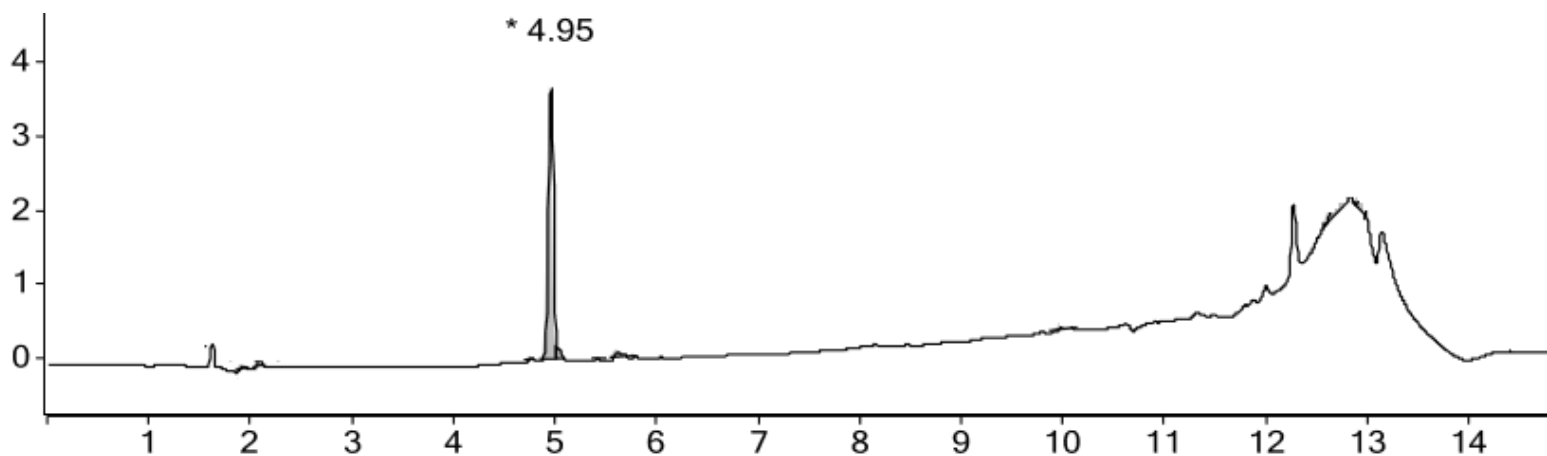
[(3*R*, 4*S*)-β-4-(H$_2$NH$_2$C)-triazolyl-Agl^3]-101.10 (4.2p)

LCMS chromatogram [5-60-90% MeOH (0.1% FA)/water (0.1% FA), 15 min]; RT = 7.9 on a CSH-C18, 4.6 X100 mm, 5 um, with a flow rate of 0.8 mL/min.

LCMS chromatogram [5-60-90% ACN (0.1% FA)/water (0.1% FA), 15 min]; RT = 6.1 on a CSH-C18, 4.6 X100 mm, 5 um, with a flow rate of 0.8 mL/min.

Annex 3: Supporting information of Article 3

[(3*R*, 4*S*)-β-4-(HOH₂C)-triazolyl-Agl³]-101.10 (4.2q)

LCMS chromatogram [5-60-90% MeOH (0.1% FA)/water (0.1% FA), 15 min]; RT = 7.2 on a CSH-C18, 4.6 X100 mm, 5 um, with a flow rate of 0.8 mL/min.
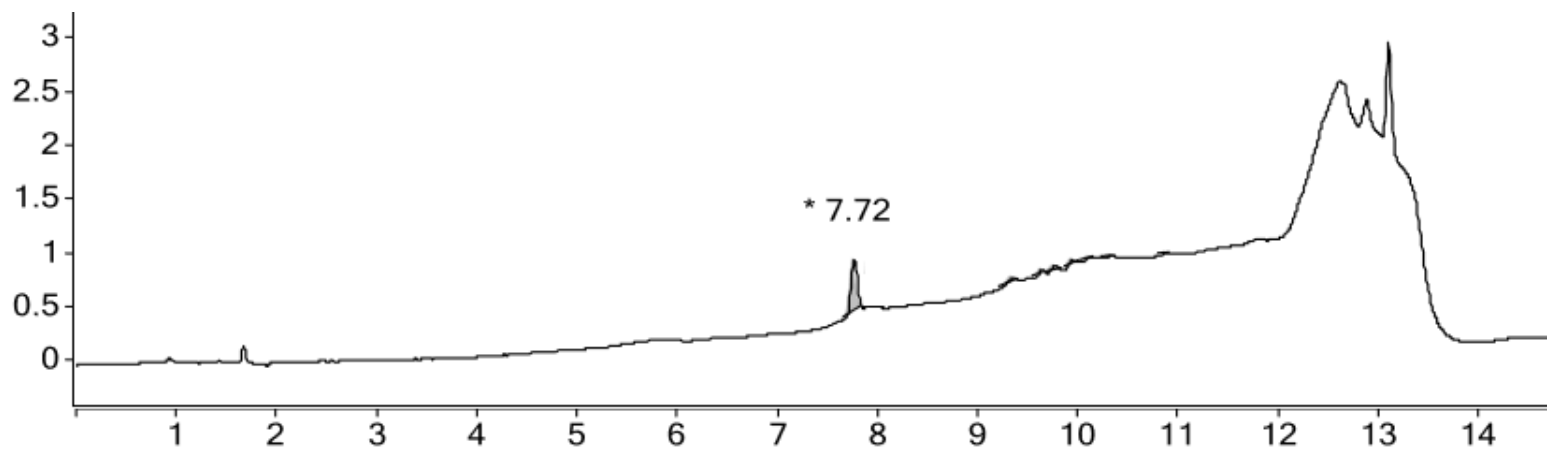
LCMS chromatogram [5-60-90% ACN (0.1% FA)/water (0.1% FA), 15 min]; RT = 5.7 on a CSH-C18, 4.6 X100 mm, 5 um, with a flow rate of 0.8 mL/min.

Annex 3: Supporting information of Article 3

Annex 4: Supporting information of chapter 5

Annex 3: Supporting information of Article 3

^{1}HNMR (500 MHz, CDCl$_3$) **5.6a**

^{13}CNMR (126 MHz, CDCl$_3$) **5.6a**
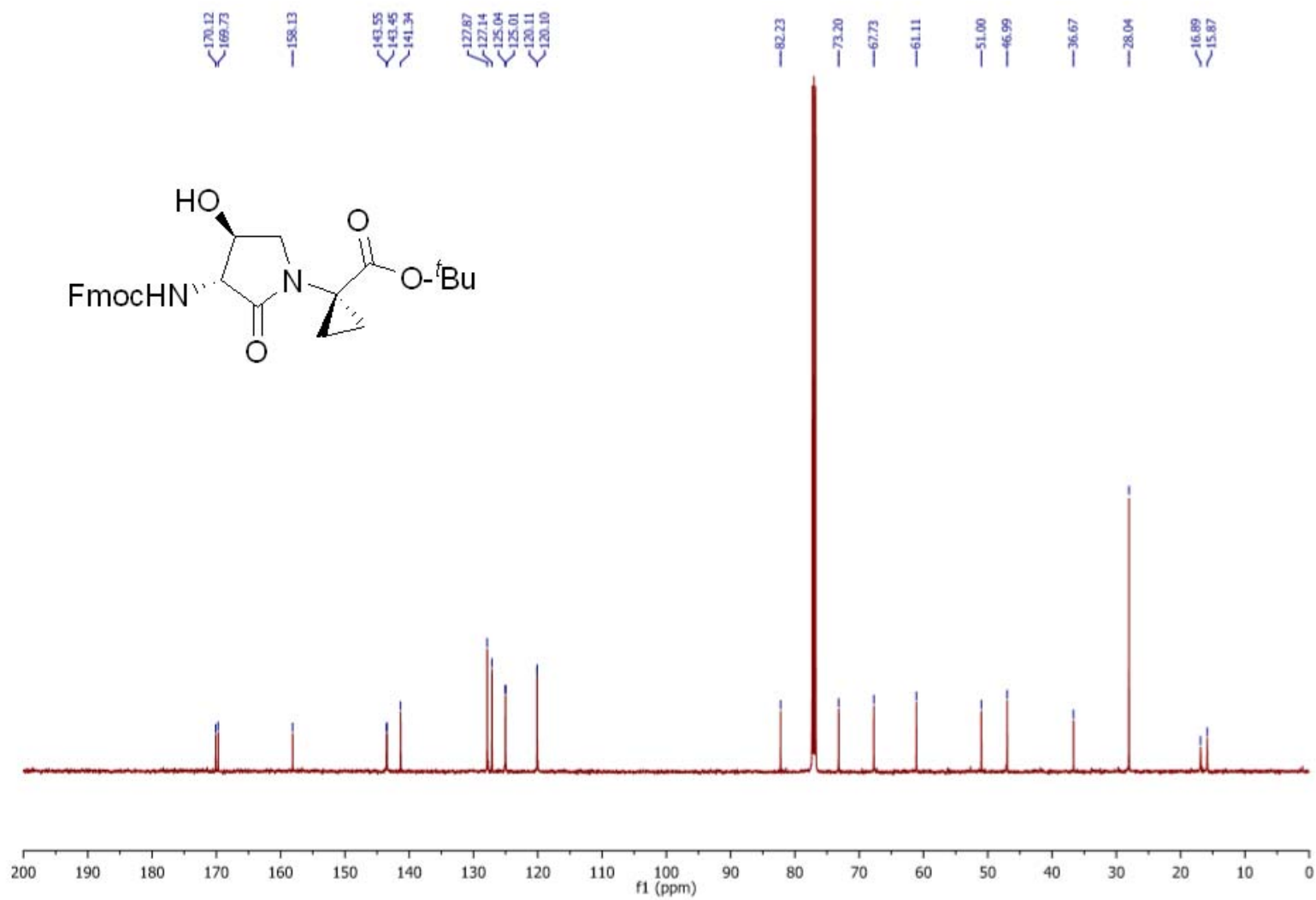
Annex 3: Supporting information of Article 3

dept (126 MHz, CDCl₃) **5.6a**

Annex 3: Supporting information of Article 3

^{1}HNMR (500 MHz, CDCl$_3$) **5.7a (Less polar)**

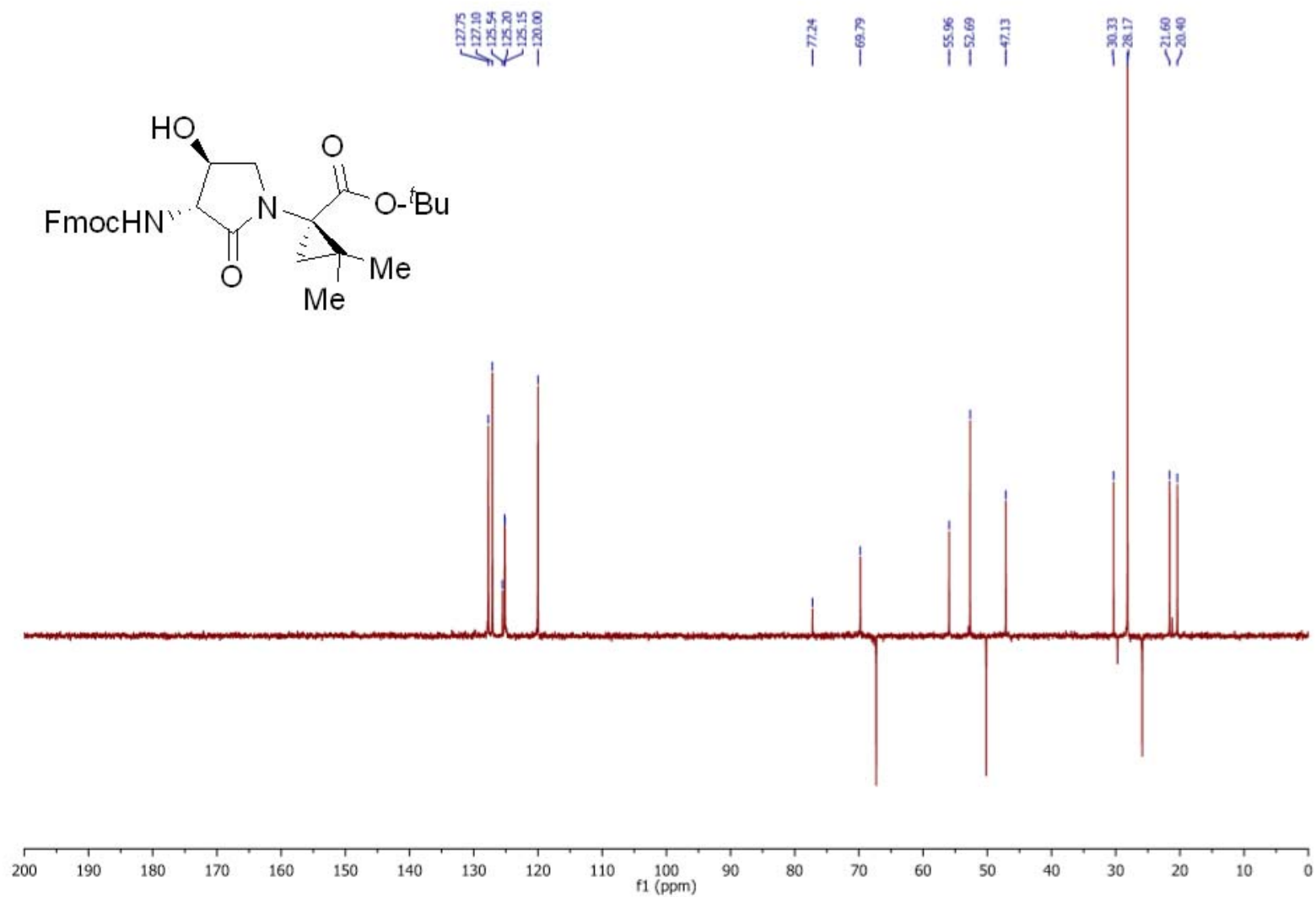4.50 4.45 4.40 4.35 4.30 4.25 4.20 4.15 4.10
f1 (ppm)

2.9 2.8 2.7 2.6 2.5
f1 (ppm)

10.0 9.5 9.0 8.5 8.0 7.5 7.0 6.5 6.0 5.5 5.0 4.5 4.0 3.5 3.0 2.5 2.0 1.5 1.0 0.5 0.0
f1 (ppm)

Annex 3: Supporting information of Article 3

^{13}CNMR (126 MHz, CDCl$_3$) **5.7a (Less polar)**
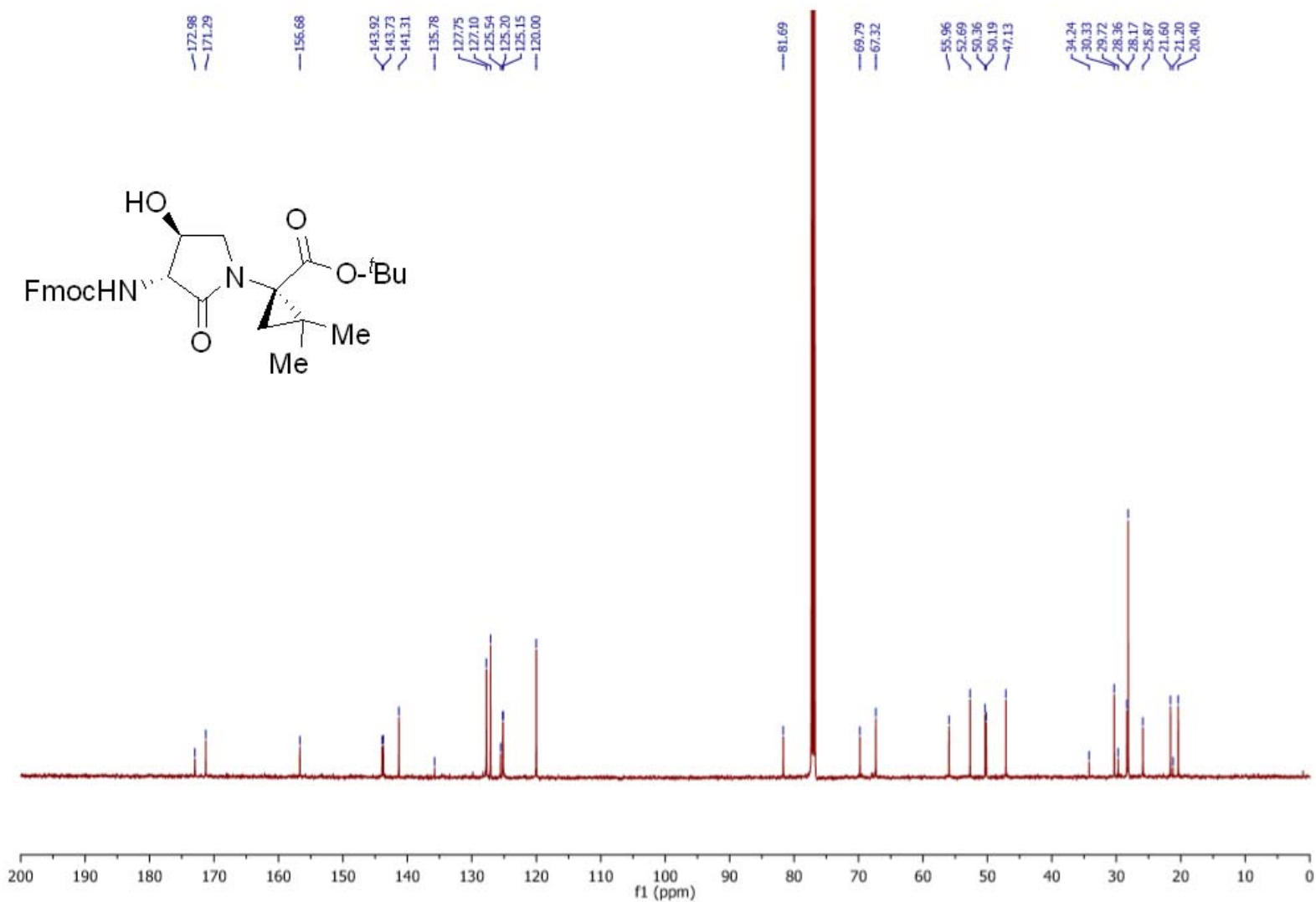
dept (126 MHz, CDCl₃) **5.6a (Less polar)**
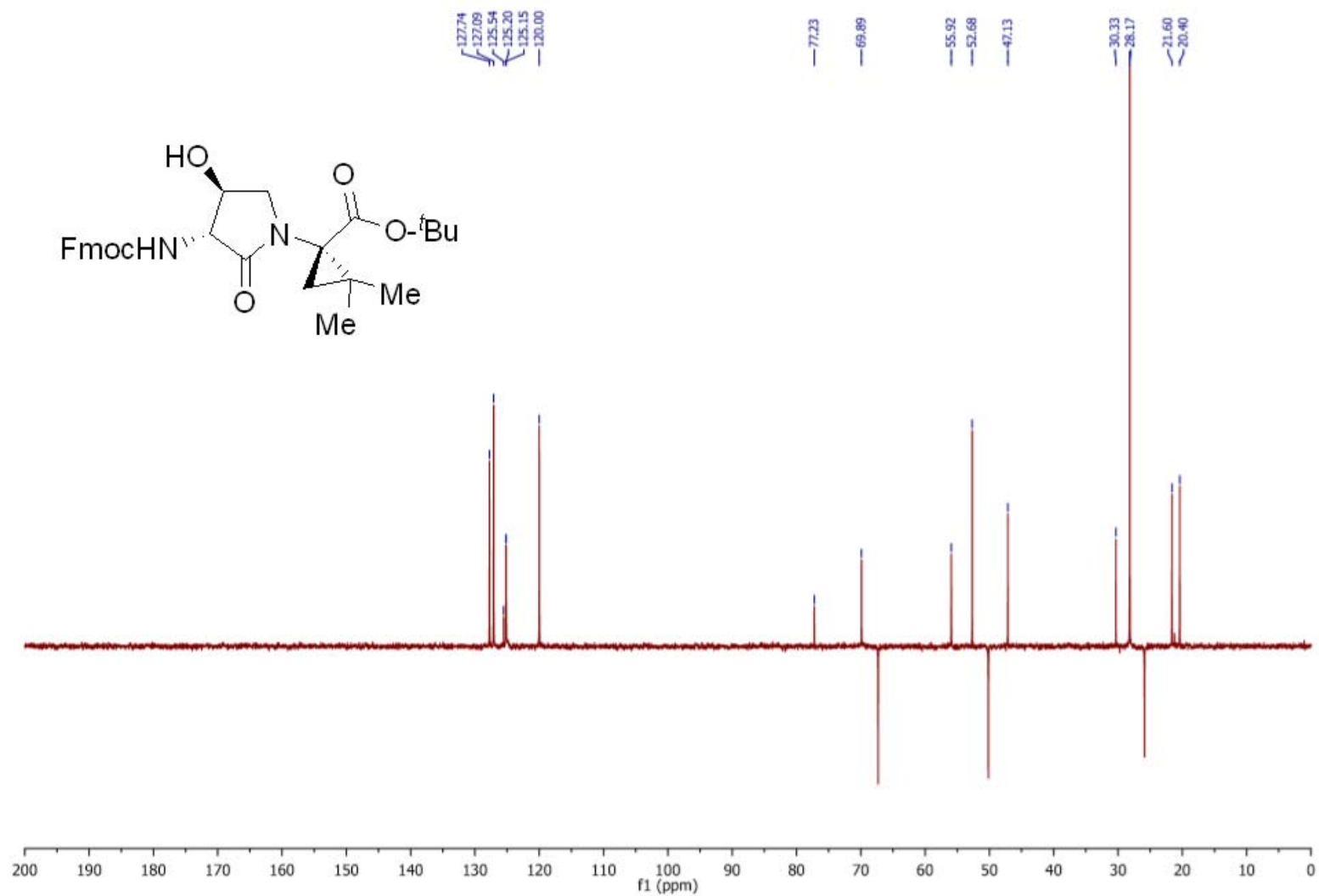
^{1}HNMR (500 MHz, CDCl$_3$) **5.7a (More polar)**
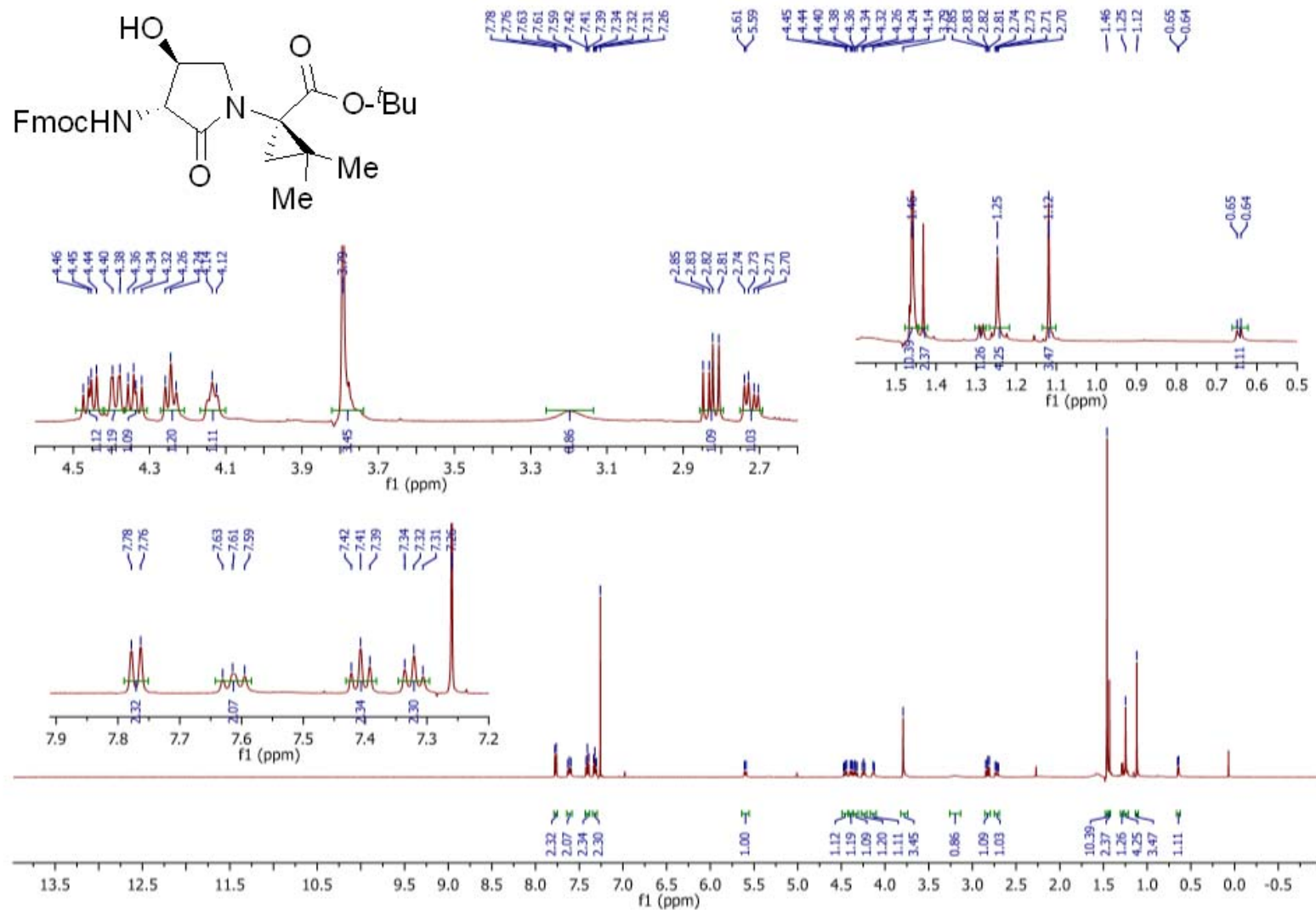
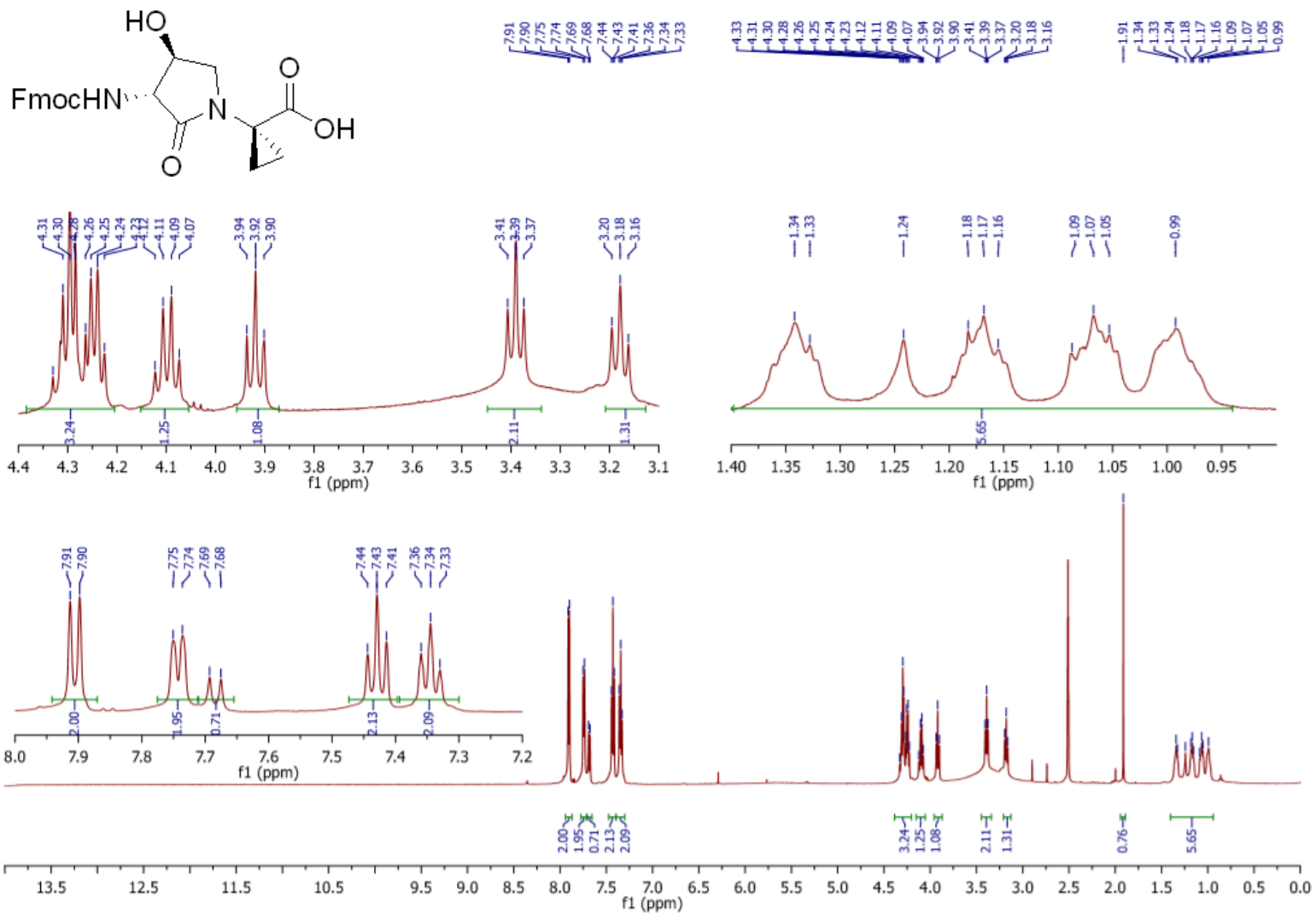^{13}CNMR (126 MHz, CDCl$_3$) **5.7a (More polar)**
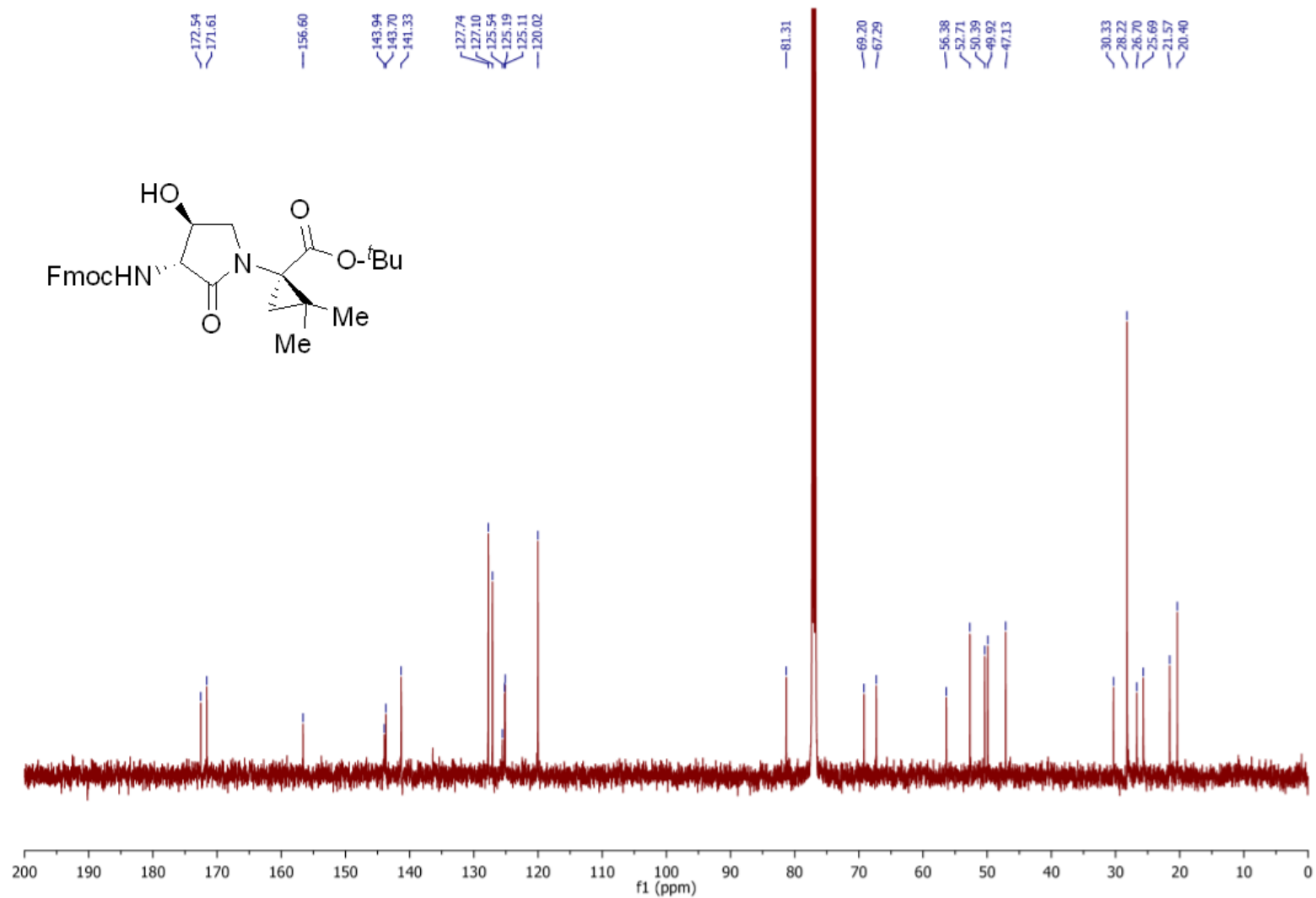
dept (126 MHz, CDCl₃) **5.6a (More polar)**

^{1}HNMR (500 MHz, CDCl$_3$) **5.6b**

Annex 3: Supporting information of Article 3

^{13}CNMR (126 MHz, CDCl$_3$) **5.6b**

200 190 180 170 160 150 140 130 120 110 100 90 80 70 60 50 40 30 20 10 0
f1 (ppm)
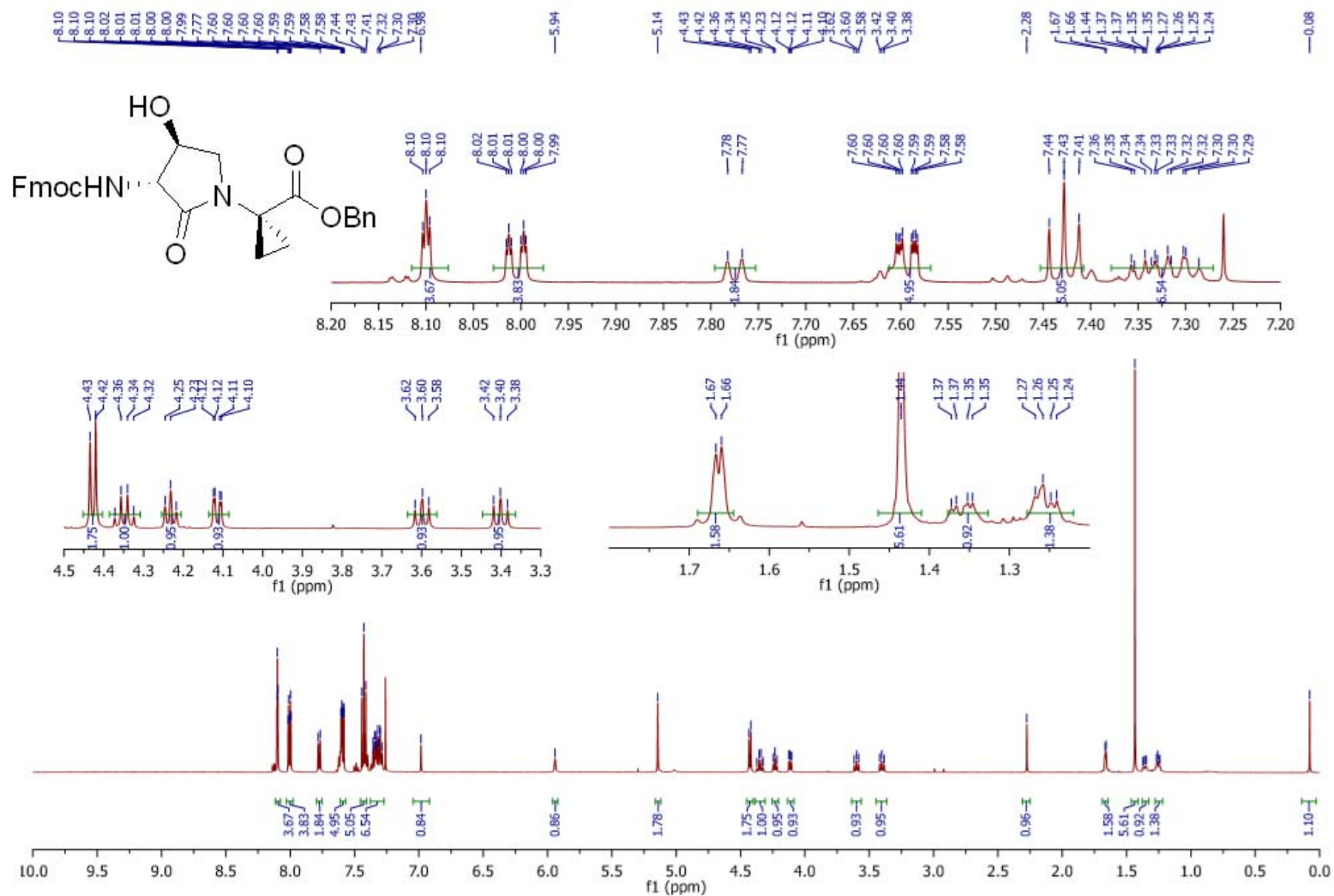
Annex 3: Supporting information of Article 3
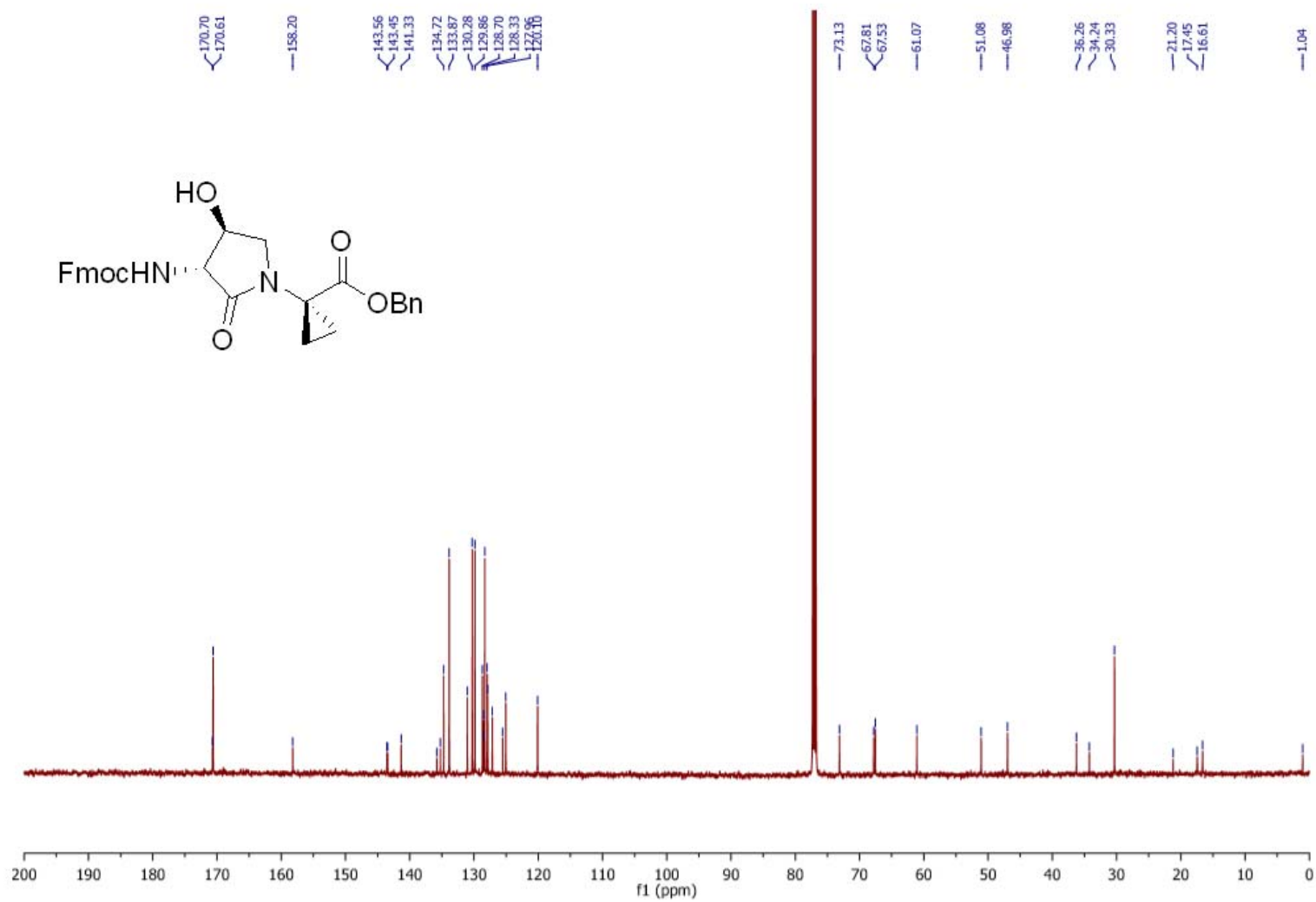
dept (126 MHz, CDCl$_3$) **5.6b**
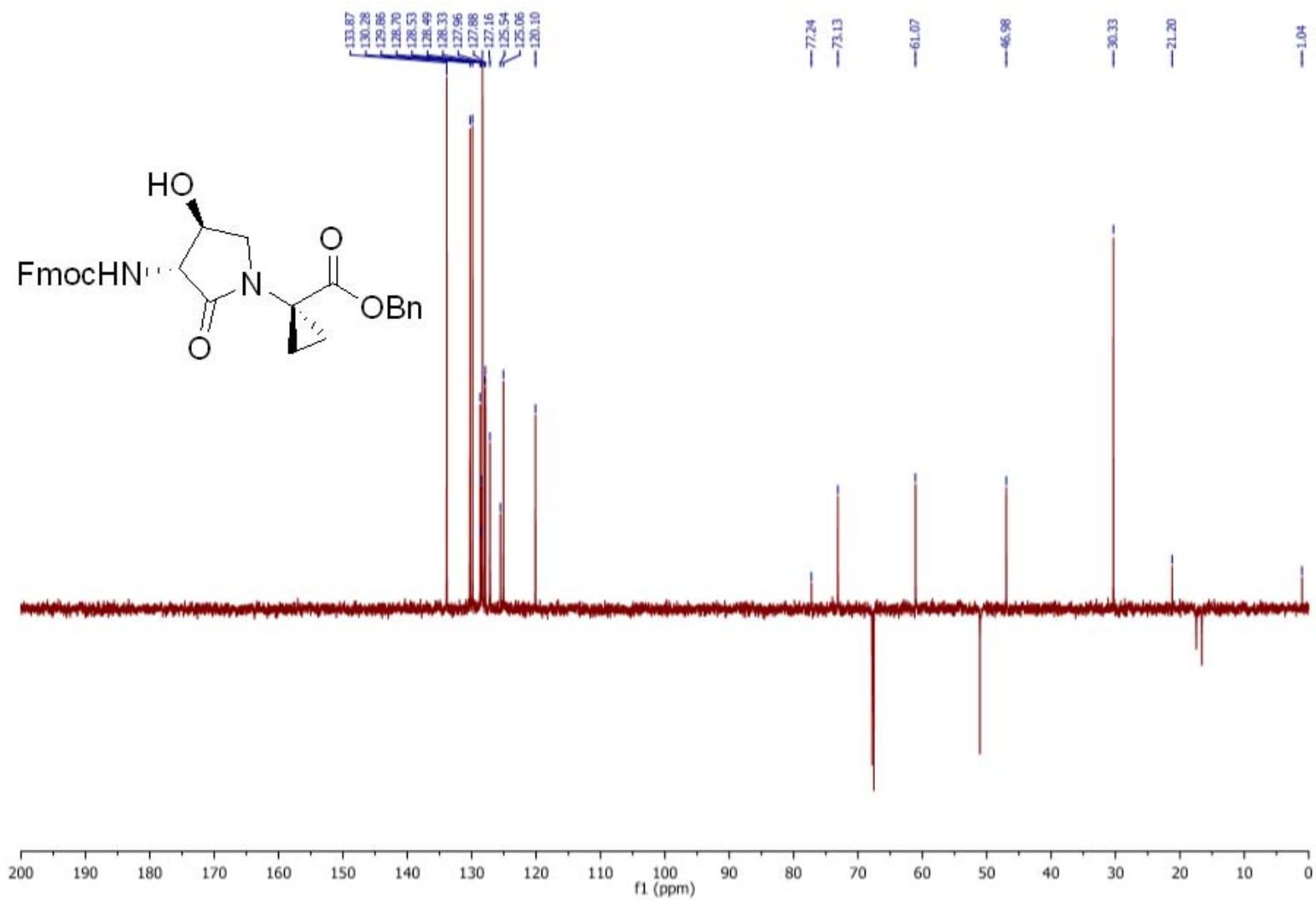
Annex 3: Supporting information of Article 3

^{1}H NMR (500 MHz, DMSO) **5.8**
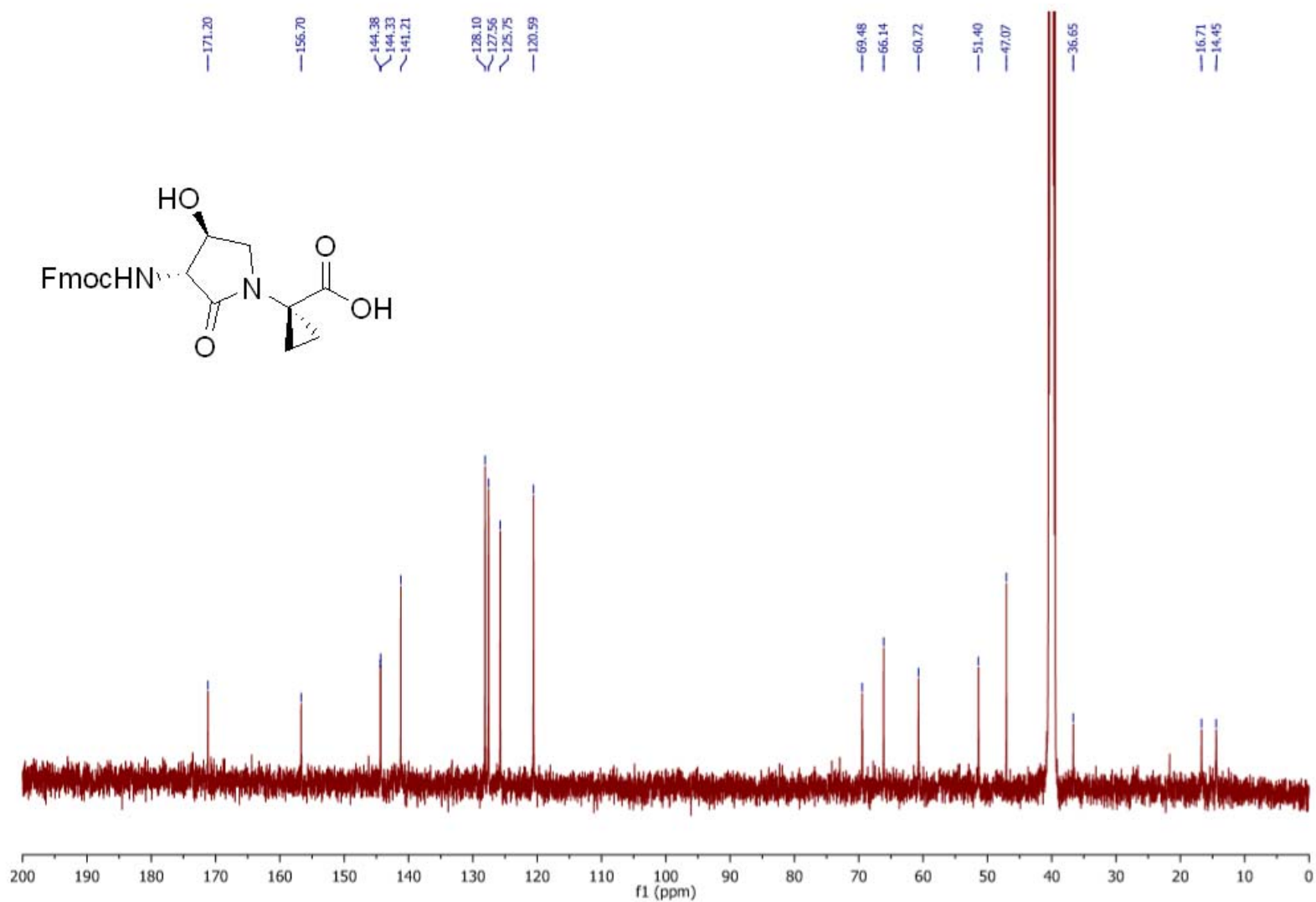
Annex 3: Supporting information of Article 3
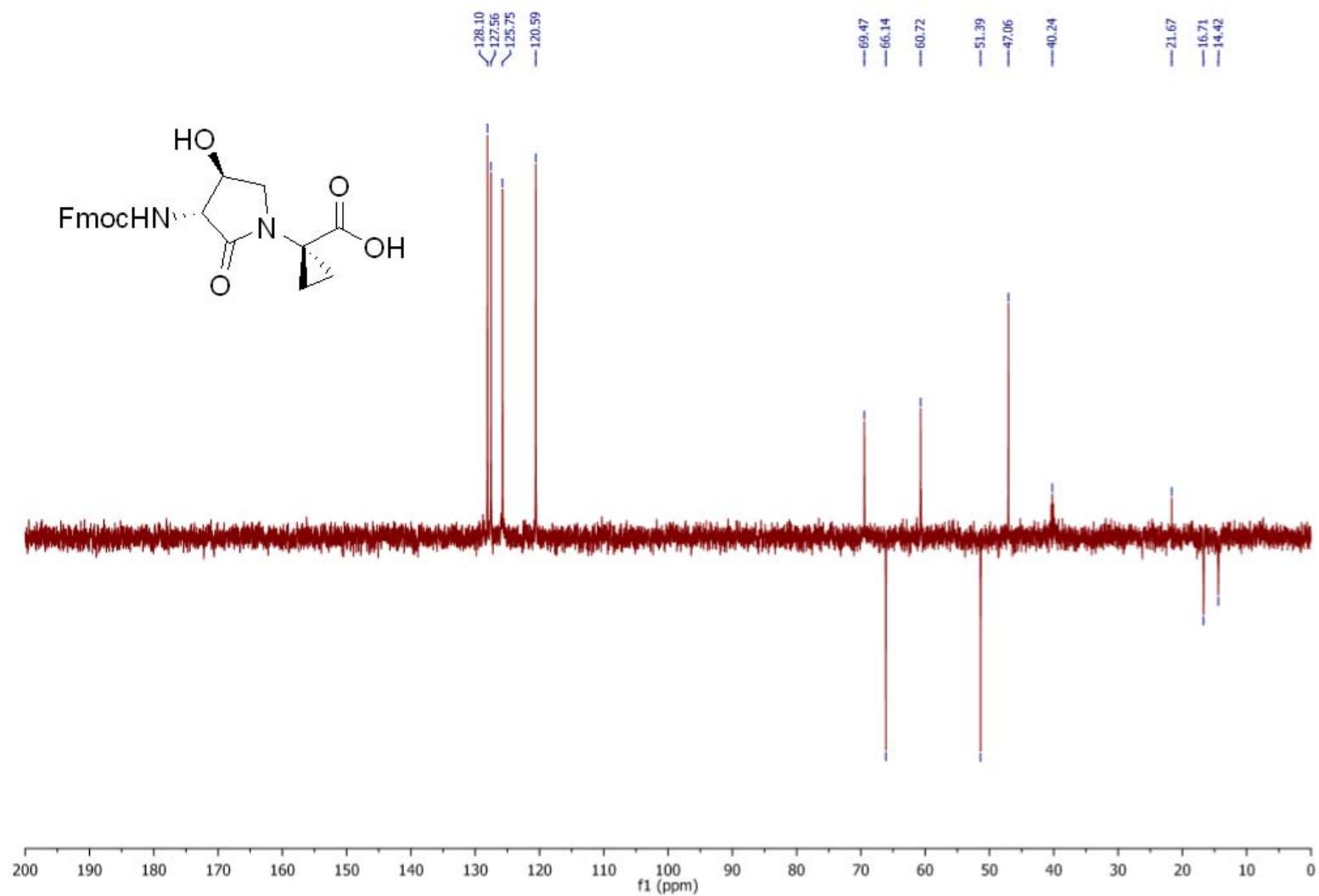
^{13}C NMR (126 MHz, DMSO) **5.8**

dept (126 MHz, DMSO) **5.8**